Dynamic Energy and Mass Budgets

in Biological Systems

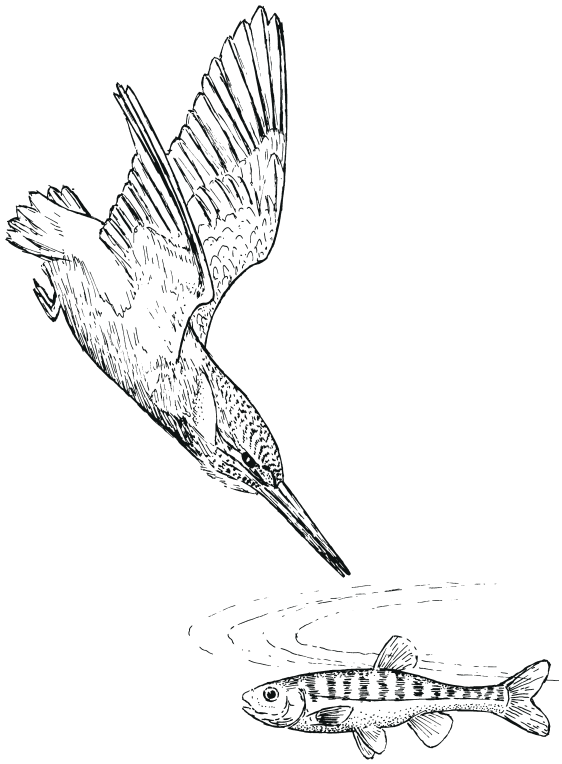

S.A.L.M. Kooijman

second edition

Dynamic Energy Budget theory unifies the commonalities between organisms as prescribed by the implications of energetics, which link different levels of biological organization (cells, organisms and populations). The theory presents simple mechanistic rules that describe the uptake and use of energy and nutrients and the consequences for physiological organization throughout an organism's life cycle, including the relationships between energetics and aging and the effects of toxicants. In this new edition, the theory is broadened to encompass the fluxes of both energy and mass. All living organisms are now covered in a single quantitative framework, the predictions of which are tested against a wide variety of experimental results at the various levels of biological organization. The theory explains many general observations, such as the body size scaling relationships of certain physiological traits, and provides a theoretical basis for the widely used method of indirect calorimetry. In each case, the theory is developed in elementary mathematical terms, but a more detailed discussion of the methodological aspects of mathematical modelling is also included, making the book suitable for biologists and mathematicians with a broad interest in both fundamental and applied quantitative problems in biology.

Bas Kooijman is Professor of Applied Theoretical Biology at the Vrije Universiteit in Amsterdam and is also head of the University's Department of Theoretical Biology. His research focuses on mathematical biology, in particular ecotoxicology which provided the framework for the original version of his Dynamic Energy Budget theory published in 1993 (*Dynamic Energy Budgets in Biological Systems - Theory and Applications in Ecotoxicology*).

From the first edition:

"This book is an excellent scientific product that informs and forces contemplation of issues relating to population and community ecology. The author has made a complex subject coherent." Thomas G. Hallam, Bulletin of Mathematical Biology

"... a very useful and general tool to select more ecologically sound process equations and parameters in ecological models." Sven Erik Jørgensen, Ecological Modelling

"The author has made a significant contribution to the problem of modelling the dynamics of biological populations at the level of the individual by synthesizing this very complicated subject into a relatively short list of general assumptions and putting the energetics of sub-models for vital rates on a solid basis." Jim Cushing, Mathematical Biosciences

"The family of idealized models offered in this book is capable of playing a role analogous to that of Lotka-Volterra models in population dynamics ... I am confident that any model(s) capable of occupying this niche will be strongly influenced by the ideas in this book." Roger Nisbet, Ecology

Cambridge university press

Dynamic Energy and Mass Budgets

in Biological Systems

S.A.L.M. Kooijman

Professor of Theoretical Biology, Vrije Universiteit,
de Boelelaan 1087, 1081 HV Amsterdam

Errata implemented 30 July 2008

Cambridge university press
Cambridge
New York *Port Chester*
Melbourne *Sydney*

Published by the Press Syndicate of the University of Cambridge
The Pitt Building, Trumpington Street, Cambridge CB2 1RP
40 West 20th Street, New York, NY 10011-4211, USA
10 Stamford Road, Oakleigh, Melbourne 3166, Australia

First published 1993

Printed in Great Britain at the University Press, Cambridge

British Library Cataloguing in publication data available

Library of Congress cataloguing in publication data available

ISBN 0 521 45223 6 hardback
ISBN 0 521 786088 paperback

Summary of contents

Contents

Preface to the second edition

The substantial progress made in many developments of the Dynamic Energy Budget (DEB) theory and its applications has prompted a new edition of the book '*Dynamic Energy Budgets in Biological systems – Theory and Applications in Ecotoxicology*'. I must admit that, while extending the theory, I did not exclude the risk that the theory would tumble over, like an overloaded Christmas tree. However, the opposite has happened; the theory has gained in logical structure, broadened its physico-chemical basis, and become in many respects simpler conceptually. I consider this to be the most reliable indication that the theory really has a strong and healthy backbone.

The most fundamental progress is in the development of a framework that accommodates both energy and mass fluxes. This provides a theoretical basis for the method of indirect calorimetry and elaboration of the coupling between energy and mass fluxes, including respiration rates. Simultaneous limitation of growth by nutrients is modelled by the construct 'Synthesizing Unit', which is a 'natural' generalization of single substrate enzyme kinetics, after re-formulation in terms of substrate fluxes rather than substrate concentrations. Extending the theory from one reserves and structural mass to several provides the proper conceptual basis to deal with autotrophs (algae, plants). These had to be omitted in the first edition. Hence, the title has be changed slightly, because now the theory covers all forms of life.

The DEB theory has been deepened as well as extended. The assumption of first-order dynamics for reserve density has been replaced by more fundamental ones about body composition. Although this change has no quantitative consequences, the conceptual gain is considerable for a theory that emphasizes mechanisms and consistency.

The material on mass fluxes has been reorganized and collected in a new chapter on the implications of energy fluxes for fluxes of essential nutrients. Extensions include an analysis of the respiration ratio and the heat increment of feeding, fermentation processes, a model for drinking and its relationship with nutrient uptake by plants, and a reanalysis of heating costs in endotherms. The material on aging has been moved to this new chapter, since aging is treated as a consequence of the flux of free radicals that originates from respiration. Less emphasis has been put on the concept of 'yield' compared to the first edition, because I now think that this ratio of two mass fluxes overly complicates the arguments for application in transient situations, where reserves play an important role. I removed a section on this concept. Another new chapter has been written to extend the single substrate, reserve and structural mass to several substrates, reserves and structural masses, which is necessary to deal with the metabolic versatility found in algae and plants.

These extensions have the property that the dynamics of several reserves can be coupled and uncoupled in a smooth way; a single reserve is a special case. This is of significance in an evolutionary context.

The material on ecotoxicity is rewritten and extended in a chapter on fluxes of non-essential nutrients and their (toxic) effects. Extensions include sublethal effects on growth and reproduction, with an analysis of the various direct and indirect pathways. I removed material that I now consider to be less important to the DEB theory, such as the correlation between concentrations of compounds in the environment and tissues, and the discussion of the logit model for effects of compounds. The methodology for estimating no-effect concentrations has already been widely applied in the analysis of routine toxicity tests. These developments are not included here to increase to focus on the DEB theory. They can be found in [519]. The concept 'fugacity' is used to derive how toxico-kinetics and effects depend on physico-chemical properties of chemical compounds.

The chapter on 'living together' is extended, with a discussion on trophic interactions between organisms, new results on the behaviour of food chains, and the 'Canonical Community' is introduced, which is meant to capture the essential features of ecosystem physiology. I removed some material that contained technical developments with little conceptual gain.

Many new biological examples are included in this second edition, and a short last chapter has been appended to discuss methodological aspects and comparisons with other approaches. Although the core of the DEB theory has not changed, its biological setting has matured considerably and still provides a rich source of inspiration, at least for me.

The inclusion of multivariate mass fluxes comes with a considerable extension of the symbol table. Consistency arguments forced me to install more stringent rules for notation: one dimension set per symbol. Changes in notation with respect to the first edition were unavoidable. I can only offer my apologies for the inconvenience to readers of the first edition, but hope that the more stringent rules help them to follow the text more easily.

Although I tried hard to avoid errors, experience tells me that they are unavoidable; the web site `http://www.bio.vu.nl/thb/deb` lists the detected errors, and again I offer my apologies for any inconvenience.

Preface

In 1978 Thea Adema asked me to develop a statistical methodology for screening toxicants for their effects on daphnid reproduction. I observed that large daphnids tend to have bigger litters than small ones and this led me to realize that reproduction cannot be modelled without including variables such as growth, feeding, food quality and so on. Since then I have found myself working on the theory of Dynamic Energy Budgets (DEB), which has rapidly covered more ground. Twenty years ago, I would not have seen any connection between topics such as feeding of daphnids, embryo development of birds and the behaviour of recycling fermenters. Now, I recognize the intimate relationship between these and many other phenomena and the fundamental role of surface/volume ratios and reserves.

DEB theory is central to eco-energetics, which is the study of the mechanisms involved in the acquisition and use of energy by individuals; this includes the many consequences of the mechanisms of physiological organization, and population and ecosystem dynamics. The related field of bioenergetics focuses on molecular aspects and metabolic pathways in a thermodynamic setting. Although the first and second laws of thermodynamics are frequently used in eco-energetics, thermodynamics is not used to derive rate equations, as is usual, for example, in non-equilibrium thermodynamics. One of the reasons is that the behaviour of individuals cannot be traced back to a restricted number of biochemical reactions. This difference in approach blocks possible cross-fertilizations between levels of organization. This barrier is particularly difficult to break down because eco-energetics usually deals with individuals in a static sense; an individual of a given size allocates energy to different purposes in measured percentages. This tradition hampers links with physiological processes. DEB theory, in contrast, treats individuals as non-linear, dynamic systems. This process-oriented approach has firm physiological roots and at the same time it provides a sound basis for population dynamics theories, as will be demonstrated in this book. The hope is that DEB theory will contribute to the cross-fertilization of the different specializations in energetics.

I like my job very much as it offers good opportunities to enjoy the diversity of life during hikes in my spare time. Many of my fellow biologists stress the interesting differences between species to such an extent that the properties they have in common remain largely hidden. I believe that this obscures the way in which a particular species deviates from the common pattern, and the causes of deviations, and urges me to stress phenomena that species seem to have in common. I fully understand the problem of being overwhelmed by the diversity of life, but I think that reactions of ecstasy, apathy or complaint hardly

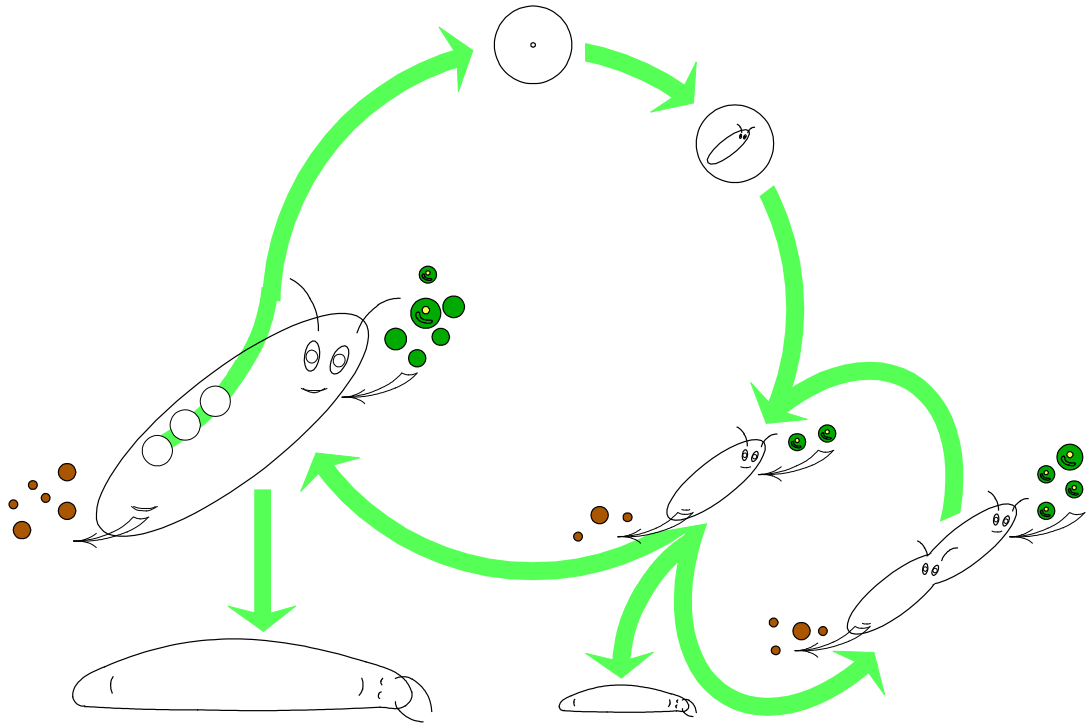

Dynamic Energy Budget theory aims to quantify the energetics of individuals as it changes during life history. The key processes are feeding, digestion, storage, maintenance, growth, development, reproduction and aging. The theory amounts to a set of simple rules, summarized in Table 3.3 on page {121}, and a wealth of consequences for physiological organization and population dynamics. Although some of the far reaching consequences turn out to be rather complex, the theory is simple, with only one parameter per key process. Intra- and inter-specific body size scaling relationships form the core of the theory and include dividing organisms, such as microbes, by conceiving them as juveniles.

contribute to insight. This book explores to what extent a theory that is not species-specific can be used to understand observations and experimental results, and it culminates in a derivation of body size scaling relationships for life history traits without using empirical arguments.

DEB theory is quantitative, so it involves mathematics; I feel no need to apologize for this, although I realize that this may be an obstacle to many biologists. My hope is that an emphasis on concepts, rather than mathematical technicalities, avoidance of jargon as much as possible and a glossary will reduce communication problems. Only in some parts of the chapter on population dynamics may the mathematics used be called 'advanced', the remainder being elementary. The text is meant for scientists and mathematicians with a broad interest in fundamental and applied quantitative problems in biology.

The *aim* is summarized in the diagram on this page. The primary aim is not to describe energy uptake phenomena and energy use in as much detail as feasible, but to evaluate consequences of simple mechanisms that are not species-specific. The choice of material included in the book was made by judging its relevance to a set of mechanisms that appeared to be tightly interlocked. This book, therefore, does not review all that is relevant to ener-

getics. It does, however, include some topics that are not usually encountered in texts on energetics, because DEB theory appears to imply predictions for the topics. Discrepancies between predictions and the actual behaviour of particular species will, hopefully, stimulate a guided search for explanations of these discrepancies. I have learned to appreciate this while developing the DEB theory. It opened my eyes to the inevitable preconceptions involved in the design of experiments and in the interpretation of results.

The emphasis is on mechanisms. This implies a radical rejection of the standard application of allometric equations, which I consider to be a blind alley that hampers understanding. Although it has never been my objective to glue existing ideas and models together into one consistent framework, many aspects and special cases of the DEB theory turned out to be identical or very similar to classic models:

author	year	page	model
Lavoisier	1780	{155}	multiple regression of heat against mineral fluxes
Arrhenius	1889	{53}	temperature dependence of physiological rates
Huxley	1891	{177}	allometric growth of body parts
Henri	1902	{43}	Michaelis–Menten kinetics
Blackman	1905	{236}	bilinear functional response
Pütter	1920	{95}	von Bertalanffy growth of individuals
Pearl	1927	{320}	logistic population growth
Fisher & Tippitt	1928	{141}	Weibull aging
Kleiber	1932	{273}	respiration scales with body weight$^{3/4}$
Mayneord	1932	{252}	cube root growth of tumours
Emerson	1950	{252}	cube root growth of bacterial colonies
Huggett & Widdas	1951	{104}	foetal growth
Weibull	1951	{255}	survival probability for aging
Best	1955	{235}	diffusion limitation of uptake
Smith	1957	{135}	embryonic respiration
Leudeking & Piret	1959	{148}	microbial product formation
Holling	1959	{73}	hyperbolic functional response
Marr & Pirt	1962	{317}	maintenance in yields of biomass
Droop	1973	{317}	reserve (cell quota) dynamics
Rahn & Ar	1974	{288}	water loss in bird eggs
Hungate	1975	{241}	digestion
Beer & Anderson	1997	{103}	development of salmonid embryos

The DEB theory not only shows how and why these models are related, it also specifies the conditions under which these models might be realistic, and it extends the scope from the thermodynamics of subcellular processes to population dynamics.

Potential *practical applications* are to be found in the control and optimization of biological production processes. In my department, for example, we use DEB theory in research on reducing sludge production in sewage treatment plants, optimising microbial product formation, the role of biota in global change, the analysis of effects of toxicants, the quantification of biodegradation of xenobiotics, and the modelling of tumour induction. Other potential applications are to be found in medicine, and many other fields.

Book organization

The first two chapters are introductory.

Chapter 1 gives the historical setting and some philosophical, methodological and technical background. Many discussions with colleagues about the way particular observations fit or do not fit into a theory rapidly evolved into ones about the philosophical principles of biological theories in general. These discussions frequently related to the problem of the extent to which biological theories that are not species-specific are possible. This chapter, and indeed the whole book, introduces the idea that the value of a theory is in its usefulness and therefore a theory must be coupled to a purpose. I have written a section on the position I take in these matters and insert throughout the book many remarks on aspects of modelling and testability to point to fundamental problems in practical work. Chapter 1 sets out the context within which DEB theory, developed in subsequent chapters, has meaning.

Chapter 2 introduces some basic concepts that are pertinent to the level of organization of the individual and to the development of DEB theory. It paves the way for testing theory against experimental data, which will occur during the development of the DEB theory. The concept 'system' is introduced and the state variables body size and energy reserves are identified as of primary importance. The relationships between different measures of body size and energy are discussed; these are rather subtle due to the recognition of storage materials. The concept 'Synthesizing Unit' is introduced and its link with classic enzyme kinetics is discussed. The concept 'generalized compound' is used to relax the principle of 'homeostasis' in order to accommodate 'storage'. Effects of temperature on physiological rates are presented and the notion of metabolic modes and life stages are discussed.

The next three chapters develop the DEB theory.

Chapter 3 describes processes of energy uptake and energy use by individuals in all life stages. The set of rules that are extracted from these descriptions constitute the DEB theory. It gives a complete specification of the transformation of food into biomass and will later be used to analyse consequences and implications. The discussion includes the processes of feeding, digestion, storage, maintenance, development and reproduction. Chapter 3 provides the meat of the DEB theory in its basic form.

Chapter 4 describes the processes of the uptake and use of essential compounds, i.e. the building blocks of life. The kinetics directly follow from the processes of energy uptake and use, via the concept of homeostasis. This chapter therefore primarily evaluates the implications of the previous chapter. Special attention is given to the process of aging because most other energetics theories select age as a primary state variable, where the focus is on the coupling between aging and energetics.

Chapter 5 extends the theory to include several substrates, reserves and structural masses to increase the metabolic versatility that is found in organisms that acquire nutrients and light independently, and have to negotiate the problem of simultaneous limitation caused by stoichiometric coupling. The various ways in which substrate can take part in metabolic transformations are discussed. The processes of photosynthesis and calcification are discussed; the implications for plant development are evaluated.

Chapter 6 considers the uptake and effects of non-essential compounds, such as toxi-

cants. Their kinetics do not follow from energy considerations. However, changes in the lipids content, dilution by growth and metabolic transformation all point to many links between uptake kinetics and energetics. The effects of toxicants on energetics interfere with their kinetics.

The next three chapters illustrate applications of the DEB theory to organismic and suborganismic levels, to comparison between species and to the population level.

Chapter 7 analyses examples of the application of DEB theory and extensions to lower levels of biological organization, showing how it can be used to improve biological insight. It repeats more or less the setup of Chapter 3, but discusses details that are essential for testing the theory against empirical data, and for interpreting data that have taxon-specific elements. A molecular mechanism is proposed for the reserve kinetics as implied by the DEB assumptions.

Chapter 8 compares the energetics of different species and studies some evolutionary implications. The DEB theory has many implications for the covariation of parameter values among species. The chapter shows how, for a wide variety of biological variables, body size scaling relationships can be derived from first principles rather than established empirically. This approach to body size scaling relationships is fundamentally different from that of existing studies. The chapter also compares different life history strategies and analyses some optimization problems.

Chapter 9 considers interactions between individuals and develops population consequences. It starts with some well known standard population dynamic theories and introduces the DEB machinery step by step. The population, after its introduction as a collection of individuals, is considered as a new entity in terms of systems analysis, with its own relationships between input, output and state. These new relationships are expressed in terms of those for individuals. The coupling between mass and energy fluxes at the population level is studied and the behaviour of food chains and of 'Canonical Communities' is discussed briefly.

Chapter 10 places the approach taken by the DEB theory in existing eco-energetic research, and highlights some differences in concepts. The general modelling strategies, as presented in Chapter 1 and applied in the book, are evaluated briefly.

The logical structure of the chapters is indicated in the diagram (right). *A first quick glance through the section on notation and symbols, page* {409}, *saves time and annoyance.* A glossary at 403 explains technical terms

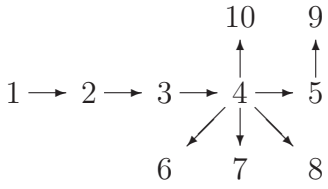

Acknowledgements

Many people have contributed to this book in different ways. I would specifically like to thank the following people.

Anneke de Ruiter, Trudy Bakker, Hanneke Kauffman, Eric Evers and Harry Oldersma have done a lot of experiments with daphnids and rotifers at the TNO laboratories, and provided the essential experimental material on energetics and toxicology for the development of DEB theory. At a later stage Cor Zonneveld and Arjan de Visser contributed to the theory by experimental and theoretical studies on pond snails, helping to fit the model to embryo development data. Nelly van der Hoeven and Lisette Enserink carried out most useful experimental work on the energetics and population dynamics of daphnids in relation to the DEB theory, while Bob Kooi, Martin Boer, Fleur Kelpin, Hans Metz, Odo Diekmann, Henk Heijmans, André de Roos, Horst Thieme, Roger Nisbet and Tom Hallam contributed significantly to the mathematical aspects of DEB-structured populations. Rob van Haren and Hans Schepers worked on mussel energetics in relation to the accumulation elimination behaviour of xenobiotics. Jacques Bedaux, Matthijs Luger, Emilia Persoon, Jens Anderson, Gineke van der Molen, Wout Slob, Inge van Leeuwen, Paul Hanegraaf and Bernd Brandt developed applications of the theory to problems in ecotoxicology, tumour biology, and biodegradation. Sigrid Bestebroer, Paul Bruijn, Christa Ratsak and Erik Muller worked on various DEB aspects of sewage water treatment. Paul Hanegraaf studied the coupling between energy and mass fluxes. Rienk-Jan Bijlsma contributed to the extension of the theory to include plants; Hugo van den Berg and Cor Zonneveld contributed to the generalization of the theory to autotrophic systems. Many students have done excellent work on specific details.

I gained a lot from productive collaboration and discussions with Ad Stouthamer, Henk van Verseveld, Hans de Hollander, Arthur Koch, Dick Eikelboom, Arnbjørn Hanstveit, Han Blok, Hans Westerhoff, Willem Stolte, Roel Riegman, Veronique Martin, Nico de With, Andries ter Maat, Nico van Straalen, Ger Ernsting, Rob Hengeveld, Peter Westbroek, Jacques Bedaux, Hans Lambers, Leo and Henk Hueck, Thea Adema, Kees Kersting, Joop Hermens, Willem Seine, Jan Kammenga, Dick Sijm, Henk Dijkstra, Jan Parmentier, Wim van der Steen, Schelten Elgersma, Dina Lika, Erik Muller and last but not least Roger Nisbet and Tom Hallam.

The work presented in this edition was supported by the Dutch Government, National Research Programme on global air pollution and climate change, contract # 013/1204.10, by the National Science Foundation, Priority Programme on Parallel Computational Methods: Biological Systems, contract # 805-44.151, and Priority Programme on Non-Linear Systems: Populaton Dynamics, contract # 61-254, and by the National Technology Foundation: Biodegradation, contract # 805.39.751 and Tumour Induction potential of Chemicals, contract # VBI.4692.

The text of the book has been improved considerably by critical comments from a number of readers, particularly Cor Zonneveld, and Sarah Price, Rob Hengeveld, Ger Ernsting, Wout Slob, Miranda Aldham-Breary, Tom Hallam, Karen Karsten, Henk Hueck, André de Roos, Bob Kooi, Martin Boer, Wim van der Steen, Emilia Persoon, Gabriëlle van Diepen, Ad van Dommelen, Mies Dronkert, and Oscar Debats. Present behind all aspects of the 20 years of work on the theory is the critical interest of Truus Meijer, whose loving patience is unprecedented. The significance of her contribution is beyond words.

S. A. L. M. Kooijman, Department of Theoretical Biology
Vrije Universiteit, de Boelelaan 1087, 1081 HV Amsterdam, the Netherlands
October 1999

Chapter 1

Energetics and models

This introductory chapter presents some general background to theoretical work in energetics. I start with an observation that feeds the hope that it is possible to have a theory that is not species-specific, something that is by no means obvious in view of the diversity of life! A brief historical setting follows giving the roots of some general concepts that are basic to Dynamic Energy Budget (DEB) theory. I will try to explain why the application of allometry restricts the usefulness of almost all existing theories on energetics. This explanation is embedded in considerations concerning philosophy and modelling strategy to give the context of the DEB theory.

1.1 Energy and mass fluxes

1.1.1 Hope for generality

Growth curves are relatively easy to produce, which may explain why the literature is full of them. Yet they remain fascinating. When environmental conditions, including temperature and food availability, are constant and the diet is adequate, organisms ranging from yeasts to vertebrates follow, with astonishing accuracy, the same growth pattern as that illustrated in Figure 1.1. This is amazing because different species have totally different systems for regulating growth. Some species, such as daphnids, start to invest, at a certain moment during growth, a considerable amount of energy in reproduction. Even this does not seem to affect their growth curve. So one wonders how the results can be so similar time and again. Is it all a coincidence, resulting from a variety of different causes, or do species have something in common despite their differences? Are these curves really similar, or is the resemblance a superficial one?

Some workers do not believe that the growth of animals, plants and other organisms can be captured in a single framework. Many concepts, such as the decomposition of mass into a storage and structural component and uptake across surface areas, are standard elements of plant production modelling [670], and equally apply to animals and micro-organisms. Thornley [920] presented arguments against a single framework. One of them is that growth is confined to specialised tissues (meristems) in plants, but this is not dissimilar to growth of the tips of fungal hyphae, or of bacterial cells for instance. Another is that

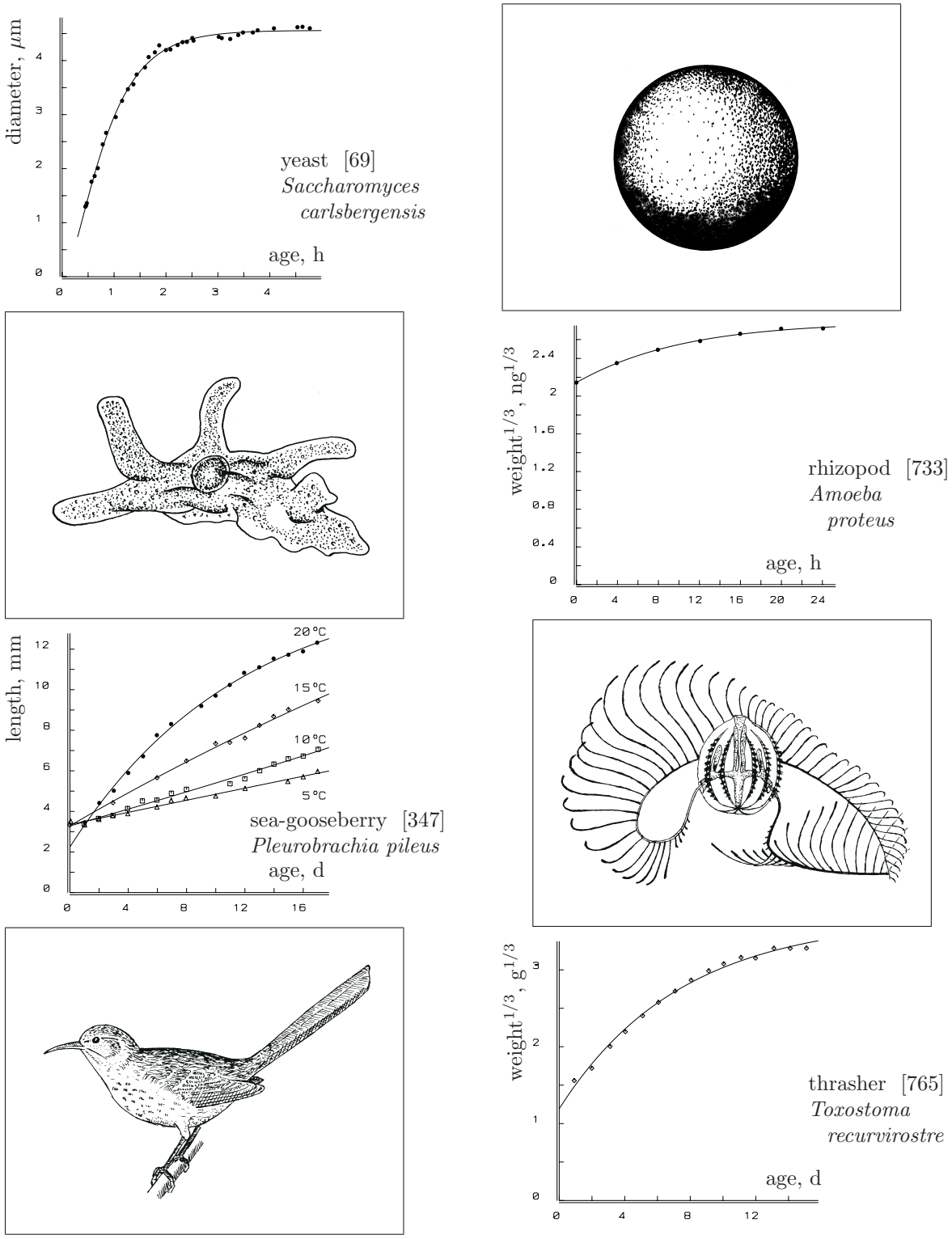

Figure 1.1: These growth curves all have the shape $L(t) = L_\infty - (L_\infty - L_0)\exp\{-\dot{r}_B t\}$, while the organisms differ considerably in their growth regulating systems. How is this possible? Data sources are indicated by entry numbers in the bibliography.)

growth is frequently indeterminate in plants, and determinate in animals. However, the wide applicability of von Bertalanffy's growth curve for animals shows that the latter is not generally true, while determinate growth can also be understood in the context of a single general framework, see {295}.

My attempts to understand similarities in growth curves led me on a breathtaking hike into many corners of biological territory. They became an entertaining puzzle: is it possible to construct a set of simple rules, based on mechanisms for the uptake and use of material by individuals, that is consistent with what has been measured? The early writers made a most useful start: growth results from processes of build-up and break-down. Break-down has something to do with making energy and elementary compounds available, so how are they replenished? What processes determine digestion and feeding? What determines food availability? Build-up results in size increase, and so affects feeding, but offspring are produced as well. This obviously affects food availability. Where does maintenance fit in? Why should there be any maintenance at all? What is the role of age? These are just some of the questions that should be addressed to satisfactorily explain of a growth curve.

The comparison of different systems that share common principles can be a most powerful tool in biology. I give two examples, which are discussed later {95,103}.

Individuals of some species, such as humans, lose their ability to grow. Cartilage tissue is replaced by bone, which makes further growth impossible. Is this why growth stops? This question cannot be answered by studying these species, because they stop growing and also change cartilage to bone. The answer should be 'no', I think, because it is possible to formulate a model for growth that applies to these species as well as to those that continue to grow, such as fish. Growth in mammals would cease even if they did not lose their ability to grow, and cartilage is replaced, possibly to obtain a mechanically better structure.

Another example is the egg shell of birds, which limits the diffusion of oxygen and, therefore, the development of the embryo, according to some authors [746]. A frequently used argument is the strong negative correlation between diffusion rates across the egg shell and diffusion resistance, when different egg sizes are compared, ranging from hummingbirds to ostriches; the product of diffusion rate and resistance does not vary a lot. Again I think that the shell does not limit the development of the embryo, because it is possible to formulate a model for embryo development that applies to birds as well as to animals without rigid egg shells. The physical properties of the egg shell are well adapted to the needs of the embryo, which causes the observed correlation.

The crux of the argument is that the same model applies to different systems and that the systems can be compared on the basis of their parameters.

1.1.2 Historical setting

Many of these questions are far from new. R. Boyle, R. Hooke and J. Mayow in the seventeenth-century were among the first to relate respiration to combustion, according to McNab [614]. The first measurements of the rate of animal heat production were made by A. Crawford in 1779, and A. L. Lavoisier and P. S. de Laplace in 1780 aimed to relate it to oxygen consumption and carbon dioxide production [614]. Interest in how metabolic rate, measured as oxygen consumption rate, depends on body size goes back at least as

far as the work of Sarrus and Rameaux [806] in 1839. They were the first to find rates proportional to surface area for warm-blooded animals [79]. Later this became known as the Rubner's surface law [793]. Pütter [740] used it in a model of the growth of individuals in 1920. He saw growth as the difference between build-up and break-down. The processes of build-up, which later became known as anabolic processes, were linked directly to the metabolic rate, which was assumed to follow the surface law. The processes of break-down, now known as catabolic processes, were assumed to proceed at a constant rate per unit of volume. Volume was thought to be proportional to weight. The growth rate then results from a weighted difference between surface area and volume. The casual way A. R. Wallace mentioned this idea in a note to E. B. Poulton (appendix 3 in [281]) suggests that its roots go back to before 1865. The resulting growth curve is presented in Figure 1.1. The fact that Pütter applied the model to fish, whereas the surface law was based on work with warm-blooded animals, generated a lot of criticism.

More data were generated with improved methods of measurement; invertebrates were also covered. Kleiber [490] found in 1932 that metabolic rates are proportional to weight to the power 0.75 and this became known as Kleiber's law. Extensive studies undertaken by Brody [119] confirmed this proportionality. Von Bertalanffy [79] saw anabolic and catabolic rates as special cases of the allometric relationship, i.e. a relationship of the type $y = \alpha x^{\beta}$, where y is a variable dependent on another variable x, usually body weight. He viewed this as a simplified approximation that could be applied to almost all types of metabolic rates, including the anabolic and the catabolic, but the constant β varies somewhat with the tissue, physiological conditions and experimental procedure. The growth curve proved to be rather insensitive to changes in β for catabolism, so, like Pütter, von Bertalanffy took the value one and classified species on the basis of the value for β of anabolism. The surface law is just one of the possibilities.

Although von Bertalanffy [78] was the genius behind the ideas of general systems theory, he never included the feeding process in his ideas about growth. I do not know why, because mass balance equations are now always bracketed together with systems. I think that the use of allometric equations, which is a step away from mechanistic explanations towards meaningless empirical regressions, obstructs new ideas in metabolic control. I will explain this in later sections. The idea of allometry goes back to Snell [865] in 1891 and, following the work of Huxley [438], it became widely known. Both Huxley and von Bertalanffy were well aware of the problems connected with allometric equations, and used them as first approximations. Now, a century later, it is hard to find a study that involves body size and does not use them.

Zeuthen [1026] was the first to point to the necessity of distinguishing between size differences within a species and between species. The differences in body size within a species, as measured in one individual at different points during development, are treated here as an integral part of the processes of growth and development. Those between species are discussed in a separate chapter on parameter values {267}, in which I show that body size scaling relationships can be deduced without any empirical arguments.

1.1.3 Energetics

The problem that everything depends on everything else is a hard one in biology, as anything left out may prove to be essential in the end. If one includes as much as possible one loses an intellectual grasp of the problem. The art is to leave out as much as possible whilst maintaining the essence. I focus the discussion on an abstract quantity, called energy, rather than a selection of the many thousands of possible compounds usually found in organisms. No selection can be inclusive, so what is the role of compounds that are left out? Jeong *et al.* [450] made a heroic attempt to model the compound-based physiology of *Bacillus* and introduced more than 200 parameters. However, many compounds have yet to be identified and the quantities and dynamics of most compounds are largely unknown. Moreover, the main components of organisms such as yeasts and vertebrates are different. So investigating compounds does not seem a promising route to understand the similarity in growth curves.

A better route would be to use the concept of energy, meaning something like 'the ability to do work', which primarily consists of driving chemical reactions against the direction of their thermodynamic decay. The term was first proposed by Thomas T. Young in 1807, according to Blaxter [92]. Energy is stored in a collection of (organic) compounds, so a full explanation requires the inclusion of mass fluxes, as I will explain on {35}. It is important to realize here that there is a close link between energy and mass flows.

Proteins in food are first decomposed into amino acids, and amino acids are polymerized to proteins again. A similar process applies to carbohydrates and lipids, which together with proteins constitute the main materials of life. The decomposition of many types of source materials into a limited number of types of central metabolites before polymerization into biomass is known as the 'funnel' concept. The rich diversity of catabolic machinery, especially among the prokaryotes, and the poor diversity of anabolic machinery was recognized by Kluyver and Donker in 1926 [493].

The role of energy in cellular metabolism, in particular the generation and use of ATP, is the main focus of bioenergetics [645]. This compound is called the energy currency of the cell. Together with NADPH and NADH, which provide reducing power, it drives the anabolic processes. Compounds involved in the decomposition processes are important for the cell in two ways: through the production of ATP from ADP and P, which is produced in anabolic processes, and through the production of elementary compounds that are substrates for anabolic processes [416]. The final stages of the catabolic processing of lipids, carbohydrates and proteins all make use of the same cellular machinery: the Krebs cycle. To some extent, these substrates can substitute each other for fuelling purposes. The cell chooses between the different substrates on the basis of their availability and its need for particular substrates in anabolic processes.

After this introduction, it perhaps comes as a surprise that ATP is not the main focus in eco-energetics. This is because ATP itself does not play a leading role in energy fluxes. It has a role similar to that of money in your purse, while your bank account determines your financial status. A typical bacterial cell has about 5×10^6 ATP molecules, which is just enough for 2 seconds of biosynthetic work [550]. The mean lifetime of an ATP molecule is about 0.3 seconds [370]. The cell has to make sure that the adenylate energy

charge $(\frac{1}{2}\ \text{ADP} + \text{ATP})\ (\text{AMP} + \text{ADP} + \text{ATP})^{-1}$ remains fairly constant (usually around 0.9, but this matter is not settled yet). It does so by coupling endergonic (energy requiring) and exergonic (energy releasing) reactions. If the energy charge is reduced, the energy yield of the reaction $\text{ATP} \rightarrow \text{ADP} + \text{P}$ declines rapidly. The situation where the energy charge as well as the concentration of $\text{AMP} + \text{ADP} + \text{ATP}$ remain constant relates to the concept of homeostasis, {30}. Cells keep their purses well filled, which makes the dynamics of the purse contents less interesting. ATP is part of the machinery used to harvest or mobilize energy.

A varying energy yield per mole of ATP does not necessarily complicate metabolic dynamics. It primarily affects the rate at which ATP is produced in energy-yielding transformations or consumed in energy-requiring transformations, and therefore also the rate at which ATP and ADP commute between the sites where these transformations occur. The analogy with money can be extended one step further: the big bank-money is in a stable currency, while the exchange rate of the small purse-money may vary. The focus on ATP/ ADP versus polymers is primarily a question of relevant time scales. Cell division cycles and stages in the development of individuals last too long for a focus on ATP.

The chemiosmotic theory was developed to explain the molecular mechanism of ATP generation. It has boosted biochemical research in cellular energetics, and it is now a central issue in all texts on molecular biology [663], although competing theories do exist [561]. The focus of bioenergetics on the processes of ATP synthesis and use, matches the classic division of metabolism into catabolic and anabolic processes very well [987]. This division, however, is less straightforward in the context of the DEB theory, where reserves play an essential role, and processes of synthesis and decomposition occur repeatedly in metabolism. Other differences exist as well. Cell size influences cellular processes through the ratio between membrane surface area to cell volume. This gives the DEB theory a natural focus on cell and life cycles. The link between activity coupled to a surface area (membrane) and mass of metabolic substrate and product coupled to volume is a cornerstone in the DEB theory for the uptake and use of energy.

1.1.4 Population energetics

If a population consists of individuals who take up and use energy in a particular way, how will it behave in a given environment? If populations are tied up in food chains or webs, how will these structures change dynamically? What new phenomena play a role at the population as opposed to the individual level?

Except for work in the tradition of mathematical demography on which modern age-structured population dynamic theory is based [157], most publications on population dynamics, up to some years ago, have dealt with unstructured populations, i.e. populations that can be characterized by the number of individuals only. So all individuals are treated as identical, and are merely counted. This also applies to microbiology publications, which basically deal with microbial populations and not with individual cells. This has always struck me as most unrealistic, because individuals have to develop before they can produce offspring. The impact of a neonate on food supplies is very different from that of an adult. In the chapter on population dynamics, {328}, I show that neonates producing neonates

themselves can dominate the dynamics of unstructured populations. This absurdity makes one wonder to what extent unstructured population models have something useful to say about real populations. Many modern views in ecology, e.g. concerning the relationship between stability and diversity, are based on models of unstructured populations.

I will use arguments from energetics to structure populations, i.e. to distinguish between different individuals. This, however, complicates population dynamics considerably, and the first question to be addressed is: does this increase in complexity balance the gain in realism? I know only one route to an answer: try it and see!

1.2 The art of modelling

1.2.1 Strategies

Before I start to develop a theory for energetics, I think it is important to explain my ideas about theories and models in general. It is certainly possible that you may disagree with part of what follows, and it is helpful to know exactly where the disagreement lies. The source of a disagreement is frequently at a point other than where it first becomes apparent. The final chapter, see {359}, evaluates the DEB theory in the light of the points of view presented in this section. I started this chapter by pointing to growth curves as an example, because they feed the hope that it is possible to build a quantitative theory that is not species-specific. My primary interest, however, is not limited to growth curves, it is far more encompassing. How do phenomena operating at different levels of organization relate to each other and how can these relationships be used to cross-fertilize different biological specializations?

Let me state first that I do not believe in the existence of objective science. The types of questions we pose and the types of observations we make bear witness to our preconceptions. There is no way to get rid of them. There is nothing wrong with this, but we should be aware of it. When we look around us we actually see mirrors of our ideas. We can try to change ourselves on the basis of what we see, but we cannot do without the projections we impose on reality. Observations and statements span the full range from facts via interpretation to abstract ideas. The more abstract the idea, the more important the mirror effect. Let me give an example of something that is not very abstract. I spend a long day looking for a particular plant species. At the end of the day luck strikes, and I find a specimen. Then I return home, using the same path, and shame, oh shame, this species turns out to be quite abundant. To make matters worse, I am quite experienced in this type of activity. So, if someone maintains that they would not miss the plants, I am inclined to think that they are simply not able to criticize their own methodology.

I do not believe in the existence of one truth, one reality. If such a 'truth' did exist, it would have so many partially overlapping aspects, that it would be impossible to grasp them all simultaneously and recognize that there is just one truth. A consequence of this point of view is that I do not accept a classification of theories into 'true' and 'false' ones. In connection with this, I regard the traditional concepts of verification and falsification as applied to theories as meaningless. Theories are always idealizations, so, when we

look hard, it must be possible to detect differences between theory-based predictions and observations. Therefore, I have taught myself to live happily with the knowledge that, if there were only one reality and if theories can only be classified into 'true' or 'false' ones, all of them would be classified as 'false'. As it is not possible to have the concept 'a bit true', believers in one reality do not seem very practical to me. Perhaps you judge this as cynical, but I do not see myself as a cynic. Discussions suggest that colleagues with a quantitative interest are more likely to share this point of view than those with a qualitative interest.

Instead of designating theories as 'true' or 'false', I classify them on the basis of their usefulness. This classification is sensitive to the specification of a purpose and to a 'state of the art'. Theories can be most useful to detect relationships between variables, but can lose their usefulness when the state of the art develops. Theories can be useful for one purpose, but totally useless for another. When theories produce predictions that deviate strongly from observations, they are likely to be classified as useless, so I do not think that this pragmatism poses a threat to science in the eyes of the apostles of K. R. Popper. Although it is satisfying to have no difference between prediction and observation, small differences do not necessarily make a theory useless. It all depends on the amount of difference and on the purpose one has in mind. A 'realistic' description then just means that observations and descriptions do not differ much. There will always be the possibility that a well fitting description rests on arguments that prove not to be realistic in the end. Perhaps you think that this is trivial, but I do not. Take for instance goodness of fit tests in statistics, where the null hypothesis is held to be true, and how they are applied, e.g. in ecological journals. The outcome of the test itself is not instructive, for the reasons given. It would be instructive, however, to have a measure of the difference between prediction and observation that allows one to judge the usefulness of the theory. Such measures should, therefore, depend on the theory and the purposes one has; it would be a coincidence to find them in a general text on statistics.

The sequence, 'idea, hypothesis, theory, law' is commonly thought to reflect an increasing degree of reliability. I grant that some ideas have been tested more extensively than others and may be, therefore, more valuable for further developments. Since I deny the existence of a totally reliable proposition, because I do not accept the concept of truth, I only use this sequence to reflect an increasing degree of usefulness. It is, however, hard and probably impossible to quantify this on an absolute scale, so I treat the terms in this sequence more or less as synonyms. Each idea should be judged separately on its merits.

Mathematics as a language is most useful for formulating quantitative relationships. Therefore, quantitative theories usually take the form of mathematical models. This does not imply that all models are theories. It all depends on the ideas behind the model. Ideally a model results, mathematically, from a list of assumptions. So, I am inclined to identify sets of assumptions with theories. The formulation of empirical models does not start with mechanistically inspired assumptions, and directly aims at models that describe data sets. Although useful for certain applications, such models have little to do with theories.

When model predictions agree with observations in a test, this supports the assumptions, i.e. it gives no reason to change them and it gives reason to use them for the time being. As explained on {14}, the amount of support such a test gives is highly sensitive

to the model structure. If possible, the assumptions should be tested one by one. From a strict point of view, it would then no longer be necessary to test the model. Practice, however, teaches us to be less strict.

People with a distaste for models frequently state that 'a model is not more than you put into it'. This is absolutely right, but instead of being a weakness, it is the single most important aspect of the use of models. As this book illustrates, assumptions, summarized in Table 3.3 on {121} have far reaching consequences that cannot be revealed without the use of mathematics. Put into other words: any mathematical statement is either wrong or follows from assumptions. Few people throw mathematics away for this reason.

The process of evolution selects for maximum numbers of offspring relative to individuals with competing genes, and indirectly for optimal efficiency. Although this general principle seems solid to me, the more detailed definition of fitness and optimality is very sensitive to the specification of the (changing) environment. There are too many examples of organisms defeating optimization. For this and other reasons I do not promote modelling that uses optimality criteria to derive a model structure for biological processes, despite the fact that such models are increasingly popular, cf. [780,878]. The types of models that seem most promising to me could be classified as functionally inspired causal models, where 'causal' refers to mechanisms (cf. {363}). Optimality considerations then only involve parameter values, not model structure. Optimality of fitness can hardly be judged in constant environments, because the produced offspring become an element of the environment; a full understanding of trait changes requires a holistic approach that incorporates the indirect side effects.

The problem that everything depends on everything else in biology has strong implications for models that represent theories. When y depends on x, it is usually not hard to formulate a set of assumptions, that imply a model that describes the relationship with acceptable accuracy. This also holds for a relationship between y and z. When more and more relationships are involved, the cumulative list of assumptions tends to grow and it becomes increasingly difficult to keep them consistent, cf. {360}. This holds especially when the same variables occur in different relationships. It is sometimes far from easy to test the consistency of a set of assumptions. For example, when a sink of material and/or energy in the maintenance process is assumed for individuals, it appears no longer possible to assume a constant conversion of prey biomass into predator biomass at the population level. It takes a few steps to see why; this is explained in the section on mass transformation, {337}.

A major trap in model building is the complexity caused by the number of variables. This trap became apparent with the advent of computers, which removed the technical and practical limitations for the inclusion of variables. Each relationship, each parameter in a relationship comes with an uncertainty, frequently an enormous one in biology. With considerable labour, it is usually possible to trim computer output to an acceptable fit with a given set of observations. This, however, gives minimal support for the realism of the whole, which turns simulation results into a most unreliable tool for making predictions in other situations. A model of the energetics of individuals can easily become too complex for use in population dynamics. If it is too simple, many phenomena at the individual level will not fit in. Then, it becomes difficult to combine realism at the individual level with

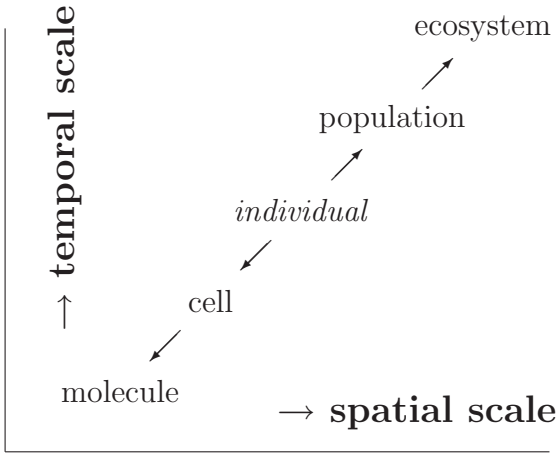

Figure 1.2: The DEB theory specifies a model for the individual, which is used to model populations in terms of individuals and ecosystems in terms of populations. We simplify while increasing the level of integration, and incorporate new processes that typically operate at that level of organization. The model for the individual serves as a constraint for modelling suborganismal processes that specify details of the (physiological) behaviour of the individual, such as regulation processes. This approach implies a link between scales in space and time, which excludes rapid processes at large spatial scales and slow processes at small spatial scales.

coherence between levels of organization. The need for compromise, which is not typical of energetics, makes modelling an art that is idiosyncratic to the modeller.

The only solution to the trap of complexity is to use nested modules. Sets of closely interacting objects are isolated from their environment and combined into a new object, a module, with simplified rules for input-output relationships. This strategy is basic to all science. A chemist does not wait for the particle physicist to finish their job, though the behaviour of the elementary particles determines the properties of atoms and molecules taken as units by the chemist. The same applies to the ecologist who does not wait for the physiologist. The existence of different specializations testifies to the relative success of the modular approach, which still amazes me. The recently proposed hierarchy theory in ecology [18,677] does basically the same within that specialization.

The problems that come with defining modules are obvious, especially when they are rather abstract. The first problem is that it is always possible to group objects in different ways to form new objects which then makes them incomparable. The problem would be easy if we could agree about the exact nature of the basic objects, but life is not that simple. The second problem with modules lies in the simplification of the input-output relationships. An approximation that works well in one circumstance can be inadequate in another. When different approximations are used for different circumstances, and this is done for several modules in a system, the behaviour of the system can easily become erratic and no longer contribute insight into the behaviour of the real thing. The principle of reduction in science relates to the attempt to explain phenomena in terms of the smallest feasible objects. I subscribe to a weaker principle: that of coherence. This aims to relate the behaviour of modules to that of their components while preserving consistency.

Another implication of a modular setup is that scales in space and time are linked [679], see Figure 1.2. It seems very hard, if not impossible, to model processes on a large spatial and a small time scale, and vice versa. The primary reason is again avoiding a large number of parameters by using modules. Using impressive computing power, it is feasible to model water transport in the earth's oceans, which seems to defeat the coupling of scales. The modelling of this physical transport, however, involves only a limited number

of parameters (and processes), given the shape of the oceans' basins, explicit external wind forcing and information on planetary rotation.

If we accept community ecology as a feasible science, I see two research strategies for riding this horse. The first one is to accept that species differ considerably in the way they take up and use resources. This would mean modelling the energetics of each species, stripping the model of most of its details in various ways, and then trying to determine the common features in population dynamics that these simplified models and the full model produce. I do not share the hope that different traits of individuals will indeed result in similar population dynamics. The second strategy, which is followed here, is to try to capture the diversity of the different species energetics into one model with different parameter values and build theories for these parameter values. The simplification step before the assemblage of populations into a community remains necessary.

1.2.2 Systems

The DEB theory is built on dynamic systems. The idea behind the concept of a system is simple in principle, but in practice some general modelling problems might arise that are best discussed here. A system is based on the idea of state variables, which are supposed to specify completely the state of the system at a given moment. Completeness is essential. The next step is to specify how the state variables change with time as a function of a number of inputs and each other. The specification usually takes the form of a set of differential equations, which have parameters, i.e. constants that are assumed to have some fixed value in the simplest case. Usually this specification also includes a number of outputs.

Parameters are typically constant, but sometimes the values change with time. This can be described by a function of time, which again has parameters that are now considered to be constant. For instance, parameters that have the interpretation of physiological rates depend on temperature; therefore, they remain constant as long as the temperature does not change. If the temperature does change, then the parameters do as well. Heat, however, is generated as a side product of metabolism. In ectotherms, i.e. animals that do not heat their body to a constant high temperature, heat production is low, because of their usually low body temperature. The body temperature usually follows that of the environment, and can thus be treated as a function of time. The situation is more complex in developing birds, which make the transition to the endothermic state some days after hatching. The hatchling's temperature is high, because of brooding; therefore, metabolism and heat production are also high. In addition, the young bird starts to invest extra energy in heating. Here, the state variables of the system interfere with the environment, but not via input; this means that the body temperature must be considered as an additional state variable.

Choosing the state variables is the most crucial step in defining a system. It is usually a lot easier to compare and test alternative formulations for the change of state variables, than different choices of state variables. Models with different sets of state variables are hardly comparable, both conceptually and in tests against data. Statistics basically deals with parameter values, and is of little use when comparing the goodness of fit of models

that differ in structure.

The variables that are easy to measure or those that will be used to test the model are not always those that should be state variables. An example is metabolic rate, which is measured as the respiration rate, i.e. oxygen consumption rate or carbon dioxide production rate. Metabolic rate is not chosen as a primary variable or parameter in the DEB theory; it only has the role of a derived variable, which is nonetheless important. This point will doubtlessly generate controversy. The metabolic rate has different components, each of which follows simple rules. The sum of these components is then likely to behave in a less simple way in non-linear models. The same holds for, for example, dry weights, which I will decompose into structural biomass and reserve materials. A direct consequence of such divisions is that experimental results that only include composite variables are difficult to interpret. For mechanistic models, it is essential to use variables that are the most natural players in the game. The relationship between these variables and those to be measured is the next problem to be solved, once the model is formulated.

Thermodynamics makes a most useful distinction between intensive variables – which are independent of size, such as temperature, concentration, density, pressure, viscosity, molar volume, and molar heat capacity – and extensive variables, which depend on size, such as mass, heat capacity and volume. Extensive variables can sometimes be added in a meaningful way if they have the same dimension, but intensive variables cannot. Concentrations, for example, can only be added when they relate to the same volume. Then they can be treated as masses, i.e. extensive variables. When the volume changes, we face the basic problem that while concentrations are the most natural choice for dealing with mechanisms, we need masses, i.e. absolute values, to make use of conservation laws. This is one of the reasons why one needs a bit of training to apply the chain rule for differentiation.

1.2.3 Physical dimensions

A few remarks on physical dimensions are needed here, because a test for dimensions is such a useful tool in the process of modelling. Remarkably, only a few texts deal with them adequately.

Models that violate rules for dealing with dimensions are meaningless. This does not imply that models that treat dimension well are necessarily useful models. The elementary rules are simple: addition and subtraction are only meaningful if the dimensions of the arguments are the same, but the addition or subtraction of variables with the same dimensions is not always meaningful; meaning depends on interpretation. Multiplication and division of variables correspond with multiplication and division of dimensions. Simplifying the dimension, however, should be done carefully. A dimension that occurs in both the numerator and the denominator in a ratio does not cancel automatically. A handy rule of thumb is that such dimensions only cancel if the sum of the variables to which they belong can play a meaningful role in the theory. The interpretation of the variable and its role in the theory always remain attached to dimensions. So the dimension of the biomass density in the environment expressed on the basis of volume is cubed length (of biomass) per cubed length (of environment); it is not dimensionless. This argument is sometimes

quite subtle. The dimension of the total number of females a male butterfly meets during its lifetime is number (of females) per number (of males), as long as males and females are treated as different categories. If it is meaningful for the theory to express the number of males as a fraction of the total number of animals, the ratio becomes dimensionless.

The connection between a model and its interpretation gets lost if it contains transcendental functions of variables that are not dimensionless. Transcendental functions, such as logarithm, exponent and sinus, frequently occur in models. pH is an example, where a logarithm is taken of a variable with dimension number per cubed length ($\ln\{\#l^{-3}\}$). When it is used to specify environmental conditions, no problems arise; it just functions as a label. However, if it plays a quantitative role, we must ensure that the dimensions cancel correctly. For example, take the difference between two pH values in the same liquid. This difference is dimensionless: $\mathrm{pH}_1 - \mathrm{pH}_2 = \ln\{\#l^{-3}\} - \ln\{\#l^{-3}\} = \ln\{\#l^{-3}\#^{-1}l^3\} = \ln\{\cdot\}$. In linear multivariate models in ecology, the pH sometimes appears together with other environmental variables, such as temperature, in a weighted sum. Here dimension rules are violated and the connection between the model and its interpretation is lost.

Another example is the Arrhenius relationship, cf. {53} where the logarithm of a rate is linear in the inverse of the absolute temperature: $\ln \dot{k}(T) = \alpha - \beta T^{-1}$, where $\dot{k}$ is a rate, T the absolute temperature and α and β are regression coefficients. At first sight, this model seems to violate the dimension rule for transcendental functions. However, it can also be presented as $\dot{k}(T) = \dot{k}_\infty \exp\{-T_A T^{-1}\}$, where T_A is a parameter with dimension temperature and $\dot{k}_\infty$ is the rate at very high temperatures. In this presentation, no dimension problem arises. So, it is not always easy to decide whether a model suffers from dimension problems.

A further example is the allometric function $\ln y(x) = \ln \alpha + \beta \ln x$, or $y(x) = \alpha\, x^\beta$, where y is some variable, x has the interpretation of body weight, the parameter β is known as the scaling exponent, and α as the scaling coefficient. At first sight, this model also seems to violate the dimension rule for transcendental functions. Huxley introduced it as a solution of the differential equation $\frac{dy}{dx} = \beta \frac{y}{x}$. This equation does not suffer from dimensional problems, nor does its solution $y(x) = y(x_1)(\frac{x}{x_1})^\beta$. However, this function has three rather than two parameters. It can be reduced to two parameters for dimensionless variables only. The crucial point is that, in most body size scaling relationships, a natural reference value x_1 does not exist for weights. The choice is arbitrary. The two-parameter allometric function violates the dimension rule for transcendental functions and should, therefore, not be used in models that represent theories. Models that violate dimension rules are bound to be purely empirical. Although this has been stated by many authors, the use of allometric functions is so widespread in energetics that it almost seems obligatory.

Many authors who use allometric functions are well aware of this problem. In discussions, they argue that they just give a description that does not pretend to be explanatory. However, they frequently use it in models that claim to be explanatory at another point. For me, this is walking in marshy country which is why I have been explicit in my point of view on theories, where there is no useful role for allometric functions. I accept that they offer a description that is sparse in parameters and frequently accurate. I also understand the satisfaction that a log-log plot can give by optically reducing the frequently huge scatter. I think, however, that they are an obstacle to understanding what is going

on. I will show that energetics does not need allometric functions and that they are at the root of many problems. One problem is that as soon as two groups of species are found to differ in the scaling exponent β, they can no longer be compared on the basis of their parameter values, because the dimensions of the parameter α differ. (The dimensions of α have a statistical uncertainty as well.) This seems most paradoxical to me, because many authors use allometric functions specifically for the purpose of comparing species, on the basis of parameter values. If one or more parameters cannot be compared for different species, because they have different dimensions, a most useful type of argument is lost. This is why allometric functions spoil the argument.

I shall frequently use dimensionless variables, rather than the original ones which bear dimensions. Although this procedure is standard when analysing the properties of models, my experience is that many biologists are annoyed by it. I will, therefore, explain briefly the rationale behind this usage.

The first reason for working with dimensionless variables is to simplify the model and get rid of as many parameters as possible. This makes the structure of the model more visible, and, of course, is essential for understanding the range of possible behaviours of the model when the parameter values change. The actual values of parameters are usually known with a high degree of uncertainty and they can vary a lot.

The second reason is to find out the parameter combinations that can actually be estimated on the basis of a given set of observations. In the model $y(x) = y(x_1)(\frac{x}{x_1})^\beta$, the parameters x_1, $y(x_1)$ and β cannot be estimated at the same time from a set of observations $\{x_i, y_i\}$, no matter how extensive the set is. When all parameter values are wanted, we need different, rather than more, observations. In many cases, knowledge about the values of all parameters is not necessary for the use of the model. One intriguing aspect is that it is not only impossible, but it is also not necessary to know the value of any parameter that has a dimension that cannot be written as product and/or ratio of the dimensions of the variables of the model; when the purpose is to test an energy-based model against observations that do not contain energies, for instance, all estimatable parameters are composed of ratios or products of parameters that contain energy in their dimension, such that the energy dimension drops out. This holds for all models that treat physical dimensions well, irrespective of how realistic they are. Some remarks on the ability to test a model must be made in this context.

The third reason for working with dimensionless variables is that numerical methods for integration and parameter estimation usually involve appropriate choices of step lengths, norm values and the like. When the step length is not dimensionless, it depends on the units of measurement in which the parameter are expressed, which is most inconvenient.

1.2.4 Statistics and support

The amount of support that a successful test of a model gives depends on the model structure and has an odd relationship with the ability to estimate parameters: the better one can estimate parameters, the less support a successful test of a model gives. This is a rather technical but vital point in work with models. I will try to make this clear with a simple model that relates y to x, and which has a few parameters, to be estimated on the basis of

a given set of observations $\{x_i, y_i\}$. We make a graph of the model for a given interval of the argument x, and get a set of curves if we choose the different values of the parameters between realistic boundaries. Two extremes could occur, with all possibilities in between:

- The curves have widely different shapes, together filling the whole x, y-rectangular plot. Here, one particular curve will probably match the plotted observations, determining the parameters in an accurate way, but a close match gives little support for the model; if the observations were totally different, another curve, with different parameter values, would have a close match.

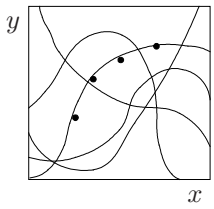

- The curves all have similar shapes and are close together in the x, y-rectangular plot. If there is a close match with the observations, this gives substantial support for the model, but the parameter values are not well determined by the observations. Curves with widely different parameter values fit equally well.

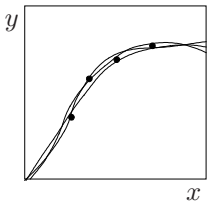

Two alternative models for biodegradation, with the same number of parameters, illustrate both situations in Figure 1.3. Of course, the choice of the model's structure is not free; it is dictated by the assumptions. I mention this problem to show that testability is a property of the theory and that nice statistical properties can combine with nasty theoretical ones and vice versa. It is essential to make this distinction.

The properties of parameter estimators also depend on the way the parameters are introduced. In the regression of y on x, the estimators for parameters a and b in the relationship $y = x^2(a + bx)$ are strongly negatively correlated when in the observations $\{x_i, y_i\}_{i=1}^n$, all $x_i > 0$; the mathematically totally equivalent relationship $y = x^2(c + b(x - \sum_i x_i^3 / \sum_i x_i^2))$ suffers much less from this problem. Replacement of the original parameters by appropriately chosen compound parameters can also reduce correlations between parameter estimates.

An increase in the number of parameters usually allows models to assume any shape in a graph. This is closely connected with the structural property of models just mentioned. So a successful test against a set of observations gives little support for such a model, unless the set includes many variables as well. A fair comparison of models should be based on the number of parameters per variable described, not on the absolute number.

Observations show scatter, which reveals itself if one variable is plotted against another. It is such an intrinsic property of biological observations that deterministic models should be considered as incomplete. Only complete models, i.e. those that describe observations which show scatter, can be tested. The standard way completing deterministic models is to add 'measurement error'. The definition of a measurement error is that, if the measurements are repeated frequently enough, the error will disappear in the mean of these observations. Such models are called regression models: $\underline{y}_i(x_i) = f(x_i|\text{pars}) + \underline{\epsilon}_i$. They are characterized by a deterministic part, here symbolized by the function f, plus a stochastic part, $\underline{\epsilon}$. The latter term is usually assumed to follow a normal probability density, with

n-th order degradation

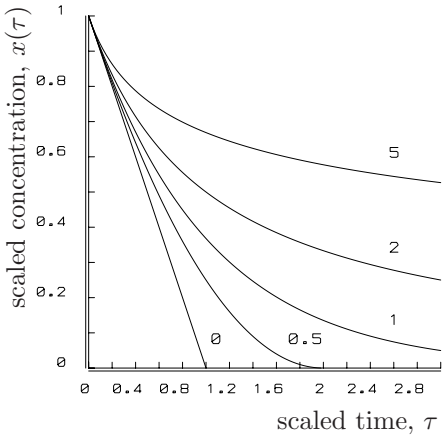

Dynamics

$$\frac{d}{dt}X = -\dot{\alpha}X^n$$

Solution

$$X(t) = \left(X_0^{1-n} - (1-n)\dot{\alpha}t\right)^{(1-n)^{-1}}$$

Special cases

$$X(t) \overset{n=0}{=} X_0 - \dot{\alpha}t \quad \text{for } t < X_0/\dot{\alpha}$$
$$X(t) \overset{n=1}{=} X_0 \exp\{-\dot{\alpha}t\}$$

Scaled solution

$$x(\tau) = (1-(1-n)\tau)^{(1-n)^{-1}}$$

with $x \equiv \frac{X}{X_0}$; $\tau \equiv t\dot{\alpha}X_0^{n-1}$

Monod degradation

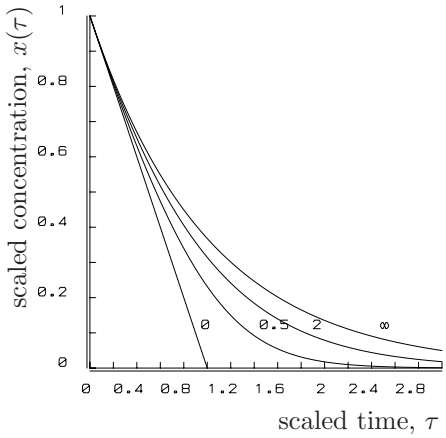

Dynamics

$$\frac{d}{dt}X = -\dot{b}\frac{X}{X_K + X}$$

Solution

$$0 = X(t) - X_0 + X_K \ln\{X(t)/X_0\} + \dot{b}t$$

Special cases

$$X(t) \overset{X_K \ll X_0}{=} X_0 - \dot{b}t \quad \text{for } t < X_0/\dot{b}$$
$$X(t) \overset{X_K \gg X_0}{=} X_0 \exp\{-\dot{b}t/X_K\}$$

Scaled solution

$$0 = x(\tau) - 1 + x_K \ln x(\tau) + (x_K + 1)\tau$$

with $x \equiv \frac{X}{X_0}; \tau \equiv \frac{t\dot{b}}{X_K + X_0}; x_K \equiv \frac{X_K}{X_0}$

Figure 1.3: The n-th order model for biodegradation of a compound X during time t is much more flexible in its morphology as a function of parameter values than the Monod model, while both models have three parameters (start concentration X_0, a rate parameter, $\dot{\alpha}$ or $\dot{b}$ and a shape parameter: the order n or the saturation constant X_K). Both models give identical $X(t)$ curves if $n = 0$ and $X_K \to 0$ and if $n = 1$ and $X_K \to \infty$. While all possible shapes of curves can be scaled between these two boundaries for the Monod model, many other shapes are possible for the n-th order model. This means that observations better determine the parameter values of the n-th order model, but that a good fit gives less support, compared to the Monod model. Moreover, the n-th order model suffers from dimension problems if n is not an integer, and has a more complex link with mechanisms, if any.

mean 0 and a fixed variance, which is one of the parameters of the model.

The interpretation of scatter as measurement error originates from physics. It is usually not realistic in biology, where many variables can be measured accurately in comparison with the amount of scatter. The observations just happen to differ from model expectations. When the scatter is large, the model is useless, despite its goodness of fit as a stochastic model. A realistic way of dealing with scatter is far from easy and usually gives rise to highly complicated models [63]. Modellers are frequently forced to compromise between realism and mathematical oversimplicity. This further degrades the strict application of goodness of fit tests for models with unrealistic stochastic components.

For lack of better ready-to-use alternatives, the tests against observations in this book will be based mainly on the regression method. This is most unsatisfactory, but such is life. I will, however, discuss two alternatives: individuals with stochastic inputs, {221}, and individuals that have different parameter values, {267,335} [63]. The motivation is that behavioural components of the feeding process are notoriously erratic, thus contributing significantly to the scatter, and individuals tend to deviate from each other in their input/output behaviour. Observations from a single individual usually have less scatter than those from different ones. The mathematics behind these alternatives is quite tedious, so I rely mainly on computer simulation studies.

I give estimates in this book for standard deviations for many parameter values that are obtained from experimental results, to roughly indicate accuracy. I follow this standard procedure with some hesitation on two grounds. The first reason to doubt the usefulness is that the value of the standard deviation is rather sensitive to the stochastic part of the model, which might not be very realistic, as discussed. The second reason is that such standard deviations do not account for correlations between parameters. A small standard deviation for a parameter, therefore, does not necessarily mean that such a parameter is known accurately, an error that is easy to make.

1.3 Summary

Similarity of growth among widely different organisms suggests the existence of common organizing principles that involve many aspects of energetics. Most of the basic questions have deep roots in the history of science. The aim of the DEB theory is to identify the main rules for the uptake and use of substrates (nutrients, light, food) that all organism have in common, and to develop a simple quantitative framework for metabolism, as it changes during the life cycle of an organism, based on elementary physico-chemical principles.

A fresh approach to the problem of revealing the common principles requires a carefully formulated philosophical position, and modelling principles that are more strict than usual. They are briefly presented. I emphasize the principle that theory-based modelling should start with the formulation of assumptions, from which mathematical descriptions are derived. The essence of modelling is that the set of assumptions is all that is used and no hidden preconceptions should slip in when deriving the mathematical description. Lack of support should be used to re-formulate assumptions.

I briefly introduce dimension analysis; statistical remarks are made in relation to em-

pirical support of models and estimation of parameter values. I explain why the standard method of allometry is of little use in the understanding of common organizing principles.

Chapter 2

Basic concepts

The purpose of this chapter is to introduce some general concepts to prepare for the development of the DEB theory in the next chapter. I present many tests against experimental data. These tests require careful interpretation of data, making use of the material presented in this chapter.

2.1 Individuals: the basic level of organization

From a systems analysis point of view, individuals are special because at this organizational level it is relatively easy to make mass balances. This is important, because the conservation law for mass and energy is one of the few hard laws available in biology. At the cellular and at the population level it is much more difficult to measure and model mass and energy flows. It is argued on {300} that life started as an individual in evolutionary history rather than as a particular compound, such as RNA. The individual is seen as an entity separated from the environment by physical barriers. Discussion should, therefore, start at the level of the individual.

2.1.1 Input/ output relationships

Any systems model relates inputs to a system with outputs of that system as a function of its state. Although many formulations suggest that the output is the result of the state of the system and its input, this cause-and-effect relationship is, in fact, a matter of subjective interpretation. The input might as well result from the state and the output; input, state and output change simultaneously, without an objective causality.

The DEB model for uptake and use of energy in terms of input/output relationships is neutral with respect to the interpretation in terms of 'supply' and 'demand'. In the 'supply' interpretation, the lead is in the feeding process, which offers an energy input to the individual. The available energy flows to different destinations, more or less as water flows through a river delta. In the 'demand' interpretation, the lead is in some process that uses energy, such as maintenance and/ or growth, which requires some energy intake. Food-searching behaviour is then subjected to regulation processes in the sense that an animal eats what it needs. I think that in practice species span the whole range from

'supply' to 'demand' systems. A sea-anemone, for example, is a 'supply' type of animal. It is extremely flexible in terms of growth and shrinkage, which depend on feeding conditions. It can survive a broad range of food densities. Japanese bonsai cultures cannot illustrate better that plants are typical supply systems as well. Birds are examples of 'demand' systems and they can only survive at relatively high food densities. The range of possible growth curves is thus much more restricted.

Even in the 'supply' case, growth may be regulated carefully by hormonal control systems. Growth should not proceed faster than the rate at which the energy and elementary compounds necessary to build the new structures can be mobilized. Models that describe growth as a result of hormonal regulation should deal with the problem of what determines the hormone levels. This requires studying organization at the individual level. The conceptual role of hormones is linked to the similarity of growth patterns despite the diversity of regulating systems. In the DEB theory, messengers such as hormones are part of the physiological machinery that an organism uses to regulate its growth. Their functional aspects can only be understood by looking at other variables and compounds.

Balance equations are extremely useful for specifying the constraints on the simultaneous behaviour of input, state and output of systems. Only precise book-keeping can avoid sources and sinks be overlooked. The possibility of formulating balance equations is a most useful aspect of the abstract quantity 'energy', cf. {35}. The conservation law for energy was originally formulated by von Mayer [600] in 1842, although its precursors go back as far as G. W. F. Leibnitz in 1693 [147]. This law is known today as the first law of thermodynamics. The law of conservation of mass was first described in a paper by A. L. Lavoisier in 1789.

2.1.2 State variables

Many models for growth have age as a state variable. Age itself has excellent properties as a measuring-tape, because it has a relatively well-defined starting point (here taken to be the start of embryogenesis and not birth, i.e. the transition from the embryonic state to the juvenile one). It can also be measured accurately. Some well-studied species only thrive on an abundant food supply, which results in well-defined and repeatable size-age curves. This has motivated a description of growth in terms of age, where food is considered as an environmental variable, like temperature, rather than a description in terms of input/ output relationships and energy allocation rules.

One frequently applied model was proposed by Gompertz [335] :

$$W(t) = W_\infty \, (W_0/W_\infty)^{\exp\{-\dot{r}_G t\}}$$

where $W(t)$ is the weight, usually the wet weight, of an individual at time t and $\dot{r}_G$ the Gompertz growth rate. The individual grows from weight W_0 asymptotically to weight W_∞. This is essentially an age-based model, which becomes visible from a comparison of alternative ways of expressing it as a differential equation: $\frac{d}{dt} \ln W = -\dot{r}_G \ln \frac{W}{W_\infty}$ or $\frac{d^2}{dt^2} \ln W = -\dot{r}_G \frac{d}{dt} \ln W$. The first equation states that the weight-specific growth rate decreases proportionally to the logarithm of weight as a fraction of ultimate weight. (Note

Figure 2.1: These talking gouramis, *Trichopsis vittatus*, come from the same brood and therefore are the same age. They also grew up in the same aquarium. The size difference resulted from competition for a limited amount of food chunks, which amplified tiny initial size differences. This illustrates that age cannot serve as a satisfactory basis for the description of growth.

that the notation $\frac{d}{dt} \ln W$ suggests a dimension problem, because it looks as if the argument of a transcendental function is not dimensionless. Its mathematically equivalent notation, $W^{-1} \frac{d}{dt} W$, shows that no dimension problem exists here.) It is hard to put a mechanism behind this relationship. The second equation states that the change in weight-specific growth rate decreases proportionally with the growth rate, which can be linked to a simple aging mechanism where the ability to grow fades according to a first-order process. In the situation of abundant food, this model usually gives an acceptable fit. The problems with this model and similar ones become apparent when growth has been measured at different food availabilities.

Figure 2.1 shows two fish from the same brood, which have lived in the same five-litre aquarium. Their huge size difference shows that age-based growth models are bound to fail. The mechanism behind the size difference in this case is the way of feeding, which involved a limited number of relatively big food chunks for the whole brood. Initially, the size differences were very small, but the largest animal always took priority over its smaller siblings, which amplified the size differences. Similar results apply to prokaryotes, which have a poor control over age-at-division at constant substrate density, but a high control over size-at-division [500].

Apart from empirical reasons for rejecting age as a state variable for the description of

growth, it cannot play the role of an explanatory variable from a physical point of view. Something that proceeds with age, such as damage caused by free radicals, cf. {140}, can play that role. One will need an auxiliary model to show in detail how such a variable depends on age. One of the problems with the Gompertz model and related ones is that growth is not caused by a difference between an uptake and a usage term. Instead, it is formulated as an intrinsic property of the organism. The environment can only affect growth through the parameter values.

When feeding is conceived as input of energy, size must be one of the state variables. A large individual eats much more than a small one, so it is hard to imagine a realistic model for growth that does not have size as one of the state variables; however, many quantities can be taken to measure size. Examples are volume, wet weight, dry weight, ash-free dry weight, amount of carbon or energy etc. Originally I thought that, to some extent, they were more or less interchangeable, depending on the species. Now, I am convinced that volume is the only natural choice to measure size in the context of the present theory, where surface areas play such an important role. A volume (organism) living in another volume (environment) is bound to communicate with it over a surface area. The DEB theory makes use of the interpretation of the size/surface-area ratio in terms of length. Masses are of considerable interest for implementing mass balances, and weights are practical for comparing theoretical predictions with data. The relationships between size measures are discussed on {31}.

Size alone is not enough to describe the process of substrate use and the implied uptake. For several reasons, energy reserves should be considered as well, even in the most simple models.

The first reason is the existence of maintenance, i.e. a continuous drain of energy necessary to keep the body going. Feeding on particles, even if these particles are molecules, implies that there are periods when no particles arrive. The capacity of a digestive system cannot realistically be made big enough to smooth out the discrete arrival process, in order to 'pay' the steady costs of maintenance. Other costs are paid as well in the absence of any food input. Spectacular examples of prolonged action without food intake are the European, North American and New Zealand eels, *Anguilla*, which stop feeding at a certain moment. Their alimentary canal even degenerates, before the 3000-km-long journey to their breeding grounds where they spawn. The male emperor penguin *Aptenodytes forsteri* breeds its egg in Antarctic midwinter for two months and feeds the newly hatched chick with milky secretions from the stomach without access to food. The male loses some 40% of its body weight before assistance from the female arrives.

The second reason for including energy reserves is that individuals react slowly to changes in their feeding conditions. Again, this cannot be described realistically with the digestive system as a buffer, because its relaxation time is too short.

The third reason is that well-fed individuals happen to have a different (chemical) body composition than those in poor feeding conditions. The type of difference depends on the species, as is discussed later. Originally I thought that, as long as food density was constant, one could do without storage. This is why the first version of the DEB model [524] did without a state variable representing energy storage. However, when growth at different food densities is compared and storage levels depend on food density, one should

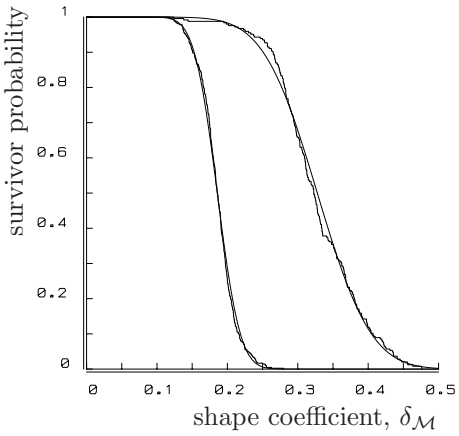

Figure 2.2: The sample survivor function (see Glossary) of shape coefficients for European birds (left) and Neotropical mammals (right). The lengths include the tail for the birds, but not for mammals. Data are from Bergmann and Helb [71] and Emmons and Feer [255]. The fitted survivor functions are those of the normal distribution.

include storage even under these simple conditions.

Size and stored energy should play a role in even the simplest model for the uptake and use of energy. Several other state variables, such as the contents of the digestive system, energy density of the blood, etc., are necessary to describe the finer details of some physiological processes, but they need not play a significant role at the population level. For the purposes of population dynamics analysis and the contribution of aging therein, it makes sense to introduce age as an auxiliary third state variable. It is also necessary to distinguish between life-stages to catch qualitative differences in energetics, cf. {59}.

2.2 Body shape: surface area/ volume relationships

The shape of organisms cannot be described accurately. For an understanding of energetics, only two aspects of size and shape are relevant, as is explained later: surface areas for acquisition processes and volumes for maintenance processes. Shape defines how these measures relate to each other. Measurements of lengths are usually easy to obtain in a non-destructive way. This also holds for weights of animals. So, the practical problem has to be solved of how these measurements relate to surface areas and volume. Contrary to volumes and weights, lengths depend on shape, and details about its measurement must be provided.

As a first crude approximation, wet weights, W_w, i.e. the weight of a living organism without adhering water, can be converted to physical volumes, V_w, by division through a fixed specific density d_{Vw}, which is close to 1 $\mathrm{g\,cm^{-3}}$. So $W_w = d_{Vw}V_w$, where d_{Vw} is taken here to be a (fixed) parameter.

If an organism does not change its shape during development, an appropriately chosen length measure, L, can be used to obtain its volume. The length is multiplied by a fixed dimensionless shape coefficient $\delta_{\mathcal{M}}$ and the result is raised to the third power: $V_w = (\delta_{\mathcal{M}}L)^3$. The shape coefficient, defined as $\mathrm{volume}^{1/3}\,\mathrm{length}^{-1}$, is specific for the particular way the length measure has been chosen. Thus the inclusion or exclusion of a tail in the length of an organism results in different shape coefficients. A simple way to obtain an approximate value for the shape coefficient belonging to length measure L is on the basis of the relationship $\delta_{\mathcal{M}} = (\frac{W_w}{d_{Vw}})^{1/3}L^{-1}$.

Table 2.1: The means and coefficients of variation of shape coefficients of European birds and mammals and Neotropical mammals.

Taxon	Source	Number	Mean tail included	cv	Mean tail excluded	cv
European birds	[131,255]	418	0.186	0.14		
European mammals	[116]	128	0.233	0.27	0.335	0.28
Neotrop. mammals	[71]	246	0.211	0.41	0.328	0.18

The following considerations may help in getting acquainted with the shape coefficient. For a sphere of diameter L and volume $L^3\pi/6$, the shape coefficient is 0.806 with respect to the diameter. For a cube with edge L, the shape coefficient takes the value 1, with respect to this edge. The shape coefficient for a cylinder with length L and diameter L_ϕ is $(\frac{\pi}{4})^{1/3}(L/L_\phi)^{-2/3}$ with respect to the length.

The shapes of organisms can be compared in a crude way on the basis of shape coefficients. Figure 2.2 shows the distributions of shape coefficients among European birds and Neotropical mammals; they fit the normal distribution closely. Summarizing statistics are given in Table 2.1, which includes European mammals as well. Some interesting conclusions can be drawn from the comparison of shape coefficients. They have an amazingly small coefficient of variation (cv), especially in birds (including sphere-like wrens and stick-like flamingos), which probably relates to constraints for flight. Mammals have somewhat larger shape coefficients than birds. They tend to be more spherical, which possibly relates to differences in mechanics. The larger coefficient of variation indicates that the constraints are perhaps less stringent than for birds. The spherical shape is more efficient for energetics because cooling is proportional to surface area and a sphere has the smallest surface area/volume ratio, namely $6/L_\phi$. When the tail is included in the length, European mammals have somewhat larger shape coefficients than Neotropical mammals, but the difference does not arise when the tail is excluded. Neotropical mammals tend to have longer tails, which is probably because most of them are tree dwellers. The temperature difference between Europe and the Neotropics does not result in mammals in Europe being more spherical to reduce cooling.

These considerations should not obscure the practical purpose of shape coefficients, which is to convert shape-specific length measures to volumetric lengths, i.e. cubic roots of volumes. In contrast to lengths, volumetric lengths do not depend on shape. Each parameter that has length in its dimensions is sensitive to the way that those lengths are measured (including or excluding extremities, etc.). As long as the comparison is made between bodies of the same shape, there is no need for concern, but as soon as different shapes are compared, it is essential to convert length to volumetric length, the rationale being that a comparison based on unit volumes of organisms is made on the basis of cells.

2.2.1 Isomorphism

Isomorphism is an important property that applies to the majority of species on Earth. It refers to conservation of shape as an individual grows in size. The shape can be any shape and the comparison is only between the shapes that a single individual takes during its development. If organisms have a permanent exoskeleton, however, there are stringent constraints on their shape [516].

Two bodies of a different size are isomorphic if it is possible to transform one body into the other by a simple geometric scaling in three dimensional space: scaling involves only multiplication, translation and rotation. This implies, as Archimedes already knew, that if two bodies have the same shape and if a particular length takes value L_1 and L_2 in the different bodies, the ratio of their surface areas is $(L_1/L_2)^2$ and that of their volumes $(L_1/L_2)^3$, irrespective of their actual shape. It is, therefore, possible to make assertions about the surface area and the volume of the body relative to some standard, on the basis of lengths only. One only needs to measure the surface area or volume if absolute values are required. This property is used extensively in this book.

Most species are approximately isomorphic. It is not difficult to imagine the physiological significance of this. Process-regulating substances in the body tend to have a short lifetime to cope with changes, so such substances have to be produced continuously. If some organ secretes at a rate proportional to its volume (i.e. number of cells), isomorphism will result in a constant concentration of the substance in the body. The way the substance exercises its influence does not have to change with changing body volume in order to obtain the same effect in isomorphs. Organisms and cells monitor their size, but the way they do this is considered to be an open problem [963, p 123]; the following argument shows that organisms and cells do not need to accumulate compounds with increasing size to monitor their size.

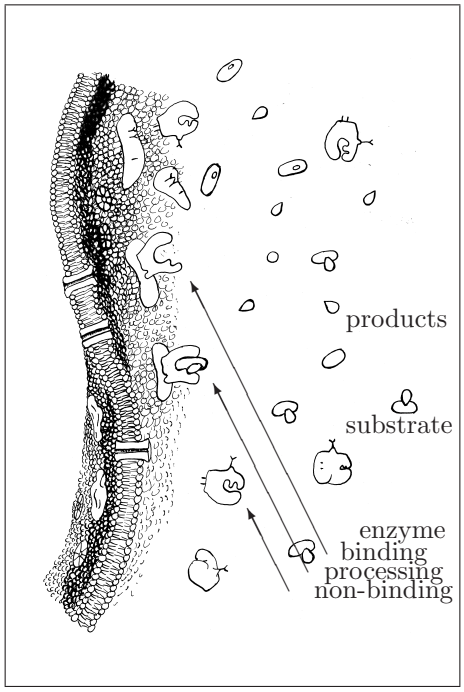

Surface-area-volume relationships play an essential role in the communication between the extensive variable body size and intensive variables such as concentrations of compounds and rates of reaction between compounds. Secreting organs 'know' their volume relative to body volume by the build up of the concentration of their products in the body. Each cell in the body 'knows' its volume by the ratio between its volume and the surface area of its membranes. This is because most enzymes only function if bound to a membrane, with their substrates and products in the cell volume as illustrated. The functional aspect is that the production of enzymes is a relatively slow process, a handicap if a particular transformation needs to be accelerated rapidly. Most enzymes can be conceived of as fluffy structures, with performance depending on the shape of the molecule's outer surface and

the electrical charge distribution over it. If bound to a membrane, the outer shape of the enzyme changes into the shape required for the catalysis of the reaction specific to the enzyme. Membranes thus play a central role in cellular physiology [316,374,985]. The change in surface area/volume ratios at a micro-scale has important kinetic implications as is shown in the discussion on structural homeostasis {246}.

Many pathways require a series of transformations and so involve a number of enzymes. The binding sites of these enzymes on the membrane are close to each other, so that the product of one reaction does not disperse in the cytosol before being processed further. The product is just handed over to the neighbouring enzyme in a process called piping. Interplay between surface areas and volumes is basic to life, not only at the level of the individual, but also at the molecular level.

2.2.2 Changing shapes

Huxley [438] described how certain parts of the body can change in size relative to the whole body, see {177}. He used allometric functions to describe this change and highlighted the problem that if some parts change in an allometric way, other parts cannot. From an energetics point of view, the change in relative size of some extremities is not very important. The total volume is of interest because of maintenance processes, and certain surface areas for acquisition processes. The fact that wing development, for instance, is delayed in birds is of little relevance to whole body growth. The basic problem is in the relationship between the size measure for the scaling of uptake rates and the volume that has to be maintained.

Some species such as echinoderms and some insects change shape over different life-stages. Plants are extreme in this, and environmental factors contribute substantially to changes in shape. Some of these changes do not cause problems because food intake is sometimes restricted to one stage only. If the shape changes considerably during development, and if volume has been chosen as the basis for size comparisons, the processes related to surface area should be corrected for these changes in shape. A convenient way to do this is to use the dimensionless shape correction function $\mathcal{M}(V)$, which stands for the actual surface area relative to the isomorphic one for a body with volume V, where a particular shape has been chosen as the reference. The derivation of this function will be illustrated for what I call V0-, and V1-morphs: idealized morphs that change in shape during growth in a particular way. Many organisms approach these idealized changes quite accurately, others can be conceived as static or dynamic mixtures of two or more of these idealized growing morphs, as will be shown.

V0-morphs

The surface area of a V0-morph is proportional to volume^0, so it remains constant. Only the surface area matters that is involved in the uptake process. A biofilm on a plane, diatoms and dinoflagellates are examples, see Figure 2.3. The outer dimensions do not increase during the synthesis of cytoplasm. The vacuoles shrink during growth of the cell, and should be

excluded from the structural volume that requires maintenance costs. The surface area of a V0-morph is A_d, say. An isomorph has surface area $A_d(V/V_d)^{2/3}$. The value V_d is a reference that is required to compare both types of morphs; at this volume they have the same surface area. The shape correction function for a V0-morph is

$$\mathcal{M}(V) = (V/V_d)^{-2/3} \tag{2.1}$$

In the section on diffusion limitation on {235}, I discuss situations where the outer boundary of the stagnant water mantle around a small organism restricts uptake. If the mantle is thick enough, the uptake will resemble that of a V0-morph, whatever the actual changes in shape of the organism.

V1-morphs

The surface area of a V1-morph is proportional to volume[1]. It (usually) grows in one dimension only, and it is possible to the orient the body such that the direction of growth is along the x-axis, while no growth occurs along the y- and z-axes. The different body sizes can be obtained by multiplying the x-axis by some scalar l. An example of a V1-morph is the filamentous hyphe of a fungus with variable length, and thus variable volume V, but a fixed diameter, see Figure 2.3. Its surface area equals $A(V) = A_d V/V_d$, where A_d denotes the surface area at $V = V_d$. The surface area of an isomorph equals $A(V) = A_d(V/V_d)^{2/3}$. So the shape correction function for V1-morphs becomes

$$\mathcal{M}(V) = \frac{A_d V/V_d}{A_d(V/V_d)^{2/3}} = (V/V_d)^{1/3} \tag{2.2}$$

It is not essential that the cross section through a filament is circular; it can be any shape, as long as it does not change during growth.

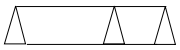

A V1-morph can also grow in two dimensions, however, as is illustrated by sheets, i.e. flat bodies with a constant, but small, height. The archaebacterium *Methanoplanus*, and Walsby's bacterium [478,965] fit this description. Several colonies, such as the sulphur bacterium *Thiopedia*, the blue-green bacterium *Merismopedia* and the green alga *Pediastrum*, also fall into this category; see Figure 2.3. How sheets grow in two dimensions does not matter: they may change wildly in shape during growth. Height must be small to neglect the contribution of the sides to the total surface area. The surface area of the sheet relates to its volume as $A(V) = 2VL_h^{-1}$, where L_h denotes the height of the sheet and the factor 2 accounts for the upper and lower surface areas of the sheet. Division by the isomorphic surface area $A(V_d)(V/V_d)^{2/3}$ gives $\mathcal{M}(V) = (V/V_d)^{1/3}$, as for filaments, i.e. V1-morphs.

Static mixtures

Cooper [174] argues that at constant substrate density *Escherichia* grows in length only, while the diameter/length ratio at division remains constant for different substrate densities. This mode of growth and division is typical for most rod-shaped bacteria, and most

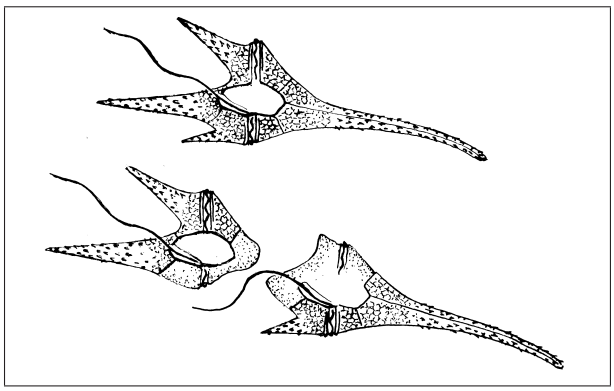

V0-morph. The dinoflagellate *Ceratium* has a rigid cell wall, which does not grow during the cell cycle, nor does the adjacent outer membrane that takes up nutrients. Cytoplasm growth is at the expense of internal vacuoles.

V1-morph. A mycelium of a fungus, such as *Mucor*, can be conceived as a branching filament, with a constant diameter. If the mycelium becomes dense, uptake is usually no longer proportional to the total filament length or number of growing tips of branches.

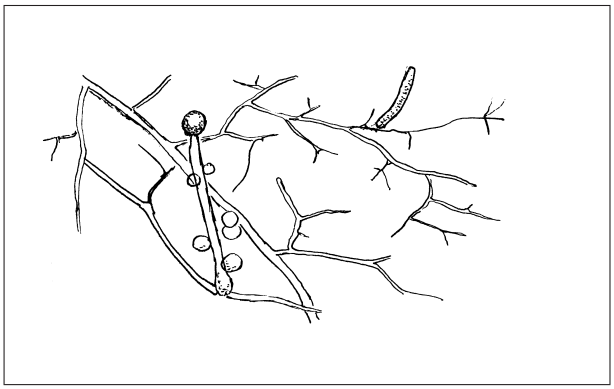

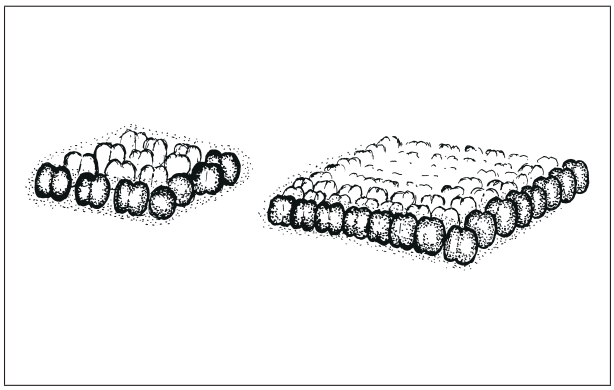

V1-morph. The blue-green bacterial colony *Merismopedia* is only one cell layer thick. Although this sheet grows in two dimensions, it is a V1-morph. The arrangement of the cells requires an almost perfect synchronization of the cell cycles.

Figure 2.3: A sample of organisms that change in shape during growth in very particular ways.

bacteria are rod-shaped. Shape and volume at division, at a given substrate density, are selected as a reference. The cell then has, say, length L_d, diameter δL_d, surface area A_d and volume V_d. The fraction δ is known as the aspect ratio of a cylinder. The index d will be used to indicate length, surface area and volume at division at a given substrate density. The shape of the rod shaped bacterium is idealized by a cylinder with hemispheres at both ends and, in contrast to a filament, the caps are now included. Length at division is $L_d = \left(\frac{4V_d}{(1-\delta/3)\delta^2\pi}\right)^{1/3}$, making length $L = \frac{\delta}{3}\left(\frac{4V_d}{(1-\delta/3)\delta^2\pi}\right)^{1/3} + \frac{4V}{\pi\delta^2}\left(\frac{(1-\delta/3)\delta^2\pi}{4V_d}\right)^{2/3}$. Surface area becomes $A = L_d^2\frac{\pi}{3}\delta^2 + \frac{4V}{\delta L_d}$. The surface area of an isomorphically growing rod equals $A_d(V/V_d)^{2/3}$. The shape correction function is the ratio of these surface areas. If volume, rather than length, is used as an argument, the shape correction function becomes

$$\mathcal{M}(V) = \frac{\delta}{3}\left(\frac{V}{V_d}\right)^{-2/3} + \left(1 - \frac{\delta}{3}\right)\left(\frac{V}{V_d}\right)^{1/3} \tag{2.3}$$

When $\delta = 0.6$, the shape just after division is a sphere as in cocci, so this is the upper boundary for the aspect ratio δ. This value is obtained by equating the volume of a cylinder to that of two spheres of the same diameter. When $\delta \to 0$, the shape tends to that of a V1-morph.

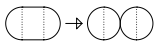

The shape correction function for rods can now be conceived as a weighted sum of those for a V0- and a V1-morph, with a simple geometric interpretation of the weight coefficients. A cylinder that grows in length only, with flat caps and an aspect ratio δ at $V = V_d$, has the shape correction function

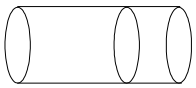

$$\mathcal{M}(V) = \frac{\delta}{\delta+2}\left(\frac{V}{V_d}\right)^{-2/3} + \frac{2}{\delta+2}\left(\frac{V}{V_d}\right)^{1/3} \tag{2.4}$$

which is again a weighted sum of correction functions for V0- and V1-morphs. For the aspect ratio $\delta \to \infty$, the shape can become arbitrary close to that of a V0-morph. The exact geometry of the caps is thus less important for surface area/volume relationships. Rods and cylinders are examples of static mixtures of V0- and V1-morphs, i.e. the weight coefficients do not depend on volume. Crusts are examples of dynamic mixtures of V0- and V1-morphs, and are discussed on {250}.

Summary

The table at the right summarises the shape correction functions for isomorphs of different dimensions. The power of the scaled volumes has an odd relationship with the dimension of isomorphy. Mixtures of V0- and V1-morphs can resemble isomorphs, depending the weight coefficients and the range of values for the scaled volume.

morph	$\mathcal{M}(V)$
V0	$(V/V_d)^{-2/3}$
V1	$(V/V_d)^{1/3}$
iso	$(V/V_d)^0$

2.3 Body size and composition

2.3.1 Homeostasis

The compounds that cells use to drive metabolism require enzymes for their chemical transformation. Compounds that react spontaneously are excluded. In this way cells achieve full control over all transformations, because they synthesize enzymes, consisting of protein, themselves. No reaction runs without the assistance of enzymes. The properties of enzymes depend on their micro-environment. So homeostasis, i.e. a constant chemical composition, is essential for full control. Changes in the environment in terms of resource availability, both spatial and temporal, require the formation of reserve pools to ensure a continuous supply of essential compounds for metabolism. This implies a deviation from homeostasis. The cell's solution to this problem is to make use of polymers that are not soluble. In this way these reserves do not change the osmotic value, and neither do they affect the capacity of monomers to do chemical work (cf. {35}). In many cases cells encapsulate the polymers in membranes, to reduce interference even further, at the same time increasing access, as many cellular activities are membrane bound (cf. {246}).

Storage and structural compounds have a limited life span in an organism, but the turnover mechanisms differ. Storage materials are continuously used and replenished, while structural materials, and in particular proteins, are continuously degraded and reconstructed. Most proteins (enzymes) have a fragile, tertiary structure, which results in very short mean functional lifetimes. Energy costs of protein turnover are included in maintenance costs. The DEB model assumes no maintenance for energy reserves. This is most obvious for freshly laid bird eggs, which are composed almost entirely of reserve materials and use practically no oxygen, as is discussed on {98,135}.

Reserve materials can be distinguished from materials of the structural mass by a change in relative abundance if resource levels change. This defining property breaks down in case of extreme starvation, when structural materials are degraded as well when reserves are exhausted. An example of this is the break down of muscle tissue, which must be considered as structural material, in mammals such as ourselves. The distinction between reserves and structural materials is meant to accommodate the fact that some materials are more mobile than others. DEB theory builds on a two-way classification. It assumes that structural mass and reserve do not change in composition; I call this assumption the *strong homeostasis* assumption; it forms the basis of the quantification of size.

The word 'reserve' to describe material perhaps suggests that this material is set aside by metabolism for later use, being metabolically inert until that moment. This meaning is *not* implied here; reserve materials can be used directly upon creation, and can have an active role in metabolism, cf. {244}. A better phrasing would possibly be 'material that is available for metabolic use', or 'reversible mass'. Rules for the actual rate of use form a cornerstone in the DEB theory.

Since the amount of reserves can change relative to the amount of structural materials, the chemical composition of the whole body can change. That is, it can change in a particular way. This is a consequence of choosing energy as a state variable rather than the complete catalogue of all compounds.

Later, {82}, I assume that homeostasis applies to the whole organism (including structural mass and reserves) from birth to death *if food density does not change and reserves are at equilibrium*. This is called the *weak homeostasis* assumption. Weak homeostasis is basically different from strong homeostasis. Strong homeostasis has nothing to do with reserve dynamics, while weak homeostasis partly specifies the reserve dynamics. The reserve dynamics will be underpinned mechanistically on the basis of the structural homeostasis assumption, see {246}. Structural homeostasis also provides an explanation for weak homeostasis. Contrary to strong homeostasis, weak homeostasis only applies at steady state. The composition of a whole organism changes during transient states, unless the reserves and structure have the same composition, which will generally not be true.

The two-way classification of compounds into permanent (structural mass) and transient (reserves) groups is too simplistic for an understanding of autotrophs, which obtain nutrients independently from the environment and are faced with the problem of how to couple them stoichiometrically to synthesize structural mass of a constant composition. In Chapter 5 on multivariate DEB models, I delineate several reserves and structural masses (roots and shoots) to accommodate autotrophs.

2.3.2 Weights

In the discussion on shape coefficients, {23}, the crude relationship $W_w = d_{Vw}V_w$ was used to relate wet weight to structural volume. This mapping in fact assumes that the compositions of structural mass and reserves are identical. Much literature is based on this relationship or on the similar one for dry weights: $W_d = d_{Vd}V_w$.

The contribution made by reserves, relative to that made by structure, to size measures depends on their nature. For example, energy allocated to reproduction, but temporarily stored in a buffer, will contribute to dry weight, but much less to wet weight [315]. While wet weight is usually easier to measure and can be obtained in a non-destructive way, dry weight has a closer link to chemical composition and mass balance implementations. I show on {125} how to separate structural body mass from reserves and determine the relative abundances of the main elements for both categories on the basis of dry weight.

The relationships between physical volume V_w, wet weight W_w and dry weight W_d with *structural* body volume V, non-allocated energy reserves E, and energy reserves allocated to reproduction E_R are

$$V_w = V + (E + E_R)\frac{w_E}{d_E\mu_E} \quad (2.5)$$

$$W_w = d_V V + (E + E_R)w_E/\mu_E \quad (2.6)$$

$$W_d = d_{Vd}V + (E + E_R)w_{Ed}/\mu_E \quad (2.7)$$

where d_* are densities, which convert volumes to weights, μ_E the chemical potential of reserves (energy per C-mole), and w_* are molecular weights (weight per C-mole, see {34}).

The contribution of reserves to weight has long been recognized, and is used to indicate the nutritional condition of fish and birds [711]. A series of coefficients has been proposed, e.g. (weight in g)×(length in cm)$^{-1}$, known as the condition factor, Hile's formula or the ponderal index [9,306,410,436].

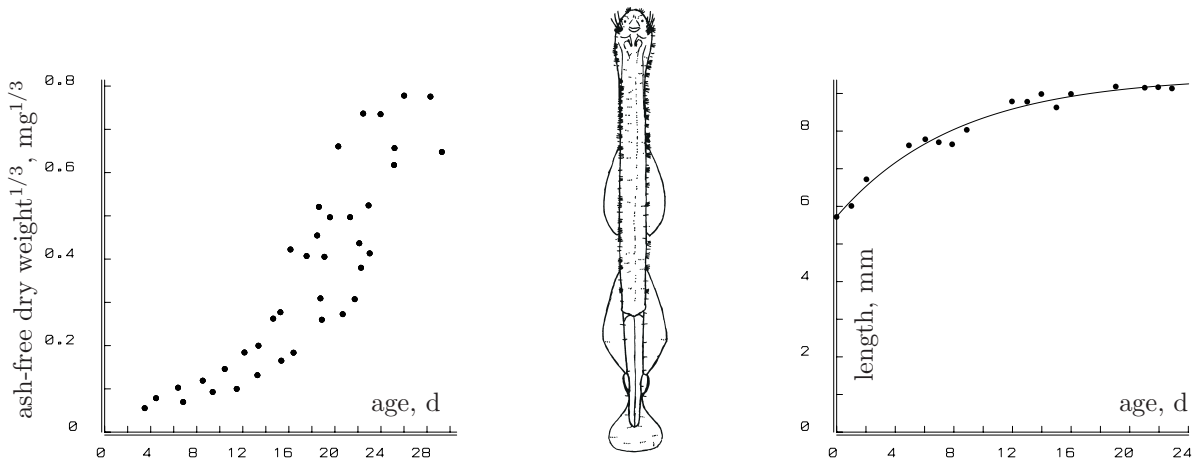

Figure 2.4: The ash-free dry weight and the length of the cheatognat *Sagitta hispida*. Data from Reeve [756,757]. The curve through the lengths is $L(t) = L_\infty - (L_\infty - L_0)\exp\{-\dot{r}_B t\}$.

Although the relationship between weight and reserves plus structural volume is more accurate than a mere proportionality, it is by no means 'exact' and depends on species-specific details. The gut contents of earthworms, shell of molluscs, exoskeleton of crustaceans do not require maintenance and for this reason they should be excluded from biovolume and weight for energetic purposes. The contribution of inorganic salts to the dry weight of small marine invertebrates is frequently substantial. Because weights combine structural and reserve mass, they should not be used to set up a theory of substrate uptake and use, and their role is restricted to link model predictions to data. The problem can be illustrated by the observation that the weight-specific maintenance costs of fungi and trees are extremely low. This does not point, however, to exceptional metabolic qualities, but to the fact that their weights include products (cell wall material, wood), that do not require maintenance. The production rates are quantified by the DEB theory, {147}, which allows weights to be decomposed into the contributions from structure, reserves and products.

Figure 2.4 illustrates an interpretation problem in the measurement of the ash-free dry weight of cheatognats. Length measurements follow the expected growth pattern closely when food is abundant, while the description of weight requires an *ad hoc* reasoning, possibly involving gut contents. Although quickly said, this is an important argument in the use of measurements within a theoretical context: if an explanation that is not species-specific competes one that is, the first explanation should be preferred if the arguments are otherwise equally convincing. Since energy reserves contribute to weight and are sensitive to feeding conditions, weights are usually much more scattered, in comparison to length measurements. This is illustrated in Figure 2.5.

The determination of the size of an embryo is complicated by the extensive system of membranes that the embryo develops in order to mobilize stored energy and materials and the decrease in water content during development [993]. In some species, the embryo can be separated from 'external' yolk. As long as external yolk is abundant, the energy reserves of the embryo without that yolk, if present at all, will, on the basis of DEB theory, turn out to be a fixed fraction of wet and dry weight, so that the embryo volume is proportional

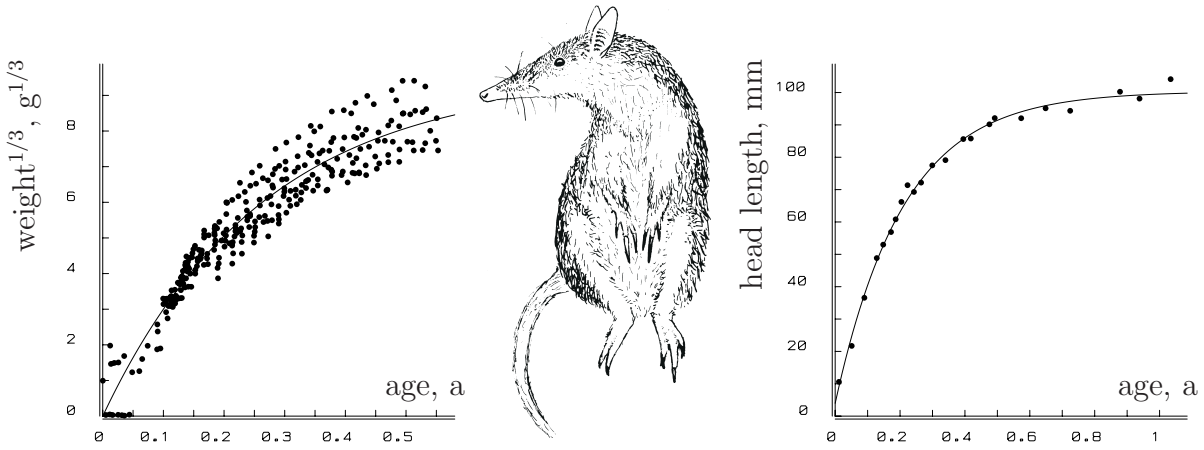

Figure 2.5: The weight to the power 1/3 and the head length of the long-nosed bandicoot *Perameles nasuta*. Data from Lyne [573]. The curves are again $L(t) = L_\infty - (L_\infty - L_0) \exp\{-\dot{r}_B t\}$.

to weight. Uncertainty about the proportionality factor will hamper the comparison of parameter values between the embryonic stage and the post-embryonic one.

Weights play no role in the DEB theory itself, but they are important for relating theoretical predictions to measurements.

2.3.3 Masses

Microbiologists frequently express the relative abundances n_{*W} of the elements hydrogen, oxygen and nitrogen in dry biomass relative to that of carbon, and conceive the combined compound so expressed as a kind of abstract 'molecule' that can be counted and written as $CH_{n_{HW}}O_{n_{OW}}N_{n_{NW}}$. For each C-atom in dry biomass, there are typically $n_{HW} \simeq 1.8$ H-atoms, $n_{OW} \simeq 0.5$ O-atoms and $n_{NW} \simeq 0.2$ N-atoms for a randomly chosen micro-organism [779]. This gives a mean degree of reduction of 4.2 and a 'molecular weight' of $w_W = 24.6$ g mol^{-1}. The latter can be used to convert dry weights into what are called 'C-moles'. The relative abundances of elements in biomass-derived sediments largely remain unaltered on a geological time scale, apart from the excretion of water. The Redfield ratio C:N:P = 105:15:1 is popular [755] in geology and oceanography, or for silica bearing organisms such as diatoms, radiolarians, silico-flagellates and (some) sponges C:Si:N:P = 105:40:15:1. This literature usually excludes hydrogen and oxygen, because their abundances in biomass-derived sediments change considerably during geological time. Other bulk elements in organisms are S, Cl, Na, Mg, K and Ca, while some 14 other trace elements play an essential role, as reviewed by Fraústo da Silva and Williams [296]. The ash that remains when dry biomass is burnt away is rich in these elements. Ash weight typically amounts to some 5% of dry weight only, and the elements C, H, O and N comprise more than 95% of the total dry weight. I focus on these four elements only, but the inclusion of more elements is straightforward. As stated before, some taxa require special attention on this point.

I denote structural mass in terms of C-moles by M_V, reserve mass by M_E, and the

ratio of reserve to structural mass by $m_E = M_E/M_V$. Table 3.4 on {122} gives useful conversions between volumes, masses and energies.

As is standard in the microbiological literature, the concept of the C-mole is extended to (simple) substrates, the difference from an ordinary mole being that it always has at most 1 C-atom.

2.3.4 Biomass composition

Reserves and structural mass are thought of as generalized compounds: rich mixtures of compounds that do not change in chemical composition. The concept rests fully on the strong homeostasis assumption. If a 'molecule' of structural biomass is denoted by $\mathrm{CH}_{n_{HV}}\mathrm{O}_{n_{OV}}\mathrm{N}_{n_{NV}}$ and a 'molecule' of energy reserves by $\mathrm{CH}_{n_{HE}}\mathrm{O}_{n_{OE}}\mathrm{N}_{n_{NE}}$, then their relative abundances in biomass consisting of structural mass M_V, reserves M_E and reserves allocated to reproduction M_{E_R} are given by

$$n_{*W} = \frac{n_{*V}M_V + n_{*E}(M_E + M_{E_R})}{M_V + M_E + M_{E_R}} = \frac{n_{*V} + n_{*E}(m_E + m_{E_R})}{1 + m_E + m_{E_R}} \tag{2.8}$$

where $*$ stands for H, O or N and $m_E = M_E/M_V$ and $m_{E_R} = M_{E_R}/M_V$ are molar reserve densities. Similarly we have $M_V = [M_V]V$ and $M_E = \mu_E^{-1}E$, where $[M_V]$ denotes the conversion coefficient from structural volume to C-mole. The molar weights of structural biovolume and energy reserves are given by

$$\begin{array}{rcll} w_V & \simeq & 12 + n_{HV} + 16n_{OV} + 14n_{NV} & \text{gram mol}^{-1} \\ w_E & \simeq & 12 + n_{HE} + 16n_{OE} + 14n_{NE} & \text{gram mol}^{-1} \end{array}$$

since the contribution of the other elements to weight is negligibly small. The problem of uncovering the relative abundances n_{*V} and n_{*E} from measurements of n_{*W}, is discussed on {125}.

The delineation of more than one type of reserve (or structural mass) comes with additional contributions to mass and weight. For n reserves, a single structural mass, and no reserves allocated to reproduction, (total) biomass can be decomposed into the masses (in C-moles)

$$\{M_{E_1}, M_{E_2}, \cdots, M_{E_n}, M_V\}$$

which together define the state of the organism. The strong homeostasis assumption states that these masses do not change in chemical composition and, therefore, they can be treated as generalized compounds.

The wet weight of the n-reserves organism amounts to $W_w = w_V M_V + \sum_i w_{E_i} M_{E_i}$, where the w's stand for the C-molar weights. The dry weight of this organism can be expressed similarly as $W_d = w_{Vd} M_V + \sum_i w_{E_i d} M_{E_i}$, where the w_{*d}'s represent the C-molar weights, after removal of water. This can be done in this way because the assumption that neither reserves nor structural biomass can change in composition means that their water fractions are constant.

The aqueous fraction of an organism is important in relation to the kinetics of toxicants. Water is treated just like any other compound in the decomposition of biomass. The

aqueous weight is the difference between wet weight and dry weight, so $W_H = W_w - W_d$. It can be written as $W_H = [W_H]V$, for

$$[W_H] = d_V - d_{Vd} + (w_E - w_{Ed})([E] + [E_R])/\mu_E = d_V - d_{Vd} + (w_E - w_{Ed})(e + e_R)[M_{Em}] \quad (2.9)$$

where $[M_{Em}] = [E_m]/\mu_E$ is the maximum molar reserve density of juveniles and adults. The volume occupied by water is $V_H = W_H/d_H \simeq (d_V - d_{Vd})V/d_H$, where d_H stands for the specific density of water, which is close to 1 $\mathrm{g\,cm^{-3}}$. The aqueous fraction of body volume V_H/V_w typically takes values between 0.7 and 0.9.

The weight of any particular chemical compound Y in the n-reserves organism can be expressed as $W_Y = w_Y(n_{YV}M_V + \sum_i n_{YE_i}M_{E_i})$, where w_Y is the molar weight of the compound Y and the n's denote the molar amounts of the compound per C-mole of reserve or structural biomass. This again is a consequence of the strong homeostasis assumption. The n's are zero if the compound does not happen to occur in that biomass components. The density of the compound in biomass can be expressed as W_Y/W_d on the basis of weights, or as $W_Y(w_Y M_V + w_Y \sum_i M_{E_i})^{-1}$ on the basis of moles per mole of carbon.

The chemical composition of biomass becomes increasingly flexible with the number of delineated reserves, and depends on the nutritional conditions of the environment. In terms of relative frequencies of chemical elements, all restrictions in the composition of (total) biomass disappear if the number of reserves exceeds the number of chemical elements minus one.

2.3.5 Energy

Energy fluxes through living systems are difficult to measure and even more difficult to interpret. Let me briefly mention some of the problems.

Although it is possible to measure the thermodynamic energy content of food through complete combustion, this only shows that the organism cannot gain more energy from food, since combustion in the body is not complete. Food has a dual role in providing the capacity to do work as well as elementary compounds for anabolism. Another problem is that of digestive efficiency. The difference between the energy contents of food and faeces is just an upper boundary for the uptake by the animal, because there are energy losses in the digestion process. Part of this difference is never used by the organism, but by the gut flora instead. Another part is lost through enhanced respiration coupled to digestion, especially of proteins, called the 'heat increment of feeding', which is discussed on {138}.

Growth involves energy investment, which is partially preserved in the new biomass. In addition to the energy content of the newly formed biomass, energy is invested to give it its structure. Part of this energy is lost during growth and can be measured as dissipating heat. This heat can be thought of as an overhead of the growth process. The energy that is fixed in the new biomass is present partly as energy bearing compounds. Cells are highly structured objects and the information contained in their structure is not measured by bomb calorimetry.

The thermodynamics of irreversible or non-equilibrium processes offers a framework for pinpointing the problem; see for instance [356,533]. While bomb calorimetry measures the change in enthalpy, Gibbs free energy is the more useful concept for quantifing the energy

performance of individuals. Enthalpy and Gibbs free energy are coupled by the concept of entropy: the enthalpy of a system equals its Gibbs free energy plus the entropy times the absolute temperature. This basic relationship was formulated by J. W. Gibbs in 1878.

To quantify entropy directly, you need to specificy the biochemical machinery completely, which is exactly what I try to avoid; one not only needs to know all chemical compounds and their amounts, but also their spatial orientation. Dörr [226], for instance, gives an entropy reduction of 0.05 eV $\simeq$ 5 kJ mol^{-1} associated with the spatial fixation of one single amino acid group of a chain molecule at 25 °C. A quick glance at the way chemists measure entropies shows us that this cannot apply to living organisms.

Yet the concept of homeostasis offers a solution to the problem of defining and measuring free energies and entropies. This solution is based on the assumption that the free energy per C-mole of structural biomass and of reserves is constant, i.e. it does not depend on the (absolute) amounts. Most chemists probably find this assumption offensive, since free energies depend on the concentration of a compound in spatially homogeneous systems. The reason for the dependence is that the molecules interfere, which affects their ability to do work in the thermodynamic sense. Yet, I think that the assumption is more than just a conceptual trick to solve problems; it is the way living cells solve the problem of a compound's capacity to do (chemical) work depending on the concentration. If this capacity changes substantially as a function of the changing cell composition, the cell would have an immensely complex problem to solve when regulating its metabolic processes. It is not just a coincidence that cells use large amounts of polymers (i.e. proteins, carbohydrates and lipids) to store bulk compounds, and small amounts of monomers to run their metabolism. Cells keep the concentration of monomers low and relatively constant, and prevent any interference that makes the monomers' capacity to do work depend on their abundance. They also solve their osmotic problems this way. Their osmotic pressure equals that of seawater, which is frequently seen as a relic of the evolutionary process: life started in the sea.

I assume that the Gibbs relationship still applies in the complex setting of living organisms. If the free energy per C-mole does not change, then neither will the entropy per C-mole, because the enthalpy per C-mole is constant. The Gibbs relationship can be used to obtain the entropy and the free energy of complex organic compounds, such as food, faeces, structural biomass and reserves, as is worked out on {155}. The mean specific Gibbs free energy (i.e. chemical potential) of biomass is -67 kJ C-mol^{-1} (pH= 7, 10^5 Pa at 25 °C, thermodynamic reference) or +474.6 kJ C-mol^{-1} (pH= 7, combustion reference) [390]. Since biomass composition is not constant, such crude statistics are of limited value and a more subtle approach is necessary to quantify dissipating heat. For many practical purposes the entropy can safely be set to zero, which implies that enthalpies can be substituted for free energies. This in consistent with the ideas of Ling [561], but not with those of Battley [54], who suggested that the entropy of bacterial biomass exceeds that of its substrate (succinic acid).

2.3.6 Storage materials

Storage material can be classified into several categories; see Table 2.2. These categories do not point to separate dynamics. Carbohydrates can be transformed into fats, for instance, see Figure 2.14. Most compounds have a dual function as a reserve pool for both energy and elementary compounds for anabolic processes. For example, protein stores supply energy, amino acids and nitrogen. Ribosomal RNA (rRNA) catalyses protein synthesis. In rapidly growing cells such as those of bacteria in rich media, rRNA makes up to 80% of the dry weight, while the relative abundance in slowly growing cells is much less. For this reason, it should be included in the storage material. I show how this point of view leads to realistic descriptions of peptide elongation rates, {244}, and growth-rate-related changes in the relative abundance of nitrogen, {125}. There is no requirement for storage compounds to be inert.

Waxes can be transformed into fats (triglycerides) and play a role in buoyancy, e.g. of zooplankton in the sea [68]. By increasing their fat/wax ratio, zooplankters can ascend to the surface layers, which offer different food types (phytoplankton), temperatures and currents. Since surface layers frequently flow in directions other than deeper ones, they can travel the Earth by just changing their fat/wax ratio and stepping from one current to another. Wax ester biosynthesis may provide a mechanism for rapidly elaborating lipid stores from amino acid precursors [805].

Unsaturated lipids, which have one or more double bonds in the hydrocarbon chain, are particularly abundant in cold water species, compared with saturated lipids. This possibly represents a homeo-viscous adaptation [833].

The amount of storage materials depends on the feeding conditions in the (recent) past, cf. {82}. Storage density, i.e. the amount of storage material per unit volume of structural biomass, tends to be proportional to the volumetric length for different species, if conditions of food (substrate) abundance are compared, as explained on {270} and tested empirically on {277}. This means that the maximum storage density of bacteria is small. However, under conditions of nitrogen limitation for instance, bacteria can become loaded with energy storage materials such as polyphosphate or polyhydroxybutyrate, depending on the species, see {172}. This property is used in biological plastic production and phosphate removal from sewage water. Intracellular lipids can accumulate up to some 70% of the cell dry weight in oleaginous yeasts, such as *Apiotrichum* [750,1024]. This property is used in the industrial production of lipids. The excess storage is due to simultaneous nutrient limitation that is associated with what is called 'luxurious' uptake.

Storage deposits

Lipids, in vertebrates, are stored in cell lysosomes in specialized adipose tissue, which occurs in rather well-defined surface areas of the body. The cells themselves are part of the structural biomass, but the contents of the vacuole are part of the reserves. In molluscs specialized glycogen storage cells are found in the mantle [395]. The areas for storage deposits are usually found scattered over the body and therefore appear to be an integral part of the structural body mass, unless super-abundant; see Figure 2.6. The occurrence of massive deposits is usually in preparation for a poor feeding season. The rodent *Glis glis* is

Table 2.2: Some frequently used storage materials in heterotrophs.

phosphates	
pyrophosphate	bacteria
polyphosphate	bacteria (*Azotobacter, Acinetobacter*)
polysaccharides	
β-1,3-glucans	
leucosin	*Chrysomonadida, Prymnesiida*
chrysolaminarin	*Chrysomonadida*
paramylon	*Euglenida*
α-1,4-glucans	
starch	*Cryptomonadida, Dinoflagellida, Volvocida*, plants
glycogen	blue green bacteria, protozoa, yeasts, molluscs
amylopectin	*Eucoccidiida, Trichotomatida, Entodiniomorphida*
trehalose	fungi, yeasts
lipoids	
poly β hydroxybutyrate	bacteria
triglyceride	oleaginous yeasts, most heterotrophs
wax	marine animals
proteins	most heterotrophs
ovalbumin	egg-white protein
casein	milk protein (mammals)
ferritin	iron storage in spleen (mammals)
cyanophycine	bluegreen bacteria
phycocyanin	bluegreen bacteria
ribosomal RNA	all organisms

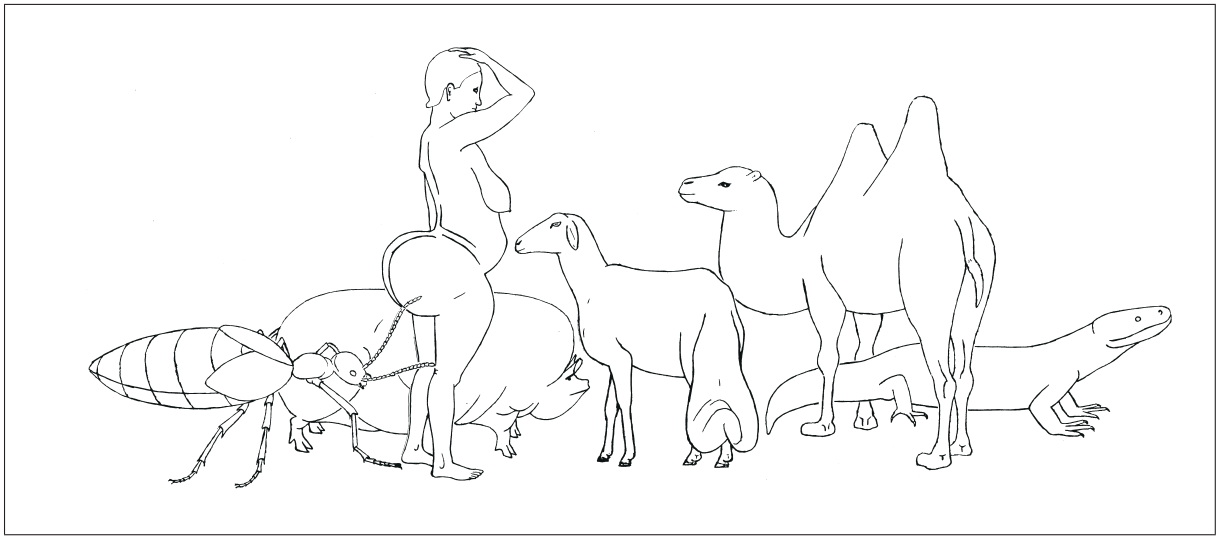

Figure 2.6: Some storage deposits are really eye-catching.

called the 'edible doormouse', because of its excessive lipid deposits just prior to dormancy, {231}. Stewed in honey and wine, doormice were a gourmet meal for the ancient Romans. Tasmania's yellow wattlebird *Anthochaera paradoxa* accumulates lipid deposits during the rich season to the extent that it has problems with flight; it then becomes exceedingly wary for a good reason [345].

In most invertebrate groups, storage deposits do not occur in specialized tissues, but only in the cells themselves in a quantity that relates to requirements. So reproductive organs tend to be rich in storage products. The mesoglea of sea-anemones, for instance, has mobile cells that are rich in glycogen and lipid, called 'glycocytes', which migrate to sites of demand during gametogenesis and directly transfer the stored materials to developing oocytes [833]. Glycogen that is stored for a long time typically occurs in rosettes, and for short time in particles [414,833]. A guild of honey ants specializes in the storage function for the colony, not unlike adipose tissue in vertebrates, see Figure 2.7.

The recently discovered anaerobic sulfur bacterium *Thiomargarita namibiensis* [822] accumulates nitrate to up 0.8 M in a vacuole of up to 750 μm in diameter; it can survive over 2 years without nitrate or sulfur at 5 °C. The bacterium *Acinetobacter calcoaceticus* accumulates polyphosphates to spectacular levels under carbon-limiting aerobic conditions, and releases phosphates under energy-limiting anaerobic conditions, which is used technically in sewage water treatment, see {174}.

Since autotrophs acquire energy and the various nutrients independently from each other, they usually store possibly limiting substrates independently in specialized organelles: the vacuoles [551]. Carbohydrate (starch) and water storage are most bulky in plants that live in seasonal environments, see Figure 2.8.

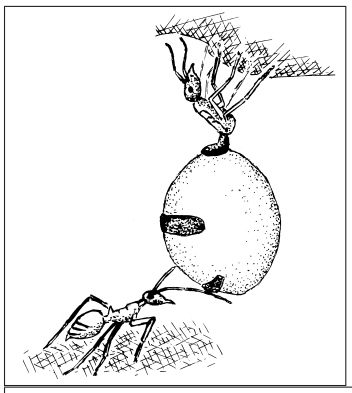

Figure 2.7: Colony members of honey ants, *Myrmecocystus*, show function differentiation. The energy storage function is taken by a guild that can be considered as the adipose tissue of the ant colony.

Figure 2.8: Plants can store large amounts of carhohydrates and/or water.

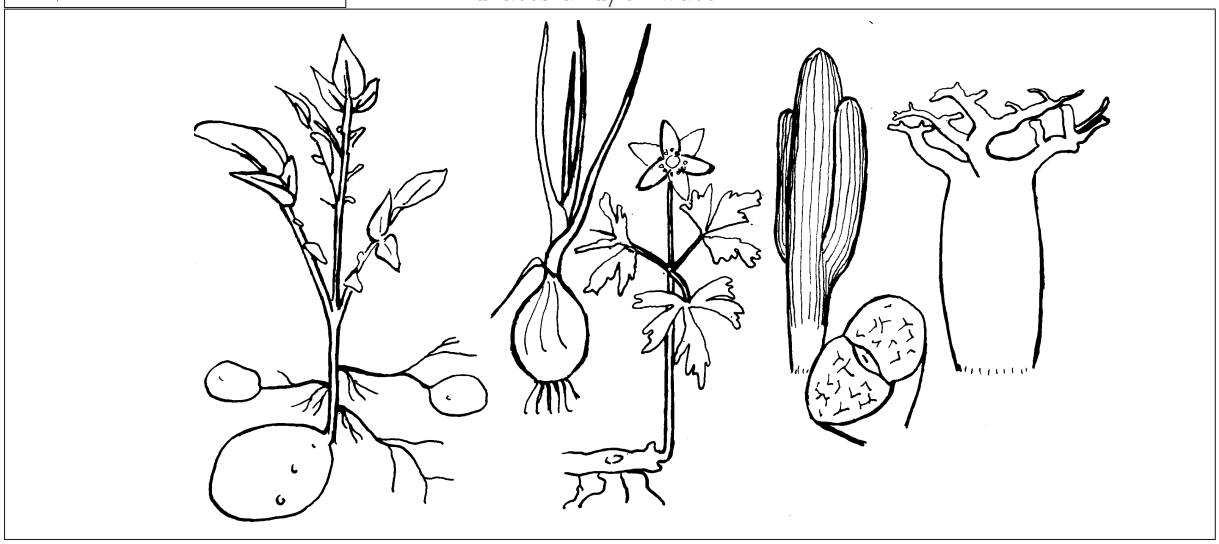

2.4 Concentrations, amounts and fluxes

When two substrates are supplementary, i.e. they are both required in fixed stoichiometric proportions, the absence of one substrate prevents the uptake of the other; think, for instance, of ammonia and carbon dioxide as substrates and amino acids as reserves. Empirical evidence frequently indicates that the uptake of the most abundant substrate (relative to the needs) is set by the least abundant substrate: the popular minimum rule of von Liebig [557]. The rule originally related biomass yields to nutrient levels, but was later applied to uptake processes [35]. However, this application becomes complex if reserves are included; the environment may not contain the substrate, but growth is not restricted because of the presence of reserves. If the role of limiting and non-limiting substrate does not switch at the same time for all individuals in the population in a variable environment, it is almost impossible to evaluate population behaviour on the basis of individual behaviour. Moreover, sharp switches are not realistic at the molecular level, because of the intrinsic stochasticity of the substrate arrival process.

Classic enzyme kinetics specifies fluxes of product in terms of substrate concentrations. This catenates two different processes, arrival process of substrate molecules to the binding site(s) of the enzyme molecules and the transformation of bounded substrate into product, which can better be dealt with separately. In homogeneous environments, arrival rates of

substrate molecules to the enzyme molecules are proportional to the concentration, on the basis of diffusive transport. The rejected substrate molecules return to the environment, which makes it difficult, if not impossible, to determine their existence. When growth is modelled as a function of mobilized reserve fluxes (see {168}), the situation is different, because this process represents arrival and replaces diffusive transport. Transformations are hard to link to concentrations in those situations.

The concept 'concentration' is rather problematic in spatially highly structured environments, such as in growing cells, where many transformations are mediated by membrane-bound enzymes. Use of concentrations should be restricted to well-mixed local environments, such as the idealized environment outside organisms. As illustrated in a model of reserve kinetics, {246}, ratios of amounts, called densities, can play a role in transformations. Densities resemble concentrations, but the compounds are not necessarily well mixed at a molecular level.

Thinking in terms of fluxes, rather than concentrations, allows us to treat light in a similar way to compounds, with stoichiometric coupling coefficients in photochemical reactions. This idea may be less wild than might first appear; cells extract a fixed amount of energy from the photons that are able to excite the pigment system, the remaining energy dissipates as heat. The light flux can be quantified in Einstein (or mole) per second, i.e. in $6.023\,10^{23}$ quanta per second [358].

Another argument for avoiding the use of concentrations as much as possible is that concentrations should be thought of as states of the system. The inclusion of concentrations of intermediary metabolites in a metabolic pathway increases the number of state variables of the system. A reduction of this number, to simplify the model, is only possible when the amounts are small enough. This problem is avoided by using fluxes, where intermediaries do not accumulate.

The following subsections introduce the concept 'Synthesizing Unit' [518], which is used to deal with transformations involving supplementary compounds {164}. However, I start with a short introduction on classic enzyme kinetics, to reveal the link with concepts that are used in that field.

2.4.1 Enzyme kinetics

Let us consider a very simple irreversible chemical transformation, where an enzyme requires one copy of each of two substrates, present in concentrations X_A and X_B, to produce a product, present in concentration X_C. Apart from the free enzyme, present in concentration X_{ab}, we have three substrate-enzyme complexes with concentrations X_{Ab}, X_{aB}, and X_{AB}. Classic enzyme kinetics states that substrate-enzyme association follows the law of mass action, so the rate is proportional to the product of the concentrations, and dissociation is a first-order process, so the rate is proportional to the concentration of the complex. Given the dissociation rate parameters $\dot{k}_A$, $\dot{k}_B$ and $\dot{k}_C$, and the association parameters $\dot{b}_A$ and $\dot{b}_B$, the change in concentration of substrates, enzyme species and product is given by

$$\begin{aligned} \frac{d}{dt}X_A &= \dot{k}_A(X_{Ab} + X_{AB}) - \dot{b}_A X_A(X_{ab} + X_{aB}) \\ \frac{d}{dt}X_B &= \dot{k}_B(X_{aB} + X_{AB}) - \dot{b}_B X_B(X_{ab} + X_{Ab}) \end{aligned}$$

$$\begin{aligned}
\frac{d}{dt}X_C &= \dot{k}_C X_{AB} \\
\frac{d}{dt}X_{ab} &= \dot{k}_C X_{AB} + \dot{k}_A X_{Ab} + \dot{k}_B X_{aB} - (\dot{b}_A X_A + \dot{b}_B X_B) X_{ab} \\
\frac{d}{dt}X_{Ab} &= \dot{k}_B X_{AB} + \dot{b}_A X_A X_{ab} - (\dot{k}_A + \dot{b}_B X_B) X_{Ab} \\
\frac{d}{dt}X_{aB} &= \dot{k}_A X_{AB} + \dot{b}_B X_B X_{ab} - (\dot{k}_B + \dot{b}_A X_A) X_{aB} \\
\frac{d}{dt}X_{AB} &= \dot{b}_A X_A X_{aB} + \dot{b}_B X_B X_{Ab} - (\dot{k}_A + \dot{k}_B + \dot{k}_C) X_{AB}
\end{aligned}$$

Steady state is reached when the substrate–enzyme complexes do not change in concentration, so $\frac{d}{dt}X_{**} = 0$. The relative abundance of enzyme-substrate complexes is now given by

$$\begin{pmatrix} \theta_{ab} \\ \theta_{Ab} \\ \theta_{aB} \\ \theta_{AB} \end{pmatrix} = \begin{pmatrix} 1 & 1 & 1 & 1 \\ x_A k_A & -x_B - k_A & 0 & 1 \\ x_B & 0 & -1 - x_A k_A & k_A \\ 0 & x_B & x_A k_A & -1 - k_A - k_C \end{pmatrix}^{-1} \begin{pmatrix} 1 \\ 0 \\ 0 \\ 0 \end{pmatrix}$$

with $x_A = X_A \dot{b}_A / \dot{k}_A$, $x_B = X_B \dot{b}_B / \dot{k}_B$, $k_A = \dot{k}_A / \dot{k}_B$, $k_C = \dot{k}_C / \dot{k}_B$, and $\theta_* = X_* / X_+$ with $X_+ = X_{ab} + X_{Ab} + X_{aB} + X_{AB}$. The appearance rate of product is for $\dot{J}_{Cm} = \dot{k}_C X_+$ given by

$$\frac{d}{dt}X_C = \dot{J}_C = \dot{J}_{Cm}\theta_{AB}$$

Two limiting cases are of special interest: the Synthesizing Unit (SU), where the substrate–enzyme dissociation rates are small, and the Rejection Unit (RU), where these rates are high, but the association rates are high as well. (Another way to obtain the same RU is when the product–enzyme dissociation rate $\dot{k}_C$ is small, and the total amount of enzyme X_+ is high, but this hardly applies to organisms.) These limiting cases give the following results:

SU: $\dot{k}_A$, $\dot{k}_B \to 0$	RU: $\dot{k}_A$, $\dot{k}_B$, $\dot{b}_A$, $\dot{b}_B \to \infty$ and $\frac{\dot{k}_A}{\dot{b}_A}$, $\frac{\dot{k}_B}{\dot{b}_B}$ constant
for $x_A = X_A \frac{\dot{b}_A}{\dot{k}_C}$ and $x_B = X_B \frac{\dot{b}_B}{\dot{k}_C}$	for $x_A = X_A \frac{\dot{b}_A}{\dot{k}_A}$ and $x_B = X_B \frac{\dot{b}_B}{\dot{k}_B}$
$\dot{J}_C = \frac{\dot{J}_{Cm}}{1 + x_A^{-1} + x_B^{-1} - (x_A + x_B)^{-1}}$	$\dot{J}_C = \frac{\dot{J}_{Cm}}{(1 + x_A^{-1})(1 + x_B^{-1})}$
$\begin{pmatrix} \theta_{ab} \\ \theta_{Ab} \\ \theta_{aB} \\ \theta_{AB} \end{pmatrix} = \begin{pmatrix} (x_A + x_B)^{-1} \\ x_A x_B^{-1} (x_A + x_B)^{-1} \\ x_B x_A^{-1} (x_A + x_B)^{-1} \\ 1 \end{pmatrix} \frac{\dot{J}_C}{\dot{J}_{Cm}}$	$\begin{pmatrix} \theta_{ab} \\ \theta_{Ab} \\ \theta_{aB} \\ \theta_{AB} \end{pmatrix} = \begin{pmatrix} (x_A x_B)^{-1} \\ x_B^{-1} \\ x_A^{-1} \\ 1 \end{pmatrix} \frac{\dot{J}_C}{\dot{J}_{Cm}}$

Despite of its popularity [55,270,271,673], the RU has a number of problems that make it less attractive than the SU. The first, but perhaps not the most important, problem is a mild form of inconsistency at the molecular level. The law of mass action is used for association between substrate and enzyme. It requires completely homogeneous mixing, which is hard to combine with infinitely large dissociation and association rates; as soon as a substrate molecule is rejected by an enzyme molecule, it becomes attracted again if the mixing rate is not infinitely large, which is obviously not realistic. Moreover, it

is hard to see in terms of molecular geometry and electrical charge distributions how a high association rate can combine with a high dissociation rate. The SU is much more natural in this respect, because the binding sites on the enzyme molecule mirror-match the substrates in shape and electrical charge, which makes it likely that the substrate-enzyme dissociation rate is small compared to the product–enzyme dissociation rate, because of the shape and charge changes during the substrates-product transition. Product molecules do not mirror-match the substrate-bindings sites in shape and electrical charge, and products, not substrates, are rejected by the enzyme.

For very large concentrations x_B, both SU and RU simplify to what is known as Michaelis–Menten kinetics (MM-kinetics): $\dot{J}_C = \dot{J}_{Cm}(1 + x_A^{-1})^{-1}$, but the convergence for SU is much faster than for RU. In fact, the RU converges really slowly to MM-kinetics, which means that substrate concentrations must exceed the saturation constant by at least an order of magnitude to become (almost) non-limiting. A substrate is defined to be non-limiting if a change in substrate concentration does not affect the production rate. Given the fact that models for uptake and use of nutrients are likely to include only a small subset of the required nutrients and compounds, the implication that compounds that are not included must be really abundant is not acceptable. Last, but not least, the multiplicative model for nutrient uptake, as implied by the RU, is found to be inconsistent with empirical data [235]. MM-kinetics, and its various generalizations, plays a central role in models for enzyme kinetics and substrate (food, nutrient) acquisition by organisms; it was first described by Henri in 1902 [398].

Given identical production rates if only one substrate is limiting (this is when the other substrate is abundant), the production rate of the RU is always smaller than that of the SU, $\dot{J}_{C,\mathrm{SU}} > \dot{J}_{C,\mathrm{RU}}$, while their ratio tends to infinity for small substrate concentrations (x_A, $x_B \to 0$).

2.4.2 Synthesizing Units

Because a Synthesizing Unit does not dissociate from substrates, it can be considered as a server, i.e. a unit handling particles. A large but fixed number of identical servers handle particles simultaneously, without interfering with each other, except by competing for the same particles (clients). The term 'server' stems from an extensive theory of applied probability calculus, known as queueing theory, which deals with this type of problem, e.g. [803,851]. The extension of the previous derivation of the dynamics of the SU to include an arbitrary number of copies of an arbitrary number of substrates becomes complex, but this is still feasible if the derivation uses the servers' point of view.

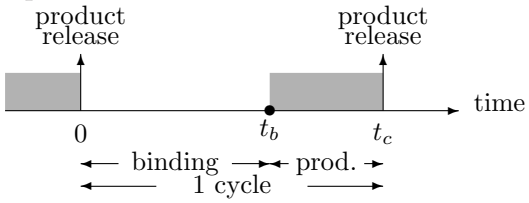

In its simplest form, the Synthesizing Unit (SU) is an enzyme or a complex of enzymes that binds a substrate molecule to deliver (synthesize) a product molecule or a set of product molecules. For simplicity's sake, I assume that the substrate molecules arrive according to a Poisson process, that the binding occurs with a fixed probability ρ if the SU is in its binding stage, and that the production stage lasts an exponentially distributed time interval. The production stage corresponds with a kind

of 'handling' time. During the production process, no substrate molecules are accepted by the SU, so the binding probability $\underline{\rho}$ for each arriving substrate molecule follows a renewal process [178], alternating between the values ρ and 0, when the SU is binding and producing, respectively. I call this SU a one substrate-one copy SU, which will be generalized to a multi substrate-multi copy SU.

Let the binding and production periods, $\underline{t}_b$ and $\underline{t}_p$, be exponentially distributed random variables, with means $\dot{J}_{Xb}^{-1}$ and $\dot{J}_{Xm}^{-1}$, respectively. The substrate molecules arrive at rate $\dot{J}_{Xa} = \dot{J}_{Xb}/\rho$, where ρ denotes the binding probability per arriving substrate molecule. The cycle period of the SU, $\underline{t}_c = \underline{t}_b + \underline{t}_p$, catenates one binding period and the subsequent production period. The inverse of its expected value, $\dot{J}_X = 1/\mathcal{E}\underline{t}_c$, equals the mean production rate, which I will call the intensity of the production process; it is defined as the ratio of the cumulative number of events in a period to the length of the period, for a large period.

When substrate molecules are sent to a one substrate-one copy SU, according to a Poisson process with intensity $\dot{J}_{Xa}$, it returns a Poisson process of rejected substrate molecules, with an intensity that alternates between values $(1-\rho)\dot{J}_{Xa}$ and $\dot{J}_{Xa}$, and a renewal process of product molecules, with intensity $\dot{J}_X = (\dot{J}_{Xm}^{-1} + \dot{J}_{Xb}^{-1})^{-1}$. The mean intensity of the rejected substrate molecules amounts to $\dot{J}_{Xa} - \dot{J}_X$. Note that for very high intensities of the arrival process, the production process approximates the value $\dot{J}_{Xm}$.

The events of substrate rejection and production are mutually dependent, but I will not work out the structure in detail, because the practical interest is not in the performance of a single SU, but a large set of independently operating SUs. The central limit theorem for the addition of independent stochastic point processes implies that the rejected substrate molecules and the product molecules of a sufficiently large set of s independent SUs converge to independent Poisson processes with constant intensities $\dot{J}_{Xa} - \dot{J}_X$ and $\dot{J}_X = ((s\dot{J}_{Xm})^{-1} + \dot{J}_{Xb}^{-1})^{-1}$, respectively. An increase in the amount of SUs has the effect of decreasing the production period; the reduction of the intensity of arriving substrate molecules per SU cancels against the increase of the binding probability. Other implementations of the step to group performance are conceivable, but these require details of the SUs' spatial organization.

Multi substrate-multi copy SU

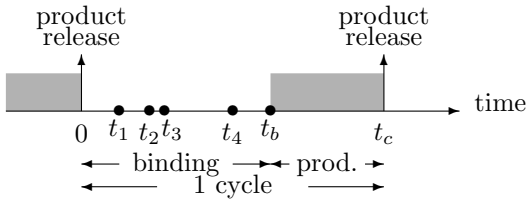

Suppose that the SU can be in a binding or in a production stage, and that it needs n copies of a single substrate X to produce a product molecule Y, while the moment at which the production stage of the SU is entered, $\underline{t}_b$, equals the moment of the n-th binding, $\underline{t}_n$, so $\underline{t}_b = \underline{t}_n$. Such a SU can be called a one substrate-multi copy SU, or n-SU. The binding period follows the Erlangian distribution $\phi_{\underline{t}_b}(t) = \frac{\dot{J}_X(\dot{J}_X t)^{n-1}}{(n-1)!}\exp\{-\dot{J}_X t\}$, which has a mean value of $\mathcal{E}\underline{t}_b = n\dot{J}_X^{-1}$. It results from adding n independently exponentially distributed random variables with parameter $\dot{J}_X$. For a mean production period $\dot{J}_{Ym}^{-1}$, the appearance of Y molecules from a single SU is a

renewal process with intensity $\dot{J}_Y = (\dot{J}_{Ym}^{-1} + n\dot{J}_X^{-1})^{-1}$. A large set of s SUs will produce a Poisson stream of Y molecules with intensity $\dot{J}_Y = ((s\dot{J}_{Ym})^{-1} + n\dot{J}_X^{-1})^{-1}$, and a Poisson stream of rejected substrate molecules of intensity $\dot{J}_X - y_{X,Y}\dot{J}_Y$, where $y_{Y,X}$ stands for the number of molecules of Y produced per processed molecule X.

The model does not specify the details of the production process. The SU might have n different binding sites, or just a single one in combination with a fast process of precursor production while the precursor molecules remain in the local environment of the SU that is under its control.

Now we are ready for the more interesting multi substrate-multi copy SU, which requires n different substrate types for the production of a single molecule, or set of molecules, Y: the $n_1, n_2, \cdots, n_n$-SU. The kinetics of the production process is based on the idea that the SU can only enter the production stage if all required substrate molecules are bound.

I will discuss two different extensions to multi substrates: sequential and parallel binding. Sequential binding hardly seems realistic, but it will help to understand parallel binding.

Sequential processing

When the SU binds the different types of substrate sequentially, in a random order, the expected waiting time to the binding of n_i molecules of type i is $n_i\dot{J}_i^{-1}$. The order of the types is not relevant, but when the SU is binding type i it continues to do so until all required molecules for the production of one product molecule are bound. This directly leads to the expected binding period

$$\mathcal{E}\underline{t}_b = \sum_{i=1}^{n} \frac{n_i}{\dot{J}_i} \tag{2.10}$$

and the mean production rate $\dot{J}_X = (\dot{J}_{Xm}^{-1} + \sum_i n_i\dot{J}_i^{-1})^{-1}$.

The interest in this mechanism is mainly in its mathematical simplicity, and its interesting properties (M. P. Boer, pers. comm.) The parallel binding period is equal to the sequential binding period minus the gain in time (compare (2.10) and (2.14)). Suppose that the substrate fluxes are proportional to the substrate concentrations X_i, as a result of some convection or diffusion process. The production rate can then be rewritten as $\dot{J}_X = \dot{J}_{Xm}(1 + \sum_i X_{Ki}/X_i)^{-1} = \dot{J}_{Xm}f_n$, where X_{Ki} denotes the saturation constant, which quantifies the affinity of the SU for substrate i, including the transport rate from the (local) environment to the SU, and the factor f_n is the scaled functional response for n types of possibly limiting substrates, which takes values between 0 and 1. (The term 'functional response' originates from ecology, and stands for the feeding rate of a predator as function of the density of prey.) The recurrent relationship $f_n = \frac{X_n f_{n-1}}{X_n + X_{Kn} f_{n-1}}$ applies, for $f_0 = 1$ and $n = 1, 2, \cdots$, which leads to $f_n = \prod_i X_i (\prod_i X_i + \sum_i X_{Ki} \prod_{j \neq i} X_j)^{-1}$.

Parallel processing

Suppose that the binding of one type of substrate does not interfere with that of another. The SU will not bind substrate i molecules, either if it already bound n_i molecules of that

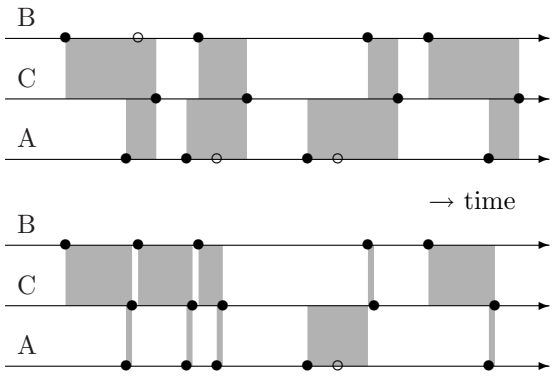

Figure 2.9: These pictures illustrate the production by a strongly binding relatively slow (upper) and a very fast (lower) 1,1-SU. The arrival events of substrate molecules A and B, and the production events of product molecules C are indicated with filled and open dots on three time-axes. Filled dots stand for acceptance, open ones for rejection. The grey areas indicate periods during which the SU is blocked for a substrate. Note that the fast SU still has substantial blocked periods.

substrate, but still has to bind other types of substrate, or if the SU is in the production stage, see Figure 2.9. Let $\underline{t}_{bi}$ denote the moment of the binding of the n_i-th molecule of substrate type i (so the binding is complete for that substrate), and $\underline{t}_b = \max_i\{\underline{t}_{bi}\}$ the moment when all required substrate molecules are bound, and the production stage is entered. The distribution function of the binding period $\underline{t}_b$ equals the product of the distribution functions of $\underline{t}_{bi}$, which are incomplete gamma functions

$$\Phi_{\underline{t}_b}(t) = \prod_{i=1}^{n} \Phi_{\underline{t}_{bi}}(t) = \prod_{i=1}^{n} \int_0^t \phi_{\underline{t}_{bi}}(t_1)\, dt_1 = \prod_{i=1}^{n} P(n_i, t\dot{J}_i) \tag{2.11}$$

where $P(n,t) = \frac{1}{\Gamma(n)} \int_0^t \exp\{-t_1\} t_1^{n-1}\, dt_1 = 1 - \exp\{-t\} \sum_{j=0}^{n-1} \frac{t^j}{j!}$ is the incomplete gamma function. The expected value of the binding period is

$$\mathcal{E}\underline{t}_b = \int_0^\infty \left(1 - \Phi_{\underline{t}_b}(t)\right)\, dt = \int_0^\infty \left(1 - \prod_{i=1}^{n} P(n_i, t\dot{J}_i)\right)\, dt \tag{2.12}$$

and the expected value of the cycle period is $\mathcal{E}\underline{t}_c = \dot{J}_{Xm}^{-1} + \mathcal{E}\underline{t}_b$. The mean production rate, therefore, occurs at intensity $\dot{J}_X = (\dot{J}_{Xm}^{-1} + \mathcal{E}\underline{t}_b)^{-1}$ for a single SU, and $\dot{J}_X = ((s\dot{J}_{Xm})^{-1} + \mathcal{E}\underline{t}_b)^{-1}$ for a set of s SUs. The intensity of the rejected substrate molecules of type i amounts to $\dot{J}_i/\rho_i - n_i\dot{J}_X$, where arriving substrate molecules of type i are bound with probability ρ_i if the SU is in the binding stage.

For two possibly limiting nutrients, so $n = 2$, (2.12) reduces to

$$\mathcal{E}\underline{t}_b = \frac{n_1}{\dot{J}_1} + \frac{n_2}{\dot{J}_2} - \sum_{i=0}^{n_1-1} \sum_{j=0}^{n_2-1} \frac{(i+j)!}{i!\, j!} \frac{\dot{J}_1^i \dot{J}_2^j}{(\dot{J}_1 + \dot{J}_2)^{i+j+1}} \tag{2.13}$$

and for three possibly limiting nutrients

$$\begin{aligned} \mathcal{E}\underline{t}_b = &\sum_{i=1}^{3} \frac{n_i}{\dot{J}_i} - \sum_{i_2>i_1=1}^{3} \sum_{i=0}^{n_{i_1}-1} \sum_{j=0}^{n_{i_2}-1} \frac{(i+j)!}{i!\, j!} \frac{\dot{J}_{i_1}^i \dot{J}_{i_2}^j}{(\dot{J}_{i_1} + \dot{J}_{i_2})^{i+j+1}} + \\ &+ \sum_{i_3>i_2>i_1=1}^{3} \sum_{i=0}^{n_{i_1}-1} \sum_{j=0}^{n_{i_2}-1} \sum_{k=0}^{n_{i_3}-1} \frac{(i+j+k)!}{i!\, j!\, k!} \frac{\dot{J}_{i_1}^i \dot{J}_{i_2}^j \dot{J}_{i_3}^k}{(\dot{J}_{i_1} + \dot{J}_{i_2} + \dot{J}_{i_3})^{i+j+k+1}} \end{aligned} \tag{2.14}$$

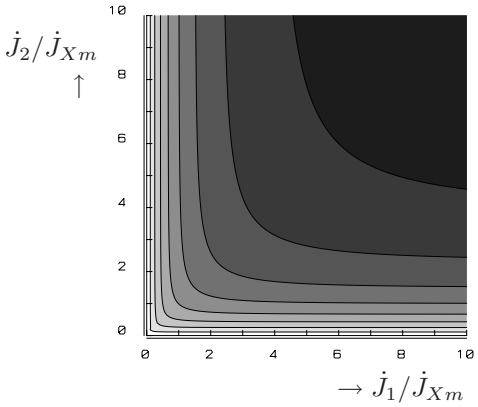

Figure 2.10: The 0.1(0.1)0.7 contours of the scaled production flux $\dot{J}_X/\dot{J}_{Xm}$ as function of the scaled substrate supply fluxes $\dot{J}_1' = \dot{J}_1/\dot{J}_{Xm}$ and $\dot{J}_2' = \dot{J}_2/\dot{J}_{Xm}$ for a 1,1-SU. The production flux for a 1,1-SU simplifies to $\dot{J}_X = \left(\dot{J}_{Xm}^{-1} + \dot{J}_1^{-1} + \dot{J}_2^{-1} - (\dot{J}_1 + \dot{J}_2)^{-1}\right)^{-1}$.

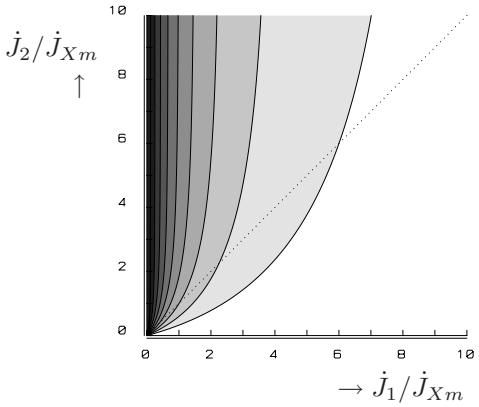

Figure 2.11: The 0.1(0.1)0.9 contours (right to left) of the flux control coefficients $\frac{\partial \ln \dot{J}_X}{\partial \ln \dot{J}_1'}$ of the substrate flux $\dot{J}_1'$ on the production flux $\dot{J}_X$ for a 1,1-SU. The flux control coefficients for substrate $\dot{J}_2$ can be obtained by interchanging the labels on the axes. The stippled line marks $\dot{J}_1 = \dot{J}_2$.

from which it is obvious how this expression generalizes for a larger number of possibly limiting substrates. There is no need to evaluate the integral in (2.12), when it comes to practical computations. Note that the first summation in the last (i.e. third) summation term in (2.14) only contains one element. The first summation in the middle summation term contains three elements.

Figure 2.10 illustrates that the 1,1-SU behaves very like a minimum operator for small substrate supply fluxes. This can be quantified using the Metabolic Control Analysis [393], which shows that the flux control coefficients $\frac{\partial \ln \dot{J}_X}{\partial \ln \dot{J}_i}$ rapidly decrease for increasing substrate concentrations, see Figure 2.11. The elasticity coefficients, which quantify the effect of a change in the SU concentration on the production flux, are $\frac{\partial \ln \dot{J}_X}{\partial \ln s} = \frac{\dot{J}_X}{s\dot{J}_{Xm}}$. When a 1,1-SU binds sequentially, the production rate is $\dot{J}_X = \left(\dot{J}_{Xm}^{-1} + \dot{J}_1^{-1} + \dot{J}_2^{-1}\right)^{-1}$, which is obviously lower than that obtained using parallel binding. An important implication of SUs behaving like a minimum operator is that abundant substrates do not matter, and only possibly limiting substrates need to be followed explicitly.

The supply fluxes of substrates to the SU can result from convection or diffusion processes, which makes it likely that they are proportional to the concentration X_i of substrate in the local environment of the SU and the number of SUs. The 1-SU then behaves quantitatively according to the familiar MM-kinetics [398,629]. Most texts on this kinetics [825,826] assume a reversible binding to the enzyme, however. For the 1-SU such an extension hardly complicates the model. The 1,1-SU requires 9 binding and dissociation rates to quantify the production process [36,625], but reversible binding becomes really complex for the multi substrate–multi copy enzymes. It requires the kinetics of all possible combinations of partially filled enzyme–substrate complexes to be specified [776], which

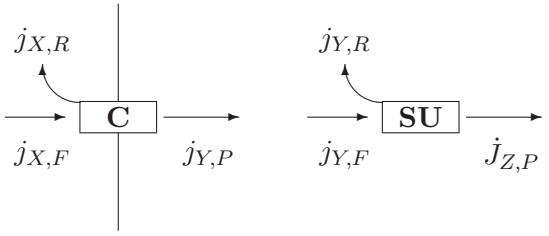

Figure 2.12: The Carrier-Synthesizing Unit complex binds substrate X in the environment reversibly and delivers product Z to the cellular metabolism. The inherent rejected fluxes of substrate X and intermediary metabolite Y are indicated, and quantified in the text.

is not only cumbersome, but also involves a huge amount of parameters. The Carrier-Synthesizing Unit complex allows reversible binding with relative ease, see below.

2.4.3 Production of generalized compounds

As might be expected, an increase in substrate concentration almost cancels against an increase in stoichiometric requirements, so $\dot{J}_X$ is rather insensitive to multiplication of both $\dot{J}_i$ and n_i by an arbitrary factor. This allows the use of SUs to quantify the production of generalized compounds. The product flux of a $\{n_i\}_1^n$-SU approximates that of a $1, 1, \cdots, 1$-SU, when we replace $\dot{J}_i$ by $\dot{J}_i/n_i$, resulting in

$$\dot{J}_X = \left(\dot{J}_{Xm}^{-1} + \sum_{i_1=1}^{n} \left(\frac{\dot{J}_{i_1}}{n_{i_1}} \right)^{-1} - \sum_{i_2>i_1=1}^{n} \left(\sum_{j=1}^{2} \frac{\dot{J}_{i_j}}{n_{i_j}} \right)^{-1} + \sum_{i_3>i_2>i_1=1}^{n} \left(\sum_{j=1}^{3} \frac{\dot{J}_{i_j}}{n_{i_j}} \right)^{-1} - \cdots \right.$$

$$\left. \cdots - (-1)^n \sum_{i_n>\cdots>i_1=1}^{n} \left(\sum_{j=1}^{n} \frac{\dot{J}_{i_j}}{n_{i_j}} \right)^{-1} \right)^{-1} \tag{2.15}$$

As is obvious from the derivation, the constraints $n_i \dot{J}_X < \dot{J}_i$ apply for all $i = 1, 2, \cdots n$.

Many applications of SUs not only involve generalized compounds, but also generalized enzymes that catalyze the transformation. They can be thought of as a set of enzymes that pass metabolites to each other, without accumulating pools of intermediary metabolites. The implication is that the transformation is halted instantaneously when one of the required substrate molecules is not (yet) available, and the SU ceases binding other substrates, until the generalized product molecule is delivered.

2.4.4 Handshaking protocols

Suppose that a substrate X is taken up from the environment by a Carrier (C), which passes its product Y to a Synthesizing Unit (SU), which delivers its product Z to the rest of the metabolism of the cell, see Figure 2.12. One molecule of substrate converts into $y_{Y,X}$ molecules of product Y or $y_{Z,X}$ molecules of product Z. I will evaluate the dynamics of the Carrier-Synthesizing Unit (CSU) complex, under various assumptions about the exchange of compounds between the two components, given c Carriers and s SUs per unit of biomass.

Three processes should be delineated: feeding F, rejection R, and production P. Appearing fluxes are taken positive (R and P), disappearing ones negative (F). Fluxes are denoted by two indices: one represents the compound, the other the process. The feeding flux is the flux of substrate molecules that arrives in the catching area of the c Carriers or s SUs.

The mass balances for the Carriers, the SUs, and the CSU complex are

$$\begin{aligned} 0 &= j_{X,F} + j_{X,R} + y_{X,Y} j_{Y,P} \\ 0 &= j_{Y,F} + j_{Y,R} + y_{Y,Z} j_{Z,P} \\ 0 &= j_{X,F} + j_{X,R} + y_{X,Y} j_{Y,R} + y_{X,Z} j_{Z,P} \end{aligned}$$

for $y_{X,Z} = y_{X,Y} y_{Y,Z}$ and $j_{Y,P} = -j_{Y,F}$. The problem now is to write all these fluxes as functions of the feeding flux $j_{X,F}$ given a specification of the interaction between the Carriers and the SUs.

The behaviour of the CSU complex depends on the handshaking protocol between the Carrier and the SU. Two extremes are evaluated. In the 'closed' protocol, the Carrier only passes its product to the SU if the SU is in the unbounded state. In the 'open' protocol, the Carrier releases its product irrespective of the state of the SU. The derivation of the behaviour of the CSU complex under both handshaking protocols starts with the changes in the binding fractions, θ_c and θ_s, among the c Carriers and the s SUs, followed by a pseudo-steady-state assumption.

Closed protocol

The changes in the binding fractions amount to

$$\frac{d}{dt}\theta_c = (\dot{k}_X + \dot{k}_Y \theta_s)(1 - \theta_c) + \rho_X j_{X,F} \theta_c / c \tag{2.16}$$

$$\frac{d}{dt}\theta_s = \dot{k}_Z (1 - \theta_s) - \rho_Y \dot{k}_Y \theta_s (1 - \theta_c) y_{Y,X} c / s \tag{2.17}$$

where ρ_X denotes the binding probability of substrate X to the Carrier, ρ_Y the binding probability of assimilated substrate Y (i.e. Carrier product) to the SU, and $\dot{k}_*$ the dissociation rates.

The fluxes can now be quantified as

$$\begin{aligned} j_{X,R} &= \dot{k}_X (1 - \theta_c) c - j_{X,F}(1 - \rho_X \theta_c) & \qquad j_{Y,R} &= (1 - \rho_Y) y_{Y,X} \dot{k}_Y (1 - \theta_c) \theta_s c \\ j_{Y,P} &= y_{Y,X} \dot{k}_Y \theta_s (1 - \theta_c) c & \qquad j_{Z,P} &= y_{Z,Y} \dot{k}_Z (1 - \theta_s) s \end{aligned}$$

Suppose now that the binding fractions are in steady state, i.e. $\frac{d}{dt}\theta_* = 0$. The binding fractions and all fluxes can then be written as functions of the feeding flux $j_{X,F}$. The result is

$$\begin{aligned} \theta_c &= \frac{2c^2 \dot{k}_X \dot{k}'_Y + 2cs \dot{k}_Y \dot{k}_Z - \ddot{k}_1 - \ddot{k}}{-2c \dot{k}'_Y j'_{X,F}}; \quad \theta_s = \frac{\ddot{k}_1 + \ddot{k}}{2cs \dot{k}_Y \dot{k}_Z} \\ \dot{k}'_Y &= \rho_Y \dot{k}_Y y_{Y,X}; \quad j'_{X,F} = \rho_X j_{X,F} - c \dot{k}_X \\ \ddot{k} &= \sqrt{\ddot{k}_1^2 - 4cs^2 \dot{k}_Y \dot{k}_Z^2 j'_{X,F}}; \quad \ddot{k}_1 = \rho_X j_{X,F}(s \dot{k}_Z + c \dot{k}'_Y) + cs(\dot{k}_Y - \dot{k}_X) \dot{k}_Z \end{aligned}$$

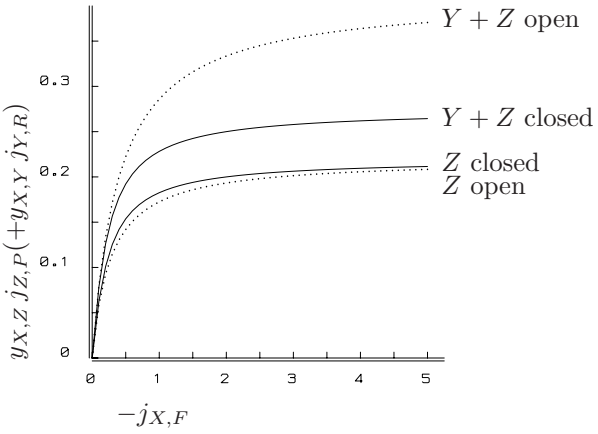

Figure 2.13: The production of product, Z, and of precursor plus product, $Y + Z$, from substrate X of a CSU complex, as functions of the substrate arrival flux, using the closed (drawn curves) or the open (dotted curves) handshaking protocol. The open protocol leads to hyperbolic production curves. The parameters are $\dot{k}_X = 0\,\mathrm{s}^{-1}$, $\dot{k}_Y = 0.4\,\mathrm{s}^{-1}$, $\dot{k}_Z = 0.7\,\mathrm{s}^{-1}$, $\rho_X = 1$, $\rho_Y = 0.8$, $y_{X,Y} = 1$, $y_{X,Z} = 1$, $c = s = 1$.

For $\rho_Y = 1$, no products Y are produced and all assimilated X is transformed into Z. For $\rho_Y = 0$, all assimilated X is transformed into Y. The binding probability ρ_Y can be tuned by inhibitors, allowing the CSU complex to branch flux X into fluxes Y and Z.

Open protocol

The changes in the binding fractions amount to

$$\frac{d}{dt}\theta_c = (\dot{k}_X + \dot{k}_Y)(1 - \theta_c) + \rho_X j_{X,F} \theta_c / c \tag{2.18}$$

$$\frac{d}{dt}\theta_s = \dot{k}_Z(1 - \theta_s) - \rho_Y \dot{k}_Y \theta_s (1 - \theta_c) y_{Y,X} c / s \tag{2.19}$$

where the ρ_* denote the binding probabilities and $\dot{k}_*$ the dissociation rates. The only difference with the closed protocol is the absence of θ_s in the change of θ_c.

Assuming a steady state for the binding fractions, the fluxes can be quantified as

$$j_{X,R} = \dot{k}_X(1 - \theta_c)c - j_{X,F}(1 - \rho_X \theta_c) \qquad j_{Y,R} = (1 - \rho_Y \theta_s) y_{Y,X} \dot{k}_Y (1 - \theta_c) c$$
$$j_{Y,P} = y_{Y,X} \dot{k}_Y (1 - \theta_c) c \qquad j_{Z,P} = y_{Z,Y} \dot{k}_Z (1 - \theta_s) s$$

Assuming a steady state again, the binding fractions can be solved through $\frac{d}{dt}\theta_* = 0$, giving all fluxes as functions of the feeding flux $j_{X,F}$.

The solutions amount to

$$\theta_c = \frac{c(\dot{k}_X + \dot{k}_Y)}{c(\dot{k}_X + \dot{k}_Y) - \rho_X j_{X,F}}; \quad \theta_s = \frac{(c(\dot{k}_X + \dot{k}_Y) - \rho_X j_{X,F}) s \dot{k}_Z}{(c(\dot{k}_X + \dot{k}_Y) - \rho_X j_{X,F}) s \dot{k}_Z - \rho_X j_{X,F} c \rho_Y \dot{k}_Y y_{Y,X}}$$

The production of Y relative to Z can be modified by the binding probability ρ_Y, as in the closed protocol, but even when $\rho_Y = 1$ the CSU complex still produces Y.

Comparison

Figure 2.13 compares the performances of the CSU complex using a closed and an open handshaking protocol between the Carrier and the SU. The closed protocol allows a slightly

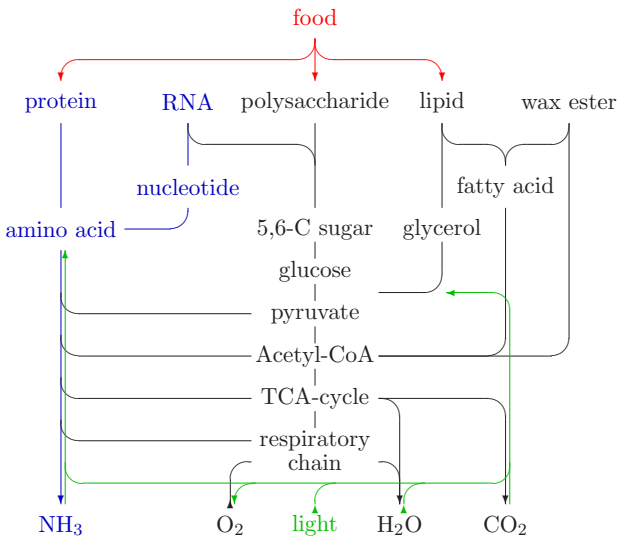

Figure 2.14: A simplified map of metabolism. The second line gives the main polymers that are used as reserves, below that are the monomers that play an active role in metabolism. The bottom line gives the main end products and external sources. Oxygen is used as an electron acceptor by the respiratory chain, but sometimes other electron acceptors are used. Most pathways are reversible, although different sets of enzymes are usually involved. Most animals can synthesize lipids from polysaccharides, but not vice versa. Heterotrophs use food to supply the reserve polymers, autotrophs use light and minerals to synthesize sugar and animo acids (in grey), mixotrophs do both. TCA = tricarboxylic-acid.

greater production rate of product Z, but less of precursor plus product, $Y + Z$. This is because the Carrier waits to dissociate from its substrate until the SU is ready for acceptance, so no precursor is 'spoiled', but the carrier is busy for longer time intervals.

The SU can be thought of as a resistance that leads to deviation of the hyperbolic production curve as a function of substrate density, making it somewhat steeper. The closed protocol is optimal for regulation of flux Y versus flux Z, while the open protocol maximizes substrate uptake, with inherent production of Y, and a slightly reduced production of Z. The closed protocol requires compact spatial organization to allow information exchange between the Carriers and the SUs with respect to the binding state of the SUs, which is not required for the open protocol.

2.5 Metabolic modes

Animals feed on complex foods (mixtures of polysaccharides, lipids and proteins), from which they extract energy, electrons, as well as all necessary 'building' blocks: carbon, nitrogen, vitamins, etc. As is the case in many other organisms, some of the amino acids, purines and pyrimidines in food are taken up and used as building blocks directly, while other amino acids are synthesized *de novo* if not available in food. They thus obtain energy from oxidation–reduction reactions, and carbon from organic compounds. This classifies them as chemo-organotrophs (chemo- is opposite to photo-; organo- is opposite to litho-; the latter dichotomy is synonymous with hetero- versus auto-). They frequently use oxygen as an electron acceptor. As a consequence, they excrete carbon dioxide and nitrogen waste, such as ammonia or urea, see Figure 2.14.

Most plants, in contrast, use light energy, and take carbon dioxide as a carbon source. This classifies them as photolithotrophs. Energy that comes from light is usually stored in polysaccharides and/or lipids, which also serve as carbon reserves. Plants use water, rather

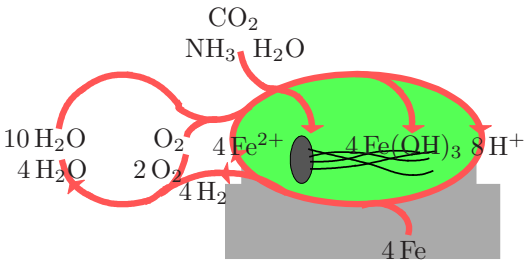

Figure 2.15: The next time you look at your car or bike, you will remember that corrosion is an example of chemolithotrophy. Most corrosion is microbe-mediated and the main culprit is the iron bacterium *Gallionella*; it uses 220 g of iron-II and produces 430 g of rust to make just 1 g of cells from carbon dioxide, water and ammonia [585]. It excretes long strands of rust at one side of the cell.

than organic compounds, as an electron donor, and, with carbon dioxide as the electron acceptor, oxygen is produced in the light. Most plants can synthesize all compounds they need from very simple minerals (nitrate, phosphate, etc), but some plants also use complex organic compounds (for instance the parasitic plants that lack chlorophyll, or the hemi-parasites that still have chlorophyll), so they combine chemo-organotrophic with photolithotrophic properties.

Bacteria, as a group, use a wide range of metabolic modes, some resembling those of animals or plants. The purple non-sulfur bacteria *Rhodospirallacea* use light as their energy source, but different kinds of organic compounds as the electron donor and acceptor. This classifies them as photo-organotrophs. Most photo-assimilable organic compounds can also be respired, but benzoate, for instance, can be used in the light, but cannot be respired [876]. Sulfur bacteria use light as an energy source, carbon dioxide as a carbon source, and H_2S, elemental sulfur or H_2 as an electron donor. Like plants, they classify as photolithotrophs. Most bacteria are chemotrophs, however, which use oxidation–reduction or fermentation reactions to fuel energy-demanding reactions. Figure 2.15 gives an example of chemolithotrophy.

Individuals of many phototrophic prokaryotes and protoctists can also activate the chemotrophic mode, depending on the environmental conditions, which somewhat degrades the usefulness of the classification. They are called mixotrophs. Figure 2.14 illustrates that organisms can differ in their assimilation strategies, but otherwise have substantial similarities in the organization of metabolism.

Some organisms, like ourselves, rapidly die when oxygen is not available. Intertidal animals (crustaceans, molluscs), animals in sediments, parasitic animals, yeasts and goldfish can survive its absence for some time, by switching from respiration to fermentation (cf. {148}), see [132] for a review. (At some stage, all need some oxygen to synthesize steroids or collagen [277]). Some bacteria do not need oxygen, but can survive in its presence, but others rapidly die when exposed to oxygen. This is because oxygen is rather reactive and can form free radicals in the cell, which are extremely reactive. Organisms can only survive in the presence of oxygen (aerobic conditions) if they 'catch' these free radicals efficiently with specialized enzymes, called superoxide dismutases (some prokaryotes use high concentrations of Mn^{2+} or other means), to convert the radicals to the highly toxic hydrogen peroxide, and subsequently back to oxygen, using the enzyme catalase. The handling of oxygen remains rather tricky, however, and is at the basis of the process of aging, cf. {139}.

From a dynamic point of view, it is important to realize that the availability of the various nutrients and light can fluctuate wildly, while autotrophs must couple them to synthesize structural biomass with a constant chemical composition. This requires the installation of auxiliary reserves, one for each nutrient (mineral) that has to be taken up, with rules for the use of these reserves and their replenishment. This is less necessary for chemo-organotrophs such as animals; an imbalance between the composition of food and their needs to synthesize structural biomass can be modelled realistically, as a first approximation, by a conversion of food into reserves that is not very efficient. This is why cows extract so little energy from grass: grass is poor in proteins. The required energy–protein balance shifts even more to the protein side if a lot of proteins are taken away from the cow in milk. It is well known that the amount of grass required to feed cows can be substantially reduced by protein supplements. The predator–prey conversion is very efficient, because the body compositions match almost exactly. The match is perfect for animals that feed on closely related species, and explains why they evolved in many taxa: mammal-eating mammals, starfish-eating starfish, comb jelly-eating comb jellies, etc.

Animals can buffer varying availabilities of food with a single reserve, because all required nutrients covary, while plants also need auxiliary reserves, because mineral nutrients and light vary independently. Since growth of structural biomass can change, the machinery to synthesize biomass would face very busy and very quiet periods if they were a fixed part of the structural biomass. (The part must be fixed on the basis of the homeostasis assumption.) If the synthesis machinery is part of the reserves, however, the fluctuations in activity would be much less, and the amount of required machinery could be 'chosen' much more economically, see {244}. This is because growth tends to increase with the reserves, as we will see. Auxiliary reserves for a particular nutrient, in contrast, can increase considerably if growth is limited by other nutrients or energy, see {172}. This is how large (auxiliary) reserves can accompany low growth rates. The homeostasis assumption also applies to each auxiliary reserve. Homeostasis for the organism as a whole decreases with an increasing number of reserves, and the composition of the body increases in flexibility.

2.6 Temperature

All physiological rates depend on the body temperature. For a species-specific range of temperatures, the description proposed by S. Arrhenius in 1889, see, e.g. [327], usually fits well

$$\dot{k}(T) = \dot{k}_1 \exp\left\{\frac{T_A}{T_1} - \frac{T_A}{T}\right\} \tag{2.20}$$

with T the absolute temperature (in Kelvin), T_1 a chosen reference temperature, the parameter T_A the Arrhenius temperature, $\dot{k}$ a (physiological) reaction rate and $\dot{k}_1$ its value at temperature T_1. So, when $\ln \dot{k}$ is plotted against T^{-1}, a straight line results with slope $-T_A$, as Figure 2.16 illustrates.

Arrhenius based this formulation on the van't Hoff equation for the temperature coefficient of the equilibrium constant and amounts to $\dot{k}(T) = \dot{k}_\infty \exp\{\frac{-E_a}{RT}\}$, where $\dot{k}_\infty$ is known as the frequency factor, R is the gas constant 8.31441 $\mathrm{J\,K^{-1}\,mol^{-1}}$, and E_a is called

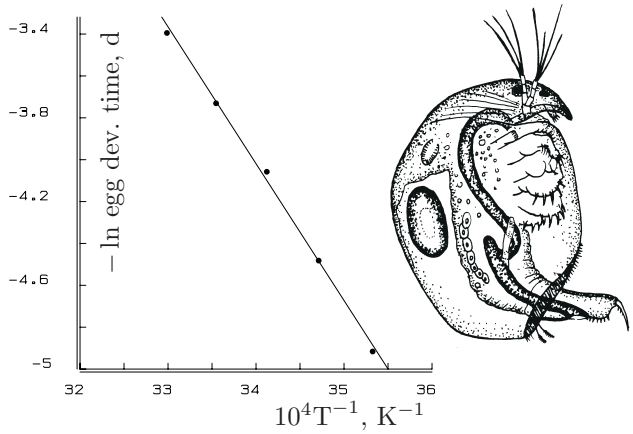

Figure 2.16: The Arrhenius plot for the development rate for eggs of the waterflea *Chydorus sphaericus*, i.e. the inverse time between egg laying and hatching. Data from Meyers [628].

the activation energy. Justification rests on the collision frequency which obeys the law of mass action, i.e. it is proportional to the product of the concentrations of the reactants. The Boltzmann factor $\exp\{\frac{-E_a}{RT}\}$ stands for the fraction of molecules that manage to obtain the critical energy E_a to react.

Glasstone *et al.* [327] studied the thermodynamic basis of the Arrhenius relationship in more detail. They came to the conclusion that this relationship is approximate for bimolecular reactions in the gas phase. Their absolute rate theory for chemical reactions proposes a more accurate description where the reaction rate is proportional to the absolute temperature times the Boltzmann factor. This description, however, is still an approximation [327,412].

The step from a single reaction between two types of particles in the gas phase to physiological rates where many compounds are involved and gas kinetics do not apply is, of course, enormous. If, however, each reaction depended in a different way on temperature, cells would have a hard time coordinating the different processes at fluctuating temperatures. The Arrhenius relationship seems to describe the effect of temperature on physiological rates with acceptable accuracy in the range of relevant temperatures. Due to the somewhat nebulous application of thermodynamics to describe how physiological rates depend on temperature, I prefer to work with the Arrhenius temperature, rather than the activation energy. I even refrain from the improvement offered by Glasstone's theory, because the small correction does not balance the increase in complexity of the interpretation of the parameters for biological applications.

Figure 2.17 shows that the Arrhenius temperatures for different rates in a single species are practically the same, which again points to the regulation problem an individual would experience if they were different. Obviously, animals cannot respire more without eating more.

In chemistry, the activation energy is known to differ widely between different reactions. Processes such as the incorporation of [^{14}C]leucine into protein by membrane-bound rat-liver ribosomes have an activation energy of 180 kJ mol^{-1} in the range 8–20 °C and 67 kJ mol^{-1} in the range 22–37 °C. The difference is due to a phase transition of the membrane lipids, [930] after [14]. Many biochemical reactions seem to have an activation energy in this range [874]. This supports the idea that the value of activation energy is a constraint for functional enzymes in cells.

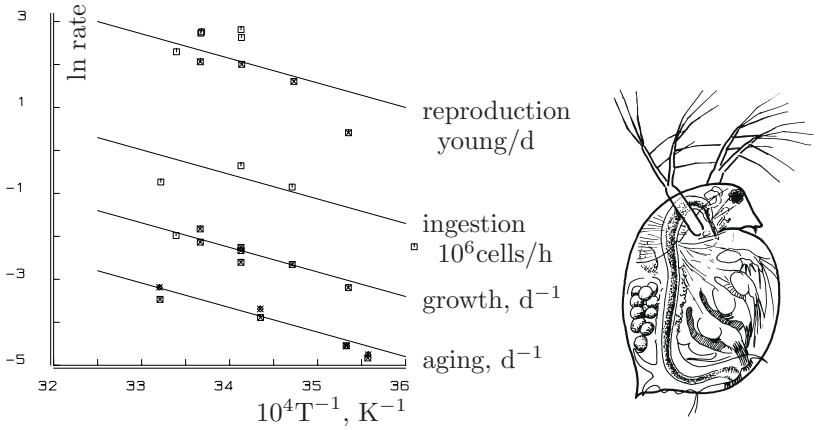

Figure 2.17: The Arrhenius plot for reproduction, ingestion, von Bertalanffy growth and Weibull aging of *Daphnia magna*; from [522]. The Arrhenius temperature is 6400 K. ◇ males, □ females. Food: the algae *Scenedesmus subspicatus* (open symbols) or *Chlorella pyrenoidosa* (filled symbols). The ingestion and reproduction rates refer to 4 mm individuals.

Table 2.3 gives Arrhenius temperatures for several species. The mean Arrhenius temperature, T_A, is somewhere between 10 000 and 12 500 K, which is consistent for the embryo development of 35 species [1030] and the von Bertalanffy growth of 250 species [515]. The value is in the upper range of values usually applied. This is because many experiments do not allow for an adaptation period. The problem is that allo-enzymes are produced with somewhat different temperature–activity relationships when temperature changes. This takes time, depending on species and body size. Without an adaptation period, the performance of enzymes adapted to one temperature is measured at another temperature, which affect the apparent Arrhenius temperature.

At low temperatures, the actual rate of interest is usually lower than expected on the basis of (2.20). If the organism survives, it usually remains in a kind of resting phase, until the temperature rises again. For many seawater species, this lower boundary is between 0 and 10 °C, but for terrestrial species it can be much higher; caterpillars of the large-blue butterfly *Maculinea rebeli*, for instance, cease to grow below 14 °C [253]. The lower boundary of the temperature tolerance range frequently sets boundaries for geographical distribution. Reef-building corals only occur in waters where the temperature never drops below 18 °C. Plants can experience chilling injury if the temperature drops below a species-specific threshold.

At temperatures that are too high, the organism usually dies. At 27 °C, *Daphnia magna* grows very fast, but at 29 °C it dies almost instantaneously. The tolerance range is sharply defined at the upper boundary. A few degrees rise of the seawater temperature, due to the intense 1998 El Niño event, caused death and the subsequent bleaching of vast areas of coral reef. It will take them decades to recover. Nisbet [666] gives upper temperature limits for 46 species of protozoa, ranging from 33 to 58 °C. Thermophilic bacteria and organisms living in deep ocean thermal vents thrive at temperatures of 100 °C or more. The width of the tolerance range depends on the species; many endotherms have an extremely small one around 38 °C.

Sharpe *et al.* [821,830] proposed a quantitative formulation for the reduction of rates at low and high temperatures, based on the idea that the rate is controlled by an enzyme that has an inactive configuration at low and high temperatures. The reaction to these

Table 2.3: Arrhenius temperatures as calculated from literature data on the growth of ectothermic organisms. The values for the mouse cells are obtained from Pirt [717]. The other values were obtained using linear regressions.

species	range (°C)	T_A (K)	type of data	source
Escherichia coli	23–37	6 590	population growth	[639]
Escherichia coli	26–37	5 031	population growth	[443]
Escherichia coli	12–26	14 388	population growth	[443]
Psychrophilic pseudomonad	12–30	6 339	population growth	[443]
Psychrophilic pseudomonad	2–12	11 973	population growth	[443]
Klebsiella aerogenes	20–40	7 159	population growth	[929]
Aspergillus nidulans	20–37	7 043	population growth	[931]
9 species of algae	13.5–39	6 842	population growth	[333]
mouse tissue cells	31–38	13 834	population growth	[969]
Nais variabilis	14–29	9 380	population growth	[460]
Pleurobrachia pileus	5–20	10 000	Bertalanffy growth	[347]
Mya arenaria	7–15	13 000	Bertalanffy growth	[24]
Daphnia magna	10–26.5	6 400	Bertalanffy growth	[515]
Ceriodaphnia reticulata	20–26.5	6 400	Bertalanffy growth	[515]
Calliopius laeviusculus	6.5–15	11 400	Bertalanffy growth	[192]
Perna canaliculus	7–17	5 530	lin. growth	[409]
Mytilus edulis	6.5–18	8 460	lin. growth larvae	[873]
Cardium edule & C. glaucum	10–30	8 400	lin. growth larvae	[483]
Scophthalmus maximum	8–15	15 000	lin. growth larvae	[453]
25 species of fish	6–29	11 190	embryonic period	[609]
Brachionus calyciflorus	15–25	7 800	embryonic period	[357]
Chydorus sphaericus	10–30	6 600	embryonic period	[628]
Canthocampus staphylinus	3–12	10 000	embryonic period	[807]
Moraria mrazeki	7–16.2	13 000	embryonic period	[807]

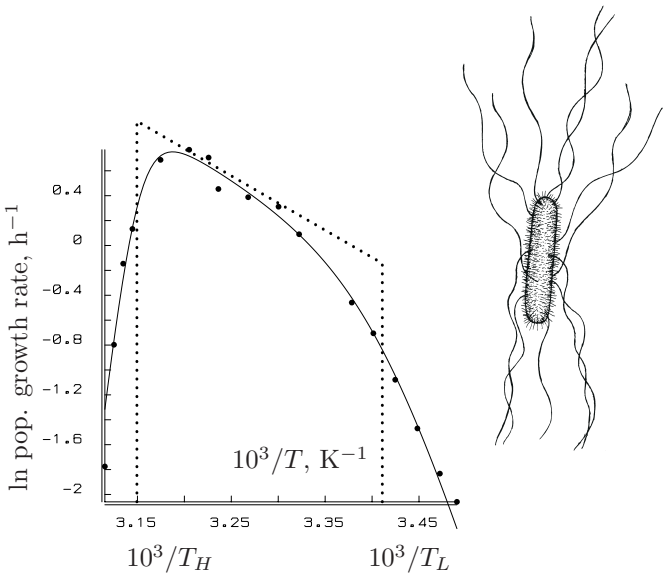

Figure 2.18: The Arrhenius plot for the population growth rate of *Escherichia coli* B/r on rich complex medium. Data from Herendeen *et al.* [401]. The Arrhenius temperature for the growth rate, and for both deactivation rates are $T_A = 4\,370$ (sd 1640) K, $T_{AL} = 20\,110$ (sd 7 940) K, and $T_{AH} = 69\,490$ (sd 8260) K. The dotted line shows the Arrhenius relationship with the same value for T_A and the population growth rate (1.94 (sd 0.11) h^{-1} at $T_1 = 310$ K), but without accounting for the deactivation, between the upper and lower boundaries of the tolerance range, $T_L = 293$ (sd 3.4) K and $T_H = 318$ (sd 0.4) K.

two inactive configurations is taken to be reversible with rates depending on temperature in the same way as the reaction that is catalysed by the enzyme, however the Arrhenius temperatures might differ. This means that the reaction rate has to be multiplied by the enzyme fraction that is in its active state, which is assumed to be at its equilibrium value. This fraction is

$$s(T)/s(T_1) \quad \text{with } s(T) = \left(1 + \exp\left\{\frac{T_{AL}}{T} - \frac{T_{AL}}{T_L}\right\} + \exp\left\{\frac{T_{AH}}{T_H} - \frac{T_{AH}}{T}\right\}\right)^{-1} \tag{2.21}$$

where T_L and T_H relate to the lower and upper boundaries of the tolerance range and T_{AL} and T_{AH} are the Arrhenius temperatures for the rate of decrease at both boundaries. All are taken to be positive and all have dimension temperature. We usually find $T_{AH} \gg T_{AL} \gg T_A$. Figure 2.18 illustrates the quantitative effect of applying the correction factor.

The existence of a tolerance range for temperatures is of major evolutionary importance; many extinctions are thought to be related to changes in temperature. This is the conclusion of an extensive study by Prothero, Berggren and others [737] on the change in fauna during the middle-late Eocene (40–41 Ma ago). This can most easily be understood if the ambient temperature makes excursions outside the tolerance range of a species. If a leading species in a food chain is the primary victim, many species that depend on it will follow. The wide variety of indirect effects of changes in temperature complicate a detailed analysis of climate-related changes in faunas. Grant and Porter [341] discuss in more detail the geographical limitations for lizards set by temperature, if feeding during daytime is only possible when the temperature is in the tolerance range, which leads to constraints on ectotherm energy budgets.

As a first approximation it is realistic to assume that all physiological rates are affected by temperature in the same way, so that a change in temperature amounts to a simple transformation of time. Accelerations, such as the aging acceleration that is introduced on {141}, must thus be corrected for temperature differences by applying the squared factor, so $\ddot{k}(T) = \ddot{k}(T_1)\exp\{-2T_A(T_1^{-1} - T^{-1})\}$. I argue, {95}, that ultimate size results from a ratio of two rates, so it should not depend on the temperature, as all rates are affected

Table 2.4: The von Bertalanffy growth rate for the waterfleas *Ceriodaphnia reticulata* and *Daphnia magna*, reared at different temperatures in the laboratory both having abundant food. The length at birth is 0.3 and 0.8 mm respectively.

	Ceriodaphnia reticulata				*Daphnia magna*			
temp	growth rate	sd	ultimate length	sd	growth rate	sd	ultimate length	s.d
°C	a^{-1}	a^{-1}	mm	mm	a^{-1}	a^{-1}	mm	mm
10					15.3	1.4	4.16	0.16
15	20.4	4.0	1.14	0.11	25.9	1.3	4.27	0.06
20	49.3	3.3	1.04	0.09	38.7	2.2	4.44	0.09
24	57.3	2.6	1.06	0.01	44.5	1.8	4.51	0.06
26.5	74.1	4.4	0.95	0.02	53.3	2.2	4.29	0.06

in the same way. Table 2.4 confirms this for two species of daphnids cultured under well standardized conditions and abundant food [515]. It is also consistent with the observation by Beverton, see appendix to [158], that the walleye *Stizostedion vitreum* matures at 2 years at the southern end of its range in Texas and at 7 or 8 years in northern Canada, while the size at maturation of this fish is the same throughout its range.

Although ultimate sizes are not rates, they are frequently found to decrease with increasing temperature. The reason may well be that the feeding rate increases with temperature, so, at higher temperatures, food supplies are likely to become limited, which reduces ultimate size. I discuss this phenomenon in more detail in relation to the Bergmann rule, {232}. For a study of the effects of temperature on size, it is essential to test for the equality of food density. This requires special precautions.

Not all rates vary with temperature in the same way. The interception of photons by chlorophyll is less effected by temperature than oxygen or carbon dioxide binding by Rubisco, which implies an enhanced electron leak at low temperatures. The solubility of oxygen in water decreases less with temperature than that of carbon dioxide, which means that the compensation point, i.e. the ratio of the carbon dioxide to the oxygen partial pressures for which photorespiration balances photosynthesis, increases with temperature [542]. This leads to an optimum relationship of photosynthesis with temperature, but the location of the optimum is highly adaptable, and can change during the season in a single individual.

Apart from effects on rate parameters, temperature can affect egg size [261] and sex. High temperatures produce males in lizards and crocodiles, and females in turtles [203,834], within a range of a few degrees.

A common way to correct for temperature differences in physiology is on the basis of Q_{10} values, known as van't Hoff coefficients. The Q_{10} is the factor that should be applied

to rates for every 10 °C increase in temperature: $\dot{k}(T) = \dot{k}(T_1)Q_{10}^{(T-T_1)/10}$. The relationship with the Arrhenius temperature is thus $Q_{10} = \exp\{\frac{10T_A}{TT_1}\}$. Because the range of relevant temperatures is only from about 0 to 40 °C, the two ways to correct for temperature differences are indistinguishable for practical purposes. If the reference temperature is 20 °C, or $T_1 = 293$ K, Q_{10} varies from 3.49 to 2.98 over the full temperature range for $T_A = 10\,000$ K.

2.7 Life-stages

Three life-stages can be distinguished in the study of mass and energy fluxes: embryo, juvenile and adult. The triggers for transition from one stage to another and details of the different stages are discussed later, {111}. This section introduces the stages.

Embryo

The first stage is the embryonic one, which is defined as a state early in the development of the individual, when no food is ingested. The embryo relies on stored energy supplies. Freshly laid eggs consist, almost entirely, of stored energy, and for all practical purposes the initial volume of the embryo can realistically be assumed to be negligibly small. At this stage it hardly respires, i.e. it uses no oxygen and does not produce carbon dioxide. (The shells of bird eggs initially produce a little carbon dioxide [99,376].) In many species, this is a resting stage. This especially holds for plants, where seeds are equivalent to eggs; seeds can be dormant for many years and the number of dormant seeds greatly exceeds the number of non-dormant individuals [371]. Many seeds (particularly berries) require to be treated by the digestive juices of a particular animal species for germination. No seedlings of the tambulacoque tree *Calvaria major* were found after the extinction of the dodo *Raphus cucullatus* at around 1690 on Mauritius. With the help of turkeys, the tree still survives artificially. Although the egg exchanges gas and water with the environment, it is otherwise a rather closed system.

Foetal development represents an exception, where the mother provides the embryo with reserve material, such as in the placentals and some species of velvet worm *Peripatus*. Complicated intermediates between reproduction by eggs and foetuses exist in fish [1017, 1018], reptiles and amphibians [88,715,886]. The evolutionary transition from egg to foetal development occurred several times independently. From the viewpoint of energetics, foetuses are embryos because they do not take food. The digestive system is not functional and the embryo does not have a direct impact on food supplies in an ecological sense. The crucial difference from an energetics point of view is the supply of energy to the embryo. In lecithotrophic species, nutrients are provided by the yolk of the ovum, whereas in matrotrophic species nutrients are provided by the mother as the foetus grows, not just in vitellogenesis. The fact that eggs are kept in the body (viviparity) or deposited in the environment (oviparity) is of no importance from an energetic perspective. (The difference is important in a wider evolutionary setting, of course.) As in eggs, a number of species of mammal have a developmental delay just after fertilization, called diapause [837].

Juvenile

The second stage in life history is the juvenile one, in which food is taken but resources are not yet allocated to the reproductive process. In some species, the developing juvenile takes a sequence of types of food or sizes of food particles. Most herbivores, for instance, initially require protein-rich diets that provide nitrogen for growth, cf. {76}. Some species, such as *Oikopleura*, seem to skip the juvenile stage. It does not feed as a larva, a condition known as lecithotrophy, and it starts allocating energy to reproduction at the moment it starts feeding. A larva is a morphologically defined stage, rather than an energy defined one. If the larva feeds, it is treated as a juvenile; if not, it is considered to be an embryo. So, the tadpole of the gastric-brooding frog *Rheobatrachus*, which develops into a frog within the stomach of the parent, should for energy purposes be classified as an embryo, because it does not feed. The switch from feeding to non-feeding as a larva seems to be made easily, from an evolutionary perspective. Sea urchins have developed a complex pattern of species that do or do not feed as a larva, even within the same genus, which comes with dramatic differences in larval morphology [1019,1020,1021]. Sperm of the sea urchin *Heliocidaris tuberculata*, which has feeding larvae, can fertilize eggs of *H. erythrogramma*, which has non-feeding larvae; the zygote develops into feeding hybrid larvae that resemble starfish larvae, similar to that of the distant ancestor of sea urchins and starfishes, some 450 Ma ago [742].

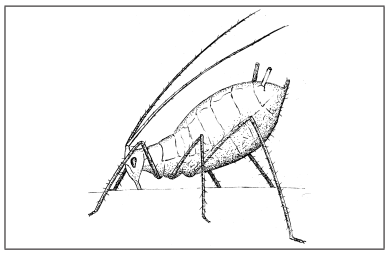

Parthenogenetic aphids have a spectacular mode of reproduction: embryos producing new embryos [481] cf. {328}. Since aphids are ovoviviparous, females carry daughters and grand-daughters at the same time. There is no juvenile stage, and the embryonic stage overlaps with the adult one. Aphids illustrate that the events of turning on feeding and reproduction matter, rather than the stages.

The word 'mammal' refers to the fact that the young usually receive milk from the mother during the first stage after birth, called the baby stage. Pigeons, flamingos and penguins also do this. The length of the baby stage varies considerably. If adequate food is available, the guinea-pig *Cavia* can do without milk [837]. At weaning the young experience a dramatic change in diet, and after weaning the growth rate frequently drops substantially. Few biochemical transformations are required from milk to building blocks for new tissue. The baby, therefore, represents a transition stage between embryo and juvenile. The baby stage relates to the diet in the first instance, cf. {76}, and not directly to a stage in energetic development, such as embryo and juvenile. This can best be illustrated by the stoat *Mustela erminea*. Although blind for some 35–45 days, the female offspring reaches sexual maturity when only 42–56 days of age, before they are weaned. Copulation occurs whilst they are still in the nest [482,837].

Asexually propagating unicellular organisms take food from their environment, though they do not reproduce in a way comparable to the production of eggs or young by most multicellular organisms. For this reason, I treat them as juveniles in this energy-based classification of stages. Although I realize that this does not fit into standard biological nomenclature, it is a logical consequence of the present delineations. I do not know of

better terms to indicate energy-defined stages, which highlights the death of literature dealing with the individual-based energetics of both micro- and multicellular organisms. This book shows that both groups share enough features to try to place them in a single theoretical framework. Some multicellular organisms, such as some annelids, triclads and sea cucumbers (e.g. *Holothuria parvula* [257]), also propagate by division. Some of them sport sexual reproduction as well, causing the distinction between both groups to become less sharp and the present approach perhaps more amenable. Some authors think that ciliates stem from multicellular organism that have lost their cellular boundaries. This feature is standard in fungi, acellular slime moulds and in the green alga *Caulerpa*. Some bacteria have multicellular tendencies [829]. All in all, no sharp separation exists between unicellular and multicellular organisms.

The eukaryotic cell cycle is usually partitioned into the interphase and mitotic phases; the latter is here taken to be infinitesimally short. The interphase is further decomposed into the first gap-phase, the synthesis phase (of DNA) and the second gap-phase. Most cell components are made continuously through the interphase, so that this distinction is less relevant for energetics. The second gap-phase is usually negligibly short in prokaryotes. Since the synthesis phase is initiated upon exceeding a certain cell size, size at division depends on growth conditions and affects the population growth rate. These phenomena are discussed in some detail on {118}, {243}.

In many species, the switch from the juvenile to the adult stage is hardly noticeable, but in the paradoxical frog, for instance, the switch comes with a dramatic change in morphology and a substantial reduction in size from 20 to 2 cm; the energy parameters differ between the stages. Holo-metabolic insects are unique in having a pupal stage between the juvenile and adult ones. It closely resembles the embryonic stage from an energetics point of view, cf. {253}. Pupae do not take food, and start synthesizing (adult) tissue from tiny imaginal disks. A comparable situation occurs in echinoderms, bryozoans, sipunculans and echiurans, where the adult stage develops from a few undifferentiated cells of the morphologically totally different larva. In some cases, the larval tissues are resorbed, and so converted to storage materials; in other cases the new stage develops independently. When *Luidia sarsi* steps off its bipinnaria larva as a tiny starfish, the relatively large larva may continue to swim actively for another 3 months, [905] in [1003]. Some jelly fishes (Scyphomedusae) alternate between an asexual stage, i.e. small sessile polyps, and a sexual stage, i.e. large free swimming medusae. Many parasitic trematods push this alternation of generations to the extreme. Mosses, ferns and relatives alternate between a gametophyte and a sporophyte stage; the former is almost completely suppressed in flowering plants. From an energetics perspective, the sequence embryo, juvenile is followed by a new sequence, embryo, juvenile, adult, with different values for energy parameters for the two sequences. The coupling between parameter values is discussed on {267}.

Adult

The third stage is the adult one, in which energy is allocated to the reproduction process. The switch from the juvenile to the adult stage, puberty, is here taken to be infinitesimally short. The actual length differs from species to species and behavioural changes are also

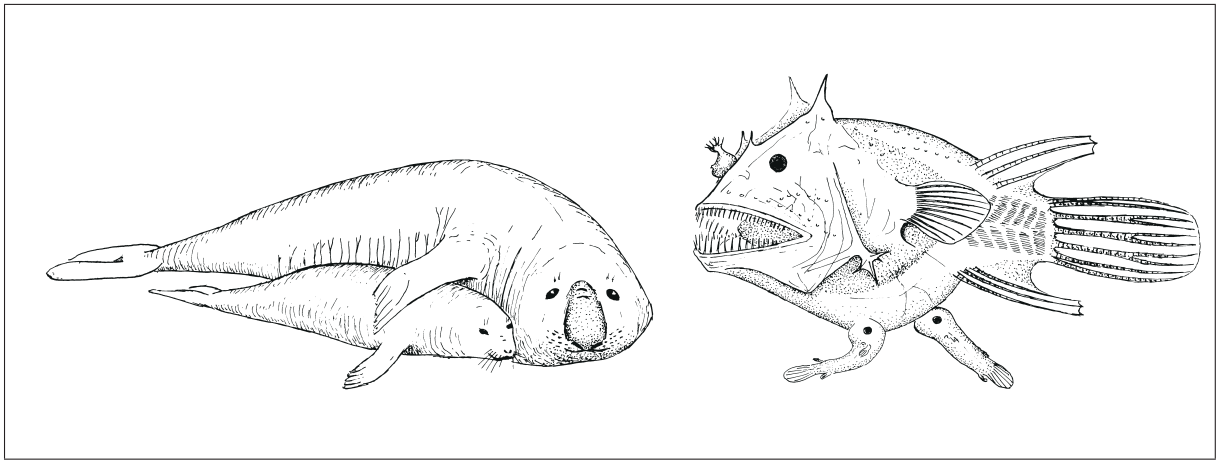

Figure 2.19: Sexual dimorphy can be extreme. The male of the southern sea elephant *Mirounga leonina* is ten times as heavy as the female, while the parasitic males of the angler fish *Haplophryne mollis* are just pustules on the female's belly.

involved. The energy flow to reproduction is continuous and usually quite slow, while reproduction itself is almost instantaneous. This can be modelled by the introduction of a buffer, which is emptied or partly emptied upon reproduction. The energy flow in females is usually larger than that in males, and differs considerably from species to species.

Some *Florideophyceae* (red algae) and *Ascomyceta* (fungi) have three sexes; most animals and plants have two, male and female, but even within a set of related taxa, an amazing variety of implementations can occur. Some species of mollusc and annelid, and most plants, are hermaphroditic, being male and female at the same time; some species of fish and shrimp are male during one part of their life and female during another part; plants such as the bog-myrtle *Myrica gale* can change sex yearly; some have very similar sexes while other species show substantial differences between males and females; see Figure 2.19. The male can be bigger than the female, as in many mammals, especially sea elephants, or the reverse can occur, as in spiders and birds of prey. Males of some fish, rotifers and some echiurans are very tiny, compared to the female, and parasitize in or on the female or do not feed at all. The latter group combines the embryo stage with the adult one, not unlike aphids. As is explained in Chapter 8 on the comparison of species on {267}, differences in ultimate size reflect differences in values for energy parameters. Parameter values, however, are tied to each other, because it is not possible to grow rapidly without eating a lot (in the long run). Differences in energy budgets between sexes are here treated in the same way as differences between species.

Reproduction, in terms of the production of offspring, does not always have a simple relationship with gamete production. All oocytes are already present at birth for future ovulations in birds and mammals, where they are arrested at Prophase I of meiosis [636] (which occurs at the transition from the second gap-phase to the mitotic phase). In some species of tapeworm, wasp and at least eighteen species of mammal (e.g. armadillo) there is a mode, called polyembryony, in which a sexually produced embryo splits into several genetically identical offspring. The opposite also occurs in several species of mammal

(e.g. pronghorn, elephant shrews, bats, viscacha), where the mother reduces a considerable number of ova to usually two, early in the development, but also later on, by killing embryos [87]. Cannibalism among juveniles inside the mother has been described for *Salamandra*, some sharks and the sea star *Patiriella*, {76}. Parent coots are known to drown some hatchlings of large litters, possibly to increase the likelihood of the healthy survival of the remaining ones.

In some species a senile stage exists, where reproduction diminishes or even ceases. This relates to the process of aging and is discussed on {139}. An argument is presented for why this stage cannot be considered as a natural next stage within the context of DEB theory.

The summary of the nomenclature used here reads:

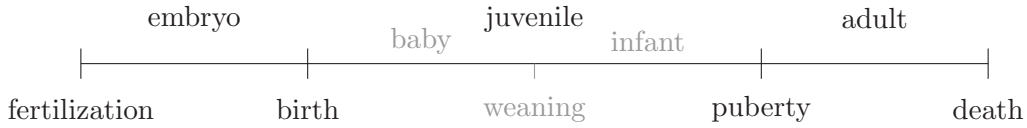

2.8 Summary

This chapter dealt with some basic concepts that are required to set up the DEB theory systematically, without too many asides.

The individual is introduced as the basic level of organization, in terms of system theoretical concepts, involving state variables, inputs and outputs. Individuals span the range from supply to demand systems.

Surface area to volume relationships are discussed, and how they can change during ontogeny. This is necessary because uptake is coupled to surface area, and maintenance to volume. The notion of the shape correction function is introduced to transform isomorphs into organisms that change in shape during growth. I argued that changes in surface area to volume relationships inform molecules about the size of the structure.

The notion of Synthesizing Units is developed from classic enzyme kinetics. It structures interactions between uptake of several reserves, on the basis of a conservation argument for time; the use of the concept 'concentration' should be restricted to well-mixed environments, and the combination of densities and fluxes should be used to understand metabolic transformations.

The various metabolic modes and life-stages of organisms are briefly introduced, and the effects of temperature on physiological rates quantified.

Chapter 3

Energy acquisition and use

This chapter discusses the mechanistic basis of different processes which together constitute the Dynamic Energy Budget (DEB) model. Further chapters evaluate consequences at the individual level. Tests against experimental data are presented during the discussion to examine the realism of the model formulations, and also to develop a feeling for the numerical behaviour of the model elements. The next chapter presents additional tests that involve combinations of processes. The sequential nature of human language does not do justice to the many interrelationships of the processes. These interrelationships are what makes the DEB model more than just a collection of independent submodels. I have chosen here to follow the fate of food, ending up with production processes. This order fits 'supply' systems, but for 'demand' systems another order may be more natural. The relationships between the different processes is schematically summarized in Figure 3.1.

The details and logic of the energy flows will be discussed in this chapter; a brief introduction will be given in this introductory section.

Food is ingested by an animal, transformed into faeces and egested. Energy derived from food is taken up via the blood, which has a low capacity for energy but a high transportation rate. Blood exchanges energy with the storage, and delivers energy to somatic and reproductive tissues. A fixed part, κ, of the catabolic flux, i.e. the energy delivered by the blood, is used for (somatic) maintenance plus growth, the rest for development and/or reproduction. The decision rule for this fork is called the κ-rule. Maintenance has priority

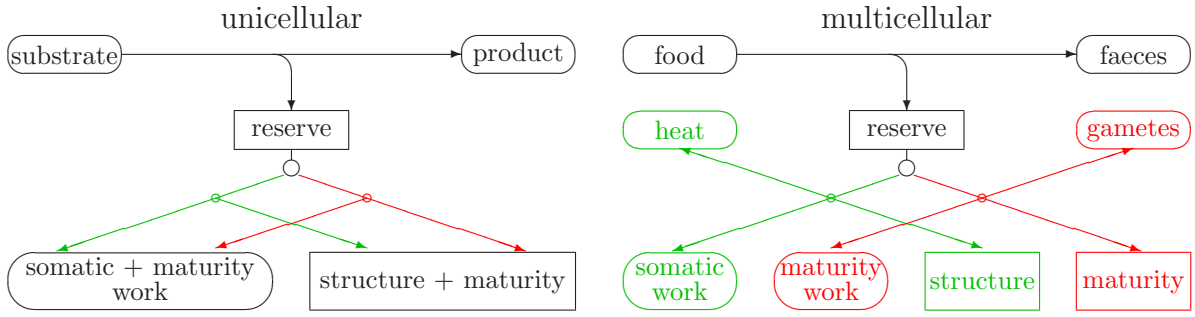

Figure 3.1: Energy fluxes through a heterotroph. The rounded boxes indicate sources or sinks. All fluxes contribute a bit to heating, but this is not indicated in order to simplify the scheme.

over growth, so growth ceases if all energy available for maintenance plus growth is used for maintenance. Energy used for development in embryos and juveniles is similarly partitioned into maintenance of a certain degree of maturation and an increase in the degree of maturity. The energy spent on increasing the degree of maturity in juveniles is allocated to reproduction in adults.

Substrate is taken up and processed by unicellulars (including prokaryotes) in a way that is conceptually comparable to how food is taken up and processed by animals, although defecation and utilization share partly the same machinery to mobilize energy. The coupling between mass and energy fluxes, particularly relevant to micro-organisms, is discussed on {125}. Autotrophs (including plants) are discussed in the multivariate extension of the DEB model, {159}.

3.1 Feeding

Feeding is part of the behavioural repertoire and, therefore, notoriously erratic compared with other processes involved in energetics. The three main factors that determine feeding rates are body size, food availability and temperature. If different types of food are available, many factors determine preferences, e.g. relative abundances, size and searching patterns, which relate to experience and nutritional aspects. For some species it is sensible to express food availability per surface area of environment, for others food per volume makes more sense, and intermediates also exist. The body size of the organism and spatial heterogeneity of the environment hold the keys to the classification. Food availability for krill, which feed on algae, is best expressed in terms of biomass or biovolume per volume of water, because this links up with processes that determine filtering rates. The spatial scale at which algal densities differ is large with respect to the body size of the krill. Baleen whales, which feed on krill, are intermediate between surface and volume feeders because some dive below the top layer, where most algae and krill are located, and sweep the entire column to the surface; so it does not matter where the krill is in the column. Cows and lions are typically surface feeders and food availability is most appropriately expressed in terms of biomass per surface area.

These considerations refer to the relevance of the dimensions of the environment for feeding, be it surface or volume. The next section discusses the relevance of the size of the organism for feeding. The significance of food density returns in the section on functional response.

3.1.1 Feeding methods

Organisms use many methods to obtain their meal; some sit and wait for the food to pass by, others search actively. Figure 3.2 illustrates a small sample of methods, roughly classified with respect to active movements by prey and predator. The food items can be very small with respect to the body size of the individual and rather evenly distributed over the environment, or the food can occur in a few big chunks. This section briefly mentions some feeding strategies and explains why feeding rates tend to be proportional

to the surface area when a small individual is compared to a large one of the same species. (Comparisons between species are made in Chapter 8, {267}.) The examples illustrate a simple physical principle: mass transport from one environment to another, namely to the organism, must be across a surface.

Bacteria, floating freely in water, are transported even by the smallest current, which implies that the current relative to the cell wall is effectively nil. Thus bacteria must obtain substrates through diffusion, {235}, or attach to hard surfaces (films) or each other (flocs, {251}) to profit from convection, which can be a much faster process. Some species develop more flagellae at low substrate densities, which probably reduces diffusion limitation (L. Dijkhuizen, pers. comm.). Uptake rate is directly proportional to surface area, if the carriers that bind substrate and transport it into the cell have a constant frequency per unit surface area of the cell membrane [7,142]. *Arthrobacter* changes from a rod shape into a small coccus at low substrate densities to improve its surface area/volume ratio. Caulobacters do the same by enhancing the development of stalks under those conditions [720].

Some fungi, slime moulds and bacteria glide over or through the substrate, releasing enzymes and collecting elementary compounds via diffusion. Upon arrival at the cell surface, the compounds are taken up actively. The bakers' yeast *Saccharomyces cerevisiae* typically lives as a free floating, budding unicellular, but under nitrogen starvation it can switch to a filamentous multicellular phase, which can penetrate solids [421]. Many protozoans engulf particles (a process known as phagocytosis) with their outer membrane (again a surface), encapsulate them into a feeding vacuole and digest them via fusion with bodies that contain enzymes (lysosomes). Such organisms are usually also able to take up dissolved organic material, which is much easier to quantify. In giant cells, such as the Antarctic foraminiferan *Notodendrodes*, the uptake rate can be measured directly and is found to be proportional to surface area [205]. Ciliates use a specialized part of their surface for feeding, which is called the 'cytostome'; isomorphic growth here makes feeding rate proportional to surface area again.

Marine polychaetes, sea-anemones, sea lilies and other species that feed on blind prey are rather apathetic. Sea lilies simply orient their arms perpendicular to an existing current (if mild) at an exposed edge of a reef and take small zooplankters by grasping them one by one with many tiny feet. The arms form a rather closed fan in mild currents, so the active area is proportional to the surface area of the animal. Sea-gooseberries stick plankters to the side branches of their two tentacles using cells that are among the most complex in the animal kingdom. Since the length of the side branches as well as the tentacles are proportional to the length of the animal, the encounter probability is proportional to a surface area.

Filter feeders, such as daphnids, copepods and larvaceans, generate water currents of a strength that is proportional to their surface area [122], because the flapping frequency of their limbs or tails is about the same for small and large individuals [726], and the current

Figure 3.2: A small sample of feeding methods classified with respect to the moving activities of prey and predator.

prey and predator inactive

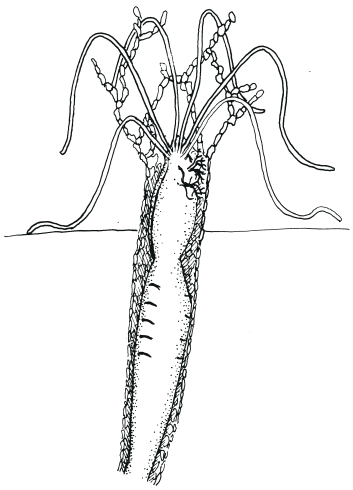

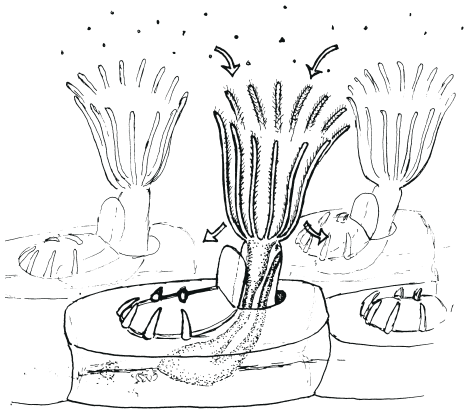

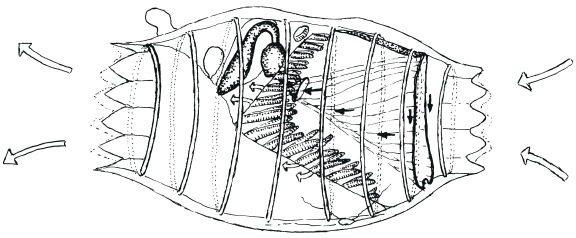

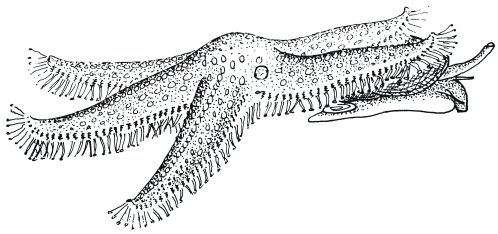

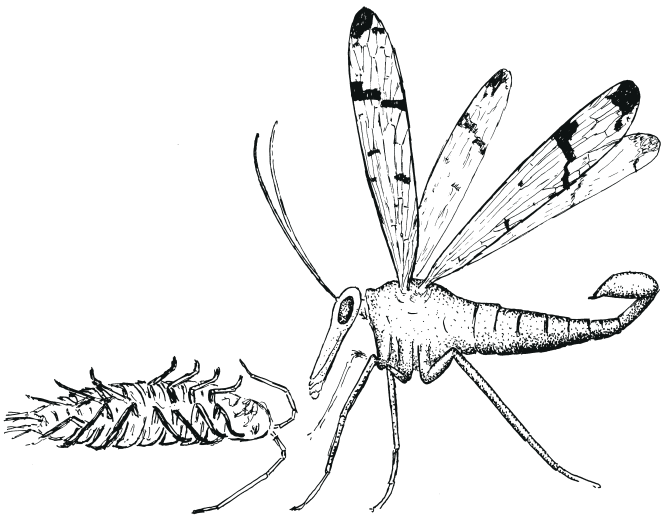

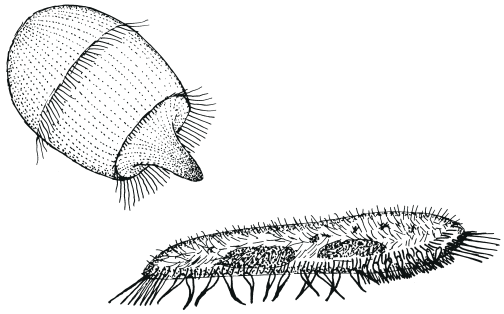

prey inactive

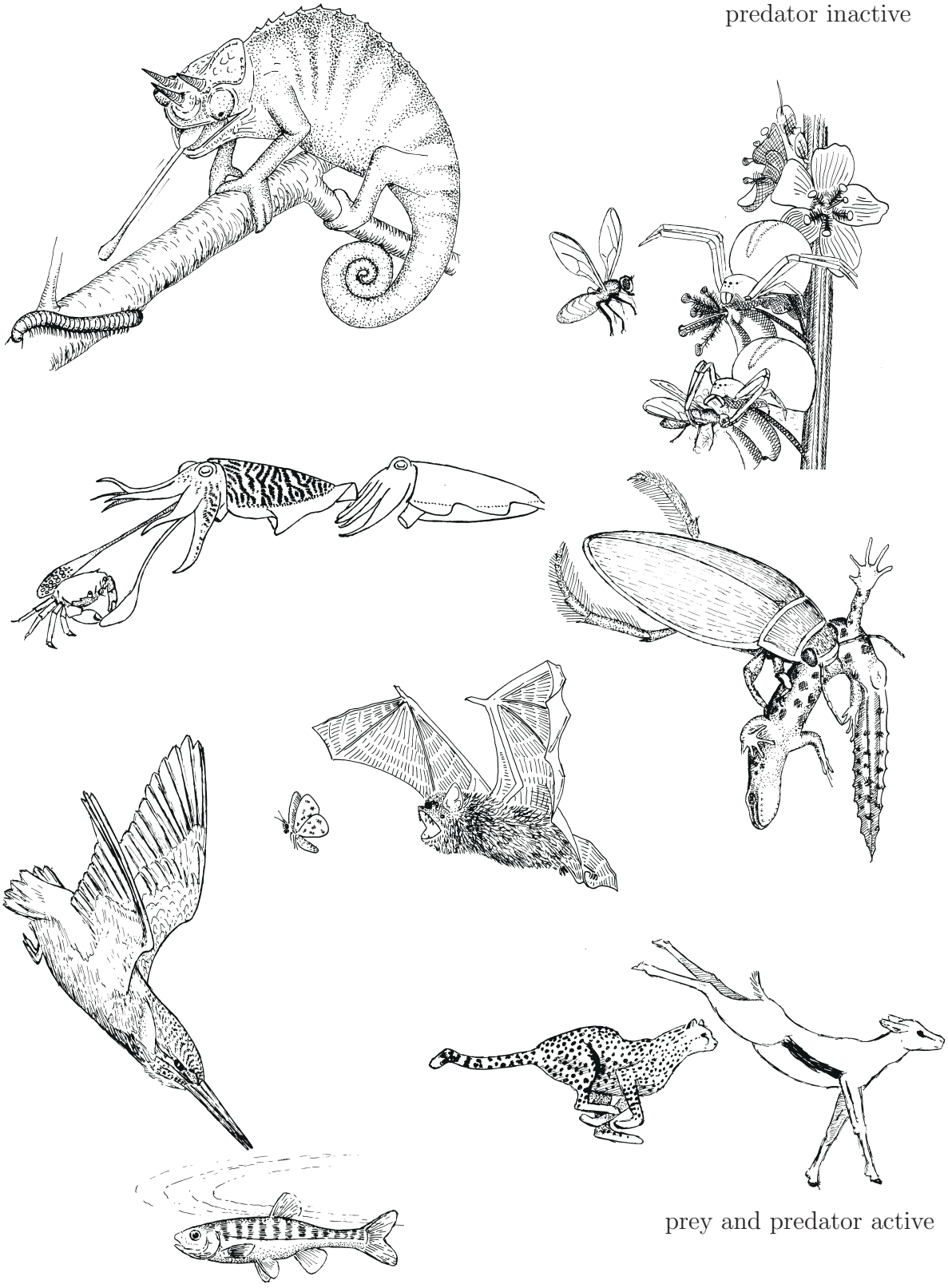
predator inactive
prey and predator active

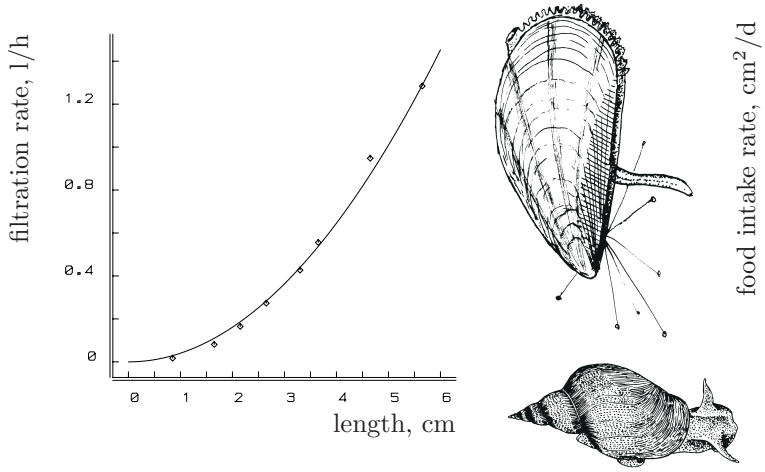

Figure 3.3: Filtration rate as a function of shell length, L, of the blue mussel *Mytilus edulis* at constant food density (40×10^6 cells l^{-1} *Dunaliella marina*) at 12 °C. Data from Winter [1006]. The least-squares-fitted curve is $\{\dot{F}\}L^2$, with $\{\dot{F}\} = 0.041$ (sd 6.75×10^{-4}) $l\,h^{-1}\,cm^{-2}$.

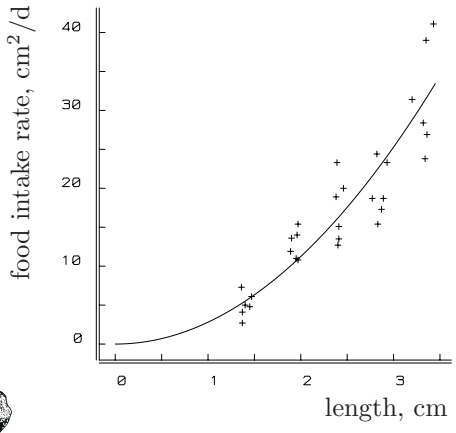

Figure 3.4: Lettuce intake as a function of shell length, L, in the pond snail *Lymnaea stagnalis* at 20 °C [1028]. The weighted least-squares-fitted curve is $\{\dot{J}_X\}L^2$, with $\{\dot{J}_X\} = 2.81$ (sd 0.093) $cm^2\,d^{-1}\,cm^{-2}$.

is proportional to the surface area of these extremities. (Allometric regressions of currents gives a proportionality with length to the power 1.74 [114], or 1.77 [249] in daphnids. In view of the scatter, they agree well with a proportionality with squared length.) The ingestion rate is proportional the current, so to squared length. Allometric regressions of ingestion rates resulted in a proportionality with length to the power 2.2 [610], 1 [727], 2.4–3 [207], and 2.4 [686] in daphnids. This wide range of values illustrates the limited degree of replicatability of these types of measurements. This is partly due to the inherent variability of the feeding process, and partly to the technical complications of measurement. Feeding rate depends on food density, as is discussed on {73}, while most measurement methods make use of changes in food densities so that the feeding rate changes during measurement. Figure 3.11 illustrates results obtained with an advanced technique that circumvents this problem [264].

The details of the filtering process differ from group to group. Larvaceans are filterers in the strict sense: they remove the big particles first with a coarse filter and collect the small ones with a fine mesh. The collected particles are transported to the mouth in a mucous stream generated by a special organ, the endostyle. Copepods take their minute food particles out of the water, one by one with grasping movements [941]. Daphnids exploit centrifugal force and collect them in a groove. Ciliates, bryozoans, brachiopods, bivalves and ascidians generate currents, not by flapping extremities but by beating cilia on part of their surface area. The ciliated part is a fixed portion of the total surface area [292], and this again results in a filtering rate proportional to squared length; see Figure 3.3.

Some surface feeding animals, such as crab spiders, trapdoor spiders, praying mantis, scorpion fish and frogs, lie in ambush; their prey will be snatched upon arrival within

reach, i.e. within a distance that is proportional to the length of a leg, jaw or tongue. The catching probability is proportional to the surface area of the predatory isomorphs. When aiming at a prey with rather keen eye sight, they must hide or apply camouflage.

Many animals search actively for their meal, be it plant or animal, dead or alive. The standard cruising rate of surface feeders tends to be proportional to their length, because the energy investment in movement as part of the maintenance costs tends to be proportional to volume, while the energy costs of transport are proportional to surface area; see {73}. Proportionality of cruising rate to length also occurs if limb movement frequency is more or less constant [736]. The width of the path searched for food by cows or snails is proportional to length if head movements perpendicular to the walking direction scale isomorphically. So feeding rate is again proportional to surface area, which is illustrated in Figure 3.4 for the pond snail.

The duration of a dive for the sperm whale *Physeter macrocephalus*, which primarily feeds on squid, is proportional to its length, as is well known to the whalers [970]. This can be understood, since the respiration rate of this endotherm is approximately proportional to surface area, as I argue on {135}, and the amount of reserve oxygen is proportional to volume on the basis of a homeostasis argument. It is not really obvious how this translates into the feeding rate, if at all; large individuals tend to feed on large prey, which occur less frequently than small prey. Moreover, time investment in hunting can depend on size as well. If the daily swimming distance during hunting were independent of size, the searched water volume would be about proportional to surface area for a volume feeder such as the sperm whale. If the total volume of squid per volume of water is about constant, this would imply that feeding rate is about proportional to surface area.

The amount of food parent birds feed per nestling relates to the requirements of the nestling, which is proportional to surface area; Figure 3.5 illustrates this for chickadees. This is only possible if the nestlings can make their needs clear to the parents, by crying louder.

Catching devices, such as spider or pteropod webs and larvacean filter houses [17], have effective surface areas that are proportional to the surface area of the owner.

All these different feeding processes relate to surface areas in comparisons between different body sizes within a species at a constant low food density. At high food densities, the encounter probabilities are no longer rate limiting, this becomes the domain of digestion and other food processing activities involving other surface areas, for example the mouth opening and the gut wall. The gradual switch in the leading processes becomes apparent in the functional response, i.e. the ingestion rate as function of food density, {73}.

3.1.2 Feeding and movement costs

As feeding methods are rather species-specific, costs of feeding will also be species-specific if they contribute substantially to the energy budget. I argue here that costs of feeding and movements that are part of the routine repertoire are usually insignificant with respect to the total energy budget. For this reason this subsection does not do justice to the voluminous amount of work that has been done on the energetics of movements [696], a field that is of considerable interest in other contexts. Alexander [13] gives a most

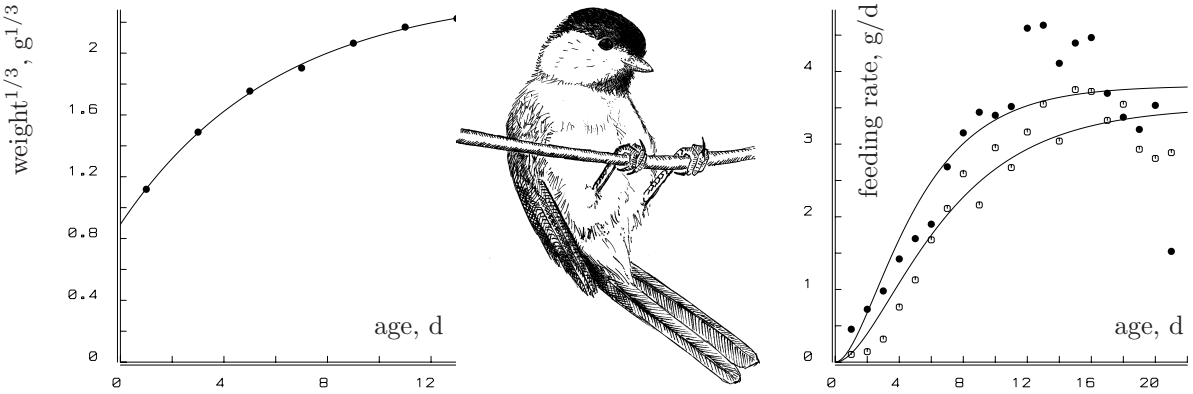

Figure 3.5: The von Bertalanffy growth curve applies to the black-capped chickadee, *Parus atricapillus* (left figure, data from Kluyver [494,862]. Brood size was a modest 5.) The amount of food fed per male (•) or female (○) nestling in the closely related mountain chickadee, *P. gambeli*, is proportional to weight$^{2/3}$ (right figure), as might be expected for individuals that grow in a von Bertalanffy way. Data from Grundel [351,862]. The last five data points were not included in the fit; the parents stop feeding, and the young still have to learn gathering food while rapidly losing weight.

readable and entertaining introduction to the subject of energetics and biomechanics of animal movement. Differences in respiration between active and non-active individuals give a measure for the energy costs of activity. The resting metabolic rate is a measure that excludes active movement. The standard or basal metabolic rate includes a low level of movement only. The field metabolic rate is the daily energy expenditure for free ranging individuals. Karasov [465] found that the field metabolic rate is about twice the standard metabolic rate for several species of mammal, and that the costs of locomotion ranges 2–15% of the field metabolic rate. Mammals are among the more active species. The respiration rate associated with filtering in animals such as larvaceans and ascidians was found to be less than 2% of the total oxygen consumption [286]. Energy investment in feeding is generally small, which does not encourage the introduction of many parameters to describe this investment. Feeding costs can be accommodated in two ways within the DEB theory without the introduction of new parameters, and this subsection aims to explore to what extent this accommodation is realistic.

The first way to accommodate feeding costs is when they are proportional to feeding rate. They then show up as a reduction of the energy gain per unit of food. One can, however, argue that feeding costs per unit of food should increase with decreasing food density, because of the increased effort of extracting it from the environment. This type of cost can only be accommodated without complicating the model structure if these costs cancel against increased digestion efficiency, caused by the increased gut residence time, cf. {239}.

The second way to accommodate feeding costs without complicating the model structure applies if the feeding costs are independent of the feeding rate and proportional to body volume. They then show up as part of the maintenance costs, cf. {89}. This argu-

ment can be used to understand how feeding rates for some species tend to be proportional to surface area if transportation costs are also proportional to surface area, so that the cruising rate is proportional to length, {71}. In this case feeding costs can be combined with costs of other types of movement that are part of the routine repertoire. A fixed (but generally small) fraction of the maintenance costs then relates to movement.

Schmidt-Nielsen [815] calculated 0.65 ml $O_2\,cm^{-2}\,km^{-1}$ to be the surface-area-specific transportation costs for swimming salmon, on the basis of Brett's work [115]. (He found that transportation costs are proportional to weight to the power 0.746, but respiration was not linear with speed. No check was made for anaerobic metabolism of the salmon. Schmidt-Nielsen obtained, for a variety of fish, a power of 0.7, but 0.67 also fits well.) Fedak and Seeherman [273] found that the surface-area-specific transportation cost for walking birds, mammals and lizards is about 5.39 ml $O_2\,cm^{-2}\,km^{-1} \simeq 118$ J $cm^{-2}\,km^{-1}$. (They actually report that the transportation costs are proportional to weight to the power 0.72 as the best fitting allometric relationship, but the scatter is such that 0.67 fits as well.) This is consistent with data from Taylor *et al.* [906] and implies that the costs of swimming are some 12% of the costs of running. Their data also indicate that the costs of flying are between those of swimming and running and amount to some 1.87 ml $O_2\,cm^{-2}\,km^{-1}$.

The energy costs of swimming are frequently taken to be proportional to squared speed on sound mechanical grounds [535], which questions the usefulness of the above-mentioned costs and comparisons because the costs of transportation become dependent on speed. If the inter-species relationship that speeds scale with the square root of volumetric length, see {275}, also applies to intra-species comparisons, the transportation costs are proportional to volume if the travelling time is independent of size.

The energy required for walking and running is found to be proportional to velocity for a wide diversity of terrestrial animals including mammals, birds, lizards, amphibians, crustaceans and insects [311]. This means that the energy costs of walking or running a certain distance are independent of speed and just proportional to distance. If the costs of covering a certain distance are dependent on speed, and temperature affects speeds, these costs would work out in a really complex way at the population and community levels.

The conclusion is that, for the purposes of studying how energy budgets change during the life span, transportation costs either show up as a reduction of energy gain from food, or as a fixed fraction of the somatic maintenance costs when these costs are proportional to structural mass.

3.1.3 Functional response

The feeding or ingestion rate, $\dot{J}_X$, of an organism as a function of food, nutrient or substrate density, X, expressed as C-moles per surface area or volume, is described well by the hyperbolic functional response

$$\dot{J}_X = f\,\dot{J}_{Xm} \quad \text{with } f \equiv (1 + X_K/X)^{-1} \tag{3.1}$$

where X_K is known as the saturation coefficient or Michaelis–Menten constant, i.e. the density at which food intake is half the maximum value, and $\dot{J}_{Xm}$ the maximum ingestion rate. This functional response, proposed by Holling [424] as type II, is illustrated in Figure

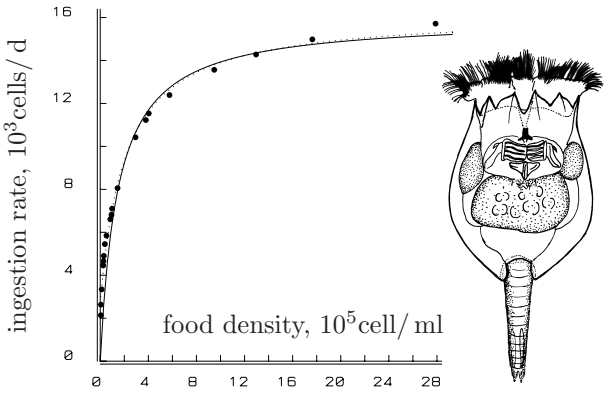

Figure 3.6: The ingestion rate, $\dot{J}_X$ of an individual (female) rotifer *Brachionus rubens*, feeding on the green alga *Chlorella* at 20 °C, as a function of food density, X. Data from Pilarska [714]. The curve is the hyperbola (3.1), with maximum feeding rate $\dot{J}_{Xm} = 15.97$ (sd 0.81) 10^3 cells d^{-1} and saturation coefficient $X_K = 1.47$ (sd 0.26) 10^5 cells ml^{-1}. The stippled curve allows for an additive error in the measurement of the algal density of $0.35\,10^5$ cells ml^{-1}.

3.6. It applies to the uptake of organic particles by ciliates (phagocytosis), the filtering of algae by daphnids, the catching of flies by mantis, the uptake of substrates by bacteria, the nutrient uptake by algae and plants, and the transformation of substrates by enzymes. Although these processes differ considerably in detail, some common abstract principle gives rise to the hyperbolic functional response: the busy period, which is characteristic of the Synthesizing Unit, cf. {43}. To reveal the connection, I rephrase the basic derivation in terms that make sense in the context of a simple model for feeding, or substrate processing, that will be generalized subsequently in various directions, cf. {160}.

Let $\dot{F}$ denote the filtering rate or the speed of an animal relative to prey particles, a rate that is taken to depend on mean particle density only, and not on particle density at a particular moment. The arrival of food particles, present in density X, equals $\dot{F}X$. The mean time between the end of a handling period and the next arrival (the binding period) is $t_b = (\dot{F}X)^{-1}$, and the mean handling period is $t_p = \dot{J}_{Xm}^{-1}$. The time required to find and eat one particle is thus given by $t_c = t_b + t_p$ and the mean ingestion rate is $\dot{J}_X = (\dot{J}_{Xm}^{-1} + (\dot{F}X)^{-1})^{-1} = \dot{J}_{Xm}X(\dot{J}_{Xm}/\dot{F} + X)^{-1}$, which is hyperbolic in the density X. The saturation coefficient is inverse to the product of the handling time and the filtering (or searching) rate, i.e. $X_K = (t_p\dot{F})^{-1} = \dot{J}_{Xm}/\dot{F}$.

This derivation can be generalized in different ways without changing the model. Each arriving particle can have an attribute that stands for its probability of becoming caught. The i-th particle has some fixed probability ρ_i of being caught upon encountering an animal if the animal is not busy handling particles, and a probability of 0 if it is. The mass of each particle does not need to be the same. The flux $\dot{J}_X$ should be interpreted as the mean mass flux (in C-moles per time), where the mass of each particle represents a random trial from some frequency distribution. It is not essential for the handling time to be the same for all particles; handling time can be conceived of as a second attribute attached to each particle, but it must be independent of food density. The condition of zero catching probability when the animal is busy can be relaxed. Metz and van Batenburg [620,621] and Heijmans [387] tied catching probability to satiation (thought to be related to gut content in the mantis). An essential condition for hyperbolic functional responses is that catching probability equals zero if satiation (gut content) is maximal.

Deviations from the hyperbolic functional response can be expected if the mass per

particle is large, while the intensity of the arrival process is small, especially if the mass scatters among the particles. An important source of deviations from the hyperbolic functional response is discussed on {235}.

A most interesting property of the hyperbolic functional response is that it is the only one with a finite number of parameters that maps onto itself. For instance, an exponential function of an exponential function is not again an exponential function. A polynomial (of degree higher than one) of a polynomial is also a polynomial, but it is of an increasingly higher degree if the mapping is repeated over and over again. The hyperbolic function of a hyperbolic function is also a hyperbolic function. (Note that the linear response function is a special case of the hyperbolic one.) In a metabolic pathway each product serves as a substrate for the next step. Neither the cell nor the modeller needs to know the exact number of intermediate steps to relate the production rate to the original substrate density, if and only if the functional responses of the subsequent intermediate steps are of the hyperbolic type. If, during evolution, an extra step is inserted in a metabolic pathway the performance of the whole chain does not change in functional form. This is a crucial point because each pathway has to be integrated with other pathways to ensure the proper functioning of the individual as a whole. If an insert in a metabolic pathway simultaneously required a qualitative change in regulation at a higher level, the probability of its occurrence during the evolutionary process would be remote. This suggests that complex regulation systems in metabolic pathways fix and optimize the kinetics that originate from the simpler kinetics on which Synthesizing Units are based.

A most useful property of the hyperbolic functional response is that it has only two parameters that serve as simple scaling factors on the food density and ingestion rate axis. So if food density is expressed in terms of the saturation coefficient, and ingestion rate in terms of maximum ingestion rate, the functional response no longer has dimensions or parameters.

Filter feeders, such as rotifers, daphnids and mussels, reduce filtering rate with increasing food density [291,726,773,774], rather than maintain a constant rate, which would imply the rejection of some food particles. They reduce the rate by such an amount that no rejection occurs because of the handling (processing) of particles. If all incoming water is swept clear, the filtering rate is found from $\dot{F}(X) = \dot{J}_X/X$, which reaches a maximum if no food is around (temporarily), so that $\dot{F}_m = \{\dot{J}_{Xm}\}V^{2/3}/X_K$, and approaches zero for high food densities. The braces stand for 'surface-area-specific', so $\{\dot{J}_{Xm}\} \equiv \dot{J}_{Xm}V^{-2/3}$ stands for the maximum surface-area-specific ingestion rate, which is considered as a parameter that depends on the composition of the diet. An alternative interpretation of the saturation coefficient in this case would be $X_K = \dot{J}_{Xm}/\dot{F}_m = \{\dot{J}_{Xm}\}/\{\dot{F}_m\}$, which is independent of the size of the animal, as long as only intra-specific comparisons are made. It combines the maximum capacity for food searching behaviour, only relevant at low food densities, with the maximum capacity for food processing, which is only relevant at high food densities.

The mean ingestion rate for an isomorph of volume V at food density X thus amounts to

$$\dot{J}_X = \{\dot{J}_{Xm}\}fV^{2/3} \text{ with } f \equiv (1 + X_K/X)^{-1} \tag{3.2}$$

When starved animals are fed, they often ingest at a higher rate for a short time [971], but this is neglected. Starved daphnids, for instance, are able to fill their guts within 7.5 minutes [314].

The ingestion rate, or substrate uptake rate for V0- and V1-morphs are found from (3.2) by multiplication of $\{\dot{J}_{Xm}\}$ with the shape correction function (2.1) or (2.2), which leads to

$$\begin{array}{lrcl} \text{V0-morph:} & \dot{J}_X & = & \{\dot{J}_{Xm}\} V_d^{2/3} f \\ \text{V1-morph:} & \dot{J}_X & = & [\dot{J}_{Xm}] f V \end{array} \tag{3.3}$$

for $[\dot{J}_{Xm}] \equiv \{\dot{J}_{Xm}\} V_d^{-1/3}$ and V_d is a fixed reference volume.

Feeding on more substrates

Several extensions are possible from one to more types of food (or substrate), see {160}. The way in which these substrates are treated can be classified independently as parallel or sequential, and substitutable or supplementary processing. Supplementary processing means that several substrates are required (at the same time, in fixed relative amounts) to synthesize reserves; the implication is that processing is halted when one of the required substrates is absent. Sequential processing means that one substrate competes with other substrates for access to the same processing unit; the implication is that the uptake rate of that substrate can be reduced by an increase in the abundance of other substrates.

3.1.4 Diet

Details of growth and reproduction patterns can only be understood in relation to selection of food items and choice of diet. The reverse relationship holds as well, especially for 'demand' systems. I will, therefore, mention some aspects briefly.

Many species change their diet during development in relation to their shifting needs with an emphasis on protein synthesis during the juvenile period and on maintenance during the adult one. Many juvenile holo-metabolic insects live on different types of food compared with adults. Wasps, for instance, are often carnivorous when juvenile, while they feed on nectar as adults; butterflies feed on leaves when juvenile, and also nectar as adults. Stickelback fish change from being carnivorous to being herbivorous at some stage during development [212]. Plant-eating ducks live on insects during the first period after hatching. The male emperor penguin *Aptenodytes* and mouth-brooding frog *Rhinoderma darwinii* provide their young initially with secretions from the stomach. Mammals live on milk during the baby stage, cf. {60}.

The first hatching tadpoles of the alpine salamander *Salamandra atra* live on their siblings inside the mother, where they are also supported by blood from her reproductive organs, and the one to four winners leave the mother when fully developed. The same type of prenatal cannibalism seems to occur in the coelacanth *Latimeria* [918], and several sharks (sand tiger sharks *Odontaspidae*, mackerel sharks *Lamnidae*, thresher sharks *Alopiidae* [749]), and the sea star *Patiriella* [143]. Some species of poison dart frog *Dendrobatus* feed their offspring with unfertilized eggs in the water-filled leaf axils of bromeliads, high up in the trees [239,240].

Shifts in food selection that relate to shifts in nutritional requirements can be modelled using at least two reserves, e.g. carbohydrates plus lipids and proteins, which differ in their contributions to maintenance costs, and in the requirements for growth. Changes in behavioural aspects, such as food selection, can then be based on efficiency arguments.

Some species select for different food items in different seasons for reasons other than changes in the relative abundance of the different food sources. This is because of the tight coupling between feeding and digestion. The bearded tit *Panurus biarmicus* is a spectacular example; it lives on the seed of bulrush, *Typha*, and reed, *Phragmites*, from September to March and on insects in summer [870,974]. This change in diet comes with an adaptation of the stomach which is much more muscular in winter when it contains stones to grind the seeds. Once converted to summer conditions, the bearded tit is unable to survive on seeds. The example is remarkable because the bearded tit stays in the same habitat all year round. Many temperate birds change habitats over the seasons. Divers, for instance, inhabit fresh water tundra lakes during the breeding season and the open ocean during winter. Such species also change prey, of course, but the change is usually not as drastic as the one from insects to seeds.

When offered different food items, individuals can select for type and size. Shelbourne [831] reports that the mean length of *Oikopleura* eaten by plaice larvae increases with the size of the larvae. Copepods appear to select the larger algal cells [897]. Daphnids do not collect very small particles, < 0.9 μm cross-section [336], or large ones, > 27 and > 71 μm; the latter values were measured for daphnids of length 1 and 3 mm respectively [140]. Kersting and Holterman [477] found no size-selectivity between 15 and 105 μm^3 (and probably 165 μm^3) for daphnids. Selection is rarely found in daphnids [771], or in mussels [291,996].

The relationship between feeding rates and diet composition gives a clue as to what actually sets the upper limit to the ingestion rate. An indication that the maximum ingestion rate is determined by the digestion rate comes from the observation that the maximum ingestion rate of copepods feeding on diatoms expressed as the amount of carbon is independent of the size of the diatom cells, provided that the chemical composition of the cells is similar [300]. The maximum ingestion rate is inversely related to protein, nitrogen and carbon contents fed to the copepod *Acartia tonsa* [431]. The observation that the maximum ingestion rate is independent of cell size on the basis of ingested volume [314] points to the capacity of gut volume being the limiting factor.

These examples should make clear that the quantitative details of the feeding process cannot be understood without some understanding of the fate of the food. This involves the digestion process in the first place, but a whole sequence of other processes follow. Regulation of (maximum) ingestion depends by definition on the need in 'demand' systems, which is especially easy to observe in species that lose the ability to grow, such as birds and mammals. Temporarily elevated food intake can be observed in birds preparing for migration or reproduction, in mammals preparing for hibernation or in pregnant mammals [940]. For simplicity's sake, these phenomena will not be modelled explicitly.

Prokaryotes show a diversity and adaptability of metabolic pathways that is huge in comparison to that of eukaryotes. Many bacteria, for example, are able to synthesize all the amino acids they require, but will only do so if these are not available from the environment.

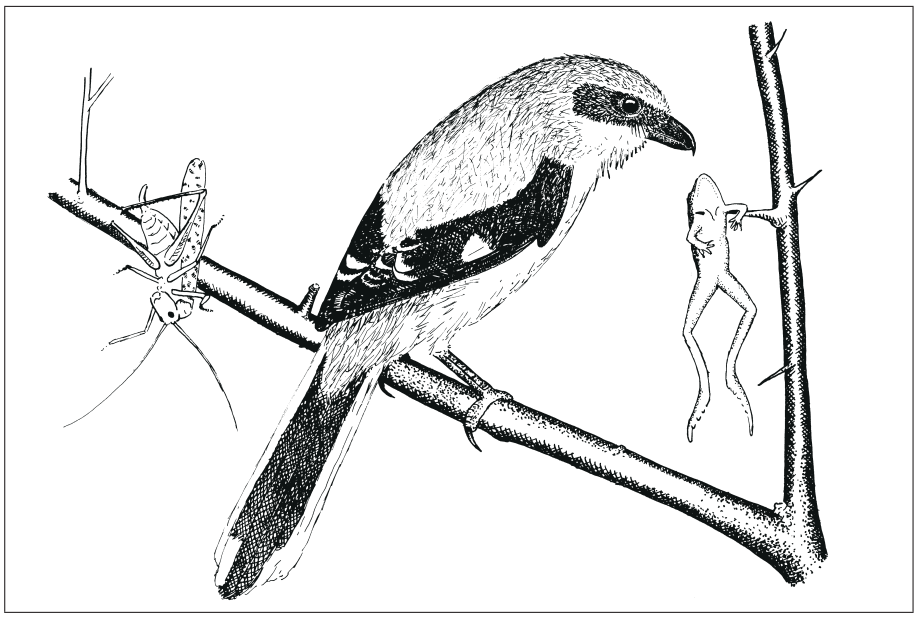

Figure 3.7: The great grey shrike *Lanius excubitor* hoards throughout the year, possibly to guard against bad luck when hunting. Many other shrikes do this as well.

The fungus *Aspergillus niger* only feeds on cellulose if no compounds are available that are easier to decompose. The relationship between food quality and physiological performance is discussed again in the treatment of food intake reconstructions {223}, dissipating heat {153} and adaptation {263}.

3.1.5 Food deposits and claims

Any general description of the feeding process must be approximate in nature. In this subsection I want to highlight briefly some important types of feeding behaviour that are likely to cause deviations from the hyperbolic functional response: stocking food and claiming resources via a territory. The importance of these types of behaviour is at the population level, where the effect is strongly stabilizing for two reasons. The first is that the predator lives on deposits if prey is rare, which lifts the pressure on the prey population under those conditions. The second one is that high prey densities in the good season do not directly result in an increase in predator density. This also reduces the predation pressure during the meagre seasons. Although the quantitative details are not worked out here because of species specificity, I want to highlight this behaviour as an introduction to other smoothing phenomena that are covered.

Many food deposits relate to survival during winter, frequently in combination with dormancy, cf. {231}. The hamster is famous for the huge piles of maize it stocks in autumn. In the German, Dutch and Scandinavian languages, the word 'hamster' is the stem of a verb meaning to stock food in preparation for adverse conditions. The English language has selected the squirrel for this purpose. This type of behaviour is much more widespread, for example in jays and shrikes, see Figure 3.7.

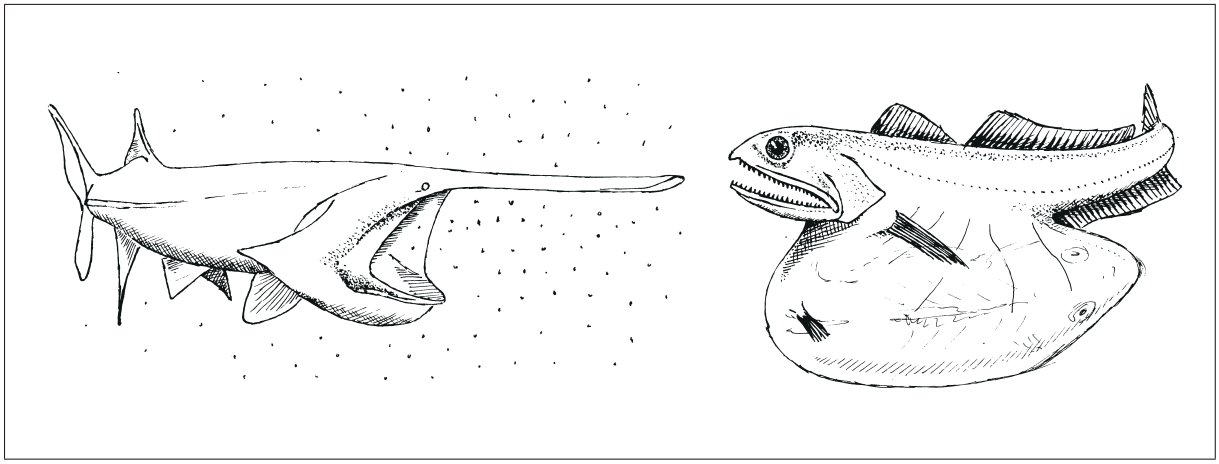

Figure 3.8: The 2 m paddlefish *Polyodon spathula* feeds on tiny plankters, while the 18 cm black swallower *Chiasmodon niger* can swallow fish bigger than itself. They illustrate extremes in buffer capacities of the stomach.

Many species defend territories just prior to and during the reproductive season. Birds do it most loudly. The size of the territories depends on bird as well as food density. One of the obvious functions of this behaviour is to claim a sufficient amount of food to fulfil the peak demand when the young grow up. The behaviour of stocking and reclaiming food typically fits 'demand' systems and is less likely to be found in 'supply' systems.

3.2 Digestion

Details of the digestion process are discussed on {239} because they do not bear directly on the specification of the DEB model. Logic of arguments requires, however, that some aspects of the digestion process are discussed here.

3.2.1 Smoothing and satiation

The capacity of the stomach/gut volume depends strongly on the type of food a species specializes on. Fish feeding on plankters, i.e. many small constantly available particles, have a low stomach capacity, while fish such as the swallower, which feed on rare big chunks of food (see Figure 3.8), have high stomach capacities. It may wait for weeks before a new chunk of food arrives. The stomach/gut volume, which is still 'environment' rather than animal, is used to smooth out fluctuations in nutritional input to the organism. Organisms attempt to run their metabolic processes under controlled and constant conditions. Food in the digestive tract and reserves inside the organism together make it possible for regulation mechanisms to ensure homeostasis. Growth, reproductive effort and the like do not depend directly on food availability but on the internal state of the organism. This even holds, to some extent, for those following the 'supply' strategy, where energy reserves are the key variable. These reserves rapidly follow the feeding conditions.

If the food in the stomach, M_s, follows a simple first-order process, the change of stomach contents is

$$\frac{d}{dt}M_s = \{\dot{J}_{Xm}\}V^{2/3}\left(f - \frac{M_s}{[M_{sm}]V}\right) \tag{3.4}$$

where $[M_{sm}]V$ is the maximum food capacity of the stomach. The derivation is as follows. A first-order process here means that the change in stomach contents can be written as $\frac{d}{dt}M_s = \dot{J}_X - t_s^{-1}M_s$, where the proportionality constant t_s^{-1} is independent of the input, given in (3.2). Since food density is the only variable in the input, t_s^{-1} must be independent of food density X, and thus of scaled functional response f. If food density is high, stomach content converges to its maximum capacity $\dot{J}_{Xm}t_s = \{\dot{J}_{Xm}\}V^{2/3}t_s$. The assumption of isomorphism implies that the maximum storage capacity of the stomach is proportional to the volume of the individual. This means that we can write it as $[M_{sm}]V$, where $[M_{sm}]$ is some constant, independent of food density and body volume. This allows one to express t_s^{-1} in terms of $[M_{sm}]$, which results in (3.4).

The mean residence time in the stomach is thus $t_s = V^{1/3}[M_{sm}]/\{\dot{J}_{Xm}\}$, and so it is proportional to length and independent of the ingestion rate. First-order dynamics implies complete mixing of food particles in the stomach, which is unlikely if fermentation occurs. This is because the residence time of each particle is then exponentially distributed, so a fraction $1-\exp\{-1\} = 0.63$ of the particles spends less time in the stomach than the mean residence time, and a fraction $1-\exp\{-\frac{1}{2}\} = 0.39$ less than half the mean residence time. This means incomplete, as well as over complete, and thus wasteful fermentation.

The extreme opposite of complete mixing is plug flow, where the variation in residence times between the particles is nil in the ideal case. Pure plug flow is not an option for a stomach, because this excludes smoothing. These conflicting demands probably separated the tasks of smoothing for the stomach and digestion for the gut to some extent. Most vertebrates do little more than create an acid environment in the stomach to promote protein fermentation, while actual uptake is via the gut. For a mass of food in the stomach of M_s, and in the gut of M_g, plug flow of food in the gut can be described by

$$\frac{d}{dt}M_g(t) = t_s^{-1}(M_s(t) - M_s(t-t_g)) \tag{3.5}$$

where t_g denotes the gut residence time and t_s the mean stomach residence time. This equation follows directly from the principle of plug flow. The first term, $t_s^{-1}M_s(t)$, stands for the influx from the stomach and follows from (3.4). The second one stands for the outflux, which equals the influx with a delay of t_g. Substitution of (3.4) and (3.2) gives $\frac{d}{dt}M_g(t) = \dot{J}_X(t) - \dot{J}_X(t-t_g) + \frac{d}{dt}M_s(t-t_g) - \frac{d}{dt}M_s(t)$. Since $0 \le M_s \le [M_{sm}]V$, $\frac{d}{dt}M_s \to 0$ if $[M_{sm}] \to 0$. So the dynamics of food in the gut reduces to $\frac{d}{dt}M_g(t) = \dot{J}_X(t) - \dot{J}_X(t-t_g)$ for animals without a stomach.

Some species feed in meals, rather than continuously, even if food is constantly available. They only feed when 'hungry' [228]. Stomach filling can be used to link feeding with satiation. From (3.4) it follows that the amount of food in the stomach tends to $M_s^* = f[M_{sm}]V$, if feeding is continuous and food density is constant. Suppose that feeding starts at a rate given by (3.2) as soon as food in the stomach is less than $\delta_{s0}M_s^*$, for some value of the dimensionless factor δ_{s0} between 0 and 1, and feeding ceases as soon as food in the

stomach exceeds $\delta_{s1} M_s^*$, for some value of $\delta_{s1} > \delta_{s0}$. The mean ingestion rate is still of the type (3.2), where $\{\dot{J}_{Xm}\}$ now has the interpretation of the *mean* maximum surface-area-specific ingestion rate, not the one during feeding. A consequence of this on/off switching of the feeding behaviour is that the periods of feeding and fasting are proportional to a length measure. This matter is taken up again on {221}.

3.2.2 Gut residence time

The volume of the digestive tract is proportional to the whole body volume in strict isomorphs. The fraction is $\simeq 11\%$ for ruminant and non-ruminant mammals [206] and $\simeq 2.5\%$ for daphnids if the whole space in the carapace is included [264]. If the animal keeps its gut filled to maximum capacity, $[M_{gm}]V$ say, and if the volume reduction due to digestion is not substantial, this gives a simple relationship between gut residence time of food particles t_g, ingestion rates $\dot{J}_X$, and body volume V

$$t_g = [M_{gm}]V/\dot{J}_X = \frac{V^{1/3}[M_{gm}]}{f\{\dot{J}_{Xm}\}} \tag{3.6}$$

This has indeed been found for daphnids [264], see Figure 3.9, and mussels [367]. Copepods [160] and carnivorous fish [451] seem to empty their gut at low food densities, which gives an upper boundary for the gut residence time. The gut residence time has a lower boundary of $V^{1/3}[M_{gm}]/\{\dot{J}_{Xm}\}$, which is reached when the throughput is at maximum rate.

Since ingestion rate, (3.2), is proportional to squared length, the gut residence time is proportional to length for isomorphs. For V1-morphs, which have a fixed diameter, ingestion rate is proportional to cubed length, (3.3), so gut residence time is independent of body volume.

Daphnids are translucent, which offers the possibility of studying the progress of digestion as a function of body length, see Figure 3.10.

3.3 Assimilation

The term 'assimilated' energy here denotes the free energy fixed into reserves; it equals the intake minus free energy in faeces and in all losses in relation to digestion. The energy in urine is included in assimilation energy, because urine does not directly derive from food and is excreted by the organism, cf. {127} and {145}. (Faeces is not excreted, because it has never been inside the organism.)

The assimilation efficiency of food is here taken to be independent of the feeding rate. This makes the assimilation rate proportional to the ingestion rate, which seems to be realistic, cf. Figure 7.15. I later discuss the consistency of this simple assumption with more detailed models for enzymatic digestion, {239}. The conversion efficiency of food into assimilated energy is written as $\{\dot{p}_{Am}\}/\{\dot{J}_{Xm}\}$, where $\{\dot{p}_{Am}\}$ is a diet-specific parameter standing for the maximum surface-area-specific assimilation rate. This notation may seem clumsy, but the advantage is that the assimilated energy that comes in at food density X is now given by $\{\dot{p}_{Am}\} f V^{2/3}$, where $f = X/(X_K + X)$ and V the body volume. It does not

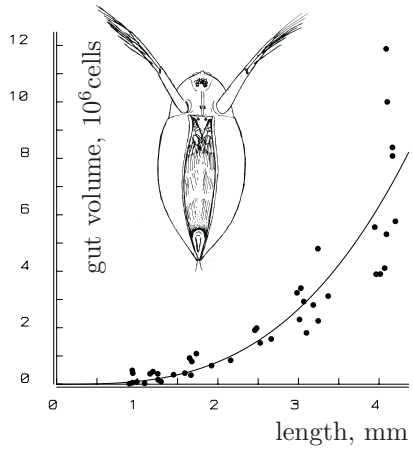

Figure 3.9: Gut volume is proportional to cubed length (right) and gut residence time is proportional to length (lower left), while the latter depends hyperbolically on food density (lower right), as illustrated for daphnids. The first two figures relate to *D. magna* feeding on the green alga *Scenedesmus* at 20 °C. Data from Evers and Kooijman [264]. The third one relates to a 2-mm *D. pulex* feeding on the diatom *Nitzschia actinastroides* at 15 °C. Data from Geller [314].

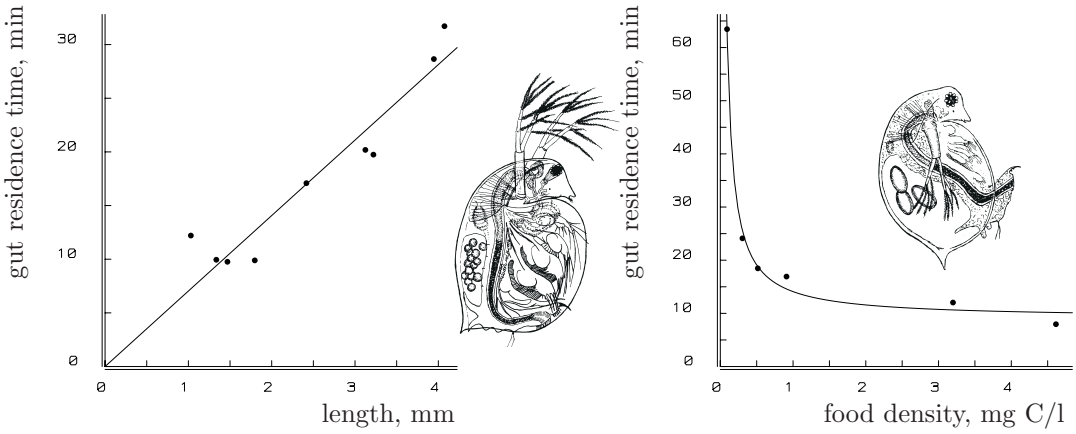

involve the parameter $\{\dot{J}_{Xm}\}$ in the notation, which turns out to be useful in the discussion of processes of energy allocation in the next few sections.

The conversion from substrate to energy in bacteria is substantially more efficient under aerobic (oxygen rich) conditions than under anaerobic ones, while metabolic costs are not affected by oxygen availability [525]. This means that the parameter $\{\dot{p}_{Am}\}$, and not $\{\dot{J}_{Xm}\}$, is directly relevant to the internal machinery, cf. {153}.

3.4 Reserve dynamics

Energy crossing the gut wall enters the blood or body fluid. Blood has a low capacity for energy (or nutrients), but a high transportation rate; it is pumped through the body many times an hour. It does not matter, therefore, where in the gut uptake takes place. Residence time of energy in the digestive tract is usually short compared to that in the energy reserves, which means that, for most practical purposes, the effect of digestion can simply be summarized as a conversion of ingested food, $\dot{J}_X = \{\dot{J}_{Xm}\} f V^{2/3}$ (in C-mole per time), into (assimilated) energy, $\dot{p}_A = \{\dot{p}_{Am}\} f V^{2/3}$ (in energy per time). The changes of energy in blood, E_{bl}, and in reserves, E, are coupled by $\frac{d}{dt} E_{bl} = \dot{p}_A - \frac{d}{dt} E - \dot{p}_C$, where $\dot{p}_C$ denotes the energy consumed by the bodily tissues and is called the catabolic power. The change in energy reserves can be positive or negative. Since the energy capacity of blood is

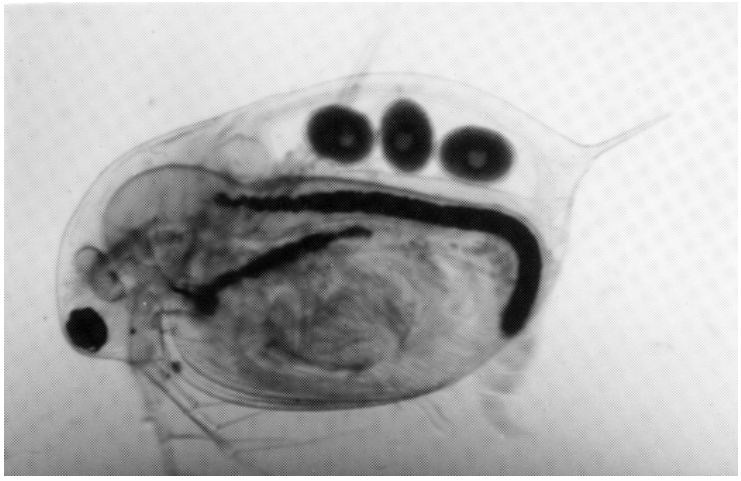

Figure 3.10: The photograph of *Daphnia magna* on the right shows the sharp transition between the chlorophyll of the green algae and the brown-black digestion products, which is typical for high ingestion rates. The relative position of this transition point depends on the ingestion rate, but not on the body length. Even in this respect daphnids are isomorphic. At low ingestion rates, the gut looks brown from mouth to anus. The paired digestive caecum is clearly visible just behind the mouth.

small, the change of energy in blood cannot have a significant impact on the whole body. It therefore seems safe to assume that $\frac{d}{dt}E_{bl} \simeq 0$, which means that the dynamics of the reserves can be written as $\frac{d}{dt}E = \dot{p}_A - \dot{p}_C$, as a very good approximation.

The dynamics of the reserves follows from three requirements: the reserve dynamics should be partitionable, the reserve density at steady state should not depend on structural body mass, and the use of reserves should not directly relate to food availability or allocation details. Since the reserve dynamics is a key element in the DEB theory, I pay due attention to the argumentation, motivation and implications for these requirements in this section.

The dynamics for the reserve density has to be set up first, in general form. It can be written as the difference between the volume-specific assimilation rate, $[\dot{p}_A]$, and some function of the state variables: the reserve density $[E] = E/V$ and the structural volume V. The freedom of choice for this function is greatly restricted by the requirement that $[E]$ at steady state does not depend on size, while $[\dot{p}_A] \propto V^{-1/3}$. It implies that the dynamics can be written as

$$\frac{d}{dt}[E] = [\dot{p}_A] - V^{-1/3}H([E]|\boldsymbol{\theta}) + ([E]^* - [E])G([E], V)$$

where $H([E]|\boldsymbol{\theta})$ is some function of $[E]$ and a set of parameters $\boldsymbol{\theta}$, that does not depend on V, and $G([E], V)$ some function of $[E]$ and V. The value $[E]^*$ represents the steady-state reserve density, which can be found from $\frac{d}{dt}[E] = 0$. Since $[E]^*$ depends on food density via the assimilation power $[\dot{p}_A]$, the requirement that the rate of use of reserves should not depend on food density implies that $G([E], V) = 0$.

The requirement that the reserve density at steady state does not depend on V is motivated by the homeostasis assumption, now applied to the biomass as a whole (reserves *and* structural biomass). This is the weak homeostasis assumption.

The mass balance for the reserve density can be written as

$$\frac{d}{dt}[E] = [\dot{p}_A] - [\dot{p}_C] - [E]\frac{d}{dt}\ln V \tag{3.7}$$

The volume-specific assimilation rate is given by $[\dot{p}_A] = \dot{p}_A/V = f\{\dot{p}_{Am}\}V^{-1/3}$, and $[\dot{p}_C]$ is the volume-specific catabolic flux, which is some function of the state variables $[E]$ and V. The third term stands for the dilution by growth, which directly follows from the chain rule for differentiation of E/V. Because maintenance (work) and growth are among the destinations of catabolic energy, one can write $\kappa([E], V)\dot{p}_C = \dot{p}_M + [E_G]\frac{d}{dt}V$, or $\frac{d}{dt}V = (\kappa([E], V)\dot{p}_C - \dot{p}_M)/[E_G]$, where $\dot{p}_M$, which is some function of V, denotes the maintenance costs and $[E_G]$ is the volume-specific costs of structure. The latter is a constant in keeping with the homeostasis assumption for structural mass. The fraction $\kappa([E], V)$ is, at this stage in the reasoning, some function of the state variables. Substitution of the expression for growth into (3.7) results in

$$\frac{d}{dt}[E] = [\dot{p}_A] - [\dot{p}_C](1 + \kappa[E]/[E_G]) + [E][\dot{p}_M]/[E_G] \tag{3.8}$$

Since the reserve density dynamics must be of the form $\frac{d}{dt}[E] = [\dot{p}_A] - V^{-1/3}H([E]|\boldsymbol{\theta})$, as shown above, the volume-specific catabolic flux can now be written as

$$[\dot{p}_C] = \frac{V^{-1/3}H([E]|\boldsymbol{\theta}) + [E][\dot{p}_M](V)/[E_G]}{1 + \kappa([E], V|\boldsymbol{\theta})[E]/[E_G]} \tag{3.9}$$

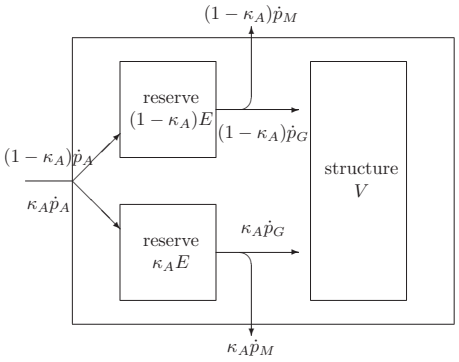

The third requirement, that of partitionability of reserve kinetics, is now used. By this I mean that the partitioning of reserves should not affect its dynamics, i.e. the sum of the dynamics of the partitioned reserves should be identical to that of the lumped one in terms of growth, maintenance, development and reproduction. The requirement originates from the fact that the reserves are generalized compounds, i.e. mixtures of various kinds of proteins, lipids, etc. Each of these compounds follows its own kinetics, which are functions of the amounts of that compound and of structural mass. The assumption that the system has only two state variables, reserves and structural mass, implies that all reserve components have identical kinetics. The strong homeostasis assumption ensures that the amount of any particular compound of the reserves is a fixed fraction, say κ_A, of the total amount of reserves. This compound must account for a fraction κ_A of the maintenance costs and growth investment, see figure, or we would end up with a more-reserve model, rather than a single-reserve model; this is a basic limitation of single-reserve models. Most physiologists would be inclined to let various fractions of the reserves, such as lipids and proteins, contribute differently to the maintenance and structure costs. The homeostasis assumption for reserves implies that this difference in treatment of fractions is only possible in models with more than one reserve, which is discussed later {168}.

The partitionability requirement represents basically a consistency argument that is inherent to the concept of generalized compound. Any whole organism model that specifies the kinetics of a set of chemical compounds but does *not* obey the partitionability requirement suffers from a serious problem: if, some day, we improve our experimental techniques

and separate a particular compound into two new chemical species, both playing a role in storage dynamics, this would affect the model structure. Properties of specific chemicals can only be taken into account in a physiological model if it deals with *all* relevant chemicals, which seems hopelessly complex to me. (Ecosystem models should not deal with individual species for the same reason.)

The partitionability requirement translates quantitatively into

$$\kappa_A[\dot{p}_C]([E], V|[\dot{p}_M], [E_G], \boldsymbol{\theta}) = [\dot{p}_C](\kappa_A[E], V|\kappa_A[\dot{p}_M], \kappa_A[E_G], \boldsymbol{\theta})$$

for an arbitrary factor κ_A in the interval $(0, 1)$. This factor not only applies to $[E]$, but also to two parameters, the specific maintenance $[\dot{p}_M]$ and structure costs $[E_G]$, because the different fractions of the reserves contribute to these costs. The factor does not apply to V and the parameters $\boldsymbol{\theta}$. We can check in (3.9) that $[\dot{p}_C]$ is partitionable if

- the function H is a first-degree homogeneous function, which means that $\kappa_A H([E]|\boldsymbol{\theta}) = H(\kappa_A[E]|\boldsymbol{\theta})$. It follows that this function can be written as $H([E]) = \dot{v}[E]$, for some constant $\dot{v}$.

- the function κ is a zero-th degree homogeneous function in E, which means that $\kappa(\kappa_A[E], V) = \kappa([E], V)$. In other words: κ may depend on V, but not on $[E]$. Later, I argue that $\kappa(V)$ is a rather rudimentary function of V, namely a constant, see {87}.

Substitution of the function H in the reserve density dynamics gives $\frac{d}{dt}[E] = [\dot{p}_A] - \dot{v}[E]V^{-1/3}$, and the reserve density at steady state is $[E]^* = V^{1/3}[\dot{p}_A]/\dot{v} = f\{\dot{p}_{Am}\}/\dot{v}$. The maximum reserve density at steady state occurs at $f = 1$, which gives the relationship $[E_m] = \{\dot{p}_{Am}\}/\dot{v}$, or $\dot{v} = \{\dot{p}_{Am}\}/[E_m]$. As $\dot{v}$ shows up time and again, I have given it a name, *energy conductance*, a result of one of many discussions with R. M. Nisbet. Its dimension is length per time and it stands for the ratio of the maximum surface-area-specific assimilation rate to the maximum volume-specific reserve energy density. The inverse, $\dot{v}^{-1}$, has the interpretation of a resistance. Conductances are often used in applied physics. Therefore, it is remarkable that the biological use of conductance measures seems to be restricted to plant physiology [455,670] and neurobiology [537]. This is probably due to the wide application of allometric functions in animal physiology, which are hard to combine with physics.

The conclusion is that the partitionability and homeostasis requirements lead to a simple first-order dynamics for the reserve density

$$\frac{d}{dt}[E] = \frac{\{\dot{p}_{Am}\}}{V^{1/3}}\left(f - \frac{[E]}{[E_m]}\right) \quad \text{or} \tag{3.10}$$

$$\frac{d}{dt}e = \frac{\dot{v}}{V^{1/3}}(f - e) \tag{3.11}$$

where the scaled reserve density $e = [E]/[E_m]$ is a dimensionless quantity, which will be used frequently.

The storage dynamics (3.10) results in the catabolic rate

$$\dot{p}_C = \dot{p}_A - V\frac{d}{dt}[E] - [E]\frac{d}{dt}V = [E](\dot{v}V^{2/3} - \frac{d}{dt}V) \tag{3.12}$$

An important property of the catabolic rate is that it does not depend directly on the assimilation rate and, therefore, not on food density. It only depends on the volume of the organism and energy reserve.

The storage residence time in (3.10) is thus $V^{1/3}/\dot{v}$, which must be large with respect to that of the stomach, $V^{1/3}[M_{sm}]/\{\dot{J}_{Xm}\}$ and the gut, $V^{1/3}[M_{gm}]/\{\dot{J}_{Xm}\}$, to justify neglecting the smoothing effect of the digestive tract.

If the energy reserve capacity, $[E_m]$, is extremely small, the dynamics of the reserves degenerates to $[E] = f[E_m]$, while both $[E]$ and $[E_m]$ tend to 0. The utilization rate then becomes $\dot{p}_C = \{\dot{p}_{Am}\}fV^{2/3}$. This case has been studied by Metz and Diekmann [623], but some consistency problems arise in variable environments, cf. {360}.

The storage dynamics for V0- and V1-morphs can be found from that of isomorphs by multiplying $\{\dot{p}_{Am}\}$ with the shape correction function $\mathcal{M}(V)$ (2.1) and (2.2), {27}. The scaled reserve density kinetics then becomes

$$\text{V0:} \quad \frac{d}{dt}e = (f-e)\dot{v}V_d^{2/3}/V \tag{3.13}$$

$$\text{V1:} \quad \frac{d}{dt}e = (f-e)\dot{v}/V_d^{1/3} = (f-e)\dot{k}_E \tag{3.14}$$

The reserve turnover rate $\dot{k}_E = [\dot{p}_{Am}]/[E_m]$, for $[\dot{p}_{Am}] = \{\dot{p}_{Am}\}V_d^{-1/3}$, is introduced for V1-morphs to simplify the notation, because it will appear frequently; it has dimension 'per time'.

An essential difference between stomach and reserves dynamics is that the first is in absolute quantities, because it relates to bulk transport, while the latter is in densities because of the homeostasis requirement. (One cannot simply divide by body volume in (3.4) to turn to densities because body volume depends on time. One should, therefore, correct for growth to observe the mass conservation law.) Note that the requirement of homeostasis for energy density is not consistent with the interpretation of reserve dynamics in terms of a simple mechanism where reserve 'molecules' react with the catabolic machinery at a rate given by the law of mass action. (This mechanism is attractive because the density of the catabolic machinery is constant, due to the concept of homeostasis.) The resulting model, known as first-order kinetics (for amounts, not for densities!), is very popular in chemistry. The organism has to adjust the reaction rate between reserves and the catabolic machinery during growth to preserve homeostasis. These adjustments are small, as long as dilution of energy density by growth is small with respect to the use of energy, i.e. if $\frac{d}{dt}\ln V \ll \dot{v}V^{-1/3}$. In practice, this condition is usually fulfilled in animals, but not necessarily in unicellulars. A more realistic mechanism, based on the structural homeostasis concept (see {246}), helps us to understand why first-order dynamics for reserve densities also applies to unicellulars.

Under conditions of prolonged starvation, organisms can deviate from the standard reserve kinetics, as is discussed on {227}.

3.5 The κ-rule for allocation

Some animals, such as birds, first reproduce long after having obtained their final size. Others, such as daphnids, continue to grow after the onset of reproduction. *Daphnia magna* starts to reproduce at a length of 2.5 mm, while its ultimate size is 5–6 mm, if well-fed. This means an increase of well over a factor eight in volume during the reproductive period. Figure 3.11 illustrates a basic problem for the energy allocation rules that such animals pose. It becomes visible as soon as one realizes that a considerable amount of energy is invested in reproductive output. The volume of young produced exceeds one-quarter of that of the mother each day, or 80% of the catabolic rate [764]. The problem is that growth is not retarded in animals crossing the 2.5 mm barrier; they do not feed much more and simply follow the surface area rule with a fixed proportionality constant at constant food densities; they do not change sharply in respiration, so it seems unlikely that they digest their food much more efficiently. So where does the energy allocated to reproduction come from?

A solution to this problem can be found in development. Juvenile animals have to mature and become more complex. They have to develop new organs and install regulation systems. The increase in size (somatic growth) of the adult does not include an increase in complexity. The energy spent on development in juveniles is spent on reproduction in adults. This switch does not affect growth and suggests the 'κ-rule': a fixed proportion κ of energy utilized from the reserves is spent on growth plus maintenance, the remaining portion $1-\kappa$ on development plus reproduction. The partitionability of reserve kinetics has led to the conclusion that κ cannot depend on the reserve density (see {85}). The argument that allocation is an intensive process, not an extensive one, suggests that κ is independent of V as well.

The mechanistic background and rationale of the κ-rule is as follows. At separated sites along the path the blood follows, somatic cells and ovary cells pick up energy. The only information the cells have is the energy content of the blood and body size, cf. {25}. They do not have information about each other's activities in a direct way. This also holds for the mechanism by which energy is added to or taken from energy reserves. The organism only has information on the energy density of the blood, and on size, but not on which cells have removed energy from the blood. This is why the parameter κ does not show up in the dynamics of energy density. The activity of all carriers that remove energy from the body fluid and transport it across the cell membrane depends, in the same way, on the energy density of the fluid. Somatic cells and ovary cells both may use the same carriers, but the concentration in their membranes may differ so that $1-\kappa$ may differ from the ratio of ovary to body weight. This concentration of active carriers is controlled, by hormones for example, and depends on age, size and environment. Once in a somatic cell, energy is first used for maintenance, the rest is used for growth. This makes maintenance and growth compete directly, while development and reproduction compete with growth plus maintenance at a higher level. The κ-rule makes growth and development parallel processes that interfere only indirectly, as is discussed by Bernardo [73], for instance.

If conditions are poor, the system can block allocation to reproduction, while maintenance and growth continue to compete in the same way, see {227}. I explain on {177}

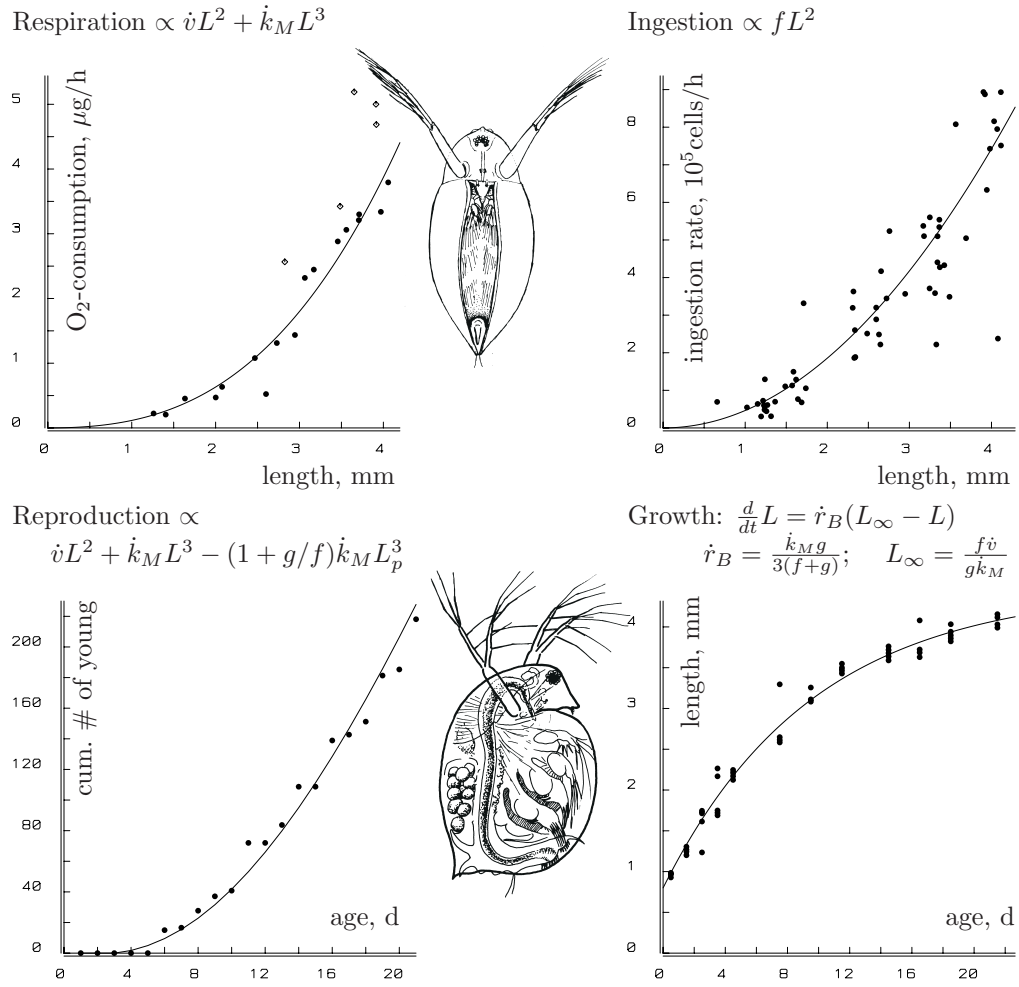

Figure 3.11: Respiration (upper left), and ingestion (upper right) as a function of body length, and reproduction (lower left) and body length (lower right) as function of age in the waterflea *Daphnia magna* at 20 °C. Original data and from [264,520]; the DEB model specifies the curves. The reproduction curve shows that *D. magna* starts to reproduce at the age of 7 d, i.e. when its length exceeds 2.5 mm. However, respiration, and ingestion do not increase steeply at this size, nor does growth decrease. Where did the substantial reproductive energy come from? The answer leads to the κ-rule. The open symbols in the graph for respiration relate to individuals with eggs in their brood pouch.

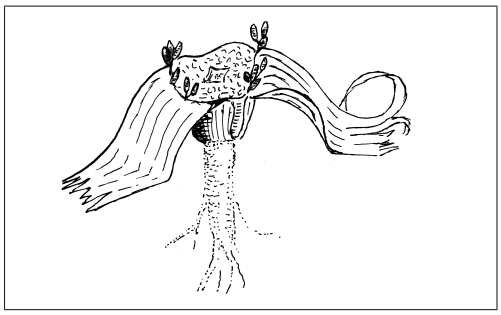

Figure 3.12: The leaves of most plant species grow during a relatively short time period, and are shed yearly, after the plant has recovered useful compounds. The leaves of some species, however, such as *Welwitschia mirabilis*, grow and weather continuously. The life span of this remarkable gymnosperm can exceed 2000 years. Leaves have a very limited functional life span, but plants have found different ways to deal with that problem.

that Huxley's allometric model for relative growth closely links up with the κ-rule.

It is important to realize that although the fraction of utilized energy spent on maintenance plus growth remains constant, the absolute size of the flow tends to increase during development at constant food densities, as does the energy flow to maintenance plus growth.

The κ-rule solves quite a few problems from which other allocation rules suffer. Although it is generally true that reproduction is maximal when growth ceases, a simple allocation shift from growth to reproduction leaves similarity of growth between different sexes unexplained, since the reproductive effort of males is usually much less than that of females. The κ-rule implies that size control is the same for males and females and for organisms such as yeasts and ciliates, which do not spend energy on reproduction but do grow in a way that is comparable to species that reproduce; see Figure 1.1. Strong support for the κ-rule comes from situations where the value for κ is changed to a new fixed value. Such a simple change affects reproduction as well as growth and so food intake in a very special way. Parasites such as the trematod *Schistosoma* in snails harvest all energy to reproduction and increase κ to maximize the energy flow they can consume, cf. {295}. Parasite-induced gigantism, coupled to a reduction of the reproductive output, is also known from trematod-infested chaetognats [652], for instance. The daily light cycle also affects the value for κ in snails, and the allocation behaviour during prolonged starvation; see {227}. The effect of some toxic compounds can be understood as an effect on κ, as is discussed on {209}.

3.6 Maintenance

The notion of maintenance costs for advanced taxa is probably as old as mankind. Duclaux [238] was the first to recognize, in 1898, that maintenance costs should be separated from production costs to understand the energetics of micro-organisms. The next reference to maintenance costs for micro-organisms stems from Sherris *et al.* [832] in 1957, in relation to mobility. In the early 1960s maintenance costs for micro-organisms received considerable attention [400,476,592,608,690,716].

Maintenance stands for a collection of processes necessary to 'stay alive'. More precisely, maintenance energy is defined as the (mean) energy requirement of an organism, excluding investments in the production processes of growth of structural mass, reproduction and development. However, all these processes have overhead costs, with which excreted

products can be associated, cf. {147}. The quantification of new structural mass or mass of offspring does not necessarily quantify the investments in these processes. Maintenance costs are species-specific and depend on the size of the organism and on body temperature.

As is customary, I use the term 'metabolism' or 'respiration' to cover non-maintenance processes as well. The realization that respiration includes growth leads, I think, to the solution of a long-standing problem: the acceptance that maintenance energy is proportional to biovolume, while metabolism or respiration is about proportional to volume to the power 0.75. I discuss this further in the section on respiration, {135}.

Maintenance costs are here taken to be independent of the growth rate. Tempest and Neijssel [911] argued that the concentration gradients of potassium and glutamic acid can involve a substantial energy requirement in prokaryotes. However, the concentrations of these compounds vary markedly with growth rate so that this energy drain is not taken to be part of maintenance here, but as part of the overhead costs of the growth process. The high costs of potassium gradients is at odds with Ling's association-induction hypothesis [561], which states that virtually all potassium in living cells exists in an absorbed state. The mechanism is via a liquid crystal type of structure for the cytoplasm [127].

As explained in the discussion of the κ-rule, {87}, development is excluded from maintenance, as it relates (partly) to a type of production process. The maintenance part of development is referred to as maturity maintenance, and is discussed in the section on development, {111}. To distinguish maturation maintenance from other maintenance costs, the latter will be called costs for somatic maintenance, if necessary.

As stated on {37}, no maintenance costs are paid over reserves. The empirical justification can most easily be illustrated by the absence of respiration in freshly laid eggs, which consist almost entirely of reserves; see Figure 3.15. The logical justification is that reserves have an intrinsic turnover; the costs are covered by overheads in assimilation and utilization. Although the difference between turnover costs for reserves and structural biomass is subtle, eggs show that the turnover costs for reserves are not equivalent to maintenance for reserves, since they do not respire when freshly laid.

Maintenance costs can generally be decomposed in contributions that are proportional to structural body volume, and to surface area.

3.6.1 Volume-related maintenance costs

Maintenance processes include the maintenance of concentration gradients across membranes, the turnover of structural body proteins, a certain (mean) level of muscle tension and movement, and the (continuous) production of hairs, feathers, scales, leaves (of trees), see Figure 3.12.

The idea that maintenance costs are proportional to biovolume is simple and rests on homeostasis: a metazoan of twice the volume of a conspecific has twice as many cells, which each use a fixed amount of energy for maintenance. A unicellular of twice the original volume has twice as many proteins to turn over. Protein turnover seems to be low in prokaryotes [499]. Another major contribution to maintenance costs relates to the maintenance of concentration gradients across membranes. Eukaryotic cells are filled with membranes, and this ties the energy costs for concentration gradients to volume. (The

argument for membrane-bound food uptake works out differently in isomorphs, because feeding involves only the outer membrane directly.) Working with mammals, Porter and Brand [728] argued that proton leak in mitochondria represents 25% of the basal respiration in isolated hepatocytes and may contribute significantly to the standard metabolic rate of the whole animal. Prokaryotes usually have an outer membrane only. Concentration gradients across the outer membrane involve maintenance costs that relate to surface areas of cells. Since prokaryotes approximately behave as V1-morphs, this hardly matters from a quantitative perspective.

The energy costs of movement are also taken to be proportional to volume if averaged over a sufficiently long period. Costs of muscle tension in isomorphs are likely to be proportional to volume, because they involve a certain energy investment per unit volume of muscle. In the section on feeding, I discuss briefly the energy involved in movement, {73}, which has a standard level that includes feeding. This can safely be assumed to be a small fraction of the total maintenance costs. Sustained powered movement such as in migration requires special treatment. Such activities involve temporarily enhanced metabolism and feeding. The occasional burst of powered movement hardly contributes to the general level of maintenance energy requirements. Sustained voluntary powered movement seems to be restricted to humans and even this seems of little help in getting rid of weight!

There are many examples of species-specific maintenance costs. Daphnids produce moults every other day at 20 °C. The synthesis of new moults occurs in the intermoult period and is a continuous and slow process. The moults tend to be thicker in the larger sizes. The exact costs are difficult to pin down, because some of the weight refers to inorganic compounds, which might be free of energy cost. Larvaceans produce new feeding houses every 2 hours at 23 °C [274], and this contributes substantially to organic matter fluxes in oceans [15,16,198]. These costs are taken to be proportional to volume. The inclusion of costs of moults and houses in maintenance costs is motivated by the observation that these rates do not depend on feeding rate [274,513], but only on temperature.

The maintenance costs, $\dot{p}_M$, are thus taken to be proportional to volume

$$\dot{p}_M = [\dot{p}_M]V \tag{3.15}$$

The volume-specific costs of maintenance, $[\dot{p}_M]$, can be allocated to a variety of processes that together are responsible for these costs.

3.6.2 Surface-area-related maintenance costs

Some specialized maintenance costs relate to surface areas of individuals.

Osmosis

Aquatic insects are chemically fairly well isolated from the environment. Euryhaline fishes, however, have to invest energy in osmoregulation when in waters that are not iso-osmotic. The cichlid *Oreochromis niloticus* is iso-osmotic at 11.6 °/$_{\circ\circ}$ and 29% of the respiration

rate at 30 °/₀₀ can be linked to osmoregulation [1016]. Similar results have been obtained for the brook trout *Salvelinus fontinalis* [303].

Homeothermy

Heat is a side product of all uses of energy, cf. {153}. In ectotherms, this heat simply dissipates without increasing the body temperature above that of the environment to any noticeable amount as long as the temperature is sufficiently low. If the environmental temperature is high, as in incubated bird eggs just prior to hatching, metabolic rates are high as well, releasing a lot more energy in the form of heat, which increases the body temperature even further, cf. {258}. This is called positive feedback in cybernetics. The rate of heat dissipation obviously depends on the degree of insulation and is directly related to surface area.

A small number of species, known as endotherms, use energy to maintain their body temperature at a predetermined high level, 27 °C in sloths, 34 °C in monothremes, 37 °C in most mammals, 39 °C in non-passerine birds, 41 °C in passerine birds. Mammals and birds change from ectothermy to endothermy during the first few days of their juvenile stage. Some species temporarily return to the ectothermic state or partly so at night (hummingbirds, insectivores) or during hibernation (poorwills [559], rodents, bats) or dry seasons (tenrecs, cf. {231}). Not all parts of the body are kept at the target temperature, especially not the extremities. The naked mole rat *Heterocephalus glaber* (see Figure 3.13) has a body temperature that is almost equal to that of the environment [569] and actually behaves as an ectotherm. Huddling in the nest plays an important role in the thermoregulation of this colonial species [1010]. The body temperature of the Grant's golden mole *Eremitalpa granti* normally matches that of the sand in which it lives, but it is able to maintain the diurnal cycle if the temperature of the sand is kept constant [570].

Many ectotherms can approach the state of homeothermy under favourable conditions by walking from shady to sunny places, and back, in an appropriate way. In an extensive study of 82 species of desert lizards from three continents, Pianka [709] found that body temperature T_b relates to ambient air temperature T_e as

$$T_b = 311.8 + (1 - \beta)(T_e - 311.8)$$

where β stands for the species-specific thermoregulatory capacity, spanning the full range from perfect regulation, $\beta = 1$, for active diurnal heliothermic species, to no regulation, $\beta = 0$, for nocturnal thigmothermic species. The target temperature of 311.8 K or 38.8 °C varies somewhat between the different sub-groups and is remarkably close to that of mammals. Many species of plants enhance the interception of radiation by turning their flowers to the moving sun. The parabolic shape of flowers helps to focus radiation on the developing ovum. Sunflowers, *Helianthus annuus*, follow the sun with their leaves and developing inflorescence, but when the flowers open they are oriented towards the east [543]. This probably relates to thermoregulation.

Several species can raise their temperature over 10 °C above that of the environment (bumble bees and moths [392], tuna fish, mackerel shark, leatherback turtles). Some species of *Arum*, which live in dark forests, heat their flowers metabolically. These examples

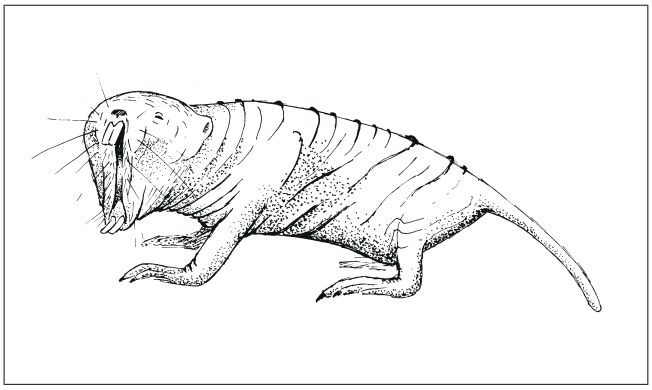

Figure 3.13: The naked mole rat *Heterocephalus glaber* (30 gram) is one of the few mammals that are essentially ectothermic. They live underground in colonies of some 60 individuals. The single breeding female suppresses reproductive development of all 'frequent working' females and of most 'infrequent working' females, a social system that reminds us of termites [571].

do make it clear that energy investment in heating is species-specific and that the regulation of body temperature is a different problem.

The 'advantages' of homeothermy are that enzymes can be used that have a narrow tolerance range for temperatures and that activity can be maintained at a high level independent of environmental temperature. At low temperatures ectotherms are easy prey for endotherms. Development and reproduction are enhanced, which opens niches in areas with short growing seasons that are closed to ectotherms. The costs depend on the environmental temperature, insulation and body size. If temperature is high and/or insulation is excellent and/or body size is large, there may be hardly any additional costs of heating; the range of temperatures to which this applies is called the thermo-neutral zone.

The costs of heating, $\dot{p}_T$, due to losses by convection or conduction can be written as

$$\dot{p}_T = \{\dot{p}_T\} V^{2/3} \tag{3.16}$$

Heat loss is not only proportional to surface area but, according to I. Newton, also to the temperature difference between body and environment. This is incorporated in the concept of thermal conductance $\{\dot{p}_T\}/(T_e - T_b)$, where T_e and T_b denote the temperature of the environment and the body. It is about 5.43 $\mathrm{J\,cm^{-2}\,h^{-1}\,{}^{\circ}C^{-1}}$ in birds and 7.4–9.86 $\mathrm{J\,cm^{-2}\,h^{-1}\,{}^{\circ}C^{-1}}$ in mammals, as calculated from [402]. The unit $\mathrm{cm^{-2}}$ refers to volumetric squared length, not to real surface area which involves shape. The values represent crude means in still air. The thermal conductance is roughly proportional to the square root of wind speed.

This is a simplified presentation. Birds and mammals moult at least twice a year, to replace their hair and feathers which suffer from wear, and change the thick winter coat for the thin summer one. Cat owners can easily observe that when their pet is sitting in the warm sun, it will pull its hair into tufts, especially behind the ears, to facilitate heat loss. Many species have control over blood flow through extremities to regulate temperature. People living in temperate regions are familiar with the change in the shape of birds in winter to almost perfect spheres. This increases insulation and generates heat from the associated tension of the feather muscles. These phenomena point to the variability of thermal conductance.

There are also other sources of heat exchange, through ingoing and outgoing radiation and cooling through evaporation. Radiation can be modulated by changes in colour, which

chameleons and tree frogs apply to regulate body temperature [569]. Evaporation obviously depends on humidity and temperature. For animals that do not sweat, evaporation is tied to respiration and occurs via the lungs. Most non-sweaters pant when hot and lose heat by enhanced evaporation from the mouth cavity. A detailed discussion of heat balances would involve a considerable number of coefficients [640,871], and would obscure the main line of reasoning. I discuss heating in connection with the water balance on {153}. It is important to realize that all these processes are proportional to surface area, and so affect the heating rate $\{\dot{p}_T\}$ and in particular its relationship with the temperature difference between body and environment.

3.7 Growth

The growth rate follows from the assumptions that have already been introduced. The κ-rule states that a fixed fraction of catabolic power is spent on somatic maintenance and growth, so

$$\kappa \dot{p}_C = [E_G] \frac{d}{dt} V + \dot{p}_M + \dot{p}_T \tag{3.17}$$

where $[E_G]$ denotes the volume-specific costs of structure, which are taken as fixed in view of homeostasis of the structural biomass. These costs thus include all types of overheads, not just the costs of synthesis. There are no costs of heating for ectotherms, so $\dot{p}_T = 0$. Substitution of (3.12), (3.15) and (3.16) gives

$$\frac{d}{dt} V = \dot{v} \frac{V^{2/3}[E]/[E_m] - V^{2/3}(V_h/V_m)^{1/3} - V/V_m^{1/3}}{[E]/[E_m] + g} \tag{3.18}$$

Note that growth does not depend on food density directly. It only depends on reserve density and body volume. The energy parameters combine in the compound parameters V_h, V_m, g and $\dot{v}$. The compound parameters appear frequently, so they are best introduced here. To aid memory, I gave them names.

The *maintenance rate constant* $\dot{k}_M \equiv [\dot{p}_M]/[E_G]$ was introduced by Marr *et al.* [592] and publicized by Pirt [716], and stands for the ratio of costs of maintenance to biovolume synthesis. It has dimension time^{-1}. It remains hidden here in the maximum volume V_m, but it frequently plays an independent role.

The *investment ratio* $g \equiv [E_G]/\kappa[E_m]$ stands for the costs of new biovolume relative to the maximum potentially available energy for growth plus maintenance. It is dimensionless.

The *maximum volume* $V_m \equiv (\frac{\dot{v}}{g\dot{k}_M})^3 = (\kappa\{\dot{p}_{Am}\}/[\dot{p}_M])^3$ applies to ectotherms. Endotherms cannot reach this volume because they lose energy through heating. The comparison of species is based on this relationship between maximum volume and energy budget parameters and is the core of the relationship between body size and physiological variables together with the invariance property of the DEB model, to be discussed later, {267}.

The *heating volume* $V_h \equiv (\{\dot{p}_T\}/[\dot{p}_M])^3$ stands for the reduction in volume endotherms experience due to the energy costs of heating. It can be treated as a simple parameter as long as the environmental temperature remains constant. Sometimes, it will prove to

be convenient to work with the scaled heating length $l_h \equiv (V_h/V_m)^{1/3}$ as a compound parameter. If the temperature changes slowly relative to the growth rate, the heating volume is just a function of time. If environmental temperature changes rapidly, body temperature can be taken to be constant again while the effect contributes to the stochastic nature of the growth process, cf. {221}. Note that (3.18) shows that the existence of a heating volume is not an extra assumption, but a consequence of the volume-bound maintenance costs and the surface-area-bound input and heating costs.

If food density X and, therefore, the scaled functional response f are constant, and if the initial energy density equals $[E] = f[E_m]$, energy density will not change. Volumetric length as a function of time since hatching where $V(0) \equiv V_b$ can then be solved from (3.18)

$$\frac{d}{dt}V^{1/3} = \frac{\dot{v}}{3(f+g)}\left(f - (V_h/V_m)^{1/3} - (V/V_m)^{1/3}\right) \tag{3.19}$$

$$V^{1/3}(t) = V_\infty^{1/3} - (V_\infty^{1/3} - V_b^{1/3})\exp\{-t\dot{r}_B\} \quad \text{or} \tag{3.20}$$

$$t(V) = \frac{1}{\dot{r}_B}\ln\frac{V_\infty^{1/3} - V_b^{1/3}}{V_\infty^{1/3} - V^{1/3}} \tag{3.21}$$

I will follow tradition and call this curve the von Bertalanffy growth curve despite its earlier origin and von Bertalanffy's contribution of introducing allometry, which I reject; see {13}. The von Bertalanffy growth rate equals

$$\dot{r}_B \equiv (3/\dot{k}_M + 3fV_m^{1/3}/\dot{v})^{-1} \tag{3.22}$$

and the ultimate volumetric length

$$V_\infty^{1/3} \equiv fV_m^{1/3} - V_h^{1/3} \tag{3.23}$$

Time t in (3.20) is measured from hatching or birth. (Note that time and age are not the same.) The von Bertalanffy growth curve results for isomorphs at constant food density and temperature and has been fitted successfully to the data of some 270 species from many different phyla; see Table 8.2 and [515]. The gain in insight since A. Pütter's original formulation in 1920 [740] is in the interpretation of the parameters in terms of underlying processes. It appears that heating costs do not affect the von Bertalanffy growth rate $\dot{r}_B$. Being a rate, high temperature does elevate it, of course. Food density affects both the von Bertalanffy growth rate and the ultimate volume. The inverse of the von Bertalanffy growth rate is a linear function of the ultimate volumetric length; see Figure 3.14. This is in line with Pütter's original formulation, which took this rate to be inversely proportional to ultimate length, as has been proposed again by Gallucci and Quinn [309].

The requirement that food density is constant for a von Bertalanffy curve can be relaxed if food is abundant, because of the hyperbolic functional response. As long as food density is higher than four times the saturation coefficient, food intake is higher than 80% of the maximum possible food intake, which makes it hardly distinguishable from maximum food intake. Since most birds and mammals have a number of behavioural traits aimed at guaranteed adequate food availability, they appear to have a fixed volume–age relationship. This explains the popularity of age-based models for growth in 'demand' systems. Later, on

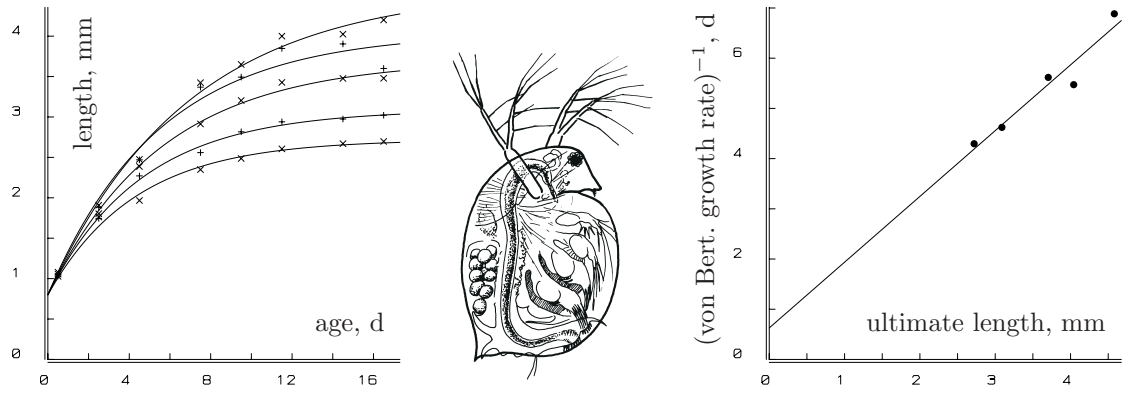

Figure 3.14: The left figure shows the length-at-age data of the waterflea *Daphnia magna* for various densities of the green alga *Chlorella* at 20 °C with von Bertalanffy growth curves. Data from [513]. The inverses of the estimated von Bertalanffy growth rates, $\dot{r}_B^{-1}$, are plotted against estimated ultimate lengths (right). The expected relationship is $\dot{r}_B^{-1} = 3/\dot{k}_M + 3\delta_{\mathcal{M}} L_\infty/\dot{v}$. The least-squares-fitted line gives estimates for the energy conductance $\dot{v}/\delta_{\mathcal{M}} = 2.29$ mm d^{-1} and for the maintenance rate constant $\dot{k}_M = 4.78$ d^{-1}, both of which seem to be too high in comparison with other species. Frequent moulting may contribute to the maintenance costs and so to the high estimate of the maintenance rate coefficient $\dot{k}_M$.

{258}, I discuss deviations from the von Bertalanffy growth curve that can be understood in the context of the present theory.

In contrast, at low food densities, fluctuations in food density soon induce deviations from the von Bertalanffy curve. This phenomenon is discussed further in the section on genetics and parameter variation, {267}. Growth ceases, i.e. $\frac{d}{dt}V = 0$, if the reserve density equals a threshold value, $[E] = (\{\dot{p}_T\} + [\dot{p}_M]V^{1/3})/\kappa\dot{v}$.

Although food availability does not influence growth directly, it does so indirectly via reserve energy. Moreover, the maximum surface-area-specific assimilation rate $\{\dot{p}_{Am}\}$, and so energy conductance $\dot{v}$, relate to the food–energy conversion. Many herbivores, such as chickens, eat animal products in the early juvenile period to gain nitrogen, which they need to synthesize proteins. They experience a shift in diet during development. Mammals feed milk to their offspring, this needs little conversion and induces growth rates that cannot be reached with their later diet. Their growth curves, therefore, kink sharply at weaning.

Animals that have non-permanent exoskeletons (arthropods, insects) have to moult to grow. The rapid increase in size during the brief period between two moults relates to the uptake of water or air, not to synthesis of new structural biomass, which is a slow process occurring during the intermoult period. This minor deviation from the DEB model relates more to size measures than to model structure.

3.7.1 Embryonic growth

The DEB model takes the bold view that the only essential difference between embryos and juveniles is that the former do not feed [514]. I will discuss eggs first, which do not take up energy from the environment. (See [141] for an excellent introduction to eggs, with

beautiful photographs.) Subsequently, I deal with foetuses, which obtain energy reserves from the mother during development.

The idea is that the dynamics for growth, (3.18) and reserve density, (3.10) also apply to embryos in eggs in the absence of food intake. The scaled functional response is thus taken to be $f = 0$. The dynamics for the reserve density then reduces to

$$\frac{d}{dt}[E] = -\dot{v}[E]V^{-1/3} \tag{3.24}$$

The initial volume is practically nil, so $V(0) = 0$. This makes the energy density infinitely large, so $[E](0) = \infty$. The (absolute) initial energy is a certain amount, $[E](0)V(0) = E_0$, which, however, is not considered to be a free parameter. Its value is determined from the condition of the energy reserves at hatching. Hatching occurs at age a_b, say, and initial energy density $[E_b]$, so $[E](a_b) = [E_b]$. The just-born juvenile still needs some energy reserves to cope with its metabolic needs. If all utilized energy is used for maintenance at hatching, a lower boundary for reserve energy density follows from $[\dot{p}_M]V_b = \dot{v}[E_b]V_b^{2/3}$, giving $[E_b] = [\dot{p}_M]V_b^{1/3}/\dot{v}$.

If food density is constant, the energy density will change from the one at hatching, called $[E_b]$, to $f[E_m]$ in juveniles. If energy density at hatching equals $f[E_m]$, the growth curve follows a von Bertalanffy curve. For initial energy densities less than $f[E_m]$, growth will be retarded compared to the von Bertalanffy growth curve; the opposite holds true for initial densities larger than $f[E_m]$. The deviation from the von Bertalanffy growth curve will not last long, because the relaxation time for energy density is proportional to length, which is small at hatching. It is tempting to take the initial energy density as equal to that of the mother at egg laying, because this results in von Bertalanffy growth at constant food density even just after hatching, and it does not require additional parameters.

Experimental evidence for the initial condition of the reserves at egg laying is inconsistent for daphnids. The triglycerides component of energy density is visible as a yellow colour and as droplets. I have observed that well-fed, yellow mothers of *Daphnia magna* give birth to yellow offspring, and poorly fed, glassy mothers give birth to glassy offspring. This is consistent with observations of Tessier *et al.* [914]. Later observations of Tessier as well as Enserink [259], however, indicate an inverse relationship between food density and energy reserves at hatching. An increase of energy investment per offspring can also result in larger offspring rather than an increased reserve density at hatching. Large-bodied offspring at low food availability has been described for the terrestrial isopod *Armadillium vulgare* [118]. Because of the relationship with energy costs of egg production, and so with reproduction rate, this response to resource depletion has implications for population dynamics. It can be viewed as a mechanism that aims to ensure adequate food supply for the existing individuals. The assumption that energy density at hatching equals that of the mother at egg formation is made here for reasons of simplicity and theoretical elegance. No theoretical barriers exist for other formulations within the context of the DEB theory. Such formulations are likely to involve species-specific empirical or optimization arguments, however, which I have tried to avoid as much as possible.

Embryo development provides an excellent opportunity to test the model for the dynamics of energy reserves, because of the huge change of energy density, which avoids the

pathological conditions that starving individuals face. As embryos do not feed, data on their development do not suffer from a major source of scatter.

Figure 3.15 shows that data on embryo weight, yolk and respiration are in close agreement with model expectations. As is discussed later, {135}, respiration is taken to be proportional to the catabolic rate. The two or three curves per species have been fitted simultaneously by Zonneveld [1030], and the total number of parameters is five excluding, or seven including, respiration. This is less than three parameters per curve and thus approaches a straight line for simplicity when measured this way. I have not found comparable data for plant seeds, but I expect a very similar pattern of development.

The examples are representative of the data collected in Table 3.1, which gives parameter estimates of some 40 species of snails, fish, amphibians, reptiles and birds. The model tends to underestimate embryo weight and respiration rate in the early phases of development. This is partly because of deviations in isomorphism, the contributions of extra-embryonic membranes (both in weight and in the mobilization of energy reserves), and the loss of water content during development. The parameter estimates for the altricial birds such as the parrot *Agapornis* should be treated with some reservation, because neglected acceleration caused by the temperature increase during development substantially affects the estimates, as discussed on {258}.

The values for the energy conductance $\dot{v}$, as given in Table 3.1, are in accordance with the average value for post-embryonic development, as given on {277}, which indicates that no major changes in energy parameters occur at birth. The maintenance rate constant $\dot{k}_M$ for reptiles and birds is about 0.08 d^{-1} at 30 °C, implying that the energy required to maintain tissue for 12 days at 30 °C is about equal to the energy necessary to synthesize the tissue from the reserves. The maintenance rate constant for fresh water species seems to be much higher, ranging from 0.3 to 2.3 d^{-1}. Data from Smith [861] on the rainbow trout *Oncorhynchus mykiss* result in 1.8 d^{-1} and Figure 3.14 gives over 10 d^{-1} for the waterflea *Daphnia magna* at 30 °C. The costs of osmosis might contribute to these high maintenance costs, as has been suggested on {91}. Although information on parameter values is still sparse, it indicates that no (drastic) changes in these values occur at the transition from the embryonic to the juvenile state.

Table 3.1 shows that about half of the reserves are used during embryonic development. The deviating values for altricial birds are artefacts, caused by the abovementioned acceleration of development by increasing temperatures. Congdon *et al.* [169] observed that the turtles *Chrysemus picta* and *Emydoidea blandingi* have 0.38 of the initial reserves at birth. Respiration measurements on sea birds by Pettit *et al.* [704] indicate values that are somewhat above the ones reported in the table. The extremely small value for the soft shelled turtle, see also Figure 3.15, relates to the fact that these turtles wait for the right conditions to hatch, after which they have to run the gauntlet as a cohort at night from the beach to the water, where a variety of predators wait for them.

The general pattern of embryo development in eggs is characterized by unrestricted fast development during the first part of the incubation period (once it has started the process) due to unlimited energy supply, at a rate that would be impossible to reach if the animal had to refill reserves by feeding. This period is followed by a retardation of development due to the increasing depletion of energy reserves. Apart from the reserves of

Figure 3.15: Yolk-free embryo weight (⋄), yolk weight (×), and respiration rate (+) during embryo development, and fits on the basis of the DEB model. Data sources are indicated.

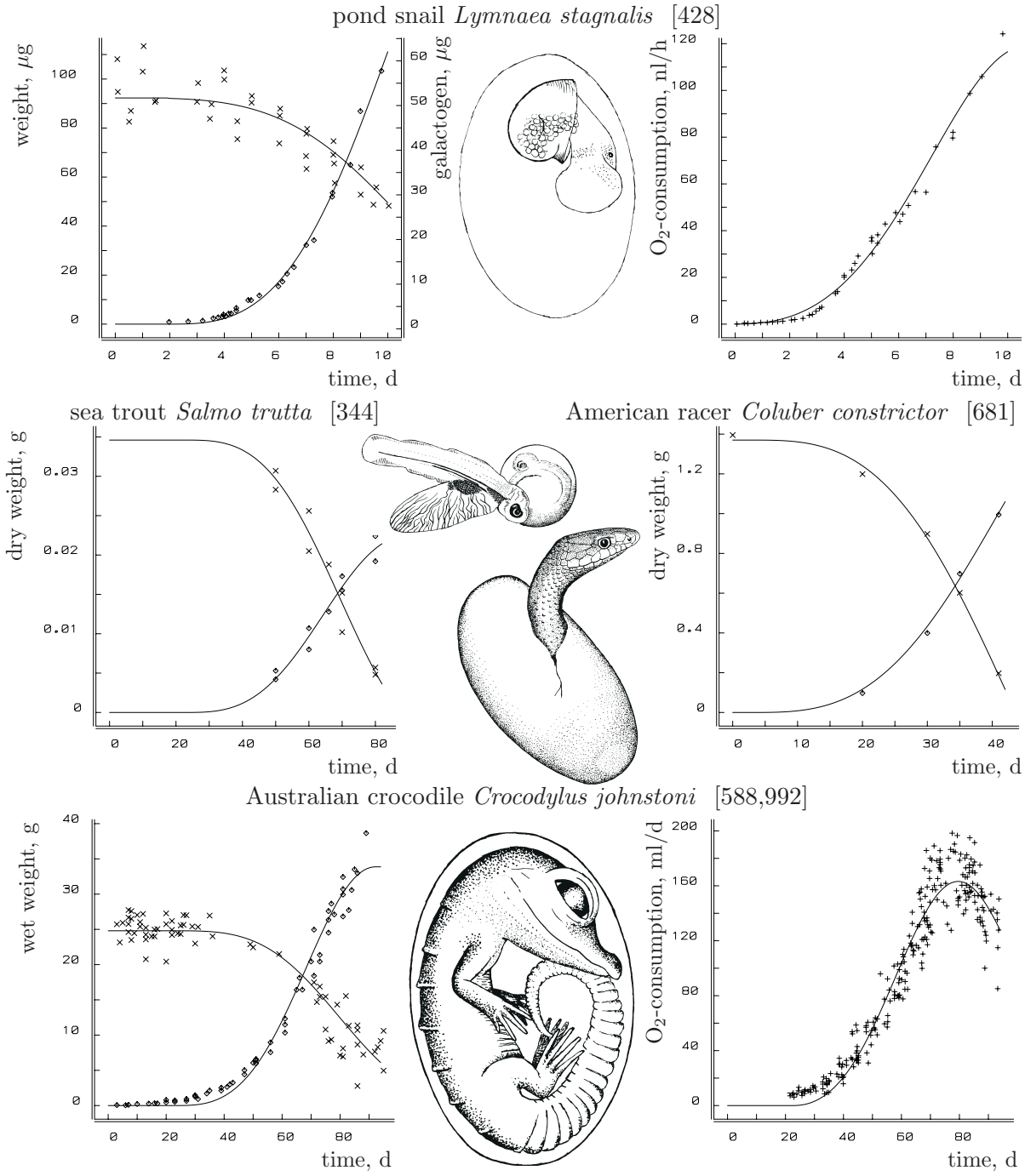

Figure 3.15 continued
New Guinea soft-shelled turtle *Carettochelys insculpta* [975]

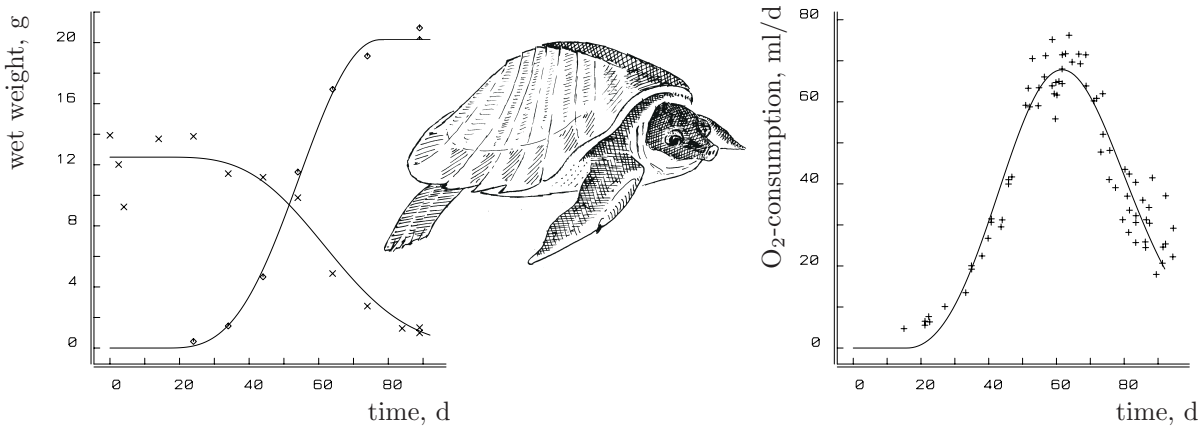

Laysan albatross *Diomedea immutabilis* [702]

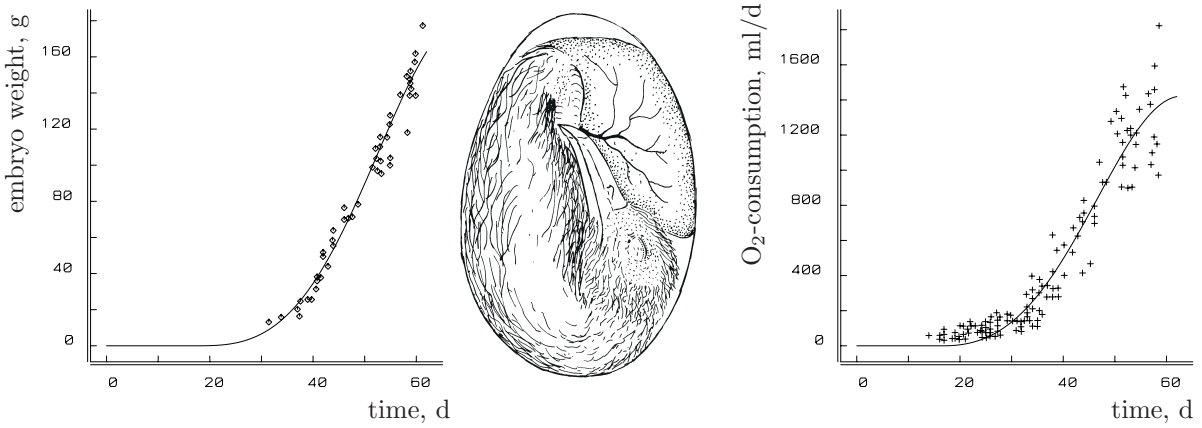

Table 3.1: Survey of re-analysed egg data, and parameter values standardized to a temperature of 30 °C, taken from [1030]. *1* P. J. Whitehead, pers. comm., 1989 ; *2* M. B. Thompson, pers. comm., 1989; 'galac.', stands for galactogen content.

species	temp. ° C	type of data	$\dot{v}_{30}$ mm d^{-1}	$\dot{k}_{M\,30}$ d^{-1}	E_b/E_0	reference
Lymnaea stagnalis	23	ED, galac, O	0.80	2.3	0.55	[428]
Salmo trutta	10	ED, YD	3.0	0.31	0.37	[344]
Rana pipiens	20	EW, O	2.5		0.87	[34]
Crocodylus johnstoni	30	EW, YW	1.9	0.060	0.31	[588]
	29, 31	O				[992]
Crocodylus porosus	30	EW, YW	2.7	0.024	0.19	[976]
	30	O				*1*
Alligator mississippiensis	30	EW, YW	2.7		0.34	[204]
	30	O				[919]
Chelydra serpentina	29	ED, YD	1.9		0.35	[681]
	29	O				[319]
Carettochelys insculpta	30	EW, YW, O	1.9	0.040	0.08	[975]
Emydura macquarii	30	EW, O	1.6	0.14	0.35	[919]
Caretta caretta	28–30	EW, O	3.0		0.65	[4,3]
Chelonia mydas	28–30	EW, O	3.0		0.57	[4,3]
Amphibolurus barbatus	29	ED, YD	0.92	0.061	0.47	[682]
Coluber constrictor	29	ED, YD	1.4		0.69	[683]
Sphenodon punctatus	20	HW, O	0.85	0.062	0.25	*2*
Gallus domesticus	39	EW, O, C	3.2	0.039	0.34	[783]
Gallus domesticus	38	EW, C	3.4		0.52	[99]
Leipoa ocellata	34	EE, YE, O	1.7	0.031	0.55	[954]
Pelicanus occidentalis	36.5	EW, O	3.2	0.10	0.77	[50]
Anous stolidus	35	EW, O	2.0	0.11	0.59	[703]
Anous tenuirostris	35	EW, O	1.8	0.20	0.59	[703]
Diomedea immutabilis	35	EW, O	2.5	0.069	0.57	[702]
Diomedea nigripes	35	EW, O	2.5	0.049	0.58	[702]
Puffinus pacificus	38	EW, O	0.92	0.084	0.61	[5]
Pterodroma hypoleuca	34	EW, O	1.9		0.20	[702]
Larus argentatus	38	EW, C	2.7	0.15	0.56	[233]
Gygis alba	35	EW, O	1.4		0.53	[701]
Anas platyrhynchos	37.5	EW	2.5	0.10	0.67	[735]
	37.5	O				[466]
Anser anser	37.5	EW	4.1	0.039	0.23	[782]
	37.5	O				[952]
Coturnix coturnix	37.5	EW, O	1.7		0.49	[952]
Agapornis personata	36	EW, O	0.8		0.79	[134]
Agapornis roseicollis	36	EW, O	0.84		0.81	[134]
Troglodytes aëdon	38	EW, O	1.4		0.82	[473]
Columba livia	38	EW	2.7		0.80	[467]
	37.5	O				[952]

EW: Embryo Wet weight YW: Yolk Wet weight ED: Embryo Dry weight
EE: Embryo Energy content YE: Yolk Energy content YD: Yolk Dry weight
O: Oxygen consumption rate C: Carbon dioxide prod. rate HW: Hatchling Wet weight

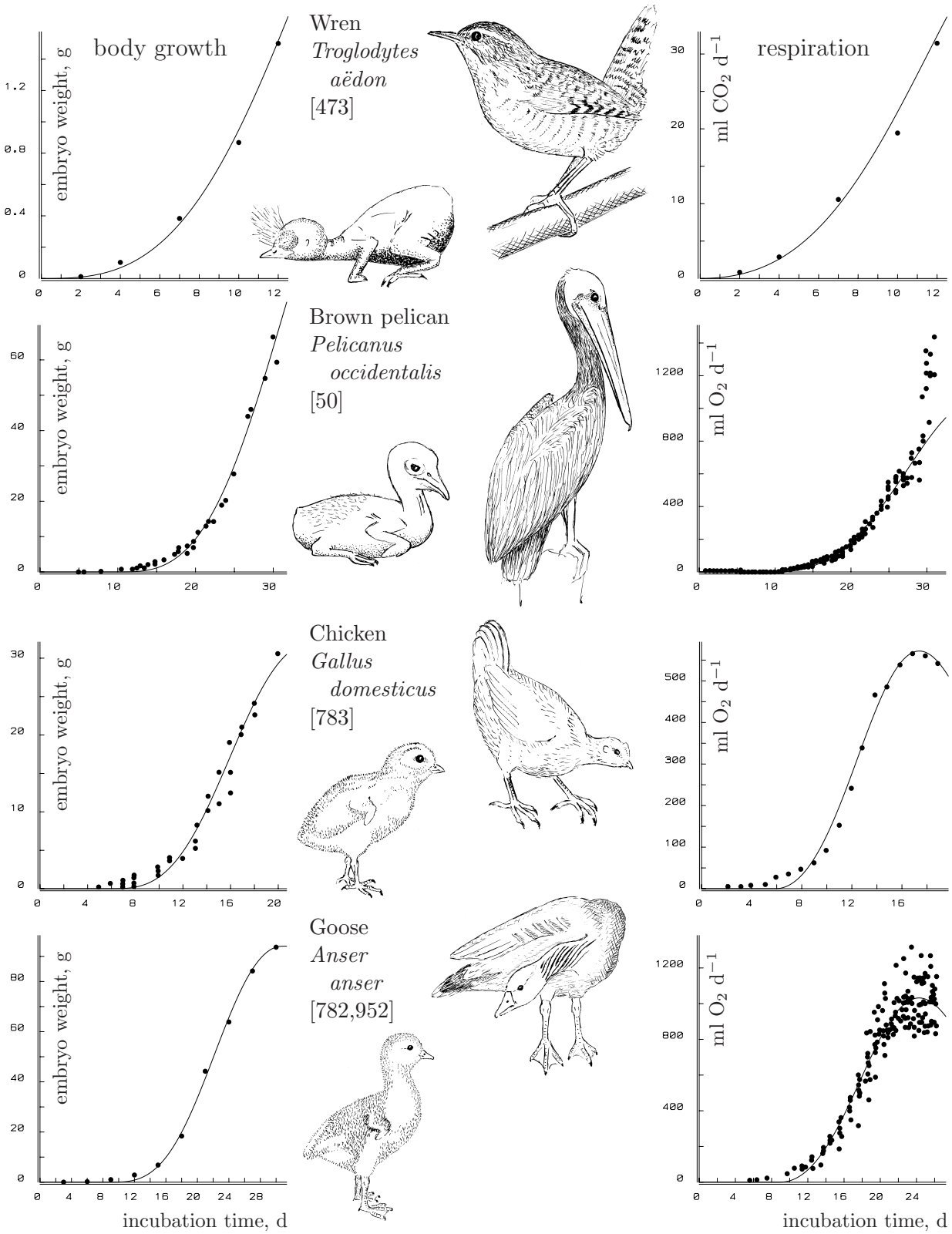

Figure 3.16: The embryonic development of altricial (wren, pelican) and precocial (chicken, goose) birds. Data from the sources indicated; fits are on the basis of the DEB model (parameters in Table 3.1). The underestimation of the initial development possibly relates to embryonic membranes. Pelican's high respiration rate just prior to hatching is attributed to internal pipping, which is not modelled. The drawings show hatchlings and adults.

Figure 3.17: Egg dimorphism occurs as standard in crested penguins (genus *Eudyptes*). The small egg is laid first, but it hatches later than the big one, which is 1.5 times as heavy. The DEB theory explains why the large egg requires a shorter incubation period. The illustration shows the Snares crested penguin *E. atratus*.

the juvenile, the model works out very similar that of Beer and Anderson [64] for salmonid embryos. In view of the goodness of fit of the model in species that do not possess shells, retardation is unlikely to be due to limitation of gas diffusion across the shell, as has been frequently suggested for birds [746]. Such a limitation also fails to explain why respiration declines in some species after its peak value, here beautifully illustrated with the turtle data. The altricial and precocial modes of development have been classified as being basically different; the precocials show a plateau in respiration rates towards the end of the incubation period, whereas the altricials do not. Figure 3.16 shows that this difference can be traced back to the simple fact that altricial birds hatch relatively early.

Large eggs, so large initial energy supplies, result in short incubation times if eggs of one species are compared. Crested penguins, *Eudyptes*, are known for egg dimorphism [967]; see Figure 3.17. They first lay a small egg and, some days later a 1.5 times bigger one. As predicted by the DEB model, the bigger one hatches first, if fertile, in which case the parents cease incubating the smaller egg, because they are only able to raise one chick. They continue to incubate the small egg only if the big one fails to hatch. This is probably an adaptation to the high frequency of unfertilized eggs or other causes of loss of eggs (aggression [967]), which occurs in this species.

Incubation periods only decrease for increasing egg size if the structural biomass of the hatchling is constant. The incubation period is found to increase with egg size in some beetle species, lizards and marine invertebrates [162,261,847]. In these cases, however, the structural biomass at hatching also increases with egg size. This is again consistent with the DEB theory, although the theory does not explain the variation in egg sizes.

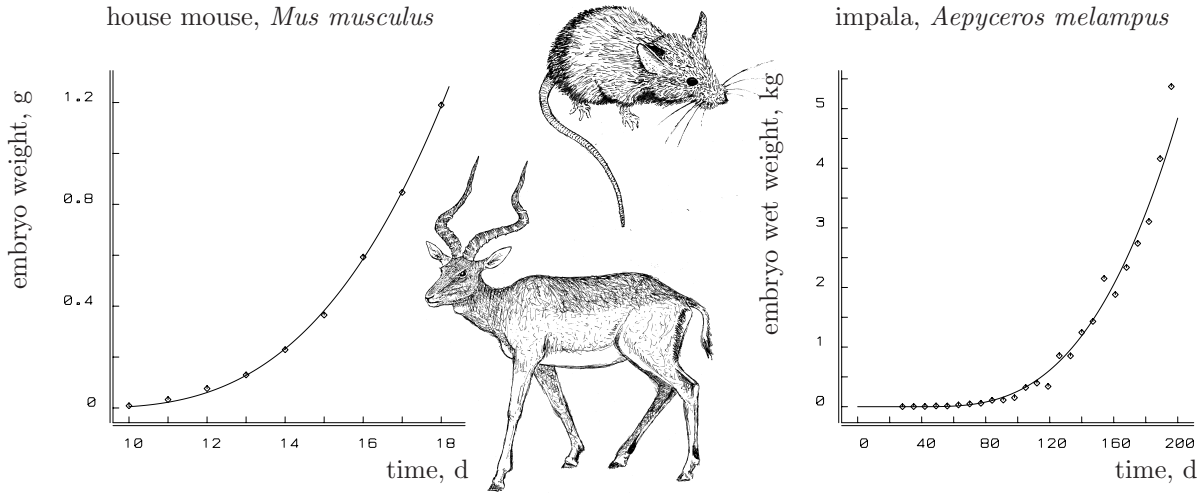

Figure 3.18: Foetal weight development in mammals. Parameters are given in Table 3.2.

Foetal development

Foetal development differs from that in eggs in that energy reserves are supplied continuously via the placenta. The feeding and digestion processes are not involved. Otherwise, foetal development is taken to be identical to egg development, with initial reserves that can be taken to be infinitely large, for practical purposes. At birth, the neonate receives an amount of reserves from the mother, such that the reserve density of the neonate equals that of the mother. So the approximation $[E] = \infty$ for the foetus can be made for the whole gestation period and the dynamics of the reserve density (3.24) not longer applies, because the foetus lives on the reserves of the mother. In other words: unlike eggs, the development of foetuses is not restricted by energy reserves. Initially the egg and foetus develop in the same way, but the foetus keeps developing at a rate not restricted by the amount of reserves till the end of the gestation time, while the development of the egg becomes retarded, due to depletion of the reserves. The approximation $[E] = \infty$ reduces the growth equation (3.18) to

$$\frac{d}{dt}V = \dot{v}V^{2/3} \quad \text{so} \tag{3.25}$$

$$V(t) = (\dot{v}t/3)^3 \tag{3.26}$$

This growth curve was proposed by Huggett and Widdas [434] in 1951. Payne and Wheeler [694] explained it by assuming that the growth rate is determined by the rate at which nutrients are supplied to the foetus across a surface that remains in proportion to the total surface area of the foetus itself. This is consistent with the DEB model, which gives the energy interpretation of the single parameter. The graph of foetal weight against age resembles an exponential growth curve, but in fact it is less steep; the model has the property that subsequent weight doubling times increase by a factor $2^{1/3} = 1.26$, while there is no increase in the case of exponential growth.

The fit is again excellent; see Figure 3.18. It is representative for the data collected in Table 3.2 taken from [1030]. A time lag for the start of foetal growth has to be incorporated,

and this delay may be related to the development of the placenta, which possibly depends on body volume as well. The long delay for the grey seal *Halichoerus* probably relates to timing with the seasons to ensure adequate food supply for the developing juvenile. Variations in weight at birth are primarily due to variations in gestation period, not in foetal growth rate. For comparative purposes, energy conductance $\dot{v}$ is converted to 30 °C, on the assumption that the Arrhenius temperature, T_A, is 10 200 K and the body temperature is 37 °C for all mammals in the table. This is a rather crude conversion because the cat, for instance, has a body temperature of 38.6 °C. Weights were converted to volumes using a specific density of $[W_w] = 1\ \mathrm{g\,cm^{-3}}$.

One might expect that precocial development is rapid, resulting in advanced development at birth and, therefore, comes with a high value for the energy conductance. The values collected in Table 3.2, however, do not seem to have an obvious relationship with altricial–precocial rankings. The precocial guinea-pig and alpaca as well as the altricial human have relatively low values for the energy conductance. The altricial–precocial ranking seems to relate only to the relative volume at birth V_b/V_m.

Egg costs

The embryo thus develops from state $(a, [E], V) = (0, \infty, 0)$ to state $(a_b, [E_b], V_b)$. The costs of structure and maintenance together with κ determine the energy costs of an egg, E_0. These costs and the incubation time thus follow from specifications at hatching. This back reasoning is necessary because the initial volume is taken to be infinitesimally small, which makes the initial reserve density infinitely large.

The derivation of the costs of an egg is a bit technical, I am afraid, because of the non-linearity of the dynamics. The costs must be evaluated in the model formulation in order to go from an energy flux allocated to reproduction to a reproductive rate in terms of a number of offspring per time. You will not miss a lot if you skip the rest of this section if you are ready to accept the result that egg costs do not involve any new parameters. Costs of breeding by the parent are not included in this derivation.

The first step in deriving the costs of an egg is to get rid of a number of parameters by turning to the dimensionless variables scaled energy density $e = [E]/[E_m]$, scaled volumetric length $l = (V/V_m)^{1/3}$ and scaled time $\tau = t\dot{k}_M$. Substitution into (3.24) and (3.18) reduces the coupled differential equations to

$$\frac{d}{d\tau}e = -g\frac{e}{l} \text{ and } \frac{d}{d\tau}l = \frac{g}{3}\frac{e-l}{e+g} \tag{3.27}$$

The ratio of these equations gives the Bernoulli equation

$$\frac{dl}{de} = -\frac{l}{3e}\frac{e-l}{e+g} \text{ or } \frac{dx}{de} = \frac{ex-1}{3e(e+g)} \tag{3.28}$$

where $x \equiv l^{-1}$ is only introduced because the resulting equation in x is of a solvable linear first order with variable coefficients. Its solution is

$$x(e) \;=\; v(e)\left(\int_{e_b}^{e} \frac{-de_1}{3(e_1+g)e_1v(e_1)} + x(e_b)\right) \tag{3.29}$$

Table 3.2: The estimated energy conductance, $\dot{v}$, and its value corrected for a temperature of 30 °C, and the time lag for the start of development, t_l, for mammalian embryos.

species (race)	$\dot{v}$ cm d^{-1}	(cv)	$\dot{v}_{30}$ mm d^{-1}	t_l d	(cv)	reference
Homo sapiens			0.84			
males	0.180	(0.3)		26.8	(2.0)	[979]
females	0.179	(0.4)		26.5	(2.9)	
Oryctolagus cuniculus	0.560	(0.9)	2.6	10.7	(1.5)	[552]
small litters	0.602	(1.5)		11.5	(2.4)	[46]
large litters	0.571	(1.5)		11.5	(2.4)	[46]
	0.504	(5.6)		10.4	(10)	[48]
Lepus americanus	0.573	(3.1)	2.7	13.1	(4.2)	[101]
Cavia porcellus	0.269	(3.3)	1.1	15.7	(8.3)	[231]
	0.239	(2.3)				[439]
Cricetus auratus	0.570	(2.1)	2.6	9.29	(1.3)	[739]
Mus musculus	0.333	(0.1)	1.5	8.45	(0.1)	[578]
Rattus norvegicus			2.5			
wistar	0.487	(0.5)		11.4	(0.3)	[279]
albino	0.531	(0.8)		12.2	(0.5)	[890]
	0.525	(0.2)		11.8	(0.2)	[434]
albino	0.568	(3.3)		12.7	(2.1)	[22]
albino	0.542	(3.1)		12.4	(2.0)	[285]
Clethrionomys glareolus	0.374	(9.3)	1.8	8.29	(11)	[177]
Aepyceros melampus	0.316	(1.2)	1.4	39.4	(3.8)	[265]
Odocoileus virginianus	0.296	(6.7)	1.3	34.9	(28)	[775]
	0.274	(1.6)		25.1	(8.5)	[944]
Dama dama	0.345	(6.4)	1.7	9.94	(46)	[30]
Cervus canadensis	0.336	(3.1)	1.5	24.9	(19)	[643]
Lama pacus	0.120	(7.6)	0.56	7.47	(83)	[280]
Ovis aries			1.9			
welsh	0.482	(5.6)		43.9	(12)	[434]
merino	0.341	(8.6)		14.9	(71)	[584]
	0.346	(4.6)		15.2	(32)	
	0.433	(4.4)		33.3	(13)	[166]
karakul	0.436	(3.7)		31.0	(13)	[245]
	0.403	(2.6)		27.5	(8.2)	[459]
hampshire ×	0.382	(1.5)		20.4	(7.9)	[1007]
Capra hircus	0.339	(6.5)	1.7	24.3	(29)	[252]
	0.365	(4.5)		31.3	(14)	[47]
Bos taurus	0.475	(2.6)	2.3	59.5	(7.5)	[1008]
Equus caballus	0.370	(11)	1.8	37.0	(81)	[627]
Sus scrofa	0.266	(0.6)		4.73	(12)	[968]
Yorkshire	0.283	(0.9)		5.49	(16)	[937]
Large white	0.383	(1.3)		23.6	(4.2)	[723]
Essex	0.321	(4.8)		14.1	(30)	
Felix catus	0.371	(1.2)	1.8	18.8	(2.3)	[176]
Pipistrellus pipistrellus			0.97			
1978	0.237	(1.9)		9.95	(2.9)	[741]
1979	0.181	(3.5)		13.7	(4.7)	
Halichoerus grypus	0.375	(10)	1.8	145	(9.2)	[405]

$$\text{with } v(e) \;=\; \exp\left\{\int_{e_b}^{e} \frac{de_1}{3(g+e_1)}\right\} = \left(\frac{g+e}{g+e_b}\right)^{1/3}$$

Substitution of $l = x^{-1}$ gives

$$\frac{1}{l} = \left(\frac{g+e}{g+e_b}\right)^{1/3}\left(\frac{1}{l_b} - \frac{(g+e_b)^{1/3}}{3g^{4/3}}\int_{\frac{e_b}{e_b+g}}^{\frac{e}{e+g}} s^{-1}(1-s)^{1/3}\,ds\right) \tag{3.30}$$

Assume that the condition at hatching is fixed at e_b and l_b and let $l \to 0$ and $e \to \infty$ such that $[E_m]V_m e l^3 = E_0$, say, which represents the energy reserves in a freshly laid egg. Solving E_0 gives, for $e_0 \equiv E_0/E_m$ with $E_m \equiv [E_m]V_m$

$$e_0 = \left(\frac{1}{l_b(g+e_b)^{1/3}} - \frac{B_{\frac{g}{e_b+g}}(\frac{4}{3},0)}{3g^{4/3}}\right)^{-3} \tag{3.31}$$

where $B_x(a,b) \equiv \int_0^x y^{a-1}(1-y)^{b-1}\,dy$ is the incomplete beta function. Its two-term Taylor expansion in $[E_G]$ around the point $[E_G] = 0$ gives

$$e_0 \simeq \frac{2^6 e_b^4}{(4e_b/l_b - 1)^3} + \frac{4e_b/l_b - 16/7}{(4e_b/l_b - 1)^4}\, g 2^6 e_b^3 \tag{3.32}$$

Incubation time

The incubation time can be found by separating variables in (3.27) and substituting in (3.30). After some transformation, the result is

$$a_b = \frac{3}{\dot{k}_M}\int_0^{x_b} \frac{dx}{(1-x)x^{2/3}(\alpha - B_{x_b}(\frac{4}{3},0) + B_x(\frac{4}{3},0))} \tag{3.33}$$

where $x_b \equiv \frac{g}{e_b+g}$ and $\alpha \equiv 3g x_b^{1/3}/l_b$. Its two-term Taylor expansion in $[E_G]$ around the point $[E_G] = 0$ gives after tedious calculation

$$a_b \simeq \frac{3\sqrt{2}}{\dot{k}_M}u^3\left(\frac{e_b}{g} + \frac{1}{4} - \frac{9}{28}u^4\right)\left(\frac{1}{2}\ln\frac{u^2+u\sqrt{2}+1}{u^2-u\sqrt{2}+1} + \arctan\frac{u\sqrt{2}}{1-u^2}\right) + \frac{9}{7\dot{k}_M}(u^4 + \ln\{1+u^4\}) \tag{3.34}$$

where u stands for $(4e_b/l_b - 1)^{-1/4}$. I owe you an apology for writing out such a dreadful expression; the essence, however, is that no new parameters show up and that (3.34) can readily be implemented in computer code.

Foetal costs and gestation time

The energy costs of producing a neonate are found by adding the costs of development, growth and maintenance plus energy reserves at birth, i.e. $[E_b]V_b$. Expressed as a fraction of the maximum energy capacity of an adult, these costs are

$$e_0 = \left(\int_0^{a_b} \dot{p}_C(t)\,dt + [E_b]V_b\right)E_m^{-1}$$

Substitution of the κ-rule, $\kappa \dot{p}_C = [E_G]\frac{d}{dt}V + [\dot{p}_M]V$ and the growth curve (3.26) results in

$$e_0 = l_b^3(g + e_b + l_b 3/4) \tag{3.35}$$

This expression does not include the costs of the placenta. These costs can easily be taken into account if they happen to be proportional to that of the rest of the foetuses; see {114}.

Gestation time (excluding any time lag) is

$$a_b = 3l_b/g\dot{k}_M = 3V_b^{1/3}/\dot{v} \tag{3.36}$$

3.7.2 Growth for non-isomorphs

The above derivation assumes isomorphism, but it can easily be extended to include changing shapes. The surface areas of organisms that change shape have to be corrected for this change by multiplying parameters accounting for surface area, $\{\dot{J}_{Xm}\}$ and $\{\dot{p}_{Am}\}$ and thus $\dot{v}$ and $V_m^{1/3}$, by the shape correction function $\mathcal{M}(V)$. These organisms are ectothermic, so $\{\dot{p}_T\} = 0$. For V0- and V1-morphs, the shape correction functions (2.1) and (2.2) transform the growth rate (3.18) into

$$\text{V0-morph:} \quad \frac{d}{dt}V = \frac{\dot{v}}{e+g}\left(eV_d^{2/3} - VV_m^{-1/3}\right) \tag{3.37}$$

$$\text{V1-morph:} \quad \frac{d}{dt}V = \frac{\dot{k}_E}{e+g}\left(e - (V_d/V_m)^{1/3}\right)V \tag{3.38}$$

where V_d is the volume at division, and V_m is defined by $V_m^{1/3} = \frac{\dot{v}}{g\dot{k}_M}$. If substrate density X and, therefore, the scaled functional response f are constant long enough, energy density tends to $[E] = f[E_m]$ and the volume of V1-morphs as a function of time since division becomes for $V(0) = V_d/2$

$$V(t) = \frac{1}{2}V_d \exp\{t\dot{r}\} \quad \text{or} \tag{3.39}$$

$$t(V) = \dot{r}^{-1} \ln\{2V/V_d\} \tag{3.40}$$

with specific growth rate $\dot{r} \equiv \dot{k}_E \frac{f-(V_d/V_m)^{1/3}}{f+g}$. The time taken to grow from $V_d/2$ to V_d is thus $t(V_d) = \dot{r}^{-1} \ln 2$.

Exponential growth can be expected if the surface area at which nutrients are taken up is proportional to volume. For V1-morphs, this happens when the total surface area is involved, or a fixed fraction of it. If uptake only takes place at tips, the number of tips should increase with total filament length to ensure exponential growth. This has been found for the fungi *Fusarium* [932], and *Penicillium* [660,718], which do not divide; see Figure 3.19. The ascomycetous fungus *Neurospora* does not branch this way [254]; it has a mycelium that grows like a crust, see {250}.

Exponential growth of individuals should not be confused with that of populations. As is discussed in the section on population dynamics {312}, all populations grow exponentially at resource densities that are constant for long enough, whatever the growth pattern

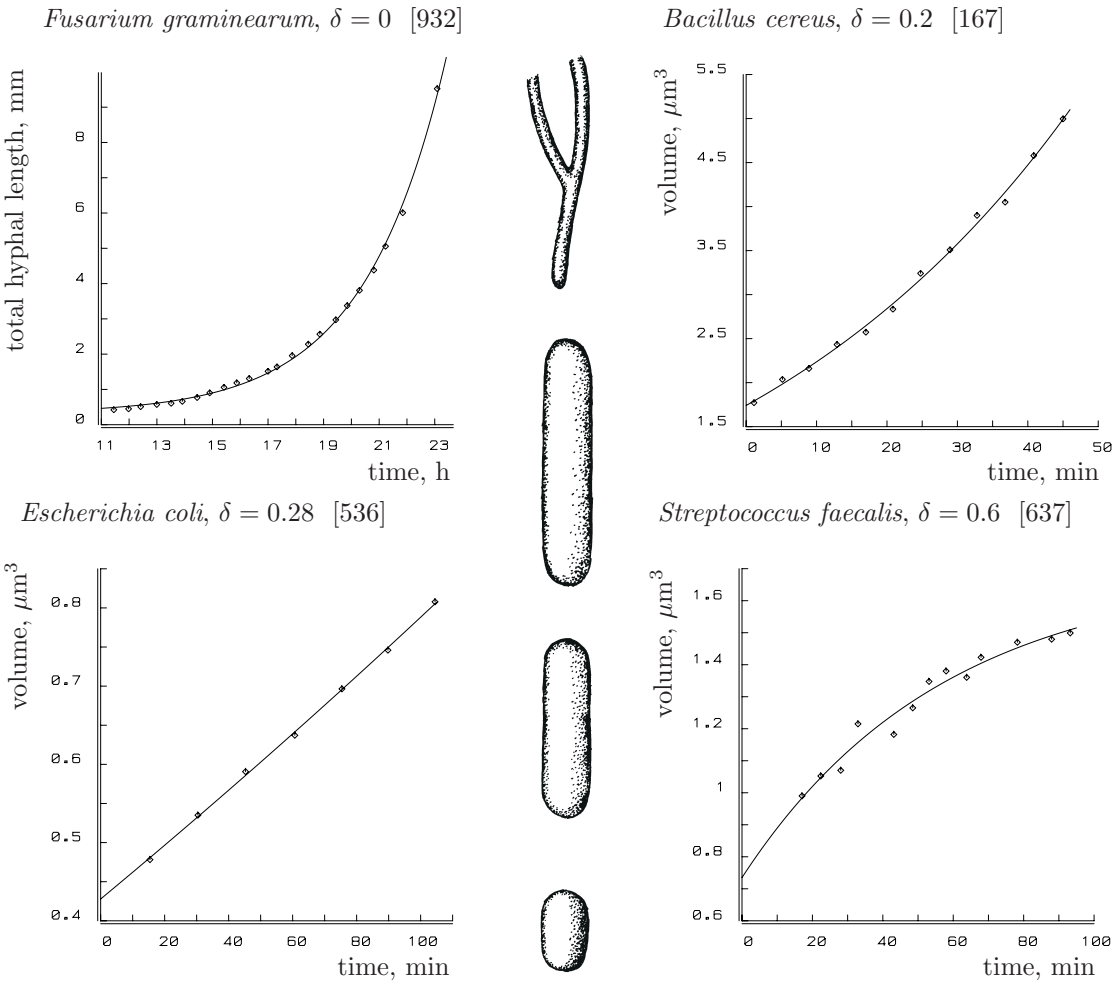

Figure 3.19: DEB-based growth curves for cells of V1-morphs and rods. The larger the aspect ratio, δ, the more the growth curve turns from the exponential to the satiation type, reflecting the different surface area/volume relationships.

of individuals. This is simply because the progeny repeats the growth/reproduction behaviour of the parents. Only for V1-morphs it is unnecessary to distinguish between the individual and the population level. This is a characteristic property of exponential growth of individuals and is discussed on {317}.

Figure 3.20 shows that the growth curves of V0-morphs are more convex than the von Bertalanffy one for isomorphs. Note that the change in *length* is a first-order process for isomorphs, while the change in *volume* is a first-order process for V0-morphs.

The same derivation for growth can be made for rods on the basis of the shape correction function (2.3)

$$\frac{d}{dt}V = \frac{\delta V_d}{3V_\infty}\frac{\dot{k}_E e}{e+g}(V_\infty - V) \tag{3.41}$$

where $V_\infty \equiv V_d \frac{\delta}{3}(e^{-1}(\frac{V_d}{V_m})^{1/3} - 1 + \frac{\delta}{3})^{-1}$ and, as before, $V_m^{1/3} \equiv \frac{\dot{v}}{g\dot{k}_M}$. If substrate density X and, therefore, the scaled functional response f are constant long enough, scaled energy

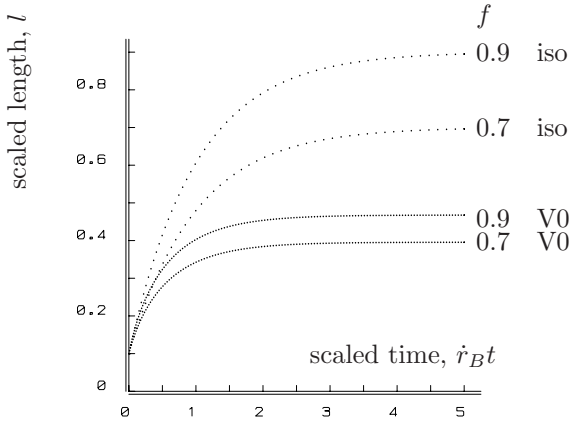

Figure 3.20: Expected growth curves for V0-morphs compared with those for isomorphs at constant substrate densities. Parameters: scaled length at birth $l_b = 0.1$, scaled functional response $f = 0.7$ and 0.9 and scaled length at division $l_d = l_b 2^{1/3}$.

density tends to $e = f$ and volume as a function of time since division becomes

$$V(t) = V_\infty - (V_\infty - V_d/2)\exp\{-t\dot{r}_r\} \tag{3.42}$$

where $\dot{r}_r \equiv \frac{V_d f \dot{k}_E \delta/3}{V_\infty(f+g)}$. The interpretation of V_∞ depends on its value.

- If $V_\infty = \infty$, i.e. if $f(1-\delta/3) = (V_d/V_m)^{1/3}$, the volume of rods grows linearly at rate $\frac{\dot{k}_E f}{f+g} V_d \frac{\delta}{3}$. This is frequently found empirically [40].
- If $0 < V_\infty < \infty$, V_∞ is the ultimate volume if the cell ceases to divide but continues to grow. For these values, $V(t)$ is a convex function and is of the same type as $V(t)^{1/3}$ for isomorphs, (3.20). Note that volume, and thus cubed length, grows skewly S-shaped for isomorphs. When V_∞ is positive, the cell will only be able to divide when $V_\infty > V_d$, thus when $f > (V_d/V_m)^{1/3}$.
- If $\delta = 0$, $V_\infty = 0$ and the rod behaves as a V1-morph, which grows exponentially.
- For $V_\infty < 0$, $V(t)$ is a concave function, tending to an exponential one. The cell no longer has an ultimate size if it ceases to divide. V_∞ is then no longer interpreted as ultimate size, but this does not invalidate the equations.

The shape of the growth curve, convex, linear or concave, thus depends on substrate density and the aspect ratio. Figure 3.19 illustrates the perfect fit of growth curves (3.42) with only three parameters: volume at 'birth', $V_d/2$, ultimate volume, V_∞, and growth rate, $\dot{r}_r$. The figure beautifully reveals the effect of the aspect ratio; the larger the aspect ratio, the more important the effect of the caps, so a change from V1-morphic behaviour to a V0-morphic behaviour. A sudden irreversible change in morphology from spherical to filamentous cells has been observed in the yeast *Kluyveromyces marxianus* [348], while no other changes could be detected. The associated increase of 30% in the maximum specific growth rate could be related to the observed increase in specific surface area.

The time required to grow from $V_d/2$ to V at constant substrate density is found from (3.42)

$$t(V) = \frac{(f+g)V_\infty}{f\dot{k}_E V_d \delta/3} \ln \frac{V_\infty - V_d/2}{V_\infty - V} \tag{3.43}$$

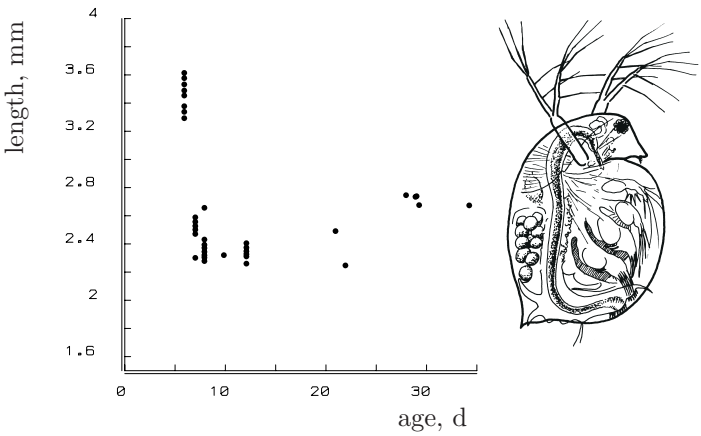

Figure 3.21: The carapace length of the daphnid *Daphnia magna* at 20 °C for 5 different food levels at the moment of egg deposition in the brood pouch. Data from Baltus [44]. The data points for short juvenile periods correspond with high food density and growth rate. They are difficult to interpret because length increase is only possible at moulting in daphnids.

3.8 Development

Now that growth has been specified, the catabolic rate for isomorphs can be evaluated from (3.12) and (3.18). It amounts to

$$\dot{p}_C = \frac{g[E]}{g + [E]/[E_m]}(\dot{v}V^{2/3} + \dot{k}_M V_h^{1/3} V^{2/3} + \dot{k}_M V) \tag{3.44}$$

Energy allocation to development is $(1-\kappa)\dot{p}_C$. Comparison of growth and reproduction at different food levels highlights a problem: the volume at the first appearance of eggs in the brood pouch of daphnids seems to be independent of food density. It appears to be almost fixed; see Figure 3.21. Let this volume be called V_p, where subscript p refers to puberty (transition juvenile/adult). The same holds for the volume at hatching, V_b, say, where subscript b refers to birth (transition embryo/juvenile). The problem is that the total energy investment in development depends on food density. Indeed, if feeding conditions are so poor that the ultimate volume is less than V_p, the cumulated energy investment in development becomes infinitely large if the organism survives long enough. This seems to be highly unrealistic.

Thieme [915] proposed a solution to this problem: split the energy allocated to development into two fluxes, the increase of the state of maturity $\dot{p}_R$ and the maintenance of a certain degree of maturity $\dot{p}_J$. The total energy investment in the increase of the state of maturity does not depend on food density for ectotherms for a special choice of the maturity maintenance costs. This can be seen most easily from (3.17), when both sides are multiplied by $(1-\kappa)/\kappa$ to obtain the investment in development

$$(1-\kappa)\dot{p}_C = \frac{1-\kappa}{\kappa}\dot{p}_M + \frac{1-\kappa}{\kappa}[E_G]\frac{d}{dt}V \tag{3.45}$$

for juvenile ectotherms ($V < V_p$ and $\dot{p}_T = 0$). If the first term of the right-hand side corresponds to maturity maintenance costs, the second one for the increase of the state of maturity depends only on size, not on food density. Since the individual does not

become more complex after attaining size V_p, the energy flow to maintain a certain degree of maturity must then be

$$\dot{p}_J = \min\{V, V_p\}[\dot{p}_M]\frac{1-\kappa}{\kappa} \tag{3.46}$$

It can be thought to relate to the maintenance of regulating mechanisms and concentration gradients, such as those found in *Hydra*, that maintain head/foot differentiation [325]. The increase in the state of maturity is not thought to affect the elemental composition of the structural biomass. If new compounds are generated in this process, their contribution to structural biomass composition is thought to be negligibly small.

It took me quite a while to accept the existence of maturity maintenance as inevitable. Although the concept sounds a little esoteric, there are two hard observations that support its existence. The first one concerns an experiment where food density is held constant at two levels, just below and above the food density that gives an ultimate size $V_\infty = V_p$. For ectotherms, such as daphnids, (3.23) implies that this food density is found from $f = (V_p/V_m)^{1/3} \equiv l_p$, so $X = X_K l_p/(1-l_p)$. If maturity maintenance did not exist, animals kept at the lower food density would never reproduce, while those at a slightly higher food density would invest in reproduction at a rate $\frac{1-\kappa}{\kappa}[\dot{p}_M]V_p$, which amounts to $4[\dot{p}_M]V_p$ for $\kappa = 0.2$, which is realistic for daphnids. This substantial difference in reproductive output as a result of a tiny difference in feeding rates has never been observed.

The second observation that points to the existence of maturity maintenance concerns pond snails, where the day/night cycle affects the fraction of utilized energy spent on maintenance plus growth [1028] such that κ at equal day/equal night, κ_{md}, is larger than that at long day/short night, κ_{ld}. Apart from the apparent effects on growth and reproduction rates, volume at the transition to adulthood is also affected. If the cumulated energy investment in the increase of maturity does not depend on the value for κ and if the maturity maintenance costs are $\frac{1-\kappa}{\kappa}\dot{p}_M$, the expected effect is $\frac{V_{p,ld}}{V_{p,md}} = \frac{\kappa_{ld}(1-\kappa_{md})}{\kappa_{md}(1-\kappa_{ld})}$, which is consistent with the observations on the coupling of growth and reproduction investments to size at puberty [1028].

Some species, such as birds, only reproduce well after the growth period. The giant petrel wanders seven years over Antarctic waters before it starts to breed for the first time. From a mathematical point of view, growth is asymptotic, so it is possible to choose V_p to be so close to V_∞ that the desired result is described adequately. This must be rejected, however, because it seems most unrealistic to have a model where decision rules depend on such small differences in volume in a world that is full of scatter [201]. The introduction of costs of maintaining a certain degree of maturity solves this problem, because the model is then energy-structured as well as size-structured. A transition from embryo to juvenile and from juvenile to adult occurs if the cumulative investment to increase the state of maturity exceeds specified amounts. After growth has ceased, this cumulative investment increases linearly, so it has no asymptote. The rate of increase of cumulated investment can be substantial, even if body size hardly increases, so this rule causes no problems for species that separate growth and reproduction in time.

The juvenile/adult transition only occurs at a fixed structural volume for the specific maturity maintenance costs (3.46), for which I have no arguments. The observed volume at transition in daphnids and pond snails does not vary much at all. It is possible, however,

to introduce a free parameter for the maturity maintenance costs, and use volume at first maturation to estimate its value, which then proves to be close to (3.46), because this value produces a volume that is independent of food density. If this free parameter has a different value, variations in volume at first maturation will result when food density varies, see {295}. This has been observed for some species [73]. Its introduction has the serious drawback that evaluating the length of incubation and juvenile periods becomes cumbersome, which causes problems especially at the population level. The fixed size transition should then be replaced by a fixed cumulative energy transition.

Little is known about the molecular machinery that is involved in the transition from the juvenile to the adult stage. Recent evidence points to a trigger role of the hormone leptin in mice, which is excreted by the adipose tissue [159]. This finding supports the direct link between the transition and energetics.

Growth and development are parallel processes in the DEB model, which links up beautifully with the concepts of acceleration and retardation of developmental phenomena such as sexual maturity [338]. These concepts are used to describe relative rates of development in species that are similar in other respects.

In embryos and juveniles, the energy spent on somatic maintenance and the maintenance of a certain degree of maturation can be combined, because both can be taken to be proportional to volume. The difference between the two only shows up in adults that still increase in size. Somatic maintenance remains proportional to size, while maturation maintenance stays constant at constant temperature. The same holds for the energy spent on growth and the increase of the degree of maturity. In embryos and juveniles, they can be combined, because both are taken to be proportional to the volume increase. This means that for non-adults the κ-rule is not quantitatively relevant, and the model simplifies to the one for micro-organisms with respect to the use of energy.

Whether or not unicellulars and particularly prokaryotes invest in cell differentiation during the cell cycle is still open to debate. Dworkin [244] reviewed development in prokaryotes and points to the striking similarities between myxobacteria and cellular slime moulds and between *Actinomyceta* and some fungi. A most useful aspect of the κ-rule is that this matter does not need to be resolved, because this investment only shows up in the parameter values and not in the model structure.

During extreme forms of starvation, many organisms shrink {230}. They can only recover enough energy from the degradation of structural mass to pay the somatic maintenance costs if they can reduce the maturity maintenance costs under those conditions. Maintenance costs can, therefore, be partitioned into reducible (maturity) and irreducible (somatic) costs.

3.9 Propagation

Organisms can achieve an increase in numbers in many ways. Sea anemones can split off foot tissue that can grow into a new individual. This is not unlike the strategy of budding yeasts. Colonial species usually have several ways of propagating. Fungi have intricate sexual reproduction patterns involving more than two sexes. Under harsh conditions some

animals can switch from parthenogenic to sexual reproduction, others develop spores or other resting phases. It would not be difficult to fill a book with descriptions of all the possibilities. I will confine the discussion to the two most common modes of propagation: via egg and foetus or vegetatively, via division.

3.9.1 Reproduction

Energy allocation to reproduction equals the allocation to development plus reproduction minus the costs of maintaining the state of maturity

$$(1-\kappa)\dot{p}_C - \dot{p}_J \tag{3.47}$$

This is a continuous energy investment. The costs of egg (or foetus) development are fully determined, as is discussed in the section on embryonic growth, {96}. The costs of producing an egg can be written as E_0/κ_R, where the dimensionless factor κ_R between 0 and 1 represents the fraction of reproduction energy that is fixed in eggs; the fraction $1-\kappa_R$ dissipates and represents the overhead involved in the conversion from the reserve energy of the mother to the initial energy available to the embryo. Since these types of energy reserves are chemically related, the overhead is likely to be small in most cases so that κ_R is close to 1. This might seem an odd way to introduce this overhead, but κ_R can also be interpreted as an egg survival probability, which can be further modulated by predation and toxic compounds, as discussed in later chapters. This is practical because egg survival is frequently governed by different processes than survival of later stages. Substitution of catabolic rate (3.44), and the maintenance costs (3.46) into (3.47) leads to a mean reproduction rate for ectotherms of

$$\dot{R} = \frac{\kappa_R}{e_0 V_m}(1-\kappa)\left(\frac{ge}{g+e}(\dot{v}V^{2/3} + \dot{k}_M V) - g\dot{k}_M V_p\right) \tag{3.48}$$

where the relative energy costs of embryo development e_0 are given in (3.31). Under no-growth conditions, i.e. when $e \leq l$, individuals can no longer follow the κ-rule, because the allocation to maintenance would no longer be sufficient. Maintenance has priority over all other expenses. Individuals that still follow the storage dynamics (3.12) under no-growth conditions must reproduce at mean rate $(\dot{p}_C - \dot{p}_M - \dot{p}_J)\kappa_R/E_0$, so

$$\dot{R} = \frac{\kappa_R}{e_0 V_m} g\dot{k}_M \left(eV_m^{1/3}V^{2/3} - \kappa V - (1-\kappa)V_p\right)_+ \tag{3.49}$$

At the border of the no-growth condition, i.e. when $e = l$, both expressions for the reproduction rate are equal, so there is no discontinuity for changing energy reserves.

At constant food density where $e = f$, the reproduction rate is, according to (3.48), proportional to

$$\dot{R} \propto V^{2/3} + \frac{\dot{k}_M}{\dot{v}}V - \frac{g+f}{f}\frac{\dot{k}_M}{\dot{v}}V_p \tag{3.50}$$

where the third term is just a constant. Comparison of reproduction rates for different body sizes thus involves three compound parameters, i.e. the proportionality constant, the

parameter $\dot{k}_M/\dot{v}$ and the third term, if all individuals experience the same food density for a long enough time. Figure 3.22 illustrates that this relationship is realistic, but that the notorious scatter for reproduction data is so large that access to the parameter $\dot{k}_M/\dot{v}$ is poor. The fits are based on guestimates for the maintenance rate coefficient, $\dot{k}_M = 0.011$ d^{-1}, and the energy conductance, $\dot{v} = 0.433$ mm d^{-1} at 20 °C. Note that if the independent variable is a length measure rather than structural body volume, the shape coefficient $\delta_{\mathcal{M}} = V^{1/3}L^{-1}$ has to be introduced since the guestimate for the energy conductance is expressed in volumetric length. For some length measure L, we have

$$\dot{R} \propto L^2 + \frac{\dot{k}_M}{\dot{v}}\delta_{\mathcal{M}}L^3 - \frac{g+f}{f}\frac{\dot{k}_M}{\dot{v}}\delta_{\mathcal{M}}L_p^3 \tag{3.51}$$

The practical significance of this remark is in the comparison between species, which is discussed later, {267}. The main reason for the substantial scatter in reproduction data is that they are usually collected from the field, where food densities are not constant, and where spatial heterogeneities, social interactions, etc., are common.

The reproduction rate of spirorbid polychaetes has been found to be roughly proportional to body weight [403]. On the assumption by Strathmann and Strathmann [896] that reproduction rate is proportional to ovary size and that ovary size is proportional to body size (an argument that rests on isomorphy), the reproduction rate is also expected to be proportional to body weight. They observed that reproduction rate tends to scale with body weight to the power somewhat less than one for several other marine invertebrate species, and used their observation to identify a constraint on body size for brooding inside the body cavity. The DEB theory gives no direct support for this constraint; an allometric regression of reproduction rate against body weight would result in a scaling parameter between 2/3 and 1, probably close to 1, depending on parameter values.

The maximum (mean) reproduction rate for ectotherms of maximum volume $V_m = (\dot{v}/g\dot{k}_M)^3$ amounts to

$$\dot{R}_m = \frac{\kappa_R}{e_0}(1-\kappa)g\dot{k}_M(1 - V_p/V_m) \tag{3.52}$$

All these expressions refer only to mean reproduction rates. Individuals are discrete units, which implies the existence of a buffer, where the energy allocated to reproduction is stored and converted to eggs at the moment of reproduction. The translation of reproduction rate into number of eggs in Figure 3.22 assumes that this accumulation is over a period of one year. The energy content of the buffer is denoted by E_R.

Some species reproduce when enough energy for a single egg has been accumulated, others wait longer and produce a large clutch. There is considerable variation in the way the reproduction buffer is handled. If the reproduction buffer is used completely, the size of the clutch equals the ratio of the buffer content to the energy costs of one young, $\kappa_R E_R/E_0$, where E_0 is given in (3.31). This resets the buffer. So after reproduction $E_R = 0$ and further accumulation continues from there. That is to say, the bit of energy that was not sufficient to build the last egg can become lost or still remains in the buffer; fractional eggs do not exist. In the chapter on population dynamics, {329,333}, I show that this uninteresting detail substantially affects dynamics at low population growth rates, which occur most frequently in nature. If food is abundant, the population will evolve rapidly

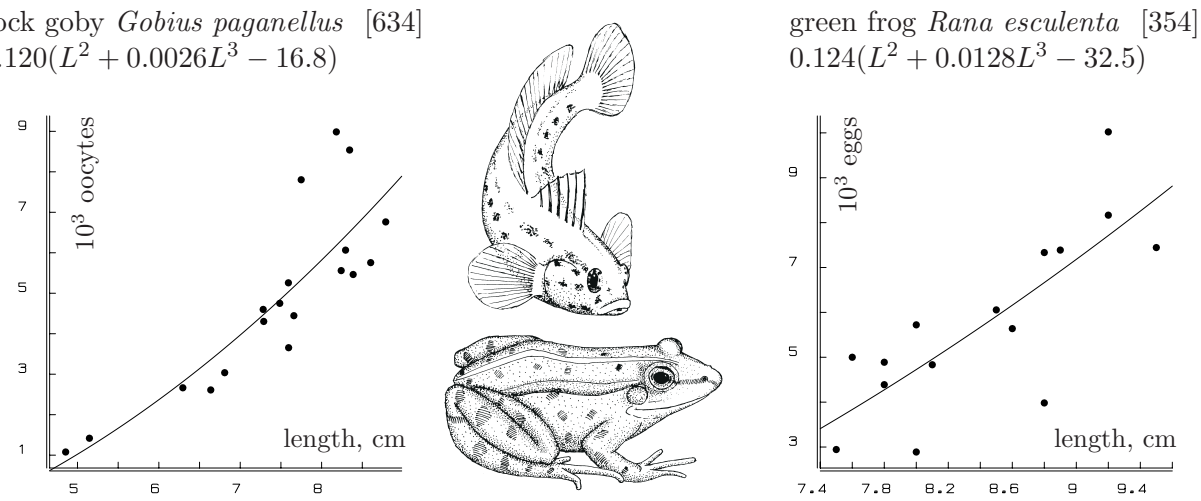

Figure 3.22: The clutch size, as a measure for the reproduction rate, as a function of body length L for two randomly selected species. The data sources and DEB-based curves are indicated. The parameter that is multiplied by L^3 in both fits has been guestimated on the basis of common values for the maintenance rate coefficient and the energy conductance, with a shape coefficient of $\delta_{\mathcal{M}} = 0.1$ for the goby and of $\delta_{\mathcal{M}} = 0.5$ for the frog. Both other parameter values represent least-squares estimates.

to a situation in which food per individual is sparse and reproduction low if harvesting processes do not prevent this.

The strategies for handling this buffer are species-specific and are affected by environmental variables. The spectacular synchronization of reproduction in corals [836], the pelagic palolo worms *Eunice viridis*, South East Asian dipterocarps and bamboo forests probably reduce losses, because potential predators have little to eat between the events. Most species are able to synchronize the moment of reproduction with seasonal cycles such that food availability just matches the demand of the offspring. Clutch size in birds typically relates to food supply during a two-month period prior to egg laying and tends to decrease if breeding is postponed in the season [617]. The laying date is determined by a rapid increase in food supply. Since feeding conditions tend to improve during the season, internal factors must contribute to the regulation of clutch size. These conclusions result from an extensive study of the energetics of the kestrel *Falco tinnunculus* by Serge Daan and co-workers [218,595,616]. I see reproductive behaviour like this for species that cease growth at an early moment in their life span, as variations on the general pattern that the DEB theory is aiming to grasp. Aspects of reproduction energetics for species that cease growth are worked out on {253} and {295}.

Under conditions of prolonged starvation, organisms can deviate from the standard reproduction allocation, as is discussed on {227}.

Cumulative reproduction

Oikopleura sports a heroic way of reproduction which leads to instant death. During its week-long life at 20 °C and abundant food, it accumulates energy for reproduction

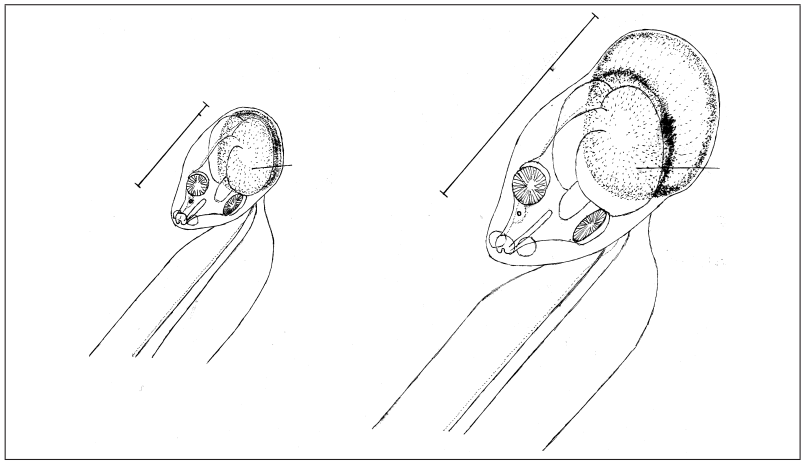

Figure 3.23: The larvacean *Oikopleura* grows isomorphically; during its short life it accumulates reproductive material at the posterior end of the trunk. The energy interpretation of data on total trunk lengths should take account of this. Larvaceans of the genus *Oikopleura* are an important component of the zooplankton of all seas and oceans and have an impact as algal grazers comparable with that of copepods.

which is deposited at the posterior end of the trunk; see Figure 3.23. This allows an easy test of the allocation rule against experimental data. Except for this accumulation of material for reproduction, the animal remains isomorphic. The total length of the trunk, L_t, including the gonads, can be partitioned into the true trunk length, L, and the length of the gonads, L_R. Since the reproduction material is deposited on a surface area of the trunk, the length of the gonads is about proportional to the accumulated investment of energy in reproduction divided by the squared true trunk length. Fenaux and Gorsky [275] measured both the true and the total trunk length under laboratory conditions. This allows us to test the consequences of the DEB theory for reproduction.

Let $e_R(t_1, t_2)$ denote the cumulative investment of energy in reproduction between t_1 and t_2, as a fraction of the maximum energy reserves $[E_m]V_m$. From Table 3.5 we know that this investment amounts for adults to

$$e_R(t_1, t_2) = \kappa_R(1-\kappa)g\dot{k}_M \int_{t_1}^{t_2} \left(\frac{g + l(t)}{g + e(t)} e(t) l^2(t) - l_p^3 \right) dt \tag{3.53}$$

Oikopleura has a non-feeding larval stage and starts investing in reproduction as soon as it starts feeding, so $L_b = L_p$. From an energetic point of view, it thus lacks a juvenile stage, and the larva should be classified as an embryo. The total trunk length then amounts to $L_t(t) = L(t) + V_R e_R(0,t)/L^2(t)$. The volume V_R is a constant that converts the scaled cumulative reproductive energy per squared trunk length into the contribution to the total length. At abundant food, the true trunk length follows the von Bertalanffy growth curve $L(t) = L_m - (L_m - L_b)\exp\{-\frac{tg\dot{k}_M}{3(1+g)}\}$ and $e(t) = 1$, where L_m denotes the maximum length, i.e. $L_m = V_m^{1/3}/\delta_{\mathcal{M}}$. If the data set $\{t_i, L(t_i), L_t(t_i)\}_{i=1}^n$ is available, the five parameters L_b, L_m, $\dot{k}_M$, g and $V_R\kappa_R$ can be estimated in principle. Dry weight relates to trunk length and reproductive energy as $W_d(t) = [W_{Ld}]L^3(t) + W_{Rd}e_R(0,t)$, where the two coefficients give the contribution of cubed trunk length and cumulative scaled reproductive energy to dry weight. If dry weight data are available as well, there are seven parameters to be estimated from three curves.

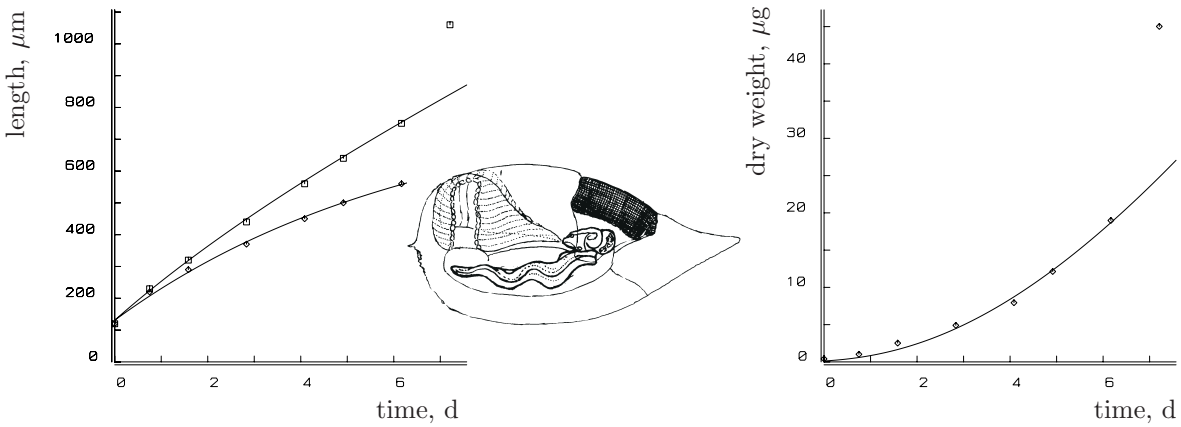

Figure 3.24: The total trunk length, L_t (□ and upper curve, left), the true trunk length, L (◇ and lower curve, left) and the dry weight (right) for *Oikopleura longicauda* at 20 °C. Data from Fenaux and Gorsky [275]. The DEB-based curves account for the contribution of the cumulated energy, allocated to reproduction, to total trunk length and to dry weight. The parameter estimates are $L_m = 822$ (sd 37) μm, $l_b = l_p = 0.157$ (sd 0.006), $\dot{k}_M = 1.64$ (sd 0.14) d^{-1}, $g = 0.4$, $V_R\kappa_R = 0.0379$ (sd 0.0083) mm^3, excluding the last L_t data point. Given these parameters, the weight data give $W_{Ld} = 0.0543$ (sd 0.0131) $\mathrm{g\,cm}^{-3}$, $W_{Rd} = 15.2$ (sd 4.20) μg, the last data point is excluded.

Figure 3.24 gives an example. The data appear to contain too little information to determine both $\dot{k}_M$ and g, so either $\dot{k}_M$ or g has to be fixed. The more or less arbitrary choice $g = 0.4$ is made here. The estimates are tied by the relationship that $\frac{\dot{k}_M g}{1+g}$ is almost constant. The high value for the maintenance rate coefficient $\dot{k}_M$ probably relates to the investment of energy in the frequent synthesis of new filtering houses.

3.9.2 Division

If propagation is by division, the situation is comparable to the juvenile stage of species that propagate via eggs. A cell divides as soon as the energy invested in the increase of the state of maturity exceeds a threshold value. If the specific maturity maintenance costs equals $\frac{1-\kappa}{\kappa}[\dot{p}_M]$, division also occurs at a fixed structural volume, say V_d. Donachie [224] pointed out that in fast growing bacteria the initiation of DNA duplication occurs at a certain volume V_p, but it requires a fixed and non-negligible amount of time t_D for completion. This makes the volume at division, V_d, dependent on the growth rate, so indirectly on substrate density, because growth proceeds during this period.

The mechanism (in eukaryotic somatic cells) of division at a certain size is via the accumulation of two mitotic inducers, cdc25 and cdc13, which are produced coupled to cell growth. (The name for the genes 'cdc' stands for cell division cycle.) If these inducers exceed a threshold level, protein kinase $\mathrm{p34}^{\mathrm{cdc2}}$ is activated and mitosis starts [642,649]. During mitosis, the protein kinase is deactivated and the concentration of inducers resets to zero. This mechanism indicates that for shorter interdivision periods, the cell starts a

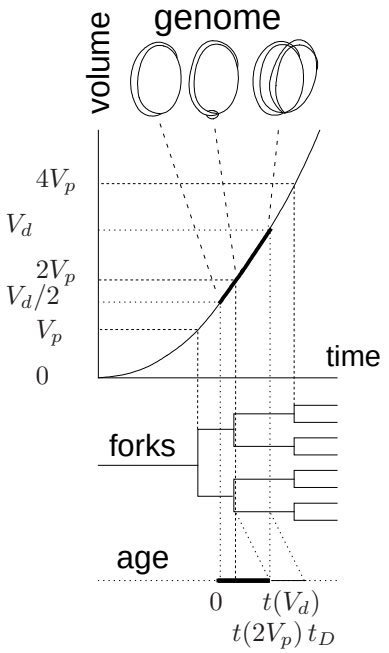

Figure 3.25: A schematic growth curve of a cell, where the fat part is used in steady state. This is the situation for $i = 2$, the number of forks switching between 1 and 3. If $V_d/V_p = 2^i$, equation (3.54) reduces to $t_D = it(2^iV_p) = it(V_d)$, with $t(2^{i-1}V_p) = 0$, which means that the time required to duplicate DNA is exactly i times the division interval. So, during each cell cycle, a fraction i^{-1} of the genome is duplicated, which implies that 2^i-1 DNA duplication forks must be visible during the cell cycle. At the moment that the number of forks jumps from $2^i - 1$ to $2^{i+1} - 1$, the cell divides and the number of forks resets to $2^i - 1$. This is obviously a somewhat simplified account, as cell division is not really instantaneous. If $V_d/V_p \neq 2^i$, the age of the cell at the appearance of the new set of duplication forks somewhere during the cell cycle is $t(2^{i-1}V_p)$, which thus has to be subtracted from $it(V_d)$ to arrive at the genome duplication time.

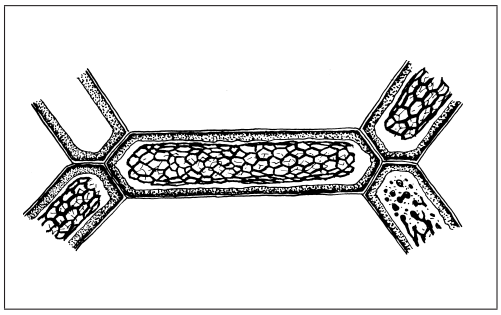

Figure 3.26: The waternet *Hydrodictyon reticulatum* forms a cylindrical sac-like net; the largest recorded size is 114 cm long and 4–6 cm broad [151]. Several thousand spores in each cell grow into small cylindrical cells, which make contact, stick together and form a minute net. The mother cells disintegrate synchronously, each giving birth to a new net. This green alga recently arrived in New Zealand, where it causes water quality problems in eutrophic fresh waters.

new DNA duplication cycle when its volume exceeds $2V_p$, $4V_p$, $8V_p$ etc. The interdivision time for *Escherichia coli* can be as short as 20 minutes under optimal conditions, while it takes an hour to duplicate the DNA. The implementation of this trigger is not simple in a dynamic environment. At constant substrate densities, the scaled cell length at division, $l_d \equiv (V_d/V_m)^{1/3}$, and the division interval, $t(l_d) \equiv t_d$, can be obtained directly. When i is an integer such that $2^{i-1} < V_d/V_p \leq 2^i$, V_d can be solved from

$$t_D = it(V_d) - t(2^{i-1}V_p) \tag{3.54}$$

Figure 3.25 illustrates the derivation.

The volume at division V_d can be found numerically when (3.21), (3.40) or (3.43) is substituted for $t(V)$ in (3.54), for isomorphs, V1-morphs or rods, respectively. If the ratio of the maturity and somatic maintenance costs does not equal $\frac{1-\kappa}{\kappa}$, the size at division must be obtained from equating the cumulative investment in maturation to a threshold level, the size at division generally increases with substrate density, even apart from delays due to DNA duplication.

Many organisms that propagate vegetatively produce spores, and the mother cell dies upon release. The number usually varies between species and growth conditions, and

frequently is a power of 2. In the green alga *Scenedesmus* it is usually 4 or 8, but in the water net, it can be several thousand, see Figure 3.26.

3.10 Summary of the basic DEB model

The assumptions on which the basic DEB model is based are listed in Table 3.3. They are arranged into two categories: general and specific. The general ones are required for the mass–energy relationships to be discussed in the next chapter; the specific ones serve to specify the basic powers.

The DEB model is built on two state variables:

- structural biomass, quantified as volume V (maximum volume V_m), mass M_V (maximum mass M_{Vm}) or scaled length $l \equiv (V/V_m)^{1/3}$ (maximum scaled length 1);
- reserves, quantified as energy density $[E]$ (maximum energy density $[E_m]$), mass M_E (maximum mass M_{Em}), relative mass $m_E \equiv M_E/M_V$, or scaled energy density $e \equiv [E]/[E_m]$.

There is not a single most useful notation for energetics. Volumes are handy in relation to surface areas, which are needed for the process of food/substrate uptake in the DEB model, while moles are handy for mass fluxes. Table 3.4 gives the conversions between volume-based and mole-based quantities, some of which are introduced in the next chapter. The specific fluxes j_* relate to the fluxes $\dot{J}_*$ by $j_* = \dot{J}_*/M_V$.

Table 3.4 can be used to deduce from (3.10) and (3.18) that the change in reserve density m_E and in structural mass M_V in terms of (specific) molar masses amount to

$$\frac{d}{dt}m_E = j_{EAm}(f - m_E/m_{Em}) \tag{3.55}$$

$$\frac{d}{dt}M_V = M_V\frac{j_{EAm}(m_E/m_{Em} - l_h) - j_{EM}/\kappa}{m_E + y_{EV}/\kappa} \tag{3.56}$$

where y_{EV} denotes the moles of reserves required to synthesize a mole of structural mass. Equation (3.55) shows that the parameter m_{Em} can be interpreted as the maximum value of the molar reserve density m_E. The scaled heating length l_h is zero for ectotherms. Changes in shape during growth affect the relationship between the maximum specific assimilation rate and the structural mass; the parameters $j_{EAm} = y_{EX}j_{XAm}$ and j_{XAm} must be multiplied by the shape correction function $\mathcal{M}$, see {29}. For isomorphs we have $j_{XAm} = \{\dot{J}_{XAm}\}M_V^{-1/3}[M_V]^{-2/3}$.

The energy fluxes, called powers, are given in Table 3.5 as functions of the scaled energy density e and scaled length l for a 3S–isomorph, i.e. a isomorph with three life stages, and in Table 3.6 for a 1S–V1–morph. These tables also assign symbols to the various powers. Notice that all powers are cubic polynomials in the (scaled) length, while the weight coefficients depend on (scaled) reserve density. Powers are indicated by symbol $\dot{p}$, molar fluxes of masses by $\dot{J}$.

Table 3.3: The assumptions that lead to the basic DEB model as formulated for multicellulars and modified for unicellulars.

General

1 Structural body mass and reserves are the state variables of the individual; they have a constant composition (strong homeostasis).

2 Food is converted into faeces, and assimilates derived from food are added to reserves. These fuel all other metabolic processes, which can be classified into three categories: synthesis of structural body mass, synthesis of gametes, and processes that are not associated with synthesis of biomass. Products that leave the organism may be formed in direct association with these three categories of processes, and with the assimilation process.

3 If the individual propagates via reproduction (rather than via division), it starts in the embryonic stage that initially has a negligibly small structural body mass (but a substantial amount of reserves).

Specific

3a The reserve density of the hatchling equals that of the mother at egg formation. Foetuses develop in the same way as embryos in eggs, but at a rate unrestricted by energy reserves.

4 The transition from embryo to juvenile initiates feeding, that from juvenile to adult initiates reproduction, which is coupled to the cessation of maturation. The transitions occur when the cumulated energy invested in maturation exceeds certain threshold values. Unicellulars divide when the cumulated energy invested in maturation exceeds a threshold value.

5 Somatic and maturity maintenance are proportional to structural body volume, but maturity maintenance does not increase after a given cumulated investment in maturation. Heating costs for endotherms are proportional to surface area.

6 The feeding rate is proportional to the surface area of the organism and the food handling time and the digestion efficiency are independent of food density.

7 The reserves must be partitionable, such that the dynamics is not affected; the use of reserves does not depend on food density; the reserve density *at steady state* does not depend on structural body mass (weak homeostasis).

8 A fixed fraction of energy, utilized from the reserves, is spent on somatic maintenance plus growth, the rest on maturity maintenance plus maturation or reproduction (the κ-rule).

9 Under starvation conditions, individuals always give priority to somatic maintenance and follow one of two possible strategies: they do not change the reserve dynamics (so continue to invest in development or reproduction), or cease energy investment in development and reproduction (thus changing reserves dynamics).

Table 3.4: Conversions between volumes, molar masses and energies in the DEB model. Volumes are indicated by V, masses in C-moles by M, energies by E, molar fluxes with $\dot{J}$, energy fluxes (powers) with $\dot{p}$. Dots refer to time^{-1}, brackets [ ] refer to volume^{-1}, while the braces { } refer to surface area^{-1}. The energy-mass coupler $\mu_{*_1*_2}$ couples energy flux $*_1$ to mass flux $*_2$ (dimension energy per mass). The chemical potential μ_* also has dimension energy per mass, but cannot be interpreted as ratio of fluxes. The mass-mass coupler $y_{*_1*_2}$ can be written as the ratio of two energy-mass couplers or of two mass fluxes. The first index of mass fluxes, $\dot{J}_{*_1*_2}$, refers to the compound, $*_1$, the second one, $*_2$, to the energy flux with which the mass flux is associated. The dimensions are indicated by l (length), m (mass), e (energy), t (time)

structural volume	$V = \frac{M_V}{[M_V]}$	l^3	max structural volume	$V_m = \left(\frac{\dot{v}}{\dot{k}_M\, g}\right)^3 = \frac{M_{Vm}}{[M_V]} = \left(\frac{\kappa y_{VX}}{\dot{k}_M}\frac{\{\dot{J}_{XAm}\}}{[M_V]}\right)^3$	l^3
reserve energy	$E = \mu_E M_E$	e	max res energy	$E_m = [E_m]V_m = \mu_E M_{Em}$	e
max res ener dens	$[E_m] = \mu_E [M_{Em}]$	$\frac{e}{l^3}$	spec struct costs	$[E_G] = \mu_{GV}[M_V]$	$\frac{e}{l^3}$
scaled length	$l = \left(\frac{M_V}{M_{Vm}}\right)^{1/3} = \left(\frac{V}{V_m}\right)^{1/3}$	-	scaled res density	$e = \frac{[E]}{[E_m]} = \frac{m_E}{m_{Em}} = \frac{M_E}{M_{Em}}$	-
max spec reserve	$m_{Em} = \frac{[M_{Em}]}{[M_V]}$	$\frac{m}{m}$	spec reserve	$m_E = \frac{M_E}{M_V} = \frac{e}{\mu_E}\frac{[E_m]}{[M_V]}$	$\frac{m}{m}$
max spec assim	$\{\dot{p}_{Am}\} = \mu_{AX}\{\dot{J}_{XAm}\}$	$\frac{e}{l^2 t}$	spec maintenance	$[\dot{p}_M] = \dot{k}_M\, \mu_{GV}\, [M_V]$	$\frac{e}{l^3 t}$
energy conduct	$\dot{v} = \frac{\{\dot{p}_{Am}\}}{[E_m]} = y_{EX}\frac{\{\dot{J}_{XAm}\}}{[M_{Em}]}$	$\frac{l}{t}$	investment ratio	$g = \frac{[E_G]}{\kappa[E_m]} = \frac{y_{EV}}{\kappa m_{Em}}$	-
maint rate coef	$\dot{k}_M = \frac{[\dot{p}_M]}{[E_G]} = j_{EM}\, y_{VE}$	$\frac{1}{t}$	turnover rate	$\dot{k}_E = \frac{[\dot{p}_{Am}]}{[E_m]} = \frac{y_{EX}}{m_{Em}} j_{XAm}$	$\frac{1}{t}$

structural mass	$M_V = V[M_V]$	m	max structural mass	$M_{Vm} = V_m[M_V] = \left(\frac{\kappa y_{VX}}{\dot{k}_M}\frac{\{\dot{J}_{XAm}\}}{[M_V]}\right)^3 [M_V]$	m
reserve mass	$M_E = \frac{E}{\mu_E} = M_V \frac{e y_{EV}}{\kappa g}$	m	max reserve mass	$M_{Em} = \frac{E_m}{\mu_E} = M_{Vm} m_{Em}$	m
$\frac{\text{assim}}{\text{food}}$ coupler	$\mu_{AX} = \frac{\{\dot{p}_{Am}\}}{\{\dot{J}_{XAm}\}} = \frac{\mu_E}{y_{XE}}$	$\frac{e}{m}$	$\frac{\text{assim}}{\text{product}}$ coupler	$\mu_{AP} = \frac{\{\dot{p}_{Am}\}}{\{\dot{J}_{PAm}\}} = \frac{\mu_E}{y_{PE}}$	$\frac{e}{m}$
res chem potential	$\mu_E = \frac{[E_m]}{[M_{Em}]}$	$\frac{e}{m}$	$\frac{\text{growth}}{\text{structure}}$ coupler	$\mu_{GV} = \frac{[E_G]}{[M_V]} = \frac{\mu_E}{y_{VE}}$	$\frac{e}{m}$
$\frac{\text{product}}{\text{reserve}}$ coupler	$y_{PE} = \frac{\mu_E}{\mu_{AP}} = \frac{j_{PA}}{j_{EA}}$	$\frac{m}{m}$	$\frac{\text{product}}{\text{food}}$ coupler	$y_{PX} = \frac{\mu_{AX}}{\mu_{AP}} = \frac{j_{PA}}{j_{XA}}$	$\frac{m}{m}$
$\frac{\text{structure}}{\text{reserve}}$ coupler	$y_{VE} = \frac{\mu_E}{\mu_{GV}} = \frac{j_{VG}}{j_{EG}}$	$\frac{m}{m}$	$\frac{\text{food}}{\text{reserve}}$ coupler	$y_{XE} = \frac{\mu_E}{\mu_{AX}} = \frac{j_{XA}}{j_{EA}}$	$\frac{m}{m}$
spec assim flux	$j_{EA} = j_{XA}\, y_{EX}$	$\frac{m}{mt}$	spec maint flux	$j_{EM} = \dot{k}_M\, y_{EV}$	$\frac{m}{mt}$

mass density	$[M_*] = \frac{M_*}{V}$	$\frac{m}{l^3}$	spec mass	$m_* = \frac{M_*}{M_V}$	$\frac{m}{m}$
$\frac{\text{energy}}{\text{mass}}$ coupler	$\mu_{*_1*_2} = \frac{\dot{p}_{*_1}}{\dot{J}_{*_2*_1}} = \eta^{-1}_{*_2*_1}$	$\frac{e}{m}$	$\frac{\text{mass}}{\text{energy}}$ coupler	$\eta_{*_1*_2} = \frac{\dot{J}_{*_1*_2}}{\dot{p}_{*_2}} = \mu^{-1}_{*_2*_1}$	$\frac{m}{e}$
$\frac{\text{mass}}{\text{mass}}$ coupler	$y_{*_1*_2} = \frac{\dot{J}_{*_1*_3}}{\dot{J}_{*_2*_3}} = y^{-1}_{*_2*_1}$	$\frac{m}{m}$	$\frac{\text{mass}}{\text{mass}}$ coupler	$\zeta_{*_1*_2} = \frac{\mu_E m_{Em}}{\mu_{*_2*_1}}$	$\frac{m}{m}$
spec flux	$j_{*_1*_2} = \frac{\dot{J}_{*_1*_2}}{M_V}$	$\frac{m}{mt}$	spec power	$[\dot{p}_*] = \frac{\dot{p}_*}{V}$	$\frac{e}{l^3 t}$

Table 3.5: The powers as specified by the DEB model for 3S-isomorph of scaled length l and scaled reserve density e at scaled functional response $f \equiv \frac{X}{X_K+X}$, where X denotes the food density and X_K the saturation constant. Their relationships are given in the diagram, where the rounded boxes indicate sources or sinks. The powers $\dot{p}_X = \dot{J}_X \mu_X$ and $\dot{p}_P = \dot{J}_P \mu_P$ for ingestion and defecation occur in the environment, not in the individual. The DEB model assumes that $\dot{J}_X \propto \dot{J}_P \propto \dot{p}_A$. The table gives scaled powers, where μ_E denotes the chemical potential of the reserves. Parameters: g investment ratio, $\dot{k}_M$ maintenance rate coefficient, κ partitioning parameter for catabolic power, l_h scaled 'heating length'. Ectotherms do not heat, i.e. $l_h = 0$.

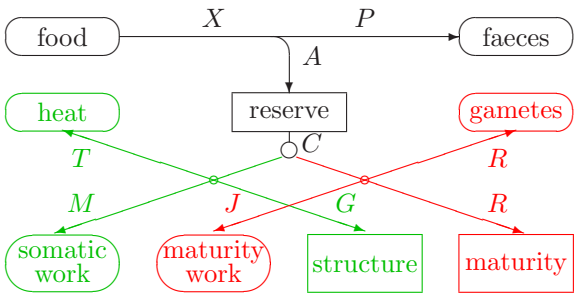

Implied dynamics for $e > l > l_b$: $\frac{d}{dt}e = \frac{f-e}{l}\dot{k}_M g$ and $\frac{d}{dt}l = \frac{e-l-l_h}{1+e/g}\frac{\dot{k}_M}{3}$

$\frac{\text{power}}{\mu_E M_{Em} \dot{k}_M g}$	embryo $0 < l \leq l_b$	juvenile $l_b < l \leq l_p$	adult $l_p < l < 1$
assimilation, $\dot{p}_A$	0	fl^2	fl^2
catabolic, $\dot{p}_C$	$el^2\frac{g+l}{g+e}$	$el^2\frac{g+l+l_h}{g+e}$	$el^2\frac{g+l+l_h}{g+e}$
somatic maintenance, $\dot{p}_M$	κl^3	κl^3	κl^3
maturity maintenance, $\dot{p}_J$	$(1-\kappa)l^3$	$(1-\kappa)l^3$	$(1-\kappa)l_p^3$
endothermic heating, $\dot{p}_T$	0	$\kappa l^2 l_h$	$\kappa l^2 l_h$
somatic growth, $\dot{p}_G$	$\kappa l^2\frac{e-l}{1+e/g}$	$\kappa l^2\frac{e-l-l_h}{1+e/g}$	$\kappa l^2\frac{e-l-l_h}{1+e/g}$
maturity growth, $\dot{p}_R$	$(1-\kappa)l^2\frac{e-l}{1+e/g}$	$(1-\kappa)l^2\frac{e-l+l_h e/g}{1+e/g}$	0
reproduction, $\dot{p}_R$	0	0	$(1-\kappa)(l^2\frac{e-l+l_h e/g}{1+e/g} + l^3 - l_p^3)$

Table 3.6: The powers as specified by the DEB model for an ectothermic 1S–V1–morph of scaled length l and scaled reserve density e at scaled functional response f. An individual of structural volume $V \equiv M_V/[M_V]$ takes up substrate at rate $[\dot{J}_{Xm}]fV$. The implied dynamics for e and l: $\frac{d}{dt}e = \frac{f-e}{l_d}\dot{k}_M g$ and $\frac{d}{dt}l = l\frac{e/l_d-1}{e/g+1}\frac{\dot{k}_M}{3}$; division occurs when $l = l_d$.

$\frac{\text{power}}{\mu_E M_{Em} \dot{k}_M g}$	juvenile
assimilation, $\dot{p}_A$	fl^3/l_d
catabolic, $\dot{p}_C$	$el^3\frac{1+g/l_d}{g+e}$
somatic maintenance, $\dot{p}_M$	κl^3
maturity maintenance, $\dot{p}_J$	$(1-\kappa)l^3$
somatic growth, $\dot{p}_G$	$\kappa l^3\frac{e/l_d-1}{1+e/g}$
maturity growth, $\dot{p}_R$	$(1-\kappa)l^3\frac{e/l_d-1}{1+e/g}$

The catabolic power equals the sum of the non-assimilative powers

$$\dot{p}_C = \dot{p}_M + \dot{p}_J + \dot{p}_T + \dot{p}_G + \dot{p}_R \tag{3.57}$$

A three-stage individual invests either in maturity growth, or in reproduction. This is why these powers have the same index, the stage determines the destination.

The dissipating power, excluding assimilation and somatic growth overheads, amounts to

$$\dot{p}_D = \dot{p}_M + \dot{p}_J + \dot{p}_T + (1 - \kappa_R)\dot{p}_R \tag{3.58}$$

where $\kappa_R = 0$ for the embryo and juvenile stages. Reproduction power $\dot{p}_R$ has a special status because reserves of the adult female are converted into reserves of the embryo which have the same composition. The efficiency of this conversion is denoted by κ_R, which means that $(1 - \kappa_R)\dot{p}_R$ is dissipating and $\kappa_R\dot{p}_R$ returns to the compound class reserve, but now of the embryo.

Chapter 4

Uptake and use of essential compounds

The previous chapter focused on energy, but energy and mass are two aspects of the same thing. Mass takes the form of many compounds, each having their own set of characteristic properties, which makes the analysis of mass more complex than that of energy.

This chapter derives the fluxes of essential compounds. The derivation holds for a broad class of models for which the general assumptions of Table 3.3, {121}, apply [517,523]. This is why I made two categories of assumptions; the specific assumptions turn out not to be essential for these derivations. They may be replaced by others, resulting in other specifications of the three basic powers (assimilation, dissipation and growth), while the derivation of how fluxes of essential compounds relate to the basic powers still applies. In other words, rules for mass fluxes do not allow supplementary assumptions on mass fluxes, such as respiration or nitrogenous waste, without creating inconsistencies. I show why fluxes of essential compounds are weighted sums of these three basic powers. Non-essential compounds differ from essential ones because their use is not regulated; they are excreted into the environment, sometimes in modified form, as analysed later, see {187}.

Just like mass fluxes, dissipating heat is a weighted sum of the three basic powers. Therefore, it can also be written as a weighted sum of three mineral fluxes: carbon dioxide, oxygen and nitrogenous waste. This relationship is the basis of the method of indirect calorimetry. After half a century of wide application, this empirical method is finally underpinned theoretically.

The aging process is discussed as a consequence of respiration, with its intimate links with energetics. Fermentation processes and the production of compounds such as alcohol are considered. A simple model for drinking by terrestrial organisms follows from the water balance.

4.1 Chemical compounds and transformations

The approach is to represent and follow chemical elements, because elements rather than compounds obey conservation laws. In particular, I follow the four most abundant elements

in living systems, C, H, O and N. These four elements happen to be the four lightest of the periodic table that can make covalently bounded compounds [156]. However, this list can be extended readily because each new element comes with a corresponding balance equation. Two sets of chemical compounds partake in three (sets of) transformations:

compounds →		minerals, $\mathcal{M}$				org. comp. $\mathcal{O}$			
transformations ↓		carbon dioxide C	water H	oxygen O	nitrogenous waste N	food X	structure V	reserves E	faeces P
assimilation	A	+	+	−	+	−		+	+
growth	G	+	+	−	+		+	−	
dissipation	D	+	+	−	+			−	

The organic compounds V and E constitute the individual, the other organic compounds and the minerals define the chemical environment of the individual. The signs indicate appearance (+) or disappearance (−); a blank indicates that the compound does not partake in that transformation.

The chemical indices of the minerals and the organic compounds are collected in two matrices $\boldsymbol{n}_{\mathcal{M}}$ and $\boldsymbol{n}_{\mathcal{O}}$, respectively. A typical element of such a matrix, $n_{*_1*_2}$, denotes the chemical index of compound $*_2$ with respect to element $*_1$. The chemical indices of the organic compounds for carbon equal 1 by definition. The strong homeostasis assumption (# 1 of Table 3.3) amounts to the condition that the chemical indices do not change.

The molecular weights of the mineral and the organic compounds are

$$\boldsymbol{w}_{\mathcal{M}}^T = (\ 12 \quad 1 \quad 16 \quad 14\ )\boldsymbol{n}_{\mathcal{M}} \quad \text{and} \quad \boldsymbol{w}_{\mathcal{O}}^T = (\ 12 \quad 1 \quad 16 \quad 14\ )\boldsymbol{n}_{\mathcal{O}} \tag{4.1}$$

The following subsections briefly discuss some features of the different compounds to supplement earlier introductions.

Mineral compounds

Oxygen and carbon dioxide

Most organisms use oxygen as an electron acceptor in the respiration chain, the final stage in the oxidation of pyruvate, see Figure 2.14. If oxygen is not available, a substantial amount of energy cannot be extracted from pyruvate, and metabolic products have to be excreted. Photosynthetic bacteria, algae and plants not only use oxygen, but also produce oxygen, see {164}. This production exceeds the consumption if light intensity is high enough. Most organisms consume and excrete carbon dioxide, consumption exceeds excretion in photosynthetic organisms in the light, and in bacteria that use methane as substrate.

Table 4.1: Various nitrogenous wastes that animals use [1009].

nitrogenous waste	formula	solubility (mM)	insects	crustaceans	fish	birds	mammals
ammonia	NH_3	52.4		○	○		
amm. bicarbonate	NH_4HCO_3	1.5		○			
urea	$CO(NH_2)_2$	39.8					○
allantoin	$C_4H_6O_3N_4$	0.015					○
allantoic acid	$C_4H_8O_4N_4$	slight					○
uric acid	$C_5H_4O_3N_4$	0.0015				○	
sodium urate	$C_5H_2O_3N_4Na_2$	0.016	○			○	
potassium urate	$C_5H_2O_3N_4K_2$	slight	○			○	
guanine	$C_4H_5ON_5$	0.0013	○			○	
xanthine	$C_5H_4O_2N_4$	0.068	○			○	
hypoxanthine	$C_5H_4ON_4$	0.021	○			○	
arginine	$C_6H_{14}O_2N_4$	3.4	○			○	

Water

Water is formed metabolically from other compounds. This rate of water production is studied first; the direct exchange of water with the environment via drinking and evaporation, and its use for transport, are discussed on {151}.

Nitrogenous waste

From an energy perspective, the cheapest form of nitrogenous waste is ammonia. Since ammonia is rather toxic at high concentrations, terrestrial animals usually make use of more expensive, less toxic nitrogenous wastes. Terrestrial isopods are an exception; Dutchmen call them 'pissebed', a name referring to the smell of ammonia that microbes produce from urine in a bed. Terrestrial eggs have to accumulate the nitrogenous waste during development; they usually make use of even more expensive, less soluble nitrogenous wastes that crystallize outside the body, within the egg shell. Table 4.1 lists the different chemical forms of nitrogenous waste. The nitrogenous waste (urine) includes its water in its chemical 'composition', for simplicity's sake.

Nitrogenous waste mainly originates from protein turnover, which is linked to somatic maintenance.

A second origin of nitrogenous waste can be assimilation, when metazoans feed on protein-rich food, and nitrogen is excreted in the transformation of food to reserves. The (energy/carbon) substrate for micro-organisms can be poor in nitrogen, such that nitrogen must be taken up from the environment, rather than excreted. Though the term nitrogenous waste not longer applies, this does not matter for the analysis; the sign of the flux defines uptake or excretion. Bacteria that live on glucose as an energy source will have

negative nitrogenous waste. In this chapter, nitrogen that is taken up independently of the energy source is assumed not to be limiting. The next chapter deals with more complex situations, where several resources can be limiting.

Organic compounds

Structural biomass, reserves

Body mass is composed of structural biomass and reserves. The chemical nature of the reserves is discussed on {37}. Observed changes in the elemental composition of the body mass, as a function of growth rate, or starvation time, can be used to obtain the elemental composition of reserves and structure, as is discussed on {134}.

Food

Food for micro-organisms is usually called 'substrate', which can be very simple chemical compounds, such as glucose. Most animals feed on plants and other animals, i.e. complex substrates. For simplicity's sake, I assume that the composition of food is constant, but this is not essential; the composition of faeces is taken to be constant as a consequence. This condition will be relaxed on {161}.

Product (faeces)

Faeces is the remains of food after it has passed through the gut. Animals add several products to these remains, such as bile and enzymes that are excreted in the gut, and excreted micro-flora formed in the gut. Mammals in particular also add substantial quantities of methane; hoatzins, an Amazonian relative of the cuckoo, smell like cows, because of the similar gut flora and digestion. I include these products in faeces, since these excretions are tightly coupled to the feeding process.

The faeces of micro-organisms is usually called 'metabolic products'. For instance, microbes degrade cellulose to lipids outside the cell in anaerobic environments; lipids play the role of faeces here. Sometimes, substrate molecules are taken up entirely, and completely metabolized to carbon dioxide and water; in this case no faeces is produced. In other cases products are formed that generally do not originate from substrate directly, but indirectly with a more complex link to the metabolic machinery of the organism. The role of such products is then similar to that of nitrogenous wastes in animals. I cope with these situations by including such products in the overheads of the three basic energy fluxes, the assimilation flux, the dissipating flux and the somatic growth flux. The number of different products can be extended in a straightforward manner, see {147}. It is not only bacteria and fungi that produce compounds that are excreted into the environment – many animals do this as well (e.g. mucus, moults); wood can be conceived as a product of plants that remains associated with the plant.

If oxygen is poorly available, a variety of products are formed and released in the environment:

product	chemical formula	rel. freq.	μ
ethanol	CH_3CH_3O	$CH_3O_{0.5}$	657
lactate	$CH_3CH_2OCHO_2$	CH_2O	442
succinate	$CHO_2CH_2CH_2CHO_2$	$CH_{1.5}O$	376
propionate	$CH_3CH_2CHO_2$	$CH_2O_{0.66}$	493
acetate	CH_3CHO_2	CH_2O	442

where the last column gives the Gibbs energy of formation in kJ/ C-mole at pH = 7 in the combustion frame of reference [389]. The kind of product depends on the species and the environmental conditions. The quantitative aspects are discussed on {148}.

4.2 Powers

The general assumptions that are listed in Table 3.3 {121} imply that the relationships between powers and mass fluxes involve three groups of basic powers

$$\dot{\boldsymbol{p}} \equiv \begin{pmatrix} \dot{p}_A \\ \dot{p}_D \\ \dot{p}_G \end{pmatrix} = \begin{cases} \text{assimilation power (coupled to food intake)} \\ \text{dissipating powers (no net synthesis of biomass)} \\ \text{growth power (somatic growth)} \end{cases}$$

Most of the dissipating power leaves the thermodynamic system of individual plus relevant compounds as heat, while a portion leaves the system in the form of nitrogenous waste or products. Part of the growth and assimilation power will also end up as dissipating heat, because of the overhead costs; growth and assimilation do not occur with 100% efficiency (see on {153}). The variety of metabolic processes can contribute to dissipating power, such as maintenance of maturity and of somatic tissue (including activity), heating, maturity growth and reproduction. It is sufficient to know that the dissipating power is a known function of the two state variables of the individual.

Reproduction power $\dot{p}_R$ has a special status because reserves of the adult female are converted into reserves of the embryo which have the same composition on the basis of assumption 1 in Table 3.3. The efficiency of this conversion is denoted by κ_R, which means that $(1-\kappa_R)\dot{p}_R$ dissipates and $\kappa_R\dot{p}_R$ returns to the compound class 'reserve', but now of the embryo. The amount of reserve that is allocated to reproduction during a very small time increment is also very small, and not enough to make one embryo. This property, which is shared by all time-continuous models, implies the existence of a buffer of reserves whose destination is reproduction. Reproduction itself, i.e. the conversion of the reserves in this buffer to embryos, is treated as an event. The overhead costs of the reproduction event are taken into account in the allocation to reproduction.

In the considerations below, the reserves and the reserves in the reproduction buffer are added together. This makes biological sense, because the buffer is still in the individual. The reason for the addition is that the assumptions in Table 3.3 imply that the sum of both fluxes is a weighted sum of the three basic powers, as we will see, but this does not necessarily hold for each of them. (It does not hold for the DEB model, for instance.) Mineral fluxes depend on the sum only. Simplicity as well as generality are maximized, this way, because organisms that propagate by division do not allocate reserves to reproduction.

Here, division is treated as an event. Details about the division only play a role at the population level, because we follow individuals up to this event. Here, I assume that division produces two identical new individuals, but this restriction can be relaxed in several respects, without affecting the main argument.

4.3 Mass balance

Let $\dot{J}_*$ denote the rate of change of the compound $*$. The conservation of mass amounts to

$$\begin{pmatrix} 0 \\ 0 \\ 0 \\ 0 \end{pmatrix} = \begin{pmatrix} 1 & 0 & 0 & n_{CN} \\ 0 & 2 & 0 & n_{HN} \\ 2 & 1 & 2 & n_{ON} \\ 0 & 0 & 0 & n_{NN} \end{pmatrix} \begin{pmatrix} \dot{J}_C \\ \dot{J}_H \\ \dot{J}_O \\ \dot{J}_N \end{pmatrix} + \begin{pmatrix} n_{CX} & n_{CV} & n_{CE} & n_{CP} \\ n_{HX} & n_{HV} & n_{HE} & n_{HP} \\ n_{OX} & n_{OV} & n_{OE} & n_{OP} \\ n_{NX} & n_{NV} & n_{NE} & n_{NP} \end{pmatrix} \begin{pmatrix} \dot{J}_X \\ \dot{J}_V \\ \dot{J}_E + \dot{J}_{E_R} \\ \dot{J}_P \end{pmatrix} \quad (4.2)$$

This can be summarized in matrix form as $\mathbf{0} = \boldsymbol{n}_{\mathcal{M}}\dot{\boldsymbol{J}}_{\mathcal{M}} + \boldsymbol{n}_{\mathcal{O}}\dot{\boldsymbol{J}}_{\mathcal{O}}$ or $\mathbf{0} = \boldsymbol{n}\dot{\boldsymbol{J}}$, for $\boldsymbol{n} = (\boldsymbol{n}_{\mathcal{M}} \vdots \boldsymbol{n}_{\mathcal{O}})$ and $\dot{\boldsymbol{J}} = (\dot{\boldsymbol{J}}_{\mathcal{M}}^T \vdots \dot{\boldsymbol{J}}_{\mathcal{O}}^T)^T$. Thus the fluxes for the 'mineral' compounds $\dot{\boldsymbol{J}}_{\mathcal{M}}$ can be written as a weighted sum of the fluxes of the organic compounds $\dot{\boldsymbol{J}}_{\mathcal{O}}$

$$\dot{\boldsymbol{J}}_{\mathcal{M}} = -\boldsymbol{n}_{\mathcal{M}}^{-1}\boldsymbol{n}_{\mathcal{O}}\dot{\boldsymbol{J}}_{\mathcal{O}} \quad (4.3)$$

with

$$\boldsymbol{n}_{\mathcal{M}}^{-1} = \begin{pmatrix} 1 & 0 & 0 & -\frac{n_{CN}}{n_{NN}} \\ 0 & 2^{-1} & 0 & -\frac{n_{HN}}{2n_{NN}} \\ -1 & -4^{-1} & 2^{-1} & \frac{n}{4n_{NN}} \\ 0 & 0 & 0 & n_{NN}^{-1} \end{pmatrix}; \quad n \equiv 4n_{CN} + n_{HN} - 2n_{ON} \quad (4.4)$$

I will now explain why the 'organic' fluxes $\dot{\boldsymbol{J}}_{\mathcal{O}}$ relate to the basic powers $\dot{\boldsymbol{p}}$ as

$$\begin{pmatrix} \dot{J}_X \\ \dot{J}_V \\ \dot{J}_E + \dot{J}_{E_R} \\ \dot{J}_P \end{pmatrix} = \begin{pmatrix} -\eta_{XA} & 0 & 0 \\ 0 & 0 & \eta_{VG} \\ \mu_E^{-1} & -\mu_E^{-1} & -\mu_E^{-1} \\ \eta_{PA} & \eta_{PD} & \eta_{PG} \end{pmatrix} \begin{pmatrix} \dot{p}_A \\ \dot{p}_D \\ \dot{p}_G \end{pmatrix}, \quad \text{or} \quad \dot{\boldsymbol{J}}_{\mathcal{O}} = \boldsymbol{\eta}_{\mathcal{O}}\dot{\boldsymbol{p}} \quad (4.5)$$

where μ_E is the chemical potential of the reserves, and $\eta_{*_1*_2}$ the mass flux of compound $*_1$ per unit of power $*_2$, i.e. the coupling between mass and energy fluxes. The latter coefficients serve as model parameters, and are collected in matrix $\boldsymbol{\eta}$.

The fluxes $\dot{J}_X = -\eta_{XA}\dot{p}_A$ and $\dot{J}_P$ follow from assumptions 2 and 3 in Table 3.3. Assimilation energy is quantified by its fixation in reserves, so reserves are formed at a rate $\dot{p}_A/\mu_E$, where μ_E stands for the chemical potential of the reserves, and $y_{XE} = \mu_E/\mu_{AX}$ stands for the C-moles of food ingested per C-mole of reserves formed, where $\mu_{AX} = \eta_{XA}^{-1}$. The rate at which work can be done by ingested food is $\mu_X\dot{J}_X$; the flux $\dot{p}_A$ is fixed in reserves, the flux $\dot{p}_A\mu_P\eta_{PA}$ is fixed in product, the rest dissipates as heat and mineral fluxes that are associated with this conversion. The coefficient $y_{PX} = \mu_{AX}\eta_{PA}$ stands for the C-mole of product that is derived directly from food per C-mole of food ingested (products can also be formed indirectly from assimilated energy).

If the individual happens to be a metazoan and the product is interpreted as faeces, then $\eta_{PD} = \eta_{PG} = 0$. Faeces production is coupled to food intake only. Alcohol production by yeasts that live on glucose is an example of product formation where $\eta_{PD} \neq \eta_{PG} \neq 0$. At this point there is no need for molecular details about the process of digestion being intra- or extra-cellular. This knowledge only affects details in the interpretation of the coefficients in $\boldsymbol{\eta}$.

The flux $\dot{J}_V = \dot{p}_G \eta_{VG}$ indicates that $\mu_{GV} = \eta_{VG}^{-1}$ is the invested energy per C-mole of structural biomass, which directly follows from assumption 1 in Table 3.3. Note that μ_V is the energy that is actually fixed in a C-mole of structural biomass, so $\mu_{GV} - \mu_V$ dissipates (as heat or via products that are coupled to growth) per C-mole.

The flux of reserves is given by $\dot{J}_E = \mu_E^{-1}(\dot{p}_A - \dot{p}_C)$: reserve energy is generated by assimilation and used by catabolism, i.e. the sum of all other metabolic powers (assumption 2 in Table 3.3). The flux of embryonic reserves (i.e. reproduction), $\dot{J}_{E_R} = \mu_E^{-1} \kappa_R \dot{p}_R$, appears as a return flux to the reserve because embryonic reserves have the same composition as adult reserves because of the strong homeostasis assumption. Since $\dot{p}_C = \dot{p}_D + \dot{p}_G + \kappa_R \dot{p}_R$, see (3.57) and (3.58), we have $\dot{J}_E + \dot{J}_{E_R} = \mu_E^{-1}(\dot{p}_A - \dot{p}_D - \dot{p}_G)$, which is the relationship given in (4.5).

Substitution of (4.5) into (4.3) shows that the mass balance equation can be re-formulated as $\mathbf{0} = \boldsymbol{n}_{\mathcal{M}} \boldsymbol{\eta}_{\mathcal{M}} + \boldsymbol{n}_{\mathcal{O}} \boldsymbol{\eta}_{\mathcal{O}}$, which provides the matrix of energy–mineral coupling coefficients $\boldsymbol{\eta}_{\mathcal{M}} = -\boldsymbol{n}_{\mathcal{M}}^{-1} \boldsymbol{n}_{\mathcal{O}} \boldsymbol{\eta}_{\mathcal{O}}$ and the mineral fluxes $\dot{\boldsymbol{J}}_{\mathcal{M}} = \boldsymbol{\eta}_{\mathcal{M}} \dot{\boldsymbol{p}}$.

The matrix $\boldsymbol{n}_{\mathcal{M}}^{-1}$ of coefficients (4.4) has an odd interpretation in terms of reduction degrees if the nitrogenous waste is ammonia. The third row, i.e. the one that relates to oxygen, represents the ratio of the reduction degree of the elements C, H, O, N to that of O_2, which is -4. That is to say, N atoms account for -3 of these reduction degrees, whatever their real values in the rich mixture of components that are present. The third row of the matrix $\boldsymbol{n}_{\mathcal{M}}^{-1} \boldsymbol{n}_{\mathcal{O}}$ thus represents the ratio of the reduction degrees of X, V, E and P to that of O. Sandler and Orbey [804] discuss the concept of generalized degree of reduction.

Figure 4.1 illustrates $\dot{\boldsymbol{J}}_{\mathcal{O}}$ and $\dot{\boldsymbol{J}}_{\mathcal{M}}$ of the DEB model as a function of the structural biomass (i.e. scaled length, see next section), when food is abundant. The embryonic reserve flux is negative, because embryos do not eat. The growth just prior to birth is reduced, because the reserves become depleted. The switch from juvenile to adult, so from development to reproduction, implies a discontinuity in the mineral fluxes, but this discontinuity is negligibly small.

4.3.1 Partitioning of mass fluxes

The mineral and organic fluxes can be decomposed into contributions from assimilation, dissipation power and growth. Let $\dot{J}_* = \dot{J}_{*A} + \dot{J}_{*D} + \dot{J}_{*G}$ for $* \in \{\mathcal{M}, \mathcal{O}\}$, and let us collect these fluxes in two matrices, then

$$\dot{\boldsymbol{J}}_{\mathcal{O}*} = \boldsymbol{\eta}_{\mathcal{O}} \, \mathbf{diag}(\dot{\boldsymbol{p}}) \quad \text{and} \quad \dot{\boldsymbol{J}}_{\mathcal{M}*} = \boldsymbol{\eta}_{\mathcal{M}} \, \mathbf{diag}(\dot{\boldsymbol{p}}) \tag{4.6}$$

where $\mathbf{diag}(\dot{\boldsymbol{p}})$ represents a diagonal matrix with the elements of $\dot{\boldsymbol{p}}$ on the diagonal, so that $\mathbf{diag}(\dot{\boldsymbol{p}})\mathbf{1} = \dot{\boldsymbol{p}}$, and $\dot{\boldsymbol{J}}_{\mathcal{M}*}\mathbf{1} = \dot{\boldsymbol{J}}_{\mathcal{M}}$, $\dot{\boldsymbol{J}}_{\mathcal{O}*}\mathbf{1} = \dot{\boldsymbol{J}}_{\mathcal{O}}$. These results are used in later sections.

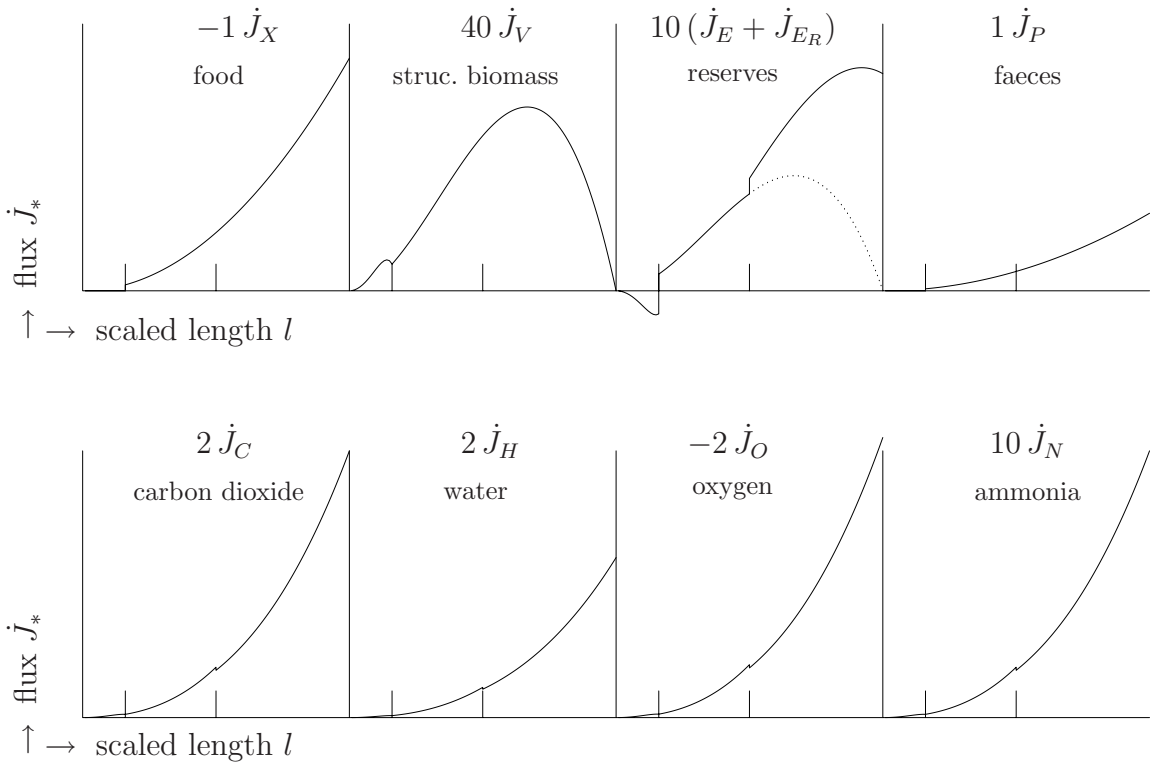

Figure 4.1: The organic fluxes $\dot{\boldsymbol{J}}_{\mathcal{O}}$ (top) and the mineral fluxes $\dot{\boldsymbol{J}}_{\mathcal{M}}$ (bottom) for the DEB model as functions of the scaled length l at abundant food ($e = 1$ for $l > l_b$; $0 < l < 1$). The various fluxes are multiplied by the indicated scaling factors for graphical purposes, while a common scaling factor involves model parameters. The parameters: scaled length at birth $l_b = 0.16$, scaled length at puberty $l_p = 0.5$ (both indicated on the abscissa), scaled heating length $l_h = 0$ (ectotherm), energy investment ratio $g = 1$, partition coefficient $\kappa = 0.8$, reproduction efficiency $\kappa_R = 0.8$. The coefficient matrices are

$$\boldsymbol{\eta}_{\mathcal{O}} = \begin{pmatrix} -1.5 & 0 & 0 \\ 0 & 0 & 0.5 \\ 1 & -1 & -1 \\ 0.5 & 0 & 0 \end{pmatrix}, \boldsymbol{n}_{\mathcal{M}} = \begin{pmatrix} 1 & 0 & 0 & 0 \\ 0 & 2 & 0 & 3 \\ 2 & 1 & 2 & 0 \\ 0 & 0 & 0 & 1 \end{pmatrix}, \boldsymbol{n}_{\mathcal{O}} = \begin{pmatrix} 1 & 1 & 1 & 1 \\ 1.8 & 1.8 & 1.8 & 1.8 \\ 0.5 & 0.5 & 0.5 & 0.5 \\ 0.2 & 0.2 & 0.2 & 0.2 \end{pmatrix}.$$

4.3.2 State versus flux

The general assumptions of Table 3.3 {121} imply that there is a direct relationship between masses and fluxes, which also holds for other specific assumptions, as long as they are consistent with the general ones, of course.

The mass of reserves and the structural biomass relate to the fluxes as $M_E(a) = M_{E0} + \int_0^a \dot{J}_E(t)\,dt$ and $M_V(a) = M_{V0} + \int_0^a \dot{J}_V(t)\,dt$. (The DEB model assumes that the initial value of the structural biomass is negligibly small, i.e. $M_{V0} = 0$.) The mass of reserves of an embryo in C-moles at age 0, M_{E0}, can be introduced as a parameter, but the DEB model obtains the value from the constraint that the reserve density of the embryo at birth equals that of the mother, i.e. $e(a_b) = f$.

The change in structural biomass M_V and reserve mass M_E relate to the powers as $\frac{d}{dt}M_V = \dot{J}_V = \dot{p}_G\eta_{VG}$ and $\frac{d}{dt}M_E = \dot{J}_E = \frac{\dot{p}_A - \dot{p}_C}{\mu_E}$. If the model for these powers implies the existence of a maximum for the structural biomass, M_{Vm}, and for the reserve mass, M_{Em}, it is extremely convenient to replace the state of the individual, M_V and M_E, by the scaled length $l \equiv (M_V/M_{Vm})^{1/3}$ and the scaled energy reserve density $e \equiv \frac{M_E M_{Vm}}{M_V M_{Em}}$. The change of the scaled state then becomes

$$\frac{d}{dt}l = \frac{\dot{p}_G\eta_{VG}}{3M_V^{2/3}M_{Vm}^{1/3}} = \frac{\dot{p}_G}{3l^2\kappa g E_m} \tag{4.7}$$

$$\frac{d}{dt}e = \frac{M_{Vm}}{M_V M_{Em}}\left(\frac{\dot{p}_A - \dot{p}_C}{\mu_E} - \frac{M_E}{M_V}\dot{p}_G\eta_{VG}\right) = \frac{1}{E_m l^3}\left(\dot{p}_A - \dot{p}_C - \dot{p}_G\frac{e}{\kappa g}\right) \tag{4.8}$$

The reproduction rate, in terms of the number of offspring per time, is given by $\dot{R} = \dot{J}_{E_R}/M_{E0}$. Therefore, the three basic powers, supplemented by the reproductive power, fully specify the individual as a dynamic system. The purpose of the specific assumptions of the DEB model is, therefore, to specify these three powers.

4.3.3 Mass investment in neonates

Several simple expressions can be obtained for changes over the whole incubation period that are useful for practical work. The initial weight (age $a = 0$) and the weight at birth (i.e. hatching, age $a = a_b$), excluding membranes and nitrogenous waste, are

$$\begin{pmatrix} W_w(0) & W_w(a_b) \end{pmatrix} = V_m \begin{pmatrix} w_E & w_V \end{pmatrix} \begin{pmatrix} [M_{Em}]e_0 & [M_{Em}]e_b l_b^3 \\ 0 & [M_V]l_b^3 \end{pmatrix} \tag{4.9}$$

where w_E and w_V denote the molecular weights of reserves and structural biomass. The scaled reserve densities e_0 and e_b are defined as $e_* \equiv E_*([E_m]V_m)^{-1}$, where E_* denotes the initial amount of reserves or the amount at hatching.

The relative weight at hatching is $W_w(a_b)/W_w(0) = (e_b + w_V/w_E)l_b^3/e_0$.

The total production of 'minerals' during incubation, $\boldsymbol{M}_{\mathcal{M}}(a_b)$, amounts to

$$\boldsymbol{M}_{\mathcal{M}}(a_b) \equiv \int_0^{a_b} \dot{\boldsymbol{J}}_{\mathcal{M}}(a)\,da = -\boldsymbol{n}_{\mathcal{M}}^{-1}\boldsymbol{n}_{\mathcal{O}} \begin{pmatrix} 0 & -[M_V]V_b & \mu_E^{-1}(E_0 - E_b) & 0 \end{pmatrix}^T \tag{4.10}$$

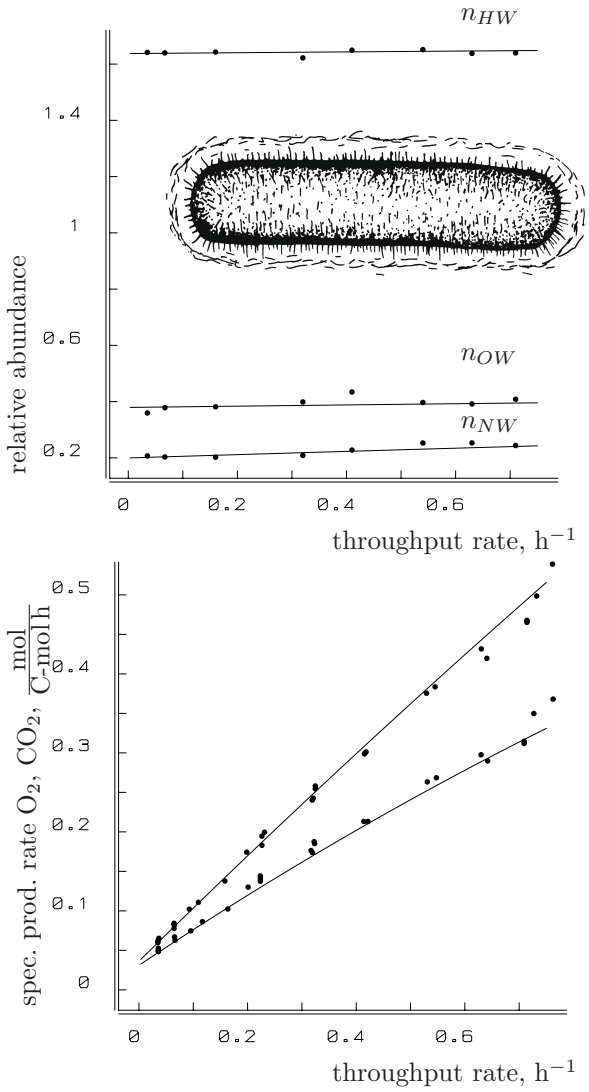

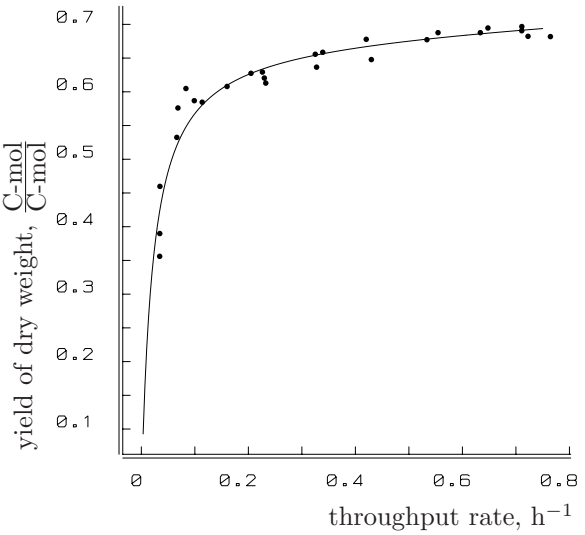

Figure 4.2: Relative abundances (upper left), molar yield of biomass dry weight (upper right), and specific O_2 consumption rate and CO_2 production rate (lower) for *Klebsiella aerogenes* growing on glycerol at 35 °C. Data from [262, 263]; fits modified from Hanegraaf [365]. Parameter estimates, given a maximum dilution rate of 1.05 h^{-1} and $g = 1$.

$\dot{k}_E$	2.11 h^{-1}	$\dot{k}_M$	0.021 h^{-1}		
y_{VE}	1.135	y_{XE}	1.490		
n_{HE}	1.66	n_{OE}	0.422	n_{NE}	0.312
n_{HV}	1.64	n_{OV}	0.379	n_{NV}	0.198

4.3.4 Composition of reserves and structural mass

Figure 4.2 illustrates that the change in composition of biomass for increasing growth rates can be used to obtain the composition of the reserves and of the structural mass. This method can be applied not only to elements but also to any chemical compound that can be measured in organisms. The relative abundance of the elements suggests that ribosomal RNA is an important component of the reserves in the prokaryote example, in view of the high population growth rate. This is discussed further on {244}. Indirect evidence can be used to obtain the amounts, without separating structure and reserve physically, see Figure 9.7.

The relative contributions of the three basic powers to the mass conversions depend on the substrate density, and therefore on throughput rate of a chemostat, as is illustrated in Figure 4.2 for the conversion process of glycerol into the bacterium *Klebsiella aerogenes* at steady state. The data on the elemental composition, and on the yield of dry weight and the specific O_2 and CO_2 fluxes, lead to the following relationship between mineral fluxes

and the three basic powers for $\dot{\boldsymbol{J}}_{\mathcal{M}+} = \dot{\boldsymbol{J}}_{\mathcal{M}*}\mathbf{1} = \dot{\boldsymbol{J}}_{\mathcal{M}}$ and $\dot{\boldsymbol{p}}_+ = \mathbf{diag}(\dot{\boldsymbol{p}})\mathbf{1} = \dot{\boldsymbol{p}}$

$$\dot{\boldsymbol{J}}_{\mathcal{M}+} = \begin{pmatrix} 0.14 & 1.00 & -0.49 \\ 1.15 & 0.36 & -0.42 \\ -0.35 & -0.97 & 0.63 \\ -0.31 & 0.31 & 0.02 \end{pmatrix} \dot{\boldsymbol{p}}_+/\mu_E \tag{4.11}$$

4.4 Respiration

Respiration, i.e. the use of oxygen or the production of carbon dioxide, is usually taken to represent the total metabolic rate in an organism. The latter is a rather vague concept, however. The conceptual relationship between respiration and use of energy has changed with time. Von Bertalanffy identified it with anabolic processes, while the Scope For Growth concept, {366}, relates it to catabolic processes. The respiration rate can now be defined concisely as the oxygen flux $\dot{J}_O = \eta_{OA}\dot{p}_A + \eta_{OD}\dot{p}_D + \eta_{OG}\dot{p}_G$, or the carbon dioxide flux $\dot{J}_C = \eta_{CA}\dot{p}_A + \eta_{CD}\dot{p}_D + \eta_{CG}\dot{p}_G$.

If product formation, such as faeces, is only linked to assimilation, the carbon dioxide production rate that is not associated with assimilation, $\dot{J}_C$ for $\dot{p}_A = 0$, follows from (4.3), (4.4) and (4.5)

$$\dot{J}_{CD} + \dot{J}_{CG} = \left(1 - n_{NE}\frac{n_{CN}}{n_{NN}}\right)\mu_E^{-1}(\dot{p}_D + \dot{p}_G) - \left(1 - n_{NE}\frac{n_{CN}}{n_{NN}}\right)\eta_{VG}\dot{p}_G \tag{4.12}$$

where the second term represents the carbon from the reserve flux that is allocated to growth and actually fixed into new tissue. The relationship simplifies if the nitrogenous waste contains no carbon ($n_{CN} = 0$). For embryos and juveniles we have $\dot{p}_G + \dot{p}_D = \dot{p}_C$, but adults fix carbon in embryonic reserves. This change at puberty results in a stepwise decrease in carbon dioxide production as illustrated in Figure 4.1. Table 3.5 gives the required powers: for adults we have the growth power $\dot{p}_G = V_m[\dot{p}_M]l^2\frac{e-l-l_h}{1+e/g}$ and the dissipating power

$$\dot{p}_D = V_m[\dot{p}_M]\left(l^3 + (\kappa^{-1} - 1)l_p^3 + l^2 l_h + (1 - \kappa_R)(\kappa^{-1} - 1)\left(l^2\frac{e - l + l_h/g}{1 + e/g} + l^3 - l_p^3\right)\right)$$

Initially, eggs hardly use oxygen, but oxygen consumption rapidly increases during development; see Figure 4.4. In juveniles and adults, oxygen consumption is usually measured in individuals that have been starved for some time, to avoid interpretation problems related to digestion. (For micro-organisms this is not possible without a substantial decrease of reserves.) The expression for the dissipating power is consistent with the observation that respiration rate increases with reserve density [488], while reserves themselves do not use oxygen. Moreover, it explains the reduction of respiration during starvation; see {227}.

The following subsection shows that respiration is a weighted sum of volume and surface area in steady-state conditions for the reserves. This is, for all practical purposes, numerically indistinguishable from the well known Kleiber's rule, which takes respiration to be proportional to weight to the power 0.75 or length to the power 2.25; see Figure 4.3.

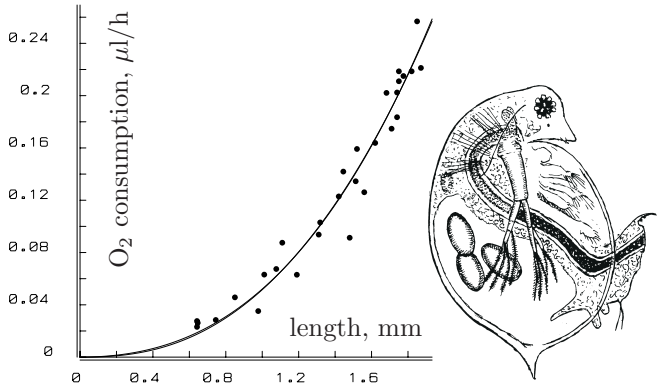

Figure 4.3: The respiration rate of *Daphnia pulex* with few eggs at 20 °C as a function of length. Data from Richman [764]. The DEB model based curve $0.0336L^2 + 0.01845L^3$ as well as the standard allometric curve $0.0516L^{2.437}$ are plotted on top of each other, but they are so similar that this is hardly visible. If you look hard, you will notice that the line width varies a little.

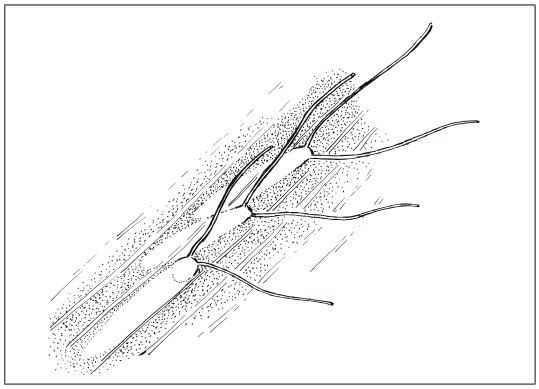

Figure 4.4: The water stick insect *Ranatra linearis* deposits its eggs in floating decaying plant material, where oxygen availability is usually poor. The eggs are easily spotted by the special respiratory organs that peek out of the plant. Just prior to hatching, eggs typically need a lot of oxygen, cf. Figure 3.15.

There are three major improvements in comparison to Kleiber's rule. This model does not suffer from dimensional problems, it provides an explanation rather than a description and it accommodates species that deviate from Kleiber's rule; endotherms respire in proportion to surface area (approximately), which has given rise to Rubner's surface law.

As already mentioned, this result solves the long standing problem of why the volume-specific respiration of ectotherms decreases with increasing size when organisms of the same species are compared. This problem has been identified as one of the central problems of biology [1009]. Many theories have been proposed, see e.g. [758] for a discussion, but all use arguments that are too specific to be really satisfactory: heating (but many species are ectothermic), muscle power (but movement costs are relatively unimportant), gravity (but aquatic species escape gravity), branching transport systems (but open circulatory systems are frequent). Peters [700] even argued that we should stop looking for a general explanation. The DEB theory, however, does offer a general explanation: the overhead of growth. A comparison of different species is covered in a later chapter, {267}, where it is shown that interspecies comparisons work out a bit differently.

The maintenance rate coefficient $\dot{k}_M$ can be estimated easily if growth data together with respiration data are collected at a constant food density. The respiration rate of embryonic and juvenile ectotherms is proportional to energy allocation to growth plus maintenance, so according to (3.17) the respiration rate is proportional to $\frac{d}{dt}V + \dot{k}_M V$. The observation that respiration is proportional to a weighted sum of volume and change in volume goes back to the 1957 Smith study [861] of salmon eggs. At constant food

density, the change in volume is of the von Bertalanffy type, which makes respiration proportional to $3\dot{r}_B(V_\infty^{1/3}V^{2/3} - V) + \dot{k}_M V$. This gives five parameters to be estimated from two data sets on respiration and growth: V_b, V_∞, $\dot{r}_B$, a proportionality constant for respiration and the maintenance rate coefficient, $\dot{k}_M$. This gives 2.5 parameters per data set, which is acceptable if the scatter is not too large.

4.4.1 Respiration Quotient

The Respiration Quotient (RQ) is of practical interest because it yields information on the relative contributions of protein, carbohydrates and lipids. The RQ for a particular compound X with chemical indices $\boldsymbol{n}_X$ can be obtained by decomposing the compound into minerals with chemical indices $\boldsymbol{n}_\mathcal{M}$. The composition of the nitrogenous waste (N), which can also contain C and O, affects the RQ if the compound contains N. The stoichiometric coefficients are $\boldsymbol{y}_{\mathcal{M}X} = (\ y_{CX} \quad y_{HX} \quad y_{OX} \quad y_{NX}\ )^T = \boldsymbol{n}_\mathcal{M}^{-1}\boldsymbol{n}_X$, and RQ$= y_{CX}/y_{OX}$.

The RQ value can be used to make inferences about the composition of reserves. Structural biomass and mainly reserves consist of three groups of polymers:

compound	symbol	formula	RQ	kJ/ g	kJ/ C-mol
polysaccharides	Ps	CH_2O	1.00	17.2	516
lipids	Li	$CH_{1.92}O_{0.12}$	0.67	38.9	616
proteins	Pr	$CH_{1.61}O_{0.33}N_{0.28}$	0.84	17.6	401

The RQ value for protein relates to urea as nitrogenous waste. The formula for lipid refers to tripalmitin. Octanol ($C_8H_{18}O$, or $CH_{2.25}O_{0.125}$) is frequently used as a chemical model for a typical animal fat, see {191}. Proteins are by far the most diverse polymers; the composition (and function) of protein differs over the taxa, the RQ varying between 0.8 and 0.9.

The chemical indices of the structural biomass and the reserves relate to that of the three groups of polymers as

$$n_{*_1*_2} = n_{*_1P_s}Y_{P_s,*_2} + n_{*_1L_i}Y_{L_i,*_2} + n_{*_1P_r}Y_{P_r,*_2} \quad *_1 \in \{C,H,O,N\}\ ,\ *_2 \in \{V,E\} \tag{4.13}$$

where $Y_{*_3*_2}$ is the molar yield of $*_3 \in \{P_s, L_i, P_r\}$, on $*_2$, and $1 = Y_{P_s,*_2} + Y_{L_i,*_2} + Y_{P_r,*_2}$. Given the composition of the three polymers, the composition of structural biomass and that of reserves have two degrees of freedom each. The constraint that the RQ is independent of the state of the individual eliminates all degrees of freedom and the value of the RQ can be directly translated into the composition of reserves and structure in terms of the three groups of polymer.

For living organisms, the situation is a bit more complex, because the ratio between the produced carbon dioxide and the consumed oxygen is not necessarily constant. The gas fluxes that are associated with the assimilation process, and so with feeding, are usually excluded from the measurements of the RQ, by starving the individual prior to the measurement. An explicit expression for the RQ can be obtained from the relationships $\dot{\boldsymbol{J}}_\mathcal{M} = \boldsymbol{\eta}_\mathcal{M}\dot{\boldsymbol{p}}$ and $\boldsymbol{\eta}_\mathcal{M} = -\boldsymbol{n}_\mathcal{M}^{-1}\boldsymbol{n}_\mathcal{O}\boldsymbol{\eta}_\mathcal{O}$. As is usually done, we set the first row of $\boldsymbol{n}_\mathcal{O}$ equal

to $\mathbf{1}^T$, set $\eta_{PD} = \eta_{PG} = 0$, and obtain

$$\text{RQ} = -\frac{\dot{J}_{CD} + \dot{J}_{CG}}{\dot{J}_{OD} + \dot{J}_{OG}} = -\frac{(\boldsymbol{n}_{\mathcal{M}}^{-1})_C \boldsymbol{n}_{\mathcal{O}} \begin{pmatrix} 0 & \dot{p}_G \eta_{VG} & -\frac{\dot{p}_D + \dot{p}_G}{\mu_E} & 0 \end{pmatrix}^T}{(\boldsymbol{n}_{\mathcal{M}}^{-1})_O \boldsymbol{n}_{\mathcal{O}} \begin{pmatrix} 0 & \dot{p}_G \eta_{VG} & -\frac{\dot{p}_D + \dot{p}_G}{\mu_E} & 0 \end{pmatrix}^T} \tag{4.14}$$

$$= \frac{1 - n_{NV} \frac{n_{CN}}{n_{NN}} - (1 - n_{NE} \frac{n_{CN}}{n_{NN}}) \frac{\mu_{GV}}{\mu_E} \left(1 + \frac{\dot{p}_D}{\dot{p}_G}\right)}{1 + \frac{n_{HV}}{4} - \frac{n_{OV}}{2} - \frac{n}{4} \frac{n_{NV}}{n_{NN}} - (1 + \frac{n_{HE}}{4} - \frac{n_{OE}}{2} - \frac{n}{4} \frac{n_{NE}}{n_{NN}}) \frac{\mu_{GV}}{\mu_E} \left(1 + \frac{\dot{p}_D}{\dot{p}_G}\right)} \tag{4.15}$$

where $(\boldsymbol{n}_{\mathcal{M}}^{-1})_*$ denotes the row of $\boldsymbol{n}_{\mathcal{M}}^{-1}$ that corresponds to compound $*$. The contribution of energetics to the RQ is thus via the ratio of growth to dissipation power. The RQ is in practice usually taken to be a constant for a particular species. Within the DEB model, the RQ is independent of the state of the animal (size l and reserve density e) if the following condition on the composition of E, V and N holds

$$\frac{1 + \frac{n_{HE}}{4} - \frac{n_{OE}}{2} - \frac{n}{4} \frac{n_{NE}}{n_{NN}}}{1 + \frac{n_{HV}}{4} - \frac{n_{OV}}{2} - \frac{n}{4} \frac{n_{NV}}{n_{NN}}} = \frac{1 - n_{NE} \frac{n_{CN}}{n_{NN}}}{1 - n_{NV} \frac{n_{CN}}{n_{NN}}} \tag{4.16}$$

in which case

$$\text{RQ} = \frac{1 - n_{NE} \frac{n_{CN}}{n_{NN}}}{1 + \frac{n_{HE}}{4} - \frac{n_{OE}}{2} - \frac{n}{4} \frac{n_{NE}}{n_{NN}}} = \frac{1 - n_{NV} \frac{n_{CN}}{n_{NN}}}{1 + \frac{n_{HV}}{4} - \frac{n_{OV}}{2} - \frac{n}{4} \frac{n_{NV}}{n_{NN}}} \tag{4.17}$$

The respiration rate (the oxygen consumption rate as well as the carbon dioxide production rate) is then proportional to the catabolic power if the contribution via assimilation is excluded. Condition (4.16) simplifies considerably if the Urination Quotient (UQ) is constant as well, see (4.29). The elemental composition of the reserves has to be equal to that of the structural biomass, if the Watering Quotient (WQ) is also independent of the state of the animal, see {146}.

4.4.2 Heat increment of feeding

The heat increment of feeding, also known as 'specific dynamic action', and many other terms, is defined (strangely enough) as the *oxygen* consumption that is associated with the feeding process. Apart from a small part that relates to the processing of proteins, the heat increment of feeding is little understood [1009]. It can be obtained, however, from the conservation law for mass. The oxygen consumption per C-mole of food is independent of the states of the animal (reserves e and size l) as

$$\frac{\dot{J}_{OA}}{\dot{J}_X} = (\boldsymbol{n}_{\mathcal{M}}^{-1})_{O*} \boldsymbol{n}_{\mathcal{O}} \begin{pmatrix} 1 \\ 0 \\ -\mu_{AX} \mu_E^{-1} \\ -\mu_{AX} \eta_{PA} \end{pmatrix} = \begin{pmatrix} -1 & -\frac{1}{4} & \frac{1}{2} & \frac{n}{4 n_{NN}} \end{pmatrix} \begin{pmatrix} n_{CX} & n_{CE} & n_{CP} \\ n_{HX} & n_{HE} & n_{HP} \\ n_{OX} & n_{OE} & n_{OP} \\ n_{NX} & n_{NE} & n_{NP} \end{pmatrix} \begin{pmatrix} 1 \\ -\frac{\mu_{AX}}{\mu_E} \\ -\frac{\mu_{AX}}{\mu_{AP}} \end{pmatrix} \tag{4.18}$$

where $(\boldsymbol{n}_{\mathcal{M}}^{-1})_{O*}$ denotes the row of $\boldsymbol{n}_{\mathcal{M}}^{-1}$ that relates to O, which is the third row. The expression shows how assimilation-associated oxygen consumption depends on the composition of food, faeces, reserves and nitrogenous waste, and the digestion efficiency through the parameters μ_{AX}, μ_{AP} and μ_E.

4.4.3 Aging as a consequence of respiration

Since age is not a state variable, the steady shift in properties due to the poorly understood process of aging is only of secondary relevance to the DEB theory. In a number of situations, however, one should consider life span, which has well recognized roots in energetics. The frequently observed correlation between life span and the inverse volume-specific metabolic rate for different species (see, e.g. [815]) has guided a lot of research. The impressive work of Finch [281] gives well over 3000 references. Animals tend to live longer at low food levels than at high ones. The experimental evidence, however, is rather conflicting on this point. For example, Ingle *et al.* [442] found such a negative relationship, while McCauley *et al.* [605] found a positive one for daphnids. This is doubtlessly due to the fundamental problem that death can occur for many reasons, such as food-related poisoning, that are not directly related to aging.

Some species such as salmon, octopus, *Oikopleura* die after (first) reproduction, cf. {262}. They are said to be semelparous species, while species that reproduce more than once are called iteroparous. The sessile colonial sea squirt *Botryllus schlosseri* follows both genetically determined strategies within one population [350]. The semelparous colonies numerically dominate the population through midsummer, while the iteroparous ones do so in late summer. Death after first reproduction, like many other causes of death, does not relate to aging.

On approaching the end of the life span, the organism usually becomes very vulnerable, which complicates the interpretation of the life span of a particular individual in terms of aging. Experiments usually last a long time, which makes it hard to keep food densities at a fixed level and to prevent disturbances. This explains why theories on aging are still in a primordial state.

In a first naïve attempt to model the process of aging, it might seem attractive to conceive the senile state, followed by death as the next step in the sequence embryo, juvenile, adult, and then tie it to energy investment in development just as has been done for the transitions to the juvenile and adult stages. This is not an option for the DEB model, since at sufficiently low food densities the adult state is never entered, even if the animal survives for nutritional reasons. This means that it would live for ever, as far as aging is concerned. Although species exist with very long life spans (excluding external causes of death [281]), this does not seem acceptable.

In view of the substantial scatter in age at death among individuals, an obvious strategy to model aging is on the basis of hazard rates. The hazard rate relates to the survival probability according to the differential equation $\frac{d}{dt}\Pr\{\underline{a}_\dagger > t\} = -\Pr\{\underline{a}_\dagger > t\}\dot{h}(t)$ or $\dot{h}(t) = -\frac{d}{dt}\ln\Pr\{\underline{a}_\dagger > t\}$. The survivor probability is thus

$$\Pr\{\underline{a}_\dagger > t\} = \exp\left\{-\int_0^t \dot{h}(t_1)\,dt_1\right\} \tag{4.19}$$

The mean life span equals $\mathcal{E}\underline{a}_\dagger = \int_0^\infty \Pr\{\underline{a}_\dagger > t\}\,dt = \int_0^\infty \exp\{-\int_0^t \dot{h}(t_1)\,dt_1\}\,dt$. This hazard rate thus ties aging to energetics, which explains for instance why dormancy prolongs life span, cf. {231}.

Attempts to relate hazard rates directly to the accumulation of hazardous compounds

formed as a spin off of respiration, such as oxidized lipids, have failed to produce realistic age-specific mortality curves: the hazard rate increases too rapidly for a given mean life span. See [486,675] for reviews on the role of secondary products from metabolism in aging. The same holds for the hazard tied to damage to membranes, if this damage accumulates at a rate proportional to volume-specific respiration. Telomers, repetitive DNA-code at the end of chromosomes, were recently found be copied incompletely in animals, which gives a reduction in their size after each cell division, and eventually leads to loss of the ability to divide. The process is controlled by telomerase; sperm has enough of this enzyme to continue division. It seems likely that telomer reduction is important in the process of differentiation and the control of organ size. Accurate descriptions of survival data where aging can be assumed to be the major cause of death seem to call for an extra integration step, however, which points to activities of changed DNA.

It has been suggested that free radicals, or related reactive oxygen species formed as a spin off of respiration, cause irreparable damage to the DNA in organisms and have a direct relationship with aging [363,368,369,877,923]. The specific activity of antioxidants correlates with life span within the mammals [28,281,995]. The structure of the antioxidant enzyme manganese superoxide dismutase has recently been solved [798]. Although too unspecific to be of much help to molecular research, for energetics purposes the free radical hypothesis specifies just enough to relate the age-specific survival probability, and so life span, to energetics. The idea is that the hazard rate is proportional to damage density, which accumulates at a rate proportional to the concentration of changed DNA, while DNA changes at a rate proportional to the catabolic rate. The catabolic rate is proportional to the respiration rate that is not associated with assimilation, and the proportionality constant is affected by the activity of the superoxide dismutases and the DNA repair efficiency. Oxygen use that is associated with assimilation is not taken into account, because it is used more locally, in specialized tissues.

Although it is not yet possible to draw firm conclusions on this point, this mechanism does provide the extra integration step that is required for an accurate description of data. It is further assumed that the cells with changed DNA do not grow and divide, while the density of affected cells is reduced owing to the propagation of the unchanged cells. This assumption is supported by the recent identification of gene *chk1* [966], whose products are involved in the detection of DNA damage; damaged DNA prevents entry into mitosis by controlling the activity of the protein that is produced by *cdc2* , cf. {118}. Because of the uncertainty in the coupling with molecular processes, I prefer to talk about damage and damage-inducing compounds, rather than wrong proteins (or their products) and DNA. Kowald and Kirkwood [529,528] followed a very similar line of reasoning, and incorporated much more detail. The present very simple model has only one parameter for the aging process. Its strength is in revealing the role of energetics in the survival probability; energy budgets parameters will show up in the survival process, which can also be obtained from data that do not relate to survival.

The amount of damage-inducing compounds (changed DNA), M_Q, accumulates from value 0 in an embryo of age 0. The non-assimilatory respiration rate is about proportional to the catabolic rate, so $\frac{d}{dt}M_Q = \eta_{QC}\dot{p}_C$, where the mass–energy coupler η_{QC} is the contribution of the volume-specific catabolic rate to the compounds per unit of energy. The

coefficient incorporates the activity of the antioxidants and the DNA repair potential. The second term stands for the dilution through growth, where cells with changed DNA become mixed with cells with unchanged DNA.

Substitution of (3.17), gives for ectotherms

$$\frac{d}{dt}M_Q = \frac{\eta_{QC}}{\kappa}\left([E_G]\frac{d}{dt}V + \dot{p}_M\right) \tag{4.20}$$

The amount of damage-inducing compounds as a function of time for ectotherms thus equals

$$M_Q(t) = \frac{\eta_{QC}}{\kappa}\left([E_G](V(t) - V(0)) + [\dot{p}_M]\int_0^t V(t_1)\,dt_1\right) \tag{4.21}$$

As explained in the section on embryonic growth, {96}, the initial volume, $V(0)$, is infinitesimally small. The accumulated damage during the embryonic stage is also negligibly small. The high generation rate of damage-inducing compounds is balanced by the high dilution rate through growth. The fact that the embryonic period is usually a very small fraction of the total life span ensures that one does not lose much information by starting from the moment of hatching.

Damage (wrong protein) accumulates at a rate proportional to the amount of damage-inducing compounds, so the damage density is proportional to $V(t)^{-1}\int_0^t M_Q(t_1)\,dt_1$. The hazard rate, $\dot{h}(t)$, is finally taken to be proportional to the damage density, which leads to

$$\dot{h}(t) = \frac{\ddot{h}_a}{V(t)}\int_0^t \left(V(t_1) - V(0) + \dot{k}_M\int_0^{t_1} V(t_2)\,dt_2\right)\,dt_1 \tag{4.22}$$

The proportionality constant $\ddot{h}_a$, here called aging acceleration, absorbs both proportionality constants leading to this formulation of the age-dependent hazard rate and is proportional to $\eta_{QC}[E_G]/\kappa$. This most useful property means that only a single parameter is necessary to describe the aging process.

Figure 4.5 shows that the fit with experimental data for male and female daphnids is quite acceptable, in view of the fact that the combined hazard curves have only one free parameter $\ddot{h}_a$ (so half a parameter per curve). The differences in survival probability of male and female daphnids can be traced back to difference in ultimate size (i.e. in the surface-area-specific maximum assimilation rate $\{\dot{A}_m\}$).

It is instructive to compare this model with that of Weibull where

$$\Pr\{\underline{a}_\dagger > t\} \equiv \exp\left\{-\int_0^t \dot{h}(t_1)\,dt_1\right\} = \exp\{-(\dot{h}_W t)^\beta\}$$

The model was first proposed by Fisher and Tippitt [283] in 1928 as a limiting distribution of extreme values, and Weibull [978] has used it to model the failure of a mechanical device composed of several parts of varying strength, according to Elandt-Johnson and Johnson [251]. The (cumulative) hazard increases allometrically with time. Like many other allometrically based models for physiological quantities, it is attractively simple, but fails to explain, for instance, why the sexes of *Daphnia* have different shape coefficients

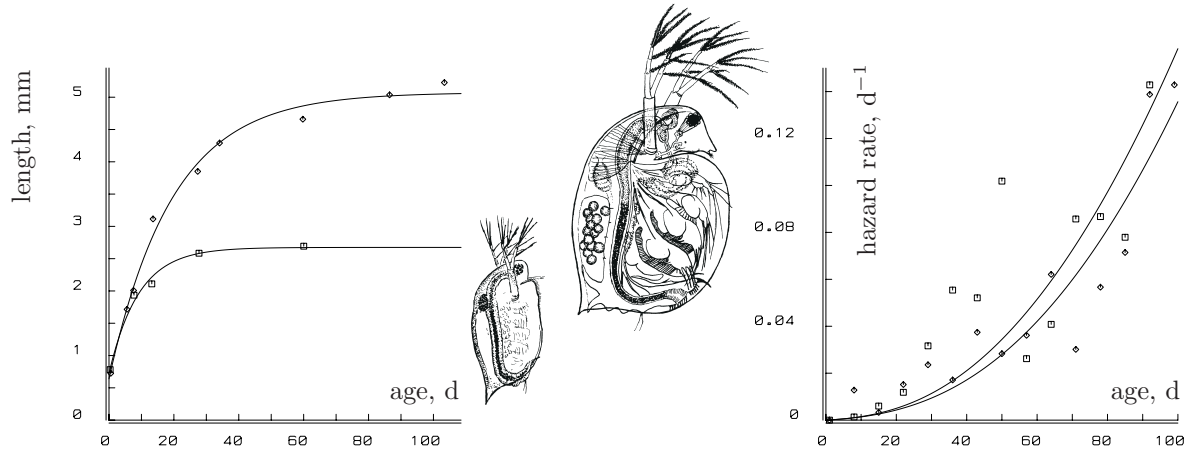

Figure 4.5: The growth curves of female (◇) and male daphnid (□)*Daphnia magna* at 18 °C and the observed hazard rates. Data from MacArthur and Baillie [574]. The growth curves are of the von Bertalanffy type with common length at birth. The hazard rates are fitted on the basis of the damage genesis discussed in the text, with a common aging acceleration of 2.587×10^{-5} d^{-2}. The difference in the hazard rates is due to the difference in ultimate lengths.

β [522]. As long as both parameters of the Weibull model can be chosen freely, i.e. if only one data set is considered, it will be hard to distinguish it from the DEB-based model. See Figure 4.6. The maintenance rate coefficient in the fit is here considered as a free parameter, so both curves then have two free parameters. This is done because the available estimate for the maintenance rate coefficient on the basis of egg development as reported in Table 3.1 is rather far out of range. The resulting estimate of $\dot{k}_M = 0.073$ d^{-1} at 20 °C is much more realistic, which in itself lends strong support to my interpretation. It can be shown that the Weibull model with shape parameter 3 results if the growth period is short relative to the mean life span, {257}.

The Gompertz model for survival $\Pr\{\underline{a}_\dagger > t\} = \exp\{\beta(1-\exp\{\dot{h}_G t\})\}$ is also frequently used as a model for aging; see e.g. [1011]. It can be mechanistically underpinned by a constant and independent failure rate for a fixed number of hypothetical critical elements. Death strikes if all critical elements cease functioning. The curvature of the survival probability then relates to the number of critical elements, which Witten [1011] found to be somewhere between 5 and 15. Their nature still remains unknown. A property of this model is that the hazard rate does not approach zero for neonates (or embryos), which does not seem to be consistent with the data [854]. Finch [281] favours the empirical description of aging rates given by the Gompertz model because its property of a constant mortality rate doubling time, $\dot{h}_G^{-1} \ln 2$, provides a simple basis for comparison of taxa.

The present formulation allows for a separation of the aging- and energy-based parameters. The estimation of the 'pure' aging parameter in different situations and for different species will hopefully reveal patterns that can guide the search for more detailed molecular mechanisms; however, many factors may be involved, cf. {216}. It has been suggested in the literature that the neural system may be involved in setting the aging rate. The fact that brain weight in mammals correlates very well with respiration rate [422] makes it difficult to identify factors that determine life span in more detail. The mechanism may

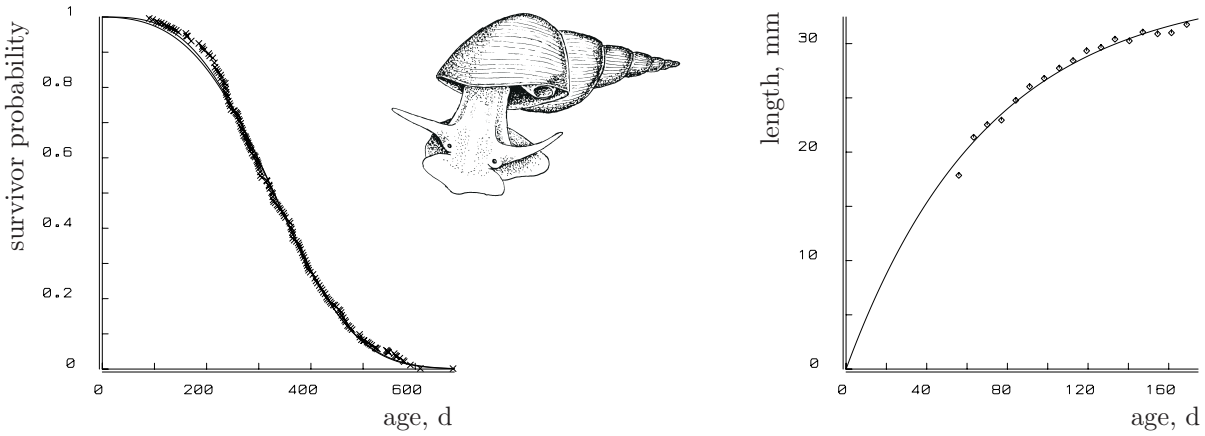

Figure 4.6: The survival probability and the growth curve of the pond snail *Lymnaea stagnalis* at 20 °C. Data from Slob and Janse [854] and Bohlken and Joosse [98,1028]. The fitted growth curve is the von Bertalanffy one, giving an ultimate length of 35 mm and a von Bertalanffy growth rate of $\dot{r}_B = 0.015$ d^{-1}. The survival curve was used to estimate both the maintenance rate constant, $\dot{k}_M = 0.073$ d^{-1}, and the aging acceleration $\ddot{h}_a = 2.563 \times 10^{-6}$ d^{-2}. The Weibull curve with shape parameter 3.1 is plotted over the DEB model to show that both curves are hard to distinguish in practice.

be again via the neutralization of free radicals.

An indication of this pathway can be found in the age-specific survival probability for humans, see Figure 4.7, which can be described well by a Weibull distribution with shape parameter 6.8. Compared with the data on ectotherms, we have here an extremely low hazard rate for the young ages, which increases rapidly after the age of 50 years. This pattern suggests that the system involved in the neutralization of free radicals is itself subjected to aging, while for ectotherms it is not necessary to build in this complication. A constant neutralization probability, combined with low mortality during growth, leads to survival curves that are close to the Weibull curve with shape parameter 3, see {255}. Aging as a result of free radicals is partially supported by the observation that the life spans of both ectotherms and endotherms correlate well with the specific activity of antioxidants [281]. It should be noted that if we compare an endotherm with a body temperature of 40 °C with that of an otherwise similar ectotherm at 20 °C, we should expect a 10 times shorter life span, on the basis of an Arrhenius temperature of 10 000 K. Endotherms, therefore, have a problem to solve, which possibly involves additional mechanisms to remove free radicals.

One of the many questions that remain to be answered is how aging proceeds in animals that propagate by division rather than by eggs. Unlike eggs, they have to face the problem of initial damage. It might be that such animals have (relatively few) undifferentiated cells that can divide and replace the damaged (differentiated) ones. A consequence of this point of view is that the option to propagate by division is only open to organisms whose differentiation of specialized cells is not pushed to the extreme. If aging affects all cells at the same rate, it becomes hard to explain the existence of dividing organisms. This is perhaps the best support for the damage interpretation of the aging process. Theories

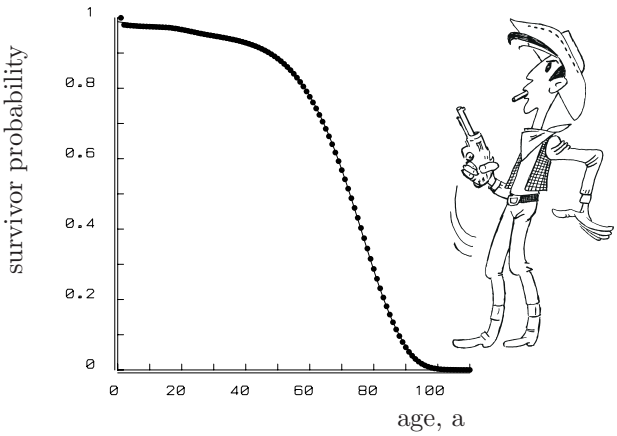

Figure 4.7: The survival curve for humans: white males in the USA in the period 1969–1971. Data from Elandt-Johnson and Johnson [251]. The fitted empirical survival curve is $q\exp\{-\dot{h}t-(\dot{h}_W t)^\beta\}$, with $q = 0.988$, $\dot{h} = 0.0013$ a^{-1}, $\dot{h}_W = 0.01275$ a^{-1} and $\beta = 6.8$. The parameter q relates to neonate survival and $\dot{h}$ to death by accident. The extreme goodness of fit suggests that the data might not be data, but model predictions.

that relate aging, for instance, to the accumulation of compounds as an intrinsic property of cellular metabolism should address this problem. The same applies to unicellulars. If accumulated damage carries over to the daughter cells, it becomes hard to explain the existence of this life style. The assumption of the existence of cells with and without damage seems unavoidable. Organisms that live in anaerobic environments cannot escape aging, because other radicals will occur that have the same effect as oxygen. Note that if one follows the fate of each of the daughter cells, this theory predicts a limited number of divisions until death occurs, so that this event itself gives no support for aging theories built on cellular programming. Only the variation in this number can to some extent be used to choose between both approaches. The present theory can be worked out quantitatively for unicellulars as follows.

Since unicellulars cannot dilute changed DNA with unchanged DNA and cannot compensate for its effect, the hazard rate for unicellulars must equal $\dot{h}(t) = \eta_{QC}\dot{p}_C/V$, where η_{QC} couples the generation of damage-inducing compounds to catabolic power. (Note that the range of the cell volume is $(V_d/2, V_d)$, so that the volume-specific respiration rate is restricted, while for embryos, where V is assumed to be infinitesimally small initially, it does not have a boundary. Dilution by growth solves this problem for embryos.) The hazard rate for V1-morphs is found from Table 3.6 {123} to be

$$\dot{h}(e) = \dot{h}_a e \frac{1+g}{e+g} \tag{4.23}$$

where $\dot{h}_a$ represents the maximum aging rate. At constant substrate densities, the scaled energy reserve density, e, equals the scaled functional response, f, so the hazard rate is constant and independent of the age of the filament. For the hazard rate of unicellular isomorphs we obtain from (3.44)

$$\dot{h}(e,l) = \dot{h}_a e \frac{1+g}{e+g} \frac{1+g/l}{1+g/l_d} \tag{4.24}$$

In contrast to V1-morphs, isomorphs experience a reduction of the hazard rate during the cell cycle.

If DNA is changed, the cell will cease functioning. This gives a lower boundary for the (population) growth rate because the population will become extinct if the division

interval becomes too long. To prevent extinction (in the long run) the survival probability to the next division should be at least 0.5, so the lower boundary for substrate density can be found from $\Pr\{\underline{a}_\dagger > t_d\} = \exp\{-\int_0^{t_d} \dot{h}(t)\,dt\} = 0.5$. The lower boundary for the substrate density for rods must be found numerically. It is tempting to relate this aging mechanism, which becomes apparent at low substrate densities only, to the occurrence of stringent responses in bacteria, as described by, for example, Cashel and Rudd [153]. This is discussed further when populations are considered, {319}.

It is intriguing to realize that the present mechanism for aging implies that organisms use free radicals to change their DNA. Although most changes are lethal or adverse, some can be beneficial to the organism. Using a selection process, the species can exploit free radicals for adaptation to changing environments. By increasing the specific activity of antioxidants, a species can prolong the life span of individuals in non-hostile environments, but it reduces its adaptation potential as a species if the environment changes. This trait defines an optimal specific activity for antioxidants that depends on the life history of the organism and the environment. Large body size, which goes with a long juvenile period, as is discussed on {287}, requires efficient antioxidants to ensure survival to the adult state. It implies that large bodied species have little adaptation potential, which is further reduced by the long generation time; this makes them vulnerable from an evolutionary perspective. It is possibly one aspect of the extinction of the dinosaurs, although not all of them were large and they may have been endothermic. Endotherms appear to combine a high survival probability of the juvenile period with a high aging rate, thus having substantial adaptation potential during the reproductive phase; they reach this by reducing the efficiency of antioxidants during puberty.

The present formulation assumes that growth ceases as soon as DNA is changed. The background is that many genes are involved in the synthesis of one or more compounds that are essential to structural biomass and so to growth. A few genes are involved in suppressing unregulated growth of cells in multicellular organisms. If such genes are affected, tumours can develop. This theory can, therefore, also be used to work out the age-dependent occurrence rate of tumours as well as the growth rate of tumours, cf. {177}.

The energy parameters can be tied to the accumulated damage to account for the well-known phenomenon that older individuals eat less and reproduce less than younger ones with the same body volume. Senescence can be modelled this way. It is a special case of a more general principle, that non-essential compounds can affect parameter values, {202}.

4.5 Nitrogen balance

Standard 'static' energy budget studies treat energy in urine similar to energy in faeces, by subtracting both from energy contained in food to arrive as metabolizable energy that is available to the animal, cf. {365}. Since the gut contents still belong to the 'outside world', this is reasonable for energy in faeces, but not for energy in urine. The DEB model leads to a different point of view, where dissipating power and anabolic power also contribute to the nitrogenous waste. The energy (and nitrogen) in urine originates from all powers, where the contributions to urine appear as overhead costs. Without reserves, the two points

of view can be translated into each other, but with reserves the two become essentially different.

If $n_{NE} < \frac{[M_V]}{\mu_E^{-1}} \frac{n_{NV}}{[E_G]}$, the flux of nitrogenous waste that relates to anabolic power, $\dot{J}_{NG}$, is negative, meaning that nitrogen is built in rather than wasted in the transformation of reserves to structural biomass. The flux of nitrogenous waste that relates to dissipating power amounts to $\dot{J}_{ND} = \frac{\dot{p}_D}{\mu_E} \frac{n_{NE}}{n_{NN}}$, which can be a substantial part of the total flux of nitrogenous waste.

4.5.1 Urination Quotient

Analogous to the Respiration Quotient, we can define the Urination Quotient (UQ) as

$$\begin{aligned} \mathrm{UQ} &= -\frac{\dot{J}_{ND} + \dot{J}_{NG}}{\dot{J}_{OD} + \dot{J}_{OG}} = -\frac{(\boldsymbol{n}_{\mathcal{M}}^{-1})_N \boldsymbol{n}_{\mathcal{O}} \begin{pmatrix} 0 & \dot{p}_G \eta_{VG} & -\frac{\dot{p}_D + \dot{p}_G}{\mu_E} & 0 \end{pmatrix}^T}{(\boldsymbol{n}_{\mathcal{M}}^{-1})_O \boldsymbol{n}_{\mathcal{O}} \begin{pmatrix} 0 & \dot{p}_G \eta_{VG} & -\frac{\dot{p}_D + \dot{p}_G}{\mu_E} & 0 \end{pmatrix}^T} && (4.25) \\ &= \frac{\frac{n_{NV}}{n_{NN}} - \frac{n_{NE}}{n_{NN}} \frac{\mu_{GV}}{\mu_E} \left(1 + \frac{\dot{p}_D}{\dot{p}_G}\right)}{1 + \frac{n_{HV}}{4} - \frac{n_{OV}}{2} - \frac{n}{4}\frac{n_{NV}}{n_{NN}} - (1 + \frac{n_{HE}}{4} - \frac{n_{OE}}{2} - \frac{n}{4}\frac{n_{NE}}{n_{NN}}) \frac{\mu_{GV}}{\mu_E} \left(1 + \frac{\dot{p}_D}{\dot{p}_G}\right)} && (4.26) \end{aligned}$$

The UQ is independent of the states of the animal (size l and reserve density e) if the following condition on the composition of E, V and N holds

$$\frac{1 + \frac{n_{HE}}{4} - \frac{n_{OE}}{2} - \frac{n}{4}\frac{n_{NE}}{n_{NN}}}{1 + \frac{n_{HV}}{4} - \frac{n_{OV}}{2} - \frac{n}{4}\frac{n_{NV}}{n_{NN}}} = \frac{n_{NE}}{n_{NV}} \tag{4.27}$$

in which case

$$\mathrm{UQ} = \frac{\frac{n_{NE}}{n_{NN}}}{1 + \frac{n_{HE}}{4} - \frac{n_{OE}}{2} - \frac{n}{4}\frac{n_{NE}}{n_{NN}}} = \frac{\frac{n_{NV}}{n_{NN}}}{1 + \frac{n_{HV}}{4} - \frac{n_{OV}}{2} - \frac{n}{4}\frac{n_{NV}}{n_{NN}}} \tag{4.28}$$

The UQ and the RQ are both constant if

$$\begin{aligned} n_{NE} &= n_{NV} && (4.29) \\ n_{HE} - 2n_{OE} &= n_{HV} - 2n_{OV} && (4.30) \end{aligned}$$

Analogous to the RQ and UQ, we can define a Watering Quotient $\mathrm{WQ} = -\frac{\dot{J}_{HD} + \dot{J}_{HG}}{\dot{J}_{OD} + \dot{J}_{OG}}$: the ratio of the water production to oxygen consumption that relates to dissipation and growth. (For terrestrial animals, the evaporation of water invokes a drinking behaviour, which is discussed on {151}.) The condition that the RQ, UQ and WQ are all independent of the state of the animal directly translates to the condition that the reserves and the structural biomass have the same elemental composition. The oxygen consumption, the carbon dioxide production, the nitrogenous waste production and the water production that relate to dissipation and growth are all proportional to the catabolic power, comparing individuals of the same species (i.e. the same parameter values), but different states (structural biomass and/or reserves).

If the RQ and the UQ are both constant, the ratio of the carbon dioxide to the nitrogenous waste production equals $\frac{\mathrm{RQ}}{\mathrm{UQ}} = \frac{n_{NN}}{n_{NE}} - n_{CN}$, excluding contributions via assimilation as before. If the WQ is constant as well, the ratio of the water to the nitrogenous waste production equals $\frac{\mathrm{WQ}}{\mathrm{UQ}} = \frac{n_{HE}}{2}\frac{n_{NN}}{n_{NE}} - \frac{n_{HN}}{2}$.

4.5.2 Ammonia excretion

Many algae take up nitrogenous compounds, such as ammonia, from the environment, but even algae also excrete ammonia, associated with maintenance and growth. This follows from the balance equation for nitrogen, given the composition of reserves and structural mass. Ammonia excretion can be quantified for V1-morphs as follows.

Let n_{NE} and n_{NV} denote the chemical indices for nitrogen in reserves and structural mass. The ammonia excretion that is associated with maintenance and growth can then be written as

$$\begin{aligned} \dot{J}_{N_H,D} + \dot{J}_{N_H,G} &= (j_{N_H,D} + j_{N_H,G})M_V = n_{NE}(\dot{p}_D + \dot{p}_G)/\mu_E - n_{NV}\dot{p}_G/\mu_{GV} \quad (4.31) \\ j_{N_H,D} + j_{N_H,G} &= n_{NE}y_{EV}(\dot{k}_E + \dot{r}) - n_{NV}\dot{r} \quad (4.32) \end{aligned}$$

with dissipating power $\dot{p}_D = M_V\mu_{GV}\dot{k}_M$ and growth power $\dot{p}_G = M_V\mu_{GV}\dot{r}$ (see Table 3.6); the mass–mass coupler y_{EV} is the ratio of two energy–mass couplers, $y_{EV} = \mu_{GV}/\mu_E$, where μ_E represents the chemical potential of the reserves, and μ_{GV} the reserve energy investment per unit increase of structural mass.

The flux of nitrogenous waste that relates to assimilation amounts to $\dot{J}_{N,A} = \eta_{NA}\dot{p}_A$, with $\eta_{NA}n_{NN} = -\eta_{XA}n_{NX} + n_{NE}/\mu_E + \eta_{PA}n_{NP}$.

4.6 Products

From a dynamic systems point of view, minerals can be considered as products, with contributions from the basic powers, apart from the fact that their fluxes can become negative (e.g. oxygen for heterotrophs). Faeces is a product as well, where the contributions from dissipating and growth powers are zero, which ties faeces production directly to assimilation. Many micro-organisms produce a variety of products via several routes. If the DEB model still applies in the strict sense, the mere fact that product formation costs energy implies that product formation must be a weighted sum of the basic powers: assimilation, dissipation (maintenance) and growth. The energy drain to product formation can then be considered as an overhead cost in these three processes.

The necessity to tie product formation to all the three energy fluxes in general becomes obvious in a closer analysis of fermentation. If product formation is independent of one or more energy fluxes, mass balance equations dictate that more than one product must be made under anaerobic conditions, and that the relative amounts of these products must depend on the (population) growth rate in a very special way. In the Monod model, which does not include maintenance and reserves (see {317}), assimilation is proportional to growth investment, which leaves just a single energy flux available to couple to

product formation. In the Marr–Pirt model, which does not include reserves, assimilation is proportional to maintenance plus growth investment, which leaves two energy fluxes available to couple to product formation. Maintenance and reserves together allow for a three-dimensional base for product formation: $\dot{J}_P = \dot{p}_A\eta_{PA} + \dot{p}_D\eta_{PD} + \dot{p}_G\eta_{PG}$, see (4.5). The quantitative aspects of products only differ from that of 'minerals' in that the weight coefficients for products are free parameters, while those for 'minerals' follow from mass conservation.

Since most unicellulars behave approximately as V1-morphs, assimilation rate and maintenance are both proportional to biomass, with constant proportionality coefficients at steady state. Leudeking and Piret [554] proposed in 1959 that product formation is a weighted sum of biomass and change in biomass (growth). They studied lactic acid fermentation by *Lactobacillus delbruekii*. The Leudeking–Piret kinetics has proved extremely useful and versatile in fitting product formation data for many different fermentations [40]. It turns out to be a special case of the DEB theory.

For practical applications where no energies are measured, it might be useful to convert powers to mass fluxes via the coefficients $\zeta_{*_1*_2} = \eta_{*_1*_2}\mu_E m_{Em}$, which leads to the specific production flux for V1-morphs

$$j_P = \zeta_{PM}\dot{k}_M g + \zeta_{PA}\dot{k}_E f + \zeta_{PG}\dot{r}g. \tag{4.33}$$

Milk of female mammals is an example of a product that is coupled to maintenance, which requires a temporal change in parameter values to describe its production. The same holds for plant secretions (e.g. resin), in response to wounds, for example.

4.7 Fermentation

Many organisms can live in anaerobic environments, partly as a relic from their evolutionary history, as life originated in a world without free oxygen. Most parasites [926,927], as well as gut and sediment dwellers [277,278] do not usually encounter much oxygen, and aquatic environments can be low in oxygen as well. Some fish [972,973] and mollusc [123] survive periods without oxygen. Parasitic helminths sport anaerobic metabolism in the core of their bodies, and aerobic metabolism in the peripheral layers, which become relatively less important during growth [925].

The mass balance equation reveals that such organisms must produce at least one product, with an elemental composition that is independent (in the sense of linear algebra) of the composition of the other 'minerals' (carbon dioxide, water and nitrogenous waste). Usually, several products are formed. Under anoxic conditions, lipids cannot be metabolized, because their degree of reduction is too high, and the respiration chain cannot be used.

The description of the formation of each product involves three parameters, namely the coupling coefficients with the three basic powers; the absence of oxygen involves three constraints. So if just one product is formed, no free parameters are left, and we can simply replace oxygen by that product. So, if the single product is ethanol, and the nitrogenous

waste ammonia, the matrix of chemical indices for the minerals and its inverse become

$$\boldsymbol{n}_{\mathcal{M}} = \begin{pmatrix} 1 & 0 & 1 & 0 \\ 0 & 2 & 3 & 3 \\ 2 & 1 & \frac{1}{2} & 0 \\ 0 & 0 & 0 & 1 \end{pmatrix} \quad \text{and} \quad \boldsymbol{n}_{\mathcal{M}}^{-1} = \begin{pmatrix} \frac{1}{3} & -\frac{1}{6} & \frac{1}{3} & \frac{1}{2} \\ -1 & \frac{1}{4} & \frac{1}{2} & -\frac{3}{4} \\ \frac{2}{3} & \frac{1}{6} & -\frac{1}{3} & -\frac{1}{2} \\ 0 & 0 & 0 & 1 \end{pmatrix}$$

Fermentation is an anaerobic process in which organic compounds act as electron donor as well as electron acceptor. Usually several products are made rather than just one. These products can be valuable substrates under aerobic conditions, but under anaerobic conditions mass balances force organisms to leave them untouched. Cellulose is fermented to products such as acetate, propionate, butyrate and valerate in cows [810], which microorganisms cannot use as substrates under anaerobic conditions (much to the benefit of the cow!). Under anaerobic conditions we have the constraints that

$$\begin{pmatrix} \mu_{AO}^{-1} & \mu_{DO}^{-1} & \mu_{GO}^{-1} \end{pmatrix} = \mathbf{0}$$

The practical implementation of these constraints in non-linear regressions is via Lagrange multipliers, which can be found in standard texts on calculus. An interesting consequence of these constraints is that there are no free parameters for product formation if just one product is made. Figure 4.8 illustrates that the DEB model accurately describes the fermentation process (biomass composition, substrate and product fluxes) with only $17/11 = 1.5$ parameter per curve. The experimental data do not obey the mass balance for carbon and oxygen in detail. Measurements of the volatile ethanol seem to be less reliable. The mass balance-based model fit of Figure 4.8 suggests that the measured values represent 75% of the real ones when the measurement error is considered as a free parameter. The saturation coefficient X_K was poorly fixed by the data, and the chosen value should be considered as an educated guess.

Yeasts appear to be relatively rich in proteins when they grow fast, but their maximum growth rate is about half that of *Klebsiella*. Three products are made by the yeast: glycerol ($n_{HP_1} = 8/3$, $n_{OP_1} = 1$), ethanol ($n_{HP_2} = 3$, $n_{OP_2} = 0.5$) and pyruvate ($n_{HP_3} = 4/3$, $n_{OP_3} = 1$). A negative parameter for product formation means that the product is consumed, rather than produced, in the corresponding energy flux. So it is possible that compounds are produced at a rate proportional to one energy flux and consumed at a rate proportional to another energy flux. No theoretical problems occur as long as there is an overall net production.

Note that the maintenance rate coefficient $\dot{k}_M$ for *Klebsiella* at 35 °C is about ten times that for *Saccharomyces* at 30 °C. The maintenance rate coefficient for fungi is usually found to be much smaller in the literature [74], which Bulthuis [138] explained by the fact that fungi make a lot of protein at high population growth rates, which costs a lot of energy. As the maintenance rate coefficient is the ratio of maintenance to structure costs, its value for fungi is low. Since protein density is coupled to the growth rate, however, the assumption of homeostasis dictates that most protein must be conceived as part of the reserves, so the costs of synthesis of structural biomass are not higher for this reason.

Figure 4.8 shows that biomass density hardly depends on the throughput rate. In practice, this also holds for most other compounds, except for the concentration of substrate.

relative abundances of the elements
H (∘), O (◇) and N (□) in the biomass

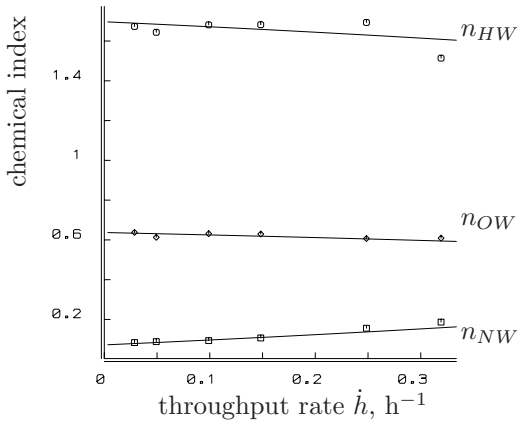

densities of substrate (glucose, ◇) and biomass (dry weight, □)

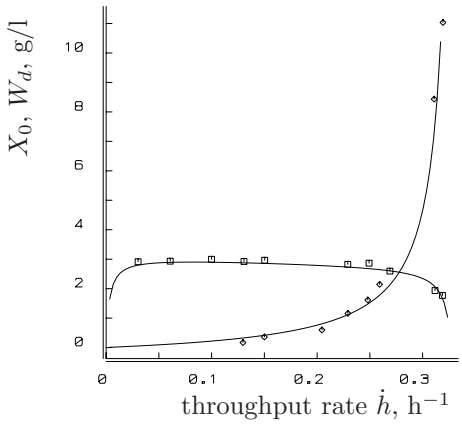

densities of products
ethanol, △, glycerol, ▽, pyruvate, ⋈

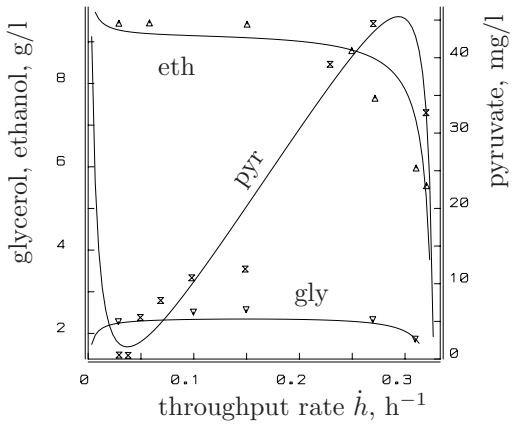

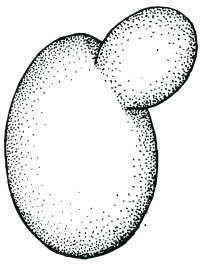

weight-specific consumption/prod. rates of glucose, □, CO_2, ◇ and ethanol, △

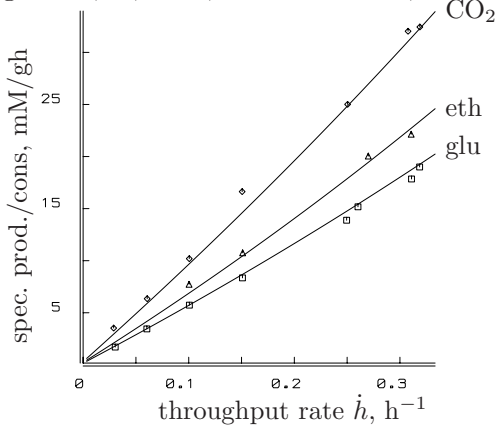

Figure 4.8: All these functions of population growth rate of *Saccharomyces cerevisiae* at 30 °C and a glucose concentration of 30 g l^{-1} in the feed have been fitted simultaneously [365]. The observation that the maximum throughput rate is 0.34 h^{-1} has also been used. Data from Schatzmann [809]. The curves are based on expectations of the DEB model, with parameters

$\dot{k}_E$	=	0.461 h^{-1}	g	=	0.385	$\dot{k}_M$	=	0.0030 h^{-1}
y_{VE}	=	1.206	y_{XE}	=	10.28	X_K	=	1.79 g l^{-1}
n_{HX_1}	=	1.70	n_{OX_1}	=	0.637	n_{NX_1}	=	0.071
n_{HE}	=	1.55	n_{OE}	=	0.572	n_{NE}	=	0.205
ethanol			glycerol			pyruvate		
$\zeta_{P_1,A}$	=	8.047	$\zeta_{P_2,A}$	=	7.398	$\zeta_{P_3,A}$	=	0.0313
$\zeta_{P_1,D}$	=	3.019	$\zeta_{P_2,D}$	=	2.711	$\zeta_{P_3,D}$	=	0.0062
$\zeta_{P_1,G}$	=	0.336	$\zeta_{P_2,G}$	=	0.972	$\zeta_{P_3,G}$	=	−0.0365

If changes in concentrations affect chemical potentials substantially, the chemical potential for substrate will be the first point to check (although substrate is usually processed intracellularly, rather than in the environment). The extremes of the substrate concentration are found for throughput rate $\dot{h} = 0$, where $X_0 = \frac{X_K g \dot{k}_M}{\dot{k}_E - g\dot{k}_M}$, and for throughput rate $\dot{h} = \dot{h}_m$, where $X_0 = X_r$ if death is negligible. The chemical potential of a compound depends on its concentration X as $\mu = \mu_{\text{ref}} + RT \ln X/X_{\text{ref}}$, where $R = 8.31441$ JK^{-1}mol^{-1} is the gas constant. The maximum relative effect of differences in concentrations of substrate on the chemical potential is

$$\frac{\mu_{X0,\max} - \mu_{X0,\min}}{\mu_{X0,\text{ref}}} = \frac{RT}{\mu_{X_0,\text{ref}}} \ln \left\{ \frac{\dot{k}_E - g\dot{k}_M}{g\dot{k}_M} \frac{X_r}{X_K} \right\}$$

In the example of Figure 4.8, where the chemical potential of glucose is 2856 kJ mol^{-1} in the combustion frame of reference, the maximum relative effect amounts to 0.00777, which is negligibly small in view of many other uncertainties. Although the effect of changes in concentrations should be tested in each practical application, in this section I will not explicitly correct chemical potentials for differences in concentrations.

4.8 Water balance

The drinking rate equals the water flux, $\dot{J}_{HX} = \dot{J}_H$ for aquatic animals, but terrestrial animals have to deal with evaporation of water. The water balance implies that the sum of the water fluxes by metabolism, evaporation and drinking amounts to zero. Embryos usually do not drink and are 'designed' such that evaporation takes care of water outflux, although small changes in water content have been found. The water content of tissues in birds gradually decreases during growth, which led Ricklefs and Webb [768] and Konarzewski [503] to model juvenile growth on the basis of the water content of the tissue. Here, we idealize the process by assuming strict homeostasis for both the structural biomass and the reserves, while focusing on juveniles and adults. Note that water emission via urine is incorporated in the composition of the nitrogenous waste, which could be large enough to let the water outflux $\dot{J}_H$ be negative and turn it into a water influx.

Evaporation has two main routes, one via water loss linked to respiration, $\dot{J}_{HO}$, and one via transpiration, $\dot{J}_{HH}$. Water loss via respiration is proportional to oxygen consumption via the amount of inhaled air, so $\dot{J}_{HO} = \dot{J}_O y_{HO}$, while transpiration is proportional to surface area, so $\dot{J}_{HH} = \{\dot{J}_{HH}\} V_m^{2/3} l^2$, where $\{\dot{J}_{HH}\}$ does not depend on the state of the animal. Both loss rates depend on water pressure in the air, temperature, wind speed and behavioural components. The DEB model leads to a drinking rate of

$$\dot{J}_{HX} = \begin{pmatrix} 0 & 1 & y_{HO} & 0 \end{pmatrix} \dot{\boldsymbol{J}}_{\mathcal{M}} + \{\dot{J}_{HH}\} V_m^{2/3} l^2 \tag{4.34}$$

This two-parameter model for the drinking process is, of course, an idealized picture which pushes the concept of homeostasis to the extreme. The water content of urine is actually rather variable, depending on environmental and behavioural factors. However, the model might be helpful as a first approximation to reveal the coupling that must exist between drinking and energetics.

Water plays an essential role in the transport of nutrients from the environment to terrestrial plants, and in the translocation of their metabolites. Its quantitative role can only be understood in a multi-variate setting, see next subsection.

4.8.1 Doubly labelled water

An ingenious method to measure the carbon dioxide flux indirectly is via the differential loss of isotopes of (injected) doubly labelled water. The method overcomes the problem that direct measurement of the carbon dioxide flux gives an instantaneous value only, and its measurement affects (the behaviour of) the animal. The interest in carbon dioxide fluxes stems from their relationship with energy fluxes, which is discussed on {155}. The method is based on the assumptions that labelled oxygen of water is exchanged (rapidly) with oxygen of carbon dioxide, and that the loss of deuterium reflects the loss of water. A few additional simplifying assumptions are also useful to obtain a simple interpretation of the results, such as labelled and unlabelled body water are completely mixed, and loss of label other than via water and carbon dioxide loss, is negligible [558].

The total water flux equals $\dot{J}_{HL} = \dot{J}_{HX} + y_{HN}\dot{J}_N$, where y_{HN} denotes the moles of water in the nitrogenous waste, per mole of nitrogenous waste. The amount of body water equals $M_H = y_{HV}M_V + y_{HE}M_E$, so that the specific rate at which deuterium is lost equals $\dot{h}_H = \dot{J}_{HL}/M_H$. An estimate for M_H can be obtained by back-extrapolation of the oxygen label density at time zero, given a known amount of injected label. The specific loss rate of deuterium, combined with the total amount of body water, leads to an estimate for total water flux $\dot{J}_{HL}$. The specific loss rate of oxygen label equals $\dot{h}_O = (\dot{J}_{HL} + 2\dot{J}_C)/M_H$, which can be used to obtain $\dot{J}_C$, when $\dot{J}_{HL}$ and M_H are known.

4.8.2 Plant–water relationships

Terrestrial plants have intimate relationships with water, and total biomass production is found to vary almost proportionally to the annual precipitation across the globe [665, page 124]. Since plants cannot move, the local availability of water is the main factor determining the distribution of plants species [1015]. Like all organisms they need water for metabolic purposes, as autotrophs they need it as electron donor, but, above all, they need it for transport [748]. From a geophysiological perspective, plants are structures that pump water from the soil into the atmosphere. The evaporation of water from the leaves generates a water flux from the roots to the shoot, which is used for internal transport and for nutrient uptake from the soil. Factors that control evaporation include temperature, relative humidity, wind speed, and water supply in the soil [801,853]. Plants can modify evaporation by stomata in the leaves, but this regulation is limited by the need to acquire carbon dioxide. Jones [455], Nobel [670] and Lambers *et al.* [542] give an excellent discussion of quantitative aspects.

Suppose that the arrival rate of nutrients at the receptor in the root, $\dot{J}_r$, is proportional to its concentration in the water, X_n, and the water flux per receptor. The water flux is proportional to the shoot area where transpiration takes place, which controls nutrient transport, and to the availability of water in the soil, X_H. The proportionality factor

includes the regulation of stomata opening by the plant, and atmospheric factors (temperature, wind, humidity). The number of receptors is proportional to the surface area of the root. The surface areas of roots and shoot are proportional to $A_r = \mathcal{M}_r(V_r)V_r^{2/3}$ and $A_s = \mathcal{M}_s(V_s)V_s^{2/3}$, respectively. The uptake rate of nutrient is proportional to the number of receptors times $\frac{\dot{k}\rho\dot{J}_r}{\dot{k}+\rho\dot{J}_r}$, where ρ is the binding probability, and $\dot{k}$ the dissociation rate between receptor and bounded nutrient. This leads to the uptake rate of nutrient

$$\dot{J}_N = \{\dot{J}_{NAm}\}A_r(1 + X_{KN}/X_N)^{-1}, \quad X_{KN} \propto (X_H A_s/A_r)^{-1} \tag{4.35}$$

The surface area of the shoot appears in the saturation 'constant' X_{KN}, which is no longer constant.

Nutrient uptake is arrested by lack of water transport in this formulation, because the saturation constant becomes very large. This mechanism gives a direct coupling between nutrient uptake and precipitation. In water-rich soils, the control of transport on nutrient uptake might be less, and in subaquatic conditions even absent. This boils down to an additive term X_0, which relates to diffusive transport of the nutrient: $X_{KN} \propto (X_0 + X_H A_s/A_r)^{-1}$.

4.9 Energy balance

The dissipating heat is usually related to oxygen consumption, by a fixed conversion of 519 ($\pm$13) kJ(mol O_2)$^{-1}$ [40]. This choice is not fully satisfactory, because it lacks a mechanistic underpinning, and because it is obviously not applicable to anaerobic conditions. The correlation between dissipating heat and carbon dioxide production has been found to be reduced by variations in the type of substrate [173]. Heijnen [389] related dissipating heat to C-moles of formed biomass. This choice is problematic because of maintenance. If substrate density is low enough, no new biomass will be produced but heat will still dissipate.

The assumption that the free energy per C-mole of structural biomass and reserves does not change implies a direct link between the dissipating heat and the free energies of structural mass and reserve. This assumption has been made palatable in the section on energy {35}, and is at the basis of a route to measure these free energies, as well as a theoretical underpinning of the method of indirect calorimetry. We first need to study the energy balance of the system 'individual plus relevant compounds'.

4.9.1 Dissipating heat

The dissipating heat $\dot{p}_{T+}$ follows from the energy balance equation

$$\begin{aligned} 0 &= \dot{p}_{T+} + \boldsymbol{\mu}_{\mathcal{M}}^T \dot{\boldsymbol{J}}_{\mathcal{M}} + \boldsymbol{\mu}_{\mathcal{O}}^T \dot{\boldsymbol{J}}_{\mathcal{O}} && (4.36)\\ &= \dot{p}_{T+} + (\boldsymbol{\mu}_{\mathcal{O}}^T - \boldsymbol{\mu}_{\mathcal{M}}^T \boldsymbol{n}_{\mathcal{M}}^{-1} \boldsymbol{n}_{\mathcal{O}}) \boldsymbol{\eta}_{\mathcal{O}} \dot{\boldsymbol{p}} && (4.37) \end{aligned}$$

where

$$\boldsymbol{\mu}_{\mathcal{M}}^T \equiv (\ \mu_C \quad \mu_H \quad \mu_O \quad \mu_N\ ) \quad \text{and} \quad \boldsymbol{\mu}_{\mathcal{O}}^T \equiv (\ \mu_X \quad \mu_V \quad \mu_E \quad \mu_P\ )$$

are the chemical potentials of the various compounds. The gist of the argument is that the energy that is allocated to reserves and structural biomass appear as parameter values, while the energy that is fixed in these masses is given by the chemical potentials, the differences appearing as dissipating heat, i.e. overhead costs.

The dissipating heat contributes to the thermal fluxes to and from the individual. The individual loses heat via convection and radiation at a rate $\dot{p}_{TT} = \{\dot{\pi}_T\}(T_b - T_e)V^{2/3} + \{\dot{\pi}_R\}(T_b^4 - T_e^4)V^{2/3}$. Here T_e denotes the absolute temperature in the environment, including a relatively large sphere that encloses the individual. For radiation considerations, the sphere and individual are assumed to have grey, opaque diffuse surfaces. T_b is the absolute temperature of the body; $V^{2/3}$ is the body surface area; $\{\dot{\pi}_T\}$ is the thermal conductance and $\{\dot{\pi}_R\} = \epsilon\sigma$ is the emissivity times the Stefan–Boltzmann constant $\sigma = 5.6710^{-8}\ \mathrm{J\,m^{-2}\,s^{-1}\,K^{-4}}$; see for instance [532]. The body temperature does not change if the energy invested in heating balances the heat loss, $\dot{p}_{T+} = \dot{p}_{TT}$. This relationship can be used to obtain the body temperature or the heating costs, given knowledge about the other components. It specifies, for instance, how a temporary increase in activity reduces heating costs, using complementary physiological information about activity efficiencies [130,977,998].

Most animals, especially the aquatic ones, have a high thermal conductance, which gives body temperatures only slightly above the environmental ones. Endotherms, however, heat their body to a fixed target value, usually some $T_b = 312$ K, and have a thermal conductance as small as $\{\dot{\pi}_T\} = 5.43\ \mathrm{J\,cm^{-2}\,h^{-1}\,K^{-1}}$ in birds and 7.4–9.86 $\mathrm{J\,cm^{-2}\,h^{-1}\,K^{-1}}$ in mammals, as calculated from [402]. The thermal conductance can be modified by environmental and behaviour factors, see e.g. [712,713].

Most endotherms are terrestrial and lose heat also via evaporation of water at a rate $\dot{p}_{TH}$, say. The relationship $\dot{p}_T > \dot{p}_{TH} + \dot{p}_{TT}$ determines the lower boundary of the thermo–neutral zone: the minimum environmental temperature at which no endothermic heating is required. It also specifies the heating requirement at a given environmental temperature. To see how, we first have to consider the water balance in more detail, to quantify the heat $\dot{p}_{TH}$ that goes into the evaporation of water. The individual loses water via respiration at a rate proportional to the use of oxygen, i.e. $\dot{J}_{HO} = y_{HO}\dot{J}_O$, see [517,942], and via transpiration, i.e. cutaneous losses. The latter route varies between 2% and 84% of the total water loss in birds, despite the lack of sweat glands [200]. Water loss, $\dot{J}_{HH}$, via transpiration is proportional to body surface area, to the difference in vapour pressure of water in the skin and the ambient air, to the square root of the wind speed, and depends on behavioural components. The heat loss by evaporation amounts to $\dot{p}_{TH} = \mu_{TH}(\dot{J}_H + \dot{J}_{HO} + \dot{J}_{HH})$, with $\mu_{TH} = 6\ \mathrm{kJ\,mol^{-1}}$. Within the thermo–neutral zone, endotherms control their body temperature among others by evaporation, through panting or sweating, which affects the water balance via enhanced drinking.

4.9.2 Indirect calorimetry

Indirect calorimetry uses measurements of oxygen consumption, carbon dioxide and nitrogen production to estimate dissipating heat $\dot{p}_{T+}$

$$\dot{p}_{T+} = \boldsymbol{\mu}_T^T \dot{\boldsymbol{J}}_{\mathcal{M}} \quad \text{with} \tag{4.38}$$

$$\boldsymbol{\mu}_T^T \equiv \begin{pmatrix} \mu_{TC} & \mu_{TH} & \mu_{TO} & \mu_{TN} \end{pmatrix} \tag{4.39}$$

Its basis is just empirical when applied to individuals, rather than pure compounds, and has ancient roots, {3}. Examples are: $\mu_{TC} = 60\ \mathrm{kJ\,mol^{-1}}$, $\mu_{TH} = 0$, $\mu_{TO} = -350\ \mathrm{kJ\,mol^{-1}}$ and $\mu_{TN} = -590\ \mathrm{kJ\,mol^{-1}}$ in aquatic animals [108] that excrete ammonia as nitrogenous waste, or $-86\frac{n_{CN}}{n_{NN}}\ \mathrm{kJ\,mol^{-1}}$ in birds [92]. For mammals, corrections for methane production have been proposed [125]. The coefficients $\boldsymbol{\mu}_T$ can be obtained by direct calorimetry, using multiple regression. The mass fluxes prove to be a weighted sum of the three basic powers, see {125}. Dissipating heat is again a weighted sum of the three powers and so of (three) mass fluxes, which justifies the method of indirect calorimetry.

Now we can reverse the argument and wonder how measurements of heat dissipation can be used to obtain the chemical potentials of the organic compounds. Substitution of (4.3) and (4.38) into (4.36) results in

$$\boldsymbol{\mu}_{\mathcal{O}}^T = (\boldsymbol{\mu}_T^T + \boldsymbol{\mu}_{\mathcal{M}}^T)\mathbf{n}_{\mathcal{M}}^{-1}\mathbf{n}_{\mathcal{O}} \tag{4.40}$$

The problem of how to obtain the relative abundances of the elements in the structural biomass and in the reserves has been discussed on {134}.

The method of indirect calorimetry can easily be adjusted for under anaerobic conditions, if a single product is excreted. The new regression coefficients $\boldsymbol{\mu}'_T$ can be found from the aerobic ones $\boldsymbol{\mu}_T$ by equating the chemical potentials $\boldsymbol{\mu}_{\mathcal{O}}$. This leads to $\boldsymbol{\mu}'^T_T = (\boldsymbol{\mu}_T^T + \boldsymbol{\mu}_{\mathcal{M}}^T)\boldsymbol{n}_{\mathcal{M}}^{-1}\boldsymbol{n}'_{\mathcal{M}} - \boldsymbol{\mu}'^T_{\mathcal{M}}$, with $\boldsymbol{n}'_{\mathcal{M}}$ the 'mineral' chemical indices with oxygen replaced by product, and $\boldsymbol{\mu}'_{\mathcal{M}}$ the chemical potentials of the minerals, with oxygen replaced by product. If the nitrogenous waste is ammonia (NH_3) and the product is ethanol ($CH_3O_{0.5}$), the chemical potentials are $\boldsymbol{\mu}'^T_{\mathcal{M}} = (0\ 0\ 657\ 0)\ \mathrm{kJ\,Cmol^{-1}}$ and $\boldsymbol{\mu}_{\mathcal{M}} = \mathbf{0}$ in a combustion frame of reference, and

$$\boldsymbol{n}_{\mathcal{M}}^{-1}\boldsymbol{n}'_{\mathcal{M}} = \begin{pmatrix} 1 & 0 & 1 & 0 \\ 0 & 1 & 1.5 & 0 \\ 0 & 0 & -1.5 & 0 \\ 0 & 0 & 0 & 1 \end{pmatrix}$$

which leads for $\boldsymbol{\mu}_T^T = (60\ 0\ -350\ -590)\ \mathrm{kJ\,mol^{-1}}$ to $\boldsymbol{\mu}'^T_T = (60\ 0\ -72\ -590)\ \mathrm{kJ\,Cmol^{-1}}$.

4.9.3 Thermodynamic constraints

Given the assumption of constant chemical potentials for the organic compounds, the second law of thermodynamics implies that the processes of assimilation, dissipation and growth are exothermic, i.e. we can decompose the dissipating heat into three positive

contributions $\dot{\boldsymbol{p}}_{T+}^T \equiv (\ \dot{p}_{TA} \quad \dot{p}_{TD} \quad \dot{p}_{TG}\ )$, with $\dot{\boldsymbol{p}}_{T+}^T \mathbf{1} = \dot{p}_{T+}$, which follow from the balance equations for these three processes

$$\mathbf{0}^T = \dot{\boldsymbol{p}}_{T+}^T + (\boldsymbol{\mu}_{\mathcal{O}}^T - \boldsymbol{\mu}_{\mathcal{M}}^T \boldsymbol{n}_{\mathcal{M}}^{-1} \boldsymbol{n}_{\mathcal{O}}) \boldsymbol{\eta}_{\mathcal{O}} \, \mathbf{diag}(\dot{\boldsymbol{p}}) \tag{4.41}$$

where $\mathbf{diag}(\dot{\boldsymbol{p}})$ is the diagonal matrix with the elements of $\dot{\boldsymbol{p}}$ on the diagonal. The sum of the three equations (4.41) returns the overall balance equations (4.38), since $\mathbf{diag}(\dot{\boldsymbol{p}})\mathbf{1} = \dot{\boldsymbol{p}}$. We see that the heat that dissipates in connection with a basic power is proportional to that power, and that the three factors that multiply the basic powers in these three balance equations should all be negative. This implies a constraint for each column of $\boldsymbol{\eta}_{\mathcal{O}}$. In a combustion frame of reference, where $\boldsymbol{\mu}_{\mathcal{M}} = \mathbf{0}$, these constraints translate to $\boldsymbol{\mu}_{\mathcal{O}}^T \boldsymbol{\eta}_{\mathcal{O}} < \mathbf{0}^T$.

4.10 Summary

The basic DEB model, as specified by the assumptions listed in Table 3.3 {121}, fully determines the fluxes of organic compounds (food, faeces, reserves and structural mass); those of mineral compounds (carbon dioxide, oxygen, water and nitrogenous waste) follow from the conservation law for atoms. The model, therefore, specifies *all* mass fluxes. These mass fluxes can all be written as weighted sums of three basic energy fluxes (powers): assimilation, dissipation and growth. Dissipating heat can also be written as weighted sums of the three basic powers, which means that dissipating heat is a also weighted sum of three mineral fluxes (carbon dioxide, oxygen and nitrogenous waste). This is well known in empiry, and used in the widely applied method of indirect calorimetry to obtain dissipating heat from the three mineral fluxes; a theoretical explanation has not been given before, as far as I know. Growth-related changes in biomass composition can be used to obtain the composition of reserves and structure, as is illustrated by examples.

Respiration is one of two mineral fluxes, carbon dioxide or oxygen. The fluxes are proportional to each other, given certain constraints on the composition of reserves, relative to structural mass. Respiration that is not associated with assimilation is then proportional to the catabolic rate. The theory also quantifies the respiration that is associated with assimilation, known as the Specific Dynamic Action; its nature is still considered to be enigmatic, but now explained in first principles.

Aging is thought to result as a byproduct of respiration via free radicals. The DEB theory specifies the quantitative aspects for multicellulars with differentiated cells on the basis of the following supplementary assumptions

1 oxygen causes net DNA damage with a certain efficiency

2 damaged DNA produces 'wrong' proteins at constant rate, which cumulate in the body

3 the hazard rate is proportional to the density of 'wrong' proteins

This results in a module for aging with just a single parameter: the aging acceleration. Unicellulars do not age gradually, but instantaneously; the parameter is the aging rate. The DEB model specifies the ontogeny of respiration, and so of aging, and how it depends on feeding and other energetic aspects. The efficiency with which oxygen causes net DNA damage seems to increase with age in endotherms, but is constant in ectotherms. Mutagenic compounds, such as nitrite, have effects very similar to those of free radicals, and accelerate aging.

Similar to other mineral fluxes, nitrogenous waste not only originates from assimilation directly, but also from maintenance (dissipation) and growth. Although this might not seem surprising, it differs from its treatment in Static Energy Budgets, see {365}, and turns out to be most useful in the analysis of trophic interactions, {304}.

Products can be included in just one single way, without changing the assumptions of Table 3.3; they, too, must be weighted sums of the three basic energy fluxes, the three weight coefficients per product are free parameters. In this way, products are included in the overhead costs of the three powers. Consequently, fermentation gives three constraints, which fully determine the three weight coefficients of a single product, or partly determine those of more products.

The drinking of water by terrestrial organisms and plants, to balance the metabolic turnover of water, can be quantified on the basis of two supplementary assumptions about water loss

---

1 water evaporates in proportion to the surface area at a rate that depends on environmental conditions (temperature, humidity, wind speed)

2 water evaporates in proportion to respiration

These assumptions apply to animals as well as plants. Drinking by plants has complex interactions with nutrient uptake and is shown to affect the saturation constant. The water balance has intimate relationships with the thermal balance, and so with the energetics of endotherms. These routes have been explored briefly.

Chapter 5

Multivariate DEB models

As long as all required nutrients and energy are available to the organism in fixed relative amounts, it can buffer temporal variations in abundance using a single reserve. This situation is approximated in organisms that eat other organisms, as discussed in the previous chapters. If energy and various nutrients are taken up independently, however, several reserves are required to buffer variations in abundance. The surface layers of seas are poor in nutrients and rich in light, while the reverse holds for the bottom of the photozone. Algal cells, which commute between these two environments on the wind-induced currents, can barely grow and survive, unless they use intracellular energy and nutrient reserves.

The purpose of this chapter is to show how the DEB theory can be extended to include several substrates, reserves and structural masses, in a way that reduces to the one-reserve, one-structure case if just one nutrient (or light) is limiting, or if nutrient abundances covary, and the reserve turnover times are identical. The concept of the Synthesizing Unit, cf. {41} will be used to show that a nutrient becomes almost non-limiting as soon as its availability exceeds that of the limiting nutrient, only by a small amount, relative to its needs. Simultaneous limitations of growth by nutrients and light only occur incidentally, and usually during a short period. This is why the simple one-reserve DEB theory can be applied so widely.

A notational problem that is inherent to fluxes of compounds is their sign. If a compound is disappearing, the sign is negative, if it is appearing it is positive, but detailed specification of the process is required. Fluxes are denoted by the symbol $\dot{J}$; the first index specifies the compound, the second index specifies the process if required. If only the compound is indicated, the flux is always taken to be positive.

Each reserve requires specifications of its assimilation process and of its contribution to maintenance costs. Together with a single structural mass, and so a single growth process, $2n+1$ powers have to be specified to delineate n reserves. Each of these powers contributes to the dissipation of heat; the fixed weight coefficients directly follow from the conservation law for energy. Product formation is directly associated with these powers, and generally requires $2n+1$ coupling parameters per product for quantification. Fluxes of non-limiting nutrients are also directly associated with the powers, and the $2n+1$ coupling parameters follow from the conservation law for mass.

To structure the model appropriately, fast processes are separated from slow ones,

and many transport processes are only included implicitly at the whole-individual level. Transport of metabolites through phloem in plants, for instance, shares important system properties with blood in animals: a small capacity is combined with a high turnover, which means that material in phloem should not play an explicit role at the whole-individual level. The transformation from nutrients and light to reserves is taken as a single step, while in fact many intermediary metabolites are formed.

5.1 Several substrates

As is widely recognized, two different substrates can be classified as substitutable or supplementary. This classification is straightforward in idealized modelling contexts, where one or more substrates are taken up from the environment and transformed into a reserve in a process called assimilation. Substrates and reserves are again taken to be generalized compounds, i.e. mixtures of chemical compounds that do not change in composition, and which can be quantified in terms of C-moles or moles. Pure chemical compounds represent a special case of generalized compounds. Two substrates are substitutable if each compound can be chemically converted into that reserve, while they are supplementary if both substrates are required simultaneously, at a fixed stoichiometry.

5.1.1 Substitutable substrates

Two substitutable substrates can compete for access to the same carrier, or they can use different carriers. (The term 'carrier' actually stands for the whole assimilation machinery, not just for the protein in the outer membrane.) This results in different uptake rates, which will be briefly discussed.

Sequential processing

Suppose that two substrates can be used as a source for the synthesis of reserves, and that substrate 1 arrives at rate $\dot{J}_1$ at a suitable carrier. Each molecule binds with fixed probability ρ_1 if the carrier is in the binding phase, and no binding occurs if the carrier is in the production phase. Substrate 2 arrives at a rate $\dot{J}_2$ and is bound with probability ρ_2. The carrier switches from the binding phase to the production phase after a successful binding of either substrate molecule, and switches back to the binding phase at rate $\dot{k}_1$ or $\dot{k}_2$, so $\dot{k}_1^{-1}$ stands for the mean handling time of a substrate 1 molecule. The dynamics of the number of carriers in the binding phase, N_0, reads

$$\frac{d}{dt}N_0 = (N - N_0)\dot{k}_X - N_0\left(\rho_1\dot{J}_1 + \rho_2\dot{J}_2\right) \tag{5.1}$$

where $N = nM_V$ stands for the total number of carriers, which is here taken to be proportional to structural mass M_V, as is appropriate for V1-morphs. The production phase lasts a period $\dot{k}_1^{-1}$ for substrate 1, and $\dot{k}_2^{-1}$ for substrate 2, so the mean transition rate from the production to the binding phase is $\dot{k}_X = (\theta_1\dot{k}_1^{-1} + (1-\theta_1)\dot{k}_2^{-1})^{-1}$, with weight coefficient $\theta_1 = \left(1 + \frac{\rho_2\dot{J}_2}{\rho_1\dot{J}_1}\right)^{-1}$.

In steady state $\frac{d}{dt}N_0 = 0$, the specific substrate assimilation rate $j_X = \dot{J}_X/M_V$ amounts to

$$j_X = n\left(\dot{k}_X^{-1} + \left(\rho_1\dot{J}_1 + \rho_2\dot{J}_2\right)^{-1}\right)^{-1} \tag{5.2}$$

Diffusion-based transport processes in the medium result in arrival rates $\dot{J}_1$ and $\dot{J}_2$ which are proportional to the concentrations X_1 and X_2 in the environment, with proportionality factors $\dot{b}_1$ and $\dot{b}_2$, say; the mechanism is based on the law of mass action. I introduce the saturation constants $X_{K*} = \dot{k}_*(\rho_*\dot{b}_*)^{-1}$, with $* \in \{1,2\}$, the scaled concentrations $x_* = X_*/X_{K*}$, and the maximum specific uptake rates $j_{*m} = n\dot{k}_*$. The specific substrate assimilation rate (5.2) can now be written as

$$j_X = \left(j_{Xm}^{-1} + (x_1 j_{1m} + x_2 j_{2m})^{-1}\right)^{-1} \tag{5.3}$$

where the maximum specific assimilation rate is given by $j_{Xm} = \theta_1 j_{1m} + \theta_2 j_{2m}$ with weight coefficient $\theta_1 = \left(1 + \frac{x_2}{x_1}\frac{j_{2m}}{j_{1m}}\right)^{-1}$ and $\theta_1 + \theta_2 = 1$. The latter weight coefficient varies with varying concentrations of substrates 1 and/or 2. The uptake of substrate has four compound parameters; the maximum specific uptake rate relates to the number of carriers and handling time, and the saturation constant relates to handling time, diffusion rate and binding probability. The uptake of substrate can be decomposed into contributions from substrates 1 and 2

$$j_X = j_1 + j_2; \quad j_1 = \theta_1 j_X; \quad j_2 = \theta_2 j_X \tag{5.4}$$

In the special case of equal handling times for both substrates, $\dot{k}_1 = \dot{k}_2 = \dot{k}_X$, or $j_{1m} = j_{2m} = j_{Xm}$, the specific assimilation rate (5.3) reduces to

$$j_X = j_{Xm}\left(1 + (x_1 + x_2)^{-1}\right)^{-1} = j_{Xm} f$$

which has three compound parameters.

Feeding on prey

The decomposition of biomass into a structural component and a reserve component implies that a predator feeds on a mixture of two compounds, rather than just a single one, even if it specializes on a single species of prey. The significance of the contribution of prey reserves to predator nutrition is obvious in the example of waterfleas feeding on algae. Most of the organic carbon of algae consists of cellulose in the cell wall, and of chlorophyll. However, the waterflea cannot digest both compounds of the structural biomass, and mainly feeds on starch and lipids. The quantitative aspects of feeding on prey differs from the general case of sequentially processed substitutable substrates by the tight coupling of the abundances structural mass and reserves. The reserves of the prey can be treated as a kind of nutritional quality of prey biomass.

Suppose that the prey's reserves do not extend the predator's handling time. If the prey does not have an energy buffer allocated to its reproduction, the assimilation power of the predator amounts to $\dot{p}_A = (\mu_{AV} + \mu_{AE} m_E^\circ)\dot{J}_X$, where μ_{AV} stands for the conversion of prey structural mass into predator assimilative power, μ_{AE} for the conversion of prey reserves into predator assimilative power, $m_E^\circ = M_E^\circ/M_V^\circ = e^\circ m_{Em}^\circ$ for the ratio of the

reserve to the structural mass of the prey, and the feeding rate $\dot{J}_X$ for the molar flux of prey structural biomass. Parameters and variables that relate to the prey are indicated with $^\circ$ to distinguish them from those of the predator.

Let $\mu_{AX} = \mu_{AV} + \mu_{AE} m^\circ_{Em}$ denote the conversion of well-fed prey biomass into assimilation power, and $\kappa_A = \left(1 + \frac{1}{m^\circ_{Em}} \frac{\mu_{AV}}{\mu_{AE}}\right)^{-1} = \left(1 + \kappa^\circ g^\circ \frac{\mu^\circ_E}{\mu^\circ_{GV}} \frac{\mu_{AV}}{\mu_{AE}}\right)^{-1}$ the fraction of the assimilative power of the predator that originates from the digestion of prey reserves, when feeding on well-fed prey. The assimilative power can then be represented as $\dot{p}_A = (1 - \kappa_A + \kappa_A e^\circ)\mu_{AX} \dot{J}_X$, so that the maximum assimilative power is $\dot{p}_{Am} = \mu_{AX} \dot{J}_{Xm}$, where $\dot{J}_{Xm}$ denotes the maximum ingestion rate in terms of structural biomass. This can be summarized as $\dot{p}_A = (1 - \kappa_A + \kappa_A e^\circ) f \dot{p}_{Am}$, since $\dot{J}_X = f \dot{J}_{Xm}$. The dynamics of the scaled reserve density of a V1-morph predator becomes

$$\frac{d}{dt} e = \dot{k}_E (f - \kappa_A f + \kappa_A e^\circ f - e) \tag{5.5}$$

Energy extracted from reserves through digestion cannot exceed the energy invested in reserves, $\mu_{AE} < \mu^\circ_E$, and energy extracted from structural biomass through digestion cannot exceed energy contained in this mass, which itself cannot exceed energy invested in the synthesis of this mass, $\mu_{AV} < \mu^\circ_V < \mu^\circ_{GV}$. Therefore $\mu_{AX} < \mu^\circ_{GV}(1 + \frac{1}{\kappa^\circ g^\circ})$, and κ_A is probably, but not necessarily, larger than $(1 + \kappa^\circ g^\circ)^{-1}$.

If the prey has a reproduction buffer, it is possible that the assimilative power exceeds $\dot{p}_{Am}$, in this scaling, which indicates that the scaled reserve density of the predator can exceed 1, in principle. The quantitative description of feeding on prey can be further detailed by accounting for the selection of prey by the predator, based on the structural biomass and reserves of the prey, and/or by allowing the handling time to depend on these state variables. In this way, the saturation constant becomes dependent on the state variables of the prey as well. Although this might be realistic in particular applications, these mechanisms are not worked out here.

Parallel processing

The situation for bacteria that feed on glucose and fructose, for instance, is different because the carriers for glucose in the outer membrane of the bacterial cell cannot handle fructose. These substrates, therefore, do not compete for access to the same carriers, and their transformation into reserves is, to some extent, independent. The uptake of substrates amounts to

$$j_X = j_1 + j_2; \quad j_1 = j_{1m}(1 + x_1^{-1})^{-1}; \quad j_2 = j_{2m}(1 + x_2^{-1})^{-1} \tag{5.6}$$

Data on the aerobic production of the yeasts *Saccharomyces cerevisiae* and *Kluyveromyces fragilis* strongly suggest the existence of two different uptake routes for glucose [365], see Figure 5.1. A low-affinity high-capacity carrier is active under anaerobic and aerobic conditions, and ethanol and acetaldehyde are produced in association with this assimilation process. A high-affinity low-capacity carrier is active under aerobic conditions only, and no products are produced in association with this assimilation process. Some strains, however,

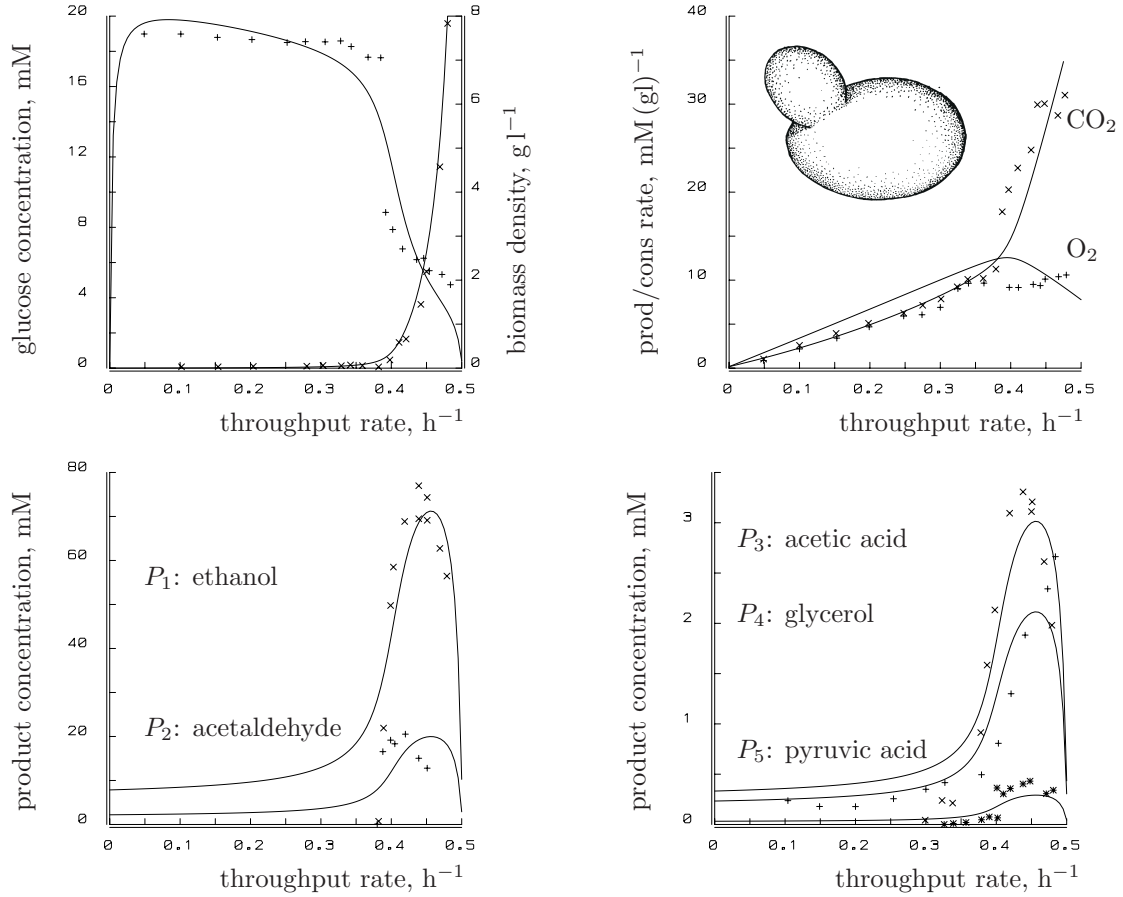

Figure 5.1: Aerobic growth and production of the yeast *Saccharomyces cerevisiae* at 30 °C in a chemostat. Data from Postma *et al.* [731,732] and Verduyn [943]. The data fits, modified from Hanegraaf [365], assume two assimilation processes for glucose, and product formation coupled to one assimilation process, which reduces the energy gain from glucose for metabolism by a factor $\kappa_A = 0.187$ (sd 0.026). The glucose concentration in the feed is 83.3 mM; the maximum throughput rate is $\dot{h}_m = 0.5$ h^{-1}; a measurement error on acetaldehyde is estimated to be 0.7 [365]. The composition of structure and reserves have been set at $n_{HV} = 1.75$, $n_{OV} = 0.61$, $n_{NV} = 0.14$, $n_{HE} = 1.7$, $n_{OE} = 0.62$, $n_{NE} = 0.23$. Parameters: $j_{Xm1} = 2.16$ (sd 0.15) mM/M h, $j_{Xm2} = 81$ (sd 13) mM/M h, $X_{K1} = 0.1$ mM, $X_{K2} = 40$ mM, $\dot{k}_E = 0.54$ (sd 0.009) h^{-1}, $\dot{k}_M = 0.003$ h^{-1}, $g = 0.050$ (sd 0.009), $\zeta_{P_1A_2} = 55$ (sd 8.9), $\zeta_{P_2A_2} = 43$ (sd 8.9), $\zeta_{P_3A_2} = 2.35$ (sd 0.8), $\zeta_{P_4A_2} = 2.47$ (sd 1.32), $\zeta_{P_5A_2} = 0.34$ (sd 1.02), $y_{EX} = 0.51$ (sd 0.035), $y_{EV} = 0.78$ (sd 0.10). The curves follow from $\dot{h} = \frac{e\dot{k}_E - g\dot{k}_M}{e+g}$; $e = \frac{j_{Xm1}f_1 + \kappa_A j_{Xm2} f_2}{j_{Xm1} + \kappa_A j_{Xm2}}$; $\kappa_A = \frac{\mu_{A_2X}}{\mu_{A_1X}}$; $W = (w_V + e w_E y_{EV}/g)\frac{\dot{h}(X_r - X)}{j_{Xm1}f_1 + j_{Xm2}f_2}$; $f_i = \frac{X}{X + X_{Ki}}$; $X_{Pi} = \frac{\zeta_{P_iA_2}\dot{k}_E f_2 (X_r - X)}{j_{Xm1}f_1 + j_{Xm2}f_2}$; $j_C = j_{Xm1}f_1(1 - y_{EX}) + j_{Xm2}f_2(1 - \kappa_A y_{EX}) + \dot{k}_M y_{EV} + \dot{h}(y_{EV} - 1) - \dot{k}_E f_2 n_C$; $j_O = j_{Xm1}f_1(y_{EX}n - 1) + j_{Xm2}f_2(\kappa_A y_{EX} n - 1) + \dot{k}_E f_2(n_C + n_H/4 - n_O/2) - \dot{k}_M y_{EV} n + \dot{h}(1 - n_{NV}/2 - n_{OV}/2 - n y_{EV})$; $n_C = \sum_i \zeta_{P_iA_2}$; $n_H = \sum_i n_{HP_i}\zeta_{P_iA_2}$; $n_O = \sum n_{OP_i}\zeta_{P_iA_2}$; $n = 1 + \frac{1}{4}n_{HE} - \frac{1}{2}n_{OE} - \frac{3}{4}n_{NE}$.

produce glycerol in association with the latter assimilation. When the process of glucose uptake and product formation is studied for increasing chemostat throughput rates under aerobic conditions, the quantitative dominance of the two carriers switches at a throughput rate of 0.2 h^{-1}, but no metabolic switches are required to capture this behaviour.

5.1.2 Supplementary substrates

When two substrates are supplementary, Synthesizing Units specify how the production rate depends on the substrate availabilities, as quantified in (2.15).

5.1.3 Photosynthesis *sensu lato*

The very extensive research on photosynthesis is usually geared to details around electron acquisition and carbon fixation. Here I also include polymer synthesis as an endpoint of the assimilation process, and assume pseudo-equilibria for the many intermediary steps. The aim is to quantify the kinetics of two transformations

$$\mathrm{CO_2 + H_2O + light \rightarrow CH_2O + O_2} \quad \left\{ \begin{array}{l} 2\,\mathrm{H_2O} + 4\,h\nu \rightarrow \mathrm{O_2} + 4\,\mathrm{H^+} + 4\,\mathrm{e^-} \\ \mathrm{CO_2} + 4\,\mathrm{H^+} + 4\,\mathrm{e^-} \rightarrow \mathrm{CH_2O} + \mathrm{H_2O} \end{array} \right.$$

$$y_{C_H,E}\mathrm{CH_2O} + y_{N_O,E}\mathrm{NO_3} \rightarrow \mathrm{CH}_{n_{HE}}\mathrm{O}_{n_{OE}}\mathrm{N}_{n_{NE}} + y_{C,E}\mathrm{CO_2} + y_{H,E}\mathrm{H_2O} + y_{O,E}\mathrm{O_2} + y_{N_H,E}\mathrm{NH_3}$$

Straightforward stoichiometry shows that

$$\begin{array}{rcl} y_{C,E} & = & y_{C_H,E} - 1; \quad y_{O,E} = -y_{C_H,E} + y_{N_O,E}\,9/4 - n_{OE}/2 - n_{NE}\,3/4 + n_{HE}/4 + 1 \\ y_{H,E} & = & y_{C_H,E} - n_{HE}/2 - y_{N_O,E}\,3/2 + n_{NE}\,3/2; \quad y_{N_H,E} = y_{N_O,E} - n_{NE} \end{array}$$

Some of these coefficients might be negative. The nitrogen source, here nitrate, can be replaced by others, of course. The carbohydrate CH_2O has the role of carbon as well as energy source for the synthesis of reserves E. This requires the implementation of a yield coefficient $y_{C_H,E} > 1$ in the second transformation, which does not depend on light directly.

The uptake of light, carbon dioxide and nitrate is quantified via their contribution in two types of reserves: carbohydrates E_C (polysaccharides and/ or lipids) and a generalized compound, E, which also contains nitrogen. These three supplementary 'nutrients' are processed in parallel, which means that an increase in the abundance of one nutrient can increase the assimilation of other. Notice that this still involves just the assimilation process. The processes of maintenance and growth run simultaneously, and contribute to the exchange of minerals between organism and environment.

Figure 5.2 gives a simplified schedule for the photosynthetic process *sensu lato*. The photopigment system of cyanobacteria, photoautotrophic protoctists and plants consists of two Photo Systems (PSs). When a photon is captured by the antenna and transferred to an unexcited PS II, it switches to the excited state, transfers an electron from water to PS I, and switches back to the unexcited state. PS I can likewise accept a photon from its antenna, and also accepts an electron from PS II, which allows it to pass an electron via NADPH to the carbon-fixation cycle (Calvin–Benson cycle). The enzyme Rubisco partakes in this cycle, and accepts the electron and a carbon dioxide molecule from its carrier, and reduces the latter to carbohydrate. Part of the carbohydrate is stored as such or excreted,

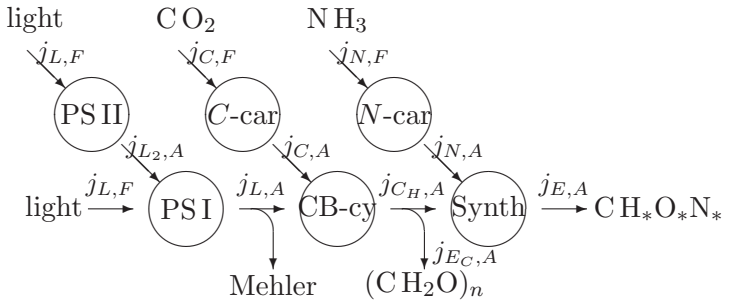

Figure 5.2: Diagram of the simplified autotrophic assimilation, where light L, carbon dioxide C and ammonia N are converted into carbohydrates E_C and (general) reserves E by Synthesizing Units (circles, see text). Photorespiration modifies the synthesis of carbohydrates. Alternative nitrogen sources can be introduced.

part is delivered to the synthesis machinery. The latter machinery also accepts ammonia from its carrier to synthesize reserves. All units behave as Synthesizing Units (SUs) {43}: PS II, the C-carrier and the N-carrier represent 1-SUs, and PS I, the Calvin–Benson cycle and the synthesizing machinery represent 1,1-SUs.

Pigment systems

For (negative) photon flux $j_{L,F}$ and large values for the flux ratios z_{L_1} and z_{L_2}, assimilated light quantifies as

$$j_{L_2,A} = j_{L_2,Am}\left(1+\frac{j_{L_2,FK}}{-j_{L,F}}\right)^{-1} \simeq -z_{L_2}j_{L,F} \quad \text{with } z_{L_2}=\frac{j_{L_2,Am}}{j_{L_2,FK}} \tag{5.7}$$

$$\begin{aligned} j_{L,A} &= j_{L_1,Am}\left(1+\frac{j_{L_1,FK}}{-j_{L,F}}+\frac{j_{L_2,AK}}{j_{L_2,A}}-\left(\frac{-j_{L,F}}{j_{L_1,FK}}+\frac{j_{L_2,A}}{j_{L_2,AK}}\right)^{-1}\right)^{-1} \\ &\simeq j_{L_1,Am}\left(1+\frac{j_{L_1,AK}}{-j_{L,F}}\right)^{-1} \quad \text{with } j_{L_1,AK}=j_{L_1,FK}+\frac{j_{L_2,AK}}{z_{L_2}}-\left(j_{L_1,FK}^{-1}+\frac{z_{L_2}}{j_{L_2,AK}}\right)^{-1} \\ j_{L,A} &\simeq -z_{L_1}j_{L,F} \quad \text{with } z_{L_1}=j_{L_1,Am}/j_{L_1,AK} \end{aligned} \tag{5.8}$$

where $j_{L_i,FK}$ and $j_{L_i,AK}$ are specific half saturation fluxes, i.e. parameters that are associated with the behaviour of SUs, and $j_{L_i,Am}$ are the maximum specific assimilation rates for photons for pigment system $i=1,2$. Although the electron input to the carbon-fixation cycle is (approximately) proportional to the light intensity, this does not mean that there is no upper limit to the light intensity that can be used, because the electrons experience increasing resistance to their use in the process of carbon-fixation. Electrons that are not used in carbon fixation or photorespiration 'leak' away via the Mehler reaction [721], also known as pseudocyclic electron transport, which involves oxygen uptake, and oxygen production of equal size [267]. The interception of light barely depends on temperature, while other metabolic processes do, which explains the need to handle spoiled electrons.

Green, purple and heliobacteria photosynthesize under anaerobic conditions, using bacteriochlorophylls and a single pigment system (PSII in purple and green non-sulfur bacteria, and PSI in green sulfur bacteria and heliobacteria). They must have an equivalent of the Mehler reaction to get rid of the excess electrons.

Carbon fixation

The output from the carbon-fixation cycle can be derived according to a similar reasoning as applied for electron production. For $x_C = X_C/X_{KC}$ we have with substitution of (5.8)

$$j_{C,A} = j_{C,Am}(1 + x_C^{-1})^{-1} = j_{C,Am} f_C \tag{5.9}$$

$$j_{C_H,A} = j_{C_H,Am}(1 + z_C^{-1}) \left(1 + \frac{j_{C,AK}}{j_{C,A}} + \frac{j_{L,AK}}{j_{L,A}} - \left(\frac{j_{C,A}}{j_{C,AK}} + \frac{j_{L,A}}{j_{L,AK}}\right)^{-1}\right)^{-1}$$

$$j_{C_H,A} = \frac{j_{C_H,Am}(1 + z_C^{-1})}{1 + z_C^{-1} f_C^{-1} + \frac{j_{L,FK}}{-j_{L,F}} - \left(z_C f_C + \frac{-j_{L,F}}{j_{L,FK}}\right)^{-1}} = j_{C_H,Am} f_{C_H} \tag{5.10}$$

with $z_C = j_{C,Am}/j_{C,AK}$, $j_{L,FK} = j_{L,AK} z_{L_1}^{-1}$, $j_{C,AK}$ the specific half saturation flux for carbon dioxide, $j_{C,Am}$ the maximum specific carbon dioxide assimilation rate, $j_{C_H,Am}$ the maximum specific carbohydrate assimilation rate.

Photorespiration

Rubisco is the most abundant enzyme on Earth, it constitutes 5–50% of the soluble protein in algal cells [267], and is involved in the fixation of carbon dioxide. Rubisco can operate in two modes on the substrate ribulose-1,5-biphosphate (RuP_2)

Carboxylase activity: $RuP_2 + CO_2 + H_2O \rightarrow 2[3P\text{-glycerate}]$

Oxygenase activity: $RuP_2 + O_2 \rightarrow 1[3P\text{-glycerate}] + 1[2P\text{-glycolate}]$

The second reaction is known as photorespiration. The net effect is that the binding of CO_2 or O_2 leads to the synthesis or degradation of carbohydrates. The binding is competitive, with widely varying relative strength among algal classes. The counterproductive effects of oxygen might be a historic accident, since Rubisco evolved in a period which was essentially free of oxygen [751]. C_4 plants, which bind carbon dioxide to an organic compound with four C-atoms in a micro-environment that is poor in oxygen, avoid photorespiration almost completely. They do not use Rubisco, but phosphoenolpyruvate (PEP) carboxylase for the binding of CO_2. Different species in the same genus can have C_3 and C_4 metabolism, and orache *Atriplex prostrata*, for instance, has both C_3 and C_4 metabolism. The oxygen use that is associated with primary carboxylation only occurs in light, and is called photorespiration. This can be modelled as follows.

Let $\boldsymbol{\theta} = \theta_{..}, \theta_{.O}, \theta_{.C}, \theta_{L.}, \theta_{LO}, \theta_{LC}$ denote the fractions of the photosynthetic system (RuP_2 plus PSs) that is in complex with nothing, oxygen, carbon, photon, photon and oxygen, or photon and carbon, respectively. The changes in the fractions are given by

$$\begin{array}{lcl} \frac{d}{dt}\theta_{..} &=& \dot{k}_O\theta_{LO} + \dot{k}_C\theta_{LC} - (j'_L + j'_O + j'_C)\theta_{..} \\ \frac{d}{dt}\theta_{.O} &=& j'_O\theta_{..} - j'_L\theta_{.O} \\ \frac{d}{dt}\theta_{.C} &=& j'_C\theta_{..} - j'_L\theta_{.C} \end{array} \qquad \begin{array}{lcl} \frac{d}{dt}\theta_{L.} &=& j'_L\theta_{..} - (j'_O + j'_C)\theta_{L.} \\ \frac{d}{dt}\theta_{LO} &=& j'_L\theta_{.O} + j'_O\theta_{L.} - \dot{k}_O\theta_{LO} \\ \frac{d}{dt}\theta_{LC} &=& j'_L\theta_{.C} + j'_C\theta_{L.} - \dot{k}_C\theta_{LC} \end{array}$$

where $j'_* = \rho_* y_{C_H*} j_*$ denotes the arrival flux j_* times the binding probability ρ_*, and the coefficient y_{C_H*} couples $*$ to C_H; $\dot{k}_O$ and $\dot{k}_C$ stand for the dissociation rates of oxygenase

and carboxylase products. The net flux of carbohydrate is found by equating the changes in fractions to zero and solving for $\boldsymbol{\theta}$. The result is

$$j_{C_H,A} = \theta_{LC}\dot{k}_C - \theta_{LO}\dot{k}_O = \frac{j'_C - j'_O}{1 + \frac{j'_C}{\dot{k}_C} + \frac{j'_O}{\dot{k}_O} + \frac{j'_C+j'_O}{j'_L} - \frac{j'_C+j'_O}{j'_L+j'_C+j'_O}} \tag{5.11}$$

For $j'_O = 0$ this reduces to $j_{C_H,A} = \left(\dot{k}_C^{-1} + {j'_L}^{-1} + {j'_C}^{-1} - (j'_L + j'_C)^{-1}\right)^{-1}$, which is identical to (5.10). At the compensation point $j'_O = j'_C$, no net synthesis of carbohydrate occurs.

Nitrogen incorporation

The incorporation of ammonia into carbohydrates finally results in the flux of reserves for $x_N = X_N/X_{KN}$

$$\begin{aligned} j_{N,A} &= j_{N,Am}(1 + x_N^{-1})^{-1} = j_{N,Am} f_N \qquad (5.12) \\ j_{E,A} &= \frac{j_{E,Am}\left(1 + z_N^{-1} + z_{C_H}^{-1} - (z_N + z_{C_H})^{-1}\right)}{1 + \frac{j_{N,AK}}{j_{N,A}} + \frac{j_{C_H,AK}}{j_{C_H,A}} - \left(\frac{j_{N,A}}{j_{N,AK}} + \frac{j_{C_H,A}}{j_{C_H,AK}}\right)^{-1}} \\ j_{E,A} &= \frac{j_{E,Am}\left(1 + z_N^{-1} + z_{C_H}^{-1} - (z_N + z_{C_H})^{-1}\right)}{1 + z_N^{-1} f_N^{-1} + z_{C_H}^{-1} f_{C_H}^{-1} - (z_N f_N + z_{C_H} f_{C_H})^{-1}} \qquad (5.13) \end{aligned}$$

with $z_N = j_{N,Am}/j_{N,AK}$ and $z_{C_H} = j_{C_H,Am}/j_{C_H,AK}$. This relationship gives the production of reserves E as a function of the three 'nutrients' light, carbon dioxide and ammonia. The production of carbohydrates E_C now amounts to $j_{E_C,A} = j_{C_H,A} - j_{E,A}$.

5.1.4 Calcification

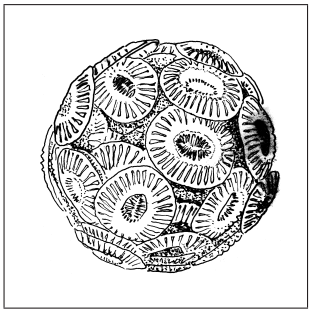

Bicarbonate is by far the dominant form of inorganic carbon in seawater. At the typical pH of about 8.3, 98% of the inorganic carbon is in this form. Few organisms can use this source, one problem is to deal with the electrical charge. Coccolithophorans, such as *Emiliania huxleyi* (right), mastered this art, by using calcium in the transformation $Ca^{2+} + 2\,HCO_3^- \rightarrow Ca\,CO_3 + CO_2 + H_2O$, where the calcium carbonate is exported by the Golgi apparatus in the form of beautifully shaped extra-cellular coccoliths, and the carbon dioxide is used as carbon substrate for the synthesis of carbohydrates and lipids (for which they obviously need water and light as well). The coccoliths accumulate in a polysaccharide layer, and are shedded at cell death. *Emiliania* is so abundant that the coccoliths can easily be seen on satellite images in huge areas in the northern Atlantic and Pacific Ocean where they bloom regularly. A substantial fraction of carbonates in rocks originates from coccoliths, and coccolithophorans may play a key role in the carbon metabolism of the Earth [986].

Since carbon dioxide is relatively rare, and the transformation of carbonate and bicarbonate to carbon dioxide is slow, and the water that envelopes the cell is stagnant,

see {235}, cells in the sea can become limited by carbon under otherwise optimal growth conditions [1013]. This points to the gain of using bicarbonate as an additional carbon source, with an inherent gradient in the CO_2/HCO_3^- ratio in the diffusive boundary layer [1014]. The process of calcification can be modelled in the context of the DEB theory by treating carbon dioxide and bicarbonate as substitutable substrates, with light as a supplementary 'substrate', for the synthesis of lipids as reserve, while calcium carbonate is formed as a product in this assimilation process. This implementation ties calcification to photosynthesis.

As long as calcium is not rate limiting, and the environment is homogeneous, the carbohydrate production amounts to

$$j_{C_H} = \left(\dot{k}_C^{-1} + (j'_C + j'_{C-})^{-1} + {j'_L}^{-1} - \left(j'_C + j'_{C-} + j'_L\right)^{-1}\right)^{-1}$$

where $j'_C = \rho_C j_C$ and $j'_{C-} = \rho_{C-} j_{C-}/2$ are the effective arrival rates of carbon dioxide and bicarbonate; and the factor 0.5 in j'_{C-} relates to the stoichiometry of the calcification process. The calcification rate now becomes

$$j_{Ca} = \frac{j_{C_H} j'_{C-}}{j'_C + j'_{C-}}$$

Calcification is also reported to occur in the dark, to some extent. This might relate to heterotrophic activity to acquire the energy for carbon fixation.

5.2 Several reserves

The number of reserves can be chosen independently of the number of nutrients, as a compromise between simplicity and realism. The case of two reserves and two nutrients serves as an example, see Figure 5.3; the model extends to more reserves and possibly limiting nutrients without causing additional problems, on the basis of the SU kinetics specified in (2.15).

The general idea is to apply the rules for SUs to quantify the transformation of nutrients to each reserve, and of reserves to structural mass. This takes $n + 1$ SUs in the case of n reserves. The rejected substrate fluxes do not pose any problem in the case of the assimilation SUs, because they are fed back into the environment. In the case of the growth SU, however, we have to specify their fate in more detail. This is why I start with the specification of growth, given the reserve densities, and then consider reserve dynamics.

5.2.1 Growth

Just like the mono-variate case, both reserve densities m_{Ei}, $i = 1, 2$, follow first-order kinetics, which means that for a reserve mass M_{Ei}, the catabolic flux, which is mobilized from the reserve, equals

$$\dot{J}_{Ei,C} = M_{Ei}(\dot{k}_{Ei} - \frac{d}{dt} \ln M_V) = M_{Ei}(\dot{k}_{Ei} - \dot{J}_{V,G}/M_V) = M_{Ei}(\dot{k}_{Ei} - j_{V,G}) \tag{5.14}$$

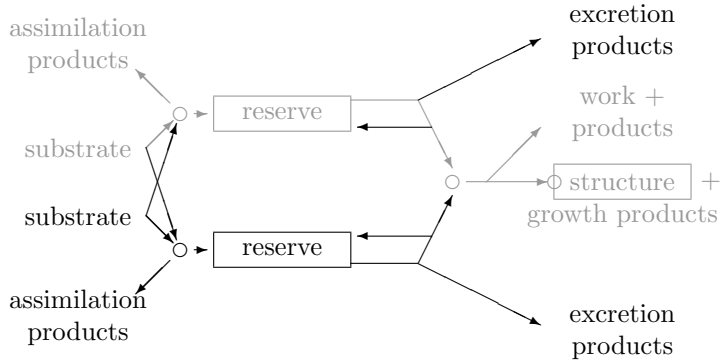

Figure 5.3: A diagram of the structure of a two-substrates, two-reserves DEB model. The circles indicate SUs. The diagram for a single-substrate, single-reserve model is in grey. Excretion products are then included in the products linked to growth and maintenance (work). The dynamics of other reserves interact with this process.

where $\dot{k}_{Ei}$ denotes the rate constant of the first-order process, and $j_{V,G} = \dot{r}$ the specific growth rate. (The first index relates to the compound, the second one to the process.) The second term in (5.14) relates to the dilution by growth, and the specific growth rate of structural mass equals the population growth for V1-morphs.

The maintenance costs $\dot{J}_{Ei,M}$ are taken to be proportional to structural mass M_V, quantified in C-moles, so $\dot{J}_{Ei,M} = j_{Ei,M} M_V$, and specific maintenance requirement $j_{Ei,M}$ for reserve i is taken to be constant. This means reserve i sends a flux $\dot{J}_{Ei,G} = \dot{J}_{Ei,C} - \dot{J}_{Ei,M}$ to the SU for growth of structural biomass, which is assumed to be fast (i.e. its $\dot{J}_{Vm}$ is large) and has high affinities for the reserve 'molecules' (i.e. $\rho_i = 1$). This does not imply, however, that the maximum growth is fast, because the dilution by growth restricts the input flux to the SU, while a maximum in the reserve density also restricts the flux to the SU. The latter results from a specification of the assimilation process.

The growth-SU merges the catabolic fluxes from the reserves stoichiometrically to produce structural mass, but stoichiometric constraints imply that the growth SU rejects some of the arriving reserve 'molecules'. The growth rate is found from (2.15) to be

$$\begin{aligned} \dot{J}_{V,G} &= \frac{d}{dt} M_V = \left(\sum_i \left(\frac{\dot{J}_{Ei,G}}{y_{Ei,V}} \right)^{-1} - \left(\sum_i \frac{\dot{J}_{Ei,G}}{y_{Ei,V}} \right)^{-1} \right)^{-1} \\ \dot{r} &= \frac{\dot{J}_{V,G}}{M_V} = \left(\sum_i \left(\frac{m_{Ei}(\dot{k}_{Ei} - \dot{r}) - j_{Ei,M}}{y_{Ei,V}} \right)^{-1} - \left(\sum_i \frac{m_{Ei}(\dot{k}_{Ei} - \dot{r}) - j_{Ei,M}}{y_{Ei,V}} \right)^{-1} \right)^{-1} \end{aligned} \quad (5.15)$$

for reserve density $m_{Ei} = M_{Ei}/M_V$ and yield coefficient $y_{Ei,V}$, which quantifies the number of C-moles of reserve i needed to synthesize a C-mole of structure. This equation can be transformed into a cubic polynomial in $\dot{J}_{V,G}$, which can easily be solved as a function of the state of the cell $\{M_{E1}, M_{E2}, M_V\}$. Note that specification of the details of the assimilation processes and the fate of the rejected reserve fluxes is required to relate the extracellular nutrient levels to reserve densities.

Figure 5.4 illustrates that the combination of first-order kinetics of reserves and a fast SU for growth is realistic. Note that cell content on phosphorus and vitamin B_{12} have been measured, rather than reserves. In view of the very small values, the reserves hardly contribute to total biomass, which can then be conceived as structural biomass. The overhead costs in the synthesis of structural mass and the maintenance costs for these

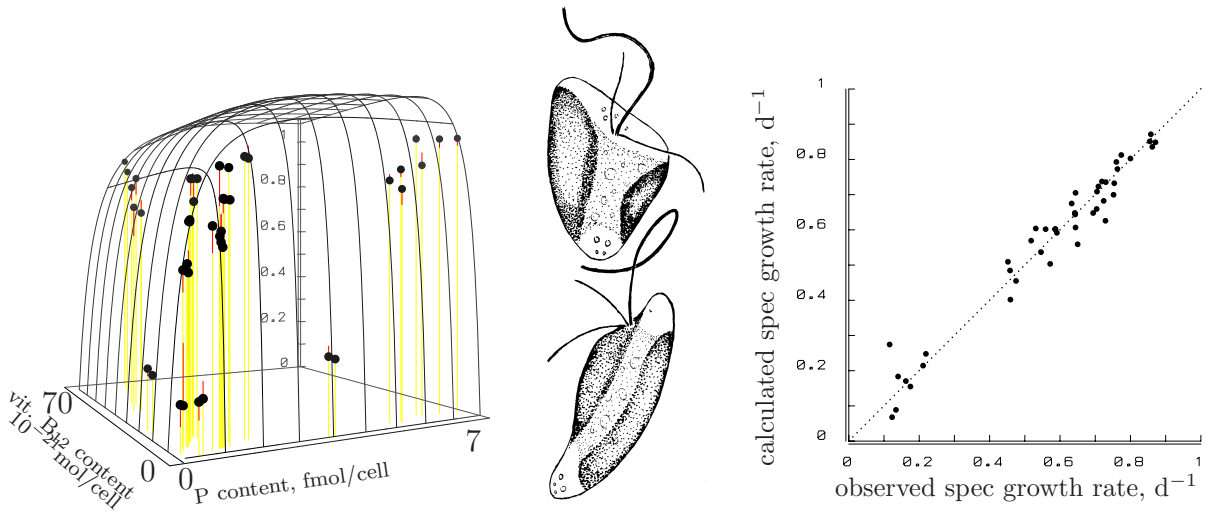

Figure 5.4: The specific growth rate $\dot{r}$ of the Haptophyte *Pavlova lutheri* as a function of the intracellular reserves of phosphorus (reserve 1) and vitamin B_{12} (reserve 2) at 20 °C (left), and the relationship between the observed growth rate and the calculated one (right). Data from Droop [235]. The parameters are given in Figure 5.5.

nutrients have been neglected.

5.2.2 Reserve dynamics

The growth-SU rejects the reserve fluxes at rates

$$\begin{aligned} \dot{J}_{Ei,R} &= \dot{J}_{Ei,C} - \dot{J}_{Ei,M} - y_{Ei,V}\dot{J}_{V,G} \\ &= M_V\left((\dot{k}_{Ei} - \dot{r})m_{Ei} - j_{Ei,M} - y_{Ei,V}\dot{r}\right) \end{aligned} \tag{5.16}$$

Each rejected reserve 'molecule' is excreted with probability $(1 - \kappa_{Ei})$ in one form or another, and fed back to the reserves with probability κ_{Ei}, so the balance equation for reserves M_{Ei} or reserve densities $m_{Ei} = M_{Ei}/M_V$ becomes

$$\begin{aligned} \frac{d}{dt}M_{Ei} &= \dot{J}_{Ei,A} - \dot{J}_{Ei,C} + \kappa_{Ei}\dot{J}_{Ei,R} \\ &= \dot{J}_{Ei,A} - (1-\kappa_{Ei})(\dot{k}_{Ei} - \dot{r})M_{Ei} - \kappa_{Ei}(j_{Ei,M} + y_{Ei,V}\dot{r})M_V \qquad (5.17) \\ \frac{d}{dt}m_{Ei} &= j_{Ei,A} - (1-\kappa_{Ei})(\dot{k}_{Ei} - \dot{r})m_{Ei} - \kappa_{Ei}(j_{Ei,M} + y_{Ei,V}\dot{r}) - \dot{r}m_{Ei} \qquad (5.18) \end{aligned}$$

If SUs behave according to (2.15) when taking up nutrients from the environment and synthesizing reserves, the assimilation rate of reserve i, $i = 1, 2$, amounts to

$$\dot{J}_{Ei,A} = j_{Ei,A}M_V = j_{Ei,Am}M_V\left(1 + \sum_j x_{ji}^{-1} - \left(\sum_j x_{ji}\right)^{-1}\right)^{-1} \tag{5.19}$$

where the scaled nutrient concentration $x_{ji} = X_j/X_{Kji}$ represents the ratio of the nutrient concentration X_j to the saturation constant X_{Kji}, which combines the affinity of substrate

j to SU i relative to the maximum assimilation rate $\dot{J}_{Ei,Am}$, and the stoichiometric requirement of product i for substrate j. If nutrient j is not required for the synthesis of reserve i, we take X_{Kji} to be infinitesimally small, which makes x_{ji} very large, and (5.19) reduces to a simple Michaelis–Menten kinetics. The uptake rate of substrate j by assimilation SU i is $y_{j,Ei}\dot{J}_{Ei,A}$. The saturation constants are independent of the cell size, while the maximum assimilation rates are proportional to the structural biomass M_V, so $\dot{J}_{Ei,Am} = j_{Ei,Am}M_V$.

In steady state, i.e. X_j is constant for long enough, we have $\frac{d}{dt}M_{Ei} = \dot{r}M_{Ei}$, so (5.17) implies

$$j_{Ei,A} = \dot{r}m_{Ei} + (1-\kappa_{Ei})(\dot{k}_{Ei} - \dot{r})m_{Ei} + \kappa_{Ei}(j_{Ei,M} + y_{Ei,V}\dot{r}) \tag{5.20}$$

which, in combination with (5.15), gives m_{E1}, m_{E2} and $\dot{r}$ as functions of the substrate concentrations x_1 and x_2. If $\kappa_{Ei} = 1$, so all reserve i molecules that are rejected by the growth SU are fed back to the reserves, non-limiting reserves would accumulate without bound.

5.2.3 Simultaneous nutrient limitation

Data from an experiment with the chemostat in steady state are used to test the simultaneous limitation model for realism. The balance equation for the nutrients in the medium of a chemostat with throughput rate $\dot{h}$ are

$$\frac{d}{dt}X_j = (X_{rj} - X_j)\dot{h} - \sum_i y_{j,Ei}\dot{J}_{Ei,A} \tag{5.21}$$

$$\frac{d}{dt}X_j^* = \sum_i (1-\kappa_{Ei})y_{j,Ei}\dot{J}_{Ei,R} + \sum_i y_{j,Ei}\dot{J}_{Ei,M} - X_j^*\dot{h} \tag{5.22}$$

where X_j is the concentration of nutrient j, X_j^* the nutrient content of excretions due to reserves that are mobilized but rejected by the growth SU and not fed back to the reserves, and (the second term) nutrients involved in maintenance losses. X_{rj} denotes the concentration of substrate j in the feed. The summation is over all reserves i. I suppose that the excreted nutrients are metabolically changed such that they cannot be reused immediately.

At steady state, the substrate concentrations X_j in the chemostat do not change, so $\frac{d}{dt}X_j = 0$, $j = 1, 2$, and

$$(X_{rj} - X_j)\dot{h} = M_V \sum_i y_{j,Ei}j_{Ei,A} \tag{5.23}$$

$$X_j^*\dot{h} = M_V \sum_i y_{j,Ei}\left((1-\kappa_{Ei})\left(\dot{k}_{Ei}m_{Ei} - (m_{Ei} + y_{Ei,V})\dot{r}\right) + \kappa_{E_i}j_{Ei,M}\right) \tag{5.24}$$

The biomass density in the chemostat follows from the fact that the specific growth rate $\dot{r} = \dot{h}$ is known. The equations (5.15), (5.19), (5.20) and (5.23) together define the biomass density M_V, the nutrient concentrations X_j and the reserve densities at steady state m_{Ei}, given the throughput rate $\dot{h}$ and the nutrient concentrations in the feed X_{rj}. Although the system consists of five coupled equations, it can be reduced to a single one in X_1 for uncoupled assimilation fluxes ($y_{1,E1} = 1$, $y_{1,E2} = 0$, $y_{2,E1} = 0$, $y_{2,E2} = 1$), while the range

of X_j is given by $(\delta_j^{-1}-1)^{-1} < X_j/X_{Kj} < X_{rj}/X_{Kj}$, with $\delta_j = \kappa_{Ej}(j_{Ej,M}+y_{Ej,V}\dot{r})/j_{Ej,Am}$. It can be shown that the resulting equation in X_1 has one or three roots, while only one root satisfies the range restriction for X_2. A bisection method can be used to arrive at a high quality initial estimate for the proper root, followed by a Newton–Raphson method to obtain that root accurately.

The details of the measurement method determine whether or not the excretions are included in the medium concentrations. In the data presented and analysed in Figure 5.5, phosphorus and cobalt (in vitamin B_{12}) were measured using isotopes. As a consequence, the measured medium concentrations include the excreted labelled phosphorus and cobalt, and correspond to $X_j + X_j^*$. The cellular contents correspond to $\sum_i y_{j,Ei}(y_{Ei,V} + m_{Ei})$. If the assimilation fluxes for phosphorus and vitamin B_{12} are not coupled, the cellular content reduces to $y_{Ej,V} + m_{Ej}$. This simplification reduces the total number of parameters to be estimated to 10 for 20 data sets, or 220 data points. The balance equation for nutrient j in the medium plus that in the cells at steady state reads

$$X_{rj} = X_j + X_j^* + \sum_i y_{j,Ei}(y_{Ei,V}M_V + M_{Ei}) = X_j + X_j^* + M_V \sum_i y_{j,Ei}(y_{Ei,V} + m_{Ei}) \quad (5.25)$$

These balance equations have been checked for the model fits in Figure 5.5, but they apply only approximately to the data, because of measurement errors. Since tiny deviations in the amount of biomass and cellular content substantially change medium concentrations, the latter has been given a low weight in the simultaneous regressions of the 20 curves in Figure 5.5.

5.2.4 Non-limiting reserves can dam up

The significance of the excretion is in avoiding the possible occurrence of 'explosion'; if a cell cannot grow because of the absence of an essential nutrient, and it would continue to take up other nutrients, the accumulation of those nutrients would be unbounded without excretion. The combination of a first-order dynamics of reserve densities and $0 \leq \kappa_{Ei} < 1$ implies the existence of an upper boundary for reserve densities if upper boundaries for the assimilation rates exist. The steady-state reserve density m_{E2} is maximal if assimilation is maximal, $j_{E2,A} = j_{E2,Am}$, while expenditure is minimal, which occurs when growth is zero, $\dot{J}_{V,G} = 0$, i.e. when $\dot{J}_{E1,C} = \dot{J}_{E1,M} = \dot{J}_{E1,A}$ or $m_{E1} = j_{E1,M}/\dot{k}_{E1}$. The maximum reserve density is found from (5.17) to be $m_{E2m} = \frac{j_{E2,Am}-\kappa_{E2}j_{E2,M}}{(1-\kappa_{E2})\dot{k}_{E2}}$. This illustrates the point that excretion is essential: $m_{Eim} \to \infty$ for $\kappa_{Ei} \to 1$. I will call the fractions κ_{Ei} recovery fractions. The density of the reserve that fully arrests growth is at minimum, and has the value $\frac{j_{E,M}}{\dot{k}_E}$. Excretion is a common feature; extracellular release of organic carbon in phytoplankton has been reported to be as high as 75 % of the totally fixed carbon [582].

The density of the limiting reserve *in*creases (hyperbolically) with the growth rate, while the non-limiting reserves can *de*crease with the growth rate. This very much depends on the recovery fraction κ_E. The reserve density of the non-limiting nutrients can build up to spectacular levels, which easily lead to the wrong conclusion that (all) reserve densities decrease with the growth rate.

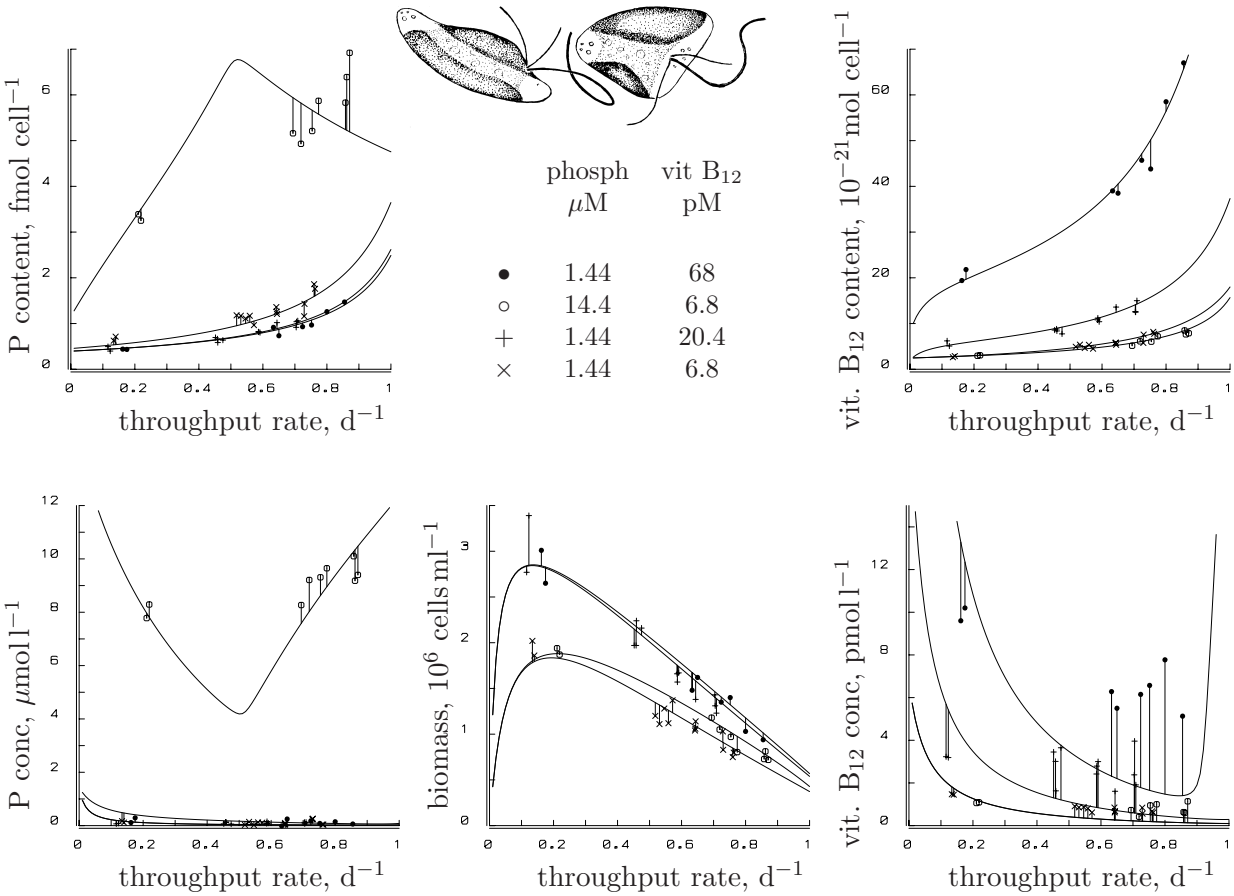

Figure 5.5: The phosphorus and vitamin B_{12} cellular contents and medium concentrations, and the biomass density, as functions of throughput rate $\dot{h}$ of the Haptophyte *Pavlova lutheri* at four levels of these nutrients in the feed. Data from Droop [235]. The parameters are the reserve turnover rates $\dot{k}_{E1} = 1.19$ (sd 0.09) d^{-1}, $\dot{k}_{E2} = 1.22$ (sd 0.09) d^{-1}, stoichiometric requirements $y_{E1,V} = 0.39$ (sd 0.05) fmol cell^{-1}, $y_{E2,V} = 2.35$ (sd 0.27) 10^{-21} mol cell^{-1}, maximum specific assimilation rates $j_{E1,Am} = 4.91$ (sd 0.14) fmol (cell d)$^{-1}$, $j_{E2,Am} = 76.6$ (sd 82) 10^{-21} mol (cell d)$^{-1}$, recovery fractions $\kappa_{E1} = 0.69$ (sd 0.08), $\kappa_{E2} = 0.96$ (sd 0.006), maintenance rates $\dot{k}_{M1} = 0.0079$ (sd 0.012) d^{-1}, $\dot{k}_{M2} = 0.135$ (sd 0.047) d^{-1}, given the saturation constants $X_{K1} = 0.017$ μM, $X_{K2} = 0.12$ pM by Droop. The simultaneously fitted curves obey mass balances, and reveal measurement errors in the vitamin concentrations.

If (traces of) all essential nutrients are required for the assimilation of each reserve, rare nutrients reduce the uptake of abundant ones and 'explosion' is avoided in almost all cases of practical interest, even if $\kappa_{Ei} = 1$; 'explosion' can still occur theoretically, in the absence of maintenance costs ($j_{Ei,M} = 0$). The DEB model accomodates, therefore, two controls on reserve accumulation: via assimilation of nutrients and via recovery.

Biological phosphate removal

The accumulation of reserves that are synthesized from non-limiting nutrients is exploited technically in the process of phosphate removal in sewage treatment plants, using *Acinetobacter calcoaceticus*. These remarkable bacteria cannot use hexoses as carbon and energy source [875]. Sewage water typically contains 10–30 mg/ l phosphorus. Under aerobic conditions, actinobacters decompose carbohydrates, such that they extract energy but little carbon. The energy is fixed in polyphosphates, by taking up phosphate. Under anaerobic conditions, energy is limiting and volatile fatty acids, such as acetates, are taken up and converted into poly 2-hydroxy butyrate (phb), while stored polyphosphates are used for energy supply in this transformation [426]. The quantitative details of this coupling are not quite clear yet; one possibility is that the rejected polyphosphate flux is used for the assimilation of phb. The excreted phosphate is technically precipitated with calcium carbonate. This gives the scope for phosphate removal by alternating between aerobic and anaerobic conditions; the specific maintenance requirement $j_{E,M}$ for phosphate is probably very small.

5.2.5 Oxygen flux

The physiological literature frequently presents Photosynthesis-Irradiance (PI) curves, where photosynthesis is usually measured via oxygen production. The rate of photosynthesis is in practice frequently measured by the rate of oxygen production, but the relationship is, however, rather indirect. The assimilation process consists of an oxygen-producing transformation that generates carbohydrate reserves, and an oxygen-consuming one that generates generalized reserves. Oxygen-consuming maintenance and two growth processes run simultaneously

$$\mathrm{CH}_{n_{HE}}\mathrm{O}_{n_{OE}}\mathrm{N}_{n_{NE}} \to \mathrm{CO}_2 + y'_{H,E}\mathrm{H}_2\mathrm{O} + y'_{O,E}\mathrm{O}_2 + n_{NE}\mathrm{NH}_3$$
$$y_{E,V}\mathrm{CH}_{n_{HE}}\mathrm{O}_{n_{OE}}\mathrm{N}_{n_{NE}} \to \mathrm{CH}_{n_{HV}}\mathrm{O}_{n_{OV}}\mathrm{N}_{n_{NV}} + y'_{C,V}\mathrm{CO}_2 + y'_{H,V}\mathrm{H}_2\mathrm{O} + y'_{O,V}\mathrm{O}_2 + y'_{N_HV}\mathrm{NH}_3$$

where straightforward stoichiometry shows that

$$\begin{aligned} y'_{H,E} &= n_{HE}/2 - n_{NE}\,3/2; \quad y'_{O,E} = -1 - n_{HE}/4 + n_{OE}/2 + n_{NE}\,3/4 \\ y'_{C,V} &= y_{E,V} - 1; \quad y'_{O,V} = y_{E,V}n_{OE}/2 - n_{OV}/2 - y_{E,V} + 1 - y'_{H,V}/2 \\ y'_{H,V} &= y_{E,V}n_{HE}/2 - n_{HV}/2 - y_{E,V}n_{NE}\,3/2 + n_{NV}\,3/2; \quad y'_{N_H,V} = y_{E,V}n_{NE} - n_{NV} \end{aligned}$$

The second growth transformation consists of a catenation between the second assimilation transformation and the first growth transformation. The significance of this delayed synthesis of generalized reserves is an increase in metabolic flexibility; the organism can produce carbohydrates in the temporary absence of a nitrogen source. Storage of carbohydrates only makes sense if nitrogen compounds are stored as well, as long as strong homeostasis applies.

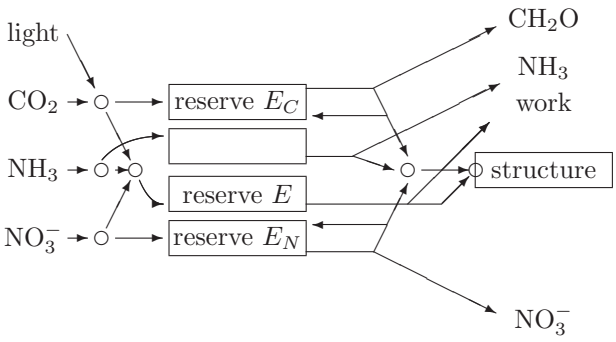

Figure 5.6: Diagram of nitrogen assimilation, where light and carbon dioxide are converted into carbohydrate reserves E_C, and nitrate into nitrate reserves E_N, which are used to synthesize structure. Ammonia can be used as an alternative nitrogen source, but barely accumulates. The circles indicate Synthesizing Units.

This all adds up to the oxygen flux

$$j_O = (m_{E_C} + y_{O,E} m_E + y_{O,E} y_{E,V} + y'_{O,V}) j_{V,G} + y'_{O,E} j_{E,M} \tag{5.26}$$

where $m_{E_C} = j_{E_C,A}/j_{V,G}$ is the carbohydrate reserve density and $m_E = j_{E,A}/j_{V,G}$ is the generalized reserve density. At steady state, these values become constant, and depend on the specification of the reserve kinetics.

If the growth SU is fast, no generalized reserves are rejected, and the specific catabolic flux from the generalized reserves, $j_{E,C_1} = m_E \dot{k}_E$, adds to the specific flux j_{E,C_2} of generalized reserves that are synthesized from carbohydrate reserves and nitrogen reserves; the sum being spent on maintenance and growth. Catabolized carbohydrates are rejected at rate $j_{E_C,C} - y_{C_H,E} j_{E,C_2}$, and a fraction κ_E returns to the carbohydrate reserves. This leads to the following relationships, where $\dot{r} = j_{V,G}$

$$\begin{aligned} j_{E,C_2} &= y_{E,V}\dot{r} + j_{E,M} - m_E \dot{k}_E \\ \frac{d}{dt} m_E &= j_{E,A} - \dot{k}_E m_E \\ \frac{d}{dt} m_{E_C} &= j_{E_C,A} - (1-\kappa_E)(\dot{k}_{E_C} - \dot{r}) m_{E_C} - \kappa_E y_{C_H,E} j_{E,C_2} - \dot{r} m_{E_C} \end{aligned}$$

The reserve densities m_E and m_{E_C} can be solved explicitly for steady state, given $\dot{r}$, and substituted into (5.26).

The interpretation of experimental data is further hampered by the common practice of presenting oxygen fluxes relative to chlorophyll, usually Chlorophyll *a*; this is practical, because chlorophyll is rather easy to measure. This compound represents, just like all other compounds in the body, a weighted sum of the generalized reserves and the structural mass: $M_{Chl} = y_{Chl,E} M_E + y_{Chl,V} M_V$, or $m_{Chl} = y_{Chl,E} m_E + y_{Chl,V}$. The chlorophyll-specific oxygen flux, therefore, amounts to j_O/m_{Chl}, which can be related to environmental and growth conditions, but involves many aspects of physiology, not just photosynthesis.

5.2.6 Ammonia–nitrate interactions

Many organisms can use several nitrogen substrates for assimilation, including ammonia, nitrite, nitrate, urea, amines and amino acids. Plants have access to nitrogen in organic compounds via mycorrhizae. Ammonia is rather toxic, so it does not accumulate as such;

it is directly assimilated into amino acids, such as glutamate and glutamine. Nitrite is also rather toxic, and has mutagenic properties, see {216}; nevertheless, it is stored by some organisms. Nitrate is first reduced to nitrite, and then to ammonia, before further use [288]. These reductions require substantial energy, which is probably the reason why ammonia is usually strongly preferred as a substrate. It is even generally believed that ammonia inhibits nitrate uptake, but this does not seem to hold true [227]. Organisms vary in their properties with respect to nitrogen uptake. The intensively studied yeast *Saccharomyces cerevisiae* cannot assimilate nitrogen oxides [963]. Some yeasts and bacteria nitrify ammonia to nitrate. Selective preferences for ammonia and nitrate can explain main patterns in plant associations [85]. Soil types differ substantially in ammonia and nitrate availability for plants [266], and their ratio strongly influences the occurrence of plant species, even at a very small spatial scale, such as the shifting mosaic of gap and understory conditions in a forest [180,534]. Probably because of its toxicity, ammonium assimilation occurs in the roots and not in the shoots of plants.

Figure 5.6 indicates how an alternative nitrogen substrate for ammonia can be implemented in a DEB framework. Ammonia is stored before use, just like nitrate, but the maximum storage capacity is very low, and the turnover rate very high. Homeostasis of structural mass requires that the product of the synthesis of ammonia and carbohydrate is identical to the generalized reserve, which means that the synthesis occurs twice: just after assimilation (prior to storage) from assimilates and after storage, just prior to synthesis of structural mass from catabolized products. The rules for sequential processing of substitutable substrates can be used to quantify the fluxes, cf. (5.3). The extra requirement of energy in the processing of nitrate can be taken into account by the stoichiometric coupling with carbohydrates, which can depend on the substrate that is used. Many applications allow a reduction of this redundancy, and a description without generalized reserves will be adequate. Ammonia is not only taken up, but is also excreted in association with growth and maintenance.

The assimilation of ammonia, nitrate and carbohydrates is given by (5.11) and (5.12). Treating ammonia and nitrogen as substitutable substrates, and complementary to carbohydrates, the specific assimilation of generalized reserves is

$$j_{E,A} = \left(j_{E,Am}^{-1} + (j'_{N_H,A} + j'_{N_O,A})^{-1} + j'^{-1}_{C_H,A} - (j'_{N_H,A} + j'_{N_O,A} + j'_{C_H,A})^{-1}\right)^{-1} \tag{5.27}$$

where $j'_{*,A} = \rho_* y_{*,E} j_{*,A}$, and $y_{C_H,E} = \theta^A_{N_H} y^{N_H}_{C_H,E} + \theta^A_{N_O} y^{N_O}_{C_H,E}$, where $\theta^A_{N_H} + \theta^A_{N_O} = 1$, and $\theta^A_{N_H} = j'_{N_H,A}(j'_{N_H,A} + j'_{N_O,A})^{-1}$. The maximum of $j_{E,A}$ is not necessarily constant: $j_{E,Am} = \theta^A_{N_H} j^{N_H}_{E,Am} + \theta^A_{N_O} j^{N_O}_{E,Am}$. Since the reduction of nitrate is rather energy consuming, and extracted from the oxidation of carbohydrates, the relationship $y^{N_H}_{C_H,E} < y^{N_O}_{C_H,E}$ holds. The requirement for carbohydrates can vary in time, and depends on the nitrogen source.

The specific catabolic rates of the four reserves are $j_{*,C} = (\dot{k}_* - j_{V,G})m_*$. The specific catabolic rate of the reserves E is $j_{E,C_1} = (\dot{k}_E - j_{V,G})m_E$. The synthesis of a compound identical to generalized reserves from catabolic products for metabolic use (maintenance and growth), j_{E,C_2} is similar to that from assimilation products (5.27), with $j_{*,C}$ replacing $j_{*,A}$. The growth SU is assumed to be fast enough to avoid spoiling of reserves, so $j_{V,G} = y_{VE}(j_{E,C_1} + j_{E,C_2} - \dot{k}_{E,M})$.

Ammonia is hardly stored, which means that rejected ammonia is not fed back to the reserves ($\kappa_{E_{NH}} = 0$), but excreted. The turnover rate $\dot{k}_{E_{NH}}$ is large; this gives an extremely low ammonia reserve, $m_{E_{NH}} \simeq 0$, and the catabolic rate equals $j_{E_{NH},C} = j_{N_H,A} - \theta^A_{N_H} y_{NE}\, j_{E,A}$. The rejected ammonia flux is $j_{E_{NH},R} = j_{E_{NH},C} - \theta^C_{N_H} y_{NE}\, j_{E,C_2}$, with $\theta^C_{N_H} + \theta^C_{N_O} = 1$ and $\theta^C_{N_O} = j'_{N_O,C}(j'_{N_H,A} - \theta^A_{N_H}\rho_{N_H} j_{E,A} + j'_{N_O,C})^{-1}$. The rejected fluxes of nitrate and carbohydrate reserves are $j_{E_{NO},R} = j_{E_{NO},C} - \theta^C_{N_O} y_{NE}\, j_{E,C_2}$ and $j_{E_C,R} = j_{E_C,C} - j_{E,C_2}$, from which fractions $\kappa_{E_{NO}}$ and κ_{E_C} are fed back to the reserves, the rest being excreted. The dynamics of the reserve densities m_{E_C} and $m_{E_{NO}}$ is given by (5.18). The specific rate of ammonium excretion amounts to $j_{N_H,E} = j_{E_{NH},R} + y_{NE}\, j_{E,M} + (n_{NE}\, y_{EV} - n_{NV}) j_{V,G}$. The middle term relates to maintenance, the third one to growth overheads.

When nitrogen is limiting, the assimilation of generalized reserves (5.27) reduces to $j_{E,A} = (j^{-1}_{E,Am} + (j'_{N_H,A} + j'_{N_O,A})^{-1})^{-1}$. The carbohydrate reserve no longer limits growth and $j_{E,C_2} = (j^{-1}_{E,Am} + (y_{EN}\,\rho_{N_H}(j_{N_H,A} - \theta^A_{N_H} y_{NE}\, j_{E,A}) + j'_{N_O,C})^{-1})^{-1} = (j^{-1}_{E,Am} + (j'_{N_H,A} - \theta^A_{N_H}\rho_{N_H} j_{E,A} + j'_{N_O,C})^{-1})^{-1}$.

The nitrogen in biomass can be decomposed into contributions from structural mass and the reserves, $n_{NW} = n_{NV} + n_{NE} m_E + m_{N_O}$. The specific nitrogen content is not constant during transient phases, but will become constant during the cell cycle in constant environments. This is an implication of the weak homeostasis assumption that is basic to the dynamics of reserves.

5.3 Several structural masses

The bill of the guillemot *Uria aalge* is just one example of non-isomorphic growth. Although of little energetical significance, the κ-rule provides the structure to describe such deviations.

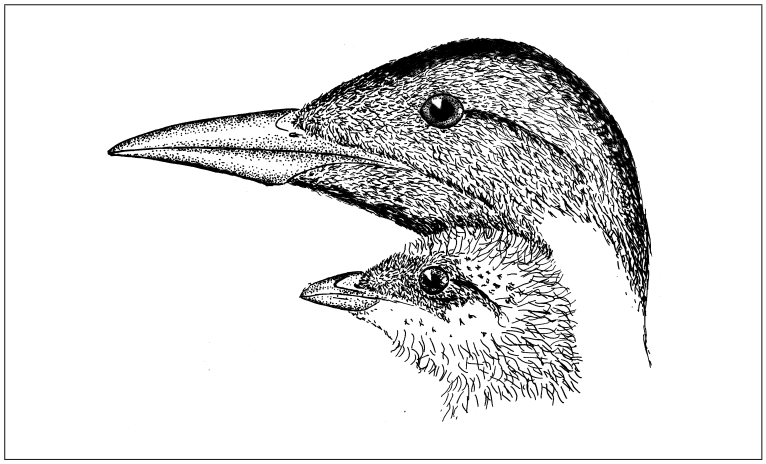

In the development of the DEB theory, only somatic and reproductive tissue have been distinguished for the sake of simplicity. The assumption of isomorphy covers other tissues as fixed fractions of the somatic tissue, conceived as a lumped sum. The elaboration below makes it clear that the mechanism behind the κ-rule implies a particular type of growth regulation. It also reveals the intimate connection between the κ-rule, {87}, and allometric growth.

In a bit more detail, the κ-rule (3.12) can be rephrased as

$$\kappa \frac{V_i}{V_+} \dot{p}_C = [E_{Gi}] \frac{d}{dt} V_i + [\dot{p}_{Mi}] V_i \tag{5.28}$$

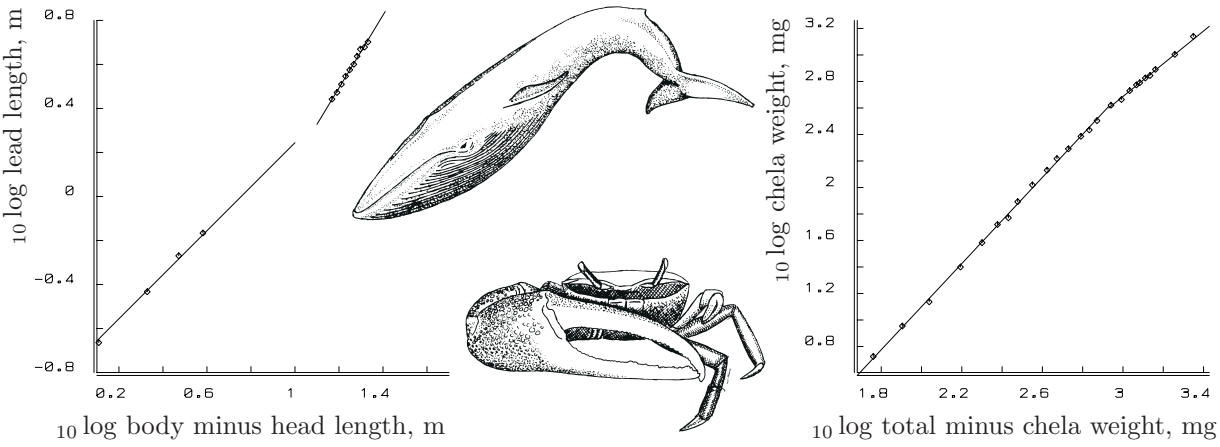

Figure 5.7: Examples of allometric growth: $\log y = a + b \log x$. Left: The head length (from the tip of the nose to the blow hole), with respect to total body length minus the head length in the male blue whale, *Balaenoptera musculus*. The first four data points are from foetuses, where growth is isomorphic ($b = 1$). Thereafter the head extends more rapidly ($b = 1.65$). Right: The weight of the large chela with respect to that of the rest of the body in the male fiddler crab *Uca pugnax*. Initially the chela grows rapidly ($b = 1.63$) until a rest of body weight of 850 mg, thereafter it slows down a little ($b = 1.23$). Data from Huxley [438].

where V_i denotes the volume of tissue (or organ or part of body) i, and $V_+ \equiv \sum_{i=1}^{k} V_i$ is the total body volume. Since blood flow is space-filling, the fraction V_i/V_+ stands for the relative length of the track followed by blood as it flows through tissue i. The basic DEB model delineates only somatic and reproductive tissue, so $k = 2$. Isomorphism implies that V_i/V_+ remains fixed, so $\kappa = \kappa_1 V_1/V_+$ has been taken, while $\frac{d}{dt}V_1 = \frac{d}{dt}V_2$. The extra uptake by reproductive tissue did not result in enhanced growth of the reproductive tissue, but in production that is lost to the body. If isomorphism is dropped as a condition and if more types of tissue are to be distinguished, (5.28) can be written as $[E_{Gi}]\frac{d}{dt}V_i = \frac{\kappa}{V_+}\dot{p}_C(1 - \frac{[\dot{p}_{Mi}]V_+}{\kappa \dot{p}_C})V_i$. Allometric growth of tissue i with respect to tissue j results, that is $\frac{dV_i}{dV_j} = \frac{[E_{Gj}]}{[E_{Gi}]}\frac{V_i}{V_j}$, if $\frac{[\dot{p}_{Mi}]V_+}{\kappa \dot{p}_C}$ is small.

Allometric growth of a body part occurs if the contribution of part i to total body volume is insignificant, because $V_+ \neq \sum_i \alpha_i V^{\beta_i}$ if $\beta_i \neq 1$ for some i, whatever the values of positive α_i's. Absolute growth requires specification of how feeding and digestion (and heating for endotherms) depend on the volume and shape of the different tissues. It is likely to become complex. Allometric growth of extremities and skeletal elements frequently occurs, as illustrated in Figure 5.7. Houck *et al.* [430] used this growth as a criterion to delineate taxa in fossil bird *Archaeopteryx*.

It is improbable, however, that whole-organism energetics is seriously affected by these relative changes. This subsection only serves to illustrate that the mechanism behind allometric growth (of appendages) is intimately connected to the κ-rule. Note that the dimensional problems that are usually connected to allometric relationships, {13}, do not apply in this implementation of allometric growth.

Isomorphs thus require growth regulation over the different body parts. Without con-

trol, allometric growth results. For isomorphs $[V_i] \equiv V_i/V_+$ must remain fixed, so that $\frac{d}{dt}V_i = [V_i]\frac{d}{dt}V_+$ must hold. For the DEB model this implies that the organism must accelerate or retard the growth of organ/tissue/part i by a factor $[V_i]\,\frac{dV_+}{dV_i} \simeq g_i \sum_j [V_j]/g_j$, with $g_i \equiv \frac{[E_{Gi}]}{\kappa_i [E_m]}$. (The approximation holds for $\dot{p}_{Mi} << \kappa_i \dot{p}_C$.) The mechanism of control may be via the density of carriers that transfer resources from the blood to the tissue. The carrier density in membranes of large tissues/parts should be less than that in small tissues/parts for a particular value.

The acceleration/retardation factor demonstrates that the carrier density does not have to change during growth. Other types of growth regulation are also possible. This discussion is only about the effects of regulation, rather than about its mechanism.

5.3.1 Organ size and function

An intriguing set of problems relates to the function–size coupling of organs. Kidneys, for instance, remove nitrogenous waste from the body, and the DEB theory predicts how the nitrogen excretion rate should depend on body size. Two lines of thought seem promising. Assuming that the relative kidney size remains constant (structural homeostasis), how should kidney function depend on kidney size such that the amount of work per unit of kidney remains constant? Can anatomical details explain this relationship? The other line of thought is to relate kidney function to kidney size from its anatomical design, and work out a regulation scheme for the kidney size such that the amount of work per unit of kidney remains constant during ontogeny. From a more abstract point of view, this type of problem has much in common with the material discussed in the section on syntrophy, {304}, where the body acts as a donor of nitrogenous waste, and the kidney as receiver.

5.3.2 Roots and shoots

The delineation of (at least) two types of structural mass is essential if we are to understand the development and growth of plants that use roots for the uptake (and excretion) of nutrients, and shoots for light uptake, gas exchange (carbon dioxide and oxygen), the evaporation of water (necessary for nutrient uptake by the roots) and reproduction. Bijlsma [85] makes a distinction between primary and secondary structures for both roots and shoots. The argument for such a refinement is to incorporate mechanical arguments to model stiffness versus transport. A simpler alternative is to use a single state variable and change stiffness via products (cellulose, lignin) that accumulate in the plant. Environmental factors can affect this production. Plants seem to follow the obvious strategy of investing relatively more in roots when water or nitrogen is limiting, and in shoots if light is limiting [126].

The interactions between the roots and shoots of plants seem to be a mixture between a two-structure organism and a symbiosis, which gives them a substantial relative flexibility in growth. Table 5.1 presents a summary of the fluxes, Figure 5.8 gives a diagram of fluxes, while Table 5.2 specifies the fluxes, as follows from the DEB theory in its simplest form. Figure 5.9 gives an example of a plant growth curve for a single choice of parameter values,

Table 5.1: The chemical compounds of the plant and their transformations and indices. The + sign means appearance, the − sign disappearance. The signs of the mineral fluxes depend on the chemical indices and parameter values. The labels on rows and columns serve as indices to denote mass fluxes and powers. The table shows the flux matrix $\dot{\boldsymbol{J}}^T$, rather than $\dot{\boldsymbol{J}}$, if the signs are replaced by quantitative expressions presented in Table 5.2.

	compounds →		minerals						shoot						root					
	↓ transformations		light	carbon dioxide	water	oxygen	ammonia	nitrate	product	structure	carbon reserve	nitrogen reserve	reserves		product	structure	carbon reserve	nitrogen reserve	reserves	
			L	C	H	O	N_H	N_O	PS	VS	E_CS	E_NS	ES		PR	VR	E_CR	E_NR	ER	
shoot	assimilation	AS	−	−	−	+					+	+	+					−		
shoot	growth	GS		+	+	−	+	+	+	+	−	−	−							
shoot	dissipation	DS		+	+	−	+	+	+		−	−	−							
shoot	reproduction	R		+	+	−	+	+			−	−	−							
	translocation	T		+	+	−	+	+			−	−	±				−	−	∓	
root	assimilation	AR		+	±	−	−	−			−						+	+	+		
root	growth	GR		+	+	−	+	+							+	+	−	−	−		
root	dissipation	DR		+	+	−	+	+							+		−	−	−		

and illustrates the effect of light restriction. Many extensions of the model are conceivable, such as limitations by other nutrients.

The proposed model has eight state variables (structure, and three reserves for root and shoot). We need generalized reserves to accomodate all micro-nutrients that are required to generate structure, and carbon and nitrogen reserves to allow nitrogen uptake during darkness. The carbon and nitrogen reserves do not necessarily consist of pure carbohydrates and nitrates, respectively; they can be thought of as generalized reserves that are enriched in these compounds. Limitation by micro-nutrients is not discussed here, so they are assumed to be non-limiting.

All reserves are initially zero except the root's generalized reserve M_{ER}, which represents the initial mass of the seed. Due to the translocation mechanism, the generalized root reserve soon partitions itself across those of shoots and roots, at a rate that depends on the values $\dot{k}_{ES}$ and $\dot{k}_{ER}$. The initial structural masses of roots and shoots are infinitesimally small, just like those of animal embryos. Flowering plants first develop one or two cotyledons, leaf-like structures that differ morphologically from normal leaves, and are usually rather thick, because of the relatively high shoot's generalized reserves, M_{ES}. When the shoot develops further, these reserves are reorganized over stem and leaves.

The generalized reserves are actively translocated between roots and shoots, as proposed by Bijlsma [85]. The translocation from one reserve to another is discussed in the section on foetal development {104}. If the reserve turnover rates $\mathcal{A}_*\dot{k}_{E*}$ are identical, and the translocation fast, the κ-rule emerges, as has been discussed in the previous section. Generally, however, these turnover rates differ because they involve surface area/volume relationships, and so the shape correction function, as discussed on {252}. The nitrogen

Table 5.2: The fluxes in and between the shoot S and the root R of a plant that experiences the forcing variables: light $\dot{J}_{L,F}$ and concentrations of carbon dioxide X_C and oxygen X_O (in the air), ammonia X_{N_H}, nitrate X_{N_O} and water X_H (in the soil). The dimensionless quantities $\mathcal{A}_S = (V_S/V_{dS})^{-1/3}\mathcal{M}_S(V_S) = (V_S/V_{dS})^{-V_S/V_{mS}}$ and $\mathcal{A}_R = (V_R/V_{dR})^{-1/3}\mathcal{M}_R(V_R) = (V_R/V_{dR})^{-V_R/V_{mR}}$ are introduced to simplify the notation, where V_{d*} are reference volumes that occur in the surface area/volume relationship, and $\mathcal{M}$ is the shape correction function, and V_{m*} parameters, see {252}. The relations $1 = \kappa_{SS} + \kappa_{RS} + \kappa_{TS}$ and $1 = \kappa_{SR} + \kappa_{TR}$ hold (the first index refers to soma, reproduction and translocation as destinations of catabolic fluxes). The fluxes $\dot{J}'_{*1,*2}$ are gross fluxes, i.e. help fluxes for specifying the net fluxes $\dot{J}_{*1,*2}$. Flux indices RS and RR refer to rejection, C_1S and C_1R to catabolism of reserves $E*$, C_2S and C_2R to catabolism of reserves E_N* plus E_C*; the other indices are listed in Table 5.1.

$\dot{J}_{E_CS,AS} = \dot{J}'_{E_CS,AS} - y^{N_O}_{C_H,ES}\dot{J}_{ES,AS}$; $\dot{J}'_{E_CS,AS} = \frac{(j'_C - j'_O)M_{VS}\mathcal{A}_S}{1+\frac{j'_C}{k_C}+\frac{j'_O}{k_O}+\frac{j'_C+j'_O}{j'_L}-\frac{j'_C+j'_O}{j'_L+j'_C+j'_O}}$

$\dot{J}_{E_NS,AS} = \dot{J}'_{E_NS,AS} - y_{E_NS,ES}\dot{J}_{ES,AS}$; $j'_L = \frac{j_{L,Am}}{1+\dot{J}_{L,AK}/\dot{J}_{L,F}}$; $j'_C = \frac{j_{C,Am}}{1+X_{KC}/X_C}$; $j'_O = \frac{j_{O,Am}}{1+X_{KO}/X_O}$

$\dot{J}_{ES,AS} = \left((y_{ES,E_NS}\dot{J}'_{E_NS,AS})^{-1} + (y^{N_O}_{ES,C_H}\dot{J}'_{E_CS,AS})^{-1} - (y_{ES,E_NS}\dot{J}'_{E_NS,AS} + y^{N_O}_{ES,C_H}\dot{J}'_{E_CS,AS})^{-1}\right)^{-1}$

$\dot{J}'_{E_NS,AS} = -y_{E_NS,E_NR}\dot{J}_{E_NR,AS}$; $\dot{J}_{E_NR,AS} = -(1-\kappa_{E_NR})\dot{J}_{E_NR,RR}$

$\dot{J}_{VS,GS} = y_{VS,ES}\left(\kappa_{SS}\dot{J}_{ES,CS} + \dot{J}_{ES,MS}\right) \equiv \dot{r}_S M_{VS}$; $\dot{J}_{ES,C_1S} = (\mathcal{A}_S\dot{k}_{ES} - \dot{r}_S)M_{ES}$

$\dot{J}_{ES,CS} = \dot{J}_{ES,C_1S} + \dot{J}_{ES,C_2S}$; $\dot{J}'_{E_CS,CS} = (\mathcal{A}_S\dot{k}_{E_CS} - \dot{r}_S)M_{E_CS}$; $\dot{J}'_{E_NS,CS} = (\mathcal{A}_S\dot{k}_{E_NS} - \dot{r}_S)M_{E_NS}$

$\dot{J}_{ES,C_2S} = \left((y_{ES,E_NS}\dot{J}'_{E_NS,CS})^{-1} + (y^{N_O}_{ES,C_H}\dot{J}'_{E_CS,CS})^{-1} - (y_{ES,E_NS}\dot{J}'_{E_NS,CS} + y^{N_O}_{ES,C_H}\dot{J}'_{E_CS,CS})^{-1}\right)^{-1}$

$\dot{J}_{ES,GS} = -y_{ES,VS}\dot{J}_{VS,GS}\theta_{ES}$; $\dot{J}_{E_CS,GS} = y^{N_O}_{C_H,ES}\dot{J}_{ES,GS}(\theta^{-1}_{ES} - 1)$; $\dot{J}_{E_NS,GS} = y_{E_NS,ES}\dot{J}_{ES,GS}(\theta^{-1}_{ES} - 1)$

$\dot{J}_{E_CS,RS} = \dot{J}'_{E_CS,CS} - y^{N_O}_{C_H,ES}\dot{J}_{ES,C_2S}$; $\dot{J}_{E_NS,RS} = \dot{J}'_{E_NS,CS} - y_{E_NS,ES}\dot{J}_{ES,C_2S}$

$\dot{J}_{ES,MS} = -j_{ES,MS}M_{VS}$; $\dot{J}_{ES,JS} = -j_{ES,JS}\min\{M_{VS}, M_{V_pS}\}$; $\theta_{ES} = \dot{J}_{ES,C_1S}\dot{J}^{-1}_{ES,CS}$

$\dot{J}_{E_CS,DS} = y^{N_O}_{C_H,ES}\dot{J}_{ES,DS}(\theta^{-1}_{ES} - 1)$; $\dot{J}_{E_NS,DS} = y_{E_NS,ES}\dot{J}_{ES,DS}(\theta^{-1}_{ES} - 1) - (1-\kappa_{E_NS})\dot{J}_{E_NS,RS}$

$\dot{J}_{ES,DS} = \theta_{ES}(\dot{J}_{ES,MS} + \dot{J}_{ES,JS})$; $\dot{J}_{ES,R} = -\theta_{ES}(\kappa_{RS}\dot{J}_{ES,CS} + \dot{J}_{ES,JS})$

$\dot{J}_{E_CS,R} = y^{N_O}_{C_H,ES}\dot{J}_{ES,R}(\theta^{-1}_{ES} - 1)$; $\dot{J}_{E_NS,R} = y_{E_NS,ES}\dot{J}_{ES,R}(\theta^{-1}_{ES} - 1)$

$\dot{J}_{E_CS,T} = -\kappa_{TS}y^{N_O}_{C_H,ES}\dot{J}_{ES,C_2S}$; $\dot{J}_{E_NS,T} = -\kappa_{TS}y_{E_NS,ES}\dot{J}_{ES,C_2S}$

$\dot{J}_{ES,T} = -\kappa_{TS}\dot{J}_{ES,C_1S} + y_{ES,ER}\kappa_{TR}\dot{J}_{ER,CR}$; $\dot{J}_{ER,T} = -\kappa_{TR}\dot{J}_{ER,C_1R} + y'_{ER,ES}\kappa_{TS}\dot{J}_{ES,CS}$

$\dot{J}_{E_CR,T} = -\kappa_{TR}y^{N_O}_{C_H,ER}\dot{J}_{ER,C_2R}$; $\dot{J}_{E_NR,T} = -\kappa_{TR}y_{E_NR,ER}\dot{J}_{ER,C_2R}$

$\dot{J}'_{N_H,AR} = \frac{M_{VR}\mathcal{A}_R j_{N_H,Am}}{1+X_{KN_H}/X_{N_H}}$; $\dot{J}_{N_O,AR} = \frac{M_{VR}\mathcal{A}_R j_{N_O,Am}}{1+X_{KN_O}/X_{N_O}}$; $X_{KN_H} = \frac{X'_{KN_H}}{1+\frac{X_H}{X_{KH}}\frac{\mathcal{A}_S}{\mathcal{A}_R}}$; $X_{KN_O} = \frac{X'_{KN_O}}{1+\frac{X_H}{X_{KH}}\frac{\mathcal{A}_S}{\mathcal{A}_R}}$

$\dot{J}_{E_CR,AR} = \dot{J}'_{E_CR,AR} - y_{C_H,ER}\dot{J}_{ER,AR}$; $\dot{J}'_{E_CR,AR} = (1-\kappa_{E_CS})y_{E_CR,E_CS}\dot{J}_{E_CS,RS}$

$\dot{J}_{E_NR,AR} = n^{-1}_{N,E_NR}(\dot{J}_{N_O,AR} - n_{N,ER}\theta_{N_O}\dot{J}_{ER,AR})$; $\dot{J}_{N,AR} = \dot{J}'_{N_H,AR} + \rho_{N_O}\dot{J}_{N_O,AR}$

$\dot{J}_{ER,AR} = \left(n_{N,ER}\dot{J}^{-1}_{N,AR} + (y_{ER,C_H}\dot{J}'_{E_CR,AR})^{-1} - (n^{-1}_{N,ER}\dot{J}_{N,AR} + y_{ER,C_H}\dot{J}'_{E_CR,AR})^{-1}\right)^{-1}$

$y_{ER,C_H} = \theta_{N_H}y^{N_H}_{ER,C_H} + \theta_{N_O}y^{N_O}_{ER,C_H}$; $\theta_{N_H} = 1 - \theta_{N_O} = J'_{N_H,AR}(J'_{N_H,AR} + \rho_{N_O}J_{N_O,AR})^{-1}$

$\dot{J}_{VR,GR} = y_{VR,ER}\left(\kappa_{SR}\dot{J}_{ER,CR} + \dot{J}_{ER,MR}\right) \equiv \dot{r}_R M_{VR}$; $\dot{J}_{ER,C_1R} = (\mathcal{A}_R\dot{k}_{ER} - \dot{r}_R)M_{ER}$

$\dot{J}_{ER,CR} = \dot{J}_{ER,C_1R} + \dot{J}_{ER,C_2R}$; $\dot{J}'_{E_CR,CR} = (\mathcal{A}_R\dot{k}_{E_CR} - \dot{r}_R)M_{E_CR}$; $\dot{J}'_{E_NR,CR} = (\mathcal{A}_R\dot{k}_{E_NR} - \dot{r}_R)M_{E_NR}$

$\dot{J}_{ER,C_2R} = \left((y_{ER,E_NR}\dot{J}'_{E_NR,CR})^{-1} + (y^{N_O}_{ER,C_H}\dot{J}'_{E_CR,CR})^{-1} - (y_{ER,E_NR}\dot{J}'_{E_NR,CR} + y^{N_O}_{ER,C_H}\dot{J}'_{E_CR,CR})^{-1}\right)^{-1}$

$\dot{J}_{ER,GR} = -y_{ER,VR}\dot{J}_{VR,GR}\theta_{ER}$; $\dot{J}_{E_CR,GR} = y^{N_O}_{C_H,ER}\dot{J}_{ER,GR}(\theta^{-1}_{ER} - 1)$; $\dot{J}_{E_NR,GR} = y_{E_NR,ER}\dot{J}_{ER,GR}(\theta^{-1}_{ER} - 1)$

$\dot{J}_{E_CR,RR} = \dot{J}'_{E_CR,CR} - y^{N_O}_{C_H,ER}\dot{J}_{ER,C_2R}$; $\dot{J}_{E_NR,RR} = \dot{J}'_{E_NR,CR} - y_{E_NR,ER}\dot{J}_{ER,C_2R}$

$\dot{J}_{E_CR,DR} = y^{N_O}_{C_H,ER}(1-\theta_{ER})\dot{J}_{ER,MR} - (1-\kappa_{E_CR})\dot{J}_{E_CR,RR}$; $\dot{J}_{E_NR,DR} = y_{E_NR,ER}(1-\theta_{ER})\dot{J}_{ER,MR}$

$\dot{J}_{ER,MR} = -j_{ER,MR}M_{VR}$; $\dot{J}_{ER,DR} = \theta_{ER}\dot{J}_{ER,MR}$; $\theta_{ER} = \dot{J}_{ER,C_1R}\dot{J}^{-1}_{ER,CR}$

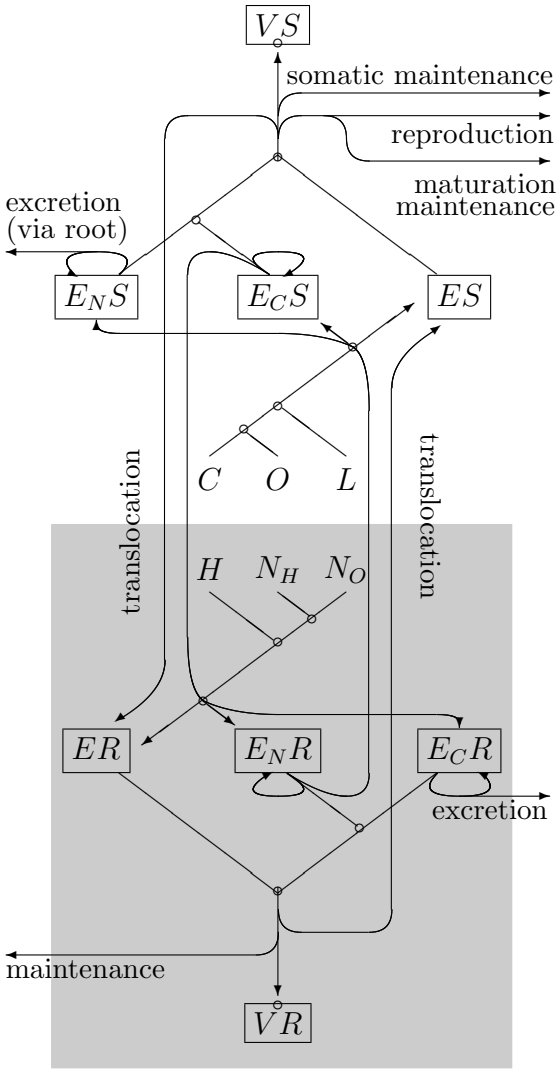

Figure 5.8: The diagram of a DEB model for the interactions between the root and the shoot of a plant. A seed has initially only an amount of generalized root-reserve ER, all other reserves and the structural masses of the root, VR, and the shoot, VS, are negligibly small; Translocation fills the generalized reserves of the shoot, ES, during the embryonic stage. Assimilation of ammonia, N_H, nitrate, N_O, carbon dioxide C, and light, L, is switched on at birth. Water, H, interferes with the uptake of nutrients from the soil; oxygen, O, interferes with the assimilation of carbon dioxide. Besides generalized reserves, carbohydrate reserves, E_CR and E_CS, and nitrogen reserves E_NR and E_NS are filled (and used) during the juvenile and adult stages. A fixed fraction of the rejected carbohydrate and nitrogen reserves are translocated, and enters via the assimilation systems. The root remains in the juvenile stage; the allocation to maturity maintenance can be combined with that to somatic maintenance, and the allocation to maturation can be combined with that to growth. The shoot generally enters the adult stage, and requires explicit treatment of these fluxes. Maturation converts to reproduction at puberty. Circles indicate SUs.

(nitrate) and carbon (carbohydrate) reserves are used independently by roots and shoots; only the 'spoils' are translocated, in a way similar to symbiontic partners, cf. {306}. The translocated fluxes partake in the assimilation of the receiver.

The synthesis of generalized reserves, as a chemical compound, occurs twice in the root and in the shoot, as described on {175}:

- The assimilation process (AS and AR). In the root, ammonia and nitrate are taken up from the soil, and carbohydrate is received from the shoot. In the shoot, nitrate is received from the root, and carbohydrate is photosynthesized. The resulting compound is stored in the reserves ER and ES, respectively. The nitrogen and carbon that cannot be transformed into generalized reserves are stored in the specialized reserves.

- The catabolic processes (C_2S and C_2R). Nitrate and carbohydrate are mobilized from the reserves; the resulting flux is merged with the mobilised generalized reserves and used for development and/or reproduction, and growth plus somatic maintenance. A fixed fraction of the nitrate and carbohydrate that is rejected by the Synthesizing

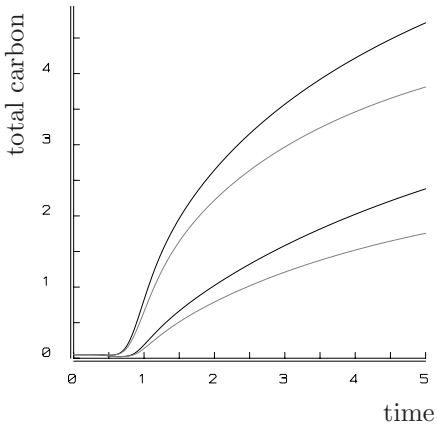

Figure 5.9: Examples of plant growth curves that result from the DEB model. The lower curves refer to root carbon, the upper ones to total plant carbon (root plus shoot). The grey curves refer to light restriction, and show that this affects the root more than the shoot. This realistic trait naturally results from the mechanism of exchange of carbohydrates and nitrogen; no optimization argument is involved. The model has a rich repertoire of growth curves, of root/shoot mass ratio ontogeny's, and of responses to changes in environmental factors, depending on parameter values.

Units that produces generalized reserves is fed back to the reserves, the remaining fraction is translocated.

The binding probability ρ_{N_O} regulates the priority of ammonia relative to nitrate in the assimilation of reserves, as is discussed on {175}. The assimilated nitrate that is not used in this pathway is stored, but ammonia that is not used is excreted ($\rho_{N_H} = 1$ is taken here). The costs of synthesis of reserves ER from ammonia or nitrate are accommodated in the conversion coefficients $y^{N_O}_{C_H,E}$ and $y^{N_H}_{C_H,E}$; nitrate has to be reduced prior to this synthesis, and the costs are covered by the oxidation of carbohydrates, which gives $y^{N_O}_{C_H,E} > y^{N_H}_{C_H,E}$.

The balance equations for the catabolic processes are

$$\dot{J}'_{E_CS,CS} - \kappa_{E_CS}\dot{J}_{E_CS,RS} = (1-\kappa_{E_CS})\dot{J}_{E_CS,RS} + \dot{J}_{E_CS,T} + \dot{J}_{E_CS,GS} + \dot{J}_{E_CS,DS} + \dot{J}_{E_CS,R}$$
$$\dot{J}'_{E_NS,CS} - \kappa_{E_NS}\dot{J}_{E_NS,RS} = \dot{J}_{E_NS,T} + \dot{J}_{E_NS,GS} + \dot{J}_{E_NS,DS} + \dot{J}_{E_NS,R}$$
$$\dot{J}_{ES,C_1S} = \dot{J}_{ES,T} + \dot{J}_{ES,GS} + \dot{J}_{ES,DS} + \dot{J}_{ES,R}; \quad \dot{J}_{ER,C_1R} = \dot{J}_{ER,T} + \dot{J}_{ER,GR} + \dot{J}_{ER,DR}$$
$$\dot{J}'_{E_NR,CR} - \kappa_{E_NR}\dot{J}_{E_NR,RR} = (1-\kappa_{E_NR})\dot{J}_{E_NR,RR} + \dot{J}_{E_NR,T} + \dot{J}_{E_NR,GR} + \dot{J}_{E_NR,DR}$$
$$\dot{J}'_{E_CR,CR} - \kappa_{E_CR}\dot{J}_{E_CR,RR} = \dot{J}_{E_CR,T} + \dot{J}_{E_CR,GR} + \dot{J}_{E_CR,DR}$$

where all fluxes are here taken to be positive. The left-hand sides specify what is leaking away from the reserves, and the right-hand sides specify the various destinations. The fluxes RS and RR on the left-hand sides specify the return fluxes of what can not be used by the SUs. The 'spoil' fluxes RS and RR on the right hand sides appear in the assimilation fluxes of the partner (root and shoot, respectively).

Assimilation in Table 5.2 should be set to zero for embryos. The root remains in the juvenile stage, the shoot is adult if $M_{VS} > M_{V_pS}$. The fluxes to reproduction (or maturation in embryos and juveniles) as specified in Table 5.2 represent outgoing fluxes from the reserves and includes overheads; a fraction κ_R of this flux is fixed in seeds, and the flux should be divided by the initial root reserve to arrive at a reproduction rate in terms of seeds per time.

If a plant lives for many years, and the resolution of the growth process is limited, the yearly shedding of leaves can be accommodated (approximately) in the constant specific maintenance costs $j_{ES,MS}$. For short-living species, this will be less satisfactory and the maintenance costs should show a cyclical pattern explicitly. Aging in plants does not follow the pattern of animals, because plants can replace cells that are hit by the aging process.

The formulation in Table 5.2 does not account for water reserves. Water controls the saturation constant of the nitrogen uptake from the soil, see {152}. Photosynthesis and photorespiration are discussed on {164}ff. Wood production can be associated with growth and maintenance.

The weight of a plant has contributions from the structure, and all reserves, but also from the accumulation products, which can have supporting functions for the structures. Their production is associated with somatic maintenance, and continues even when growth of the structure ceases. In that case, weights do not have an asymptote. Chlorophyll is part of the structure and the generalized reserves of the shoot. The prime in the conversion coefficient $y'_{ER,ES}$ from root to shoot reserves indicates that $y'_{ER,AS} \neq y'_{ES,AR}$; root reserves have no chlorophyll and other differences in composition exist as well.

5.4 Summary

The DEB model can be extended in a straightforward way to deal with several substrates (nutrients), reserves and structural masses, using the rules for the behaviour of Synthesizing Units (SUs) on the basis of the following supplementary assumptions

1 Each reserve has an assimilation SU, and each structural mass a growth SU for their synthesis from substrates.

2 A fixed part of any catabolic flux that is rejected by a growth SU adds to the originating reserve, the rest is excreted.

3 Each structural mass requires a fixed mass-specific maintenance. The maintenance requirements, therefore, have a fixed stoichiometry; each catabolic flux contributes to maintenance, but the costs are reserve-specific.

4 A single reserve can fuel the synthesis of several structural masses by partitioning the catabolic flux; a straightforward generalization of the κ-rule.

The resulting dynamics allows a rich repertoire, because of the flexible behaviour of SUs. Two routes exist for the convergence to a single-substrate, single-reserve DEB model: a single substrate and reserve is limiting growth, or the abundances of the various substrates covary and all rejected catabolic fluxes are excreted. The transition of limiting to (almost) non-limiting behaviour of substrate and/or reserve is rather sharp, as results from the rules for the behaviour of SUs.

The limiting reserve *in*creases with the growth rate, but the non-limiting reserves can *de*crease with the growth rate as a consequence of the damming, which depends on the fraction of reserves that is excreted.

Photosynthesis is quantified as a two-step process: from light, water and carbon dioxide to carbohydrate and from carbohydrate and nitrogen compounds to (generalized) reserves. The rejected carbohydrates and nitrogen compounds are stored separately. Photorespiration follows naturally from competitive binding of carbon dioxide and oxygen to Rubisco.

Calcification is described, where carbon dioxide and bicarbonate are sequentially processed, substitutable substrates for photosynthesis, and calcification is stoichiometrically coupled with bicarbonate uptake.

The interaction between ammonia and nitrogen has been worked out, because of its ecological importance. The nitrogen compounds are treated as substitutable substrates in the synthesis of generalized reserves. The latter compound is synthesized from ammonia, nitrate and carbohydrate reserves prior to storage from assimilates, and prior to growth from catabolic fluxes. The ammonia reserves have an extremely low capacity.

The production and use of oxygen is shown to have a rather indirect relationship with photosynthesis, although it is widely used as a quantifier.

The growth of body parts can be very close to the widely applied allometric growth on the basis of the multivariate extension of the κ-rule.

A model for plant growth is proposed, which represents a mixture between a bivariate structured individual and a symbiosis between root and shoot; the generalized reserves are actively translocated, while each has its own nitrogen and carbohydrate reserve, where the partner receives the 'spoils', as in a symbiontic relationship.

Chapter 6

Uptake and effects of non-essential compounds

Non-essential compounds differ from essential ones by the absence of regulated use. The first purpose of this chapter is to show how energetics interferes with many aspects of the uptake and effects of non-essential compounds and how the DEB theory can be used to specify these processes in a quantitative way. It provides the methodology to translate effects on individual performance to effects on populations and ecosystems. After a brief introduction of biological aspects, this chapter starts with a one-compartment model, in which the physiological change of the organism is first neglected. The kinetics is then made more realistic by incorporating physiological interactions as specified by the DEB model. Then follows a discussion of the inverse relationship, i.e how toxins affect the energetics of individuals and the consequences for the population.

The need to characterize the effects of compounds and extrapolate them to the population and ecosystem level originates from the huge problems that humans are creating in their environment at the moment. It is relatively easy to determine effects on individuals in the laboratory, whereas the real problems are at the ecosystem level. This calls for models to link them. The purposes are to analyse how bad a particular pollution event or situation is, to set priorities for cleaning up the mess and to set norm values for the maximum emission of compounds into the environment for industry and transport. We can only be extremely modest in our claims to understand long-term effects at the ecosystem level.

Bio-toxins

The study of effects of chemical compounds is relevant not only to the assessment of environmental risk, but also to fundamental ecology and evolution. The appearance of oxygen as a *by-product* of photosynthesis in the atmosphere has probably been fatal for most pre-Cambrian organisms. Botulin, one of the most potent toxins known, is produced by the bacterium *Clostridium botulinum* and causes frequent casualties among fish and birds in fresh waters. The soil bacterium *Bacillus thuringiensis* produces a toxin that kills insects effectively [425]. The bacterium *Vibrio alginolyticus* excretes tetrodotoxin,

which is a potent toxin that several unrelated organisms use for various purposes. The dinoflagellate *Pfiesteria piscicida* excretes toxins that kill significant numbers of fish in the coastal areas of the West Atlantic.

Some bacteria quickly transform sugar into acetate for later consumption, while acetate suppresses the growth of competitors. *Sphagna*, a class of mosses that dominate in peat land, suppress other plant growth by lowering the pH [187]. Natural growth-suppressing compounds that are produced by fungi, such as penicillin, are intensively applied in medicine.

The production of cyanides, alkaloids and other *secondary metabolic products* by plants obviously functions to deter herbivores. This is not always fully successful, and herbivores sometimes use these toxins to deter predators. Heliconid caterpillars accumulate toxins from passion flowers, and advertise this with bright warning colours. The protection from predation is sometimes so effective that similar species, that cannot handle the toxins metabolically, mimic the colour pattern to acquire the same protection. This is Batesian mimicry, well known in the case of the monarch butterfly *Danaus plexippus* (which accumulates toxins from euphorbids); its colours are adopted by the viceroy *Limenitus archippus* [938]. The male rattlebox moth *Utetheisa ornatrix* has another striking use of toxins; he supplies his mate with plant-derived pyrrolizidine alkaloids, together with his sperm, which will protect her against predation for several hours.

The reason why the Australian brushtail possum *Trichosurus vulpecula* turned into a pest in New Zealand, but not in Australia, is probably because it does not feed on *Eucalyptus* leaves there, but on trees that lack the cyanides that restrict its reproduction in Australia. The tannins of acorns effectively block digestion by the European red squirrel *Sciurus vulgaris*, for instance, but the American grey squirrel *Neosciurus carolinensis* found a way to deal with this defence of the oak and so managed to outcompete the red squirrel in parts of Europe [576].

Like plants, many species of animal use toxins to *protect* themselves against predation; most nudibranchs (snails of the subclass *Opistochranchia*) accumulate nematocysts from their cnidarian prey for protection, while their prey use these formic acid harpoons to collect food; termites [734], arrow frogs (*Dendrobatidae*), and some birds (the hooded pitohui, *Pitohui dichrous* [256]) produce and accumulate chemicals to protect themselves against predators. The tetraodontid fish *Fugu vermicularis* and the starfish *Astropecten polyacanthus* use tetrodotoxin for this purpose [922]. Cephalopods excrete a mixture of ink and toxins to confuse and paralyse an approaching predator; *Peripatus* emits some glue when offended.

Examples of chemical offence are easy to find. Snakes, wasps, spiders, centipedes, cone shells and many other organisms use venoms to *kill* offensively. Tetrodotoxin is used by chaetognats and the blue ringed octopus *Hapalochlaena maculata* to capture prey via sodium channel blocking. Mosquitos and leeches use chemicals to prevent blood from coagulating.

The ability of the parasitic bacterium *Wolbachia* to *induce* parthenogenesis in normally sexually reproducing species (doubtlessly via chemical interference) has recently attracted a lot of attention [641]. The parasitic cirripede *Sacculina* converts a male crab *Carcinus* into a female, with all secondary sex characteristics, but the allocation to reproduction

is converted to the parasite. Many parasites use endocrine disrupters to interfere in the host's allocation of resources.

Biology is full of examples of chemical warfare with sometimes striking responses and defence systems [6]. This collection of random examples serves to illustrate the wide occurrence of chemicals that affect organisms; the function of their production being frequently rather obscure.

6.1 One-compartment kinetics

The simplest, and frequently realistic, model for toxicokinetics is the one-compartment uptake/elimination model [997] in a variable environment. This model forms the basis of most work that has been done in ecotoxicity and environmental risk assessment; see Thomann and Mueller [916] for a lucid introduction. One-compartment models do not always give a satisfactory fit with experimental data. For this reason more-compartment models have been proposed [188,330,446,802]; because of their larger number of parameters, the fit is better, but an acceptable physical identification of the compartments is usually not possible. These models, therefore, contribute little to our understanding of kinetics as a process. A more direct link with the physiological properties of the organism and with the lipophilicity of the compound seems an attractive alternative, which does not, however, exclude more-compartment models. As usual, the problem is not so much in the formulation of those complex models but in the useful application. Too many parameters can easily become a nuisance if few, scattered, data are available.

A chemical compound is usually present in the environment in several, and sometimes many, chemical species. Molecules of many compounds can dissociate into ions, which easily bind to ligands that are usually abundantly present, and can transform into other compounds. These species differ in their availability to the organism, which makes the subject of toxicokinetics in natural environments a rather complex one. The compound can enter the organism via different routes: directly from the environment across the skin, via specialized surfaces that play a role in gas exchange, via food, etc. In the aquatic environment uptake directly from water is especially important for hydrophilic organic compounds [129], and metals [102,103,772]. In aquatic animals that are chemically isolated from their environment, such as aquatic insects, birds and mammals, the common uptake route is via food. Walker [961] gives a discussion of uptake routes. The compound can leave the organism using the uptake routes in reverse direction, or via reproductive output and/or products (e.g. moults in arthropods, milk in mammals). Several taxon-specific mechanisms occur. Collembola, for instance, can accumulate metal in mid-gut epithelium and excrete this tissue periodically as part of the moult [729,730]. This epithelium contains granules, probably filled with calcium phosphate, which may be excreted into the gut lumen. These granules probably play a role in the excretion of an overload of lead in the food [457,894].

Avoiding disencouragement, we start simple and focus on the well-mixed aquatic environment where the compound is present in just one chemical species at a concentration $c_d(t)$. Suppose that inside the organism the compound is also present in just one chemical species, and that the exchange between the different body parts is fast. The compound can

be present in different concentrations in the different organs, but the ratio of the concentrations in different organs is fixed. In such a situation, it suffices to follow the kinetics via the mean concentration in the body, $[M_Q](t)$, which is defined as the ratio of the amount of the compound in the body to the body volume V.

Suppose that the concentration in the tissue follows a simple one-compartment process, i.e. uptake is proportional to environment concentration and elimination is proportional to tissue concentration. The uptake kinetics is the same as in the Lotka–Volterra model for the uptake of food, {314}, and can be considered as a linear approximation of the hyperbolic functional response for low concentrations. If growth is negligibly small

$$\frac{d}{dt}[M_Q] = \dot{k}_e(P_{Vd}c_d(t) - [M_Q]) \quad \text{or} \tag{6.1}$$

$$\frac{d}{dt}c_V = \dot{k}_e(c_d(t) - c_V) \tag{6.2}$$

where $\dot{k}_e$ is the elimination rate (dimension time^{-1}). The product $\dot{k}_e P_{Vd}$ is the uptake rate (dimension $\frac{\text{volume of environment}}{\text{volume of tissue} \cdot \text{time}}$). The product $\dot{k}_e[M_Q]V$ is interpreted as elimination flux (dimension mass time^{-1}) and the product $\dot{k}_e P_{Vd}c_d(t)V$ is the uptake flux (dimension mass time^{-1}). Index V refers to the structural body volume, and d to the dissolved fraction in the environment; both are preparations for more complex situations that are discussed later. P_{Vd} is the partition coefficient: the ultimate ratio of the concentrations in the tissue to that in the environment, also known as the bioconcentration coefficient. It is treated as a constant, which can be less than 1. The interpretation of this partition coefficient refers to the steady-state situation. A better definition for P_{Vd}, which I use here, is the ratio of the uptake to the elimination rate. Both definitions are equivalent for simple one-compartment models, but not for more elaborate ones. Although many texts treat the bioconcentration coefficient as a dimensionless one, it actually has dimension environmental volume$\times$(body volume)$^{-1}$ because the sum of both types of volume does not have a useful role to play. Most texts in fact use environmental volume$\times$(body dry weight)$^{-1}$, or for soils environmental dry weight$\times$(body dry weight)$^{-1}$.

The concentration $c_V \equiv [M_Q]P_{dV}$, with $P_{dV} = P_{Vd}^{-1}$ is proportional to the tissue concentration, but has the dimensions of an environment concentration. It has a very useful role in practical applications, because the tissue concentration frequently plays the role of a hidden variable, because it is not measured.

The explicit expression of $[M_Q](t)$ in terms of $c_d(t)$ is found from (6.1) to be

$$[M_Q](t) = [M_Q](0)\exp\{-t\dot{k}_e\} + \dot{k}_e P_{Vd}\int_0^t \exp\{-(t-t_1)\dot{k}_e\}c_d(t_1)\,dt_1 \tag{6.3}$$

If $c_d(t)$ is actually constant, (6.3) reduces to

$$[M_Q](t) = [M_Q](0)\exp\{-t\dot{k}_e\} + \left(1 - \exp\{-t\dot{k}_e\}\right)P_{Vd}c_d \quad \text{or} \tag{6.4}$$

$$c_V(t) = c_V(0)\exp\{-t\dot{k}_e\} + \left(1 - \exp\{-t\dot{k}_e\}\right)c_d \tag{6.5}$$

which is known as the accumulation curve.

6.2 Partition coefficient

The concept of one-compartment kinetics has many hidden implications. This section discusses how the partition coefficient, the ionization constant and the acidity affect the exchange parameters. This section can be skipped without loss of continuity.

The most obvious property of chemicals for the understanding of toxicokinetics is the n-octanol/water partition coefficient, P_{ow}, which can be estimated from the chemical structure of the compound. Octanol serves as a model for typical lipids of animals, although the model in not always perfect [842]. It has a density of 827 $\mathrm{g\,dm^{-3}}$, and a molecular weight of 130 Dalton, so that 1 $\mathrm{dm^3}$ of octanol contains 6.36 mol. Most comparisons are restricted to the interval $(10^2, 10^6)$ for the P_{ow}. The size of the molecule tends to increase with P_{ow} and, if the P_{ow} is larger than 10^6, the molecules are generally too big to enter cells easily [170].

6.2.1 Kinetics as a function of partition

The molecular details of the transport of a compound between two matrices, such octanol and water, directly lead to the relationship between the elimination rate and P_{ow}; the P_{ow} has information about the steady state, the elimination rate about the waiting time to reach that steady state. Let us focus on a closed system that evolves to a steady state.

Suppose that N molecules of a compound are distributed over two matrices, and that they can freely travel from one matrix to the other. Both matrices occupy a unit of volume. $N_0(t)$ molecules are present in matrix 0 and $N_1(t) = N - N_0(t)$ molecules in matrix 1 at time t. If first-order kinetics applies, and the total number of molecules $N = N_0(t) + N_1(t)$ is constant, the change of N_0 is given by

$$\frac{d}{dt}\begin{pmatrix} N_0 \\ N_1 \end{pmatrix} = \begin{pmatrix} -\dot{k}_{01} & \dot{k}_{10} \\ \dot{k}_{01} & -\dot{k}_{10} \end{pmatrix}\begin{pmatrix} N_0 \\ N_1 \end{pmatrix} \quad \text{or} \tag{6.6}$$

$$\frac{d}{dt}N_0 = \dot{k}_+(N_0^* - N_0) \tag{6.7}$$

with $\dot{k}_+ = \dot{k}_{01} + \dot{k}_{10}$ and the equilibrium value for N_0 is $N_0^* = N\dot{k}_{10}/\dot{k}_+$. An implicit assumption is that the compound is homogeneously distributed within each matrix.

Suppose now that the exchange rates are proportional to the ratio of the binding forces to the two matrices, i.e. $\dot{k}_{01} = \dot{k}\rho_1/\rho_0$ and $\dot{k}_{10} = \dot{k}\rho_0/\rho_1$, where ρ_i is the binding force of the compound to molecules of matrix i, $i \in \{0, 1\}$, and $\dot{k}$ is a proportionality constant that depends on the properties of the compound, but not on those of the matrix. Although phrased differently, the setting is identical to the concept of fugacity, the escaping tendency of a compound from a phase, that has been successfully used to describe the behaviour of compounds in the environment [580]; it has a simple thermodynamic interpretation [530].

The definition of the partition coefficient is $P_{01} = N_0^*/N_1^*$. Since $N_0^*/N_1^* = N_0^*/(N - N_0^*) = \dot{k}_{10}/\dot{k}_{01} = \rho_0^2/\rho_1^2$, we have that $\rho_0/\rho_1 = \sqrt{P_{01}}$. The result directly follows that $\dot{k}_{01} = \dot{k}\sqrt{P_{10}}$ and $\dot{k}_{10} = \dot{k}\sqrt{P_{01}} = \dot{k}/\sqrt{P_{10}}$.

The bioconcentration coefficient P_{Vd} for fish relates to the octanol/water partition coefficient as $P_{Vd} = 0.048\,P_{ow}$, [579]. Hawker and Connell [382] found the allometric

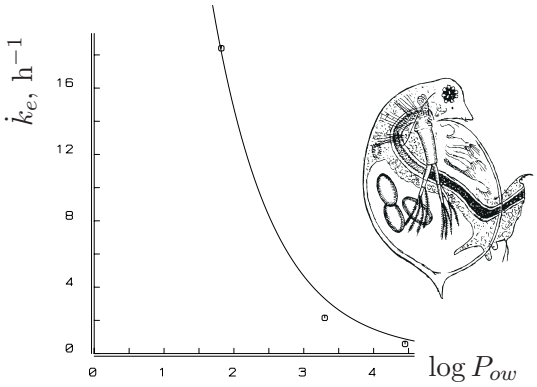

Figure 6.1: The elimination rate in *Daphnia pulex* is approximately proportional to $1/\sqrt{P_{ow}}$ for the compounds isoquinoline, acridine, and benz(a)acridine at 21 °C. Data from Southworth *et al.* [868].

relationships $P_{Vd} = 0.0484\, P_{ow}^{0.898}$ for daphnids and $P_{Vd} = 0.0582\, P_{ow}^{0.844}$ for molluscs in the range $10^2 \leq P_{ow} \leq 10^6$. The scatter in the data is big enough for the relationship $P_{Vd} = 0.02\, P_{ow}$ to apply to both daphnids and molluscs. The proportionality factor directly relates to the fat content. In general we can say that $P_{Vd} = m_o P_{ow}$, where m_o stands for the mass-specific octanol equivalent of the organism, which seems to be taxon-specific. High correlations between P_{Vd} and m_o have been found for fenitrothion in a variety of algae [475], for instance.

Hawker and Connell [381,382] related the elimination rate $\dot{k}_e$ to P_{ow} and found $\dot{k}_e = 8.851\, P_{ow}^{-0.663}$ d^{-1} for fish, $\dot{k}_e = 113\, P_{ow}^{-0.507}$ d^{-1} for *Daphnia pulex* and $\dot{k}_e = 9.616\, P_{ow}^{-0.540}$ d^{-1} for molluscs. The proportionality factor is inversely proportional to the volumetric length of the animal (see below), which explains the wide range of values. The results for daphnids are most reliable, because they all have the same body size in this case, and confirm the expectation $\dot{k}_e \propto P_{ow}^{-1/2}$, which is based on first-order kinetics. Some workers proposed diffusion layer models where the uptake rate depends hyperbolically on the membrane–water partition coefficient [287], but the derivation neglects the link between diffusion rates and partition coefficients. Others take elimination rates inversely proportional to the animal–water partition coefficient [329,916], with the odd implication that the uptake rate is independent of the partition coefficient. This is not consistent with first-order kinetics, where the two media play roles that are exchangeable, which implies a skew-symmetrical relationship between the uptake and elimination rates as functions of the partition coefficient; the square root relationship is the only one that satisfies the skew symmetry.

The DEB theory predicts that the density of octanol equivalents increases with the body size of the different species of animal because the specific maximum reserve capacity $[E_m]$ increases with a volumetric length, cf. {270}, and reserves are relatively rich in lipids. These are only general trends and many exceptions occur. The eel *Anguilla* is much fatter than other fish of similar size, for instance. Data from Hendriks [397] confirm the general trend; see Figure 6.2.

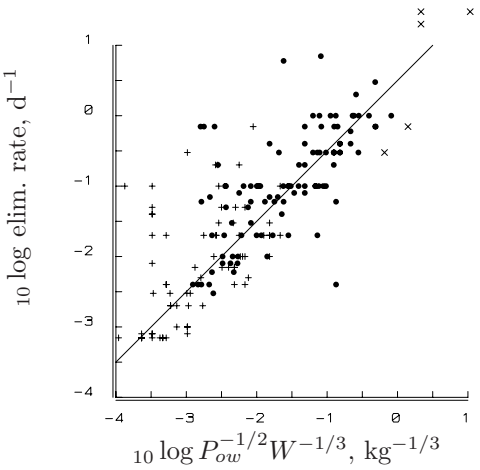

Figure 6.2: The elimination rate depends on the n-octanol–water partition coefficient P_{ow} and the weight W of an organism. It is roughly proportional to $P_{ow}^{-1/2}W^{-1/3}$ with proportionality constant $\sqrt{10}$ $\mathrm{d}^{-1}\mathrm{kg}^{-1/3}$ for 181 halogenated organic compounds in fish. Data compiled by Hendriks [397]. The marker codes are: $P_{ow} \leq 10^2$ (×), $10^2 \leq P_{ow} < 10^6$ (•), $10^6 \leq P_{ow} \leq 10^8$ (+). The range of fish weights is 0.1–900 g. No corrections for differences in temperature have been made, nor for differences in fat content of the fish.

6.2.2 Kinetics as a function of ionization

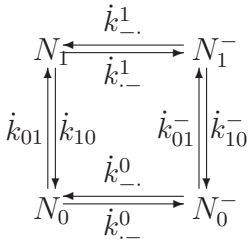

The situation is a bit more complex when the compound can be present in molecular as well as in ionic form. Let N_i^- denote the number of ions in matrix i, and $\dot{k}^i_{\cdot-}$ and $\dot{k}^i_{-\cdot}$ the ionization and de-ionization rates in matrix i, and $\dot{k}^-_{01}$ the transport rate of the ionic form from matrix 0 to matrix 1. The dynamics now becomes

$$\frac{d}{dt}\begin{pmatrix} N_0 \\ N_0^- \\ N_1 \\ N_1^- \end{pmatrix} = \begin{pmatrix} -\dot{k}^0_{\cdot-} - \dot{k}_{01} & \dot{k}^0_{-\cdot} & \dot{k}_{10} & 0 \\ \dot{k}^0_{\cdot-} & -\dot{k}^0_{-\cdot} - \dot{k}^-_{01} & 0 & \dot{k}^-_{10} \\ \dot{k}_{01} & 0 & -\dot{k}^1_{\cdot-} - \dot{k}_{10} & \dot{k}^1_{-\cdot} \\ 0 & \dot{k}^-_{01} & \dot{k}^1_{\cdot-} & -\dot{k}^1_{-\cdot} - \dot{k}^-_{10} \end{pmatrix} \begin{pmatrix} N_0 \\ N_0^- \\ N_1 \\ N_1^- \end{pmatrix} \tag{6.8}$$

The definition of the ionization constant in matrix i is $10^{-\mathrm{pK}_i} = 10^{-\mathrm{pH}_i} N_i^{-*}/N_i^*$, where pH_i stands for the pH in matrix i. Suppose that the processes of ionization and de-ionization are fast with respect to the transport processes, i.e. $N_i^-(t)/N_i(t) = \dot{k}^i_{\cdot-}/\dot{k}^i_{-\cdot} = 10^{\mathrm{pH}_i - \mathrm{pK}_i} = P^i_{-\cdot}$. This seems to be acceptable because ionization and de-ionization do not require macro-scale movements of molecules. This implies that $N_i(t) + N_i^-(t) = (1 + P^i_{-\cdot})N_i(t)$ and $\frac{d}{dt}(N_i(t) + N_i^-(t)) = (1 + P^i_{-\cdot})\frac{d}{dt}N_i(t)$. Suppose also that the ratio of the binding forces of the ionic forms to the molecules of both matrices equals that of the molecular forms, so $\dot{k}^-_{01} = \dot{k}^-\rho_1/\rho_0$ and $\dot{k}^-_{10} = \dot{k}^-\rho_0/\rho_1$. Substitution into (6.8) gives

$$\frac{d}{dt}\begin{pmatrix} N_0 + N_0^- \\ N_1 + N_1^- \end{pmatrix} = \begin{pmatrix} -\dot{k}'_{01} & \dot{k}'_{10} \\ \dot{k}'_{01} & -\dot{k}'_{10} \end{pmatrix} \begin{pmatrix} N_0 + N_0^- \\ N_1 + N_1^- \end{pmatrix} \tag{6.9}$$

with $\dot{k}'_{01} = \frac{\dot{k}+\dot{k}^- P^0_{-\cdot}}{1+P^0_{-\cdot}} \frac{\rho_1}{\rho_0}$ and $\dot{k}'_{10} = \frac{\dot{k}+\dot{k}^- P^1_{-\cdot}}{1+P^1_{-\cdot}} \frac{\rho_0}{\rho_1}$ denoting the overall specific exchange rates of molecules plus ions between the matrices. The partition coefficient being defined as $P_{01} = \frac{N_0(\infty)+N_0^-(\infty)}{N_1(\infty)+N_1^-(\infty)}$, $P_{01} = \left(\frac{\rho_0}{\rho_1}\right)^2$ only holds if $\dot{k}^- = \dot{k}$. This is very unlikely, however, and the previously derived result for molecules without ionic forms does not apply to ionizing

ones. Generally we have

$$P_{01} = \frac{\dot{k}'_{10}}{\dot{k}'_{01}} = \frac{1 + P^0_{-\cdot}}{\dot{k} + \dot{k}^- P^0_{-\cdot}} \frac{\dot{k} + \dot{k}^- P^1_{-\cdot}}{1 + P^1_{-\cdot}} \frac{\rho_0^2}{\rho_1^2} \tag{6.10}$$

Suppose now that we change the pH in matrix 1 (e.g. the environment), while the pH in matrix 0 (e.g. the organism) is kept fixed. If the pH in matrix 1 is extremely low, say $\mathrm{pH}_1 = -\infty$, or $P^1_{-\cdot} = 10^{\mathrm{pH}_1 - \mathrm{pK}_1} = 0$, and all of the compound is present in molecular form, (6.10) reduces to $P_{01} = \frac{1+P^0_{-\cdot}}{\dot{k}+\dot{k}^- P^0_{-\cdot}} \dot{k} \frac{\rho_0^2}{\rho_1^2}$. If, on the other hand, the pH in matrix 1 is extremely high, say $\mathrm{pH}_1 = \infty$, or $P^1_{-\cdot} = \infty$, and all of the compound is present in ionic form, (6.10) reduces to $P_{01} = \frac{1+P^0_{-\cdot}}{\dot{k}+\dot{k}^- P^0_{-\cdot}} \dot{k}^- \frac{\rho_0^2}{\rho_1^2}$. It directly follows that (6.10) can be rewritten as

$$P_{01}(\mathrm{pH}_1) = \frac{P_{01}(-\infty) + P_{01}(\infty) 10^{\mathrm{pH}_1 - \mathrm{pK}_1}}{1 + 10^{\mathrm{pH}_1 - \mathrm{pK}_1}} \tag{6.11}$$

which shows how the partition coefficient depends on the pH in matrix 1 (environment), where $P_{01}(-\infty)$ and $P_{01}(\infty)$ play the role of parameters, on the assumption that the pH in matrix 0 (organism) is independent of the pH in matrix 1.

Substitution into the expressions for $\dot{k}'_{10}$ and $\dot{k}'_{01}$, with $\dot{k}^-/\dot{k} = \dot{k}^-_{10}/\dot{k}_{10} = \dot{k}^-_{01}/\dot{k}_{01}$, results in

$$\dot{k}'_{10} = \dot{k} \sqrt{\frac{1 + \frac{\dot{k}^-_{10}}{\dot{k}_{10}} P^1_{-\cdot}}{1 + P^1_{-\cdot}} \frac{1 + \frac{\dot{k}^-_{10}}{\dot{k}_{10}} P^0_{-\cdot}}{1 + P^0_{-\cdot}} P_{01}} \quad \text{and} \quad \dot{k}'_{01} = \dot{k} \sqrt{\frac{1 + \frac{\dot{k}^-_{01}}{\dot{k}_{01}} P^0_{-\cdot}}{1 + P^0_{-\cdot}} \frac{1 + \frac{\dot{k}^-_{01}}{\dot{k}_{01}} P^1_{-\cdot}}{1 + P^1_{-\cdot}} P_{10}} \tag{6.12}$$

It directly follows that

$$\dot{k}'_{01}(\mathrm{pH}_1) = \sqrt{\frac{\dot{k}'^2_{01}(-\infty) + \dot{k}'^2_{01}(\infty) 10^{\mathrm{pH}_1 - \mathrm{pK}_1}}{1 + 10^{\mathrm{pH}_1 - \mathrm{pK}_1}}} \tag{6.13}$$

where $\dot{k}'_{01}(-\infty) = \dot{k} \sqrt{\frac{1 + \frac{\dot{k}^-_{01}}{\dot{k}_{01}} P^0_{-\cdot}}{1 + P^0_{-\cdot}} P_{10}}$ and $\dot{k}'_{01}(\infty) = \dot{k} \sqrt{\frac{1 + \frac{\dot{k}^-_{01}}{\dot{k}_{01}} P^0_{-\cdot}}{1 + P^0_{-\cdot}} \frac{\dot{k}^-_{01}}{\dot{k}_{01}} P_{10}}$ denote the exchange rates if all the compound is present in, respectively, the molecular and the ionized form in matrix 1, and the pH in matrix 0 is fixed.

When applied to toxicokinetics, one matrix corresponds to animal tissue, and one to fresh or sea water. Ionized and un-ionized (molecular) forms of a compound are taken up at different rates, while the pH affects their relative abundance and so the toxicokinetics [504]. If ions hardly exchange, so $\dot{k}^-_{10} = \dot{k}^-_{01} = 0$, knowledge about $\dot{k}_{10}$ or $\dot{k}_{01}$ is then no longer required; knowledge about pH_i, pK_i and $P_{ow} = P_{wo}^{-1}$ can be used to relate elimination rates of different compounds to each other, where octanol serves as a chemical model for animal tissue. Octanol is a good model compound to study lipophilicity, but a poor model to study the ionization tendency. The derivation above shows that compounds that can ionize must be compared with care; an increase in lipophilicity frequently comes with a decrease in ionization tendency. It also shows how the pH affects the elimination rate and the partition coefficient via $P^i_{-\cdot} = 10^{\mathrm{pH}_i - \mathrm{pK}_i}$. This can be useful for comparing the toxicokinetics of a single compound under different environmental conditions. Homeostasis ensures that the pK and pH in animal tissue hardly depend on the environmental conditions.

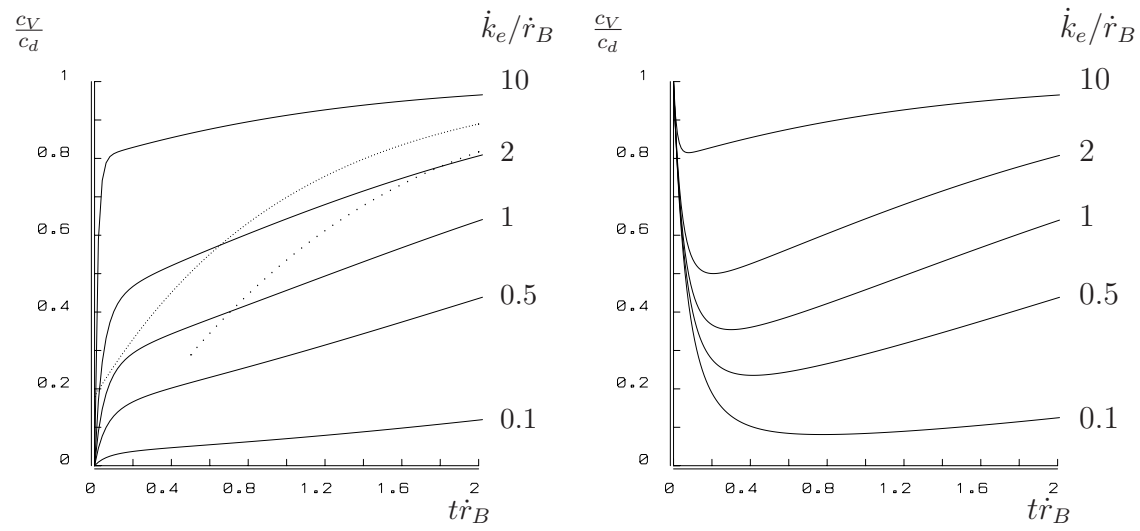

Figure 6.3: Uptake and elimination during growth. The scaled tissue concentrations start from $c_V(0) = 0$ (left), or $c_V(0) = c_d$ (right), where c_d stands for the environment concentration. The different curves represent different choices for the value of the elimination rate $\dot{k}_e$, relative to the von Bertalanffy growth rate $\dot{r}_B$. The finely dotted curve represents (scaled) body length and the coarsely dotted curve the (scaled) reproduction rate. The (scaled) lengths at the start of exposure and reproduction are realistic for the water flea *Daphnia magna* and the value $t\dot{r}_B = 2$ corresponds with 21 d for *D. magna* at 20 °C. All curves in both graphs have an asymptote at the value 1. If the product of the von Bertalanffy growth rate and the exposure time $t\dot{r}_B > 0.4$, the curves in the left and right panels are almost identical, i.e. independent of the initial tissue concentration. The deviations from $c_V = c_d$ can therefore be attributed to 'dilution by growth'.

6.3 Energetics affects toxicokinetics

6.3.1 Dilution by growth

Body growth affects the toxicokinetics even at very low values, as Figure 6.3 illustrates. The physics of the transport processes strongly suggests that uptake and elimination are proportional to the surface area of the organism; it thus links up beautifully with the structure of the DEB model. Since the elimination rate is also proportional to the tissue concentration, thus to the amount per volume, it is proportional to the ratio of the surface area to the volume, thus inversely proportional to the volumetric length. This is why the elimination rate must be divided by a scaled length if the body size changes, as has been experimentally verified [841,844]. The change in scaled tissue concentration c_V is given by

$$\frac{d}{dt}c_V = \frac{\dot{k}_e}{l}(c_d - c_V) - c_V \frac{d}{dt}\ln l^3 \tag{6.14}$$

where the term $c_V \frac{d}{dt}\ln l^3$ accounts for the dilution by growth. If food density is constant, the DEB model reduces to $\frac{d}{dt}l = (f-l)\dot{r}_B$, where $\dot{r}_B$ is the von Bertalanffy growth rate. This model still classifies as a one-compartment kinetics model with time-varying coefficients.

Newman and Mitz [662] found that the elimination rate of zinc in guppies was about

proportional to weight$^{-0.42}$ (which is consistent with the expected proportionality with length^{-1}, in view of the scatter), but the zinc-uptake rate was about proportional to weight$^{-0.9}$. This has the unexpected consequence that the bioconcentration coefficient is proportional to weight$^{-0.48}$. The elimination rate of mercury did not seem to depend on the size of the mosquitofish, while the mercury-uptake rate tended to decrease with size, so that the bioconcentration coefficient also decreases with size [661]. Boyden [107] also found negative correlations between body size and concentrations of cadmium, copper, iron, lead and zinc in some species of mollusc, but no correlations for cadmium, iron, nickel, lead and zinc in other species of mollusc and a positive correlation for cadmium in *Patella vulgata*.

The kinetics of these metals seems to interfere with the metabolism in a more complex way. The substantial scatter in the data hampers firm conclusions from being drawn. When the experimental protocol involves a shift up and thus a transition from low to high concentrations of contaminant, negative correlations between body size and concentrations of contaminant can be expected if elimination and uptake rates decrease with body size: it takes longer for big bodies to reach equilibrium. This mechanism can at best only explain part of the observations.

6.3.2 Changes in lipid content

Changes in lipid content, and thus in energy reserves, affect toxicokinetics. Since energy kinetics has a direct link with food uptake, and uptake of a compound from food can be substantial, the link between toxicokinetics with food uptake and reserves kinetics is here discussed in the context of the DEB model. Changes in lipid content frequently occur in uptake experiments; it is practically impossible to feed a cohort of blue mussels in a two-month uptake/elimination experiment adequately in the laboratory; at the end of the experiment, the lipid content is reduced substantially. This affects the kinetics of lipophilic compounds.

Accumulation of lipophilic compounds and partitioning between different organs can be explained by the occurrence of stored lipids. Schneider [816] found large differences of poly-chlorinated biphenyl (PCB) concentrations in different organs of the cod, but the concentrations did not differ when based on the phospholipid-free fraction of extractable lipids. Models for feeding-condition-dependent kinetics have been proposed [359,362,545], but they have a large number of parameters. The application of the DEB model involves relatively few parameters, because of the one-compartment kinetics and instantaneous partitioning of the compound in the organism, as proposed by Barber *et al.* [45] and Hallam *et al.* [359]. The assumption that compounds are partitioned instantaneously is supported by a study of the elimination rate of 4,4′-dichlorobiphenyl (PCB15) in the pond snail *Lymnaea stagnalis* [1000]; Wilbrink *et al.* found that elimination rates are equal for different organs, implying that ratios of concentrations in different organs do not change. The fact that structural biomass consists of organs that have different partition coefficients for the xenobiotic is covered by the assumptions of isomorphism, homeostasis and instantaneous partitioning. The combination of these three assumptions implies that the concentration–time curve in one organ can be obtained from that in another organ by

applying a fixed multiplication factor.

The amount of compound in the body can be partitioned as $M_Q = M_{QV} + M_{QE} + M_{QR}$ in contributions from structural body volume, M_{QV}, reserves, M_{QE}, and the reproduction buffer, M_{QR}. The latter contribution can be substantial in species like the blue mussel, which reproduces once a year and discharges half its body mass at spawning. Again, we assume instantaneous partitioning of the compound over these compartments, and introduce partition coefficients based on moles of compound per C-mole of body compartment. Since the reproduction buffer has the same chemical composition as the reserves, the amount of compound can be written as

$$M_Q = M_{QV}\left(1 + \frac{[M_{Em}]}{[M_V]} P_{EV}(e + e_R)\right) = M_{QV} P_{WV} \tag{6.15}$$

where P_{EV} denotes the partition coefficient between reserves and structural biomass on the basis of C-moles. The factor P_{WV}, which depends on the (changing) reserve density, can formally be considered as a partition coefficient between the total body mass and the structural body mass.

According to the DEB model, ingestion of food occurs at rate $\dot{k}_X = fl^2\dot{k}_{Xm}$. Suppose that the compound is present in food at concentration c_X (mole per C-mole). Egestion of faeces occurs at rate $\dot{k}_P = fl^2\dot{k}_{Pm}$, with $\dot{k}_{Pm}$ the maximum specific egestion rate. Suppose that the compound is present at concentration c_P in the fresh faeces, and that $\frac{c_X}{c_P} = P_{XP}$ is constant. The partition coefficient P_{XP} can be conceived as a measure of the extraction efficiency of the compound from food. The uptake flux via food amounts to $c_X\dot{k}_X - c_P\dot{k}_P = c_X\dot{k}_X - c_X\dot{k}_X\frac{\dot{k}_{Pm}}{\dot{k}_{Xm}}P_{PX} = c_X fl^2(\dot{k}_{Xm} - \dot{k}_{Pm}P_{PX}) = c_X fl^2\dot{k}_e P_{VX}$, where $\dot{k}_e$ denotes the elimination rate from the body, and $P_{VX} \equiv (\dot{k}_{Xm} - \dot{k}_{Pm}P_{PX})\dot{k}_e^{-1}$ is introduced to simplify the notation.

Suppose that the compound is present in the dissolved form at concentration c_d (mole per volume), while the exchange rates between water and body are again taken to be proportional to surface area. The nature of the uptake can be passive or active, but the rate is taken to be proportional to the concentration in the environment and/or to food uptake. Allowing for these two uptake routes, and for dilution by growth, the kinetics amounts to

$$\frac{d}{dt}[M_Q] = \frac{\dot{k}_e}{l}P_{Vd}c_d + \frac{\dot{k}_e}{l}P_{VX}fc_X - [M_Q]\left(\frac{\dot{k}_e}{l}P_{VW} + \frac{d}{dt}\ln l^3\right) \tag{6.16}$$

$$\frac{d}{dt}c_V = \frac{\dot{k}_e}{l}(c_d + P_{dX}fc_X - P_{VW}c_V) - c_V\frac{d}{dt}\ln l^3 \tag{6.17}$$

where the partition coefficient $P_{VW} = P_{WV}^{-1}$ is given in (6.15), $\frac{\dot{k}_e}{l}P_{Vd}$ is the uptake rate from the water, $\frac{\dot{k}_e}{l}P_{VX}f$ is the uptake rate from the food, $\frac{\dot{k}_e}{l}$ is the elimination rate from the body, $P_{dX} = P_{VX}/P_{Vd}$, and $c_V = [M_Q]P_{dV}$, as before. The definition of the partition coefficient P_{Vd} is the ratio of the uptake rate from water to the elimination rate; it is no longer interpreted as the ultimate ratio of the concentration in the body to that in the water. Likewise, P_{dX} is not interpreted as the ultimate ratio of the concentration in the

food to that in the water. For $P_{VW} = 1$ and $P_{dX} = 0$, (6.17) reduces to (6.14), and for $l = f$ it further reduces to (6.2). The model still classifies as a one-compartment model with time-varying coefficients.

Since most measurements are done on the basis of weights, the kinetics of the variable $\langle M_Q \rangle_w = [M_Q]/[W_w]$ is of practical interest; it represents the number of moles per unit of wet weight. Like the total amount of compound, wet weight can be decomposed into the contributions made by the structural body volume, the reserves and the reproduction buffer, as done in (2.6). The change in concentration on the basis of weights is

$$\frac{d}{dt}\langle M_Q \rangle_w = \frac{1}{[W_w]}\frac{d}{dt}[M_Q] - \langle M_Q \rangle_w w_E \frac{[M_{Em}]}{[W_w]}\left(\frac{d}{dt}e + \frac{d}{dt}e_R\right) \tag{6.18}$$

where the second term relates to the change in weight, as implied by $[W_w] = d_V + w_E[M_{Em}](e + e_R)$, cf. (2.6). Apart from the initial conditions, this specifies the dynamics in the period between the moments of spawning or reproduction. At such moments, (wet) weight as well as the amount of xenobiotic compounds are discontinuous, because the buffer of energy allocated to reproduction is emptied, possibly together with its load of xenobiotic compound. The most simple assumption is to let the compound in that buffer transfer to the egg. If reproduction occurs at time t_R, and if t_R^- denotes a moment just before t_R, and t_R^+ just after, the ratio of the concentrations of compound equals

$$\frac{\langle M_Q \rangle_w(t_R^+)}{\langle M_Q \rangle_w(t_R^-)} = \frac{d_V + w_E[M_{Em}]P_{EV}(e + e_R)}{d_V + w_E[M_{Em}]P_{EV}e}\,\frac{d_V + w_E[M_{Em}]e}{d_V + w_E[M_{Em}](e + e_R)} \tag{6.19}$$

The first factor corresponds to the ratio of xenobiotic masses in moles, the second factor to the ratio of body weights. This result can be larger or smaller than 1, depending primarily on the partition coefficient P_{EV}. If the moments of reproduction are frequent enough to neglect the contribution of e_R to wet weight and compound load, $\frac{d}{dt}e_R$ can be replaced by $e_0\dot{R}$, which can be left out if the reproductive output is negligibly small.

The elimination route via reproduction can be very important for rapidly reproducing species, such as daphnids. Even in guppies it can be noticeable [843]. It is also possible that no compound is transduced through the reproduction process, as has been found for 4,4′-DCB in *Lymnaea* [1000]. This implies a (sudden) increase of the concentration at reproduction.

The change of concentration at reproduction has, of course, an intimate relationship with the initial conditions for the offspring, which depend on the feeding conditions and the loading of the mother. Experience with chronic toxicity tests shows that most effects occur at hatching, which means that an egg must be considered to be rather isolated, chemically, from its environment apart of course, from gas exchange. An extreme consequence is that the amount of compound at egg formation is the same as that at hatching. This means that the concentration at hatching relates to that of the mother just after reproduction as

$$\langle M_Q \rangle_w(a_b) = \langle M_Q \rangle_w(t_R^+)\frac{P_{EV}V_m}{P_{WV}V_b}e_0 \tag{6.20}$$

where the ratio P_{WV} is given in (6.15) and should now be evaluated at $e_R = 0$.

The parameters that relate to the kinetics of the compound are the elimination rate $\dot{k}_e$, and the partition coefficients P_{Vd}, P_{VX} and P_{EV}. In addition, there are a number of parameters that relate volumes to weights. The third class of parameters is from the DEB model via the expressions for $\frac{d}{dt}l$, $\frac{d}{dt}e$ and $\frac{d}{dt}e_R$. Not all parameters are required to fit the model to experimental data. If food density and c_d/c_X do not change, for instance, and the reproduction buffer plays a minor role, P_{WV} is constant, and the four toxicokinetic parameters combine in just two compound parameters $(P_{Vd}+P_{VX}c_X/c_d)/P_{VW}$, and $\dot{k}_e P_{VW}$. It is obvious that additional physiological knowledge will help us to interpret experimental results, especially if the physiological condition changes during the experiment. Although some of the physiological parameters can be estimated from uptake/elimination curves in principle, an independent and more direct estimation is preferable.

Figures 6.4 and 6.5 illustrate the performance of the model to describe the uptake/elimination behaviour of the compounds hexachlorobenzene (octanol/water partition coefficient $\log P_{ow} = 5.45$ [797]) and 2-monochloronaphthalene ($\log P_{ow} = 3.90$ [678]). The mussels and fish were not fed during the experiment, which implies that their energy reserves decreased during this time. The fish depleted its energy reserves faster, because it was smaller than the mussel and its temperature was higher. As a result of the decrease in reserves, the fish started to eliminate the compound during the accumulation phase of the experiment. The model successfully describes this phenomenon. The experiments were short enough to assume that the size of the test animals did not change and that the energy allocation to reproduction was negligibly small during the experiment. The concentration of xenobiotic compounds in the water changed during accumulation. A cubic spline was, therefore, fitted to these concentrations and used to obtain the concentrations in the wet weight.

6.3.3 Bioconcentration coefficient

The bioconcentration coefficient, BC, is an important concept in the kinetics of xenobiotics. It is used among other things as a crude measure to compare xenobiotic compounds and species and to predict effects. For aquatic species and hydrophilic compounds, it is usually defined as the ratio of the concentration in the organism to that in the water, which are both taken to be constant. For terrestrial species and/or lipophilic compounds, it is usually defined as the ratio of the concentration in the organism to that in the food. Applying the BC concept is a bit complicated in the present context, because the concentration in the organism does not become stationary, because of growth and reproduction, even if the concentration in the environment is constant, i.e. in water, food and at constant food density. If the growth rate is low in comparison to the exchange rates, the compound can be in pseudo-equilibrium, but its concentration still depends, generally, on the size of the organism. In addition, reproduction causes a cyclic change in concentration. The oscillations become larger if the organism accumulates its reproductive output over a longer time period. If food density is constant for a long enough period, we have $e = f$ and $\frac{d}{dt}e = 0$. The ultimate concentration on the basis of wet weight then reduces for low growth and

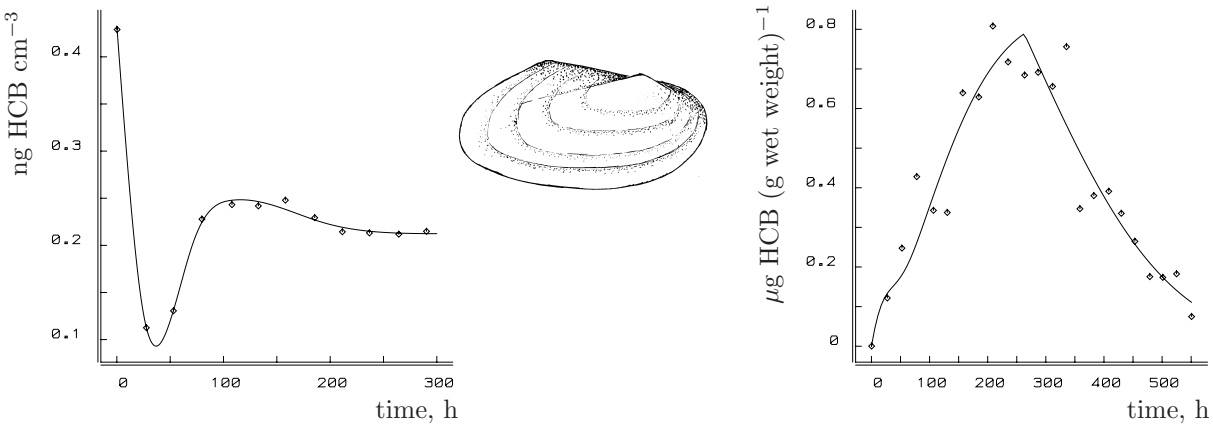

Figure 6.4: Measured concentration of hexachlorobenzene (HCB) in water and in a starving 6.03 cm^3 freshwater mussel *Elliptio complanata* at 20 °C during a 264 h uptake/elimination experiment. Data from Russel and Gobas [797]. The least-squares-fitted curves are the cubic spline function for concentrations in the water and the model-based expectation for the concentration in the wet weight. From [521].

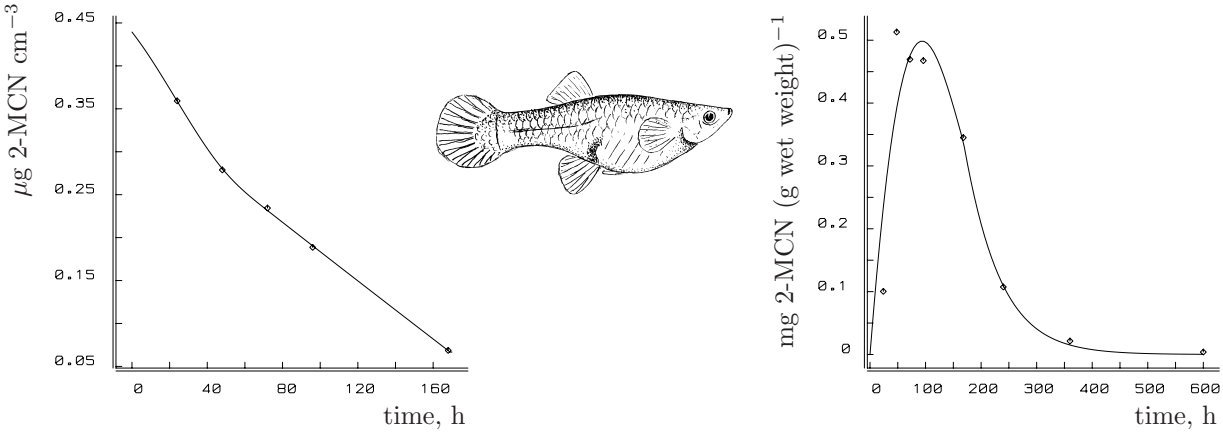

Figure 6.5: Measured concentration of 2-monochloronaphthalene (2-MCN) in water and in a starving 0.22 cm^3 female guppy *Poecilia reticulata* at 22 °C during a 168 h uptake/elimination experiment. Data from Opperhuizen [678]. The least-squares-fitted curves are the cubic spline function for the concentrations in the water and the model-based expectation for the concentration in the wet weight. From [521].

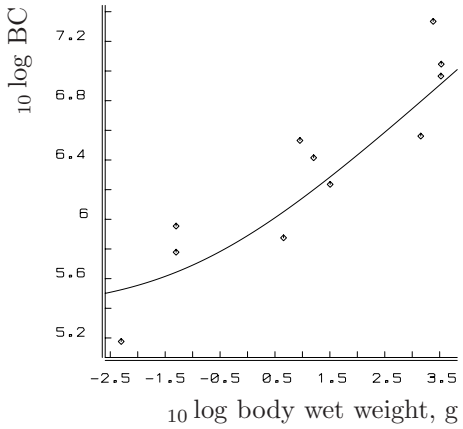

Figure 6.6: Bioconcentration coefficients (BCs) for PCB153 in aquatic organisms in the field, as given in [521]. Data from Oliver and Niimi [664,676] and from the Dutch Ministry of Public Works and Transport. The curve represents the least-squares fit of the linear relationship between the BC and the volumetric length. $P_{VX}\mathcal{V}^{1/3} = 46$ mm.

reproduction rates to

$$\langle M_Q \rangle_w \rightarrow \frac{P_{Vd}c_d + P_{VX}fc_X}{[W_w]}\left(1 + \frac{[M_{Em}]}{[M_V]}P_{EV}f\right) \tag{6.21}$$

This expression can be used to predict how BC depends on body size if species are compared on the basis of the theory presented on {269}. Since P_{VX} is proportional to $\dot{J}_{Xm}$, BC is expected to be linear in the volumetric length. The trend in $[E_m]$ almost cancels out. Figure 6.6 illustrates that the BC for the highly lipophilic compound 2,4,5,2′,4′,5′ hexachlorobiphenyl (PCB153) for aquatic animals is indeed linear in the volumetric length.

This expectation is thus based solely on differences in the uptake of the amount of food. Accumulation in the food chain occurs particularly in terrestrial habitats, and more debatably in aquatic ones. Since top predators tend to have the largest body size, it can be difficult to distinguish food chain effects from body size effects. Food chain effects operate through the partition coefficient for food/water, and body size effects act via the uptake of food.

6.3.4 Metabolic transformations

If compounds are metabolized, the usual effect is that the products are less lipophilic than the original compound, so P_{EV} is reduced. In this way, the product will be eliminated at a higher rate. If the metabolic transformation behaves as a first-order process, this only affects the value of the elimination rate, and not the model structure. It has long been recognized, however, that elimination frequently involves a metabolic activity that can be satiated [958,959,960]. Many compounds, such as salicylurate [555,556], are found to have a capacity-limited elimination route. Wagner [957] used Michaelis–Menten (MM) kinetics to describe the elimination of ethanol from human serum, i.e.

$$\frac{d}{dt}[M_Q] = \dot{k}_e P_{Vd} c - \frac{\dot{k}_e [M_Q]}{1 + [M_Q]/[M_Q]_M} \quad \text{or} \tag{6.22}$$

$$\frac{d}{dt}c_V = \dot{k}_e c - \frac{\dot{k}_e c_V}{1 + c_V/c_M} \tag{6.23}$$

with $c_V = [M_Q]P_{Vd}$, $c_M = [M_Q]_M P_{Vd}$, P_{Vd} being the ratio of the uptake to the elimination rate, and $\dot{k}_e$ and $[M_Q]_M$ or c_M are the parameters of the MM-elimination. The concentration c_M has the interpretation of the maximum sustained concentration in the environment that can be 'handled' by the organism. If the concentration exceeds this value, the concentration in the organism will build up continuously.

The MM-elimination route can supplement a first-order elimination route, which gives

$$\frac{d}{dt}c_V = \dot{k}_e c - \dot{k}_l c_V - \frac{\dot{k}_e c_V}{1 + c_V/c_M} \tag{6.24}$$

The first-order elimination route might relate to respiration, and can be taken proportional to the respiration rate $\dot{k}_C$ of the organism. The MM-elimination route might relate to excretion by the kidney or the liver, and taken proportional to the excretion rate of nitrogenous waste $\dot{k}_N$ of the organism, for instance. A coupling of elimination with exudate excretion in algae has been suggested [840]. These couplings with the energy budget reveal how these parameters change with size during growth, or with the nutritional status, and how they differ from one species to another. We can again allow for dilution by growth, cf. (6.14), and different uptake routes and changes in lipid content, cf. (6.17). Needless to say, we then need a rather elaborate series of measurements, because of the six parameters that have to be estimated.

Note that (6.24) collapses to first-order kinetics if $c_V \ll c_M$, and if $c_V \gg c_M$, with elimination rate $\dot{k}_e + \dot{k}_l$ or uptake rate $\dot{k}_e c - \dot{k}_e c_M = \dot{k}_e(c - c_M)$, respectively. If c_V varies in a rather small window around c_M, (6.24) approximates first-order kinetics, with elimination rate $\dot{k}_l + \dot{k}_e/4$. In all those cases, c_M cannot be estimated; we need a rather big window for measurements of c_V around c_M for that purpose. Problems disappear if the elimination flux via the MM-route can be measured directly, by measuring the compound or its products, in the urine, for instance.

6.4 Toxicants affect energetics

Only two types of effects are of primary, ecotoxicological, interest: those that affect survival and those that affect reproduction. These effects determine population dynamics, and thus production and existence. Due to the coupling between the various processes of energy uptake and use, many other effects of compounds have an indirect effect on reproduction. For instance, the conservation law for energy implies that a reduction of food uptake has indirect effects on reproduction. The DEB model describes the routes that translate these effects into an effect on reproduction; allocation to reproduction depends on reserve density, which depends on feeding rate, which depends on body size, which depends on growth. Maintenance competes with growth for allocation, so effects on maintenance can be translated into effects on growth, and thus into effects on reproduction. Small individuals eat less than large ones, so less energy is available for reproduction. Effects on feeding, growth and maintenance indirectly affect reproduction on the basis of the DEB model. These types of effects relate directly to energetics. Their consequences can be evaluated

by changing one or more parameter values of the DEB model. Such a study is not very different from a more general one on the evolutionary implications of parameter settings.

The environmental relevance of mutagenic effects is still in debate. A frequently heard opinion from some industrialists is that mutagenic effects have no environmental impact at all, stating that the direct effect on survival is negligibly small and the loss of gametes does not count from an ecological point of view. The way aging is treated within the DEB model closely links up with mutagenic effects, particularly if the free radical mechanism is correct. Mutagenic compounds have about the same effect on organisms as free radicals. As a consequence, mutagenic effects can be studied by changing aging acceleration (in the case of metazoans). The DEB model offers the possibility of evaluating the consequences of mutagenic effects along the same lines as the effects on energy fluxes. I have already mentioned the setting of aging acceleration as a compromise between the life span of individuals and the evolutionary flexibility of the genome. The effects of changes in aging acceleration must then be found over a time scale of many generations and involve interspecies relationships. This makes such effects extremely hard to study, both experimentally and theoretically. The lack of reliable models for this time scale makes it difficult to draw firm conclusions. The fact that mutagenic compounds tend to be rather reactive and, therefore, generally have a short life in the environment is part of the problem, which perhaps makes them less relevant to the problem of environmental pollution if emissions are only incidentical.

The significance of mutagenic effect on human health is widely recognized, particularly in relation to the occurrence of tumours and cancer. The Ames test is frequently applied to test compounds for mutagenic effects. The DEB model offers a framework for interpreting the sometimes unexpected results from these tests. The Ames test is discussed on {214} for this reason, in a subsection of the section on effects on populations, as it is basically aimed at this level of organization.

The environmental significance of teratogenic effects, i.e. effects on the development of organisms, is even less well recognized than the significance of mutagenic effects. Fortunately, only a few compounds seem to have a teratogenic effect as their primary one, and these fall outside the scope of this book.

Each physiological process has its own tolerance range for any compound. The upper boundaries can be ordered, which means that at low tissue concentrations that produce effects, only one physiological process is affected, while at high tissue concentrations many processes are affected. As long as the partitioning of the compound over the various body fractions is fast with respect to the uptake/elimination kinetics for the whole animal, it is not essential to specify the tissue or organ in which the most sensitive physiological process is affected. This only becomes essential if the partitioning is slow. This makes multi-compartment models as a basis for effect studies so much more complex to apply: we have to know a great deal more. Notice that one-compartment models can handle different concentrations in different organs as long as partitioning is fast. Observed deviations from one-compartment kinetics with constant coefficients frequently relate to the variations in the coefficients, not necessarily to the presence of more compartments.

Basic to the description of small effects of toxicants is the notion that each molecule that exceeds the tolerance range contributes to the same extent to the effect. Interactions between the molecules only occur at higher tissue concentrations. Hence, the effect size is,

as a first approximation, a linear function of the tissue concentration. This point of view relates to the Taylor approximation for non-linear functions that describe how effect size relates to tissue concentrations: we use only the first term of the Taylor approximation at the upper boundary of the tolerance range. The theorem by Taylor states that we can describe any non-linear function in a given interval arbitrarily well with an appropriate polynomial function if we include enough higher order terms. So when we want to improve the description of effects, if they happen to deviate from a linear relationship with tissue concentrations, we simply include the squared term, the cubed term, etc. Such improvements will rapidly become counterproductive because we increase the number of parameters that must be estimated and because higher tissue concentrations will affect more physiological processes. So we are increasing precision at the wrong points. Practice teaches that very good descriptions can be obtained by just taking effect size to be linear in the tissue concentration, even at rather high effect sizes, provided that we focus on the correct physiological process.

An approach to modelling effects that has proven to be rather successful is to tie the occurrence of effects to the concentration in the tissue. Combined with the idea that the compound partitions instantaneously over the different body fractions, as is discussed in the previous section, it no longer matters if the effects originate from the disfunctioning of one or more particular organs, or of the whole body. If the concentration in one particular organ exceeds some threshold, it will at the same time exceed another threshold in another organ. This is of course no longer true if partitioning is a slow process with respect to the uptake and elimination rate of the compound.

The simple observation that the effects of a mildly toxic compound that strongly accumulates cannot be distinguished from those of a strongly toxic compound that poorly accumulates teaches us that the partition coefficients do not occur as independent parameters in effect models. However, the elimination rate does; it shows up as the rate at which effects build up to their ultimate levels during exposure. If the effects build up rapidly, such as for surfactants, the elimination rate is high. A rapid build-up should not be confused with a high toxicity, however; the uptake rate and the toxicity of the compound also affect these properties. The elimination rate can thus be estimated from effect data. If the elimination rate is known from toxicokinetic data, this knowledge can be used to analyse effect data.

6.4.1 No effects

Organisms have evolved in a chemically varying environment; consequently they can cope with varying concentrations of any particular compound, as long as the variations are within a certain range. The upper boundary for this range, i.e. the internal no-effect concentration, might be zero for particular compounds. Each molecule of such compounds induces effects with a certain probability, but for most compounds, the upper boundary is positive. The lower boundary is zero for most compounds, because they are not necessary for life. Elements such as copper are required, so the lower boundary for copper is positive. Effects of a shortage of a compound resemble those of an overdose in their kinetics. The founder of ecotoxicology, Sprague [872] studied the effects of toxicants in bioassays, using

oxygen shortage as an example. Although many interrelationships exist between nutrition and toxic effects, the upper boundary of the tolerance range attracted most attention in ecotoxicology, because of its application in risk assessment studies, while ecology focused on the lower boundary (see White [991]).

The No-Effect Concentration (NEC) is a concept that is specific to the organization level of the individual. Even if each molecule has an effect, regulation systems in the individual cancel these effects; if a compound affects the binding capacity of blood for oxygen molecule by molecule, the individual reacts by producing more haemoglobin, or functionally related compounds. So, effects at low concentrations will not show up in oxygen-rich environments. This example also illustrates that the NEC can depend on environmental conditions.

6.4.2 Effects on survival

For some reason, not all individuals show effects of the same intensity at the same time if exposed to the compound in a certain concentration or at a certain dose. Part of the differences can be explained by differences in physiological condition, lipid content and size. It is possible to remove most but not all differences by strict standardization of the organisms that are used for the experiments.

A solution to these problems can be found in a stochastic approach to the occurrence of effects on a single individual, much along the same lines as is done for the modelling of aging. The survival of a single individual is then described in terms of a hazard rate that depends on the concentration of the compound in the organism, i.e. the hazard rate is

$$\dot{h}_c \propto ([M_Q]_{0,l} - [M_Q])_+ \quad \text{and/or} \quad \dot{h}_c \propto ([M_Q] - [M_Q]_{0,u})_+ \tag{6.25}$$

where $[M_Q]_{0,l}$ and $[M_Q]_{0,u}$ stand for the lower and the upper boundary of the concentrations of compound that do not affect survival.

The proportionality constant that describes the effect on the hazard rate probably differs for shortages and excesses. This relates to differences in mechanisms. If the concentration exceeds the tolerance range substantially, it is likely that death will strike via other mechanisms than for small excesses. This restricts the applicability of the model to relatively small ranges of concentration. In practice, however, very wide concentration ranges are frequently used, as in range-finding tests on a routine basis.

In the rest of this subsection, I assume that $[M_Q]_{0,l} = 0$ for simplicity's sake, and reduce the notation $[M_Q]_{0,u}$ to $[M_Q]_0$. The idea for hazard modelling can be worked out quantitatively as follows for a constant concentration in the environment.

Because of the general lack of knowledge about relevant concentrations in tissue, those in the environment will be used to specify the hazard rate. If the initial concentration in the tissue is negligibly small and if the concentration of compound in the tissue follows simple first-order (i.e. one-compartment) kinetics (6.2), the hazard rate at constant concentration c in the environment is

$$\dot{h}_c = \dot{b}_\dagger (c_V - c_0)_+ = \dot{b}_\dagger ((1 - \exp\{-t\dot{k}_e\})c - c_0)_+$$

The proportionality constant $\dot{b}_\dagger$ is the killing rate with the dimension (environment concentration $\times$ time)$^{-1}$. It is a measure of the toxicity of the compound with respect to survival.

The NEC $c_0 \equiv [M_Q]_0 P_{dV}$ in the environment is the highest concentration that will never result in an effect if the concentration is constant. If $c > c_0$, but constant, and if the initial concentration in the tissue is 0, effects start to show at $t_0 = -\dot{k}_e^{-1} \ln\{1 - c_0/c\}$, the moment at which the concentration in the tissue exceeds the NEC. In the absence of 'natural' mortality, the survival probability q for $c > c_0$ and $t > t_0$ is

$$q(c,t) = \exp\left\{-\int_0^t \dot{h}_c(t_1)\, dt_1\right\} \tag{6.26}$$

$$= \exp\left\{\dot{b}_\dagger \dot{k}_e^{-1} c(\exp\{-t_0\dot{k}_e\} - \exp\{-t\dot{k}_e\}) - \dot{b}_\dagger(c - c_0)(t - t_0)\right\} \tag{6.27}$$

This equation has three parameters, which are of all of practical interest: the NEC c_0, the killing rate $\dot{b}_\dagger$ and the elimination rate $\dot{k}_e$. The more elaborate description of the DEB-based kinetics could be used to describe survival patterns in more detail. Practical limitations are likely to ruin such an attempt if no measurements for the concentration in the tissue are available. An appropriate experimental design can usually avoid such complications.

Figure 6.7 illustrates the application of (6.27) to the results of some standard toxicity tests. Note that this formulation implies that the concentration–response relationships become steeper for longer exposure periods.

An interesting special case concerns extremely small elimination rates, so $\dot{k}_e \to 0$, and $P_{Vd} \to \infty$, such that the uptake rate $\dot{k}_e P_{Vd} = \dot{k}_{dV}$ remains fixed. The accumulation process reduces to $\frac{d}{dt}[M_Q] = \dot{k}_{dV} c$, so that $[M_Q](t) = \dot{k}_{dV} ct$ if the initial concentration in the tissue is negligibly small. The NEC (in the environment) is now 0, because a very small concentration in the environment will result ultimately in a very high concentration in the tissue. A NEC in the tissue, i.e. the upper boundary of the tolerance range, still exists, of course, and is exceeded at $t_0 = [M_Q]_0(\dot{k}_{dV} c)^{-1}$. The hazard rate amounts to $\dot{h}_c = \ddot{b}_\dagger c(t - t_0)_+$. The relationship between the killing acceleration $\ddot{b}_\dagger$ and the killing rate $\dot{b}_\dagger$, in the case that $\dot{k}_e \neq 0$, is $\ddot{b}_\dagger = \dot{b}_\dagger \dot{k}_e$. The survival probability is

$$q(c,t) = \exp\{-\ddot{b}_\dagger c(t - t_0)^2/2\} \tag{6.28}$$

For small NECs in the tissue, so $t_0 \to 0$, this represents a Weibull distribution with shape parameter 2. The only difference with the survival probability related to aging, cf. {255}, is the extra accumulation step of products made by affected DNA, which results in a Weibull distribution with shape parameter 3.

In this special case, the full response surface in the concentration-exposure time-plane is described by just one parameter, the killing acceleration $\ddot{b}_\dagger$. One step towards more elaborate models is the introduction of the upper boundary of the tolerance range, via $[M_Q]_0/\dot{k}_{da}$ in t_0. Next comes the introduction of the elimination rate $\dot{k}_e$, which allows a new parameter basis: $\dot{b}_\dagger$, $\dot{k}_e$ and c_0. Then follow changes in the chemical composition (and size) of the animal by introduction of the partition coefficients P_{EV} and P_{PX}, and/or a separation of uptake routes via the dissolved fraction $\{\dot{k}_{dV}\}$ or via food $\{\dot{k}_{xV}\}$. Finally, we should allow for metabolic transformations. So the level of model's complexity can be fully trimmed to the need and/or practical limitations. The more complex the model is, the more one needs to know (and measure) about the behaviour of the compound in the

guppies (*Poecilia reticulata*) in dieldrin
$\dot{b}_\dagger = 0.038\ \mathrm{l}\,\mu\mathrm{g}^{-1}\,\mathrm{d}^{-1}$, $\dot{k}_e = 0.712\ \mathrm{d}^{-1}$, $c_0 = 4.49\ \mu\mathrm{g}\,\mathrm{l}^{-1}$

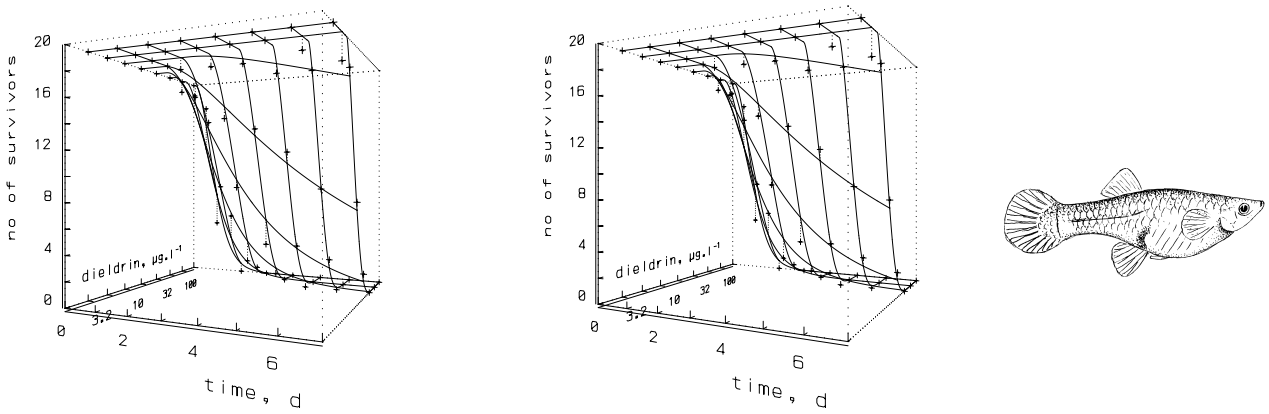

gammarids (*Chaetogammarus marinus*) in 3,4-dichloroaniline
$\dot{b}_\dagger = 0.40\ \mathrm{l}\,\mathrm{mg}^{-1}\,\mathrm{d}^{-1}$, $\dot{k}_e = 0.335\ \mathrm{d}^{-1}$, $c_0 = 1.41\ \mathrm{mg}\,\mathrm{l}^{-1}$

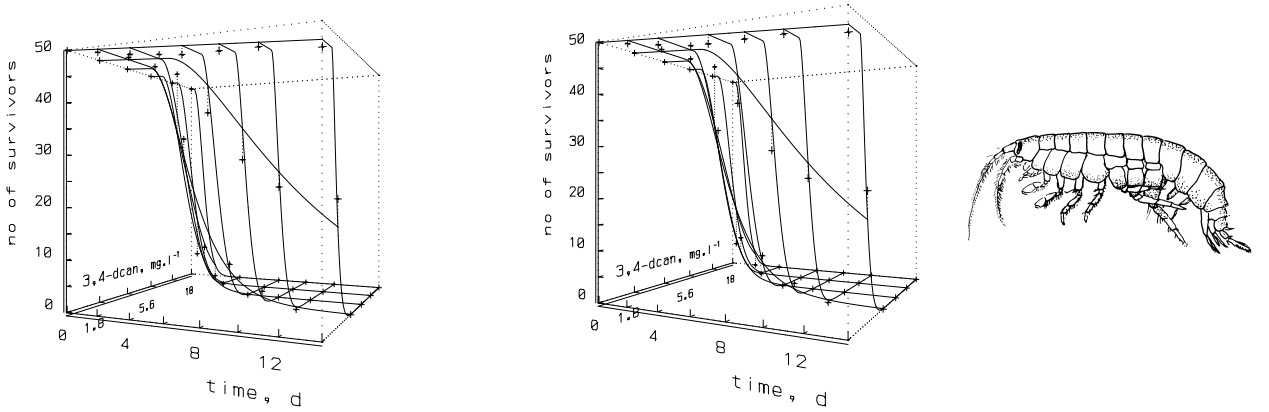

daphnids (*Daphnia magna*) in potassium dichromate
$\dot{b}_\dagger = 0.40\ \mathrm{l}\,\mathrm{mg}^{-1}\,\mathrm{d}^{-1}$, $\dot{k}_e = 0.125\ \mathrm{d}^{-1}$, $c_0 = 0.26\ \mathrm{mg}\,\mathrm{l}^{-1}$

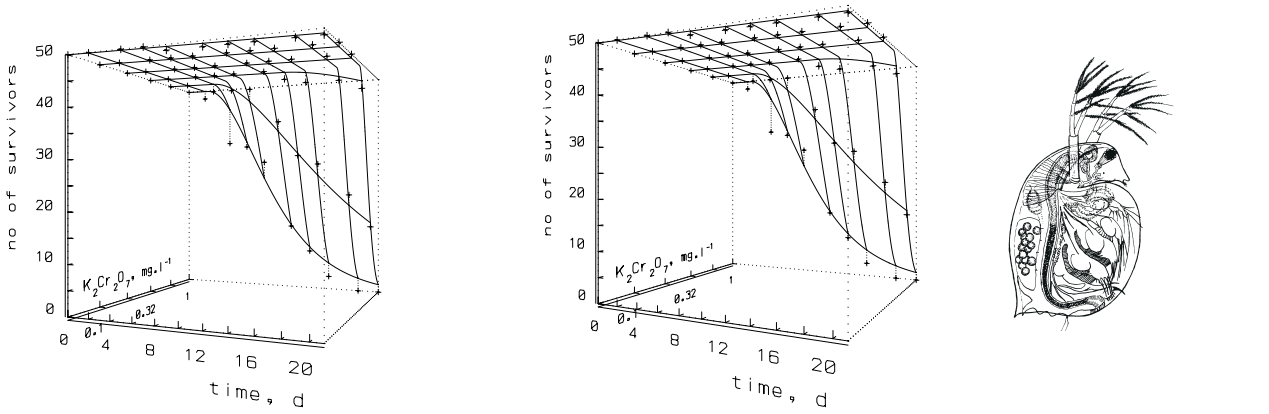

Figure 6.7: Stereo view of the number of surviving individuals, z-axis, as a function of exposure time, x-axis, to toxic compounds, y-axis. The expected number of surviving individuals is based on the idea that the hazard rate is proportional to the concentration in the tissue that exceeds the NEC under first-order kinetics. Unpublished data, kindly provided by Ms Adema (IMW–TNO laboratories).

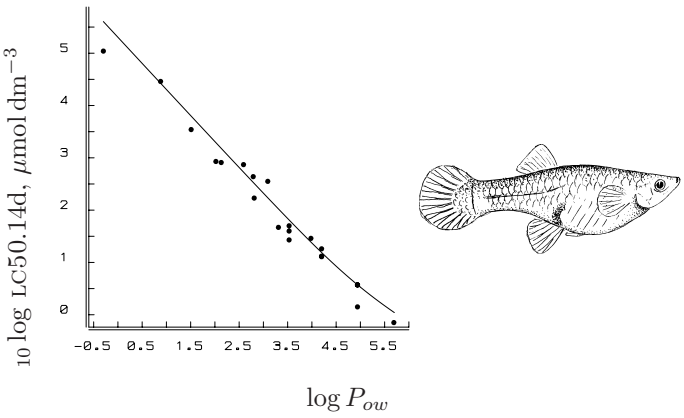

Figure 6.8: The 14 days LC50 values as a function of octanol-water partition coefficient for guppies (*Poecilia reticulata*) exposed to 21 chlorinated aromatic and other some chlorinated hydrocarbons whose P_{ow} ranged from $10^{-0.22}$ (pentachlorobenzene) to $10^{5.21}$ (acetone). (Data from Könemann [504]). The calculations are based on the assumptions that the elimination rates equal $50/\sqrt{P_{ow}}$ d^{-1}, the killing rates equal $10^{-6.6}P_{ow}$ d$^{-1}\mu$mol^{-1}dm^3 and the NECs are zero (see text).

environment, changes in the nutritional status of the animals, growth, reproduction, etc. If experimental research and model-based analysis of results are combined in the proper way, one will probably feel an increasing need to define precise experimental conditions and avoid complicating factors, such as uncontrolled changes in exposure.

This description of effects on survival makes the theory on competing risks available for direct application to toxicity and links up smoothly with standard statistical analyses of hazard rates; see for instance [51,179,197,463,606]. The significance of a toxic stress for a particular individual depends on other risks, such as aging and starvation. If $\dot{h}$ stands for the hazard tied to aging as before, and $\dot{h}_p$ for other risks, such as predation, an obvious instantaneous measure for the significance of the toxic stress is

$$\dot{h}_c(\dot{h} + \dot{h}_c + \dot{h}_p)^{-1}$$

Ionization and P_{ow}

Since the stress value is linear in the number of molecules in the organism, it follows directly from (6.11) that the killing rate and the NEC depend on the pH and the pK as

$$\dot{b}_\dagger(\mathrm{pH}) = \frac{\dot{b}_\dagger(-\infty) + \dot{b}_\dagger(\infty)10^{\mathrm{pH-pK}}}{1 + 10^{\mathrm{pH-pK}}}; \quad c_0^{-1}(\mathrm{pH}) = \frac{c_0^{-1}(-\infty) + c_0^{-1}(\infty)10^{\mathrm{pH-pK}}}{1 + 10^{\mathrm{pH-pK}}}$$

where $\dot{b}_\dagger(-\infty)$ and $\dot{b}_\dagger(\infty)$ stand for the killing rate if all of the compound were present in, respectively, the molecular and the ionized form and pK is the dissociation coefficient. A similar relationship has been proposed by Könemann [504] for LC50^{-1}, where the LC50 is defined as the concentration $c_{L50}(t)$ for which $q(c_{L50}(t), t) = 0.5$ holds; it is frequently used as a quantifier for lethal effects.

Since the equilibrium tissue concentration is proportional to P_{ow}, we should expect to find that the killing rate $\dot{b}_\dagger \propto P_{ow}$, the tolerance concentration $c_* \propto P_{ow}^{-1}$ and the NEC $c_0 \propto P_{ow}^{-1}$. The empirical study by de Wolf [1012] supports these expectations.

Könemann [505] observed that the 14 days log LC50 of the guppy *Poecilia reticulata* for 50 'industrial chemicals' is LC50 $= 0.0794\, P_{ow}^{-0.87}$ mol dm^{-3}. To understand this relationship,

we have to realize that for a large elimination rate, so a small P_{ow}, the 14 days LC50 is close to the ultimate value, but for a large P_{ow}, the ultimate LC50 is much lower than the LC50.14d. Taking these complexities into account, Figure 6.8 confirms that $\dot{b}_\dagger \propto P_{ow}$ and $\dot{k}_e \propto P_{ow}^{-0.5}$ are indeed consistent with the finding by Könemann (see). Unfortunately, the data of Figure 6.8 did not allow us to check the relationship for the NEC. Although the NECs had been set to zero, adopting the function NEC $= 10P_{ow}^{-1}$ mmol dm^{-3} hardly changes the result. The conclusion is that the quantitative structure–effects relationships for LC50s follow from first principles.

6.4.3 Effects on growth and reproduction

Toxic effects of chemicals change the allocation via the parameter values. Since the processes of assimilation (i.e. the combination of feeding and digestion), growth, maintenance and reproduction are intimately interlinked, changes in any of these processes will result in changes in reproduction [519]. Two classes for the mode of action of compounds will be distinguished: direct and indirect effects on reproduction.

When reproduction is affected directly, assimilation, growth and maintenance are not affected. There are two closely related routes within the DEB framework to affect reproduction directly. One is via survival of each ovum, and the other is via the energy costs of each egg.

Direct effects on reproduction

The survival probability of each ovum is affected as discussed in the previous section on effects on survival, except that the sensitive period is taken to be relatively short and fixed rather than the whole life span. (Age zero refers to the moment at which the ovum starts to develop, rather than the moment of hatching or birth.) The combination of an effect on the hazard rate of the ovum and a fixed sensitive period results in a survival probability that depends on the local environment of the ovum. This leads to another important difference with the previous section: the local environment of the ovum is the tissue of the mother rather than the environment concentration. The relevant concentration, therefore, changes in time even if the environment concentration is constant. The toxicity parameters that appear in the survival probability of an ovum are the NEC, as before, and the tolerance concentration, which is inversely related to the product of the killing rate and the length of the sensitive period. The elimination rate defines how the effect builds up during exposure.

In terms of number of eggs per time, the reproduction rate equals the ratio of the energy allocated to reproduction and the energy costs of an egg. If the compound affects the latter, it can be modelled by making the energy costs a (linear) function of the tissue concentration. The model is mathematically different from the hazard model but behaves quantitatively rather similarly, as is illustrated in Figure 6.9.

Indirect effects on reproduction

Allocation to reproduction starts as soon as the cumulative investment in the increase of the state of maturity exceeds some threshold value. Since direct effects on reproduction

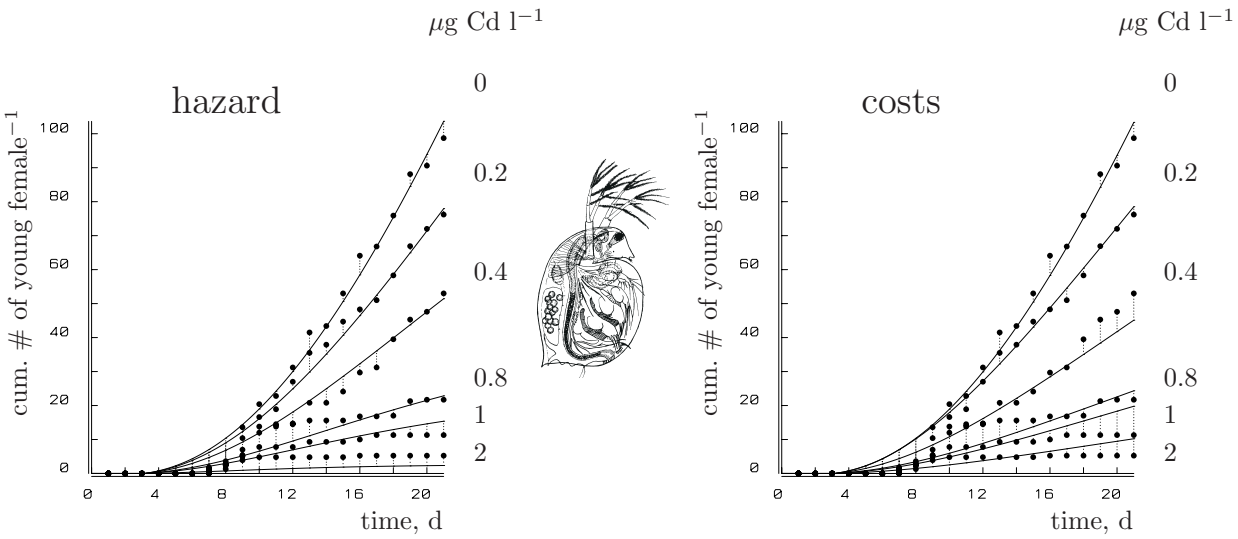

Figure 6.9: Direct effects of cadmium on *Daphnia* reproduction. The mean cumulated number of young per female daphnid as a function of the exposure time to several concentrations of cadmium. The fitted curves represent least-squares fits of the hazard (left) and the cost (right) model for effects on reproduction to the same data.

Given an elimination rate of $\dot{k}_e = 0.05$ d^{-1}, the estimated values for the NEC c_0, the tolerance concentration c_* and the maximum reproduction rate $\dot{R}_m$ in the control are

	c_0,μg l^{-1}	c_*,μg l^{-1}	$\dot{R}_m$,d^{-1}
hazard	0.023	0.166	13.1
cost	0.047	0.069	13.1

only affect the translation from energy allocated to reproduction into number of offspring, these modes of action do not affect the time of onset of reproduction. Indirect effects on reproduction via assimilation, maintenance and growth do delay the onset of reproduction. The occurrence of such delays is the best criterion for distinguishing direct from indirect effects.

Indirect effects on reproduction all follow the same basic rules: the relevant parameter (surface-specific assimilation rate, volume-specific maintenance costs or volume-specific costs of structure) is taken to be a linear function of the tissue concentration. Since the assimilation rate represents a source of income rather than costs, it is assumed to *decrease* linearly with the tissue concentration rather than increase, see Figure 6.10. This is consistent with the effect of oxygen on the assimilation of autotrophs: photorespiration subtracts from photosynthesis, see {166}.

The effects on the reproduction rate as a function of environment concentration and exposure time all work out rather similarly and have the same three toxicity parameters: NEC, tolerance concentration and elimination rate. If growth is measured during exposure, or if the animals' size at the end of the exposure period is measured, it is possible to identify the mode of action. The differences in effects on reproduction are too small to identify the mode of action on the basis of effects on reproduction alone. Figure 6.11 compares the three indirect effect models fitted to the same data. It shows that the models differ little in terms of goodness of fit.

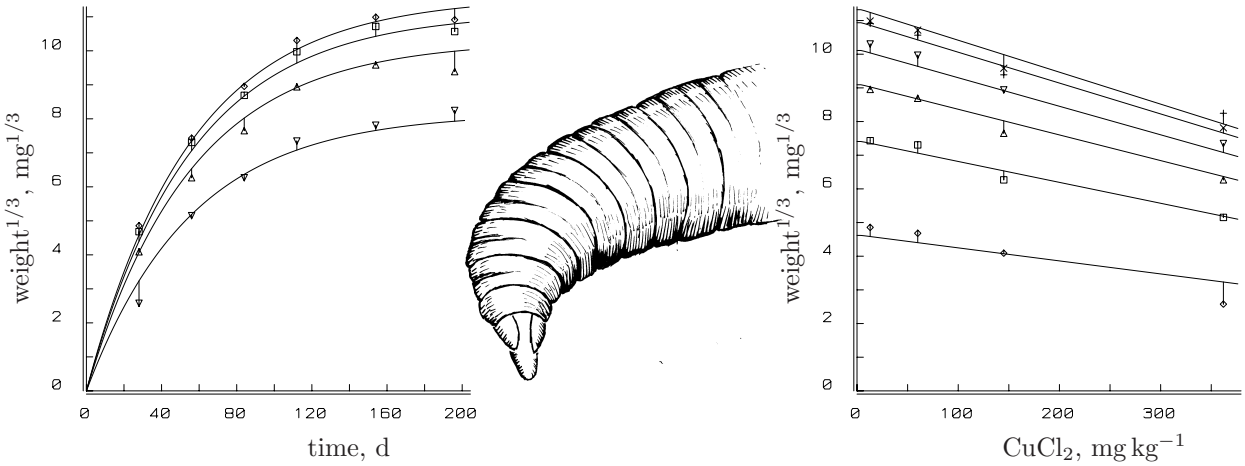

Figure 6.10: The effect of $CuCl_2$ on the assimilation of *Lumbricus rubellus*. Data kindly provided by Mrs C. Klok [492] and fits by J. J. M. Bedaux. The newly hatched worms were exposed in sandy loam soil and fed *ad libitum* with *Alnus* leaves at 15 °C and 90% relative humidity. Parameter values: $W_b = 0$ mg, $W_m = 11.66^3$ mg, $\dot{r}_B = 0.018$ d^{-1}, $g = 1$, $c_0 = 4.45$ mg kg^{-1}, $c_A = 1193$ mg kg^{-1}, $\dot{k}_e = \infty$ d^{-1}.

Stress value

The quantitative aspects of the various modes of action can be summarized as follows. The compound affects a single target parameter value at low concentrations via the dimensionless stress value $s = c_*^{-1}(c_V - c_0)_+ = (c_V/c_* - s_0)_+$, where c_V is the scaled tissue concentration (that has the dimensions of an environment concentration), c_0 the NEC and c_* the tolerance concentration. The tolerance concentration is a parameter that has the dimension of an environment concentration, and it belongs to a specific physiological target parameter; its name refers to the fact that the value decreases for increasing toxicity of the compound.

The DEB model identifies the following target parameters: the maximum specific assimilation rate $\{\dot{p}_A\}$, the specific maintenance rate $[\dot{p}_M]$, the costs of structure $[E_G]$, the costs of reproduction E_0, and the hazard of the ovum $\dot{h}$ (during a short period). It is conceivable that other parameters can be affected as well, such as the threshold for the cumulative investment in development that triggers the stage transition. These primary parameters can be written as simple functions of the stress value, and occur in a number of compound parameters that define the post-embryonic growth and reproduction process via

$$\frac{d}{dt}e = (f-e)\frac{\dot{k}_{Ms}g_s}{l} \tag{6.29}$$

$$\frac{d}{dt}l = (l_{ms}e - l)\frac{\dot{k}_{Ms}g_s}{3(e+g_s)} \tag{6.30}$$

$$\dot{R}_s(l) = \frac{\dot{R}_{ms}}{1-l_p^3}\left(\left(\frac{l_{m0}}{l_{ms}}\right)^3 \frac{el^2}{g+e}\left(\frac{\dot{k}_{M0}}{\dot{k}_{Ms}}g_0 + l\right) - l_p^3\right)_+ \tag{6.31}$$

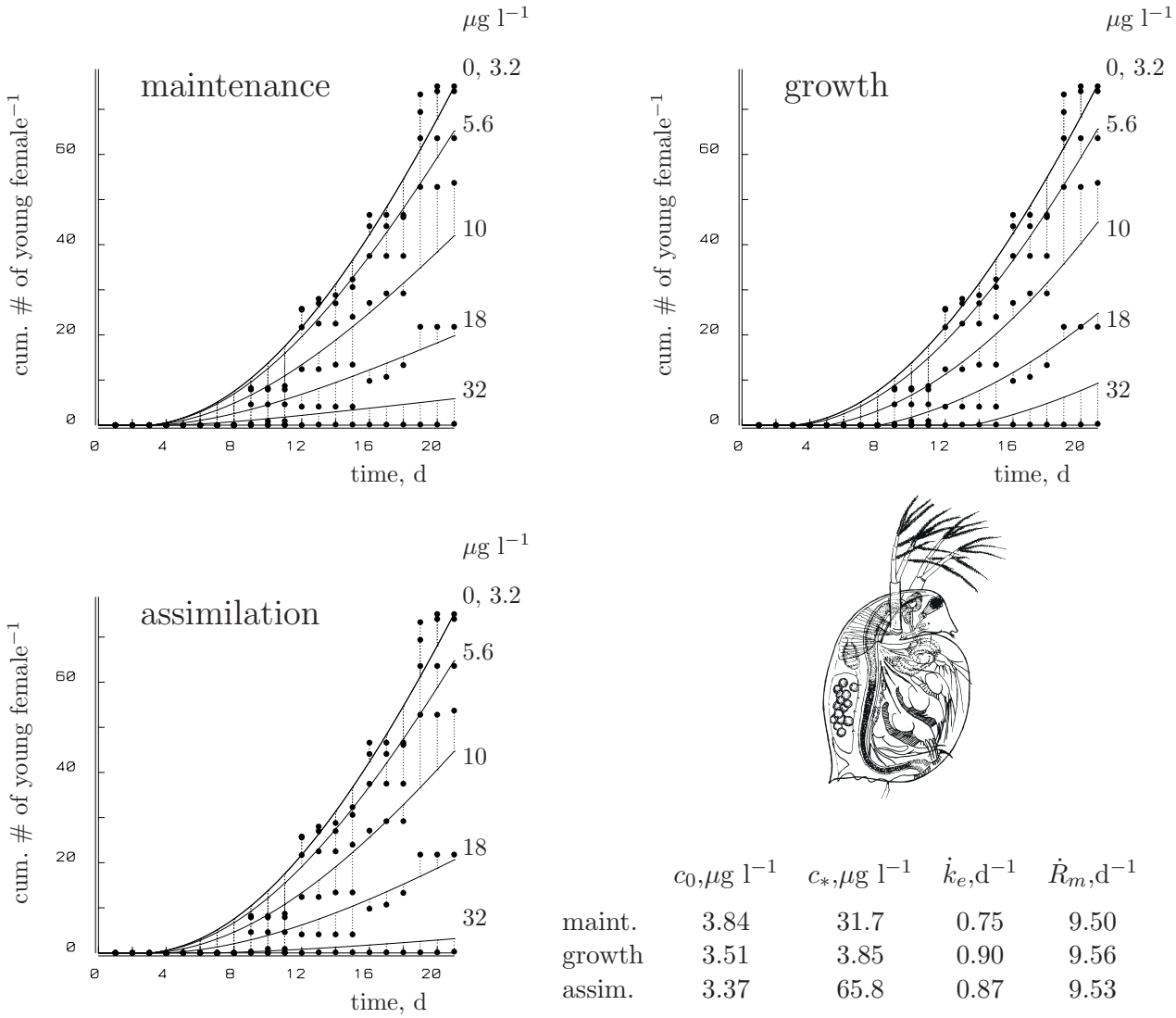

	c_0,μg l^{-1}	c_*,μg l^{-1}	$\dot{k}_e$,d^{-1}	$\dot{R}_m$,d^{-1}
maint.	3.84	31.7	0.75	9.50
growth	3.51	3.85	0.90	9.56
assim.	3.37	65.8	0.87	9.53

Figure 6.11: Indirect effects of 3,4-dichloroaniline on *Daphnia* reproduction. The mean cumulated number of young per female daphnid as a function of the exposure time to several concentrations of 3,4-dichloroaniline. The fitted curves represent least-squares fits of the model for effects on reproduction via maintenance, growth and assimilation to the same data. The estimated values for the NEC c_0, the tolerance concentration c_*, the elimination rate $\dot{k}_e$ and the maximum reproduction rate $\dot{R}_m$ in the control are given in the table of parameters.

where the index s indicates that the compound parameter depends on the stress value through multiplication of the value without stress (index 0) by a factor that is given in the table

model	target	$\frac{\dot{R}_{ms}}{\dot{R}_{m0}}$	$\frac{g_s}{g_0}$	$\frac{\dot{k}_{Ms}}{\dot{k}_{M0}}$	$\frac{l_{ms}}{l_{m0}}$
hazard	$\dot{h}_{\text{ovum}}$	$\exp\{-s\}$	1	1	1
costs	κ_R	$(1+s)^{-1}$	1	1	1
maint.	$[\dot{p}_M]$	$(1+s)\frac{1-l_p^3(1+s)^3}{1-l_p^3}$	1	$1+s$	$(1+s)^{-1}$
struct.	$[E_G]$	1	$1+s$	$(1+s)^{-1}$	1
assim.	$\{\dot{p}_{Am}\}$	$\frac{1-l_p^3(1-s)^{-3}}{1-l_p^3}$	$(1-s)^{-1}$	1	$1-s$

Growth and reproduction under stress, as given in (6.29), (6.30) and (6.31), should be supplemented with the scaled toxicokinetics (6.2), (6.14), (6.17), (6.23) or (6.24) and the initial conditions, to complete the specification. The dynamics of sublethal effects are thus characterized by just two parameters, the NEC c_0 and the tolerance concentration c_*, and at least one toxicokinetic parameter, the elimination rate $\dot{k}_e$. Additional parameters can be included in more elaborate descriptions of toxicokinetics. Although the stress value can change in time, because of a varying tissue concentration, none of these three parameters depends on exposure time, but the resulting effects can already be quite complex in transient environments.

6.4.4 Receptor-mediated effects

Up till now, the effect of a compound has been taken directly proportional to the tissue concentration. In a number of cases, the effect might be more complex, and does not only relate to the actual tissue concentration, but also to its (recent) history. A simple model on the basis of receptors gives an example.

Suppose that the total number of receptors N_+ in an organism remains constant, and that the compound transforms functional receptors into non-functional ones at a rate that is proportional to the 'meeting frequency' between the compound and the number of functional receptors. Non-functional receptors can resume their functioning at a given probability rate, or the organism can produce new functional receptors at a rate that is proportional to the number of non-functional receptors. Let $N_n(t)$ denote the number of non-functional receptors, and $N_f(t)$, the number of functional ones, while $N_n(t) + N_f(t) = N_+$. The change in the number of non-functional receptors then amounts to

$$\frac{d}{dt}N_n = \dot{b}_{fn}c_V N_f - \dot{r}_{nf}N_n = \dot{b}_{fn}c_V N_+ - (\dot{r}_{nf} + \dot{b}_{fn}c_V)N_n \tag{6.32}$$

with $\dot{r}_{nf}$ the specific recovery rate, $\dot{b}_{fn}$ the knock-out rate, and c_V the scaled tissue concentration. The stress value can be taken linear in the number of non-functional receptors, $s = N_s^{-1}(N_n - N_0)_+ = (N_n/N_s - s_0)_+$, where the parameter N_s scales the number of non-functional receptors to the stress, and N_0 is the number of non-functional receptors that

does not result in an effect on the stress. If we start with unexposed individuals, we have $N_n(0) = 0$, $N_f(0) = N_+$ and $c_V(0) = 0$. This formulation can be combined with a simple first-order kinetics for the tissue concentration, if the amount of compound involved in the binding process is negligibly small.

The model has the interesting property that the amount of memory of the effect is tunable. For large values of $\dot{b}_{fn}$ and $\dot{r}_{nf}$, the number of non-functional receptors is in pseudo steady state, the amount of memory is negligibly small, and the stress is a hyperbolic function of the tissue concentration, rather than a linear one, since $N_n \simeq N_+ \left(1 + \frac{\dot{r}_{nf}}{\dot{b}_{fn} c_V}\right)^{-1}$. If $\dot{r}_{nf} \gg \dot{b}_{fn}$ and N_s is small, or the concentration is small, the model converges to the earlier one, where the effect depends linearly on the actual tissue concentration.

Receptor-mediated effects on survival can be modelled by simply taking the hazard rate as being proportional to the stress, which amounts to the coupled differential equations for the scaled number of non-functional receptors $n_n = N_n/N_+$ and the survival probability q

$$\frac{d}{dt} n_n = \dot{b}_{fn} c_V - (\dot{r}_{nf} + \dot{b}_{fn} c_V) n_n; \quad \frac{d}{dt} q = -q(\dot{k}_\dagger n_n - \dot{h}_0)_+$$

on the assumption that all of the compound in tissues contributes to knocking out receptors, but that the individual can handle a threshold level of non-functioning receptors.

6.4.5 Mutagenic effects

Ames test

The *Salmonella* test, also known as the Ames test, is a popular test for the mutagenic properties of a compound [19,591]. It is discussed here because the results of the test can sometimes only be understood if energy side-effects are taken into account, for which the DEB model gives a useful framework [420].

The test is carried out as follows. Bacteria (mutants of *Salmonella typhimurium*) that cannot produce the amino acid histidine are grown on an agar plate with a small amount of histidine but otherwise large amounts of all sorts of nutrients. When the histidine becomes depleted, these histidine auxotrophs stop growing at a colony size of typically 8–32 cells. Histidine auxotrophic bacteria can undergo a mutation enabling them to synthesize the necessary histidine themselves, as can the wild strain. They become histidine-prototrophic and continue to grow, even if the histidine on the plate is depleted. (They only synthesize histidine if it is not available in the environment.) Colonies that contain histidine-prototrophs are called revertant colonies and can eventually be observed with the naked eye when the colony size is thousands of cells. The number of revertant colonies relates to the concentration of the compound that has been added to the agar plate and its mutagenic capacity.

Liver homogenate of metabolically stimulated rats is sometimes added to simulate mutagenicity for vertebrates. The primary interest in mutagenicity is because of human health problems, as explained. Vertebrates have many metabolic pathways that prokaryotes do not have. Enzymes in this homogenate sometimes transform non-mutagenic compounds into mutagenic ones, sometimes they do the opposite or have no effect at all.

Some initial histidine is necessary, because bacteria that do not grow and divide do not seem to mutate, or, at least, the mutation is not expressed. This ties mutation frequency to energetics. It is a most remarkable observation, with many consequences. Since maintenance processes also involve some protein synthesis, one would think that mutations should also be expressed if growth ceases, but observation teaches otherwise. If a compound is both mutagenic and reduces growth, the moment of histidine depletion is postponed, so that effective exposure time to the mutagenic compound is increased. Some brands of agar contain small amounts of compounds that become (slightly) mutagenic after autoclaving. This gives a small mutagenic response in the blank. If a test compound only affects growth and is not mutagenic at all, the number of revertant colonies will increase with the concentration of test compound. Such responses make it necessary to model the combined mutation/growth process for the interpretation of the test results.

The rest of this section gives a simple account, appropriate for DEB V1-morphs from a culture that resembles the (initial) growth conditions on the agar plate. For a more detailed account; see [420]. A description for DEB rods would be more accurate but also more complex and would hide the message.

Suppose that the initial amount of histidine on a plate is just enough for the synthesis of N_h cells. Figure 9.7 shows that the histidine reserves are small enough to be neglected. If the inoculum size on the plate is N_0, the number of cells develops initially as $N(t) = N_0 \exp\{\dot{r}t\}$. Histidine thus becomes depleted at time $t_h = \dot{r}^{-1} \ln\{1 + N_h/N_0\}$. If the mutation rate per unit of DNA is constant, say at value $\dot{h}_M$, the probability of at least one mutation occurring in the descendants of one auxotrophic cell becomes for low mutation rates

$$1 - \exp\left\{-\dot{h}_M \int_0^{t_h} (N(t)/N_0)\, dt\right\} = 1 - \exp\left\{-\frac{\dot{h}_M N_h}{\dot{r} N_0}\right\} \simeq \frac{\dot{h}_M N_h}{\dot{r} N_0} \tag{6.33}$$

The probability of back mutation is small enough to be neglected. The expected number of revertant colonies is N_0 times (6.33), so that the number of revertant colonies is hardly affected by the inoculum size. The effect of an increase in the number of micro-colonies on the plate is cancelled by the resulting reduction of exposure time.

A consequence of the assumption that the mutation frequency per unit of DNA is constant is that the mutations are independent of each other. This means that the number of revertant colonies on a plate follows a binomial distribution, which is well approximated by the Poisson distribution for low mutation rates. (There are typically less than 100 revertant colonies with a typical inoculum size of 10^8 per plate.)

The significance of this expression is that the effect of inoculum size and the amount of histidine become explicit. Variations in these variables, which are under experimental control, translate directly into extra variations in the response. If a compound affects the population growth rate, it also affects the expected number of revertant colonies. I refer to the subsection on population growth rates, {217}, for a discussion of how individual performance (substrate uptake, maintenance, growth) relates to population growth rates. This defines how effects on individual performance translate into effects on population growth rates. This remark not only applies to effects of the test compound, but also to the nutritional quality of the agar.

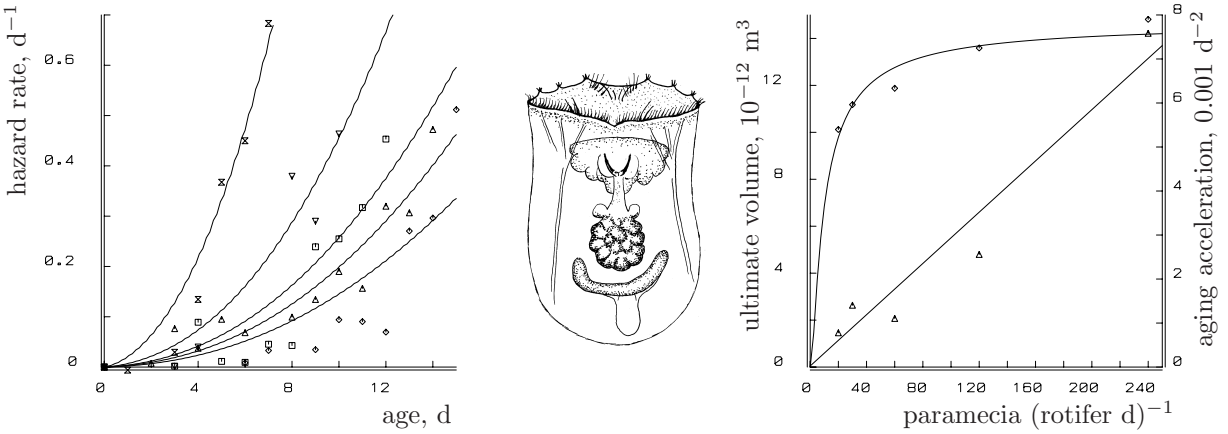

Figure 6.12: The hazard rates for the rotifer *Asplanchna girodi* for different food levels: 20 (◇) 30 (△) 60 (□) 120 (▽) and 240 (⋈) paramecia rotifer^{-1} d^{-1} at 20 °C. Data from Robertson and Salt [777]. The one-parameter hazard curves are based on the scaled food densities as estimated from the ultimate volumes (◇, right), which give f = 0.877, 0.915, 0.955, 0.977, 0.988. The resulting five aging accelerations are plotted in the right figure (△). They proved to depend linearly on food density, with an intercept that is consistent with the aging acceleration found for daphnids.

The mutation rate is usually found to be proportional to the concentration of test compound. This means that each molecule has a certain probability of causing a mutation. Deviations from this relationship can usually be related to changes in the stability of the compound on the plate. Many mutagenic compounds are rather reactive, so the concentration usually decreases substantially before t_h. Others, such as nitrite, diffuse to the deeper layers of the agar plate and become less available to the bacteria in the upper layer. It is easy to circumvent this problem by adding the compound to the (thick) nutritive bottom layer when it is still liquid, rather than to the (thin) top layer. However, this would increase the financial costs of the test. If metabolic activation is applied, the concentrations of the original compound and the products are likely to become complex compound-specific functions of time. One strategy for interpreting the test results is to analyse and model the time stability of compounds in the Ames test. A better strategy would be to change the experimental procedure in such a way that these complexities do not occur.

Food-induced aging acceleration

Some data sets, such as that of Robertson and Salt [777] on the rotifer *Asplanchna girodi* feeding on the ciliate *Paramecium tetraurelia*, indicate that the hazard rate increases sharply with food density. See Figure 6.12. Although the shapes of the hazard curves are well described by (4.22), this equation does not predict the extreme sensitivity to food density. This particular data set shows that aging acceleration is linear in the food density, which suggests that something that is proportional to food density affects the build-up of damage-inducing compounds or the transformation of these compounds into damage. One

possibility is nitrite derived from the lettuce used to culture the ciliates; nitrite is known for its mutagenic capacity [420].

6.4.6 Effects of mixtures

The toxicity of mixtures of compounds is of substantial practical interest, which explains the wide interest in the subject. A compound that can be present in molecular and ionic forms can be thought of as a mixture. Since the stress value is assumed to depend linearly on the tissue concentration, the evaluation of effects of binary mixtures of compounds within the DEB context is relatively straightforward. If two compounds have the same physiological target parameter, and do not interact, a natural choice for the stress value would be

$$s = (c_{V1}/c_{*1} + c_{V2}/c_{*2} - s_0)_+ \tag{6.34}$$

where c_{V1} and c_{V2} are the scaled tissue concentrations of compounds 1 and 2, c_{*1} and c_{*2} are the tolerance concentrations, and s_0 is the stress value that the organism can handle, without showing effects. The idea is that the threshold s_0 reflects the physiological flexibility of the organism, rather than an absence of effects at the molecular level. Such a mechanism would suggest $s = (c_{V1} - c_{01})_+/c_{*1} + (c_{V2} - c_{02})_+/c_{*2}$, which has one parameter more. Since the elimination rates can differ for the two compounds, such an extra parameter would add up to at least six toxicity parameters for the dynamic effects of the mixture if there is no interaction between the compounds.

Compounds can interact in complex ways in their toxic effects. Hewlett and Plackett [407] found that the insecticide thanite intensifies biochemically the toxicity of aprocarb, but that the inverse was not the case. Excluding this type of complex interaction, we can think of the stress value as some non-linear function of the two tissue concentrations, where we are interested in small stress values only. For this purpose, we can introduce an interaction term as is standard in the analysis of variance, and arrive at

$$s = \left(\frac{c_{V1}}{c_{*1}} + \frac{c_{V2}}{c_{*2}} + \frac{c_{V1}c_{V2}}{C_*} - s_0\right)_+ \tag{6.35}$$

where the parameter C_* (dimension: squared environment concentration) is inversely proportional to an interaction term, analogous to the model of the analysis of variance. It can be positive, in the case of synergism, and negative, if the compounds counteract. For effects on the hazard rate, this translates to

$$\dot{h}_c = (\dot{b}_{\dagger 1}c_{V1} + \dot{b}_{\dagger 2}c_{V2} + \dot{B}_\dagger c_{V1}c_{V2} - \dot{h}_0)_+ \tag{6.36}$$

where $\dot{B}_\dagger$ is the interaction parameter, and $\dot{h}_0$ the hazard rate that measures the stress value with which the animal can cope without effects on survival.

6.4.7 Population consequences of effects

The general theory to evaluate properties of individuals in terms of dynamics of populations is discussed on {303}ff. Here I only remark that different modes of action translate differently to consequences for the population, which can be understood intuitively as follows.

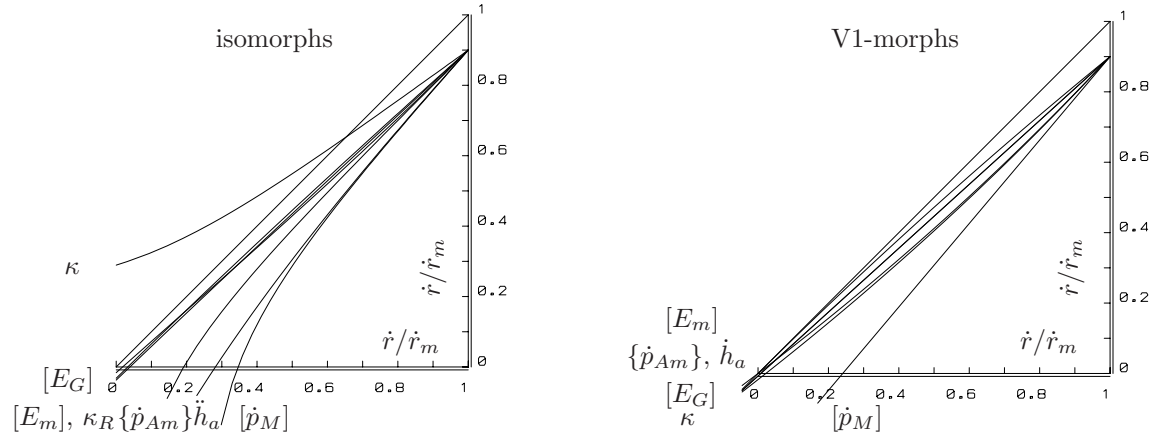

Figure 6.13: Population growth rate in a stressed situation is plotted against that in a blank situation, when only one energy parameter is affected at the same time for reproducing isomorphs (left) and dividing filaments (right). The effect of compounds with different modes of action is standardized such that the maximum population growth rate is 0.9 times that in the blank. Food density is assumed to be constant. Relative effects in isomorphs on structure costs $[E_G]$, reserve capacity $[E_m]$ and reproduction κ_R are almost independent of the feeding conditions, while those on assimilation $\{\dot{p}_{Am}\}$, maintenance $[\dot{p}_M]$ and survival $\ddot{h}_a$ are much stronger under poor feeding conditions. The effect on the partitioning fraction κ is different from the rest and probably does not correspond to an effect of a toxic compound. The relative effects on filaments are largely comparable to those on isomorphs for growth and maintenance. Effects on assimilation $[\dot{p}_{Am}]$ coincide with effects on survival $\dot{h}_a$.

If the population is at its carrying capacity, $\dot{r} = 0$, and reproduction and loss rates are both very low, food availability completely governs the reproduction rate. All resources are used for maintenance. Effects on maintenance, therefore, show up directly in this situation, but effects on growth and reproduction remain hidden, unless the effect is so strong that replacement is impossible. If the population is growing at a high rate, energy allocation to maintenance is just a small fraction of available energy. Even considerable changes in this small fraction will, therefore, remain hidden, but effects on production rates are now revealed. These principles are illustrated in Figure 6.13. They imply that at a constant concentration of compound in the environment, the effect at the population level depends on food availability and thus is of a dynamic nature. This reasoning does not yet use the more subtle effects of uptake via food as opposed to those via the environment directly.

The effects at low population growth rates can be studied if the population is at its carrying capacity. If food supply to a fed-batch culture is constant, the number of individuals at carrying capacity is proportional to the food supply rate, cf. Figure 9.16. If the loss rate, and so the reproduction rate, is small, the ratio of the food supply rate to the number of individuals is a good measure of the maintenance costs. Figure 6.15 illustrates that some compounds, such as vanadium and bromide, affect these maintenance costs, while others do not and 'only' cause death in this situation. It also shows that the effect is almost linear in the concentration, as are the effects on survival, aging and mutagenicity.

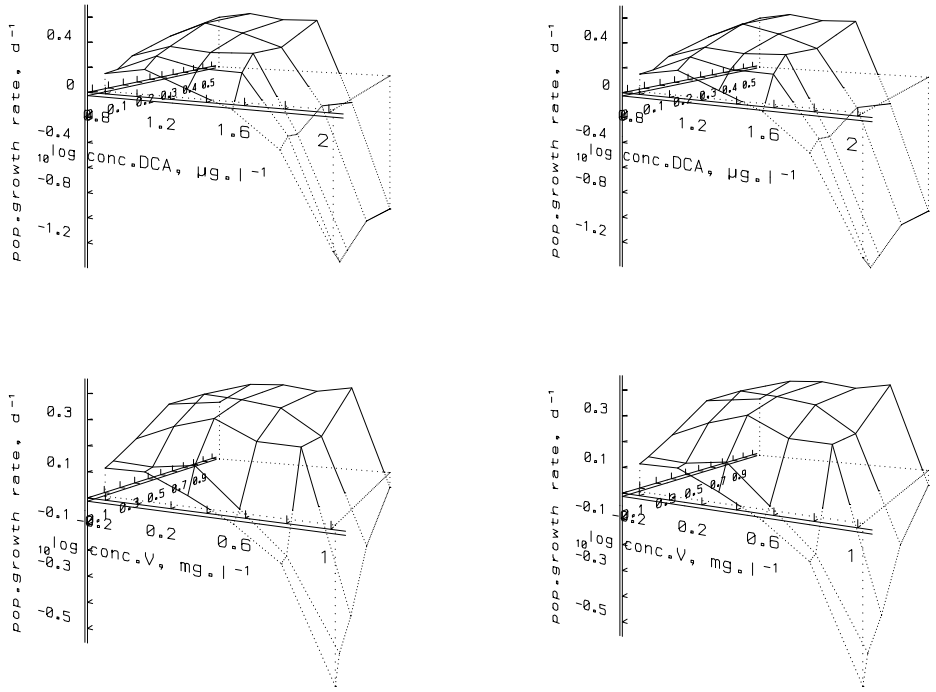

Figure 6.14: Stereo view of the population growth rate of the rotifer *Brachionus rubens* (z-axis) as a function of food density (y-axis) and concentration of toxic compound (x-axis): 3,4 dichloroaniline (above) and potassium metavanadate (below). Food density is in 1.36×10^9 cells *Chlorella pyrenoidosa* per litre, temperature is 20 °C. The difference in shape of the response surfaces is due to differences in the mode of action of the compounds, as predicted by the DEB theory.

6.5 Summary

Non-essential compounds are taken up in a similar way to essential ones, the difference is in their use: non-essential ones are not used, but eliminated. The concentrations in the environment are usually small enough to let the uptake rate be proportional to the concentration, and densities in the body are usually small enough to let the elimination rate be proportional to the density in the body. On the basis of the fugacity argument, this first-order kinetics provides the rules for how kinetic parameters co-vary among compounds with the octanol–water partition coefficient, and the ionization constant.

Energetics modifies the kinetics in a number of ways: dilution by growth, changes in the body's lipid content, the existence of several uptake and elimination routes, and metabolic transformation. Since the exchange rate with the environment is proportional to the surface area of the body, these various modifications link up beautifully with the structure of the DEB model, and are evaluated in this chapter.

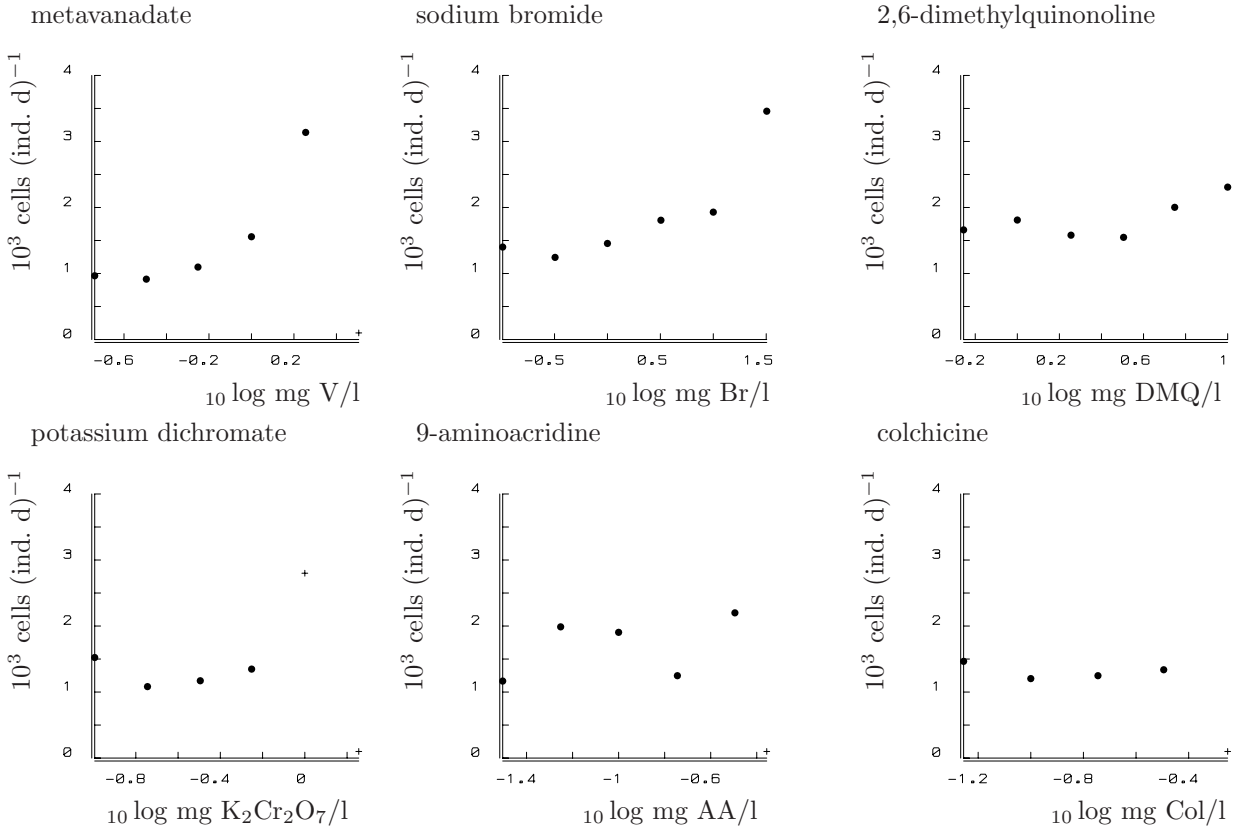

Figure 6.15: The ratio of the food supply rate for a population of daphnids to the number of individuals at carrying capacity in fed-batch cultures as a function of the concentration of compound at 20 °C. The crosses, +, refer to the occurrence of mortality. Only compounds that affect maintenance give a positive response.

Non-essential compounds can modify energetics in a number of ways, by changing one or more parameters of the DEB model. Small changes in the parameter values can taken to be linear in the density of non-essential compounds in the body, on the basis of the Taylor approximation. The changes can be effectuated by multiplying the appropriate parameter(s) with a time-varying stress factor. This quantifies the direct and indirect effects of compounds on energetics dynamically as a function of the concentration in the environment and exposure time, and provides the basis of the estimation of NECs of non-essential compounds. This is of substantial value for Environmental Risk Assessment for toxicants produced by humans.

The description of the effects of non-essential compounds in terms of changes in the parameter values allows the effects of compounds on individuals to be translated into those on populations. Effects at the molecular level have a NEC of zero, because each molecule can react. At the individual level, it is generally larger than zero, because individuals can handle small physiological handicaps. At the population level, effects can vary with food levels even if toxicokinetics is in full steady state; this depends on the mode of action of the compound.

Chapter 7

Case studies

The purpose of this chapter is to place the DEB theory in a wider context and to evaluate combinations of primary processes and their consequences. The last three chapters treated them one by one, as far as possible, to reveal and explain the basic structure of the theory. Now the models for the primary processes will gain colour as the processes change together in a variable environment. Each section can be read independently, and deals with a problem that may have taxon-specific elements. Some applications aim to illustrate how particular measurements can be interpreted within the context of the DEB theory; some aim to show how mechanisms that are included can interact and explain observed phenomena; other applications are in fact extensions of the DEB theory in various directions to reveal constraints for modelling processes at a lower level of organization, and to show how such processes give some background for the assumptions on which the DEB model is based.

Although the sections cover a range of topics, many important ones are painfully lacking, which only reflects that the theory is still in a stage of development. My hope is that it is possible to reduce the dazzling amount of seemingly complex eco-physiological phenomena to a small set of simple underlying principles that can be based on lower levels of organization help to structure modelling attempts at the biochemical level.

7.1 Changing feeding conditions

Food density is never really constant, as experienced by an individual. The relative size of food particles with respect to the individual and the food density itself are important. Moreover, feeding frequently takes the form of meals. The next subsections analyse phenomena at an increasing time scale.

7.1.1 Scatter structure of weight data

For simplicity's sake, the processes of feeding and growth have been modelled deterministically, so far. This is not very realistic, as (feeding) behaviour especially is notoriously erratic. This subsection discusses growth if feeding follows a special type of random process, known as an alternating Poisson process or a random telegraph process. Because of the resulting complexity, I rely here on computer simulation studies.

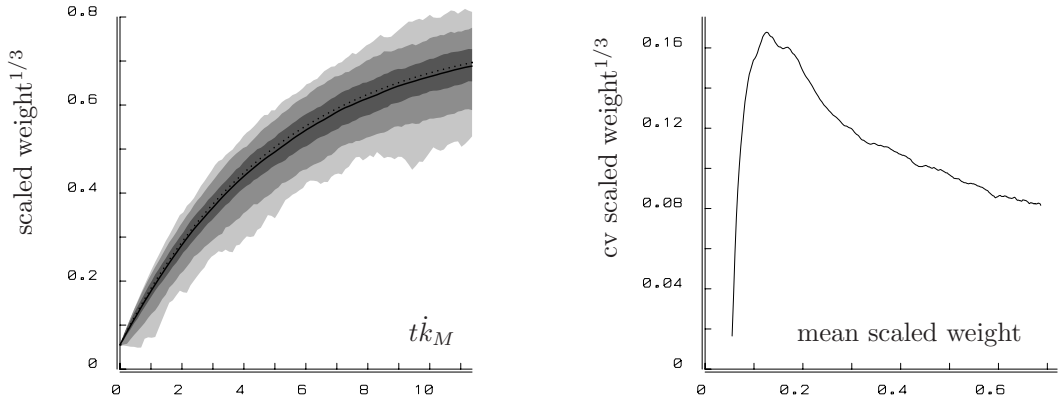

Figure 7.1: Computer-simulated scaled weight$^{1/3}$, $(W_w/d_V V_m)^{1/3}$, is plotted against scaled time in the left figure, if feeding follows an alternating Poisson process. The shade areas give frequency intervals of 99, 90 and 50%, the drawn curve gives the mean and the dotted one gives the deterministic growth curve, if feeding is constant at the same mean level. The coefficient of variation is given in the right figure. The parameters are $\lambda_0 = 11.666$, $\lambda_1 = 5$, $g = 1$, $l_b = 0.05$ and $w_E[M_{Em}]/d_V = 0.5$. The small difference between the mean and deterministic curves relates to the step size of the numerical integration (Mrs F. D. L. Kelpin, pers. comm.).

Suppose that feeding occurs in meals that last an exponentially distributed time interval $\underline{t}_1$ with parameter $\dot{\lambda}_1$, so $\Pr\{\underline{t}_1 > t\} = \exp\{-t\dot{\lambda}_1\}$. The mean length of a meal is then $\dot{\lambda}_1^{-1}$. The time intervals of fasting between the meals is also exponentially distributed, but with parameter $\dot{\lambda}_0$. Food intake during a meal is copious, so the scaled functional response switches back and forth between $f = 1$ and $f = 0$. The mean value for f is $\mathcal{E}\underline{f} = \dot{\lambda}_0(\dot{\lambda}_0 + \dot{\lambda}_1)^{-1}$. This on/off process is usually smoothed out by the digestive system, but let us here assume that this is of minor importance. According to (4.8), (4.7), and Table 3.5, growth in scaled length of juveniles (that are able to shrink) is given by

$$\frac{d}{d\tau}e = \frac{g}{l}(f - e) \quad \text{and} \quad \frac{d}{d\tau}l = \frac{g}{3}\frac{e - l - l_h}{e + g}$$

where $\tau = t\dot{k}_M$ is the scaled time. A single parameter, g, is involved in this growth process, while two others, λ_0 and λ_1, occur in the description of the on/off process of f. (Note that the λ's do not have dots, because scaled time is dimensionless.) The process is initiated with $l(0) = l_b$ and $e(0)$ equals the scaled energy density of a randomly chosen adult.

Figure 7.1 shows the results of a computer simulation study, where scaled weight relates to scaled length and scaled energy density, according to (2.6) as

$$W_w(d_V V_m)^{-1} = (1 + e w_E[M_{Em}]/d_V) l^3$$

The resemblance of the scatter structure with experimental data is striking, see for instance Figure 2.5. This does not imply, however, that the feeding process is the only source of scatter. Differences of parameter values between individuals are usually important as well. The results do suggest a mechanism behind the generally observed phenomenon that scatter in weights increases with the mean.

7.1.2 Step up/down in food availability

The difference between age-based and size-based models becomes apparent in situations of changing food densities. As long as food density remains constant, size-based models can always be converted into age-based ones, which makes it impossible to tell the difference.

Figure 7.2 shows the result of an experiment with *Daphnia magna* at 20 °C, exposed to constant high food densities with a single instantaneous switch to a lower food density at 1, 2 or 3 weeks. The reverse experiment with a single switch from low to high food densities has also been done, together with continuous exposure to both food densities. Figure 3.14 has already shown that the maintenance rate coefficient $\dot{k}_M$ and energy conductance $\dot{v}$ can be obtained by comparing growth at different constant food densities. These compound parameters, together with ultimate and maximum lengths and the common length at birth, have been obtained from the present experiment without a switch. These five parameters completely determine growth with a switch, both up and down, leaving no free parameters to fit in this situation. The excellent fit strongly supports to the DEB theory.

7.1.3 Mild starvation

If a growing individual is starved for some time, it will (like the embryo) continue to grow (at a decreasing rate) till it hits the non-growth boundary of the state space ($e = l$). Equation (3.30) describes the e, l-path. Depending on the amount of reserves, the change in volume will be small for animals not far from maximum size. Strömgren and Cary [899] found that mussels in the range of 12–22 mm grew 0.75 mm. If the change in size is neglected, the scaled reserve density changes as $e(\tau) = e(0) \exp\{-g\tau/l\}$ and the growth of scaled length is $\frac{d}{d\tau} l = \frac{g}{3} \frac{\exp\{-g\tau/l\} - l/e(0)}{\exp\{-g\tau/l\} + g/e(0)}$. Figure 7.3 confirms this prediction.

Respiration during starvation is proportional to the use of reserves; see {135}. It should, therefore, decrease exponentially in time at a rate of $\dot{v} V^{-1/3}$ if size changes can be neglected. See (3.10). Figure 7.4 confirms this prediction for a daphnid. If a shape coefficient of $\delta_{\mathcal{M}} = 0.6$ is used to transform the length of the daphnid into a volumetric one, the energy conductance becomes $\dot{v} = 0.6 \times 1.62 \times 0.23 = 0.22$ mm d^{-1}. This value seems to be somewhat small in comparison with the mean energy conductance of many species, cf. {277}. The next section suggests an explanation in terms of changes in allocation rules to reproduction during starvation.

7.1.4 Food intake reconstruction

Many data sets on growth in the literature do not provide adequate information about food intake. Sometimes it is really difficult to gain access to this type of information experimentally. The blue mussel *Mytilus edulis* filters what is called 'particulate organic matter' (POM). Apart from the problem of monitoring the POM concentration relevant to a particular individual, its characterization in terms of nutritional value is problematic. The relative abundances of inert matter, bacteria and algae change continuously. In the search for useful characterizations, it can be helpful to invert the argument: given an observed size and temperature pattern, can the assimilation energy be reconstructed in

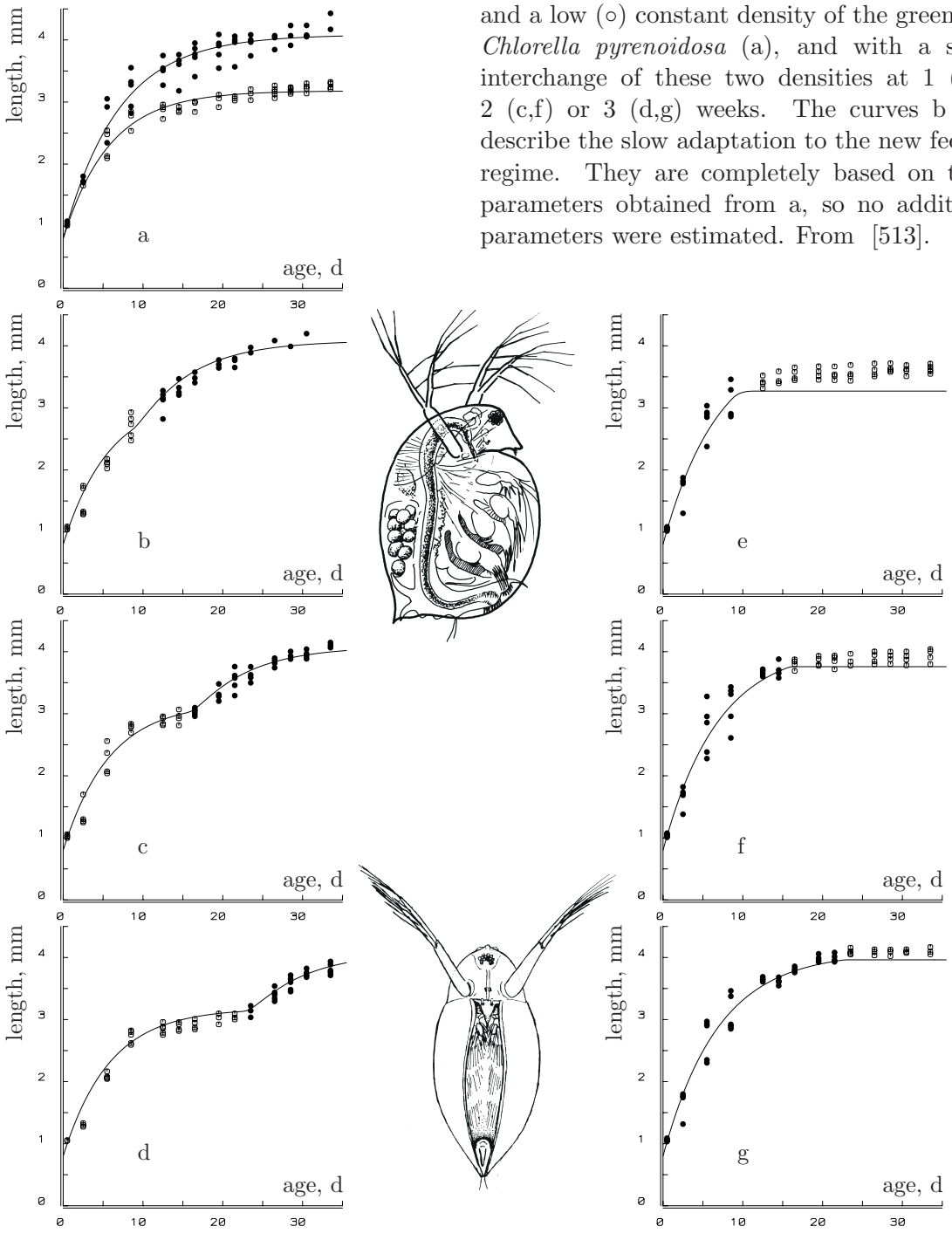

Figure 7.2: Length-at-age for the waterflea *Daphnia magna* at 20 °C feeding at a high (•) and a low (○) constant density of the green alga *Chlorella pyrenoidosa* (a), and with a single interchange of these two densities at 1 (b,e), 2 (c,f) or 3 (d,g) weeks. The curves b to g describe the slow adaptation to the new feeding regime. They are completely based on the 5 parameters obtained from a, so no additional parameters were estimated. From [513].

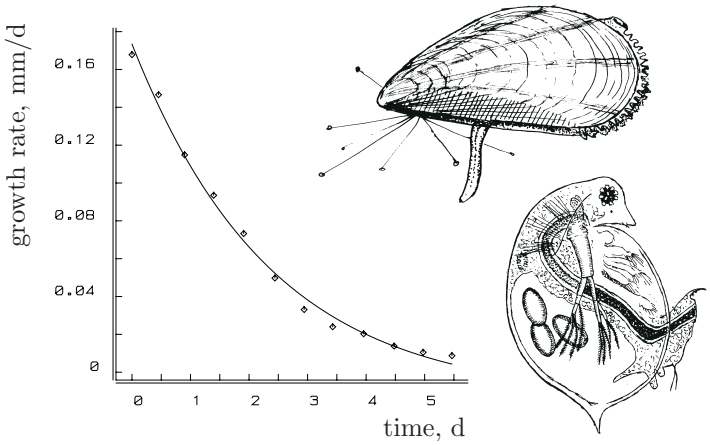

Figure 7.3: Growth rate in the starved mussel *Mytilus edulis* at 21.8 °C. Data from Strömgren and Cary [899]. The parameter estimates (and standard deviations) are $\frac{g}{e(0)} = 12.59$ (1.21), $\dot{k}_M = 2.36$ (0.99) 10^{-3} d^{-1} and $\dot{v} = 2.52$ (0.183) $\mathrm{mm\,d^{-1}}$.

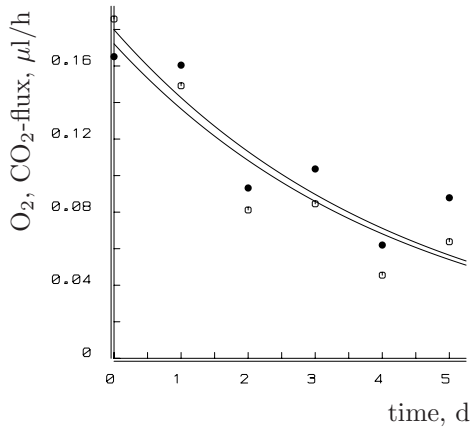

Figure 7.4: The oxygen consumption rate (•) and the carbon dioxide production rate (○) in starved *Daphnia pulex* of 1.62 mm at 20 °C. Data from Richman [764]. The exponential decay rate is 0.23 (0.032) d^{-1}.

order to relate it to measurements of POM? The practical gain of such a reconstruction is in the use of correlation measures to determine the nutrition value of bacteria, alga, etc. Since the correlation coefficient is a linear measure, a direct correlation between bacteria numbers and mussel growth, for instance, only has limited value because assimilation and growth are related in a complex way, whereas bacteria numbers and assimilation are related linearly.

Kautsky [468] measured mussels from four size classes kept individually in cages (diameter 10 cm) at a depth of 15 m in the Baltic at a salinity of $7\,{}^{\circ}/_{\circ\circ}$. Suppose that (the mean) food density changes slowly enough to allow an approximation of the energy reserves with $e = f$. The growth equation (4.7) then reduces to

$$\frac{d}{dt}l = \frac{(f(t)-l)_+}{3(f(t)+g)} g \dot{k}_{M\,15} (T(t) > T_0) \exp\left\{T_A \left(\frac{1}{288} - \frac{1}{T(t)}\right)\right\} \tag{7.1}$$

where $\dot{k}_{M\,15}$ is the maintenance rate coefficient at the chosen reference temperature of 15 °C = 288 K and T_0 is at the lower end of the tolerance range. The next step is to choose cubic spline functions to describe the observed temperature pattern $T(t)$ and the unobserved scaled functional response $f(t)$. The reconstruction of $f(t)$ from length–time data then amounts to the estimation of the knot values of the spline at chosen time points, given realistic choices for the growth parameters. Figure 7.5 shows that the simultaneous least-squares fit of the numerically integrated growth description (7.1) is acceptable in view of the scatter in the length data (not shown), which increases in time in the upper size class in the original data. The scaled functional response (i.e. the hyperbolically transformed food abundance in terms of its nutritional value) appears to follow the temperature cycle during the year. Such a reconstructed food abundance can be correlated with POM and

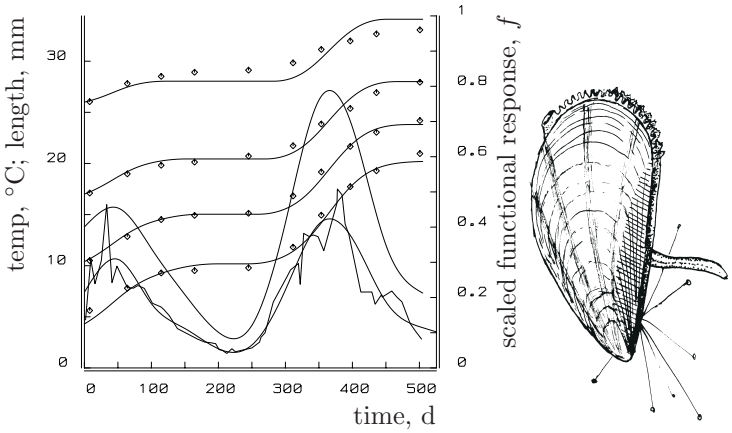

Figure 7.5: The reconstruction of the scaled functional response since the first of August from mean length–time data for four length classes of the mussel *Mytilus edulis* as reported by Kautsky [468] (upper four curves). The reconstruction (the curve in the middle with two peaks) is based on a cubic spline description of the measured temperature (lower curve and capricious line) and the parameter values $L_m = 100$ mm, $g = 0.13$, $\dot{k}_{M\,15} = 0.03$ d^{-1} and $T_A = 7600$ K.

chlorophyll measurements to evaluate their significance for the mussel.

If food intake changes too fast to approximate the reserve density with its equilibrium value, the reserve density should be reconstructed as well. Figure 7.6 illustrates this for the penguin. The von Bertalanffy growth is shown to apply to the adelie penguin, which indicates that body temperature is constant and food is abundant. The deviation at the end of the growth period probably relates to the refusal of the parents to feed the chicks in order to motivate them to enter the sea. The small bodied adelie penguin manages to synchronize its breeding cycle with the local peaks in plankton density in such a way that it is able to offer the chicks abundant food. Typically there are two such peaks a year in northern and southern cold and temperate seas. The plankton density drops sharply when the chicks are just ready to migrate to better places. This means that a larger species, such as the king penguin, is not able to offer its chicks this continuous wealth of food, because its chicks require a longer growth period (see Chapter 8 on comparison of species for an explanation, {267}). So they have to face the meagre period between plankton peaks. (Food for king penguins, squid and fish, follows plankton in abundance.) The parents do not synchronize their breeding season with the calendar; they follow a 14–17 month breeding cycle [845]. The largest living penguin, the emperor penguin, also has to use both plankton peaks for one brood, which implies a structural deviation from a simple von Bertalanffy growth curve.

Given weight–time data, food intake can be reconstructed on the basis of the DEB theory. The relationship between (wet) weights, volumes and energy reserves is given in (2.6). For juveniles, where $E_R = 0$, we have $[W_w] = d_V + w_E[M_{Em}]e$ and specific wet weight is thus not considered to be a constant. Growth according to (3.18) and (3.10) is given by

$$\frac{d}{dt}W_w = [W_w]\frac{d}{dt}V + w_E[M_{Em}]V\frac{d}{dt}e \tag{7.2}$$

$$= \dot{v}V^{2/3}\left(\frac{[W_w]}{e+g}\left(e - l_h - (V/V_m)^{1/3}\right) + [W_{Ew}](f-e)\right) \tag{7.3}$$

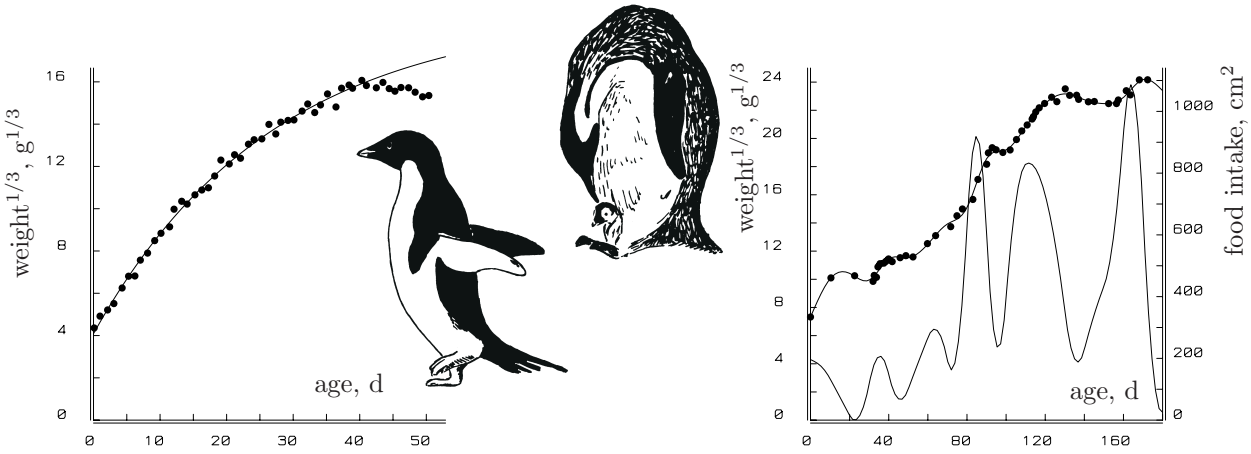

Figure 7.6: Weight ontogeny of the small adelie penguin *Pygoscelis adeliae* (left) and the large emperor penguin *Aptenodytes forsteri* (right). Data from Taylor [909] and Stonehouse [887]. The adelie data follow the fitted von Bertalanffy growth curve, which suggests food abundance during the nursery period. The cubic spline through the emperor data is used to reconstruct food intake $fV^{2/3} = \dot{J}_X/\{\dot{J}_{Xm}\}$. $d_V = 0.3$ g cm^{-3}, $w_E[M_{Em}] = 0.7$ g cm^{-3}, $g = 0.1$, $\dot{v} = 0.6$ cm d^{-1}, $l_h = 0.01$, $V_m = 6000$ cm^3, $e_0 = 0.6$.

Solution of f and substitution of (3.10) gives

$$f = e + \frac{[W_w]^{2/3}}{\dot{v}[W_{Ew}]W_w^{2/3}} \frac{d}{dt} W_w - \frac{[W_w]/[W_{Ew}]}{g+e} \left(e - l_h - \left(\frac{W_w}{V_m[W_w]} \right)^{1/3} \right) \tag{7.4}$$

$$\frac{[M_{Em}]w_E}{[W_w]} \frac{d}{dt} e = \frac{d}{dt} \ln W_w - \frac{\dot{v}}{g+e} \left((e - l_h) \left(\frac{[W_w]}{W_w} \right)^{1/3} - V_m^{-1/3} \right) \tag{7.5}$$

The steps to reconstruct feeding are as follows: first fit a cubic spline through the weight data, which gives $W_w(t)$ and so $\frac{d}{dt} W_w(t)$. Use realistic values for $e(0)$, d_V, $w_E[M_{Em}]$, g, V_m, l_h and $\dot{v}$ and recover $e(t)$ through numerical integration of (7.5) and then $f(t)$ by substitution. Figure 7.6 gives an example. The peaks in the reconstruction will probably be much sharper if the chick's stomach contents are taken into account. This reconstruction can be useful in cases where feeding behaviour that is hard to observe directly is studied and knowledge concerning energetics from captive specimens is available. The significance of this example is to show that the DEB theory hardly poses constraints for growth curves in general. The simple von Bertalanffy growth curve only emerges under the conditions of constant food density and temperature.

7.1.5 Prolonged starvation

If the reserve density drops below the non-growth barrier $e = l$, a variety of possible physiological behaviours seems to occur, depending on the species and environmental factors. Deviation from the κ-rule is necessary, because the standard allocation to growth plus maintenance is no longer sufficient for maintenance, even if growth ceases. Pond snails seem to continue energy allocation to reproduction during prolonged starvation under a

light:dark 16:8 cycle (summer conditions, denoted by LD), but they cease reproduction under a 12:12 cycle (spring/autumn conditions, denoted by MD) [98,1028]. This makes sense because under summer conditions, an individual can expect high primary production, so, if it has consumed a plant, it will probably find another one in the direct neighbourhood. Under spring/autumn conditions, however, it can expect a long starvation period. By ceasing allocation to reproduction, it can increase its survival period by a factor of two; see Figure 7.8. Another aspect is that offspring have a remote survival probability if there is no food around. They are more vulnerable than the parent, as follows from energy reserve dynamics. These dynamics can be followed on the basis of the assumption that LD snails do not change the rule for utilization of energy from the reserves, and neither MD nor LD snails cut somatic maintenance.

Any switch in a continuous-time model is a nuisance to analyse, and special care has to be taken to specify what exactly happens at the switch to be mathematically consistent. If an individual ceases reproduction during starvation, any consistent specification of $\frac{d}{dt}e$ must be continuous in f, e and l. One possibility is by first obeying maturity maintenance requirements, then switching on reproduction gradually if food intake increases from a low level. Other consistent specifications are possible. This amounts to the following specifications for the scaled powers $p'_* \equiv \dot{p}_*(\dot{k}_M g[E_m]V_m)^{-1}$ and the scaled reserve density dynamics of an ectotherm ($l_h = 0$, cf. Table 3.5):

	$e < l$	$e = l$	$e > l$
p'_A	fl^2	fl^2	fl^2
$p'_{G_m} + p^*_R$	0	$((1-\kappa)l^3 - p_{M_m})_+$	$(1-\kappa)(\frac{e-l}{1+e/g}l^2 + (l^3 - l_p^3)_+)$
p'_G	0	0	$\kappa\frac{e-l}{1+e/g}l^2$
p'_{M_m}	0	$\min\{(p_A - p_{M_s})_+, (1-\kappa)\min\{l^3, l_p^3\}\}$	$(1-\kappa)\min\{l^3, l_p^3\}$
p'_{M_s}	κl^3	κl^3	κl^3
$\frac{d}{dt}e(\dot{k}_M g)^{-1}$	$f/l - \kappa$	$(p_A - p_{M_s} - p_{M_m} - p_R)l^{-3}$	$f/l - e/l$

If starvation is complete and volume does not change, i.e. $f = 0$ and l is constant, the energy reserves will be $e(t) = e(0)\exp\{-g\dot{k}_M t/l\}$; see (4.8). Dry weight is a weighted sum of volume and energy reserves, so according to (2.7) for LD snails we must have

$$W_d(l,t) = V_m l^3(d_{Vd} + w_{Ed}[M_{Em}]e(0)\exp\{-g\dot{k}_M t/l\}) \tag{7.6}$$

if the buffer of energy allocated to reproduction is emptied frequently enough (E_R small). For MD snails, where $e(t) = e(0) - ([\dot{p}_M]/[E_m])t$, dry weight becomes

$$W_d(l,t) = V_m l^3(d_{Vd} + w_{Ed}[M_{Em}](e(0) - t[\dot{p}_M]/[E_m])) \tag{7.7}$$

So the dry weight of LD snails decreases exponentially and that of MD snails linearly. Figure 7.7 confirms this. It also supports the length dependence of the exponent.

When storage levels become too low for maintenance, some species can decompose their structural biomass to some extent. If feeding conditions then become less adverse, recovery may be only partial. The distinction between structural biomass and energy reserves fades at extreme starvation. The priority of storage materials over structural

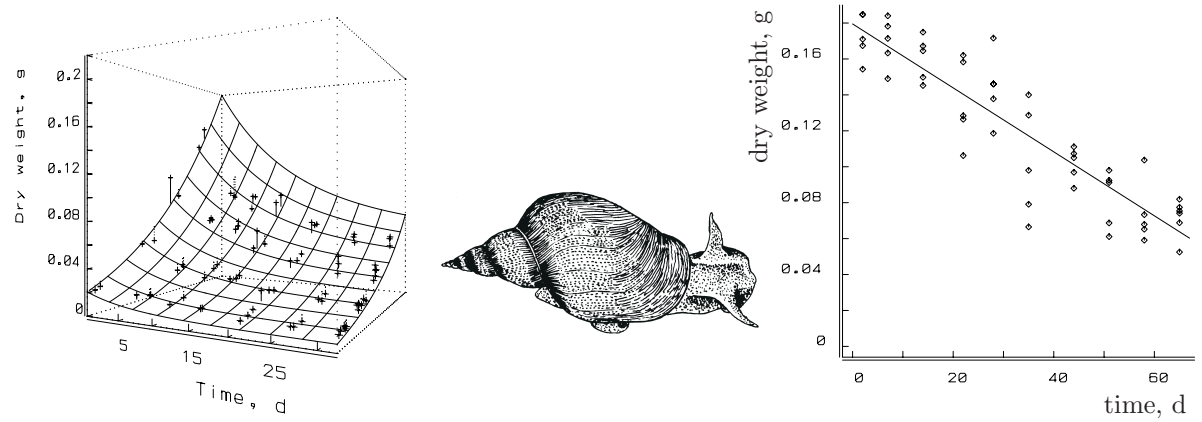

Figure 7.7: Dry weight during starvation of long-day (LD, left) and mid-day (MD, right) pond snails *Lymnaea stagnalis* at 20 °C. The left figure gives dry weights (z-axis) as a function of starvation time (x-axis) and length (y-axis: 1.6–3.3 cm). In the right figure, the length of the MD pond snails was 3 cm. From [1028]. The surface and curve are fitted DEB-based expectations.

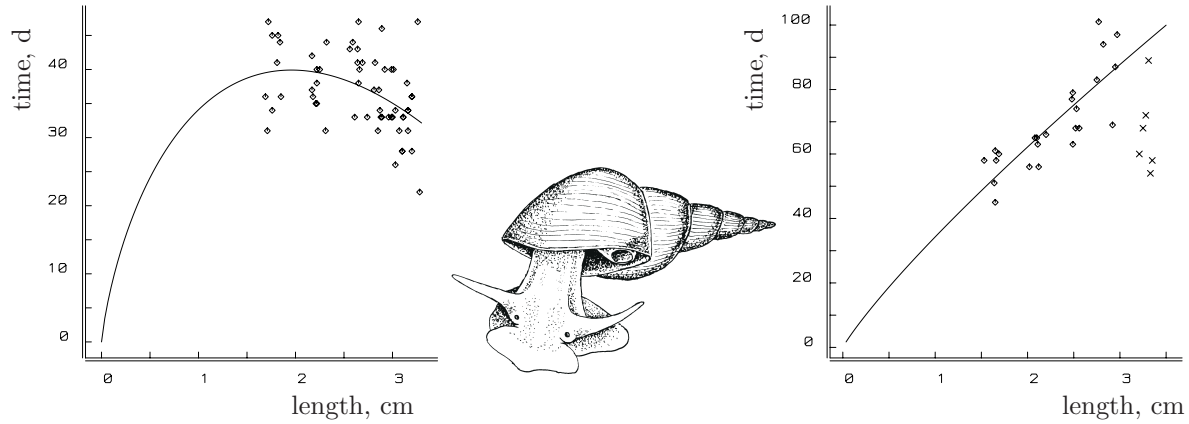

Figure 7.8: Survival time during starvation of LD (left) and MD (right) pond snails as a function of length. From [1028]. The data points × in the right figure are not included in the DEB-based fit. These large individuals had deformations of the shell.

biomass is perhaps even less strict in species that shrink during starvation. Species with (permanent or non-permanent) exoskeletons usually do not shrink in physical dimensions, but the volume-specific energy content nonetheless decreases during starvation.

If we exclude the possibility of prolonging life through decomposition of structural body mass, and if death strikes when the utilization rate drops below the maintenance level, the time till death by starvation can be evaluated.

In animals such as LD snails, that do not change storage dynamics, the utilization rate, $-\frac{d}{dt}[E]$, equals the maintenance rate, $[\dot{p}_M]$ for $[E]/[E_m] = V^{1/3}[\dot{p}_M]/\{\dot{p}_{Am}\}$ or $e = \kappa l$. Since $e(t) = e(0)\exp\{-\dot{k}_M t g/l\}$, death strikes at $t_\dagger = \frac{l}{\dot{k}_M g}\ln\frac{e(0)}{\kappa l}$. This only holds if the length increase is negligibly small.

In animals such as MD snails, which change storage dynamics to $\frac{d}{dt}e = -[\dot{p}_M]/[E_m]$ or $e(t) = e(0) - t[\dot{p}_M]/[E_m]$, death strikes when $e = 0$, that is at $t_\dagger = e(0)[E_m]/[\dot{p}_M] = \frac{e(0)}{\kappa\dot{k}_M g}$. This only holds as long as there is no growth, so $e(0) < l$. In practice, this is a more stringent condition than the previous one. The first part of the starvation period usually includes a period where growth continues, because $e > l$. This complicates the analysis of starvation data, as illustrated in the following example. In a starvation experiment with MD snails, individuals were taken from a standardized culture and initially fed *ad libitum* for 4 days prior to complete starvation. If we assume that food density in the culture has been constant, so $e(0) = f_c$, say, with f_c being about 0.7, and $f = 1$ during the 4 days prior to the starvation experiment, the change in length is negligibly small. The initial storage density is $e(0) = 1-(1-f_c)\exp\{-4\dot{k}_M g/l\}$, according to (3.10). The time till growth ceases is found again from (3.10) and the boundary condition $l = e(0)\exp\{-t\dot{k}_M g/l\}$. (Although the length increase is negligibly small, energy allocation to growth can be substantial.) After a period $l(\kappa\dot{k}_M g)^{-1}$ death will strike, so

$$t_\dagger = \frac{l}{\dot{k}_M g}\left(\frac{1}{\kappa} + \ln\left\{l^{-1}\left(1-(1-f_c)\exp\{-4\dot{k}_M g/l\}\right)\right\}\right) \tag{7.8}$$

Figure 7.8 confirms model predictions for the way survival time depends on length in LD and MD snails, and shows that MD snails can prolong life by a factor of two by not reproducing during starvation. In contrast to the situation concerning embryonic growth, this confirmation gives little support to the theory, because the shape of the survival time–length curve is very flexible for the LD case, although there are only two free parameters. The upper size class of the MD snails has been left out of the model fit, because the shape of their shell suggested a high age, which probably affected energy dynamics.

7.1.6 Shrinking

Many species can, to some extent, shrink in structural mass during starvation, as a way to pay their somatic maintenance costs. Even animals with a skeleton, such as shrews of the genus *Sorex*, can exhibit a geographically varying winter size depression, known as the Dehnel phenomenon [317]. Molluscs seem be to able to reduce shell size [230]. During starvation, isomorphs mobilize a power $e\{\dot{p}_{Am}\}V^{2/3}$ from the reserves, and V1-morphs $eV[E_m]\dot{k}_E$. Shrinking releases a power $-\mu_V[M_V]\frac{d}{dt}V$ from the structure, where

$\frac{d}{dt}V \leq 0$. Assuming that the individual does not invest in reproduction under these conditions, somatic maintenance has to be paid at a rate $[\dot{p}_M]V = \dot{k}_M[E_G]V$.

The (negative) growth is found from $\kappa e\{\dot{p}_{Am}\}V^{2/3} = \dot{k}_M[E_G]V + [E_G]\frac{d}{dt}V$, which gives $\frac{d}{dt}V = eV^{2/3}\kappa\{\dot{p}_{Am}\}/[E_G] - \dot{k}_M V$. Substitution into the total dissipating power gives a total rate of $e\{\dot{p}_{Am}\}V^{2/3} - \mu_V[M_V]\frac{d}{dt}V = e\{\dot{p}_{Am}\}V^{2/3}(1 - \kappa\mu_V[M_V]/[E_G]) + \dot{k}_M V\mu_V[M_V]$, which should exceed the somatic maintenance costs. The latter cannot be paid if $e\{\dot{p}_{Am}\}V^{2/3}(1 - \kappa\mu_V[M_V]/[E_G]) + \dot{k}_M V\mu_V[M_V] < \dot{k}_M V[E_G]$, i.e. $e < \alpha V^{1/3}[\dot{p}_M]/\{\dot{p}_{Am}\}$ for $\alpha = \frac{1-\mu_V[M_V]/[E_G]}{1-\kappa\mu_V[M_V]/[E_G]}$. This prediction rests on energy considerations only, but maintenance costs also have a mass aspect, and the specific maintenance costs $[\dot{p}_M]$ might depend on the source, i.e. reserves or structure. The growth rate at death by starvation is $\frac{d}{dt}V = \dot{k}_M V(\alpha\kappa - 1)$.

The second law of thermodynamics ensures that $[E_G] > \mu_V[M_V]$, and so $0 < \alpha \leq 1$. This implies that, for $\kappa = 1$, the individual cannot fully pay the somatic maintenance costs by shrinking. The maturity maintenance costs can considered to be reducible maintenance costs, while the somatic maintenance costs are mandatory.

7.1.7 Dormancy

Some species manage to escape adverse feeding conditions (and/or extreme temperature or drought) by switching to a torpor state in which growth and reproduction cease, while maintenance (and heating) costs greatly diminish. The finding that metabolic rate in homeotherms is proportional to body weight during hibernation [470] suggests that maintenance costs are reduced by a fixed proportion.

As heating is costly, a reduction in the body temperature of endotherms saves a lot of energy. Bats and hummingbirds lower their body temperature in a daily cycle. This probably relates to the relatively long life span of bats (for their size) [281]. Although most bird embryos have a narrow temperature tolerance range, swifts survive significant cooling. This relates to the food-gathering behaviour of the parents. Dutch swifts are known to collect mosquitoes above Paris at a distance of 500 km, if necessary. During hibernation, not only is the body temperature lowered, but other maintenance costs are reduced as well.

Hochachka and Guppy [415] found that the African lungfish *Protopterus* and the South American lungfish *Lepidosiren* reduce maintenance costs during torpor in the dry season, by removing ion channels from the membranes. This saves energy expenses for maintaining concentration gradients over membranes, which proves to be a significant part of the routine metabolic costs. This metabolic arrest also halts aging. The life span of lungfish living permanently submerged, so always active, equals the cumulative submerged periods for lungfish that are regularly subjected to desiccation. This is consistent with the DEB interpretation of aging.

If maintenance cannot be reduced completely in a torpor state, it is essential that some reserves are present, {37}. This partly explains why individuals frequently survive adverse conditions as freshly laid eggs, because the infinitesimally small embryo requires little maintenance; it only has to delay development. The start of the pupal stage in holometabolic insects is also very suitable for inserting a diapause in order to survive adverse

conditions, {253}.

7.1.8 Emergency reproduction

The determination of sex in some species is coupled to dormancy in a way that can be understood in the context of the DEB model. Daphnids use special winter eggs, packed in an ephippium. The diploid female daphnids usually develop diploid eggs that hatch into new diploid females. If food densities rapidly switch from a high level to a low one and the energy reserves are initially high, the eggs hatch into diploid males, which fertilize females that now produce haploid eggs [855]. After fertilization, the 'winter eggs' or resting eggs develop into new diploid females. The energy reserves of a well-fed starving female are just sufficient to produce males, to wait for their maturity and to produce winter eggs.

The trigger for male/winter egg development is not food density itself, but a change of food density. If food density drops gradually, females do not switch to the sexual cycle [512], cf. Figure 9.16. Sex determination in species such as daphnids is controlled by environmental factors, so that both sexes are genetically identical [136,385]. Mrs D. van Drongelen and Mrs J. Kaufmann informed me that a randomly assembled cohort of neonates from a batch moved to one room proved to consist almost exclusively of males after some days of growth, while in another cohort from the same batch moved to a different room all individuals developed into females as usual. This implies that sex determination in *Daphnia magna*, and probably in all other daphnids and most rotifers as well, can be affected even after hatching. More observations are needed. Male production does not seem to be a strict prerequisite for winter egg production [491]. Kleiven, Larsson and Hobæk [491] found that crowding and shortening of day length also affect male production in combination with a decrease in food availability at low food densities. The females that hatch from winter eggs grow faster, mature earlier and reproduce at a higher rate than those from subitaneous eggs [27]; the size at maturation and the ultimate body size are also larger for the exephippial generation. The physiological nature of these interesting differences is still unknown.

The switch to sexual reproduction as a reaction to adverse feeding conditions frequently occurs in unrelated species, such as slime moulds, myxobacteria, oligochaetes (*Nais*) and plants. The difference between emergency and suicide reproduction, see {262}, is that the individual can still switch back to standard behaviour if the conditions improve.

7.1.9 Geographical size variations

The energy constraints on distribution, apart from barriers to migration, consist primarily of the availability of food in sufficient quantity and quality. The second determinant is the temperature, which should be in the tolerance range for the species for a long enough period. If it drops below the lower limit, the species must adopt adequate avoidance behaviour (migration, dormancy) to survive.

The minimum food density for survival relates to metabolic costs. If an individual is able to get rid of all other expenses, mean energy intake should not drop below $[\dot{p}_M]V+\{\dot{p}_T\}V^{2/3}$ for an individual of volume V, so the minimum ingestion rate, known as the maintenance

ration, should be $\frac{\{\dot{J}_{Xm}\}}{\{\dot{p}_{Am}\}}([\dot{p}_M]V + \{\dot{p}_T\}V^{2/3})$. For a 3-mm daphnid at 20 °C this minimum ingestion rate is about six cells of *Chlorella* (diameter 4 μm) per second [511]. The minimum scaled food density X/X_K is $x_s = \frac{l_h+l}{1/\kappa-l_h-l}$.

This minimum applies to mere survival for an individual. For prolonged existence, reproduction is essential to compensate at least for losses due to aging. The ultimate volumetric length, $fV_m^{1/3} - V_h^{1/3}$, should exceed that at puberty, $V_p^{1/3}$, which leads to the minimum scaled food density $x_R = \frac{l_h+l_p}{1/\kappa-l_h-l_p}$.

Several factors determine food density. It is one of the key issues of population dynamics. The fact that von Bertalanffy growth curves frequently fit data from animals in the field indicates that they live at relatively constant (mean) food densities. In the tropics, where climatic oscillations are at a minimum, many populations are close to their 'carrying capacity', i.e. the individuals produce a small number of offspring, just enough to compensate for losses. It also means that the amount of food per individual is small, which reduces them in ultimate size. Towards the poles, seasonal oscillations divide the year into good and bad seasons. In bad seasons, populations are thinned, so in the good seasons a lot of food is available per surviving individual. Breeding periods are synchronized with the good seasons, which means that the growth period coincides with food abundance. So food availability in the growth season generally increases with latitude [540]. The effect is stronger towards the poles, which means that body size tends to increase towards the poles for individuals of one species. Figure 7.9 gives two examples. Other examples are known from, for instance, New Zealand including extinct species such as the moa *Dinornis* [137]. Note that size increase towards the poles also comes with a better ability to survive starvation and a higher reproduction rate, traits that will doubtlessly be of help in coping with harsh conditions.

Geographical trends in body sizes can easily be distorted by regional differences in soils, rainfall or other environmental qualities affecting (primary) production. Many species or races differ sufficiently in diets to hamper a geographically based body size comparison. For example, the smallest stoats are found in the north and east of Eurasia, but in the south and west of North America [482]. The closely related weasels are largest in the south, both in Eurasia and in North America. Patterns like these can only be understood after a careful analysis of the food relationships. Simpson and Boutin [846] observed that muskrats *Ondatra zibethicus* of the northern population in Yukon Territory are smaller and have a lower reproduction rate than the southern population in Ontario. They could relate these differences to feeding conditions, which were better for the southern population, in this case.

Bergmann [70] observed the increase in body size towards the poles in 1847, but he explained it as an effect of temperature. Large body size goes with small surface area/volume ratios, which makes endotherms more efficient per unit body volume. This explanation has been criticized [613,818,824]. It is indeed hard to see how this argument applies in detail. Animals do not live on a unit-of-body-volume basis, but as a whole individual [613]. It is also hard to see why the argument applies within a species only, and why animals with body sizes as different as mice, foxes and bears can live together in the Arctic. The tendency to increase body size towards the poles also seems to occur in

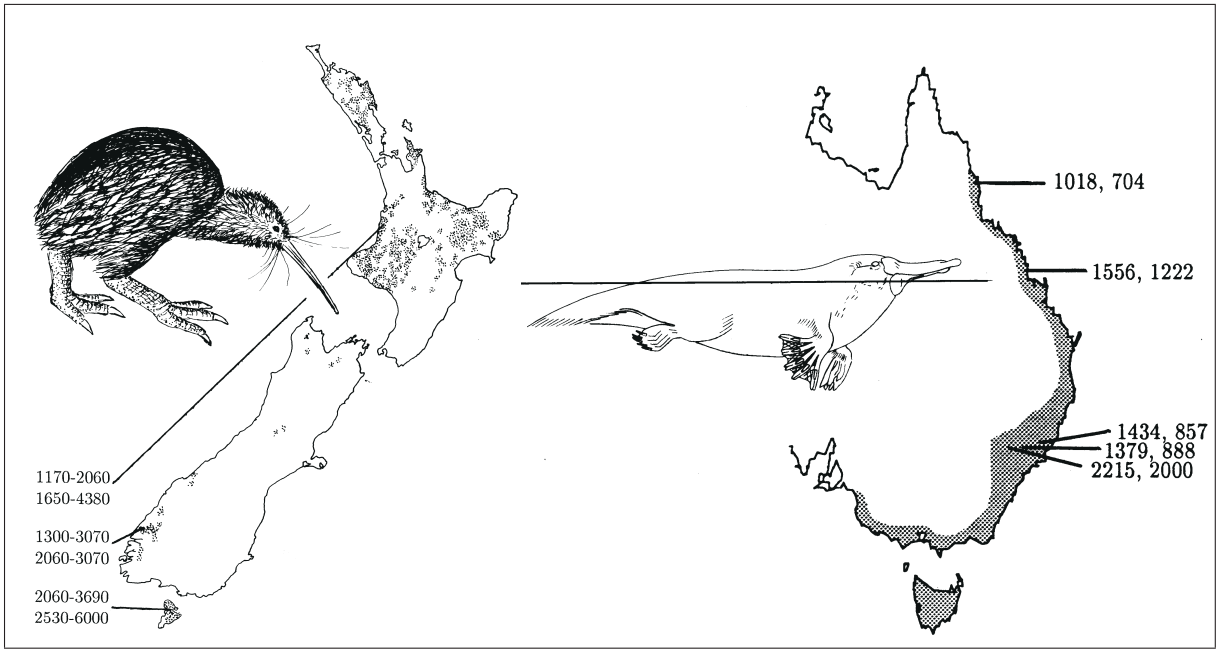

Figure 7.9: The brown kiwi *Apteryx australis* in subtropical north of New Zealand is lighter than in the temperate south. The numbers give ranges of weights of male and female in grams, calculated from the length of the tarsus using a shape coefficient of $\delta_{\mathcal{M}} = 1.817\ \mathrm{g}^{1/3}\,\mathrm{cm}^{-1}$. Data from Fuller [305]. A similar gradient applies to the platypus *Ornithorhynchus anatinus* in Australia. The numbers give the mean weights of male and female in grams as given by Strahan [895]. The DEB theory relates adult weights to food availability and so to the effect of seasons. This interpretation is supported by the observation that platypus weight increases with seasonal differences at the same latitude in New South Wales. The seasons at the three indicated sites are affected by the Great Dividing Range in combination with the easterly winds.

ectotherms, which requires a different explanation. The DEB theory offers an alternative explanation for the phenomenon because of the relationship between food availability and ultimate body volume. Temperature alone works in the opposite direction within this context. If body temperature has to be maintained at some fixed level, individuals in the Arctic are expected to be smaller while living at the same food density, because they have to spend more energy on heating, which reduces their growth potential. The effect will, however, be small since insulation tends to be better towards the poles.

It is interesting to note that species with distribution areas large enough to cover climatic gradients generally tend to split up in isolated races or even subspecies. This can be seen as a form of adaptation, cf. {263}. The differences in ultimate size have usually become genetically fixed. This is typical for 'demand' systems where regulation mechanisms set fluxes at predefined values which are obtained through adaptation. Within the DEB theory this means that the parameter values are under genetic control and that the minimum food level at which survival is possible is well above the level required for maintenance. The matter is taken up again on {291}.

7.2 Diffusion limitation

The purpose of this subsection is to show why small deviations from the hyperbolic functional response can be expected under certain circumstances, and how the functional response should be corrected.

Any submerged body in free suspension has a stagnant water mantle of a thickness that depends on the roughness of its surface, its electrical properties and on the turbulence in the water. The uptake of nutrients by cells that are as small as that of a bacterium can be limited by the diffusion process through this mantle [498]. Logan [563,564] related this limitation to the flocculation behaviour of bacteria at low food densities. The existence of a diffusion-limited boundary layer is structural in Gram-negative bacteria such as *Escherichia* [496], which have a periplasmic space between an inner and outer membrane. The rate of photosynthesis of aquatic plants [858,989] and algae [770] can also be limited by diffusion of CO_2 and HCO_3^- through the stagnant water mantle that surrounds them. Coccolithophores, such as *Emiliania*, have a layer of polysaccharides with coccoliths (i.e. calcium carbonate platelets), which might limit diffusion. Since diffusion limitation affects the functional response, it is illustrative to analyse the deviations a bit more in detail. For this purpose I re-formulate some results that originate from Best [81] and Hill and Whittingham [411] in 1955.

7.2.1 Homogeneous mantle

Suppose that the substrate density in the environment is constant and that it can be considered as well mixed beyond a distance l_1 from the centre of gravity of a spherical cell of radius l_0. Let X_1 denote the substrate density in the well-mixed environment and X_0 that at the cell surface. The aim is now to evaluate uptake in terms of substrate density in the environment, given a model for substrate uptake at the cell surface.

The build-up of the concentration gradient from the cell surface is fast compared with other processes, such as growth; the gradient is, therefore, assumed to be stationary.

The conservation law for mass implies that the flux $\dot{X}(l)$ at distance l from the centre of gravity of the cell obeys the relationship $4\pi l_1^2 \dot{X}(l_1) = 4\pi l_2^2 \dot{X}(l_2)$ for any two choices of distances l_1 and l_2. From the choice $l_1 = l$ and $l_2 = l + dl$ follows $l^2 \frac{d}{dl}\dot{X} + 2l\dot{X} = 0$. According to Fick's diffusion law, the mass flux over a sphere with radius l is proportional to the substrate density difference in the adjacent inner and outer imaginary tunics (i.e. 3D-annulus), so $\dot{X} \propto -\frac{d}{dl}X$. This leads to the relationship $l^2 \frac{d^2}{dl^2}X + 2l\frac{d}{dl}X = 0$ or $\frac{d}{dl}\left(l^2 \frac{d}{dl}X\right) = 0$, which is known as the Laplace equation. The boundary conditions $X(l_0) = X_0$ and $X(l_1) = X_1$ determine the solution $X(l) = X_1 - (X_1 - X_0)\frac{1-l_1/l}{1-l_1/l_0}$.

The mass flux at l_0 is, according to Fick's law, $4\pi l_0^2 \dot{D} \frac{d}{dl}X(l_0)$, where $\dot{D}$ is the diffusivity. It must be equal to the uptake rate $\dot{J}_X = \dot{J}_{Xm} X_0/(X_K + X_0)$. This gives the relationship between the density at the cell surface and the density in the environment as a function of the thickness of the mantle

$$X_0 = g(X_1|X_K, X_{K1}) = \frac{1}{2}X_c + \frac{1}{2}\sqrt{X_c^2 + 4X_1 X_K} \tag{7.9}$$

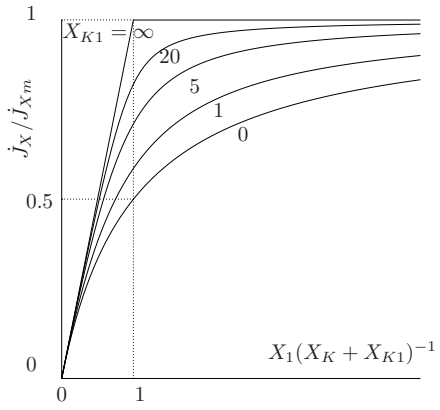

Figure 7.10: The shape of the functional response depends on the value of the mantle saturation coefficient; it can vary from a Holling type II for small values of the mantle saturation coefficient, to Holling type I for large values.

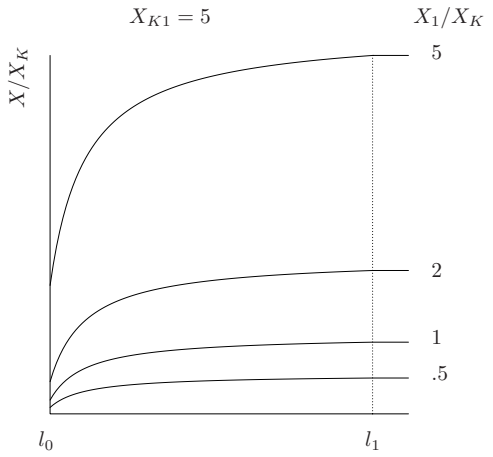

Figure 7.11: Substrate density as a function of the distance from the cell centre in the case of a homogeneous water mantle, for different choices for the substrate densities X_1 in the well-mixed medium.

with $X_c \equiv X_1 - X_K - X_{K1}$ and $X_{K1} = \frac{\dot{J}_{Xm}}{4\pi \dot{D} l_0}\left(1 - \frac{l_0}{l_1}\right)$. Since the cell can only 'observe' the substrate density in its immediate surroundings, X_0 must be taken as the argument for the hyperbolic functional response and not X_1. Measurements of substrate density, however, refer to X_1, which invites one to write the functional response as a function of X_1, rather than X_0, so $\dot{J}_X(X_1) = \dot{J}_{Xm}\frac{g(X_1|X_K,X_{K1})}{X_K+g(X_1|X_K,X_{K1})}$.

The extent to which a stagnant water mantle changes the uptake rate and the shape of the functional response depends on the value of the mantle saturation coefficient X_{K1}, and therefore on the thickness of the mantle relative to the size of the individual and the diffusivity relative to the maximum uptake rate. If the mantle saturation coefficient is small, the mantle has hardly any effect, i.e. $X_0 \to X_1$ for $X_{K1} \to 0$, and the functional response is of the hyperbolic type. If it is large, however, the functional response approaches Holling's type I [424], also known as Blackman's response [89], where the ingestion rate is just proportional to food density up to some maximum; see Figure 7.10 and 7.11. This exercise thus shows that the two types of Holling's functional response are related and mixtures are likely to be encountered. This response is at the root of the concept of limiting factors, which still plays an important role in eco-physiology.

The uptake rate depends on the size of the individual in a rather complex way if diffusion is rate limiting. Figure 7.12 illustrates that irregular surfaces are smoothed out. For relatively thick water mantles and at low substrate densities, especially, it is not important that the cell is spherical. The approximate relationship $V \simeq l_0^3\pi 4/3$ will be appropriate for most rods. The rod then behaves as a V0-morph, since the boundary of the mantle is limiting the uptake and hardly changes during growth of the cell.

Increasing water turbulence and active motion by flagellas will reduce the thickness of the water mantle. Its effect on mass transfer is usually expressed by the Sherwood

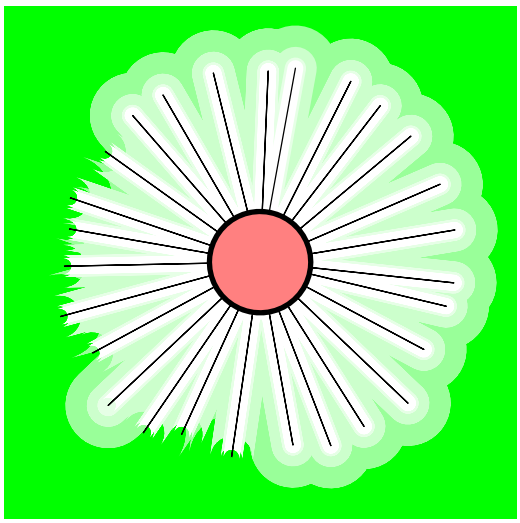

Figure 7.12: Irregular surfaces that catch food are smoothed out by a water mantle if (Eddy) diffusion through this layer limits the uptake rate; the thicker the mantle, the more efficient the smoothing. This is here illustrated for a heliozoan, which has thin protoplasm-covered spines that help to catch small food particles (bacteria, algae, microorganisms).

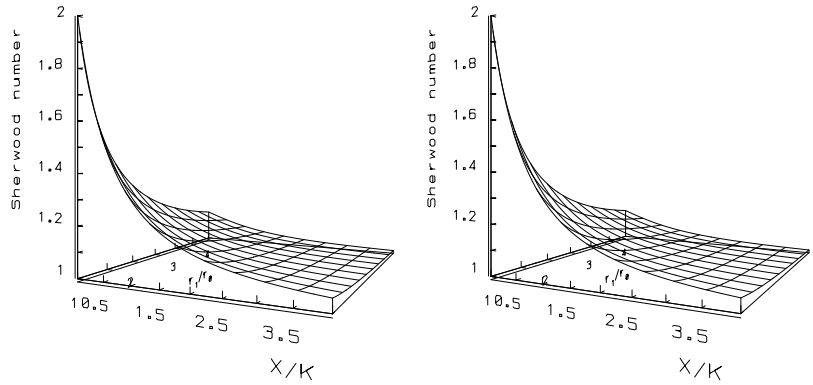

Figure 7.13: Stereo view of the substrate uptake rate of a cell in suspension relative to that in completely stagnant water, as a function of the substrate density in the medium (x-axis) and the thickness of the water mantle (y-axis). Parameter choice: $\dot{J}_{Xm} = 4\pi \dot{D} X_K l_0$

number, which is defined as the ratio of mass fluxes with to those without turbulence. If $X_1 \ll X_K$, the Sherwood number is independent of substrate density, and amounts to $\left(1 + \frac{X_{K1}/X_K}{1-l_0/l_1}\right)(1 + X_{K1}/X_K)^{-1}$. For larger values of X_1, the Sherwood number becomes dependent on substrate density and increasing turbulence will less easily increase mass transfer, because uptake will be rate limiting; see Figure 7.13. This probably defines the conditions for producing sticky polysaccharides which result in the development of films of bacteria on hard substrates or of flocs. If a cell attaches itself, it loses potentially useful surface area for uptake, but increases mass transfer via convection. Although the quantitative details for the optimization of uptake can be rather complex, the qualitative implication that cells usually occur in free suspension when substrate densities are high, and in flocs when they are low can be understood from Sherwood numbers.

Since diffusivity is proportional to (absolute) temperature, see e.g. [33], and uptake rates tend to follow the Arrhenius relationship, {53}, the temperature dependence of diffusion-limited uptake is likely to depend on temperature in a more complex way.

It is conceivable that slowly moving or sessile animals exhaust their immediate surroundings in a similar way to that described here for bacteria in suspension, if the transport of food in the environment is sufficiently slow. Trapping devices suffer from this problem

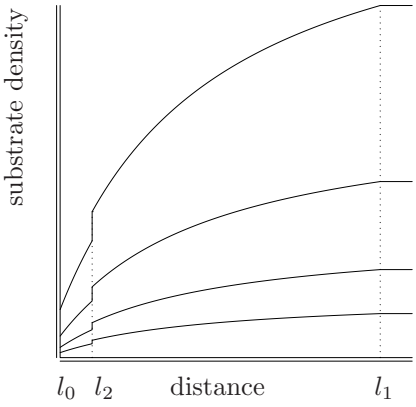

Figure 7.14: Substrate density as a function of the distance from the cell centre for a Gram-negative bacterium. The inner membrane is at distance l_0, the outer membrane at distance l_2, and beyond distance l_1 the medium is completely mixed. Four different choices for substrate densities X_1 in the medium have been made, to illustrate that the higher X_1 the more the substrate density at the inner membrane X_0 is reduced.

too [448]. Patterson [692] showed by changing the flow rate that the physical state of the boundary layer surrounding the symbiosis of coral and algae directly affects nutrient transfer. The shape, size and polyp-wall thickness of scleractinian corals could be related to diffusion limitation of nutrients. Some processes of transport can be described accurately by diffusion equations, although the physical mechanism may be different [674,852].

7.2.2 Mantle with barrier

For Gram-negative bacteria, which have an inactive outer membrane with a limited permeability for substrate transport, the relationship between the substrate density at the active inner membrane and that in the well-mixed environment is a bit more complicated. On the assumption that the substrate flux through the outer membrane is proportional to the difference of substrate densities on either side of the outer membrane, the permeability affects the mantle saturation coefficient X_{K1}, i.e. $X_{K1} = \frac{\dot{J}_{Xm}}{4\pi\dot{D}l_0}\left(1 - \frac{l_0}{l_1} + \frac{l_0\dot{D}}{l_2^2\dot{P}}\right)$, where l_2 is the radius at which the outer membrane occurs and $\dot{P}$ is the permeability of that membrane (dimension length.time^{-1}). The periplasmic space is typically some 20–40% of the cell volume [657], so that $l_0/l_2 \simeq 0.9$. If $l_2\dot{P} \gg \dot{D}$, the resistance of the outer membrane for substrate transport is negligible. Figure 7.14 illustrates how substrate density decreases towards the inner membrane.

7.2.3 Non-homogeneous mantle

Suppose now that the cell has, besides a stagnant water mantle, also a layer of polysaccharides, where the diffusivity has value $\dot{D}_0$, while it has value $\dot{D}_2$ in the water mantle. Suppose that the boundary of the layer is at distance l_2 from the cell centre, so $l_0 < l_2 < l_1$. The substrate density at the boundary of the polysaccharide layer can now be solved by equating the uptake rate to the flux at the cell membrane. This value can be substituted when the flux at the layer boundary is set equal to the uptake rate. The relationship between X_0 and X_1 is still given by (7.9), but the mantle saturation constant is now

$X_{K1} = \frac{\dot{J}_{Xm}}{4\pi \dot{D}_2 l_2}\left(1 - \frac{l_2}{l_1}\right)\left(1 + \frac{\dot{D}_2 l_1}{\dot{D}_0 l_2}\frac{1-l_2/l_0}{1-l_1/l_2}\right)$. So, just like the barrier in the preceding section, inhomogeneities in the mantle only affect the mantle saturation coefficient, not the shape of the functional response.

7.3 Digestion

Microflora is likely to play an important role in the digestion process of all herbivores. It can provide additional nutrients by fermenting carbohydrates and by synthesizing amino acids and essential vitamins. Daphnids are able to derive structural body components and lipids from the cellulose of algal cell walls [817], though it is widely accepted that daphnids, like almost all other animals, are unable to produce cellulase. Endogenous cellulase production is only known to occur in some snails, wood-boring beetles, shipworms and thysanurans [569]. The leaf-cutting ant *Atta* specifically cultures fungi, probably to obtain cellulase [594]. Bacteria have been found in the guts of an increasing number of crustaceans [653], but not yet in daphnids [817]. In view of the short gut residence times for daphnids, it is improbable that the growth of the daphnid's gut flora plays an important role. Digestion of cellulose is a slow process, and the digestive caecum is situated in the anterior part of the gut. Daphnids, therefore, probably produce enzymes that can pass through cell walls, because they do not have the mechanics to rupture them.

Many studies of energy transformations assume that the energy gain from a food item does not depend on the size of the individual or on the ingestion rate. The usefulness of this assumption in ecological studies is obvious, and the DEB model uses it as well. In view of the relationship of gut residence time to both size and ingestion rate, this assumption needs further study.

The nutritional gain from a food particle has been observed to depend on gut residence time [764,812]. These findings are suspect for two reasons, however. The first reason is that assimilation efficiencies are usually calculated per unit of dry weight of consumer, while the energy reserves contribute increasingly to dry weight with increasing food density, but do not affect digestion. The second reason is that, while the nutritional value of faecal pellets may decrease with increasing gut residence time, it is not obvious whether the animal or the gut microflora gains from the difference. I discuss here to what extent digestion is complete and the composition of faeces does not change if the composition of food does not change.

When animals such as daphnids are fed with artificial resin particles mixed through their algal food, the appearance of these particles in the faeces supports the plug flow type of model for the digestion process, as proposed by Penry and Jumars [264,697,698].

The shape of the digestive system also suggests plug flow. The basic idea is that materials enter and leave the system in the same sequence and that they are perfectly mixed radially. Mixing or diffusion along the flow path is assumed to be negligible. (This is at best a first approximation, because direct observation shows that particles sometimes flow in the opposite direction.)

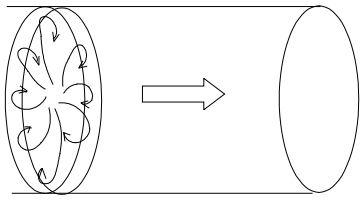

Suppose that a thin slice of gut contents can be followed during its travel along the tube-like digestive tract, under conditions of a constant ingestion rate. The small changes in the size of the slice during the digestion process are ignored. The gut content of a 4-mm *D. magna* is about 0.1 mm^3, while the capacity is about 6.3×10^5 cells of *Scenedesmus*, see Figure 3.9, of some 58 μm^3 per cell, which gives a total cell volume of 0.0367 mm^3. The cells occupy some 37% of the gut volume, which justifies the neglect of volume changes for the slice. The volume of the slice of thickness L_λ is $V_s = \pi L_\lambda L_\phi^2/4$, where L_ϕ is the diameter of the gut, and $\pi L_\lambda L_\phi$ is the surface area of contact between slice and gut.

Suppose that the gut wall secretes enzymes into the slice, which catalyse the transformation of food X into faeces and a product P, which can be absorbed through the gut wall. The rate of this transformation, called digestion, is taken proportional to the concentration of active enzymes which have been secreted. If the secretion of enzymes is constant and the deactivation follows a simple first-order process, the amount M_g of active enzyme in the slice will follow $\frac{d}{dt}M_g = \{\dot{J}_g\}\pi L_\lambda L_\phi - \dot{k}_g M_g$, where $\{\dot{J}_g\}$ is the (constant) secretion rate of enzyme per unit of gut wall surface area and $\dot{k}_g$ is the decay rate of enzyme activity. The equilibrium amount of enzyme is thus $M_g = \{\dot{J}_g\}\pi L_\lambda L_\phi/\dot{k}_g$ and I assume that this equilibrium is reached fast enough to neglect changes in the concentrations of active enzyme. So the enzyme concentration is larger in smaller individuals because of the more favourable surface area/volume ratio of the slice.

A simple Michaelis–Menten kinetics for the change in the amount of food gives $\frac{d}{dt}M_X = -\dot{k}_X y_{Xg} f_X M_g$, where $f_X = M_X/(M_{KX} + M_X)$ is the scaled functional response for digestion. The compound parameter $\dot{k}_X y_{Xg}$ is a rate constant for digestion.

If the absorption of product through the gut wall again follows Michaelis–Menten kinetics, the change of the amount of product in the slice is given by $\frac{d}{dt}M_P = -y_{PX}\frac{d}{dt}M_X - \dot{k}_P y_{Pc} f_P M_c$ with $f_P \equiv M_P/(M_{KP} + M_P)$ the scaled functional response for absorption and $M_c = \{M_c\}\pi L_\lambda L_\phi$ the amount of carriers in the gut wall with which the slice makes contact, while the surface-area-specific number of carriers $\{M_c\}$ is taken to be constant. The parameter $\dot{k}_P y_{Pc}$ is a rate constant for absorption. This two-step Michaelis–Menten kinetics for digestion with plug flow has been proposed independently by Dade *et al.* [191].

The digestion process in the slice ends at the gut residence time t_g, given in (3.6), which decreases for increasing ingestion rate and is minimal for the scaled functional response for feeding $f = 1$. The conservation law for mass can be used to deduce that the total amount of product taken up from the slice equals $M_{Pu}(t_g) = ((M_X(0) - M_X(t_g))y_{PX} - M_P(t_g))$, where $M_X(0)$ denotes the amount of food in the slice at ingestion. An ideal gut will digest food completely ($M_X(t_g) = 0$) and absorb all product ($M_P(t_g) = 0$).

To evaluate to what extent food density in the environment and the size of the organism affect digestion, via gut residence time and gut diameter, it is helpful to define the digestion and uptake efficiency $M_{Pu}(t_g)(y_{PX}M_X(0))^{-1}$. For isomorphs, where gut diameter L_ϕ is proportional to whole body length L, the energy uptake from food is independent of body size. A shorter gut residence time in small individuals is exactly compensated by a higher enzyme concentration. This is because the production of short-living enzymes is taken to be proportional to the surface area of the gut. An obvious alternative would be a long-living enzyme that is secreted in the anterior part of the digestive system. If this part is a

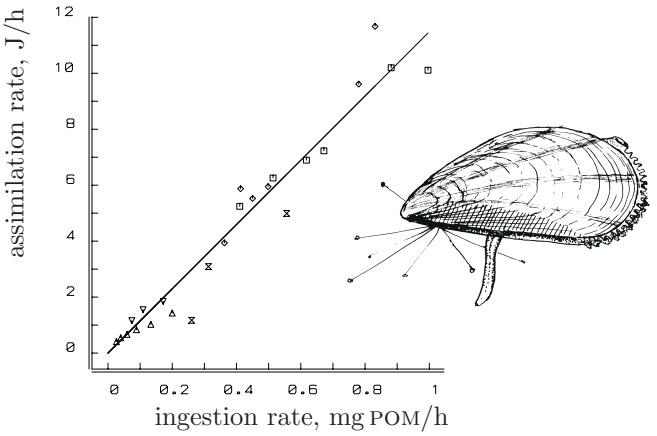

Figure 7.15: The assimilation rate as a function of ingestion rate for mussels (*Mytilus edulis*) ranging from 1.75 to 5.7 cm. Data from [58,59,103,383,485], figure from [367]. All rates are corrected to 15 °C. The fitted line is $\dot{p}_A = \dot{k}_X\{\dot{p}_{Am}\}/\{\dot{J}_{Xm}\}$ with $\{\dot{p}_{Am}\}/\{\dot{J}_{Xm}\} = 11.5$ (sd 0.34) J mg POM^{-1}.

fixed proportion of the whole gut length the result of size independence is still valid.

Efficiency depends on food density as long as digestion is not complete. The undigested amount of food $M_X(t_g)$ can be solved implicitly and a relationship results between the rate of enzyme secretion and the ingestion rate of food items by imposing the constraint that the $M_X(t_g)$ must be small. So it relates ingestion rate to food quality.

If the saturation coefficient M_{KX} of the digestion process is negligibly small, digestion becomes a zero-th order process, and the amount of food in the slice decreases linearly with time (and distance). This has been proposed by Hungate [435], who modelled the 42 hour digestion of alfalfa in ruminants. Digestion is complete if $t_g > M_X(0)(\dot{k}_X y_{Xg} M_g)^{-1}$, and so $\dot{k}_g \dot{J}_{Xm} < \dot{k}_X y_{Xg} \dot{J}_g$, where $\dot{J}_g$ denotes the total enzyme production by the individual; both $\dot{J}_{Xm}$ and $\dot{J}_g$ are proportional to $V^{2/3}$ for an isomorph.

The above model can be extended easily to cover a lot of different enzymes in different sections of the gut, without becoming much more complicated, as long as the additivity assumptions of their mode of action and their products hold. Food usually consists of many components that differ in digestibility. Digestion can only be complete for the animal in question if the most resistant component is digested.

The existence of a maximum ingestion rate implies a minimum gut residence time. With a simple model for digestion, it is possible to relate the digestive characteristics of food to the feeding process, on the assumption that the organism aims at complete digestion. The energy gain from ingested food is then directly proportional to the ingestion rate, if prolonged feeding at constant, different, food densities is considered. See Figure 7.15. Should temperature affect feeding in a different way than digestion, the close harmony between both processes would be disturbed, which would lead to incomplete digestion under some conditions.

7.3.1 Comparison of substrates

When different substrates are compared, the conversion efficiency of substrate to biomass tends to be proportional to the chemical potential μ_X, on the basis of C-moles. It seems reasonable to assume that μ_{AX} is proportional to the chemical potential of substrate. If we tie the maximum reserve capacity $[E_m]$ to $[\dot{p}_{Am}]$, see {270} for arguments, the specific energy conductance $\dot{k}_E$ becomes independent of the chemical potential and the molar yield

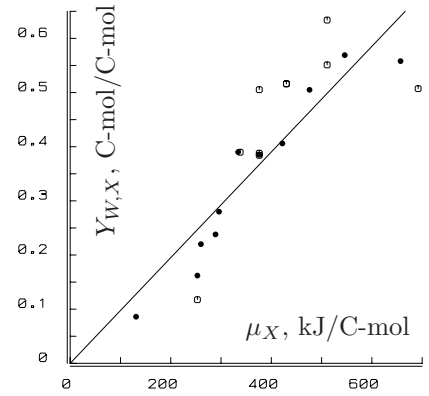

Figure 7.16: The molar yield of biomass corrected for a fixed population growth rate of $\dot{r} = 0.2$ h^{-1} is proportional to the chemical potential of substrate, expressed per C-mole in combustion reference. Data from Rutgers [799] for *Pseudomonas oxalaticus* (•) and from van Verseveld, Stouthamer and others [615,946,947,948,949] for *Paracoccus denitrificans* (○) under aerobic conditions with NH_4^+ as the nitrogen source, corrected for a temperature of 30 °C. No product, or a negligible amount, is formed during these experiments [946].

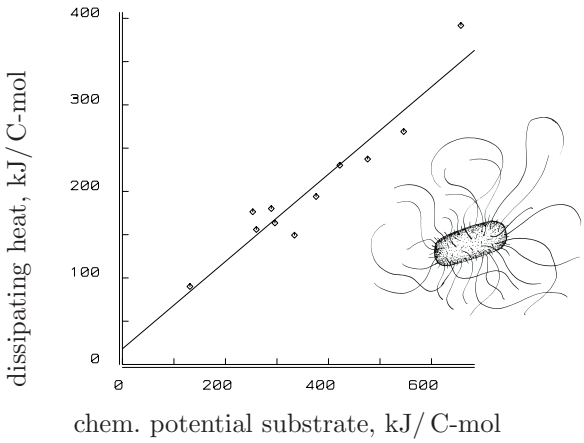

Figure 7.17: The amount of dissipating heat at maximum population growth rate is linear in the free energy per C-mole of substrate on the basis of combustion reference (pH = 7). Data from Rutgers [799] and Heijnen and van Dijken [389,390] for *Pseudomonas oxalaticus*, growing aerobically at 30 °C on a variety of substrates.

of biomass becomes proportional to the chemical potential for a fixed value of $\dot{r}$ via $[E_m]$ in g and in $[M_{Em}]$. This is confirmed in Figure 7.16.

The dissipating heat $\dot{p}_{T+}$ is found from

$$0 = \dot{p}_{T+} + (\boldsymbol{\mu}_{\mathcal{O}}^T - \boldsymbol{\mu}_{\mathcal{M}}^T \boldsymbol{n}_{\mathcal{M}}^{-1} \boldsymbol{n}_{\mathcal{O}}) \boldsymbol{\eta}_{\mathcal{O}} \dot{\boldsymbol{p}}(e,1) M_{V+}/M_{Vm}$$

If the population is growing at maximum rate, we have that $f = e = 1$, and

$$\dot{\boldsymbol{p}}(1,1) = \begin{pmatrix} \frac{\dot{k}_E}{g} & \dot{k}_M & \frac{\dot{k}_E - \dot{k}_M g}{1+g} \end{pmatrix} \mu_{GV} M_{Vm}$$

When different substrates are compared, the dissipating heat tends to increase with the free energy of substrate. This is to be expected, because the maximum volume-specific assimilation rate $[\dot{p}_{Am}]$ and the maximum reserve capacity $[E_m]$ are proportional to the free energy per C-mole of substrate μ_X, see on {241}, so, the reserve turnover rate $\dot{k}_E$ is independent of μ_X, $g \propto \mu_X^{-1}$, and the dissipating heat at maximum population growth rate is approximately linear in μ_X if the combustion frame of reference is used. This frame of reference is necessary because a high free energy of substrate corresponds with a high degree of reduction, which requires more oxygen to release the energy. In the combustion reference, this extra use of oxygen does not affect the relationship between free energy of substrate and heat dissipation. This is confirmed by the data of Rutgers [799]; see Figure 7.17.

The idea that the type of substrate and environmental conditions affect the substrate/energy conversion μ_{AX} (and $[E_m]$) but nothing else is consistent with analyses of data from Pirt [716], who plotted the inverse of the yield against the inverse of the population growth rate and obtained the linear relationship formulated by Marr *et al.* [592]. According to the DEB theory for V1-morphs with small reserve capacities $[E_m]$, this relationship is $\frac{1}{Y_{WX}} = \frac{\mu_{GV}}{\mu_{AX}}(1 + \frac{\dot{k}_M}{\dot{r}})$. As S. J. Pirt noted, this relationship is linear in $\dot{r}^{-1}$, but the slope depends on the substrate-energy conversion μ_{AX}. Pirt found a wide range of 0.083–0.55 h^{-1} on a weight basis for two species of bacteria growing on two substrates, aerobically and anaerobically. The ratio of the slope to the intercept equals the maintenance rate coefficient, $\dot{k}_M$, which does not depend on the substrate-energy conversion. Pirt's data fall in the narrow range of 0.0393–0.0418 h^{-1} [513]. These findings support the funnel concept, which states that a wide variety of substrates is decomposed to a limited variety of building blocks, which depend of course on the nature of the substrate and environmental conditions; these products are then built into biomass, which only depends on internal physiological conditions, subject to homeostasis.

7.4 Cell wall and membrane synthesis

The cell has to synthesize extra cell wall material at the end of the cell cycle. Since the cell grows in length only, the growth of surface material is directly tied to that of cytoplasmic material. Straightforward geometry shows that the change in surface area A of a rod with aspect ratio δ and volume at division V_d is given by $\frac{d}{dt}A = (16\pi\frac{1-\delta/3}{\delta V_d})^{1/3}\frac{d}{dt}V$. So the energy costs of structure can be partitioned as $[E_G] = [E_{GV}] + \{E_{GA}\}(16\pi\frac{1-\delta/3}{\delta V_d})^{1/3}$, where $\{E_{GA}\}$ denotes the energy costs of the material in a unit surface area of cell wall and $[E_{GV}]$ that for the material in a unit volume of cytoplasm. For reasons of symmetry, it is more elegant to work with $[E_{GA}] \equiv \{E_{GA}\}V_d^{-1/3}$ rather than $\{E_{GA}\}$. The dimensions of $[E_{GV}]$ and $[E_{GA}]$ are then the same: energy per volume. At the end of the cell cycle, when cell volume is twice the initial volume, the surface material should still increase from $A(V_d)$ to $2A(V_d/2) = (1 + \delta/3)A(V_d)$. This takes time, of course. If all incoming energy not spent on maintenance is used for the synthesis of this material, the change in surface area is given by $\frac{d}{dt}A = \frac{\dot{k}_E}{g_A}(fA - V_d/V_m^{1/3})$, where $g_A \equiv [E_{GA}]/\kappa[E_m]$. So $A(t) = (A(0) - V_d/fV_m^{1/3})\exp\{tf\dot{k}_E/g_A\} + V_d/fV_m^{1/3}$. The time it takes for the surface area to reach $(1 + \delta/3)V_d^{2/3}$, starting from $A(0) = V_d^{2/3}$, equals

$$t_A = \frac{g_A}{f\dot{k}_E}\left(\ln 2 + \ln\frac{V_\infty - V_d/2}{V_\infty - V_d}\right) \tag{7.10}$$

For the time interval between subsequent divisions, $t(V_d)$ must be added, giving

$$t_d = \frac{g_A}{f\dot{k}_E}\ln 2 + \left(\frac{g_A}{f\dot{k}_E} + \frac{(f+g)V_\infty}{f\dot{k}_E V_d\delta/3}\right)\ln\frac{V_\infty - V_d/2}{V_\infty - V_d} \tag{7.11}$$

The extra time for cell wall synthesis at the caps is not significant for filaments, as their caps are comparatively small. Neither does it play a significant role in unicellular eukaryotic

isomorphs, because they do not have cell walls to begin with. The cell's volume is full of membranes in these organisms, so the amount of membrane at the end of the cell cycle does not need to increase as abruptly as in bacteria, where the outer membrane and cell wall (if present) are the only surfaces. Comparable delays occur in ciliates for instance, where the cell mouth does not function during and around cell division.

Cooper [175] and Koch [500] argued that the weight increase of bacterial cells is always of the exponential type, apart from minor contributions of cell wall, DNA, etc. If the activity of the carriers for substrate uptake is constant during the cell cycle, an implication of this model is that carriers should be produced at a rate proportional to the growth rate, and consequently to cell volume rather than to surface area. This would increase the number of carriers per unit of surface area of active membrane during the cell cycle. At the end of the cell cycle the number of carriers per unit of surface area should (instantaneously) drop by a factor of $(1 + \delta/3)^{-1}$ due to the production of the new membrane without carriers that separates the daughter cells. This factor amounts to $5/6 = 0.83$ for cocci and 1 for V1-morphs. The factor stands for the ratio of the surface area of a body with volume V_d to two times the surface area of a body with volume $V_d/2$; so it is $2^{-1/3} = 0.79$ for isomorphs. To my knowledge, such a reduction has never been demonstrated. The carrier density is assumed to be constant in the DEB theory. If the carrier density in the membrane is constant in the case of exponential growth (in non-V1-morphs), the carrier activity should increase during the cell cycle. This requires the loss of homeostasis and/or complex regulation of carrier activity. In the DEB theory, the carrier activity is constant during the cell cycle. Although exponential growth of the cell seems an attractively simple model at first sight, theory to tie the growth rate to nutrient levels no longer comes naturally for such an extreme 'demand' type of system. Moreover, phenomena such as the small cell size in oligotrophic oceans, the growth of stalks in *Caulobacter*, the removal of disused DNA need other explanations than given in this book. Another point is of course that, if bacteria increased their weight exponentially, they would deviate from unicellular eukaryotes in this respect, where exponential growth is obviously untenable, cf. Figure 1.1. The problem of what makes prokaryotes fundamentally different from eukaryotes in terms of energetics should then be addressed.

7.5 Protein synthesis

RNA, mainly consisting of ribosomal RNA, is an example of a compound known to increase in abundance with the growth rate [495]. This property is used to measure the growth rate of fish, for example [135,432]. In prokaryotes, which can grow much faster, the increase in rRNA is much stronger. This section will, therefore, focus on prokaryotes. Within the DEB model, we can only account for this relationship when (part of the) RNA is included in the energy reserves. This does not seem unrealistic, because when cells experience a decline in substrate density and thus a decline in energy reserves, they are likely to gain energy through the degradation of ribosomes [199]. It also makes sense, because the kinetics of reserve energy density is assumed to be first order, which implies that the use of reserves increases with their density. The connection between the abundance of RNA,

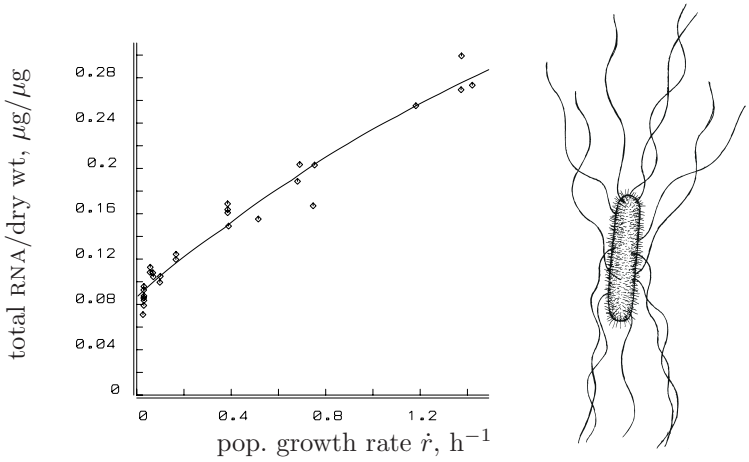

Figure 7.18: The concentration of RNA as a function of the population growth rate in *E. coli*. Data from Koch [495]. The least-squares estimates of the parameters are $\theta_e = 0.44$ (sd 0.05), $\theta_v = 0.087$ (sd 0.005) and $[W_{Ed}]/[W_{Vd}] = 20.7$ (sd 5.4).

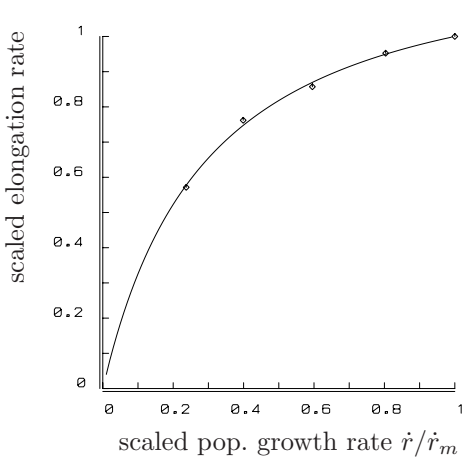

Figure 7.19: Elongation rate in *E. coli* for $\delta = 0.3$, $l_d = 0.24$ (sd 0.019), $g = 32.4$ (sd 91.9). Data from Bremer and Dennis [113]. Both elongation rate and population growth rate are expressed as fractions of their maximum value of $\dot{r}_m = 1.73$ h^{-1} with an elongation rate of 21 aa s^{-1}rib^{-1}.

i.e. the apparatus for protein synthesis, and energy density is, therefore, a logical one. No assumption of the DEB model implies that the energy reserves should be inert materials that only wait for further use. The analysis of the data from Esener in the section on mass–energy coupling, {125}, also points to the conclusion that rRNA can be a significant part of the reserves in bacteria.

The dynamics of RNA is most easy to describe when RNA constitutes a fixed fraction of the energy reserves. This is also the simplest condition under which homeostasis for energy reserves holds in sufficient detail to apply to RNA. The rate of RNA turnover is completely determined by this assumption. It also has strong implications for the translation rate and the total number of translations made from a particular RNA molecule.

RNA as a fraction of dry weight is given in Figure 7.18. If the weight of RNA is a fraction θ_v of the dry weight of structural biomass and a fraction θ_e of the dry weight of the energy reserves, the fraction of dry weight that is RNA equals

$$W_{RNA}/W_d = \frac{\theta_v[W_{Vd}]V + \theta_e[W_{Ed}]fV}{[W_{Vd}]V + [W_{Ed}]fV} = \frac{\theta_v + \theta_e f[W_{Ed}]/[W_{Vd}]}{1 + f[W_{Ed}]/[W_{Vd}]}$$

The parameters of Figure 9.8 were used to relate $\dot{r}$ to f. This indicates that at least in *E. coli* most RNA is part of the reserves, and about half the energy reserves consist of RNA.

The mean translation rate of a ribosome, known as the peptide elongation rate, is proportional to the ratio of the rate of protein synthesis to the energy reserves, E. The rate of protein synthesis is proportional to the growth rate plus part of the maintenance rate, which is higher the lower the growth rate in bacteria [892]. The peptide elongation rate is plotted in Figure 7.19 for *E. coli* at 37 °C. If the contribution of maintenance to protein synthesis can be neglected, the elongation rate at constant substrate density is

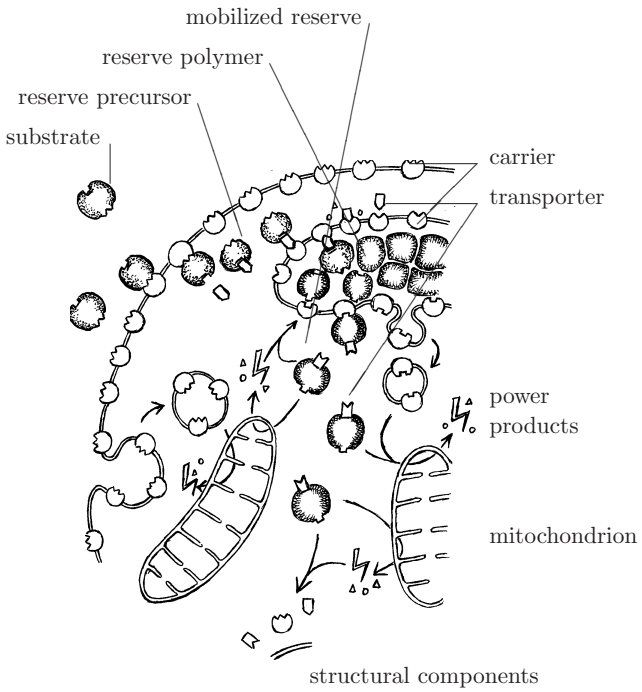

Figure 7.20: In combination with the structural homeostasis hypothesis, the following rules imply a molecular mechanism for first-order kinetics for reserve density: (generalized) substrate is taken up by substrate carriers from the environment, converted into a reserve precursor and added to (generalized polymer) reserves. Reserve carriers mobilize reserves at a constant rate per carrier and a fixed fraction of this flux is used for the synthesis of reserve carriers; the rest of this flux is used for maintenance and growth, where reserves are the source of energy (via decomposition in mitochondria) as well as building blocks for structural mass (including substrate carriers). The carrier density in the membranes does not change and carriers have a limited life span. The turnover of substrate carriers is paid via maintenance.

proportional to the ratio of the growth rate $\frac{d}{dt}V$ to the stored energy $[E_m]fV$. As shown by (3.41), the elongation rate in a rod of mean volume should be proportional to $\dot{r}/f$ at population growth rate $\dot{r}$. The relationship allows the estimation of the parameter l_d, which is hard to obtain in another way.

The lifetime of a compound in the reserves is exponentially distributed with a mean residence time of $(\dot{k}_E(\frac{\delta}{3}\frac{V_d}{V} + 1 - \frac{\delta}{3}))^{-1}$. The mean residence time thus increases during the cell cycle. At division it is $\dot{k}_E^{-1}$, independent of the (population) growth rate. The total number of transcriptions of a ribosome, in consequence, increases with the population growth rate. Outside the cell, RNA is rather stable. The fact that the RNA fraction of dry weight depends on feeding conditions indicates that an RNA molecule has a restricted life span inside the cell.

7.6 Structural homeostasis

This section presents a mechanism that explains why the dynamics of the reserve density, i.e. the ratio of the reserves to the structural volume, follows a first-order process and how the assumption of weak homeostasis can be substantiated. The mechanism behind this reserve dynamics can be simple if the growth rate is small and dilution by growth plays no role: each reserve 'molecule' has a constant probability of being utilized. If the growth rate is large, however, as can be the case for unicellulars, a special mechanism is required to explain why dilution by growth is not involved in the use of reserves. One such a mechanism can be as follows.

Suppose that the reserves of an isomorphic cell are localized in vesicles, see Figure 7.20. Reserves are there because carriers in the outer membrane of the cell (or in membranes

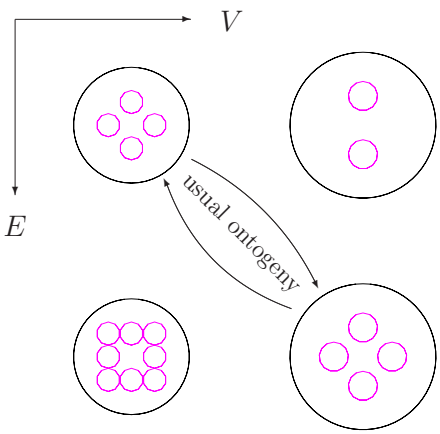

Figure 7.21: The structural cell volume V is growing to the right by a factor two, i.e. the cell diameter is growing by a factor $2^{1/3}$. The (energy) reserve E is growing to the bottom by a factor two, i.e. the number of vesicles is growing by a factor two. Structural homeostasis is obtained if the total amount of membranes in the vesicles is proportional to $EV^{-1/3}$. This implies that the number of vesicles reduces, if the structural cell volume grows, but not the amount of reserves. In that case, the reserve density does not change at constant substrate concentration: structural homeostasis implies weak homeostasis.

that wrap digestive vesicles) bind substrate outside the cell; substrate is then (possibly) converted to reserve precursors, and transporters, gliding along the cytomatrix [165], deliver these precursors to carriers in the membranes of reserve vesicles. The latter carriers release reserve molecules in the vesicle and operate in a way that the reserve precursor density in the cytosol remains constant, for instance because the transporter density is constant. This implies that the rate of transformation of reserve precursors into reserves equals the rate at which enzymes that are located in the outer membrane of the cell bind substrate molecules from the environment and release reserve precursors into the cytosol. The number of such enzyme molecules in the outer membrane is just proportional to the amount of outer membrane; carrier synthesis has in practice been found to be coupled to membrane synthesis, and not directly to growth of the cytoplasm [217].

Reserves are mobilized by other enzymes in the membranes of reserve vesicles. The density of these enzymes in the membranes (i.e. the number of enzyme molecules per surface area of membrane) is constant, i.e. independent of the amount of membranes M_C quantified in C-moles, reserves E or structural cell mass M_V. The enzymes take reserve molecules from the vesicle content and release reserve products into the cytosol to fuel cellular metabolism.

The DEB model assumes that the change in reserves equals the difference between the assimilation energy $\dot{p}_A$ and the catabolic energy $\dot{p}_C$ (i.e. the catabolic power is defined as the energy flux that is mobilized from the reserves). The κ-rule states that a fixed fraction κ of the catabolic energy is spent on growth, $\dot{p}_G = \mu_{GV}\frac{d}{dt}M_V$, plus maintenance, i.e. $\dot{p}_M$. I assume a similar rule for the synthesis and breakdown of membranes. This amounts to

$$\frac{d}{dt}E = \dot{p}_A - \dot{p}_C(E,V) \tag{7.12}$$

$$\frac{d}{dt}M_C = \dot{p}_C(E,V)\eta_{CC} - M_C\dot{k}_C \tag{7.13}$$

$$\frac{d}{dt}M_V = \dot{p}_C(E,V)\eta_{VC} - M_V\dot{k}_M \tag{7.14}$$

where $\dot{p}_C$ denotes the catabolic power of the cell, η_{CC} the conversion efficiency of catabolic power into membrane, $\dot{k}_C$ the specific decay rate of membrane, $\eta_{VC} = \mu_{CV}^{-1}$ the conversion

efficiency of catabolic energy into structural biomass, and $\dot{k}_M$ the maintenance rate coefficient (i.e. $\dot{k}_M = [\dot{p}_M]/[E_G]$). There is no need to distinguish whether structural biomass is first formed and then degraded, or whether maintenance costs are paid before synthesis occurs, since both possibilities result in the same kinetics.

From (7.12) and (7.14), it follows that

$$\frac{d}{dt}[E] = [\dot{p}_A] - [\dot{p}_C] - [E]([\dot{p}_C]\eta_{VG}/[M_V] - \dot{k}_M) \quad \text{or} \tag{7.15}$$

$$[\dot{p}_C] = \frac{[\dot{p}_A] - \frac{d}{dt}[E] + \dot{k}_M[E]}{1 + [E]\eta_{VG}/[M_V]} \tag{7.16}$$

for $[E] \equiv E/V$, $[\dot{p}_C] \equiv \dot{p}_C/V$ and $[\dot{p}_A] \equiv \dot{p}_A/V$. The ratio $\eta_{VG}/[M_V]$ quantifies the efficiency of the conversion of catabolic energy into structural biovolume, since $[M_V]$ stands for the number of C-moles per unit of biovolume.

Suppose that the number of vesicles n and their radius change fast with respect to the change in V_C and that the radius is proportional to the radius of the cell, i.e. proportional to the ratio of volume to surface area. This fast coupling between the linear dimensions of vesicles and cell is called the structural homeostasis assumption, see Figure 7.21. Because the membranes wrap the reserves, one must have that $E = nV[E_n]$ (or $[E] = n[E_n]$) and

$$M_C = nV^{2/3}\{M_{Cn}\} = [E]V^{2/3}\{M_{Cn}\}/[E_n] \quad \text{or} \tag{7.17}$$

$$\frac{d}{dt}M_C = \left(V^{2/3}\frac{d}{dt}[E] + \frac{2}{3}V^{-1/3}[E]\frac{d}{dt}V\right)\frac{\{M_{Cn}\}}{[E_n]} \tag{7.18}$$

where $[E_n]$ and $\{M_{Cn}\}$ are conversion constants. Note that the assumption of the fast coupling between the linear dimensions of the vesicles and the cell is equivalent to the assumption that the number of vesicles is proportional to the reserve density.

From (7.13) and (7.18) and from (7.16), we obtain

$$[\dot{p}_C] = \mu_{CC}V^{-1}\left(\frac{d}{dt}M_C + M_C\dot{k}_C\right) \tag{7.19}$$

$$= \frac{\{M_{Cn}\}V^{-1/3}}{[E_n]\eta_{CC}} \frac{\frac{d}{dt}[E] + (\dot{k}_C - \frac{2}{3}\dot{k}_M)[E]}{1 - \frac{2}{3}\frac{\{M_{Cn}\}\eta_{VC}}{[E_n]\eta_{CC}[M_V]}[E]V^{-1/3}} \tag{7.20}$$

$$\frac{d}{dt}[E] = \frac{[\dot{p}_A] - [E]\left(V^{-1/3}\dot{v}\left(1 - \frac{2}{3}\frac{\dot{k}_M}{\dot{k}_C} + \frac{2}{3}\frac{\eta_{VC}}{[M_V]}\frac{[\dot{p}_A]}{\dot{k}_C} + [E]\frac{\eta_{VC}}{[M_V]}\right) - \dot{k}_M\right)}{1 + \frac{\dot{v}}{\dot{k}_C}V^{-1/3}(1 + \frac{1}{3}\frac{\eta_{VC}}{[M_V]}[E])} \tag{7.21}$$

for $\dot{v} \equiv \frac{\{M_{Cn}\}\dot{k}_C}{[E_n]\eta_{CC}}$.

Suppose that the membrane kinetics is fast with respect to the reserve kinetics, so $\eta_{CC} \to \infty$ and $\dot{k}_C \to \infty$, such that $\eta_{CC}/\dot{k}_C$ remains fixed. The consequence is that the amount of membrane is in pseudo-equilibrium, i.e. $\frac{d}{dt}M_C \to 0$, and the specific membrane activity is constant, i.e. $[\dot{p}_C]/[M_C] = \dot{k}_C/\eta_{CC}$. In other words: each enzyme in the membrane binds a reserve 'molecule' inside a vesicle and releases a reserve product 'molecule' outside the vesicle into the cytosol at a rate that does not depend on the amount of reserves

or the structural volume of the cell. The amount of membranes per structural cell volume equals $[M_M^*] = [E]V^{-1/3}\{M_{Cn}\}/[E_n]$, which implies that the energy costs of membrane turnover are included in the overhead of the catabolic power. Since the membrane density is proportional to an inverse length measure, strict chemical homeostasis is lost if the membrane composition differs from the structural biomass.

In the limit, (7.21) reduces to

$$\frac{d}{dt}[E] = [\dot{p}_A] - [E]\left(V^{-1/3}\dot{v}(1 + [E]\eta_{VC}/[M_V]) - \dot{k}_M\right) \tag{7.22}$$

If $[E]\eta_{VC} \ll [M_V]$ (so $[E_m]\eta_{VC} \ll [M_V]$, or $g \equiv \frac{[E_G]}{\kappa[E_m]} \gg 1$) and $\dot{k}_M \ll \dot{v}V^{-1/3}$ (so $\dot{k}_M \ll \dot{v}V_m^{-1/3} = \dot{k}_M g$, which again gives $g \gg 1$), we finally obtain

$$\frac{d}{dt}[E] = [\dot{p}_A] - \dot{v}[E]V^{-1/3} \tag{7.23}$$

Since $[\dot{p}_A] = f\{\dot{p}_{Am}\}V^{-1/3}$, we have the maximum reserve density $[E_m] = \{\dot{p}_{Am}\}\frac{[E_n]\eta_{CC}}{\{M_{Cn}\}\dot{k}_C}$. This relationship shows that the maximum reserve density is an extensive quantity, i.e. a physical design parameter, because $\{\dot{p}_A\}$ is such a parameter, while the four other parameters are intensive quantities. The body size scaling rules, as implied by the DEB theory (see {267}), show that the inequality $g \gg 1$ is likely to apply to the very small organisms since $[E_G]$ and κ do not depend on body size and $[E_m]$ is proportional to volumetric length, so that g is inversely proportional to volumetric length.

The effect of dilution by growth on the dynamics of the reserves is small if $\frac{d}{dt}\ln V \ll \dot{v}V^{-1/3}$. Using $V^{-1}\frac{d}{dt}V = [M_V]^{-1}\frac{d}{dt}M_V$, and $\frac{d}{dt}M_V = \mu_E^{-1}y_{VE}\dot{p}_G$, we obtain from Table 3.5 that $V^{-2/3}\frac{d}{dt}V = \frac{\dot{v}}{g}\frac{e-l-l_h}{1+e/g}$. This quantity is much smaller than $\dot{v}$ if $g \gg -l - l_h$. So, the dilution is negligible if g is large. Dilution by growth can never become important because fast growth cannot combine with a small change of energy reserves, because the costs of growth are paid from the change in energy reserves.

For a V1-morphic cell, we have that $M_C = nV[M_{Cn}^*] = [E]V[M_{Cn}^*]/[E_n]$ and

$$[\dot{p}_C] = \frac{[M_{Cn}^*]}{[E_n]\eta_{CC}}\frac{\frac{d}{dt}[E] + (\dot{k}_C - \dot{k}_M)[E]}{1 - \frac{[M_{Cn}^*]\eta_{VC}}{[E_n]\eta_{CC}[M_V]}[E]} \tag{7.24}$$

$$\frac{d}{dt}[E] = \frac{[\dot{p}_A] - [E]\left(\dot{k}_E\left(1 + \frac{[\dot{p}_A]}{\dot{k}_C}\frac{\eta_{VC}}{[M_V]} - \frac{\dot{k}_M}{\dot{k}_C} + [E]\frac{\eta_{VC}}{[M_V]}\right) - \dot{k}_M\right)}{1 + \dot{k}_E/\dot{k}_C} \tag{7.25}$$

$$= [\dot{p}_A] - [E](\dot{k}_E(1 + [E]\eta_{VC}) - \dot{k}_M) \quad \text{for} \quad \dot{k}_C \to \infty \tag{7.26}$$

$$\simeq [\dot{p}_A] - [E](\dot{k}_E - \dot{k}_M) \quad \text{for} \quad g \gg 1 \tag{7.27}$$

where $\dot{k}_E \equiv \frac{[M_{Cn}^*]\dot{k}_C}{[E_n]\eta_{CC}}$ and $[\dot{p}_A] = f[\dot{p}_{Am}]$. The membrane-specific activity equals $[\dot{p}_C]/[M_C] = \dot{k}_C/\eta_{CC}$, just as for isomorphic cells.

The essential element in the proposed mechanism of first-order dynamics for reserve density, and weak homeostasis, is a spatial micro-structure that is subjected to structural homeostasis. Although many reserves are actually wrapped by membranes, even in

prokaryotes [553, p 31], membranes are not essential elements in the proposed mechanism. What is essential is that the (polymer) reserves in a single droplet or granule can only be assessed from the outside, so the relative accessibility decreases with the size of the granule. The key element is thus the change in the surface area/volume ratio at a micro scale.

7.7 Growth of dynamic mixtures of morphs

Some organisms change in shape during growth in a complex fashion. Frequently it is still possible, however, to take these changes in shape into account in a rather simple way.

7.7.1 Crusts

Crusts, i.e. biofilms of limited extent that grow on hard surfaces, are mixtures of V0-morphs in the centre and V1-morphs in the periphery where the new surface is covered. Bacterial colonies on an agar plate, conceived as super-organisms, are crusts. When crusts grow, an increasing proportion of the biomass behaves as a V0-morph. With an extra assumption about the transfer of biomass from one mode of growth to the other, the growth of the crust on a plate is determined and can be worked out as follows for constant substrate density.

Let L_ϵ denote the width as well as the thickness of the outer annulus of the circular crust of radius L_r that is growing exponentially in an outward direction. The width and the thickness of the outer annulus remain constant. This biomass thus behaves as a V1-morph; all other biomass in the centre of the crust behaves as a V0-morph. The surface area of the crust is $A_r(t) = \pi L_r^2(t)$, and of the exponentially growing annulus $A_\epsilon(t) = \pi\left(L_r^2(t) - (L_r(t) - L_\epsilon)^2\right) = \pi\left(2L_r(t)L_\epsilon - L_\epsilon^2\right)$. The total surface area is growing at rate $\frac{d}{dt}A_r = \dot{r}A_\epsilon$, so the radius is growing at rate

$$\frac{d}{dt}L_r = \dot{r}L_\epsilon\left(1 - \frac{L_\epsilon}{2L_r}\right)$$

from which it follows that the diameter of the crust is growing linearly in time for $L_\epsilon \ll L_r$. This linear growth in diameter has been observed experimentally by Fawcett [272], and the linear growth model originates from Emerson [254] in 1950 according to Fredrickson *et al.* [297]. Figure 7.22 shows that this linear growth applies to lichen growth on moraines. Richardson [763] discusses the value of gravestones for the study of lichen growth, because of the reliable dates. Lichen growth rates are characteristic of the species, so the diameter distribution of the circular patches can be translated into arrival times, which can then be linked to environmental factors, for instance.

If substrate transport in the vertical direction on the plate is sufficient to cover all maintenance costs, and transport in the horizontal direction is small, the growth rate of the V0-morph on top of an annulus of surface area dA is

$$\frac{d}{dt}V = \frac{f\{\dot{p}_{Am}\}\,dA - [\dot{p}_M]V}{[E_G] + [E_m]f}$$

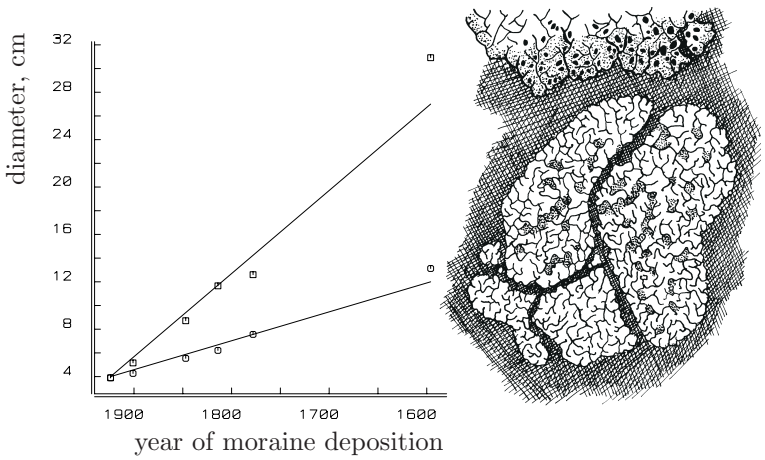

Figure 7.22: The lichens *Aspicilia cinerea* (above) and *Rhizocarpon geographicum* (below) grow almost linearly in a period of more than three centuries on moraine detritus of known age in the European Alps. Data from Richarson [763]. Linear growth is to be expected from the DEB model, when such lichens are conceived as dynamic mixtures of V0- and V1-morphs.

The denominator stands for the volume-specific costs of structural biomass and reserves. Division by the surface area of the annulus gives the change in height L_h of the V0-morph on the top of an annulus of surface area $dA = V_d^{2/3}$; the height is found from (3.37) by substituting $V = L_h V_d^{2/3}$

$$\frac{d}{dt}L_h = \frac{\dot{v}}{e+g}(e - V_m^{-1/3}L_h) \text{ or } \frac{d}{dt}l_h = 3\dot{r}_B(f - l_h)$$

with the scaled height $l_h \equiv L_h V_m^{-1/3}$. The initial growth rate in scaled height is $3\dot{r}_B(f - l_\epsilon)$. The parameter $l_\epsilon \equiv L_\epsilon V_m^{-1/3}$ can be eliminated, on the assumption that the growth rate in the outward direction equals the initial growth rate in the vertical direction, which gives $l_\epsilon = l_d/2$ for $l_d \ll f$. For $l_d \ll l_r$ with $l_r \equiv L_r V_m^{-1/3}$, the end result amounts to

$$l_h(t, l_r) = f - (f - l_d/2)\exp\left\{\frac{l_r}{f - l_d} - 3\dot{r}_B t\right\} \tag{7.28}$$

The scaled height of the crust is thus growing asymptotically to f. Different crust shapes can be obtained by accounting for horizontal transport of biomass and diffusion limitation of food transport to the crust.

The spatial expansion of geographical distribution areas of species, such as the musk rat in Europe, and of infectious diseases, cf. [104,105,386], closely resembles that of crusts. Although these population phenomena differ in many respects from the growth of crusts as (super) individuals, the reason why the expansion proceeds at a constant rate is basically the same from an abstract point of view: material in the border area grows exponentially, but the inner area hardly contributes to the expansion.

7.7.2 Flocs and tumours

Growth in the thickness of a biofilm on a plane, which behaves as a V0-morph, is thus similar to that of a spherical biofilm on a small core in suspension, which behaves as an isomorph as long as mass transport in the film is sufficiently large to consider the biomass as homogeneous. Films are growing in a von Bertalanffy way in both situations, if growth

via settling of suspended cells on the film is not important. Note that if maintenance is small, so that the asymptotic depth of the film is large, the increase in diameter is linear with time, so that volume increases as time^3, as has been found for foetuses in (3.26) by different reasoning. This mode of growth was called the 'cube root' phase by Emerson [254], who found it applicable to submerged mycelia of the fungus *Neurospora*. The model was originally formulated by Mayneord for tumour growth [601], and frequently applied since then [541,619,879,990].

If mass transport in a spherical biofilm on a small core in suspension is not large, the biomass in the centre will become deprived of substrate by the peripheral mass, and die from starvation. Such a film is called a (microbial) floc. A concentration gradient of substrate develops in the living peripheral mass, such that the organisms at the living/dead boundary layer just receive enough substrate to survive, and do not grow. The organisms at the outer edge grow fastest. The thickness of the living layer directly relates to the transport rate of substrate, and so depends on the porosity of the floc. Flocs again behave as dynamic mixtures of V0- and V1-morphs, and, just like crusts, the floc diameter eventually grows linearly in time at constant substrate densities in the environment, if it does not fall apart because of the increasing mechanic instability. This can be seen as follows.

Let L_ϵ denote the thickness of the thin living layer of a spherical floc of radius L_r. The thickness remains constant, while the living mass is growing exponentially at rate $\dot{r}$. The outer layer behaves as a V1-morph, the kernel as a degenerated V0-morph. The total volume of the floc is $V_r(t) = \frac{4}{3}\pi L_r^3(t)$ and of the living layer $V_\epsilon(t) = \frac{4}{3}\pi\left(L_r(t)^3 - (L_r(t) - L_\epsilon)^3\right) = \frac{4}{3}\pi\left(3L_r^2(t)L_\epsilon - 3L_r(t)L_\epsilon^2 + L_\epsilon^3\right)$. The growth of the floc is given by $\frac{d}{dt}V_r = \dot{r}V_\epsilon$, so the radius is growing at rate

$$\frac{d}{dt}L_r = \dot{r}L_\epsilon\left(1 - \frac{L_\epsilon}{L_r} + \frac{L_\epsilon^2}{3L_r^2}\right)$$

For $L_r \gg L_\epsilon$, the change in the radius L_r becomes constant, and the floc grows linearly in time. The steady-state population growth rate of flocs can be obtained analytically, given a fixed size at fragmentation into n parts. The dead volume increases with $\frac{d}{dt}V_\dagger(t) = 4\pi(L_r(t) - L_\epsilon)^2\frac{d}{dt}L_r(t)$. B. W. Brandt (pers. comm.) showed that the combination of diffusive transport of substrate into the floc, and uptake that is a hyperbolic function of the substrate density leads to a living layer of thickness $\left(\frac{\dot{D}X_k}{2j_{Xm}X_1}\right)^{1/2}\int_{x_\dagger}^{x_0}\left(y - x_\dagger + \ln\frac{1+x_\dagger}{1+y}\right)^{-1/2}dy$, where $\dot{D}$ is the diffusion coefficient, the scaled substrate density at the living/ dead boundary is $x_\dagger = \frac{[\dot{p}_M]}{[\dot{p}_{Am}]-[\dot{p}_M]}$ with specific maintenance power $[\dot{p}_M]$ and specific maximum assimilation power $[\dot{p}_{Am}]$, scaled substrate concentration $x_0 = X_0/X_K$ with saturation constant X_K, biomass density in the floc X_1 and maximum specific substrate uptake rate $[j_{Xm}]$ [109].

7.7.3 Roots and shoots

The modelling step from algae to plants involves a number of extensions that primarily relate to the fact that plants take up nutrients through roots, while shoots (including leaves) are used for light and carbon dioxide uptake and water transpiration, which affect internal nutrient and metabolite transport. This makes the allocation of resources to root versus

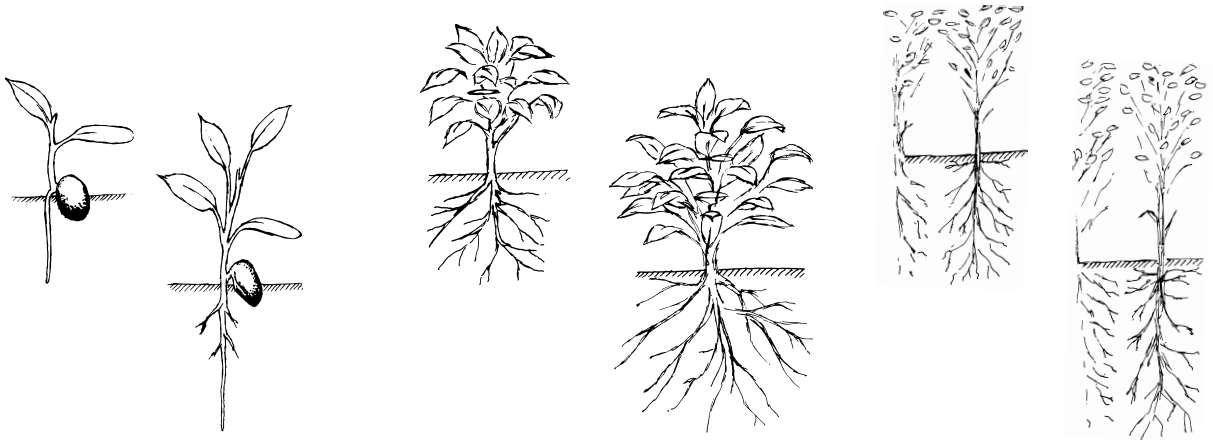

Figure 7.23: Just after germination, plants usually grow as V1-morphs, but when the number of leaves increases, self-shading becomes important, and the plant gradually behaves as an isomorph. If they make contact with other plants, and leaves and roots form a closed layer, they behave as V0-morphs; an increase in mass no longer results in an increase of surface area that is effectively involved in nutrient or light uptake.

shoot growth of special interest, as well as shape changes that affect surface area/ volume relationships via the scaling of assimilation and maintenance, respectively, with structural mass. As illustrated in Figure 7.23, most plants naturally develop from a V1-morphic, via an isomorphic, to a V0-morphic growth during their life cycle. Procumbant plants almost skip the isomorphic phase and directly develop from V1- to V0-morphic growth, similar to crusts [85]. Climbing plants seem to stay in the V1-morphic phase.

These changes in shape can be incorporated using the shape correction function $\mathcal{M}(V)$, which can be chosen differently for roots and shoots. Given the wild diversity of plant shapes and the extreme extent of local adaptations, it is hard to see how a choice can be based on mechanistic arguments. Empirical and convenience arguments can hardly be avoided at this point. A simple choice would be $\mathcal{M}(V) = (V/V_d)^{1/3-(V/V_m)^\beta}$, which starts from V1- and ends with V0-morphic growth when it reaches its maximum volume V_m.

7.8 Pupa and imago

Insects do not grow in the adult stage, called the imago. They are thus much less flexible in their allocation of energy. Holometabolic insects (butterflies, wasps, beetles, flies) have a pupal stage between the juvenile and the adult one, which has a development pattern that strongly resembles that of the embryo or, more specifically, the foetus, since the energy reserves at eclosion are usually quite substantial so that there is hardly any growth retardation due to reserve depletion. This resemblance to a development pattern is not a coincidence because the adult tissue develops from a few tiny imaginal disks, the structural biomass of the larva being first converted to reserves for the pupa. So the initial structural volume of the pupa is very small indeed. Since no energy input from the environment occurs

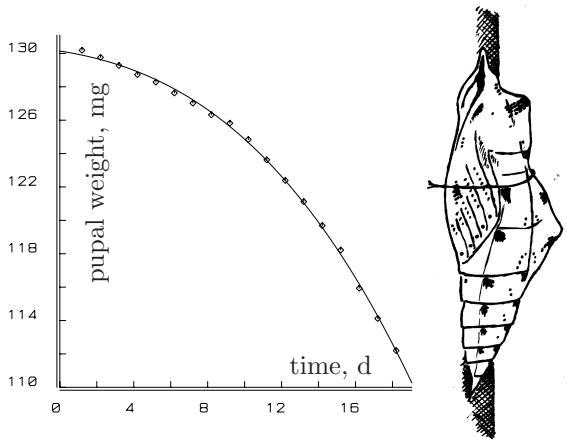

Figure 7.24: The wet weight development of the male pupa of the green-veined white butterfly *Pieris napi* at 17 °C until eclosion, after having spent 4 months at 4 °C. Data from Forsberg and Wiklund [290]. The fitted curve is $W_w(t) = 130.56 - (\frac{7.16+t}{9.61})^3$, with weight in mg and time in days, as is expected from the DEB theory.

until development is completed, pupal weight decreases, reflecting the use of energy. This can be worked out quantitatively as follows.

As discussed under foetal development {104}, growth is given by $\frac{d}{dt}V = \dot{v}V^{2/3}$, so that, if temperature is constant, $V^{1/3}(t) = V_0^{1/3} + t\dot{v}/3$, where V_0 represents the structural volume of the imaginal disks. The energy in the reserves decreases because of growth, maintenance and development, so that

$$E(t) = E_0 - \frac{[E_G]}{\kappa}V(t) - \frac{[\dot{p}_M]}{\kappa}\int_0^t V(t_1)\,dt_1 \tag{7.29}$$

$$= E_0 - \frac{[E_G]}{\kappa}(V_0^{1/3} + t\frac{\dot{v}}{3})^3 - \frac{[\dot{p}_M]}{4\kappa\dot{v}}(V_0^{1/3} + t\frac{\dot{v}}{3})^4 + \frac{[\dot{p}_M]}{4\kappa\dot{v}}V_0^{4/3} \tag{7.30}$$

Together with the contribution of the structural volume, this translates via (2.6) into the wet weight development

$$W_w(t) = w_E\frac{E_0}{\mu_E} - (gw_E[M_{Em}] - d_V)\left(V_0^{1/3} + t\frac{\dot{v}}{3}\right)^3 - \frac{w_E[M_{Em}]}{4V_m^{1/3}}\left(\left(V_0^{1/3} + t\frac{\dot{v}}{3}\right)^4 - V_0^{4/3}\right) \tag{7.31}$$

Tests against experimental data quickly show that the contribution of the third term, which relates to maintenance losses, is too small to be noticed. So the weight-at-time curve reduces to a three-parameter one. It fits the data excellently, see Figure 7.24. Just as in foetuses, the start of the development of the pupa can be delayed, in a period known as the diapause. The precise triggers that start development are largely unknown.

Imagos do not grow, so if the reserve dynamics (3.10) still applies, the catabolic rate reduces to $\dot{p}_C = \{\dot{p}_{Am}\}V^{2/3}e$. If food density is constant or high, and aging during the pupate state is negligible, the change in damage inducing compounds is

$$\frac{d}{dt}[M_Q] = \mu_{QC}^{-1}[\dot{p}_C] = \mu_{QC}^{-1}\{\dot{p}_{Am}\}V^{-1/3}f = \frac{[E_G]\dot{k}_M f}{\kappa\mu_{QC}l}$$

where $l \equiv (V/V_m)^{1/3}$ and $V_m^{1/3} \equiv \kappa\{\dot{p}_{Am}\}/[\dot{p}_M]$ as before. Note that, in this case, V_m cannot be interpreted as the maximum body volume and κ cannot be interpreted as a partition coefficient. Energy derived from food is spent on (somatic plus maturity) maintenance at a constant rate (at constant temperature) in imagos; the rest is spent on reproduction. The

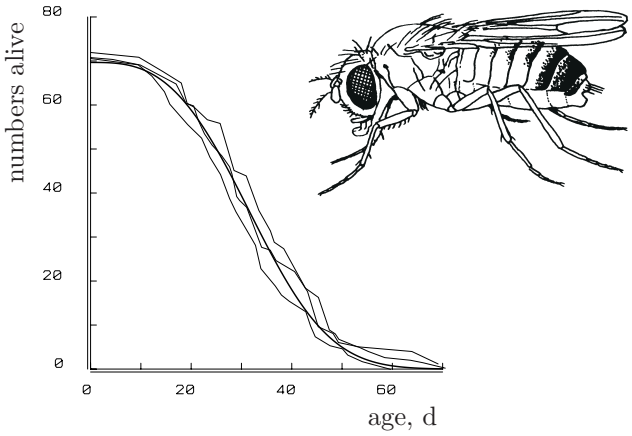

Figure 7.25: The survival curves of the female fruit fly *Drosophila melanogaster* at 25 °C and unlimited food. Data from Rose [788]. The fitted survival curve is $\exp\{-(\dot{h}_i t)^3\}$ with $\dot{h}_i = 0.0276$ (sd 0.00026) d^{-1}.

loss of the interpretations for V_m and κ is not a problem; the term $[\dot{p}_M]/\kappa$ represents the sum of the somatic and maturity volume-specific maintenance costs, so $V_m^{1/3}$ represents the ratio of the maximum surface-area-specific assimilation rate to the volume-specific total maintenance costs.

The hazard rate and the survival probability simplify to

$$\dot{h}(t) = \frac{t^2}{2}\ddot{h}_a \dot{k}_M f/l \tag{7.32}$$

$$\Pr\{\underline{a}_\dagger > a_p + t | \underline{a}_\dagger > a_p\} = \exp\left\{-\frac{1}{6}t^3 \ddot{h}_a \dot{k}_M f/l\right\} = \exp\left\{-(\dot{h}_i t)^3\right\} \tag{7.33}$$

for aging rate $\dot{h}_i \equiv (\frac{1}{6}\ddot{h}_a \dot{k}_M f/l)^{1/3}$, and age at puberty a_p. This is thus the Weibull model with a fixed shape parameter of 3. The mean age at death as an imago then equals $\Gamma(\frac{1}{3})(3\dot{h}_i)^{-1} \simeq 1.62(\ddot{h}_a \dot{k}_M f/l)^{-1/3}$, where Γ stands for the gamma function $\Gamma(x) \equiv \int_0^\infty t^{x-1} \exp\{-t\}\, dt$.

Experimental results of Rose, Figure 7.25, suggest that this is realistic. He showed that longevity can be prolonged in female fruit flies by selecting offspring from increasingly older females for continued culture [788]. It cannot be ruled out, however, that this effect has a simple nutrient/energy basis with little support for evolutionary theory. Selection for digestive deficiency also results in a longer life span. Reproduction, feeding, respiration and, therefore, aging rates must be coupled because of the conservation law for energy. This is beautifully illustrated with experimental results by Ernsting and Isaaks [260], who collected carabid beetles *Notiophilus biguttatus* from the field shortly after eclosion, kept them at a high and a low level of food supply (springtail *Orchesella cincta*) at 16 h 20 °C:8 h 10 °C, and measured survival and egg production. A third cohort was kept at 10 °C at a high feeding level. They showed that the respiration rate of this 4–7 mg beetle is linear in the reproduction rate: $0.84 + 0.041\dot{R}$ in $\mathrm{J\,d^{-1}}$ at 20/10 °C and $0.57 + 0.051\dot{R}$ at 10 °C. This linear relationship is to be expected for imagos on the basis of the aforementioned interpretations. It allows a reconstruction of the respiration rate during the experiment from reproduction data and a detailed description of the aging process. This is more complex than the Weibull model, because metabolic activity was not constant, despite standardized experimental conditions. The quantitative details are as follows.

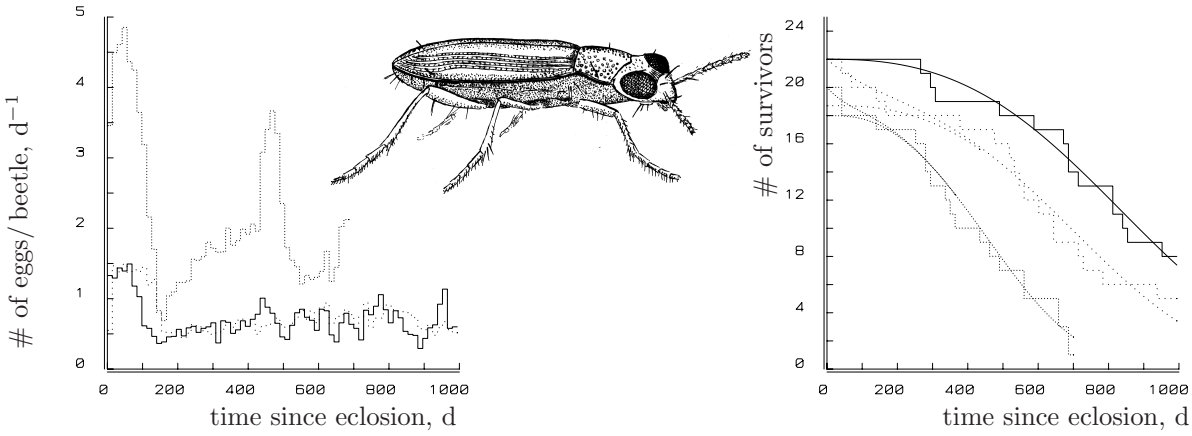

Figure 7.26: The reproduction rate (left figure) of the carabid beetle *Notiophilus biguttatus* feeding on a high density (stippled graphs) of springtails at 20/10 °C (densely stippled) and at 10 °C (sparsely stippled) and a lower density (drawn graph) at 20/10 °C. The survival probability of these cohorts since eclosion is given in the right figure. Data from G. Ernsting, pers. comm. and [260]. The survival probability functions (right) are based on the observed reproduction rates with estimated parameter $\ddot{h}_a e_0 (\kappa_R g l^3)^{-1} = 0.63$ (0.02) a^{-2} for high food level and high temperature, 0.374 (0.007) a^{-2} for low food level and high temperature, 0.547 (0.02) a^{-2} for high food level and low temperature. The contribution of maintenance costs to aging is determined from respiration data. A small fraction of the individuals at the high food levels died randomly at the start of the experiments.

The catabolic rate is subdivided into the maintenance and reproduction costs as

$$\dot{p}_C = \dot{p}_M/\kappa + \dot{R}E_0/\kappa_R = (\dot{k}_M + \dot{R}e_0(g\kappa_R l^3)^{-1})[E_G]V/\kappa$$

where the scaled egg cost e_0 is given in (3.31). This gives the hazard rate and survival probability

$$\begin{aligned} \dot{h}(t) &= \frac{1}{2}\ddot{h}_a \dot{k}_M t^2 + \frac{\ddot{h}_a e_0}{\kappa_R g l^3} \int_0^t \int_0^{t_1} \dot{R}(t_2)\, dt_2\, dt_1 \\ \Pr\{\underline{a}_\dagger > a_p + t | \underline{a}_\dagger > a_p\} &= \exp\left\{ -\frac{1}{6}\ddot{h}_a \dot{k}_M t^3 - \frac{\ddot{h}_a e_0}{\kappa_R g l^3} \int_0^t \int_0^{t_1} \int_0^{t_2} \dot{R}(t_3)\, dt_3\, dt_2\, dt_1 \right\} \end{aligned}$$

Although e_0 depends on the reserve energy density of the beetle, and so on feeding behaviour, variations will be negligibly small for the present purpose since food-dependent differences in egg weights have not been found. The low temperature cohort produced slightly heavier eggs, which is consistent with the higher respiration increment per egg. The estimation procedure is now to integrate the observed $\dot{R}(t)$ three times and to use the result in the estimation of the two compound parameters $\frac{1}{6}\ddot{h}_a \dot{k}_M$ and $\ddot{h}_a e_0 (\kappa_R g l^3)^{-1}$ of the survivor function from observations.

Figure 7.26 confirms this relationship between reproduction, and thus respiration, and aging. The contribution of maintenance in respiration is very small and could not be estimated from the survival data. The mentioned linear regressions of respiration data

against the reproduction rate indicate, however, that $\kappa_R g \dot{k}_M l^3/e_0 = 0.84/0.041 = 20.4$ d^{-1} at 20/10 °C or $0.57/0.051 = 11$ d^{-1} at 10 °C. This leaves just one parameter $\ddot{h}_a e_0 (\kappa_R g l^3)^{-1}$ to be estimated from each survival curve. The beetles appear to age a bit faster per produced egg at high than at low food density. This might be caused by eggs being more costly at high food density, because of the higher reserves at hatching. Another aspect is that, at high food density, the springtails induced higher activity, and so higher respiration, by physical contact. Moreover, the substantial variation in reproduction rate at high food density suggests that the beetles had problems with converting the energy allocated to reproduction to eggs, which led to an increase in κ_R and a higher respiration per realized egg. Note that these variations in reproduction rate are hardly visible in the survival curve, which is due to triple integration. The transfer from the field to the laboratory seemed to induce early death for a few individuals at the high food levels. This is not related to the aging process but, possibly, to the differences with field conditions.

The Weibull model for aging with a fixed shape parameter of 3 should not only apply to holometabolic insects, but to all ectotherms with a short growth period relative to the life span. Gatto *et la.* [312] found, for instance, a perfect fit for the bdelloid rotifer *Philodina roseola* where the growth period is about 1/7-th of the life span. Notice that constant temperature and food density are still necessary conditions for obtaining the Weibull model.

The presented tests on pupal growth and survival of the imago support the applicability of the DEB theory to holometabolic insects, if some elementary facts concerning their life history are taken into account. This suggests new interpretations for experimental results.

7.9 Changing parameter values

Parameter values are usually constant, by definition, but environmental and internal factors might make them vary in time. Such variations occur at different time scales, and some variations are permanent.

Several changes have already been introduced, and are briefly recapitulated in this introduction. Starvation can induce changes energy allocation through κ, and prolonged starvation can invoke drastic qualitative changes. Choices of diet are frequently predictable, and sometimes relate to the life stage; this comes with changes in (maximum) ingestion rate and assimilation energy. During pregnancy and the lactation period, and prior to migration, the maximum ingestion and assimilation rates can be elevated, which involves hormonal control. Toxicants and parasites can affect parameter values. Although not worked out quantitatively, parameter values can be coupled to the aging process, where maintenance, reproduction and feeding usually tend to decrease with age.

Some changes are briefly discussed in the next subsections, to reveal possible interpretations of data in the light of the DEB theory. They are arranged on an increasing time scale.

7.9.1 Changes due to body temperature

Empirical growth curves of birds frequently deviate from the von Bertalanffy growth curve, even if food is abundant. Does this falsify the DEB theory? Not necessarily. The body temperature of endotherms can be well above the environmental temperature. If insulation or heat transfer from mother to chick changes in time, deviations from the von Bertalanffy growth curve are to be expected. Altricial birds provide an excellent case to illustrate the problem of the energy interpretation of growth measurements in the case of an unknown body temperature. This section offers partial solutions to the interpretation problem.

Birds become endothermic around hatching; precocial species usually make the transition just before hatching, and altricial ones some days after. The ability to keep the body temperature at some fixed level is far from perfect at the start, so the body temperature depends on that of the environment and the behaviour of the parent(s) during that period. Unless insulation of the nest is perfect, the parents cannot heat the egg to their own body temperature. There will be a few degrees difference, but this is still a high temperature, which means that the metabolic rate of the embryo is high. So it produces an increasing amount of heat as a byproduct of its general metabolism before the start of endothermic heating.

The process of pre-endothermic heating can be described by: $\frac{d}{dt}T_b = \alpha_T \dot{p}_{T+} - \dot{k}_{be}(T_b - T_e)$, where T_b is the body temperature of the embryo, T_e the temperature of the environment, α_T the heat generated per unit of utilized energy and $\dot{k}_{be}$ the specific heat flux from the egg to the environment. The latter is here taken to be independent of the body size of the embryo, because the contents of the egg are assumed to be homogeneous with respect to the temperature. (The Brunnich's guillemot seems to need a 40 °C temperature difference between one side of the egg and the other to develop [760].)

Figure 7.27 illustrates the development of the lovebird *Agapornis*, with changing body temperature ($T_A = 10\,\mathrm{kK}$). The curves hardly differ from those with a constant temperature, but the parameter estimates differ substantially. The magnitude of the predicted temperature rise depends strongly on the parameter values chosen. The information contained in the data of Figure 7.27 did not allow a reliable estimation of all parameters; the predicted temperature difference of 4 °C is arbitrary, but not unrealistic.

It is interesting that the red-headed lovebird, *A. pullaria* from Africa, and at least 11 other parrot species in South America, Australia and New Guinea breed in termite nests, where they profit from the heat generated by the termites. Breeding Golden-shouldered parrots, *Psephotus chrysopterygius*, in captivity failed frequently, until it became known that one has to heat the nest to 33 °C for some days before hatching and for two weeks after.

The significance of this exercise is the following: the least-squares-fitted curves remain almost exactly the same, whether or not the body temperature changes, but the parameter estimates for, for example the energy conductance, differ considerably. It follows that these data are not suitable for estimating energy parameters unless the temperature is known as a function of time. This holds specially for altricial birds because they hatch too early to show the reduction in respiration rate that gives valuable information about parameter values. The few studies on bird development that include temperature measurements

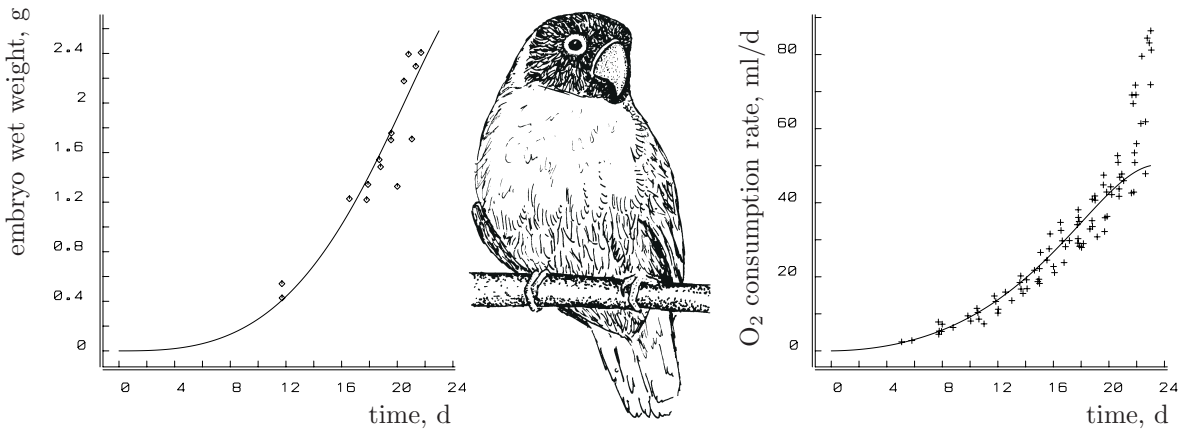

Figure 7.27: Embryo weight and respiration ontogeny in the parrot *Agapornis personata*. Data from Bucher [134]. The curves are DEB model predictions accounting for a temperature increase of 4 °C during development; see text. The temporary respiration increase at day 23 relates to hatching. This detail is not part of the model.

indicate that the temperature change during incubation is not negligibly small. Drent [233] found an increase from 37.6 to 39 °C in the precocial herring gull *Larus argentatus*.

The change in body temperature also causes deviations from the simplest formulation of the DEB model after hatching in some species. My conjecture is that they are the main reason why the (empirical) logistic growth curve fits better than the von Bertalanffy curve for birds living at food abundance; as body temperature is measured in only a few exceptional studies, it makes sense to study the inverse argument. Given the observed growth pattern and the DEB model, can the body temperature ontogeny be recovered at abundant food?

At abundant food, (4.7) reduces to $\frac{d}{dt}l = \dot{r}_B(1-l)$, where the von Bertalanffy growth rate $\dot{r}_B = \frac{\dot{k}_M}{3}\frac{g}{1+g}$ is now considered not as a constant but as a function of time, since the temperature and thus the maintenance rate coefficient $\dot{k}_M$ change. Integration gives

$$l(t) = 1 - (1 - l(0)) \exp\left\{-\int_0^t \dot{r}_B(t_1)\, dt_1\right\} \text{ with} \tag{7.34}$$

$$\dot{r}_B(t) = \dot{r}_{B\infty} \exp\{T_A(T_\infty^{-1} - T_b(t)^{-1})\} \tag{7.35}$$

where $\dot{r}_{B\infty}$ is the ultimate growth rate when the body temperature is kept constant at some target temperature in the range 39 – 41 °C, or $T_\infty = 312$ (non-passerines) or 314 K (passerine birds). Body temperature is thus given by

$$T_b(t) = \left(\frac{1}{T_\infty} - \frac{1}{T_A} \ln \frac{\frac{d}{dt}l}{\dot{r}_{B\infty}(1-l)}\right)^{-1} \tag{7.36}$$

Given an observed growth and size pattern, this equation tells us how to reconstruct the temperature. The reconstruction of body temperature, therefore, rests on the assumption of (time inhomogeneous) von Bertalanffy growth (7.34) and an empirical description of the

observed growth pattern. It is a problem, however, that both the growth rate and the length difference with its asymptote 1 vanish, which means that their ratio becomes undetermined if inevitable scatter is present. General purpose functions such as polynomials or splines to describe size-at-age are not suitable in this case.

A useful choice for an empirical description of growth is

$$\frac{d}{dt}l = \frac{\dot{r}_{B\infty}}{\delta_l}(l^{-\delta_l} - 1)l \quad \text{or} \quad l(t) = (1 - (1 - l(0)^{\delta_l})\exp\{-\dot{r}_{B\infty}t\})^{1/\delta_l} \tag{7.37}$$

because it covers both von Bertalanffy growth (shape parameter $\delta_l = 1$), and the frequently applied logistic growth ($\delta_l = -3$) and all shapes in between. For the shape parameter $\delta_l = 0$, the well-known Gompertz curve arises: $l(t) = l(0)^{\exp\{-\dot{r}_B t\}}$. Nelder [658] called this model the generalized logistic equation. It was originally proposed by Richards [761] to describe plant growth. The graph of volume as a function of age is skewly sigmoid, with an inflection point at $V/V_\infty = (1 - \delta_l/3)^{3/\delta_l}$ for $\delta_l \leq 3$. Substitution of (7.37) into (7.36) gives

$$T_b(t) = \left(\frac{1}{T_\infty} - \frac{1}{T_A}\ln\frac{1}{\delta_l}\frac{1 - l^{-\delta_l}}{1 - l^{-1}}\right)^{-1} \tag{7.38}$$

Note that if growth is of the von Bertalanffy type, so $\delta_l = 1$, this reconstruction amounts to $T_b(t) = T_\infty$, which does not come as a surprise. This interpretation of growth data implies that the growth parameters of the logistic, Gompertz and von Bertalanffy growth curves are comparable in their interpretation and refer to the target body temperature. The DEB theory gives the physiological backgrounds. Figure 7.28 gives examples of reconstructions, which indicate that the body temperature at hatching can be some 10 °C below the target and it increases almost as long as growth lasts. The reconstruction method has been tested on several data sets where the body temperature has been measured during growth [1029]. It has been found to be quite accurate given the scatter in the temperature data. Figure 7.28 gives one example. Although the Arrhenius temperature can be estimated from combined weight/temperature data, its value proved to be poorly defined.

An important conclusion from this exercise is that deviations from von Bertalanffy growth at constant food abundance in birds can be explained by changes in body temperature.

7.9.2 Changes at puberty

Growth curves suggest that some species, e.g. humans, change the partition coefficient κ and the maximum surface-area-specific assimilation rate $\{\dot{p}_{Am}\}$ at puberty in situations of food abundance; see Figure 7.29. These changes amount to changes in the ultimate length and the von Bertalanffy growth rates via $L_m = (\kappa\{\dot{p}_{Am}\}/[\dot{p}_M] - V_h^{1/3})/\delta_{\mathcal{M}}$ and $\dot{r}_B = [\dot{p}_M](3[E_G] + \kappa[E_m])^{-1}$. Suppose that the volume-specific maintenance costs $[\dot{p}_M]$, the volume-specific structure costs $[E_G]$, and the heating volume V_h do not change at puberty. Table 3.1 suggests that $\dot{k}_M \equiv [\dot{p}_M]/[E_G]$ will be about 0.1 d^{-1} at 37 °C. If a man of 180 cm weighs 75 kg and if half this weight is structural biomass, the shape coefficient is approximately $\delta_{\mathcal{M}} = 0.19$. For $V_h^{1/3}$ is 10 cm, the observed changes in ultimate length

Great skua, *Catharacta skua*
$\dot{r}_{B\infty} = 0.111$ (0.009) d^{-1}, $\delta_l = -1.159$(0.326)

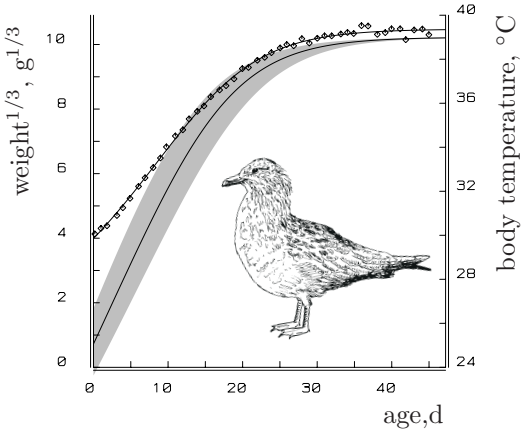

Long-tailed skua, *Stercorarius longicaudus*
$\dot{r}_{B\infty} = 0.267$ (0.035) d^{-1}, $\delta_l = -2.538$ (0.804)

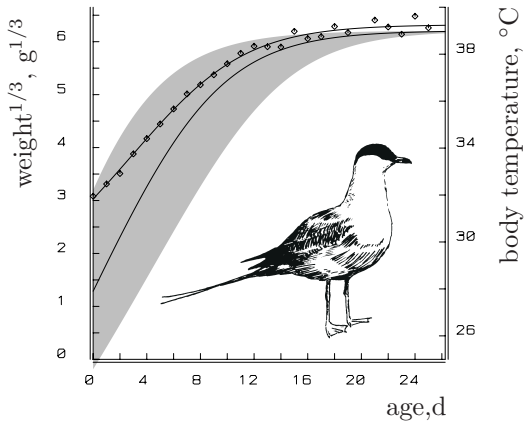

Manx shearwater, *Puffinus puffinus*
$\dot{r}_{B\infty} = 0.114$ (0.008) d^{-1}, $\delta_l = -2.483$ (0.467)

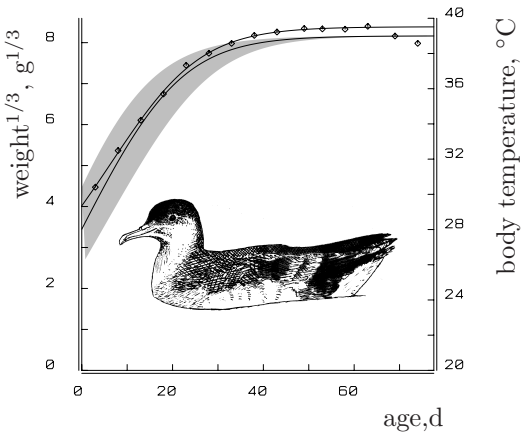

Guillemot, *Uria aalge*
$\dot{r}_{B\infty} = 0.125$ (0.037) d^{-1}, $\delta_l = -0.883$ (1.707)

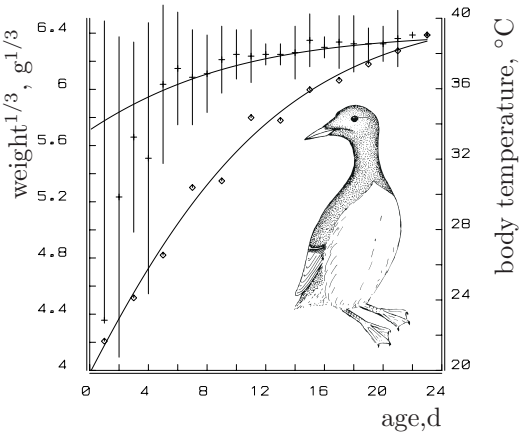

Figure 7.28: The empirical, generalized, logistic growth curves have been fitted to measured data for some birds. The von Bertalanffy growth rate $\dot{r}_{B\infty}$ at the ultimate body temperature and shape parameter δ_l are given. On the basis of these fits the body temperature was reconstructed, on the assumption that $T_\infty = 312$ K and $T_A = 10$ kK. The shaded areas around the body temperature curves indicate the 95% confidence interval based on the marginal distribution for k. The reconstruction method is tested on the guillemot data (lower right figure) where measured body temperatures were available. The bars indicate the standard deviation. Both temperature parameters, $T_\infty = 312.3$ (sd 2.32) K and $T_A = 8.225$ (sd 16.3) kK, have been estimated from the combined weight/temperature data. Data from Furness, de Korte in [308], Thompson in [121] and [583] respectively.

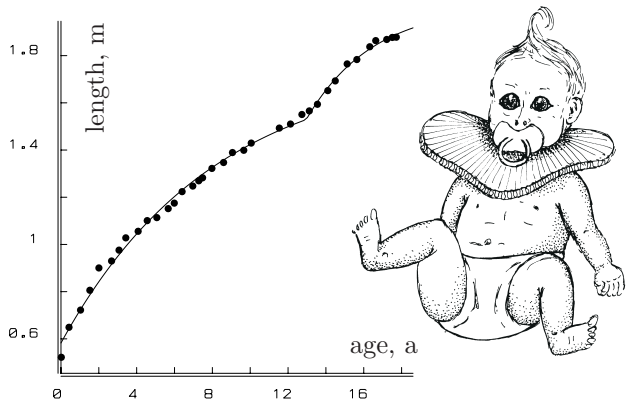

Figure 7.29: Length-at-age of man, de Montbeillard's son, in the years 1759-1777. Data from Cameron [149]. The curve is the von Bertalanffy one with an instantaneous change of the ultimate length from 177 (sd 4.6) cm to 201 (sd 8.2) cm and of the von Bertalanffy growth rate from 0.123 (sd 0.0093) a^{-1} to 0.285 (sd 0.094) a^{-1} at the age of 13 (sd 0.215) a.

and the von Bertalanffy growth rate correspond with a change by a factor 2.8 for $\{\dot{p}_{Am}\}$ and by a factor 0.426 for κ. This analysis can only be provisional. Deviations from strict isomorphism may affect estimates.

7.9.3 Changes in response to the photoperiod

The allocation of energy to reproduction in the pond snail *Lymnaea stagnalis* depends on the photoperiod, as is discussed in 'prolonged starvation', {227}. The photoperiod also affects the allocation under non-starvation conditions. This is obvious from the ultimate length. Snails kept under a 12 h:12 h cycle (MD conditions) have a larger ultimate length than under a 16 h:8 h cycle (LD conditions) [1028]. MD snails also have a smaller von Bertalanffy growth rate and a smaller volume at puberty, cf. {112}, but MD and LD snails are found to have the same energy conductance of $\dot{v} \simeq 1.55$ mm d^{-1} at 20 °C. This is a strong indication that the photoperiod only affects the partition coefficient κ.

7.9.4 Suicide reproduction

Like *Oikopleura*, salmon, eel and most cephalopods die soon after reproduction. The distribution of this type of behaviour follows an odd pattern in the animal kingdom. Tarantula males die after first reproduction, but the females reproduce frequently and can survive for 20 years. Death after first reproduction does not follow the Weibull-type aging pattern and probably has a different mechanism. Because the (theoretical) asymptotic size is not approached in cephalopods, they also seem to follow a different growth pattern. I believe, however, that early death, not the energetics, makes them different from iteroparous animals. The arguments are as follows.

Starting not close to zero, the surface area in von Bertalanffy growth is almost linear in time across a fairly broad range of surface areas. This has led Berg and Ljunggren [69] to propose an exactly linear growth of the surface area for yeast until a certain threshold is reached; see Figure 1.1. Starting from an infinitesimally small size, however, which is realistic for most cephalopods, length is almost linear in time, so the volume increases with cubed time: $V(t) = (\frac{\dot{v} f t}{3(f+g)})^3$. Over a small trajectory of time, this closely resembles exponential growth, as has been fitted by Wells [982], for instance.

Squids show a slight decrease in growth rate towards the end of their life (2 or perhaps 3 years [900]), just enough to indicate the asymptotic size, which happens to be very different for female and male in *Loligo pealei*. It will be explained in the section of primary scaling relationships, {270}, that the costs of structure $[E_G]$ in the von Bertalanffy growth rate $\dot{r}_B = \frac{[\dot{p}_M]/3}{[E_G]+\kappa[E_m]f}$ hardly contribute in large-bodied species because they are independent of asymptotic length, while maximum energy density is linear therein. So $\dot{r}_B \simeq \frac{[\dot{p}_M]}{3\kappa[E_m]f}$. The product $\dot{r}_B V_\infty^{1/3} \simeq \dot{v}/3$ should then be independent of ultimate size. On the basis of data provided by Summers [900], the product of ultimate length and the von Bertalanffy growth rate was estimated to be 0.76 and 0.77 $\mathrm{dm\,a^{-1}}$ for females and males respectively. The equality of these products supports the interpretation in terms of the DEB model. The fact that the squids die well before approaching the asymptotic size only complicates parameter estimation.

A large (theoretical) ultimate volume goes with a large maximum growth rate. If the maximum growth rates of different species are compared on the basis of size at death, the octopus *Octopus cyana* grows incredibly quickly, as argued by Wells [982]. Assuming that the maximum growth rate is normal, however, a (theoretical) ultimate volume can be inferred by equating $\dot{r}_B V_\infty^{1/3}$ for the octopus to that for the squid, after correction of temperature differences. Summers did not indicate the temperature appropriate for the squid data, but on the assumption that it has oscillated between 4 and 17 °C and that $T_A = 12.5$ kK, the growth rate has to be multiplied by 9.3 to arrive at the temperature that Wells used, i.e. 25.6 °C. The data of Wells indicate a maximum growth rate of $\frac{4}{9}\dot{r}_B V_m = 25.5\ \mathrm{dm^3\,a^{-1}}$. The ultimate volume is thus $\left(\frac{9\times25}{4\times9.3\times0.77}\right)^{3/2} = 22\ \mathrm{dm^3}$ for the octopus. This is three times the volume at death.

7.9.5 Adaptation

Figure 7.30 illustrates that prolonged exposure to limiting amounts of glucose eventually results in substantially improved uptake of glucose from the environment by bacteria. The difference in saturation constants between a 'wild' and an adapted population can amount to a factor of 1000. The outer membrane adapts to the specialized task of taking up a single type of substrate, which may jeopardize a rapid change to other substrates. This adaptation process takes many cell division cycles, as is obvious from the measurement of population growth rates, which itself takes quite a few division cycles.

When substrate is absent for a sufficiently long period of time, the metabolic machinery that deals with handling those substrates can be deleted from DNA, see {294}. This is a route to speciation, which leads to permanent changes in parameter values.

7.10 Summary

A variety of aspects are discussed to show how the basic DEB model can be applied and extended to deal with details of energetics.

- Reactions to variations in food levels depend on the time scale of starvation; allocation

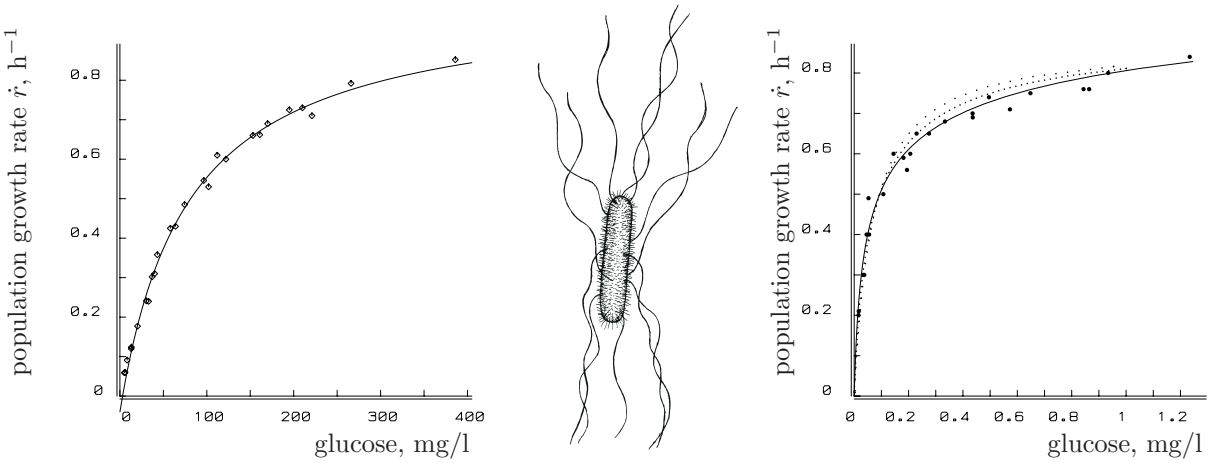

Figure 7.30: The population growth rate of *Escherichia coli* on glucose limited media. Schulze and Lipe's culture [823], left, had been exposed to glucose-limitation just prior to the experiment, while that of Senn [827], right, had been pre-adapted for a period of three months. The coarsely stippled curve in the right graph does not account for a time lapse between sampling from the continuous culture and measurement of the concentration of glucose [647]; the finely stippled one accounts for a time lapse of 0.001 h; the drawn one for a time lapse of 0.01 h.

rules are affected first, then follow reserve dynamics, and dormancy. The Bergman rule is explained as an adaptation to variation patterns in food availability.

- Transport processes in the environment can modify functional responses, and build up spatial structures.
- Constraints on digestion are discussed for an efficiency that is independent of body size and food density. The digestion of substrates is compared on the basis of chemical potentials.
- The synthesis of material that relates to surface area requires a waiting time that can be expressed in terms of energetic costs, and affects the population growth rate.
- RNA is mainly part of the reserves; reserve turnover gives excellent predictions for elongation rates of proteins.
- A mechanism is proposed for reserve dynamics and weak homeostasis, called structural homeostasis, which couples the size of subcellular structures to cell size. The role of membranes is an essential element in the mechanism that leads to first-order dynamics of reserve densities, with a turnover rate that is inversely proportional to length.
- The growth of organisms that change shape in rather complex but predictable ways, because of the spatial structure that develops during transport of substrate, is analysed.
- Pupae and imagos are discussed as examples of modifications in life stage patterns, and the implied consequences for reproduction and aging.

- Changes of parameter values are discussed that can occur at the various time scales; the evolutionary time scale involves changes that lead to speciation, as discussed in the next chapter.

Chapter 8

Comparison of species

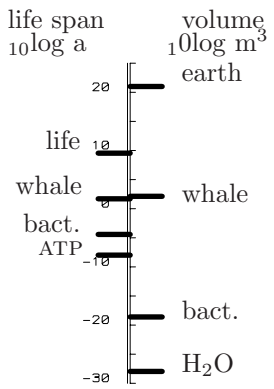

The range of body sizes is enormous. A bacterium with full physiological machinery has a volume of about 0.25×10^{-18} m^3. Some parasitic forms are much smaller. The blue whale has a volume of up to 135 m^3. A sequoia may even reach a volume of 2000 m^3, but one can argue that it is not all living material. Ironically, the organism with the largest linear dimensions is usually classified as a 'micro-organism': the fungus *Armillaria bulbosa* is reported to occupy at least 15 hectares and exceeds 10 Mg or 10 m^3 [860]. The factor between the volumes of bacterium and whale is 5.4×10^{20}, that between the volume a water molecule occupies in liquid water and that of a bacterium is 'only' 10^{10}. The interdivision interval of a bacterium can be as short as 20 min; the life span of whales may exceed 100 a [281], while some plants live for several millennia.

These differences in size and life span reflect differences in physiological processes, which the DEB theory tries to capture. The DEB model has structural body volume as a state variable. This implies that parameters that occur in the description of the process of energy uptake and use are independent of the body volume of a particular individual. Ultimate body volume, and in particular the maximum body volume, can be written as a simple compound parameter. This is why (some) parameters of the DEB model must have a (simple) relationship with ultimate body volume. This powerful argument is so simple that it can easily be overlooked. A comparison of the energetics of different species, ranging from bacteria to whales, reduces, in the DEB theory, to a comparison of sets of parameter values. This is different from comparison within a species, where we have only one set of parameter values, though different body volumes. This chapter deals with theory of parameter values, which includes body size scaling relationships, optimization problems and evolutionary aspects.

8.1 Genetics and parameter variation

The parameter values undoubtedly have a genetically determined component, which can to some extent be modulated phenotypically. As I hopefully made clear, the processes of feeding, digestion, maintenance, growth and reproduction are intimately related. They

involve the complete cellular machinery. Although mechanisms for growth which involve just one gene have been proposed [225], the many contributing processes make it likely that thousands are involved. This restricts the possibilities of population genetic theories dealing with auxiliary characters that do not have a direct link with energetics. (This is not meant to imply that such theories cannot be useful for other purposes.) In the context of quantitative genetics, some instructive points should be mentioned here. For this purpose a particular property of the DEB model, which I call the invariance property (just to have a name to refer to), should be discussed first. This property is at the basis of body size scaling relationships to be discussed later. These relationships express how species-specific characters depend on body size.

The invariance property of the DEB model is that two species with parameter sets that differ in a very special way behave identically with respect to energetics as long as food density is strictly constant. So they will have exactly the same energy dynamics, volume and reproduction ontogenies, and so on, for all life stages. The derivation of the relationship between both parameter sets is simple if two individuals are compared with the same body volume and with a maximum-surface-area-specific ingestion rates that differ by a 'zoom' factor z, so $\{\dot{J}_{Xm}\}_2 = z\{\dot{J}_{Xm}\}_1$. To behave identically, the ingestion rates must be equal: $\dot{J}_{X2} = \dot{J}_{X1}$. Since their volumes are equal, $V_2 = V_1$, (3.2) implies that $f_2 = f_1/z$ or $X_{K2} = zX_{K1} + (z-1)X$. Since the assimilation rates must be the same, $\dot{p}_{A2} = \dot{p}_{A1}$, it follows that $\{\dot{p}_{Am}\}_2 = z\{\dot{p}_{Am}\}_1$. They must have the same storage dynamics, so (3.10) implies $[E_m]_2 = z[E_m]_1$. Identical growth defined by (3.18) implies that the other parameters should be the same, so $V_{b2} = V_{b1}$, $V_{p2} = V_{p1}$, $V_{h2} = V_{h1}$, $\kappa_2 = \kappa_1$, $[\dot{p}_M]_2 = [\dot{p}_M]_1$ and $[E_G]_2 = [E_G]_1$.

If food density is not strictly constant, but fluctuates a little, both species behave in a different manner as far as energy is concerned. This is due to the non-linear relationship between the scaled functional response f and food density X. The change of f with respect to X is $\frac{d}{dX} f = X_K(X_K + X)^{-2} = (1-f)^2/X_K$. So if f approaches 1, the change in the ingestion rate, and so in the energy reserve density, becomes negligibly small. This overall homeostasis is probably selectively advantageous, because it implies that regulation systems have a much easier job to coordinate the various processes of energy allocation, which allows for optimization. The mechanism is not unlike the restriction of the tolerance range for the temperature of enzymes of homeotherms relative to heterotherms.

The invariance property has an interesting consequence with regard to selection processes. At a constant food density, the (constant) surface-area-specific ingestion rate, surface-area-specific assimilated energy, and reserve energy density can be regarded as achieved physiological characters. Fluctuations in reserve density, that result from fluctuations in food density, reduce substantially for decreasing maximum feeding rates. The reduction reflects an increase in homeostasis and allows a better regulation of metabolic activity. This may drive selection to a (genetic) fixation of the maximum feeding and assimilation rates and the reserve capacity to the realized values, a phenomenon known as 'dwarfing'. This mechanism possibly explains the Bergmann rule, as discussed on {232}.

The parameter values for different individuals are likely to differ somewhat. Differences in ultimate volume at constant food density testify to this. To what extent this has a genetic basis is not clear, but the heredity of size in different races of dogs and transgenic

mice and turkeys reveals the genetic basis of growth and size. Phenotypic factors exist as well. An important statistical implication is that parameter estimates can in principle no longer be based on means: the mean of von Bertalanffy curves with different parameters is not a von Bertalanffy curve. This problem obviously grows worse with increasing scatter. The modelling of parameter variation can easily introduce a considerable number of new parameters. To select just one or two parameters to solve this problem seems arbitrary. An attractive choice might be to conceive the factor z, just introduced, to be a stochastic variable, which couples four energy parameters. This introduces stochasticity only at fluctuating food densities.

8.2 Body size scaling relationships

The standard way to study body size scaling relationships is allometric: apply linear regression to the logarithmically transformed quantity of interest as a function of the logarithm of total body weight [146,612,700,815]. I have already given my reservations with respect to the physical dimensions, {13}, but I also object to the application of regression methods. My objections have a deeper root than the presence of 'measurement error' in the independent variable, which is usually the whole body wet weight. The dependent variable, i.e. some quantity of interest, can be considered to be a compound parameter for a particular species, and this can hardly be conceived of as a random variable. Each species of the (limited) set living on Earth happens to have a particular value for the quantity under consideration. This value is a result of evolutionary processes. Values of related species are thus likely to be dependent in a statistical sense. Moreover, evolutionary theory aims to explain a particular value while the application of regression methods implies that you leave the deviation in the black box. The random deviation from the (allometric) deterministic function, which regression analysis treats as 'measurement error', does not have a meaningful biological interpretation. A consequence of this point of view is that statistical tests on the 'exact' value of the scaling exponent must be considered to be misleading.

I prefer a different approach to the subject of body size scaling relationships which is implicit in the DEB theory. Although the relationships are mostly not of the allometric type if log–log plotted, straight lines approximate the result very well. To facilitate a comparison with the literature, I will refer frequently to the allometric (dimensionless) scaling exponent.

The tendencies discussed in the next few sections can be inferred on the basis of general principles of physical and chemical design. On top of these tendencies, species-specific adaptations occur that cause deviations from the expected tendencies. A general problem in body size scaling relationships is that large bodied species frequently differ from small bodied species in a variety of ways, such as behaviour, diet, etc. These life styles require specific adaptations, which hamper simple inter-species comparison. McMahon [611] applied elasticity arguments to deduce allometric scaling relationships for the shape of skeletal elements. Godfrey *et al.* [331] demonstrated, for mammals, that deviations from a simple geometrical upscaling of skeletal elements is due to size-related differences

Table 8.1: The relationship between the parameters of the DEB model for species 1 and 2 according to the invariance property (upper panel) and according to the primary scaling relationships (lower panel). The ratio of the ultimate volumetric body lengths of species 1 and 2 equals the zoom factor z.

X_{K2}	$=$	$X_{K1}z + X(z-1)$	$\{\dot{J}_{Xm}\}_2$	$=$	$\{\dot{J}_{Xm}\}_1 z$	$[\dot{p}_M]_2$	$=$	$[\dot{p}_M]_1$	$\{\dot{p}_T\}_2$	$=$	$\{\dot{p}_T\}_1$
$V_{b2}^{1/3}$	$=$	$V_{b1}^{1/3}$	$\{\dot{p}_{Am}\}_2$	$=$	$\{\dot{p}_{Am}\}_1 z$	$[E_G]_2$	$=$	$[E_G]_1$	$\ddot{h}_{a2}$	$=$	$\ddot{h}_{a1}$
$V_{p2}^{1/3}$	$=$	$V_{p1}^{1/3}$	$[E_m]_2$	$=$	$[E_m]_1 z$	κ_2	$=$	κ_1	κ_{R2}	$=$	κ_{R1}
X_{K2}	$=$	$X_{K1}z$	$\{\dot{J}_{Xm}\}_2$	$=$	$\{\dot{J}_{Xm}\}_1 z$	$[\dot{p}_M]_2$	$=$	$[\dot{p}_M]_1$	$\{\dot{p}_T\}_2$	$=$	$\{\dot{p}_T\}_1$
$V_{b2}^{1/3}$	$=$	$V_{b1}^{1/3}z$	$\{\dot{p}_{Am}\}_2$	$=$	$\{\dot{p}_{Am}\}_1 z$	$[E_G]_2$	$=$	$[E_G]_1$	$\ddot{h}_{a2}$	$=$	$\ddot{h}_{a1}$
$V_{p2}^{1/3}$	$=$	$V_{p1}^{1/3}z$	$[E_m]_2$	$=$	$[E_m]_1 z$	κ_2	$=$	κ_1	κ_{R2}	$=$	κ_{R1}

in life styles.

8.2.1 Primary scaling relationships

The parameter values of the DEB model tend to depend on maximum body volume in a predictable way that does not use any empirical argument. This makes it possible to predict how physiological quantities that can be written as functions of DEB parameters depend on maximum body volume. The core of the argument is that parameters that relate to the physical design of the organism are all proportional to volumetric maximum length, while the rest are size independent. The latter parameters relate to molecular processes, which are thus essentially density based. Reaction rates as described by the law of mass action depend on meeting frequencies between particles and do not depend on the (absolute) size of the organism. The difference between physical design and density-based parameters relates to the difference between intensive and extensive quantities.

The parameter values of a reference species number 1 with maximum body volume $V_{m,1}$ have an extra index to compare the parameter set with that of another species, number 2, with maximum body volume $V_{m,2}$. The primary scaling relationships are given in Table 8.1 and are compared with the relationships from the invariance property of the DEB model. This property is that parameter sets that differ in a special way that involves an arbitrary factor z result in identical energetics at strictly constant food densities, cf. {267}. A striking resemblance exists between the relationships of parameter sets on the basis of the primary scaling relationships and the invariance property. The only deviations are in size at birth and puberty, and in the saturation constant.

From the primary scaling relationships, other scaling relationships can be derived for all processes to which the DEB theory applies. Maximum volume itself is just one, though eye catching, compound parameter. Maximum volume is a result of energy uptake and use, not a factor determining these processes. Maximum volume can serve as a paradigm to compare species: $V_{m2} = (\kappa_2\{\dot{p}_{Am}\}_2/[\dot{p}_M]_2)^3 = (\kappa_1 z\{\dot{p}_{Am}\}_1/[\dot{p}_M]_1)^3 = z^3 V_{m1}$. One possible interpretation of the arbitrary zoom factor z is thus the ratio between the ultimate length

measures of two species. Although it is usual and convenient to study how physiological quantities and life histories depend on body size, it is essential to realize that all, inclusive of body size itself, depend on the coupled processes of energy uptake and use. Before I discuss how other compound parameters depend on body size, it is instructive to review the primary parameters first.

Molecular biology stresses again and again the similarities of cells, independent of the body size of the organism. It thus seems reasonable to assume that cells of equal size have about the same maintenance costs. Since the maintenance of cells is probably a major part of the maintenance of the whole individual, it seems natural that volume-specific maintenance is independent of body size. The same holds for the costs of growth. The values of $[\dot{p}_M]$, $\{\dot{p}_T\}$, $[E_G]$, κ and $\ddot{h}_a$ for a particular growing individual could in principle differ (a bit) for each time increment. The DEB model, however, assumes that these process parameters are constant. The assumption that they are independent of ultimate volume is the only one that is consistent with the structure of the DEB model.

Since κ and $[\dot{p}_M]$ are independent of maximum body size, $\{\dot{p}_{Am}\}$ has to be proportional to the cubic root of the ultimate volume, because of the relationship $V_m^{1/3} = \kappa\{\dot{p}_{Am}\}/[\dot{p}_M]$. This relationship makes $\{\dot{p}_{Am}\}$ a physical design parameter. The parameters $\{\dot{J}_{XAm}\}$ and $[E_m]$ are also physical design parameters, because the ratio of them to $\{\dot{p}_{Am}\}$ relates to density-based molecular processes. Since the DEB model in fact assumes that digestion is complete (else digestion efficiency would depend on feeding level, cf. {239}), and the ratio $\{\dot{p}_{Am}\}/\{\dot{J}_{XAm}\}$ represents digestion efficiency, $\{\dot{J}_{XAm}\}$ has to be proportional to $\{\dot{p}_{Am}\}$ and so to the cubic root of the ultimate volume as well. The same holds for the reserve capacity parameter $[E_m]$, because the ratio $\{\dot{p}_{Am}\}/[E_m]$ stands for energy conductance. Like digestion efficiency, it could in principle change (a bit) for each time increment in a growing individual, but it is assumed to be constant in the DEB model. Both ratios could have been introduced as the primary parameters, which would turn maximum assimilation rate and storage capacity into compound parameters. This is mathematically totally equivalent. Such a construction would leave V_b, V_p, $\{\dot{J}_{XAm}\}$ and X_K as the only parameters relating to the physical design of the organism.

The body size dependence of the saturation coefficient is less easy to see, because species differ so much in their feeding behaviour. At low food densities this constant can be interpreted as the ratio of the maximum ingestion to the filtering rates in a filter feeder such as *Daphnia*. If maximum beating rate is size independent, as has been observed, the filtering rate is proportional to surface area. Since the maximum specific ingestion rate $\{\dot{J}_{XAm}\}$ scales with a length measure, the saturation coefficient X_K should scale with a length measure as well. More detailed modelling of the beating rate would involve 'molecular' density-based formulations for the filtering process, which turns the saturation coefficient into a derived compound parameter. This is not attempted here, because the formulations would only apply to filtering, while many species do not filter.

The argument that the life stage parameters V_b and V_p (and V_d for dividers) are expected to be proportional to maximum volume V_m is that the threshold for investment in the increase of the state of maturity is proportional to volume, so the ratio of these threshold levels to volume is an intensive measure. These life stage parameters show, however, an extremely wide range of variation among different taxa. Huge fishes can lay very small eggs

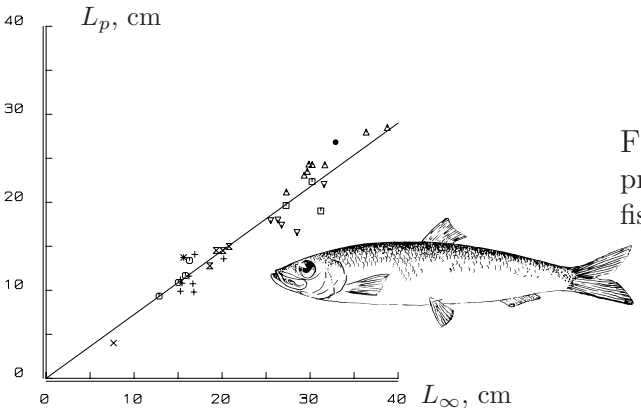

Figure 8.1: The length at first reproduction is proportional to the ultimate length in clupoid fishes. Data from Blaxter and Hunter [91].

△	*Clupea*	▽	*Sardinella*
•	*Brevoortia*	+	*Engraulis*
○	*Sprattus*	⋆	*Centengraulis*
□	*Sardinops*	×	*Stolephorus*
⧖	*Sardina*		

and thus have small values for V_b. For example, the ocean sunfish *Mola mola* can reach a length of 4 m and can weigh more than 1500 kg, it can produce clutches of 3×10^{10} tiny eggs. The other extreme within the bony fishes is the ovoviviparous coelacanth *Latimeria chalumnae*, which can reach a length of 2 m and a weight of 100 kg. It produces eggs with a diameter of 9 cm in clutches of some 26. (If we include the cartilaginous fish, the whale shark *Rhincodon typus* wins with a 12–18 m length, more than 8165 kg weight and eggs of some 30 cm.) The tendency of egg size to be proportional to ultimate size only holds for related species at best, as within the squamate reptiles [835]. This matter will be discussed further under r and K strategies, {292}. The size at first reproduction seems to vary much less, see Figure 8.1.

The gist of the argument for primary scaling relationships is that they can be derived from the structure of the DEB model and they do not involve empirical arguments.

8.2.2 Secondary scaling relationships

This section gives examples of the derivation of body size scaling relationships of a variety of eco-physiological phenomena that can be written as a compound parameter of the DEB model. The derivation follows the same path time and again and has the following structure. The quantity of interest is written as a function of scaled state variables (e and l) and primary parameters. Food density is taken to be high ($f = 1$) and the scaled reserve density is set at equilibrium ($e = 1$). I now append index 1 to all primary parameters to identify the reference species and multiply the primary parameters that scale with maximum body length with $(\mathcal{V}/V_{m1})^{1/3}$, where $\mathcal{V}$ stands for the maximum body size of the species of interest.

Body weight

Since the independent variable in body size scaling relationships is standard wet weight, we should first consider how wet weight relates to the primary parameter values. From (2.6) it follows for $[E] = [E_m]$ that $W_w = (d_V + (1 + e_R)[E_m]w_E/\mu_E)V$. The maximum volumetric length is $(\kappa\{\dot{p}_{Am}\} - \{\dot{p}_T\})/[\dot{p}_M]$, see (3.23) for $f = 1$, so that the maximum wet weight equals

$$W_w \simeq (d_V + w_E[M_{Em}])(1 - l_h)^3 V_m$$

at abundant food for isomorphs that have a relatively small amount of reserves allocated to reproduction ($[E_R] \ll [E_m]$).

Wet weights are sensitive to body composition. The structural body mass and in particular water content and type of reserve materials are different in unrelated species. This hampers comparisons that include species as different as jelly fish and elephants. If comparisons are restricted to related species, for example among mammals, the structural volume–weight conversion d_V will be independent of body volume, while $w_E[M_{Em}]$ increases with volumetric length, because it includes the maximum reserve capacity. Since $\{\dot{p}_{Am}\}$ increases with a volumetric length, while κ, $\{\dot{p}_T\}$ and $[\dot{p}_M]$ are independent of body volume, this means that the volume-specific wet weight $[W_w] \equiv W_w/V$ increases with body volume for two reasons. The first is the increasing contribution of energy reserves, the second is the decreasing effect of volume reduction due to heating. The last reason only applies to endotherms, of course.

To quantify how the specific wet weight depends on structural body volume, I append index 1 to specify the set of parameter values for a reference species, and obtain a wet weight of a species with a maximum structural volume $\mathcal{V}$

$$W_w(\mathcal{V}) \simeq (d_{V1} + w_E[M_{Em}]_1(\mathcal{V}/V_{m1})^{1/3}) \left(1 - (V_{m1}/\mathcal{V})^{1/3} l_h\right)^3 \mathcal{V}$$

Respiration

Respiration rate should be discussed first for historical reasons; see Kleiber's law on {4}. The scaling exponent has been found to be 0.66 for unicellulars, 0.88 for ectotherms and 0.69 for endotherms [706]. The exact value differs among authors taking their data from the literature. The variations are due, in part, to differences in the species included and in the experimental conditions under which respiration rates were measured. For crustaceans Vidal and Whitledge [950] present values of 0.72 and 0.85, and Conover [171] gives 0.74. If species ranging from bacteria to elephants are included, the value 0.75 emerges. It has become an almost magic number in body size scaling relationships. Many explanations have been proposed; some are based on muscle tension [611] or running speed [736], for instance. West *et al.* [984] derived the value 0.75 from an ingenious optimization argument. This value minimizes the (negligible) transport costs of material through a space-filling, self-isomorphic, fractal-like branching system of tubes, where the final branches (the capillaries in a circulatory system) are assumed to be body size invariant in terms of size and flux. The volume of tissue that each capillary serves does depend on body size, however, which makes the argument less consistent. The observed scaling of respiration rates with body size do also involve species, however, that have an open circulatory system (so, no capillaries), or no circulatory system at all, such as micro-organisms, cnidarians, nematodes, annelids, molluscs. The derivation assumes that the cross-sectional area of the branching fractal remains constant, which implies that the flow in the capillaries equals that in the aorta, which is in fact much lower [11].

As for intra-species relationships, I find these explanations not completely satisfactory, because mechanics plays only a minor role in energy budgets and the argument is too specific, since it applies to a very much restricted group of species. As mentioned, respiration rates are usually thought to reflect routine metabolic costs. It is no wonder that the

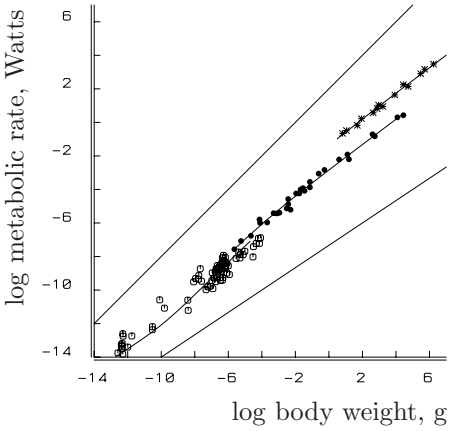

Figure 8.2: The metabolic rate of unicellulars (∘, at 20 °C), ectotherms (•, at 20 °C) and endotherms (∗, at 39 °C) as a function of body weight. Modified from Hemmingsen [247,396]. The difference between this figure and the many others of the frequently reproduced data set is that the curves relate to DEB-based expectations, and are not allometric regressions. Nonetheless they appear almost as straight lines. The lower line has slope of 2/3, the upper one a slope of 1.

explanation for why the scaling exponent is less than one for ectotherms is still a hot issue. I hope to have made it clear by now that costs other than routine metabolic ones also contribute to respiration, which makes it possible for respiration to scale with an exponent less than one, while routine metabolic costs scale with an exponent of one.

The carbon dioxide production of well-fed animals that is not associated with assimilation is given by (4.12). If we compare individuals with the same parameter set, this expression shows that the mineral fluxes, and so the oxygen consumption rate and the carbon dioxide production rate, depend on structural body length via the powers $\dot{p}_D$ and $\dot{p}_G$, which are both weighted sums of surface area and volume, i.e. of l^2 and l^3. This is nothing new. If we compare species of different (maximum) body size, however, we keep the state variables constant, and vary the parameters that depend on the maximum structural body volume. In the respiration rate (4.12), $V_m^{1/3}$, l_h^{-1} and g^{-1} are proportional to structural body length; none of the other parameters depend on maximum structural body volume. Generally, this again results in a scaling of respiration somewhere between a surface area and a volume, but it is rather critical which individuals are included. If we include only fully grown individuals of ectothermic species, the dissipating and growth powers no longer depend on the investment ratio g, and respiration is proportional to structural body volume. Even in this case, however, the weight-specific respiration decreases with body weight, because of the increasing contribution of reserves to body weight. Growth is asymptotic, however, and if individuals are selected with a structural length of some fixed fraction of the maximum possible one, the contribution of surface area will be more important.

In conclusion, the respiration rate will appear almost as a straight line in a double-log plot against body weight, the slope being somewhere between 0.66 and 1, depending on the species and the relative size of the individuals that have been included, see Figure 8.2. The scaling relationship for unicellulars is less informative, because assimilation is included and respiration depends sensitively on substrate composition (which is unknown to me). Surface-bound heating costs dominate in endotherms, so a plot that includes them will be close to a line with slope 0.66. The slope for the *Bathyergidae*, a family of rodents that are practically ectothermic, see Figure 3.13, is found to be close to 1 [571], as expected.

Maximum ingestion rate

The maximum ingestion rate for an individual of volume V is $\dot{J}_{Xm} = \{\dot{J}_{Xm}\}V^{2/3}$, so $\dot{J}_{Xm\mathcal{V}} = \{\dot{J}_{Xm}\}_1 V_{m1}^{-1/3}\mathcal{V}$. The maximum ingestion thus scales allometrically with body volume, but with a scaling exponent of 0.66 for intra-species comparisons and 1 for inter-species comparisons. Farlow [268] gives an empirical scaling exponent of 0.88, but value 1 also fits the data well. For endotherms especially, a scaling exponent of somewhat less than 1 is expected for weight as the independent variable, because of the increase in volume-specific weight, as explained. In a thorough study of scaling relationships, Calder [146] coupled the inter-specific ingestion rate directly to the respiration rate, without using an explicit model for energy uptake and use. The present DEB-based considerations force one to deviate from intuition.

Gut capacity

Within a species, isomorphy implies a gut capacity that is a constant fraction of body volume. This must also hold for inter-species comparisons, as long as body design and diet are comparable and this has been found for birds and mammals [146]. The mean gut residence time of food particles is thus independent of body size as a consequence, because ingestion rate is proportional to body size, while it was found to be proportional to a length measure for intra-species comparisons. This is of major ecological significance for herbivores, because it determines which type of food can be digested. The poorly digestible substrates can only be used successfully by animals with a big body size. The giant sauropods of the Jurassic fed mainly on cycads and conifers, which require long gut residence times for digestion. Giant carnivores probably evolved in response to giant herbivores; the explanation of their body size probably relates to the survival of meagre periods.

Maximum filtering rate

The filtering rate is maximal at low food densities. If particle retention is complete, it is given by $\dot{F}_m = \dot{J}_{Xm}/X_K = V^{2/3}\{\dot{J}_{Xm}\}/X_K$. So, $\dot{F}_{m\mathcal{V}} = \mathcal{V}^{2/3}\{\dot{J}_{Xm}\}_1/X_{K1}$. This was found by Brendelberger and Geller [114].

Speed

Since biomechanics is not part of the DEB theory, this is not the right place for a detailed discussion on Reynolds and Froude numbers, although interesting links are possible. Speed of movement has only a rather indirect relationship with feeding or other aspects that bear on energy budgets. A few remarks are, therefore, made here.

McMahon and Bonner [612] found that the speed of sustained swimming for species ranging from larval anchovy, via salmon, to blue whales scales with the square root of volumetric length; they underpinned this finding with mechanical arguments. Since the energy costs of swimming are proportional to squared speed and to surface area, cf. {73}, the total costs of movement would scale with cubed length, or $\mathcal{V}$, for a common travelling

time. This is consistent with the DEB theory, where the costs of travelling are taken to be a fixed fraction of the maintenance costs.

A similar result appears to hold for the speed of flying, but by a somewhat different argument. The cruising speed, where the power to fly is minimal, is proportional to the square root of the wing loading [912]. If a rough type of isomorphy applies, comparing insects, bats and birds, wing loading, i.e. the ratio of body mass to wing area, scales with length, so that cruising speed scales with the square root of length [612].

Arguments for why the standard cruising rate for walking tends to be proportional to length, are given on {71,73}. If energy invested in movement is proportional to volume and taken to be part of the maintenance costs, the intra- and inter-species scaling relationships work out in the same way.

Maximum diving depth

Birkhead [86] found that the maximum diving depth for auks and penguins tends to be proportional to volumetric length. This can be understood if diving depth is proportional to the duration of the dive; the latter is proportional to length, cf. {71} by the argument that the respiration rate of these endotherms is about proportional to surface area and oxygen reserves to volume.

Minimum food density

The minimum food density at which an isomorph of body volume V can live for a long time is found from the condition that energy derived from ingested food just equals the maintenance costs, so $\dot{J}_X\{\dot{p}_{Am}\}/\{\dot{J}_{Xm}\} = \dot{p}_M$, or $f_\dagger = \frac{X_\dagger}{X_K+X_\dagger} = \frac{[\dot{p}_M]}{\{\dot{p}_{Am}\}}V^{1/3}$. The solution is $X_\dagger = \frac{V^{1/3}X_K[\dot{p}_M]/\{\dot{p}_{Am}\}}{1-V^{1/3}[\dot{p}_M]/\{\dot{p}_{Am}\}}$. At this food density, the individual can only survive, not reproduce. For different species, we obtain the condition $X_{\dagger\mathcal{V}} = \frac{\mathcal{V}^{1/3}X_{K1}[\dot{p}_M]_1/\{\dot{p}_{Am}\}_1}{1-V_{m1}^{1/3}[\dot{p}_M]_1/\{\dot{p}_{Am}\}_1}$. Minimum food density, also called the threshold food density, is thus proportional to volumetric length. An important ecological consequence is that, at a given low food density, small individuals can survive, while the large ones can not. This explains, for instance, why bacteria in oligotrophic seas are so small.

This result only applies to situations of constant food density. If it is fluctuating, storage capacity becomes important, which tends to increase with body size; see {227}. The possibility of surviving in dynamic environments then works out to be rather complex. Stemberger and Gilbert [882] found that the threshold food density tends to increase with body size for rotifers, as expected, but Gliwicz [328] found the opposite for cladocerans. This result can be explained, however, by details of the experimental protocol. The threshold food density was obtained by plotting the growth rate against food density and selecting the value where growth is nil. Growth at the different food densities was measured from two-day-old individuals exposed to a constant food density for four days. The reserves at the start of the growth experiment, which depend on culture conditions, will contribute substantially to the result.

Maximum growth

The maximum growth in cubed scaled length is $\frac{d}{dt}l^3 = \frac{4}{27}\frac{g\dot{k}_M}{1+g}(1-l_h)^3$, see Table 3.5. The maximum growth rate for different species equals

$$\frac{4}{27}\frac{\dot{k}_{M1}g_1}{(\mathcal{V}/V_{m1})^{1/3}+g_1}(\mathcal{V}^{1/3}-V_{h1}^{1/3})^3$$

and is thus about proportional to volume$^{2/3}$. This fits Calow and Townsend's data very well [148].

von Bertalanffy growth rate

The von Bertalanffy growth rate at high food density is $\dot{r}_{B\mathcal{V}} = (3/\dot{k}_{M1} + 3\mathcal{V}^{1/3}/\dot{v}_1)^{-1}$ for different species. It decreases almost linearly with volumetric length. This is consistent with empirical findings; see Figure 8.3. The parameters and data sources are listed in Table 8.2. This table is extensive because the fit with the von Bertalanffy growth curve is used to support the argument that it is possible to formulate a theory that is not species-specific, {1}. If one collects growth data from the literature, an amazingly large fraction fits the von Bertalanffy curve despite the fact that most data sets are from specimens collected in the field. Since it is hard to believe that food density has been constant during the growth period, this suggests that food has been abundant; this is relevant for population dynamics.

If the von Bertalanffy growth rate is plotted against maximum volumetric length, the scatter is so large that it obscures their relationship. This is largely due to differences in body temperature. A fish in the North Sea with a yearly temperature cycle between 3 and 14 °C grows much more slowly than a passerine bird with a body temperature of 41 °C. This is not due to fundamental energy differences in their physiology. If corrected to a common body temperature according to the Arrhenius relationship with an Arrhenius temperature of 12.5 kK, the expected relationship is revealed and the differences between fishes and birds disappear. Since temperature had not been measured in most cases, I had to estimate it in a rather crude way. For most molluscs and fish data I used general information on local climate and guessed water temperatures (which depend on the, frequently unknown, depth). The body temperatures of birds and mammals have also been guessed. Uncertainties about temperature doubtlessly contributed the most to the remaining scatter. The corrected rates are not meant as predictions of actual growth rates at this body temperature because most North Sea fish and birds would die almost instantaneously if the temperature was realized. The average energy conductance, $\dot{v}$, of 261 species at 37 °C appears to be 5.49 mm d^{-1}, 0.885 mm d^{-1} at 25 °C, or 0.433 mm d^{-1} at 20 °C. This is the best evidence that the maximum storage capacity increases with volumetric length, just as the maximum surface-area-specific assimilation rate does.

The contribution of maintenance to the von Bertalanffy growth rate is small for large bodies, which explains why the von Bertalanffy growth rate is about proportional to $\mathcal{V}^{-1/3}$, as Ricklefs [767] found for birds for instance.

Table 8.2: The von Bertalanffy parameters and their standard deviations as calculated by non-linear regression. The shape coefficient converts the size measure used to volumetric length. For shape coefficient 1, the data refer to wet weight, except for *Saccharomyces*, *Actinophrys* and *Asplanchna*, where volumes were measured directly. The data for *Mnemiopsis* and *Calanus* refer to dry weight. The other data are length measures, mostly total body length. Where the standard deviation is not given, the parameters from the authors are given. Temperatures in parentheses were inferred from the location on Earth. Where two temperatures are given, a sinusoidal fluctuation between these extremes is assumed. In the column 'sex': f=female, m=male, l=larva.

species	sex	length mm L_∞	sd mm	shape coeff $\delta_\mathcal{M}$	rate a^{-1} $\dot{r}_B$	sd a^{-1}	location NS	location EW	temp °C	source
Ascomyceta										
Saccharomyces carlsbergensis		4.59e-3	2.16e-5	0.806	11830	318	lab	lab	30	[69]
Heliozoa										
Actinophrys spec.		0.0043	2.2e-5	1	2891	368	lab	lab		[904]
Rhizopoda										
Amoeba proteus		2.79	0.016	0.01	832.2	56.9	lab	lab	23	[733]
Ciliata										
Paramecium caudatum		2.969	0.062		1638	210	lab	lab	17	[813]
Ctenophora										
Pleurobrachia pileus	fm	15.04	0.436	0.702	33.27	2.49	lab	lab	20	[346]
Mnemiopsis mccradyi	fm	8.851	0.927	3.90	11.61	1.88	lab	lab	26	[757]
Rotifera										
Asplanchna girodi	f	0.2400	7.32e-4	1	193.7	4.92	lab	lab	20	[777]
Annelida										
Dendrobeana veneta	fm	14.5	0.24	1	12.04	0.73	lab	lab	20	H. Bos, pc
Mollusca										
Aplysia californica	fm	112.2	6.05	1	4.840	0.871	lab	lab	18–20	[699]
Urosalpinx cinerea	fm	30.94	1.31	0.397	0.8116	0.11	31S	152E	-1–25	[294]
Achatina achatina	fm	106.5	2.45	0.543	1.121	0.0770	5N	0E	(25)	[418]
Helix aspera	fm	25.06	0.498	0.68	1.098	0.0960	lab	lab	(18–20)	[195]
Patella vulgata	fm	46.93	0.306	0.310	0.4296	7.91e-3	54N	4.40W	(4–17)	[1022]
Monodonta lineata	fm	21.92	0.130	0.716	0.6213	0.0171	52.25N	4.05W	(4–17)	[1004]
Biomphalaria pfeifferi	fm	7.538	0.0497	1	4.879	0.201	lab	lab	25	[626]
Lymnaea stagnalis	fm	15.37	0.0584	1	10.81	0.204	lab	lab	20	[856]
Helicella virgata	fm	9.888	0.215	1	3.316	0.163	35S	139E	11–16	[722]
Macoma baltica		21.57	0.154	0.423	3.00	0.0869	41.31N	70.39W	10.56	[326]
Cerastoderma glaucum		29.24	1.86	0.558	2.221	0.380	40.50N	14.10E	13–30	[444]
Venus striatula		37.76	25.1	0.471	0.1961	0.210	55.50N	4.40W	6–13	[23]
Ensis directus		142.2		0.187	0.5830		54.35N	8.45E	4–17	[903]
Mytilus edulis		95.92	2.02	0.394	0.1045	5.109e-3	53.36N	9.50W	7–17	[778]
Placopecten magellanicus		162.3	1.01	0.388	0.1671	2.842e-3	47.10N	53.36W	0–18	[577]
Perna canaliculus		191.2	10.6	0.394	0.3555	0.0342	36.55S	174.47E	17	[409]
Hyridella menziesi		74.62	2.05	0.400	0.1331	8.38e-3	36.55S	147.47E		[447]
Mya arenaria		91.31		0.407	0.1866		41.39N	70.42W	(4–17)	[124]
Loligo pealei	f	455.3	39.5	0.398	0.4201	0.0551	41.31N	70.39W	(4–17)	[900]

Loligo pealei	m	918.2	111	0.398	0.2122	0.0315	41.31N	70.39W	(4–17)	[900]
Brachiopoda										
Terebratalia transversa		48.39	1.09	0.640	0.3140	0.0163	47.30N	122.5W	(4–17)	[684]
Crustacea										
Daphnia pulex	f	2.366	0.0192	0.526	44.25	2.10	lab	lab	20	[764]
Daphnia longispina	f	2.951	0.0260	0.520	61.32	2.92	lab	lab	25	[442]
Daphnia magna	f	5.136	0.0970	0.526	35.04	1.83	lab	lab	20	[513]
Daphnia magna	m	2.813	0.0440	0.526	66.80	5.11	lab	lab	20	[513]
Daphnia cucullata	f	1.049	0.0214	0.480	58.25	9.71	lab	lab	20	[951]
Daphnia hyalina	f	1.717	0.0399	0.520	47.52	5.93	lab	lab	20	[951]
Ceriodaphnia pulchella	f	0.7503	0.0122	0.520	39.89	5.04	lab	lab	20	[951]
Ceriodaphnia reticulata	f	1.038	0.0210	0.520	49.28	3.30	lab	lab	20	[513]
Chydorus sphaericus	f	0.4115	1.10e-3	0.560	52.63	0.969	lab	lab	20	[951]
Diaphanosoma brachyurum	f	1.380	0.0198	0.520	46.50	3.72	lab	lab	20	[951]
Leptodora kindtii	f	8.632	0.204	0.300	26.96	2.64	lab	lab	20	[951]
Bosmina longirostris	f	0.5289	0.0215	0.520	38.73	6.50	lab	lab	20	[951]
Bosmina coregoni	f	0.4938	0.0104	0.520	66.90	9.59	lab	lab	20	[951]
Calanus pacificus		6.295	1.02	0.215	8.863	1.89	lab	lab	12	[680]
Dissodactylus primitivus	f	11.02	0.410	0.635	1.025	0.0732	lab	lab	(18)	[719]
Dissodactylus primitivus	m	9.013	0.212	0.635	1.362	0.0742	lab	lab	(18)	[719]
Euphasia pacifica		12.91	2.35	0.197	1.008	0.369	lab	lab	10	[596]
Homarus vulgaris		186.6	6.99	0.939	0.05543	3.36e-3	lab	lab	10	[406]
Cancer pagurus	f	9.707	0.385	1	0.2711	0.0122	50.30N	2.45W	(5–18)	[67]
Cancer pagurus	m	115.6	0.513	1	0.3513	0.0174	50.30N	2.45W	(5–18)	[67]
Dichelopandalus bonnieri		25.73	1.97	0.882	0.4795	0.0824	54N	4.40W	(4–17)	[8]
Gammarus pulex	m	4.355	0.0570	1	3.300	0.177	lab	lab	15	[901]
Gammarus pulex	f	4.089	0.0554	1	2.218	0.123	lab	lab	15	[901]
Calliopius laeviusculus		15.27	0.699	0.262	13.52	1.96	lab	lab	15	[192]
Uniramia										
Tomocerus minor		3.903	0.0848	0.351	6.600	0.379	lab	lab	20	[458]
Orchesella cincta		3.652	0.0858	0.351	4.948	0.351	lab	lab	20	[458]
Isotomata viridis		3.034	0.0751	0.351	6.52	0.469	lab	lab	20	[458]
Entomobrya nivalis		1.981	0.0830	0.351	3.416	0.418	lab	lab	20	[458]
Lepidocyrtus cyaneus		1.181	0.0666	0.351	9.840	2.17	lab	lab	20	[458]
Orchesella cincta		1.281	0.0151	1	6.817	0.354	lab	lab	20	[449]
Phaenopsectra coracina		1.745	0.147	1	2.388	0.779	63.14N	10.24E	4	[1]
Diura nanseni		2.782	0.0460		6.328	0.536	60.15N	6.15E	0–20	[37]
Capnia pygmaea		1.024	0.0967		2.493	0.663	60.15N	6.15E	1–20	[37]
Locusta migratoria		10.82	0.237	1	44.82	7.36	lab	lab	23–36	[568]
Chironomus plumosus	f	4.053	0.272	1	21.88	5.50	lab	lab	15	[441]
Chironomus plumosus	m	3.211	0.0415	1	52.74	4.77	lab	lab	15	[441]
Cheatognata										
Sagitta hispida	fm	9.431	0.150	0.15	44.80	5.25	lab	lab	21	[756]
Echinodermata										
Lytechenus variegatus		46.10	0.147	0.70	3.913	0.199	18.26N	77.12W	26–29	[471]
Echinocardium cordatum		34.50	0.425	0.696	0.4590	0.0232	53.10N	4.15E	5–12	[241]
Echinocardium cordatum		36.70	0.375	0.696	0.5320	0.0259	53.40N	4.30E	5–14	[241]
Echinocardium cordatum		44.90	0.405	0.696	0.4960	0.0212	54.15N	4.30E	5–16	[241]
Tunicata										
Oikopleura longicauda	fm	0.829	0.049	0.520	56.56	6.62	lab	lab	20	[275]
Oikopleura dioica		0.952	0.327	0.560	63.97	37.3	lab	lab	20	[275]
Chondrichthyes										
Raja montaqui	fm	695.9	11.0	0.184	0.1874	0.0140	52–54N	3–7E	(4–17)	[423]

Raja brachyura		1589	213	0.184	0.1018	0.0261	52–54N	3–7E	(4–17)	[423]
Raja clavata	f	1303	107	0.184	0.09297	0.0163	52–54N	3–7E	(4–17)	[423]
Raja clavata	m	952.7	29.8	0.184	0.1557	0.0145	52–54N	3–7E	(4–17)	[423]
Raja erincea		542.9	32.6	0.184	0.2787	0.0542	41.05N	73.10W	1–19.1	[762]
Prionace glauca		4230		0.165	0.1100		48N	7W	(5–18)	[885]
Osteichthyes										
Accipenser stellatus		2120	30.5	0.198	0.05396	1.46e-3	(45.10N)	(28.30E)	(4–23)	[76]
Clupea sprattus		157.0	0.557	0.200	0.5847	4.60e-3	52.30N	2E	(4–17)	[440]
Coregonus lavaretus		397.3	8.39	0.203	0.3295	0.0221	54.35N	2.50W	(5–15)	[39]
Salvelinus willughbii	f	385.4	72.9	0.225	0.2495	0.0973	54.20N	2.57W	(5–15)	[302]
Salvelinus willughbii	m	328.9	12.7	0.224	0.3545	0.0366	54.20N	2.57W	(5–15)	[302]
Salmo trutta		585.8	18.0	0.216	0.4769	0.0411	53.15N	4.30W	(4–17)	[436]
Salmo trutta		576.2	20.6	0.240	0.2921	0.0253	57.40N	5.10W	5–12.8	[150]
Salmo trutta		420.2	3.13	0.240	0.4157	0.0107	54.20N	2.57W	(5–15)	[182]
Oncorhynchus tschawytscha		155.2	11.9	1	0.9546	0.217	36S	147E	(11–16)	[144]
Thymallus thymallus		459.6	8.44	0.240	0.4656	0.0224	52.09N	2.41W	(5–15)	[394]
Esox lucius	f	948.7	88.3	0.209	0.2101	0.0718	50.17N	3.39W	(5–15)	[111]
Esox lusius	m	703.6	13.0	0.209	0.4016	0.0455	50.17N	3.39W	(5–15)	[111]
Esox masquinongy		2091	848	0.199	0.04503	0.0263	44N	79W	(5–15)	[644]
Rutilus rutilus		441.6	15.8	0.258	0.1661	0.0116	52.30N	0.30E	(5–15)	[181]
Leuciscus leuciscus		252.6	2.32	0.258	0.3329	0.0131	52.30N	0.30E	(5–15)	[181]
Barbus grypus		1036	25.2	0.206	0.1265	6.59e-3	35.75N	44.7E	(17–30)	[9]
Abramis brama		546.0		0.225	0.1142		53.15N	2.30W	(5–15)	[334]
Gambusia holbrookii	f	61.72	2.34	0.250	0.9366	0.216	38.40N	9.40W	(5–25)	[293]
Poecilia reticulata	f	50.58	1.14	0.252	1.667	0.0690	lab	lab	21	[939]
Merluccius merluccius		1265	78.4	0.222	0.2075	0.0184	55.45N	5W	(8–12)	[38]
Lota lota		1009	60.3	0.193	0.09768	0.0103	53N	98W	(5–15)	[408]
Gadus merlangus	f	898.6	12.2	0.222	0.08626	2.07e-4	54N	4.40W	(8–12)	[106]
Gadus merlangus	m	772.8	9.03	0.222	0.08626	2.07e-4	54N	4.40W	(8–12)	[106]
Gadus morhua		1089	43.2	0.222	0.1308	9.26e-3	40N	60W	10	[502]
Gadus aeglefinus		106.5		1	0.2000		53–57N	0–7E	(4–17)	[82]
Atherina presbyter		124.0	3.20	0.238	1.091	0.109	51.55N	1.20W	(5–18)	[935]
Gasterosteus aculeatus		52.41	2.62	0.250	1.019	0.249	52.20N	3W	(4–17)	[456]
Pungitius pungitius		41.28	1.03	0.200	1.777	0.468	52.20N	3W	(4–17)	[456]
Nemipterus marginatus		232.8	35.8	0.243	0.5047	0.227	6N	116E	(26–30)	[693]
Labrus bergylta		509.2	8.64	0.258	0.07170	3.30e-3	54N	4.40W	(4–17)	[219]
Ellerkeldia huntii		152.1	10.8	0.319	0.3350	0.0791	35.30S	174.40E	(12–22)	[454]
Lepomis gibbosus		61.86	9.04	1	0.1415	0.0342	45.40N	89.30W	(5–15)	[638]
Lepomis macrochirus		71.62	16.8	1	0.1292	0.0467	45.40N	89.30W	(5–15)	[638]
Perca fluviatilis		317.9	22.5	0.25	0.1615	0.0242	56.10N	4.45W	8–14	[828]
Tilapia species		129.6	20.7	1	3.542	1.10	31.30N	35.30E	(37)	[572]
Liza vaigiensis		746.3	31.8	0.258	0.1758	0.0147	17S	145E	(18–27)	[342]
Mugil cephalus		595.0	27.2	0.258	0.3350	0.0370	17S	145E	(18–27)	[343]
Valamugil seheli		635.3	35.0	0.258	0.2725	0.0291	17S	145E	(18–27)	[343]
Seriola dorsalis		1373	30.7	0.231	0.1155	5.72e-3	33N	118W	(15–20)	[57]
Ammodytes tobianus		140.9	1.98	0.147	0.7305	0.0595	50.47N	1.02W	5–18	[753]
Thunnus albacares		2745	636	0.266	0.1481	0.0509	0–10N	165E	(26–30)	[672]
Thunnus thynnus		3689	448	0.266	0.06623	0.0144	53–57N	0–7E	(4–17)	[928]
Coryphoblennius galerita		69.55	2.72	0.250	0.4011	0.0598	50.20N	4.10W	(5–18)	[635]
Pomatoschistus norvegicus		48.80	0.770	0.252	2.466	0.305	56.20N	5.45W	(8–14)	[324]
Gobio gobio		154.9	15.9	0.250	0.7519	0.495	51N	2.15W		[587]
Gobio gobio		174.8	3.84	0.250	0.4165	0.0321	51.50N	8.30W	(4–17)	[474]
Gobius cobitis		213.9	14.9	0.295	0.2082	0.0385	48.45N	4W	(5–18)	[321]

Gobius paganellus		79.89	1.94	0.200	0.4790	0.0463	54N	4.40W	(4–17)	[634]
Lesueurigobius friesii		65.82	0.623	0.252	0.5628	0.0349	55.45N	5W	8–12	[655]
Lesueurigobius friesii		63.72	0.409	0.252	0.6826	0.0322	56.20N	5.45W	(8–14)	[322]
Blennius pholis		150.5	3.36	0.250	0.2464	0.0176	50.20N	4.10W	(5–18)	[635]
Arnoglossus laterna		93.55	3.06	0.200	0.4544	0.0895	56.15N	5.40W	(8–14)	[323]
Hypoglossus hypoglossus		632.7	54.7	1	0.04797	6.04e-3	59N	152W	(3–14)	[867]
Scophthalmus maximus	f	669.4	14.2	0.266	0.2165	0.0298	53–57N	0–7E	(3–14)	[453]
Scophthalmus maximus	m	495.3	6.93	0.272	0.3247	0.0222	53–57N	0–7E	(3–14)	[453]
Pleuronectes platessa		142.1		1	0.09500		53–57N	0–7E	(4–17)	[82]
Solea vulgaris		78.41		1	0.4200		53–57N	0–7E	(4–17)	[82]
Amphibia										
Rana tigrina	l	12.79	0.670	1	15.75	1.88	lab	lab	30–33	[196]
Rana sylvatica	l	8.201	0.154	1	30.97	6.64	36.05N	81.50W	21–26	[1001]
Triturus vulgaris	l	26.40		0.353	3.960		59.30N	10.30E	-5–14	[222]
Triturus cristatus	l	40.40		0.353	4.080		59.30N	10.30W	-5–14	[222]
Reptilia										
Emys orbicularis	f	182.1	1.98	0.500	0.2707	0.0124			(22)	[168]
Emys orbicularis	m	161.8	1.56	0.500	0.3453	0.0172			(22)	[168]
Vipera berus		539.0	33.0	0.075	0.3734	0.0657			(20)	[299]
Eunectes notaeus	f	3283	50.9	0.075	0.2552	0.0165	lab	lab	(20)	[705]
Eunectes notaeus	m	2946	94.5	0.075	0.2030	0.0251	lab	lab	(20)	[705]
Aves										
Eudyptula minor nov.		114.7	5.67	1	15.60	2.69			39.5	[484]
Pygoscelis papua		191.8	3.35	1	15.31	0.965			39.5	[955]
Pygoscelis antarctica		163.6	5.29	1	16.88	2.12			39.5	[955]
Pygoscelis adeliae		159.9	7.77	1	15.47	2.81			39.5	[955]
Pygoscelis adeliae		188.7	3.47	1	14.32	0.698			39.5	[909]
Aptenodytes patagonicus		250.0		1	8.508	0.164			39.5	[889]
Pterodroma cahow		63.16	0.465	1	62.96	1.55			39.5	[1005]
Pterodroma phaeopygia		79.2	0.93	1	20.08	3.43			39.5	[372]
Puffinus puffinus		83.90	0.069	1	41.55	2.87			39	[121]
Diomedea exulans		229.1	1.02	1	5.541	0.176			39.5	[924]
Oceanodroma leucorhoa		41.53	0.282	1	26.37	1.58			39.5	[769]
Oceanodroma furcata		44.73	0.339	1	23.28	1.16			39.5	[97]
Phalacrocorax auritus		149.5	6.31	1	18.18	1.81			39.5	[242]
Phaethon rubricaudata		101.1	1.45	1	13.03	0.923			39.5	[211]
Phaethon lepturus		72.79	1.12	1	18.77	2.03			39.5	[211]
Sula sula		80.01	1.18	1	11.82	1.53			39.5	[211]
Sula bassana		172.7	2.50	1	12.41	0.639			39.5	[659]
Cionia cionia		158.0	6.10	1	18.36	2.35			39.5	[183]
Phoeniconaias minor		116.8	3.01	1	11.31	1.30			39.5	[75]
Florida caerulea		68.19	1.16	1	42.63	3.61			39.5	[983]
Anas platyrhynchos		117.3	0.330	1	17.75	0.410			39.5	[404]
Anas platyrhynchos		151.3	0.353	1	17.04	0.307			39.5	[404]
Anas platyrhynchos		145.5	1.94	1	10.26	0.680			39.5	[631]
Anas platyrhynchos		154.8	1.65	1	13.14	4.56			39.5	[794]
Anser anser		181.5	2.99	1	7.895	0.626			39.5	[631]
Buteo buteo	f	103.7	1.17	1	27.57	1.34			39.5	[725]
Buteo buteo	m	95.99	1.11	1	27.90	1.45			39.5	[725]
Falco subbuteo		66.16	0.689	1	46.77	3.57			39.5	[84]
Meleagris gallopavo		256.1	9.89	1	4.340	0.782			39.5	[164]
Meleagris gallopavo		296.2	26.2	1	3.657	1.18			39.5	[164]
Phasianus colchicus	f	100.3	1.86	1	6.610	0.738			39.5	[631]

Phasianus colchicus	m	118.8	4.25	1	5.004	0.746	39.5	[631]
Gallus domesticus	f	136.5	1.24	1	4.625	0.209	39.5	[687]
Gallus domesticus	m	153.5	2.22	1	4.522	0.305	39.5	[687]
Bonasia bonasia		85.17	2.68	1	7.807	0.740	39.5	[72]
Colinus virginianus		56.90	0.328	1	10.81	0.427	39.5	[789]
Coturnix coturnix		55.41	0.761	1	14.94	0.784	39.5	[117]
Rallus aquaticus		51.66	0.730	1	14.45	0.0882	39.5	[838]
Gallinula chloropus		67.05	1.20	1	20.00	1.72	39.5	[258]
Philomachus pugnax	f	47.41	1.04	1	39.46	2.75	39.5	[811]
Philomachus pugnax	m	59.94	2.18	1	29.09	2.97	39.5	[811]
Haematopus moquini		103.4	5.69	1	10.63	1.40	39.5	[417]
Chlidonias leucopterus		42.76	0.502	1	66.39	4.08	39.5	[464]
Sterna fuscata		57.94	0.364	1	22.21	1.07	39.5	[128]
Sterna dougalli		50.15	1.12	1	33.97	3.77	39.5	[549]
Sterna hirundo		46.74	1.10	1	35.29	4.76	39.5	[549]
Rissa tridactyla		76.07	0.715	1	32.98	1.79	39.5	[597]
Larus argentatus		115.1	1.70	1	16.53	0.791	39.5	[869]
Catharacta skua		131.3	4.64	1	17.42	2.37	39.5	[888]
Catharacta skua		100.5	0.610	1	40.69	3.12	39	[308]
Catharacta maccormicki		104.8	0.310	1	60.29	3.18	39	[308]
Stercorarius longicaudus		83.90	0.069	1	41.55	2.87	30	[308]
Ptychoramphus aleuticus		59.66	0.373	1	23.73	0.913	39.5	[945]
Cuculus canoris		45.49	0.884	1	49.29	4.00	39.5	[1023]
Cuculus canoris		50.26	1.45	1	38.56	3.68	39.5	[1023]
Cuculus canoris		52.02	7.20	1	42.11	2.12	39.5	[1023]
Cuculus canoris		52.44	1.40	1	39.91	3.60	39.5	[1023]
Glaucidium passerinum	f	42.36	0.309	1	46.98	2.02	39.5	[820]
Glaucidium passerinum	m	41.86	0.484	1	41.57	2.51	39.5	[820]
Asio otus		64.94	0.596	1	36.54	1.77	39.5	[999]
Tyto alba		68.25	1.18	1	21.68	2.70	39.5	[349]
Strix nebulosa		98.26	0.960	1	16.43	0.730	39.5	[630]
Steatornis capensis		94.59	5.24	1	12.96	2.39	39.5	[866]
Apus apus		37.44	0.274	1	45.55	2.88	39.5	[981]
Selasphorus rufus		16.33	0.475	1	58.44	9.88	≤ 41	[172]
Amazilia fimbriata		16.12	0.110	1	69.86	3.54	≤ 41	[380]
Ramphastos dicolorus		70.11	1.89	1	28.52	4.01	39.5	[112]
Sturnus vulgaris		40.83	0.332	1	82.71	5.04	41	[988]
Bombycilla cedrorum		34.16	0.392	1	73.37	4.31	41	[765]
Petrochelidon pyrrhonota		31.19	0.520	1	69.64	6.40	41	[765]
Toxostoma curvirostre		36.62	0.695	1	49.82	3.62	41	[765]
Tyrannus tyrannus		35.53	0.673	1	59.43	4.60	41	[648]
Sylvia atricapilla		25.59	0.142	1	108.2	11.7	41	[80]
Garrulus glandarius		52.34	2.85	1	39.82	8.52	41	[479]
Campylorhynchus brunneicap.		32.79	0.200	1	65.85	6.70	41	[766]
Emberiza schoeniclus		25.88	0.238	1	138.7	12.1	41	[93]
Troglodytes aedon		22.29		1	105.9		41	[29]
Phylloscopus trochilus		22.41	0.576	1	76.78	8.86	41	[819]
Parus major		27.47	0.207	1	59.90	2.33	41	[43]
Parus ater		23.40	0.232	1	75.74	3.88	41	[565]
Motacilla flava		9.910	0.298	2.913	55.19	4.42	41	[220]
Agelaius phoeniceus	f	35.94	0.951	1	75.16	7.58	41	[185]
Agelaius phoeniceus	m	40.66	0.529	1	65.28	2.74	41	[185]
Gymnorhinus cyanocephalus		44.84	0.596	1	49.68	2.97	41	[52]

Eremophila alpestris		30.81	1.24	1	75.98	10.9	41	[62]
Mammalia								
Macropus parma		148.6	0.615	1	2.736	0.0942	35.5	[602]
Macropus fuliginosus		261.6	34.8	1	2.397	0.910	35.5	[724]
Trichosurus caninus		137.8	1.06	1	1.754	0.561	35.5	[433]
Trichosurus vulpecula		139.3	1.34	1	3.715	0.184	35.5	[573]
Perameles nasuta		100.5	0.967	0.961	4.743	0.175	35.5	[573]
Setonix brachyurus		116.6		1	1.728	0.117	35.5	[936]
Suncus murinus	f	26.58	0.160	1	30.92	1.37	37	[237]
Suncus murinus	m	29.88	0.267	1	20.64	1.27	37	[237]
Sorex minutus		65.00		0.294	32.97	0.674	36	[437]
Desmodus rotundus		30.68	0.175	1	8.775	0.277	(35.5)	[814]
Homo sapiens	m	1648	58.5	0.244	0.1490	0.0158	37	[149]
Lepus europaeus		148.3	1.60	1	5.034	0.530	37	[120]
Oryctolagus cuniculus		116.6	1.11	1	6.507	0.272	37	[936]
Notomys mitchellii		27.09	0.412	1	21.54	1.64	38	[184]
Notomys cervinus		23.85	0.456	1	23.94	3.00	38	[184]
Notomys alexis		27.43	0.382	1	20.03	1.24	38	[184]
Pseudomys novaehollandiae		24.88	0.101	1	13.00	0.386	38	[472]
Castor canadensis		234.4	1.64	1	5.117	0.365	38	[10]
Mus musculus		34.24	0.474	1	15.09	0.924	38	[687]
Mus musculus	f	31.87	0.129	1	22.33	1.31	38	[687]
Mus musculus	m	33.98	0.118	1	26.66	1.28	38	[687]
Rattus fuscipes		171.5	4.08	0.280	9.333	0.843	38	[908]
Rattus norvegicus		75.23	0.301	1	9.286	0.279	38	[687]
Tachyoryctes splendens		64.87	0.992	1	8.231	0.680	38	[743]
Balaenoptera musculus		37810	5420	0.188	0.05884	0.0208	37	[857]
Balaenoptera musculus	f	26200		0.188	0.2240		37	[562]
Balaenoptera musculus	m	25000		0.188	0.2160		37	[562]
Balaenoptera physalus	f	22250		0.180	0.2220		37	[562]
Balaenoptera physalus	m	21000		0.180	0.2221		37	[562]
Balaenoptera borealis	f	15300		0.197	0.1337		37	[562]
Balaenoptera borealis	m	14800		0.197	0.1454		37	[562]
Delphinapterus leucas	f	3056	54.4	0.254	0.2700	0.0399	37	[320]
Delphinapterus leucas	m	3589	86.5	0.254	0.1876	0.0227	37	[320]
Canis domesticus		387.2	1.46	1	4.168	0.120	37	[687]
Lutra lutra	f	178.1	1.32	1	2.870	0.156	37	[884]
Lutra lutra	m	197.7	1.38	1	2.692	0.143	37	[884]
Pagaphilus groenlandicus		486.4	7.44	1	0.4787	0.0673	37	[546]
Mirounga leonina	m	5580	356	0.254	0.1492	0.0265	37	[547]
Mirounga leonina	f	2933	42.7	0.254	0.3094	0.0480	37	[547]
Mirounga leonina	m	1799	149	1	0.1185	0.0278	37	[133]
Mirounga leonina	f	704.0	20.4	1	0.3661	0.0982	37	[133]
Leptonychotes weddelli		685.4		1	0.3001	0.0184	37	[133]
Loxodonta a.africana	f	1392	14.5	1	0.1016	8.16e-3	37	[548]
Loxodonta a.africana	m	1723	45.4	1	0.07173	7.81e-3	37	[548]
Rangifer tarandus	f	470.2	1.84	1	1.263	0.0589	37	[607]
Rangifer tarandus	m	534.4	4.39	1	1.000	0.0617	37	[607]
Bos domesticus	f	815.4	3.66	1	0.9957	1.73e-3	38.5	[687]
Alces alces		712.6	12.7	1	0.5930	0.159	37	[399]

An interesting application of the scaling of the von Bertalanffy growth rate with body

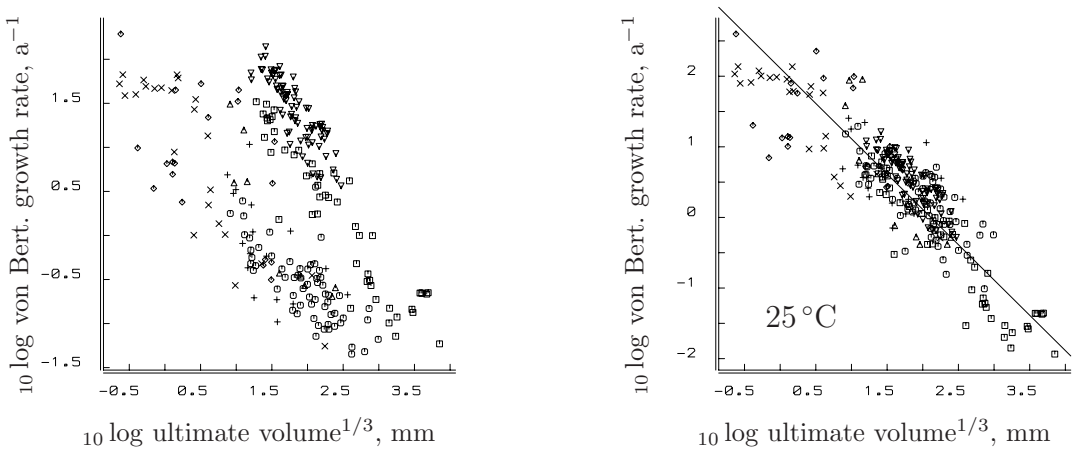

Figure 8.3: The von Bertalanffy growth rate as a function of maximum volumetric length. The left figure shows the rate as estimated from the original data, while the right figure gives the rates corrected to a common body temperature of 25 °C. The markers refer to ▽ birds, □ mammals, △ reptiles and amphibians, ○ fishes, × crustaceans, + molluscs, ◇ others. The line has slope −1, which is expected on the basis of the DEB theory.

size is in speculations about the body temperature of dinosaurs. It relates to the question of whether or not dinosaurs were endotherms, which is still a topic of considerable controversy [269]. The blood vessels in bones [42], the bone structure [49], and predator/ prey ratios [268] resemble those of birds and mammals, the general morphology points to a very active life style [41], all indications that dinosaurs were endotherms [209]; the absence of respiratory turbinates in dinosaurs is recently taken as evidence that they were ectotherms with no need to recover water from their breath [792], the micro-distribution of oxygen isotope in bones led some to conclude that the body temperature varied considerably in a 5-Mg *Tyrannosaurus* [633], and many speculations about growth and reproduction rates of dinosaurs are based on the low ectothermic levels [152]. The problem of sufficient heat loss in big dinosaurs in hot mesozoic climates was stressed by others. Although some dinosaurs weighed up to 100 Mg [25], big dinosaurs were not born big, not all of them were big as adults and they also roamed in cold climates [139]. Studies by Alexander [12] showed that

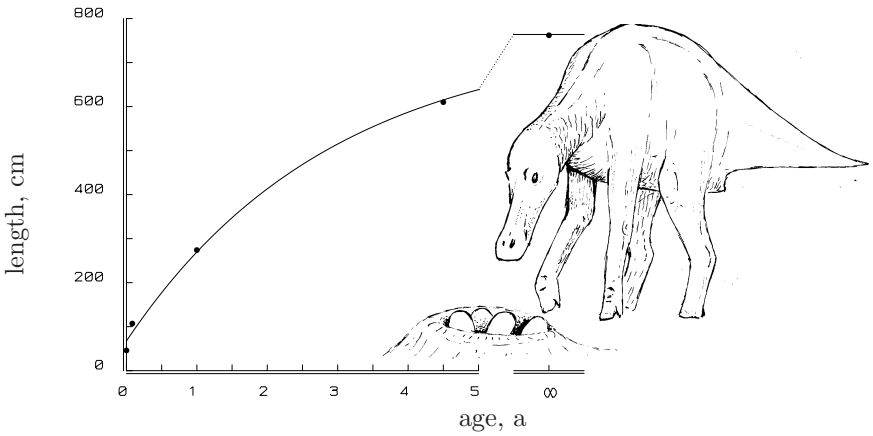

Figure 8.4: The measured length-at-age for the maiasaur (data by Horner, based on age estimates from bone structure [738]) and the fitted von Bertalanffy growth curve (ultimate length 7.6 m, von Bertalanffy growth rate 0.347 a^{-1}). This suggests a body temperature of 37.6 °C, see text.

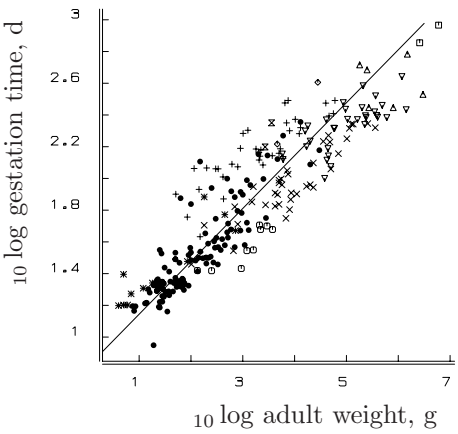

Figure 8.5: The gestation time of eutherian mammals tends to be proportional to volumetric length (line). Data from Millar [632]. The times have been corrected for differences in relative birth weight, i.e. birth weight as a fraction of adult weight, by multiplying by the ratio of the mean relative birth weight$^{1/3}$, 0.396, to the actual relative birth weight$^{1/3}$. The symbols refer to $*$ *Insectivora*, $+$ *Primates*, $\diamond$ *Edentata*, $\circ$ *Lagomorpha*, $\bullet$ *Rodentia*, $\times$ *Carnivora*, $\square$ *Proboscidea*,$\boxtimes$ *Hyracoidea*, $\triangle$ *Perissodactyla*, $\triangledown$ *Artiodactyla*.

the body temperature of small dinosaurs would exceed the environmental temperature by a few degrees only.

Maiasaurs fit the von Bertalanffy growth curve very well, see Figure 8.4. This indicates that the body temperature was constant during their life span. What is the body temperature for which the observed growth rate fits the mean pattern for all 260 species? Corrected for a body temperature of 25 °C, the mean energy conductance was found to be $\dot{v} = 0.3$ m a^{-1} and a maintenance rate coefficient $\dot{k}_M = 2.5$ a^{-1} is typical for terrestrial vertebrates (the latter value affects the calculations only a little). If the weight of a maiasaur of length 7.6 m is estimated at some 2.82 Mg, we arrive at an expected von Bertalanffy growth rate of $\dot{r}_B = 0.063$ a^{-1} at 25 °C, while the observed value is $\dot{r}_B = 0.347$ a^{-1}, see Figure 8.4. The Arrhenius temperature of $T_A = 12.5$ kK leads to an estimated body temperature for the maiasaur of $12.5(\frac{12500}{298} - \ln \frac{0.347}{0.063})^{-1}$ kK or 37.6 °C. I think that a range of plus or minus 2 °C indicates acceptable values. The result is consistent with inferences from incubation times, {287}. It would be most interesting to have data for smaller species and/or species in cold climates, but this will probably remain a wish.

Minimum embryonic period

Because the DEB model is volume structured rather than age structured, the length of the various life stages is closely tied to growth. The gestation time is proportional to volume$^{1/3}$, excluding any delay in implantation. Weasels and probably armadillos are examples of species that usually observe long delays, possibly to synchronize the juvenile period with favourable environmental conditions. Figure 8.5 illustrates that the expected scaling relationship is appropriate for 250 species of eutherian mammals. The mean energy conductance was found to be 2 mm d^{-1} at some 37 °C. This is less than half the mean-temperature-corrected value found from the von Bertalanffy growth rates of juveniles and adults, a difference that must be left unexplained at this moment.

Incubation time (3.34) depends on volume in a more complex way, but it is also approximately proportional to body volume$^{1/3}$, or alternatively to egg volume$^{1/4}$; the scaled egg costs e_0 do not depend on body size, so that egg costs themselves $E_0 = e_0 E_m$ scale with $\mathcal{V}^{4/3}$ or $\mathcal{V} \propto E_0^{3/4}$ so that $a_b \propto \mathcal{V}^{1/3} \propto E_0^{1/4}$. Figure 8.6 gives the log–log plot for

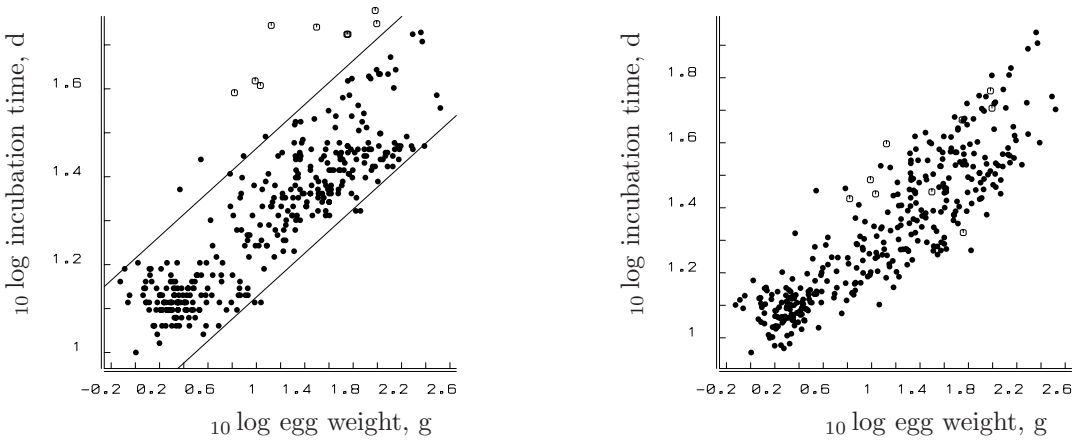

Figure 8.6: The incubation time for European breeding birds as a function of egg weight (left figure). Data from Harrison [373]. The lines have a slope of 0.25. The tube noses (∘) sport long incubation times. If corrected for a common relative volume at birth (right figure), this difference largely disappears.

the species that breed in Europe. These data are very similar to those of Rahn and Ar [744], who included species from all over the world. Although the scatter is considerable, the data are consistent with the expectation. Note that, within a species, large eggs hatch earlier than small ones, though one needs to look for species with egg dimorphism to find a large enough difference between egg weights.

The tube noses *Procellariiformes* incubate longer, while they also have relatively heavy eggs, and so relatively large chicks. If corrected for this large volume at birth, their incubation time falls within the range of other species. This correction has been done by calculating the egg weight first, from $([W_w]\pi/6)$(egg length)(egg breadth)^2. (Data from Harrison [373].) The weight at birth is about 0.57 times the initial egg weight [953]. The scaled length at birth is about $(W_b/W_\infty)^{1/3}$. (This is not 'exact' because of the weight-volume conversion and the volume reduction due to heating.) Bergmann and Helb [71] give adults weights. The incubation time is then corrected for differences in scaled length at birth on the basis of (3.34) for small values of the investment ratio g and a common value for the scaled length at birth, 0.38.

The application of the DEB model has been useful in identifying the proper question, which is not why the incubation time of tube noses is that long, but why they lay so large an egg. The bird champion in this respect is the kiwi *Apteryx*, which produces eggs of 350–400 g, while the adult weight is only 2200 g. It has an incubation period of a respectable 78 days. The relatively low incubation temperature of 35.4 °C extends incubation in comparison to other birds, which usually incubate at 37.7 °C [145,146]. This accounts for some 17–20 days extension with an Arrhenius temperature of 10–12.5 kK, however, most of this long incubation relates to the very large relative size of the egg. The relative size of the egg itself is a result of the energy uptake and use pattern. This matter is taken up again in the discussion on strategies, {293}.

If one or more primary parameters are known, the value of a certain compound parameter such as the (minimum) incubation time can be predicted with much more accuracy.

On the basis of growth data for the cassin's auklet during the juvenile phase, I predicted an incubation period of 40 days [514], not knowing that it has been measured and actually found to be 37–42 days [589]. It is more difficult to verify my prediction of an incubation period for the maiasaur of 145 days if it was ectothermic. This calculation accounted for a birth length of 35 cm with an adult length of 700 cm [427], while the Nile crocodile has a birth length of 20 cm, an adult length of 700 cm and an incubation period of 80–90 days [353]. If true, the maiasaur must have been a very patient animal! A higher (body) temperature doubtlessly reduces the incubation time considerably, cf. {283}.

The reptilian champion in incubation time is the tuatara *Sphenodon punctatus* where the 4-g hatchling leaves the egg after 15 months. The low temperature, 20–25 °C, contributes to this record.

The European cuckoo is a breeding parasite which parks each of its many eggs in the nest of a 'host', which has an adult body weight of only 10% of that of the cuckoo. The eggs of the host are one-half to three-quarters the size of that of the cuckoo. On the basis of egg size alone, therefore, the cuckoo egg should hatch later than the eggs of the host, while in fact it usually hatches earlier despite the later date of laying. If the relative size of the egg with respect to the adult is taken into account, the DEB theory correctly predicts the observed order of hatching. The essence of the reasoning is that, since the cuckoo is much larger than the host, the cuckoo uses the reserves at a higher rate (i.e. $\{\dot{p}_{Am}\}$ is larger), and, therefore, it grows faster in the absolute sense. Growth is so much faster that the difference in birth weight with the chicks of the host is more than compensated. In non-parasitic species of the cuckoo family, the eggs are much larger [1023], which indicates that the small egg size is an adaptation to the parasitic way of life. The extra bonus for the European cuckoo is that it can produce many small eggs (about 20–25), which helps it to overcome the high failure rate of this breeding strategy.

Minimum juvenile period

The juvenile period at high food density for different species is

$$a_{p\mathcal{V}} = \frac{1}{\dot{r}_{B\mathcal{V}}} \ln \frac{V_{m1}^{1/3} - (V_{h1}V_{m1}/\mathcal{V})^{1/3} - V_{b1}^{1/3}}{V_{m1}^{1/3} - (V_{h1}V_{m1}/\mathcal{V})^{1/3} - V_{p1}^{1/3}}$$

It increases almost linearly with length. This relationship fits Bonner's data, as given in Pianka [100,708] very well; however, this data set uses actual lengths, rather than the more appropriate volumetric ones.

The Guinness book of World Records mentions the striped tenrec *Hemicentetes semispinosus*, see Figure 8.7, as the mammal with the shortest juvenile period [544]. The cuis *Galea musteloides*, a 300- to 600-g South American hystricomorph rodent, usually ovulates at some 50 days, but sometimes does so within 11 days of birth [837,962]. Many smaller mammals have a longer juvenile period, which points to the fact that body scaling relationships only give tendencies and not reliable predictions.

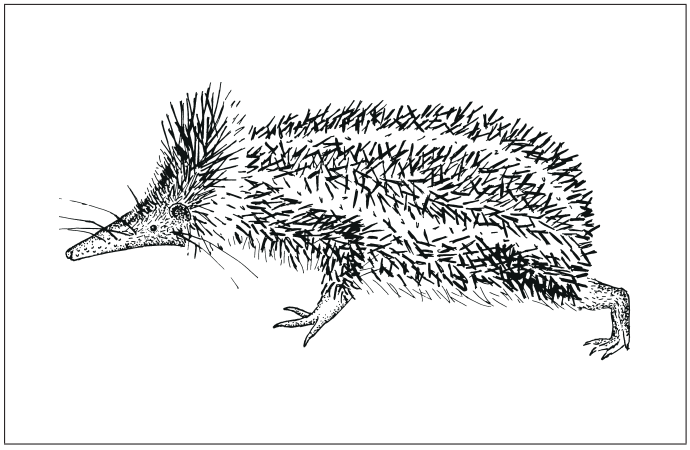

Figure 8.7: The striped tenrec *Hemicentetes semispinosus* is a curious 'insectivore' of 110 g from the rain forests of Madagascar that feeds on arthropods and earthworms and finds its way about using sonar. Walking in the forest, you can spot it easily by its head shaking, not unlike that of an angry lizard. Its juvenile period of 35 days is the shortest among mammals. The gestation period is 58 days [250].

Energy investment in an egg

For small values of the energy investment ratio g, the scaled energy investment e_0 in a single egg, as given in (3.32), is independent of maximum body volume, so that, for the unscaled energy investment $E_{0\mathcal{V}} = E_{01}(\mathcal{V}/V_{m1})^{4/3}$. This does not necessarily translate into the egg weight being proportional to body weight$^{4/3}$, because the energy content, i.e. the chemical composition, may also show scaling relationships. The larger species also have to observe mechanical constraints, and small species can have problems with heating themselves during development. This may cause deviations from expected tendencies. The volume of the hatching young is proportional to the maximum volume of the adult (if corrected for the volume reduction due to heating in endotherms), according to primary scaling relationships. The European birds have egg weights approximately proportional to adult weights. Calder [146] and Rahn *et al.* [747] obtained egg weights proportional to adult weights$^{0.77}$; Birkhead [86] found that the egg weight of auks is proportional to adult weight$^{0.72}$.

Water loss from eggs

The use of energy (stored in lipids, etc.) relates to the water that will evaporate from bird eggs. Part of this water is formed by the oxidation of energy-rich compounds, and part of it consists of the watery matrix in which the compounds are embedded for the purpose of giving enzymes the correct environment and for transport of the products. The total loss of water during the incubation period, therefore, reflects the total use of energy $E_0 - E_b$. Since, like the energy investment in a single egg E_0, the amount of energy at birth $E_b = [E_m]V_b$ is also proportional to $\mathcal{V}^{4/3}$, the loss of water must be a fixed proportion of egg volume. Rahn, Ar and Paganelli [26,745] found that it is some 15% of the initial egg weight. If the use of energy relates to water loss directly, one would expect the initial loss rate to be small and build up gradually. The egg usually decreases linearly in weight, as Gaston [310] found for the ancient murrelet *Synthliboramphus antiqua*. This is to be expected on physical grounds, of course. The specific density of an egg can be used to determine the length of time it has been incubated. This process of water loss implies that the water content of the reserves changes during incubation, but its range is rather restricted. The

functional and physical aspects of water loss from eggs thus coincide beautifully.

Maximum reproductive rate

The maximum reproductive rate, as given in (3.52), is $\dot{R}_{m\mathcal{V}} = \dot{R}_{m1}(V_{m1}/\mathcal{V})^{1/3}$ for the different species. This is a beautiful example showing that the size relationships within a species work out differently from those between species. Intra-species comparisons show that large individuals reproduce at a higher rate than small ones, while the reverse holds for inter-species comparisons. Like most of the other scaling relationships mentioned in this chapter, this only reflects tendencies that allow substantial deviations. The trade-off between a small number of large young and a large number of small young is obvious.

The partition coefficient κ does not depend on body size; thus, a small species spends the same fraction of energy that it utilizes from its reserves on reproduction as a large species. (That is, if the energy required to maintain maturity is negligibly small.) Most studies do not deal with dynamic models for energy allocation, however, but with static ones. Such studies aim to describe the (instantaneous) allocation of resources to the various end points, given an individual of a certain size. If we express the energy spent on reproduction as a fraction of the energy taken up from the environment (at constant food density), this fraction decreases with increasing body volume. This is because ingestion rate increases with volume, see {275}, and utilized energy (respiration rate) with a weighted sum of surface area and volume. This illustrates once again the importance of explicit theories for the interpretation of data.

Starvation

In the section on prolonged starvation {227}, the time till death by starvation for an individual with an initial scaled energy density of $e(0) = l$ was found to be $t_\dagger = \dot{v}^{-1}V^{1/3}\ln\kappa^{-1}$ or $t_\dagger = \dot{v}^{-1}V^{1/3}\kappa^{-1}$ depending on its storage dynamics during starvation. In the first expression the individual does not change its storage dynamics, and in the second one it spends energy on maintenance only. The corresponding survival times for different species are thus $t_{\dagger\mathcal{V}} = \dot{v}_1^{-1}\mathcal{V}^{1/3}\ln\kappa_1^{-1}$ or $t_{\dagger\mathcal{V}} = \dot{v}_1^{-1}\mathcal{V}^{1/3}\kappa_1^{-1}$. They are thus proportional to volume$^{1/3}$. Threlkeld [921] found a scaling exponent of 1/4, but 1/3 also fits the data well.

Constant food densities thus select for small body volume, because small volume aids survival at lower food densities; fluctuating food densities select for large body volume, because a large body volume gives better survival over prolonged starvation. Brooks and Dodson [122] observed that, in the absence of predators, the larger species of zooplankton dominate. The DEB theory suggests that the explanation does not lie in the size dependence of threshold food density (because this would operate the other way round), but in the length of periods for which no animal can find sufficient food. This has been confirmed experimentally by Goulden and Hornig [340].

Life span

Growth never stops in the most elementary formulation of the DEB model, but it is practical to consider the moment at which body volume exceeds $(1-\epsilon)^3V_\infty$ as the end of the growth

period, for some chosen small fraction $\epsilon = 0.05$, say. The length of the growth period at constant food density is given in (3.21) and amounts to $\dot{r}_B^{-1} \ln \epsilon(1 - l_b/f)$. It thus increases with volumetric length for different species, just as the juvenile period. The mean life span of ectotherms with a relatively short growth period that die from aging is found from (7.33) to be $\frac{1}{3}\Gamma(\frac{1}{3})(\frac{1}{6}\ddot{h}_a\dot{k}_M)^{-1/3}$ for $l = f$. The mean life span is thus independent of the maximum body volume of a species. Finch [281] concluded that the scanty data on life spans of ectotherms do not reveal clear-cut relationships with body volume. Large variations in life spans exist, both within and between taxa. The ratio of the growth period to the mean life span is $5.55\ddot{h}_a^{1/3}\dot{k}_M^{-2/3}(1 + f/g) \ln \epsilon(1 - l_b/f)$ and increases with volumetric length. If this ratio approaches 1, life span tends to increase with maximum body volume in a sigmoid manner.

In the section on aging, {139}, I discussed the coupling between the effectiveness of antioxidants, life spans and genetical flexibility. If aging allows long life spans, individuals are likely to have effective means for dealing with a threatening environment, such as avoidance behaviour for dangerous situations (learning), physiological regulation to accommodate changes in diet, temperature and so on. This is likely to involve large brain size and thus an indirect coupling between brain size and life span. The brain may also be involved in the production of antioxidants or the regulation thereof, which makes the link between brain size and life span more direct. Birds have larger brain-to-body-weight ratios than mammals and live twice as long. The life spans both of mammals and birds tend to scale empirically with weight$^{0.2}$ [146,281], which is close to volume$^{1/3}$. Although I have not worked out aging for endotherms quantitatively, this is consistent with the DEB-based expectation, because surface-bound heating costs dominate respiration, and thus aging. Brain size is found, empirically, to be approximately proportional to surface area in birds and mammals [146]. Mammals tend to have higher volume-specific respiration rates than birds [980], which contributes to the difference in mean life span and jeopardizes easy explanations.

It must be stressed that these life span considerations relate to aging, though it is doubtful that aging is a major cause of death under field conditions. Suppose that size and age independent of death dominate under those conditions and that food web interactions work out such that the population remains at the same level while food is abundantly available. To simplify the argument, let us focus on species that have a size at first maturation close to the ultimate size. The death rate can then be found from the characteristic equation (9.33) for $\dot{r} = 0$ and $\Pr\{\underline{a}_\dagger > a\} \simeq \exp\{-\dot{h}a\}$ and $\dot{R}(a) \simeq (a > a_p)\dot{R}_{m\mathcal{V}}$. Substitution gives $\exp\{-\dot{h}_{\mathcal{V}} a_{p\mathcal{V}}\} = \dot{h}_{\mathcal{V}}/\dot{R}_{m\mathcal{V}}$. I have shown already that the age at first maturation $a_{p\mathcal{V}}$ increases almost linearly with length, {287}, and the maximum reproduction rate $\dot{R}_{m\mathcal{V}}$ decreases with length, {289}. The death rate $\dot{h}_{\mathcal{V}}$ must, therefore, decrease with length, so that the life span $\dot{h}_{\mathcal{V}}^{-1}$ increases with length.

These considerations help to explain the results of Shine and Charnov [835], who showed that the product of the von Bertalanffy growth rate and the life span, $\dot{r}_{B\mathcal{V}}/\dot{h}_{\mathcal{V}}$, is independent of body size for snakes and lizards. Charnov and Berrigan [158] argued that the ratio of the juvenile period to the life span is also independent of body size. They tried to understand this empirical result from evolutionary arguments. Since the juvenile period is approximately proportional to length as well, {287}, the ratio of this period to

the life span is roughly independent of body size. The present derivation also specifies the conditions under which the result is likely to be found, without using evolutionary arguments.

8.2.3 Tertiary scaling relationships

Primary and secondary scaling relationships follow directly from the invariance property of the DEB model. The class of tertiary scaling relationships invokes indirect effects via the population level. The assumptions that lead to the DEB model, Table 3.3, must for tertiary scaling relationships be supplemented with assumptions about individual interactions. Chapter 9, on 'living together', considers the most simple one: interaction is via the resource only, {303}. This makes tertiary scaling relationships a weaker type. Body size scaling relationships are usually much less obvious at the community level [190], because of a multitude of complicating factors. Nonetheless, they can be of interest for certain applications.

Abundance

Geographical distribution areas are frequently determined by temperature tolerance limits; see {53}. Temperature and food abundance also determine species abundance in more subtle ways.

Since both the maximum ingestion rate and maintenance costs are proportional to body volume, abundance is likely to be inversely proportional to body volume, so $N \propto \mathcal{V}^{-1}$. This has been found by Peters [700], but Damuth [193] gives a scaling of -0.76. This relationship can only be an extremely crude one. Abundances depend on primary production levels, positions in the food web, etc. Nee *et al.* [656] point to the relationships between phylogenetic position, position in food webs and abundances in birds.

Distribution

High food densities go with large ultimate body sizes within a species. If different geographical regions which differ systematically in food availability are compared, geographical races can develop in which these size differences are genetically fixed. Since high food densities occur more frequently towards the poles and low food densities in the tropics, body sizes between these races follow a geographical pattern known as the Bergmann rule; see {232}.

It is tempting to extend this argument to different species feeding on comparable resources. This is possible to some extent, but another phenomenon complicates the result. Because of the yearly cycle of seasons, which are more pronounced towards the poles, food tends to be more abundant towards the poles in the good season, but at the same time the length of the good season tends to shorten. The time required to reach a certain size (for instance the one at which migration is possible) is proportional to volumetric length. This implies that maximum size should be expected at the polar side of the temperate regions, depending on parameter values, migratory behaviour, endothermism, etc. This probably

holds for species such as geese, which migrate to avoid bad seasons. Geist [313] reported a maximum body weight at some 60° latitude and smaller weights both at higher and lower latitudes for New World deer and races of wolves. He found a maximum body size for sheep at some 50° latitude. Ectotherms that stay in the region can 'choose' the lower boundary of the temperature tolerance range such that they switch to the torpor state as soon as the temperature drops to a level at which food becomes sparse. This reduces the growth rate, of course, but not the ultimate body size. Whether the mean body size in a population is affected then depends on harvesting mechanisms.

Population growth rate

Since the (maximum) reproduction rate decreases with a length measure and the juvenile period increases with a length measure, the maximum population growth rate decreases somewhat faster than a length measure, especially for the small species. A crude approximation is the implicit equation obtained from (9.34)

$$\exp\{-\dot{r}_{\mathcal{V}} a_{p1} (\mathcal{V}/V_{m1})^{1/3}\} = (\mathcal{V}/V_m)^{1/3} \dot{r}_{\mathcal{V}} / \dot{R}_{m1}$$

For dividing isomorphs, the population growth rate is inversely proportional to the division interval, which corresponds to a juvenile period from an energetics point of view. This gives $\dot{r}_{\mathcal{V}} = \dot{r}_1 (\mathcal{V}/V_{m1})^{-1/3}$. Fenchel [276] obtained an empirical scaling of weight$^{-1/4}$ for protozoa, and Niklas [665] obtained a value of (gram C)$^{-0.213}$ for blue-green bacteria and (gram C)$^{-0.22}$ for unicellular algae. Correction for the contribution of reserves in the size measures gives results very close to the expected scaling relationship.

8.3 Allocation strategies

Several comparisons of strategies have already been made to support statements during model development and analysis; this section presents some additional strategies, that would disrupt the flow of arguments if discussed in other chapters.

8.3.1 r versus K strategy

The ecological literature is full of references to what is known as r and K strategies, as introduced by MacArthur and Wilson [575]. The symbol r refers to the population growth rate and K to the carrying capacity; these two parameters occur in the logistic growth equation, which plays a central role in ecology. Under the influence of Pianka [707], organisms are classified relative to each other with respect to a number of coupled traits, the extremes being an 'r-strategist' and a 'K-strategist'. Many of these traits can now be recognized as direct results of body size scaling relationships for eco-physiological characteristics. The search for factors in the environment selecting for r or K strategies can, as a first approximation, be translated into that for factors selecting for a small or large body size.

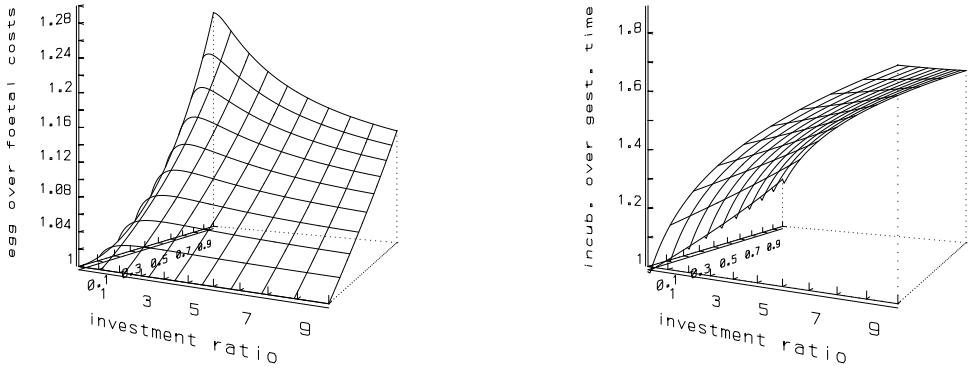

Figure 8.8: The energy costs of producing an egg relative to that of a foetus (left) and incubation time relative to gestation time (right), as a function of the investment ratio g and scaled length at birth l_b (plotted on the y-axis) at high energy density at birth, $e_b = 1$.

8.3.2 Small versus large eggs

Most optimization arguments lead to the uninspiring result that reproduction rate or population growth rate is maximized by producing an infinitely large number of infinitesimally small young. No energy argument seems to forbid this possibility. It is hard to understand why it pays to produce (few) large eggs. One possibility is in accounting for a changing spatially heterogeneous environment. Reproduction is usually synchronized with a favourable season, which is usually short. The reason why the crossbill breeds in midwinter in Scotland, for instance, is that it feeds its young with spruce seeds, which are mature early in spring. This habitat is not always favourable for them; if the seeds are finished, they have to move out. The same holds for ducks breeding in Iceland, where the adult starts to incubate while there is still snow. When the chicks hatch, food is available, but not for long; soon after they are able to fly, the conditions grow worse and they are forced to migrate to the sea. These examples are obvious, but the principle is probably quite common. The selection constraint is, therefore, a maximum period for completing development up to a stage allowing for migration.

It is consistent with the structure of the DEB model that such a stage can be tied to a certain body volume. That the time needed to reach such a volume is strongly reduced by laying large eggs is obvious from the expression for the juvenile period. The fact that birds with large eggs, such as shearwaters and the kiwi, also have long incubation times does not devalue the argument. The DEB model shows that the time taken for the chick to reach a certain size would be even longer if the eggs were smaller. This insight is one of the gains of formalized reasoning, where all relevant variables can be considered at the same time. Another aspect to consider for endotherms is that small young have a hard time maintaining a high body temperature.

8.3.3 Egg versus foetus

The ratio of the energy costs of egg to foetus production is shown in Figure 8.8 in the case of high reserve density at birth, $e_b = 1$. This figure also shows the ratio of the incubation and gestation time. For very small investment ratios, g, the latter ratio becomes

$$\frac{\sqrt{2}e_b u^3}{l_b}\left(\frac{1}{2}\ln\frac{u^2+u\sqrt{2}+1}{u^2-u\sqrt{2}+1}+\arctan\frac{u\sqrt{2}}{1-u^2}\right)$$

with $u \equiv (4e_b/l_b - 1)^{-1/4}$. For very small scaled lengths at birth, this ratio becomes $B_{x_b}(\frac{1}{3},0)x_b^{-1/3}/3$, with $x_b \equiv \frac{g}{e_b+g}$. The development of the embryo in an egg is somewhat retarded at the end of incubation, because of the diminishing reserves. This means that the incubation period is somewhat longer than the corresponding gestation period and that the cumulative costs at birth of an egg are somewhat higher than those of a foetus. This comparison assumes that all parameters are equal. Another difference is that, when breeding, the incubating individual is more restricted in its freedom than the pregnant mother.

8.3.4 Versatility versus specialization

Bacteria as a group are much more diverse in their metabolism than eukaryotes. Within the α-subgroup of the purple non-sulphur bacteria, there is a wide variety of complex metabolic pathways, each involving a considerable number of genes [891]. This can only be understood by assuming that the ancestor of this group possessed all the pathways for, for example denitrification, aerobic and anaerobic photosynthesis, methylotrophy, etc. During evolution, most species lost one or more of these traits; This brings us to the problem of understanding why it can be beneficial for species to cut out DNA that is not used in a particular environment rather than leaving it unused.

As shown in Figure 8.9, the DEB model offers an explanation; the population growth rate decreases for increasing DNA duplication time t_D, particularly at high substrate levels. As the growth process continues during DNA duplication, the cell becomes larger the longer the DNA duplication period, if DNA duplication is triggered once the cell reaches a certain specific size. Since the uptake of substrate relates to surface area, and the surface-area/volume ratio grows worse the larger the cell, the cell is better off reducing the time required to duplicate DNA. The effect of the DNA duplication time on the population growth rate is less at low substrate levels, because the division intervals are extended under these circumstances.

Cutting out disused DNA is just one way to reduce the DNA duplication time [893]. Another possibility is to maintain two chromosomes that are duplicated simultaneously, as in *Rhodobacter sphaeroides* [902], or, more frequently, to maintain megaplasmids [298, 452,891].

The evolutionary significance of a high population growth rate is probably found in the spatial and temporal heterogeneity of the environment. Useful substrates for heterotrophs are usually rare. If a plant or animal dies, the locally present microbes will grow at a high rate over a short period. If the subsequent selection processes thin randomly, the

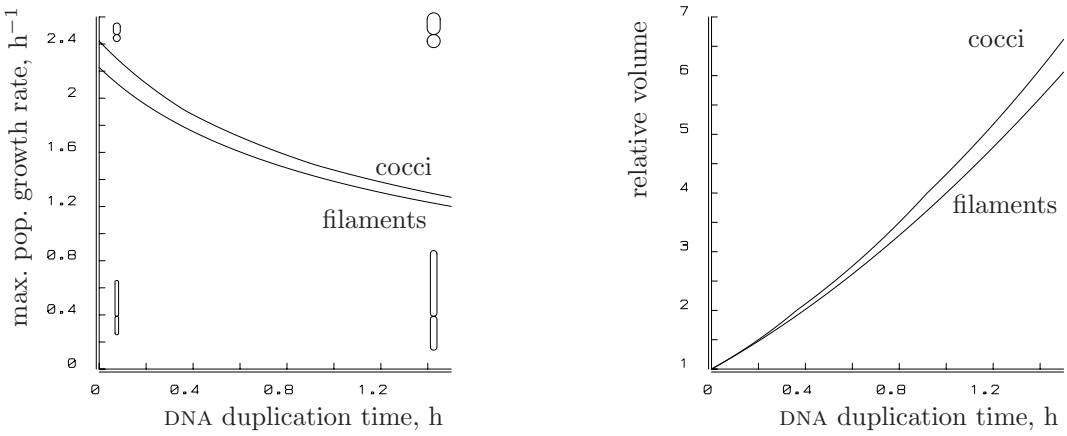

Figure 8.9: Maximum population growth rate decreases for increasing DNA duplication times. The curves are for aspect ratio $\delta = 0$, and 0.6. The aspect ratio is specified just prior to division and is fixed. Cell shape and relative size are indicated just before and after division for $\delta = 0.1$ and 0.6, at a doubling time of 0 and 1.5 h. Cell volume at division relative to the volume that triggers DNA duplication, V_d/V_p, is given in the right figure. Numerical studies show that the figure is independent of parameter values for l_p, g and $\dot{k}_M$, given maximum population growth rate.

most abundant species has the best opportunity of surviving until the next time substrate becomes available. Since the ratio of the numbers grows exponentially at a rate equal to the difference in the population growth rates, small differences can be significant for long growth periods.

8.3.5 Growth versus reproduction: determinate growth

The relative amount of effort spent on reproduction differs from one species to another. Even within a species, it can depend on environmental conditions. Based on work with Mrs K. Lika, this subsection compares the consequences of two allocation strategies in animals: indeterminate growth, where growth continues during the reproductive stage, and determinate growth, where growth is stopped during the reproductive stage. Both animals are otherwise similar, and have no differences during the embryonic stage, when no food uptake occurs, and the juvenile one, when no allocation to reproduction occurs. Both strategies frequently occur, even among rather closely related species: cladocerans sport indeterminate growth (*Daphnia magna* can grow by a factor two in length, that is a factor eight in volume, during the reproductive period), while copepods sport determinate growth.

Embryo and juvenile stages

The age at birth a_b and the energy costs per egg E_0 vary somewhat with the food density, because the reserve density at birth is taken to equal that of the mother: $[E_b] = f[E_m]$ at steady state. This applies to both allocation strategies that are compared. For simplicity's sake, I here take a_b constant and neglect maintenance costs during the embryonic stage,

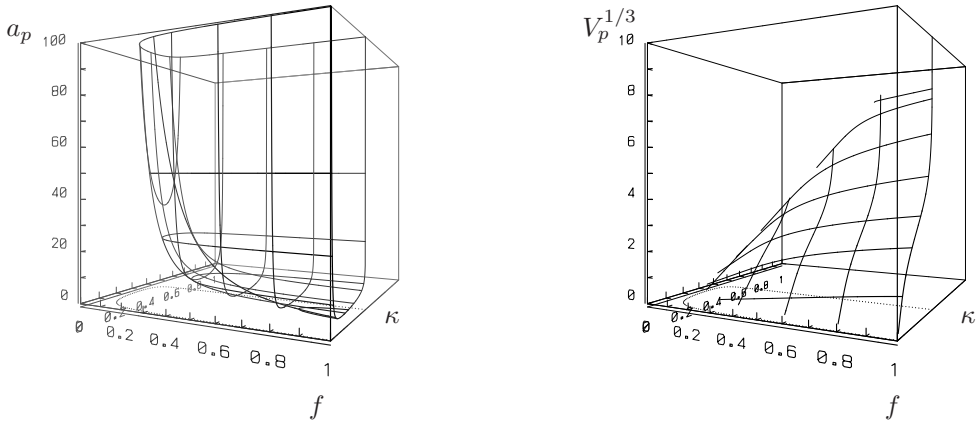

Figure 8.10: The age at puberty a_p (left) and length at puberty $V(a_p)^{1/3}$ (right) as functions of scaled functional response f, and partition coefficient κ. The parameter values are $V_b^{1/3} = 0.8$ mm, $[\dot{p}_M]/[E_m] = 0.1\ \mathrm{d}^{-1}$, $[\dot{p}_J]/[E_m] = 0.15\ \mathrm{d}^{-1}$, $E_p/[E_m] = 10\ \mathrm{mm}^3$, $\{\dot{p}_{Am}\}/[E_m] = 2.5\ \mathrm{mm\,d}^{-1}$, $[E_G]/[E_m] = 0.02$.

which results in the energy costs per egg $E_0 = ([E_G] + [E_m]f)V_b$. Up to the age at puberty a_p, the determinate animal is identical to the indeterminate one. At constant food density the volume $V(a)$ is given by

$$V(a) = \left(V_\infty^{1/3} - (V_\infty^{1/3} - V_b^{1/3})\exp\{-\dot{r}_B a\}\right)^3 \tag{8.1}$$

with $\dot{r}_B = (3[E_G] + 3\kappa f[E_m])^{-1}[\dot{p}_M]$ and $V_\infty^{1/3} = fV_m^{1/3}$ and $V_m^{1/3} = \frac{\kappa\{\dot{p}_{Am}\}}{[\dot{p}_M]}$, where κ is the fraction of catabolic power that is allocated to somatic maintenance plus growth, as opposed to maturity maintenance plus maturation or reproduction.

The age at puberty a_p is reached when the cumulative investment in maturation exceeds a threshold value: $E_p = \int_{a_b}^{a_p} ((1-\kappa)\dot{p}_C(a) - [\dot{p}_J]V(a))\ da$, where E_p is the threshold value for energy invested in maturation, $\dot{p}_C$ the catabolic power and $[\dot{p}_J]$ is the specific maturation maintenance cost. The catabolic power is defined as the power that is released from the reserves to fuel metabolism. Substitution gives

$$E_p = (1-\kappa)f\left(\{\dot{p}_{Am}\}\int_{a_b}^{a_p} V^{2/3}(a)\,da - [E_m]\,(V(a_p) - V_b)\right) - [\dot{p}_J]\int_{a_b}^{a_p} V(a)\,da \tag{8.2}$$

If $[\dot{p}_J] = \frac{1-\kappa}{\kappa}[\dot{p}_M]$, the relationship (8.2) reduces to $E_p = [E_G](V(a_p) - V_b)\frac{1-\kappa}{\kappa}$, which reveals that $V(a_p)$ does not depend on the scaled functional response f. The stage transition occurs when cumulative investment in maturation exceeds a fixed threshold, while at the same time structural mass exceeds a fixed threshold; age at puberty a_p does depend on f, however. For other values of $[\dot{p}_J]$, $V(a_p)$ does depend on f, and κ, and stage transition no longer occurs at a fixed structural mass.

Figure 8.10 illustrates how the age and length at puberty depend on the scaled functional response f and the partitioning fraction κ. The value of κ for which the length at puberty does not depend on the feeding rate is $\kappa = (1 + [\dot{p}_J]/[\dot{p}_M])^{-1} = 0.4$, which is just

outside the range for which maturity can be reached for this parameter combination (see also Figure 8.11). The volume at puberty can differ up to a factor of 6 from the ultimate volume at indeterminate growth for this choice of parameter values.

Adult stage

The hazard rate has a direct relationship with energetics, and relates to mean life span through $\mathcal{E}\underline{a}_\dagger = \int_0^\infty \Pr\{\underline{a}_\dagger > a\}\, da = \int_0^\infty \exp\{-\int_0^a \dot{h}(t)\, dt\}\, da$. For a reproduction rate $\dot{R}(a)$, the life span reproduction amounts to

$$N_R = \int_{a_p}^\infty \dot{R}(a) \Pr\left\{\underline{a}_\dagger > a\right\}\, da \tag{8.3}$$

Constant fraction allocation

In the constant fraction allocation strategy, a constant fraction κ of catabolic energy is allocated to somatic maintenance plus growth during all life stages. During the embryonic and juvenile stage, a constant fraction is allocated to maturity maintenance plus maturation; the investment in maturation switches to reproduction after the cumulated energy investment in maturation exceeds a certain threshold E_p. Maturity maintenance does not increase after the switch, but is proportional to volume before the switch. Somatic maintenance is always proportional to volume.

The reproduction rate is

$$\dot{R}(a) = \frac{\kappa_R}{E_0}\left(\frac{(1-\kappa)f}{\kappa f/[E_G] + 1/[E_m]}\left(\frac{\{\dot{p}_{Am}\}}{[E_m]} V^{2/3}(a) + \frac{[\dot{p}_M]}{[E_G]} V(a)\right) - [\dot{p}_J] V(a_p)\right) \tag{8.4}$$

while the volume $V(a)$ is given by (8.1).

If the aging acceleration is small enough, such that the period of substantial growth is short with respect to the life span, the hazard rate and the survival probability can be approximated by

$$\dot{h}(a) = \frac{\ddot{h}_a[\dot{p}_M]}{2\kappa[E_G]}(a - a_p)^2; \quad \Pr\{\underline{a}_\dagger \geq a\} = \exp\left\{-\frac{\ddot{h}_a[\dot{p}_M]}{6\kappa[E_G]}(a - a_p)^3\right\}$$

for $a \geq a_p$.

The mean life span equals

$$\mathcal{E}\underline{a}_\dagger = a_p + \Gamma\left(\frac{1}{3}\right)\left(\frac{6\kappa[E_G]}{27\ddot{h}_a[\dot{p}_M]}\right)^{1/3} \simeq a_p + 1.62\left(\frac{\kappa[E_G]}{\ddot{h}_a[\dot{p}_M]}\right)^{1/3} \tag{8.5}$$

Bang-bang allocation

The bang-bang allocation strategy is the same as the fixed-fraction allocation one, but growth is ceased at certain volume V_p; all catabolic energy is then allocated to maintenance (somatic plus maturity) plus reproduction. This leads to the reproduction rate

$$\dot{R} = \frac{\kappa_R}{E_0}\left(f\{\dot{p}_{Am}\} V^{2/3}(a_p) - ([\dot{p}_M] + [\dot{p}_J]) V(a_p)\right) \tag{8.6}$$

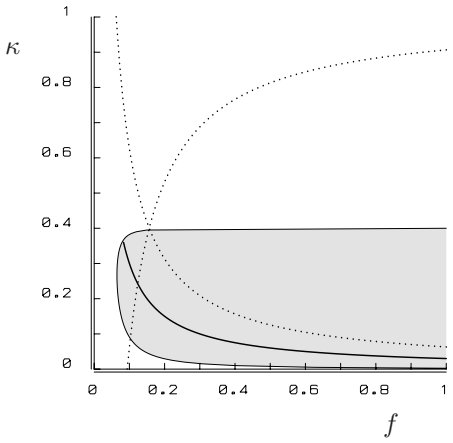

Figure 8.11: The grey area indicates the combination of values for the scaled functional response f and the partitioning fraction κ, for which the adult state is reached; the age at puberty is infinitely large at its border. The fat curve represents values for f and κ where the reproduction rate of the determinate animal equals that of a fully grown indeterminate one. The dotted curves represent boundaries for which the neonate just can pay somatic and maturity maintenance costs. Parameter values: see Figure 8.10.

If the aging acceleration is small enough, such that survival to puberty is almost sure, the hazard rate and the survival probability for the determinate animal can be approximated for $a \geq a_p$ by

$$\dot{h}(a) = \frac{\ddot{h}_a\{\dot{p}_{Am}\}f}{2[E_G]V^{1/3}(a_p)}(a-a_p)^2; \quad \Pr\{\underline{a}_\dagger \geq a\} = \exp\left\{-\frac{\ddot{h}_a\{\dot{p}_{Am}\}f}{6[E_G]V^{1/3}(a_p)}(a-a_p)^3\right\}$$

The mean life span is

$$\mathcal{E}\underline{a}_\dagger = a_p + \Gamma\left(\frac{1}{3}\right)\left(\frac{6[E_G]V^{1/3}(a_p)}{27\ddot{h}_a\{\dot{p}_{Am}\}f}\right)^{1/3} \simeq a_p + 1.62\left(\frac{[E_G]V^{1/3}(a_p)}{\ddot{h}_a\{\dot{p}_{Am}\}f}\right)^{1/3} \tag{8.7}$$

and the life span reproduction simplifies to $N_R = \dot{R}(\mathcal{E}\underline{a}_\dagger - a_p)$.

Comparison of reproduction and life span

Assuming that aging allows, the reproduction rate of the fully grown indeterminate animal exceeds that of the determinate one if

$$(1-\kappa)V_\infty - V_\infty^{1/3}V^{2/3}(a_p) + \kappa V(a_p) \geq 0 \tag{8.8}$$

Somatic maintenance costs can only be paid by the neonate if $V_\infty \geq V_b$. Maturity can only be maintained by the neonate if $V_\infty \geq V_b\left(\frac{\kappa}{1-\kappa}\frac{[\dot{p}_J]}{[\dot{p}_M]}\right)^3$. Reproduction is only initiated if $V_\infty > V(a_p)$. For very low feeding rates, the ultimate size can drop below the size at birth, as implied by the model assumptions. Figure 8.11 illustrates that the reproduction rate of a fully grown indeterminate animal exceeds that of the determinate one for all biologically meaningful combinations of f and κ, given the parameter values. The area left of the concave (upper-left to lower-right) dotted curve is less relevant, because this is where the ultimate size is below that of the neonate. The area left of the convex (lower-left to upper-right) dotted curve represents values for f and κ where neonates cannot maintain their state of maturity.

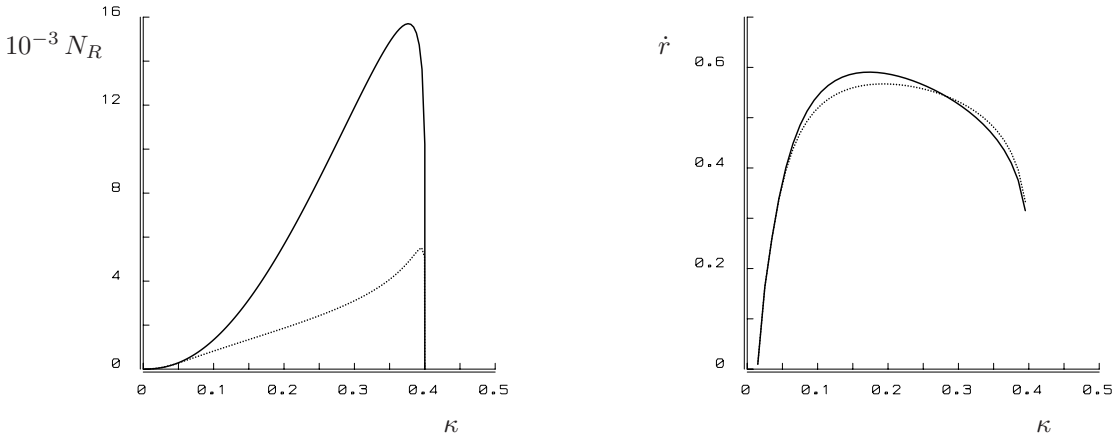

Figure 8.12: The life span reproduction N_R (left) and the population growth rate $\dot{r}$ (right) of the indeterminate (solid) and the determinate (dotted) animals as a function of the partitioning fraction κ at abundant food ($f = 1$). Parameters: see Figure 8.10, and $\kappa_R = 1$, $\ddot{h}_a = 5\,10^{-7}$ d^{-1}.

Comparison of (8.5) and (8.7) shows that the life span of the indeterminate animal exceeds that of the determinate one if $V_\infty > V(a_p)$, which is always the case. The reason is in the decreasing specific oxygen consumption for increasing body size, {135}. The assumption that death by aging is negligibly small before puberty obviously breaks down when the juvenile period becomes excessively large.

Figure 8.12 gives the life span reproduction and the population growth rate as a function of the partition coefficient at abundant food ($f = 1$), and shows that the differences between both allocation rules are substantial for the life time reproduction, but small for the population growth rate, given this choice of parameter values.

The bang-bang allocation will probably lead to larger population growth rates for high death rates, because reproduction is larger just after maturation and the contribution of the early offspring to the population growth rate is more important than that made by later offspring. This is because the early offspring will reproduce earlier as well, the interest upon interest principle. Selection for high population growth rates can be expected in situations of alternating periods of food abundance, followed by starvation with random thinning.

The difference between determinate and indeterminate growth disappears if the switch to the adult stage is outside the growth period, so the body size at puberty is close to the ultimate body size. Copepods, which cannot grow once they start reproduction, in fact follow the von Bertalanffy growth curve quite well. The difference with daphnids, which keep their growth potential, only becomes apparent if the animals are continuously exposed to low food densities during their juvenile stage, and then exposed to high food densities during the adult stage. This might be a rather artificial situation, with little relevance to field ecology. Holometabolic insects cannot grow after the pupal stage, and juveniles and adults feed on different diets; the coupling of energetic properties between adults and juveniles still awaits further study in the context of the DEB theory.

8.4 Evolutionary aspects

Comparing species ultimately leads to speculations about the origin of life. Such speculations are relatively straightforward in the context of the DEB theory, because it is not species-specific. Therefore, it probably also applies to the very first forms of life. So it does not suffer from the problem inherent to collections of species-specific models for energetics: if model 1 applies to species A and model 2 to species B, what model would apply to the common ancestor of species A and B if changes during evolution are gradual? This problem only has a solution if models 1 and 2 can be converted to each other in a continuous way, which poses severe constraints on the structure of models that make sense in an evolutionary context.

For didactical reasons, I introduced the DEB theory in this book starting with a single type of reserve. Present-day organisms that can be described by a single type of (generalized) reserve probably evolved from organisms with more reserves that gradually became coupled. The DEB model has this evolutionary consistency, as can be deduced from (5.18). The partitionability requirement of reserve dynamics is crucial here. If $\kappa_{Ei} = \kappa_E$, and $\dot{k}_{Ei} = \dot{k}_E$, and we introduce $\sum_i m_{Ei} = m_E$, $\sum_i j_{Ai} = j_A$, $\sum_i j_{Mi} = j_M$, and $\sum_i n_{Vi} = n_V$, equation (5.18) can be summed over all reserves to obtain

$$\frac{d}{dt} m_E = j_A - (1-\kappa_E)(\dot{k}_E - j_G) m_E - \kappa_E (j_M + n_V j_G) - j_G m_E \overset{\kappa_E \to 0}{=} j_A - \dot{k}_E m_E$$

This shows how organisms can gradually couple the dynamics of several reserves, and obtain a higher degree of homeostasis. A first-order process for reserve density only arises if reserve 'molecules' that are rejected by the growth-Synthesizing Unit are not fed back to the reserves. The coupling of reserves is attractive to an organism if the availabilities of nutrients are coupled as well. If food consists of animal prey, this coupling is almost perfect, and the conversion is efficient because the composition of prey resembles that of the consumer. If food consists of plant material, the coupling is still considerable, but, since the compositions of plant and consumer differ more, the conversion is less efficient.

The very first cells probably did not have an advanced structure, so they are likely to have been isomorphically growing spheres. The cells probably did not have an advanced system for dividing into two equal parts either. The surface tension of the (outer) membrane prohibits the separation of very small daughter cells. In turbulent environments protocells cannot grow to a large size before being torn apart into daughter cells that are not very different in size. In less turbulent environments cells can grow to larger sizes, while the daughter cells are able to differ more in size.

The formation of bi-layered membranes could have occurred and still does occur abiotically, especially on agitated surfaces of water, such as in coastal areas. Modern cells have phospholipid membranes that are impermeable to most compounds and exchange material with the environment through ion channels, which are complex proteins (in organisms alive today). Such exchange, therefore, requires a rather advanced machinery for protein synthesis which was probably RNA based. (Ling [561] argues, however, that uptake is largely determined by properties of the cytoplasm and that membranes are not that impermeable.) Since the discovery that RNA can catalyse its own splicing in the absence of proteins [155],

most authors now agree that RNA appeared earlier than proteins [671], even though the abiotic synthesis of such complex RNA has not been demonstrated. It is hard to see how RNA in the environment could have been of much significance. Its concentration as well as that of its substrates (amino acids) were doubtlessly extremely low. The accumulation of the products inside membranes of protocells could hardly have been significant. The situation is obviously much better for RNA molecules captured in protocells with a membrane, provided that the membrane is permeable to amino acids and other substrates. DNA appeared later to fulfil the function of an archive for RNA.

Growth can occur abiotically via the accumulation of compounds in the membranes from the environment. Originally these compounds were probably rarely subjected to chemical transformation. If RNA was present in the protocells that catalyzed transformations, such that accumulation was enhanced, positive selection of such protocells would be a fact. The catalytic role of proteins then comes next. The energy required for transformations can originally have been extracted from fermentation processes in an anoxic world. These organisms gave rise to chemo-autotrophs. According to de Duve [243], endogenic reactions were originally fuelled by thioesters. Photosynthesis possibly developed, at least $3.5\,10^9$ years ago, from phototactic chemo-autotrophs in hydrothermal environments [667]. The oxygen-requiring respiratory chain probably developed from the machinery required for nitrification. The accumulation rate of substrate at low concentrations was probably proportional to the surface area of the membrane just as it still is. Protocells will have grown in the 'cube root' phase, see {252}, because maintenance processes were relatively unimportant.

The general picture of the evolution of metabolic systems that emerges is more or less as follows. Initially metabolism became increasingly independent of temporary variations in the nutritional quality of the environment by increasing their storage capacity for the various nutrients; temporary peaks in the availability of a nutrient can only be used if other nutrients are not essential for this uptake, so the number of reserves equals the number of essential nutrients. Then followed a phase where organisms increased their control over the uptake of resources by increasing their taxis, and homeostasis abilities at the same time. It allowed them to use specialized enzymes to catalyse particular transformations, so increasing and regulating the rate of these transformations. The proper functioning of these enzymes requires a steady turnover, and so maintenance costs, which are further increased by the taxis activities. These maintenance requirements have tight links with storage capacities in varying environments to ensure the integrity of the metabolic system.

The animal line of development perfectioned the control over uptake by feeding on other organisms, which gives an almost perfect coupling of resources. This allowed animals to eliminate many routes of metabolite synthesis, to couple the use of various reserves such that a single generalized reserve emerged, and an almost perfect homeostasis was reached. This specialization came hand in hand with an increase of the taxis abilities, through the development of advanced motor systems and senses, which need a nervous system for information processing and muscle control. They used this nervous system to increase their control over homeostasis as well. This more active life style increased the maintenance costs, which is no problem as long as it leads to higher assimilation as well.

The plant line of development specialized in increasing the adaptive abilities. Plants

became extremely flexible in morphology, with direct links to the control over uptake of the various nutrients and light (roots versus shoots). They invented the use of products (wood, silica) to solve mechanical problems, and learned to use animals to solve the problem of finding partners in the reproduction process, and of exporting seeds to uncolonized areas, while being confined to a particular site. They also learned to use fungi to capture nutrients that are locked in organic compounds, and some use bacteria to make dinitrogen biologically available.

The increase in biodiversity allowed a specialization of functions, which enhanced metabolic versatility, by using other species or their activities; compare mixotrophs with a producer-consumer-decomposer community, for instance. The processes of syntrophy and even more advanced forms of symbiosis developed early in evolution and have been reestablished many times since then, resulting in loose and tight links between virtually all organisms. This will be explored in the next chapter.

8.5 Summary

The most amazing aspect of the DEB theory is that, while it deals with mechanisms, rules are implied for the covariation of parameter values among species. This rests on a classification of parameters as intensive or extensive, such that ratios of extensive ones are intensive. When expressed in the proper dimensions, the extensive parameters scale with a volumetric length. The reasoning is closely linked to an invariance property of the DEB model: two parameter sets may differ in a very special way, while the resulting energetics are identical at constant food levels.

The scaling of each of the primary parameters is derived, and then that of functions of these parameters, and finally that of quantities that relate more indirectly to primary parameter values and involve interactions between organisms and properties of the environment. They all capture observed scaling relationships very well. The functions of parameters relate to many aspects of life history, and physiological quantities, such as respiration. Many fruitless attempts have been made to explain why respiration scales with body weight to the power 0.75 (approximately). The explanation offered by the DEB theory is that the inter-specific scaling results from an increasing contribution made by the reserves to body weight; the intra-specific scaling results in the decreasing contribution of growth to the energy budget for increasing body weight.

I argue that many discussions in the literature about investments in offspring in fact relate to body size scaling relationships. Allocation to growth versus reproduction is discussed in some greater depth to reveal the coupling of traits in the context of the DEB theory. These couplings cause deviations from the general opinion that the 'optimal' strategy for growth versus reproduction is the bang-bang strategy: first grow, then reproduce. This turns out not to hold generally.

The chapter closes with a short discussion about evolutionary aspects that pertain to the structure of models for energetics. It emphasizes the importance of the partitionability assumption of the DEB theory, and the evolutionary implications. I sketch some patterns in the evolutionary development of energetics in the light of the animal–plant dichotomy.

Chapter 9

Living together

The primary purpose of this chapter is to evaluate the consequences of the DEB model for individuals at the population and higher levels if extremely simple rules are defined for the interaction between individuals and the energy balance of the whole system. The first section deals with trophic interactions between species, and the constraints on parameter values that ensure a stable coexistence. Then follows a discussion of population dynamics, food chains and (simple) ecosystems.

9.1 Trophic interactions

The DEB theory can be used to analyse the dynamics of systems with complex types of mass exchange between the participants in trophic relationships, a rich spectrum ranging from competition to predation. The present aim is to discuss some constraints in these patterns that ensure weak homeostasis of structural masses: the relative abundance of the structural masses of the participating species is independent of the substrate densities in the environment *at steady state*.

Trophic relationships are hard to classify; all relationships seem to be unique at close inspection. They are usually based on the judgement of being beneficial for one or both partners, and many different definitions exist for particular inter-species relationships. The oxpecker *Buphagus* feeds on insects that are attracted to wounds of giraffes, antelopes and other bovids; it is not difficult to see why the thin-skinned small antelopes make evident that they do not really appreciate this 'help' from the birds: oxpeckers try to keep wounds attractive for insects. I observed what solution oxpeckers have when wounds are in short supply. I will refrain from a judgement of benefits, and discuss the various relationships purely on the use of substrates. This is not meant to imply, however, that non-trophic relationships are of little importance to population dynamics.

9.1.1 Competition

When two species feed on the same substrate in a well mixed environment, they are said to compete for that substrate. The ratio of the structural masses of two competing V1-morphs is constant, despite variations in the substrate concentration, if the specific population

growth rates are identical, so $\dot{r}_1 = \dot{r}_2$, for $\dot{r}_i = \frac{f_i \dot{k}_{Ei} - g_i \dot{k}_{Mi}}{f_i + g_i}$, for $i = 1, 2$, and f_i is the scaled functional response. The growth rates are only equal if $X_{K1} = X_{K2}$, $[\dot{p}_{Am1}] = [\dot{p}_{Am2}]$, $\dot{k}_{M1} = \dot{k}_{M2}$, $\dot{k}_{E1} = \dot{k}_{E2}$ and $g_1 = g_2$. In other words, the ratio is only constant if the species are virtually identical in all their energetic properties. The significance of this remark is that syntrophic relationships allow more differences between the species to maintain weak homeostasis. The strict constraints for weak homeostasis explain why pure forms of inter-species competition are rare; most competing species have partially overlapping diets, and differ in preferences. Competition is perhaps most frequent among primary producers, but even they differ in preferences for the various chemical species of nutrients (ammonia versus nitrate, organic nitrogen, etc.).

The literature on population dynamics stresses the competitive exclusion principle: the number of competing species cannot exceed the number of substrates at steady state. The theoretical value of the result is limited, however. Real steady states are rare; complex systems easily have cyclical behaviour, even in homogeneous environments. Changes in feeding conditions come with changes in biomass composition, and the number of substrates is actually large, even if the number of species is small. Lack of sustainable diversity in community models is only problematic in models with simplistic views on chemical aspects.

9.1.2 Syntrophy

Two species have a syntrophic relationship if a recipient species lives off the products of a donor species. The term commensalism is frequently used when the donor does not experience adverse effects. Syntrophy is very common, but the coupling varies from very direct to indirect. Many species of insects and fungi are coprophagic, i.e. they live off animal faeces (its production is coupled to assimilation). A rich diversity of animals and fungi live off fallen tree leaves (their production is coupled to maintenance). The nitrifying bacteria *Nitrosomonas* and *Nitrobacter* oxidize ammonia to nitrite, and nitrite to nitrate, respectively, while other groups (*Pseudomonas*, *Micrococcus*, *Thiobacillus*) convert nitrate to dinitrogen. An even more indirect coupling exists between plants and oceanic diatoms, where plants mobilize silica from rocks [90], which diatoms require to make frustules; terrestrial plants allow diatoms to play a leading role in the plankton of the oceans.

The house dust mite *Glycyphagus demesticus* lives, with help of the fungus *Aspergillus repens*, off human skin flakes (their production is coupled to maintenance); these mites frequently cause allergic reactions in humans, which might stimulate flake production. The moth *Hypochrosis* drinks tears of big mammals, such as Asian elephants and, incidentically, humans, but stimulates tear production at the same time. The sucking of mammalian blood by mosquitos or of plant saps by mistletoes or aphids is only a small step further towards a biotrophic relationship.

Methanogens were originally believed to be able to grow on propionate, butyrate and alcohols longer than methanol [1027]. For example *Methanobacillus omelianskii* seemed to oxidize ethanol (C_2H_6O) to acetate ($C_2H_3O_2^-$) and use the electrons to reduce CO_2 to CH_4. This 'species' turned out to consist of two, which use substrates and produce products as follows

Donor	$2\,C_2H_6O + 2\,H_2O + O_2 \rightarrow 2\,C_2H_3O_3^- + 2\,H^+ + 4\,H_2$
Recipient	$4\ H_2 + CHO_3^- + H^+ \rightarrow CH_4 + 3\,H_2O$
Sum	$2\,C_2H_6O + CHO_3^- + O_2 \rightarrow 2\,C_2H_3O_3^- + H^+ + CH_4 + H_2O$

The donor needs the activities of the recipient to keep the concentration of its product, hydrogen, down to extremely low levels. This is required to extract energy from the degradation of ethanol. This pair serves as an example of a syntrophic relationship, which will be analysed quantitatively for V1-morphs. What are the constraints on the production of hydrogen such that the biomass ratio between the species does not change, and the two species behave as a single one, at least in steady state? The interest in the question is to derive evolutionary constraints on the origin of syntrophy.

Direct transfer

The donor obtains its substrate from the environment and the recipient receives product from the donor, which serves as substrate. They grow at specific rates

$$\dot r_1 = \frac{f\dot k_{E1} - \dot k_{M1} g_1}{f + g_1} \quad \text{and} \quad \dot r_2 = \frac{\frac{\dot k_{E2} j_P}{j_{P,Am2}} \frac{M_{V1}}{M_{V2}} - \dot k_{M2} g_2}{\frac{j_P}{j_{P,Am2}} \frac{M_{V1}}{M_{V2}} + g_2}$$

where f stands for the scaled functional response of the donor, and $j_P = \zeta_{PM}\dot k_{M1} g_1 + \zeta_{PA}\dot k_{E1} f + \zeta_{PG} g_1 \dot r_1$ for the specific flux of product from the donor to the recipient, see (4.33). The flux of product is thus $j_P M_{V1}$, while the maximum flux that can be handled by the recipient is $j_{P,Am2} M_{V2}$; the ratio of the two quantifies the scaled reserve density (at steady state). The first assumption is that all product can be handled.

Weak homeostasis is obtained if M_{V1}/M_{V2} remains constant, so if $\dot r_1 = \dot r_2$, independent of the substrate availability of the donor. The first observation is that $\dot r_1 = 0$ if $f = g_1 \dot k_{M1}/\dot k_{E1}$, and $\dot r_2 = 0$ if

$$\frac{M_{V1}}{M_{V2}} = \frac{g_2}{g_1} \frac{\dot k_{M2}}{\dot k_{M1}} \frac{j_{P,Am2}}{\dot k_{E2}} \frac{1}{\zeta_{PM} + \zeta_{PA}}$$

This constraint can be substituted into the expression for $\dot r_2$ and allows $\dot r_1 = \dot r_2$ for $f = g_1 \frac{\dot k_{M1} + \dot r_1}{\dot k_{E1} - \dot r_1}$, to be written as

$$(1 + \dot r_1/\dot k_{M2}) \dot k_{M1} g_1 (\zeta_{PM} + \zeta_{PA}) = (1 - \dot r_1/\dot k_{E2}) j_P$$

Substitution of j_P shows that this constraint can be re-written as a third-order polynomial in $\dot r_1$ being equal to zero, which only holds if all coefficients are equal to zero. This leads to $\zeta_{PG} = 0$, $\zeta_{PA} \neq 0$, $\dot k_{E1} = \dot k_{E2} = \dot k_E$ and $\frac{\zeta_{PM}}{\zeta_{PA}} \left(\frac{\dot k_{M1}}{\dot k_E} + \frac{\dot k_{M1}}{\dot k_{M2}} \right) = 1 - \frac{\dot k_{M1}}{\dot k_{M2}}$.

The conclusion is that homeostasis can be achieved if no product formation is associated with donor growth, the turnover rates are equal, and a simple constraint applies to the parameter values. The ratio of the structural masses to the reserves can be expressed as simple functions of parameters at steady state

$$\frac{M_{V1}}{M_{V2}} = \frac{g_2}{g_1} \frac{1 + \dot k_{M2}/\dot k_E}{1 + \dot k_{M1}/\dot k_E} \frac{j_{P,Am2}}{\zeta_{PA} \dot k_E} \quad \text{and} \quad \frac{M_{E1}}{M_{E2}} = \frac{M_{Em1}}{M_{Em2}} \frac{g_1}{g_2} \frac{1 + \dot k_{M1}/\dot k_E}{1 + \dot k_{M2}/\dot k_E} \left(1 + \frac{g_1}{f} \frac{\dot k_{M2} - \dot k_{M1}}{\dot k_{M2} + \dot k_E} \right)^{-1}$$

The ratio of the reserves is only independent of substrate availability for the donor if the maintenance rate coefficients are equal ($\dot{k}_{M2} = \dot{k}_{M1}$), that is when $\zeta_{PM} = 0$. The conclusion is that the conditions for weak homeostasis are much less stringent, compared to a competition relationship.

Indirect transfer

Suppose that the donor and the recipient live in a chemostat of throughput rate $\dot{h}$ which is fed with medium containing ethanol in concentration X_{Sr}, and other substrates that might be necessary, except for hydrogen. The donor delivers its product into the well-mixed chemostat. Changes in biomass ratios of donor and recipient are still possible given the constraints of homeostasis if the saturation constant of the recipient for the product is not very small.

The changes in the concentrations of ethanol (substrate S), hydrogen (product P), and structural biomass of species 1 and 2 are for $f_1 = (1+X_{KS}/X_S)^{-1}$ and $f_2 = (1+X_{KP}/X_P)^{-1}$

$$\frac{d}{dt}X_S = (X_{Sr} - X_S)\dot{h} - \zeta_{SA} f_1 \dot{k}_{E1} X_{V1}; \quad \frac{d}{dt}e_i = (f_i - e_i)\dot{k}_{Ei}, \quad i \in \{1,2\} \tag{9.1}$$

$$\frac{d}{dt}X_P = (\zeta_{PM}\dot{k}_{M1}g_1 + \zeta_{PA}\dot{k}_{E1}f_1 + \zeta_{PG}\dot{r}_1 g_1)X_{V1} - \zeta_{PA} f_2 \dot{k}_{E2} X_{V2} - X_P\dot{h} \tag{9.2}$$

$$\frac{d}{dt}X_{V1} = (\dot{r}_1 - \dot{h})X_{V1} \quad \text{with } \dot{r}_1 = \frac{\dot{k}_{E1}e_1 - \dot{k}_{M1}g_1}{e_1 + g_1} \tag{9.3}$$

$$\frac{d}{dt}X_{V2} = (\dot{r}_2 - \dot{h})X_{V2} \quad \text{with } \dot{r}_2 = \frac{\dot{k}_{E2}e_2 - \dot{k}_{M2}g_2}{e_2 + g_2} \tag{9.4}$$

The expressions for the specific growth rate follow from the DEB theory, as does the production of product (here hydrogen), which is, generally, a weighted sum of the three basic powers. At steady state we have $\dot{h} = \dot{r}_1 = \dot{r}_2$, and the problem is to find the weight coefficients ζ_{P*} for the production of hydrogen such that X_{V2}/X_{V1} does not depend on $\dot{h}$.

The steady-state scaled functional responses are $f_{S1} = g_1\frac{\dot{k}_{M1}+\dot{h}}{\dot{k}_{E1}-\dot{h}}$ and $f_{P2} = g_2\frac{\dot{k}_{M2}+\dot{h}}{\dot{k}_{E2}-\dot{h}}$, from which follow the concentrations $X_S = X_{KS}f_{S1}/(1-f_{S1})$ and $X_P = X_{KP}f_{P2}/(1-f_{P2})$. The ratio of the biovolume densities of species 2 and 1 at steady state is

$$\frac{X_{V2}}{X_{V1}} = \frac{\zeta_{PM}\dot{k}_{M1}g_1 + \zeta_{PA}\dot{k}_{E1}f_{S1} + \zeta_{PG}\dot{h}g_1}{\zeta_{PA}\dot{k}_{E2}f_{P2}} + \frac{\zeta_{SA}\dot{k}_{E1}f_{S1}}{\zeta_{PA}\dot{k}_{E2}f_{P2}}\frac{X_P}{X_{Sr} - X_S}$$

The ratio varies within a limited range only, for varying throughput rate $\dot{h}$ and substrate concentration X_{Sr}, if the saturation constant X_{KP} is small, and the constraints apply for weak homeostasis at direct transfer.

9.1.3 Symbiosis

Two species have a symbiontic relationship if the syntrophic one is reciprocal. It is extremely common; think for instance of the micro flora in digestive tracts of animals, or a mycorrhiza in and around plant roots. A discussion of its frequently amazing forms can

easily fill a book, and most relationships are probably still unknown. The term mutualism is frequently used to indicate a relationship that is reciprocally 'beneficial', without a direct trophic basis that is reciprocal, such as ant–plant relationships, where plants provide protein granules, and ants take care of plant-eating insects. Another example is the plant–pollinator relationship, where plants provide nectar and pollen, and the pollinator (insects, bats, birds) takes care of directed pollen dispersal. These cases represent syntrophic relationships as far as the use of substrates is concerned.

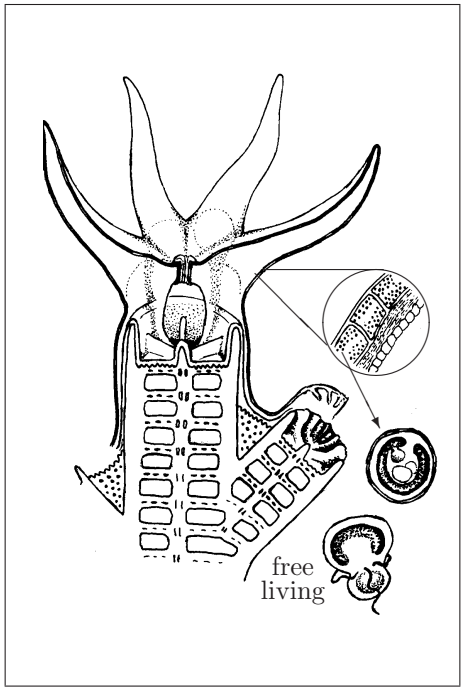

Algae frequently go for symbiontic relationships with plants, animals, and other protoctists [759]. Many (tropical) coelenterate species host endosymbiontic dinoflagellates named zooxanthellae [907], which can still live independently from the host [223]. Scleractinian corals hosting *Symbiodinium* species are the dominant reef builders. Chloroplasts, including that of *Symbiodinium*, are considered to be endosymbionts themselves. Membrane compositions reveal that chloroplasts of the endosymbiontic dinoflagellate *Amphidinium wigrense* are similar to the cryptomonad endosymbionts of *Gymnodinium acidotum*, which have lost their nucleus [1002]; the chloroplasts of these cryptomonads are possibly derived from a rhodophyte, which encapsulated a prokaryote. Such multiple nestings are frequent [850]. The view of the eukaryotic cell as an integrated symbiontic community is taking ground [590]. An analysis of trophic interactions in a symbiosis has relevance for cellular biology in general. This motivates a more detailed discussion here.

The algal symbionts receive ammonia and carbon dioxide from the host and return lipids and glycerol [53,881], which supplement the prey taken by the host. The host can increase the inorganic carbon supply for the symbionts, using the enzyme carbonic anhydrase, which catalyses the interconversion of CO_2 to HCO_3^- [651]. This reduces the carbon dioxide concentration in the host and increases its uptake from the environment. The transfer of bicarbonate to the symbiont is coupled to the calcification process, $Ca^{2+} + 2\,HCO_3^- \rightarrow CaCO_3 + CO_2$, where the carbonate is precipitated by the host and the carbon dioxide is used by the symbiont, cf. {167}. Symbionts are also found to have heterotrophic abilities [881] for compounds that are likely to be formed during fermentation processes. In oligotrophic environments, hosts can increase production by one to two orders of magnitude, with the help of symbionts [364].

The stabilizing mechanism in the host–symbiont relationship is that the symbiont requires ammonia from the host for growth, and the host requires carbohydrates from the symbiont for *extra* growth that is allowed by food supply. The symbiont cannot grow if it supplies enough carbohydrates to the host to allow the host to use all the ammonia itself; the host generates ammonia, and the symbiont only receives the 'spoils' [364]. This priority in use is reciprocal, and also applies to carbohydrates.

Table 9.1: The chemical compounds of the symbiosis and their transformations and indices. The + signs mean appearance, the − signs disappearance. The signs of the mineral fluxes depend on the chemical indices and parameter values. The labels on rows and columns serve as indices to denote mass fluxes and powers. The table shows the flux matrix $\dot{\boldsymbol{J}}^T$, rather than $\dot{\boldsymbol{J}}$, if the signs are replaced by quantitative expressions presented in Table 9.2.

compounds →			minerals					org. comp.			host		symbiont	
↓ transformations			light	carbon dioxide	water	oxygen	ammonia	faeces	food	carbohydrate	structure	reserves	structure	reserves
			L	C	H	O	N	P	X	C_H	VH	EH	VS	ES
host	assim 1	A_1H		+	+	−	+	+	−			+		
	assim 2	A_2H		+	+	−	−			−		+		
	growth	GH		+	+	−	+				+	−		
	dissip	DH		+	+	−	+					−		
symb.	assim	AS	−	−	−	+	−			+				+
	growth	GS		+	+	−	+						+	−
	dissip	DS		+	+	−	+							−
	carbon	C		1				1	1	1	1	1	1	1
	hydrogen	H			2		3	n_{HP}	n_{HX}	2	n_{HVH}	n_{HEH}	n_{HVS}	n_{HES}
	oxygen	O		2	1	2		n_{OP}	n_{OX}	1	n_{OVH}	n_{OEH}	n_{OVS}	n_{OES}
	nitrogen	N					1	n_{NP}	n_{NX}		n_{NVH}	n_{NEH}	n_{NVS}	n_{NES}

A number of simplifying assumptions are made:

- Bicarbonate is included in CO_2, which in fact stands for inorganic carbon. The complex biochemistry of calcification is simplified to a proportionality with the CO_2 that is taken up from the environment. The reported coupling of coral calcification to nitrogen metabolism [186] is taken into account by the full assimilation process, which requires light, inorganic carbon as well as nitrogen.

- Nitrate is assumed not to be present in the environment; it can be included in the nitrogen flux to the symbiosis, if the (variable) nitrate/ammonium ratio is taken into account in the assimilation costs $y_{C_H,ES}$ and $y_{C_H,EH}$.

- Water and oxygen are non-limiting; the performance of the symbiosis is only affected by light, CO_2, ammonia and food. The composition of food is constant. Self shading is neglected; light is used proportional to the mass of symbiont, and independent of the surface area of the host.

- Each partner has only one reserve, so the state variables are M_{VH}, M_{EH}, M_{VS}, M_{ES}. The symbiont does not store nitrogen separately; this seems realistic due to lack vacuoles [752]. It, therefore, makes little sense to store carbohydrates as a separate reserve.

Table 9.2: The fluxes in a symbiosis between a heterotrophic isomorphic host H and an autotrophic V1-morphic symbiont S, which experiences the light flux $\dot{J}_{L,F}$, and the densities of inorganic carbon X_C, nitrogen X_N and food X. The reserves enter the fluxes via $m_{EH} = M_{EH}/M_{VH}$ and $m_{ES} = M_{ES}/M_{VS}$. The parameter M_{Vd} just serves as reference for M_{VH} to scale j_{EH,A_1Hm}, j_{N,A_2Hm}, j_{C,A_2Hm} and $\dot{k}_{EH}$.

$\dot{J}_{C,A_1H} = -\dot{J}_{X,A_1H} - \dot{J}_{P,A_1H} - \dot{J}_{EH,A_1H}$; $\dot{J}_{N,A_1H} = -n_{N,X}\dot{J}_{X,A_1H} - n_{N,P}\dot{J}_{P,A_1H} - n_{N,EH}\dot{J}_{EH,A_1H}$;
$\dot{J}_{P,A_1H} = y_{P,EH}\dot{J}_{EH,A_1H}$; $\dot{J}_{X,A_1H} = -y_{X,EH}\dot{J}_{EH,A_1H}$; $\dot{J}_{EH,A_1H} = \frac{j_{EH,A_1Hm}}{1+X_K/X}(M_{VH}/M_{Vd})^{2/3}$;
$\dot{J}_{N,F} = -\frac{j_{N,A_2Hm}}{1+X_{KN}/X_N}(M_{VH}/M_{V_d})^{2/3}$; $\dot{J}_{C,F} = -\frac{j_{C,A_2Hm}}{1+X_{KC}/X_C}(M_{VH}/M_{V_d})^{2/3}$;
$\dot{J}_{C,A_2H} = \dot{J}_{C_H,AS} - \dot{J}_{EH,A_2H}$; $\dot{J}_{N,A_2H} = -y_{N,EH}\dot{J}_{EH,A_2H}$; $\dot{J}_{C_H,A_2H} = -y_{C_H,EH}\dot{J}_{EH,A_2H}$;
$\dot{J}_{EH,A_2H} = \left((y_{EH,N}\dot{J}_{N,A_+H})^{-1} + (y_{EH,C_H}\dot{J}_{C_H,AS})^{-1} - (y_{EH,N}\dot{J}_{N,H} + y_{EH,C_H}\dot{J}_{C_H,AS})^{-1}\right)^{-1}$;
$\dot{J}_{N,A_+H} = \dot{J}_{N,A_1H} + \dot{J}_{N,GH} + \dot{J}_{N,DH} + (J_{N,+S})_+ - \dot{J}_{N,F}$; $\dot{J}_{N,+S} = \dot{J}_{N,AS} + \dot{J}_{N,GS} + \dot{J}_{N,DS}$;
$\dot{J}_{C,GH} = (y_{EH,VH} - 1)\dot{J}_{VH,GH}$; $\dot{J}_{N,GH} = (n_{N,EH}\, y_{EH,VH} - n_{N,VH})\dot{J}_{VH,GH}$;
$\dot{J}_{EH,GH} = -y_{EH,VH}\dot{J}_{VH,GH}$; $\dot{J}_{VH,GH} = M_{VH}\frac{(M_{Vd}/M_{VH})^{1/3}\dot{k}_{EH}m_{EH} - j_{EH,DH}/\kappa_H}{m_{EH}+y_{EH,VH}/\kappa_H}$;
$\dot{J}_{C,DH} = -\dot{J}_{EH,DH}$; $\dot{J}_{N,DH} = -n_{N,EH}\dot{J}_{EH,DH}$; $\dot{J}_{EH,DH} = -j_{EH,DH}M_{VH}$;

$\dot{J}_{C,AS} = -\dot{J}_{C_H,A_+S}$; $\dot{J}_{C,A_+S} = \dot{J}_{C,+H} + \dot{J}_{C,GS} + \dot{J}_{C,DS}$;
$\dot{J}_{C,+H} = -\dot{J}_{C,F} + \dot{J}_{C,A_1H} + \dot{J}_{C,A_2H} + \dot{J}_{C,GH} + \dot{J}_{C,DH}$;
$\dot{J}_{N,AS} = -n_{N,ES}\dot{J}_{ES,AS}$; $\dot{J}_{N,A_+S} = (\dot{J}_{N,+H})_+ + \dot{J}_{N,GS} + \dot{J}_{N,DS}$
$\dot{J}_{N,+H} = \dot{J}_{N,A_+H} + \dot{J}_{N,A_2H}$; $\dot{J}_{C_H,AS} = \dot{J}_{C_H,A_+S} - y_{C_H,ES}\dot{J}_{ES,AS}$;
$\dot{J}_{C_H,A_+S} = \left(\dot{J}_{C,A_+S}^{-1} + (y_{C_H,L}\dot{J}_{L,F})^{-1} - (\dot{J}_{C,A_+S} + y_{C_H,L}\dot{J}_{L,F})^{-1}\right)^{-1}$;
$\dot{J}_{ES,AS} = \left((y_{ES,N}\dot{J}_{N,A_+S})^{-1} + (y_{ES,C_H}\rho_{C_H}\dot{J}_{C_H,A_+S})^{-1} - (y_{ES,N}\dot{J}_{N,A_+S} + y_{ES,C_H}\rho_{C_H}\dot{J}_{C_H,A_+S})^{-1}\right)^{-1}$;
$\dot{J}_{C,GS} = (y_{ES,VS} - 1)\dot{J}_{VS,GS}$; $\dot{J}_{N,GS} = (n_{N,ES}\, y_{ES,VS} - n_{N,VS})\dot{J}_{VS,GS}$;
$\dot{J}_{ES,GS} = -y_{ES,VS}\dot{J}_{VS,GS}$; $\dot{J}_{VS,GS} = M_{VS}\frac{\dot{k}_{ES}m_{ES} - j_{ES,DS}}{m_{ES}+y_{ES,VS}}$;
$\dot{J}_{C,DS} = -\dot{J}_{ES,DS}$; $\dot{J}_{N,DS} = -n_{N,ES}\dot{J}_{ES,DS}$; $\dot{J}_{ES,DS} = -j_{ES,DS}M_{VS}$

- Both assimilation processes of the host are parallel; that from carbohydrates and ammonia is fast (these substrate fluxes already have upper boundaries).

- The binding probabilities of all substrates to the Synthesizing Units are taken to be close to one, except that of carbohydrate by the symbiont, which is possibly tunable by the host [229].

- The environment is treated as homogeneous. Flow regimes and diffusive boundary layers usually modify feeding and nutrient uptake [691].

Table 9.2 specifies the fluxes of 11 compounds as indicated in Table 9.1. The fluxes are determined by 19 parameters, and chemical indices, as functions of four enviromental variables: light, inorganic carbon, nitrogen and food. The symbiosis can live fully heterotrophic as well as fully autotrophic; as a consequence, it can take up significant amounts of inorganic nitrogen [691]. Figure 9.1 shows that calcification can enhance growth; its measured yearly maximum is 4 kg $CaCO_3$ $m^{-2}a^{-1}$, or 3–5 mm a^{-1} [864]; its daily maximum is three

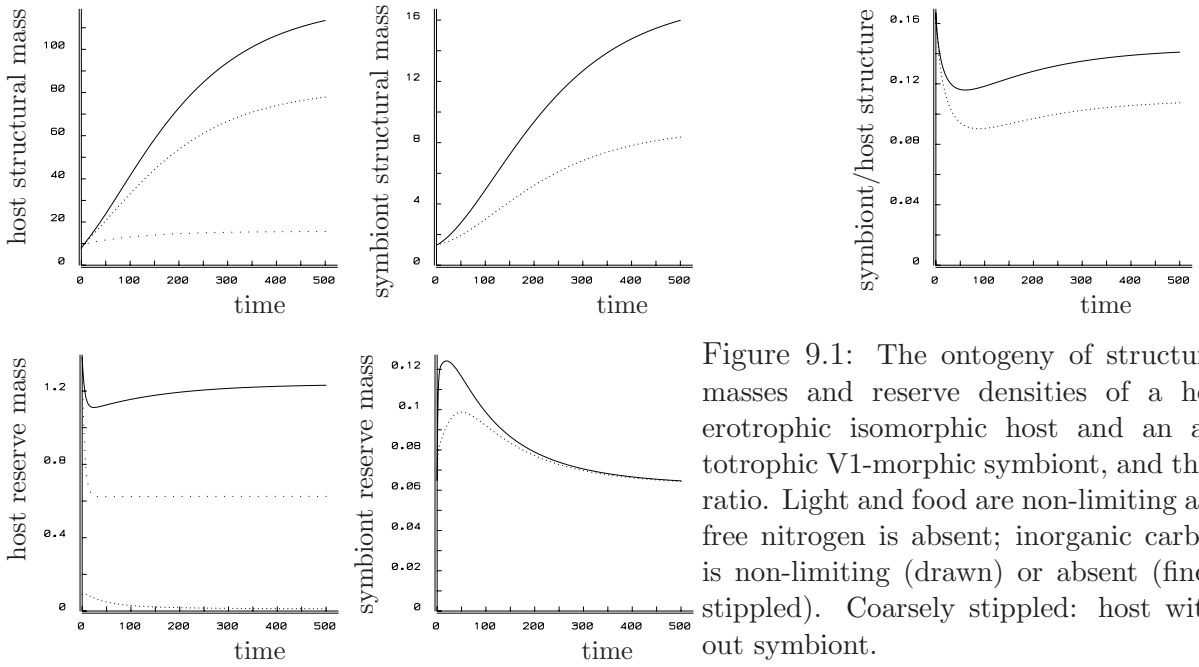

Figure 9.1: The ontogeny of structural masses and reserve densities of a heterotrophic isomorphic host and an autotrophic V1-morphic symbiont, and their ratio. Light and food are non-limiting and free nitrogen is absent; inorganic carbon is non-limiting (drawn) or absent (finely stippled). Coarsely stippled: host without symbiont.

times as high [863]. The chosen parameter values are just provisional; the figure only serves to illustrate the model structure.

Although the reproduction of the host has been taken into account by the parameter κ_H, the reproduction flux is not listed explicitly. The fluxes associated with assimilation A_2H and AS are given implicitly, and must be obtained numerically. This is hardly a handicap in practice, because a simple Newton Raphson procedure turns out to be converging rapidly starting from $\dot{J}_{C,A_2H} = \dot{J}_{N,A_2H} = 0$. The change in state is given by $\frac{d}{dt}\mathbf{M} = \dot{\boldsymbol{J}}\mathbf{1}$. The specification allows the following assertions

- The symbiont does not grow if

  $\dot{J}_{N,+S} = 0$, in which case $\dot{J}_{N,+H} = 0$ as well; all ammonia released in maintenance is used for assimilation; $\dot{J}_{N,+H} = 0$ if $\dot{J}_{N,A_+H} + \dot{J}_{N,A_2H} = 0$.

  $m_{ES} = j_{ES,DS}/\dot{k}_{ES}$; the reserves just cover the maintenance costs. Reserves do not change if $\dot{k}_{ES}M_{ES} = \dot{J}_{ES,AS}$; assimilation equals the catabolic rate.

- The host does not grow if $m_{EH} = \frac{j_{EH,DH}}{\kappa_H \dot{k}_{EH}} \left(\frac{M_{VH}}{M_{Vd}}\right)^{1/3}$; reserves do not change if $\dot{k}_{EH}(M_{Vd}/M_{VH})^{1/3}M_{EH} = \dot{J}_{EH,A_1H} + \dot{J}_{EH,A_2H}$.

- The ratio of the structural masses of symbiont and host does not change if their specific growth rates are equal, so if $j_{VS,GS} = j_{VH,GH}$.

- The flux ratio $\dot{J}_{EH,A_2H}(\dot{J}_{EH,A_1H} + \dot{J}_{EH,A_2H})^{-1}$ quantifies the photo- *versus* heterotrophic activity of the host. It is fully phototrophic if $\dot{J}_{X,F} = 0$. The host gains nothing from the symbiont if $\dot{J}_{C_H,AS} = 0$, or if $\dot{J}_{C_H,A_+S} = \dot{J}_{ES,AS}$. Muscatine *et al.* [650] proposed a related measure: the fractional contribution of translocated zooxanthellae C to animal daily respiratory C requirements CZAR $= \dot{J}_{C_H,AS}\dot{J}^{-1}_{C,+H}100\%$.

- The effect of calcification can be evaluated under the various feeding conditions ($\dot{J}_{L,F}$, $\dot{J}_{N,F}$ and $\dot{J}_{X,F}$) with the fraction $\frac{\dot{J}_{EH,A_1H}+\dot{J}_{EH,A_2H}\text{given } \dot{J}_{C,F}=0}{\dot{J}_{EH,A_1H}+\dot{J}_{EH,A_2H}\text{given } \dot{J}_{C,F}=-\infty}$.
- The host is of no use for the symbiont if it captures no prey, and competes with the symbiont for nitrogen.

Figure 9.1 reveals an important implication of the specification of fluxes in Table 9.2: the symbiont/host ratio of structural masses hardly varies. No other regulation seems to be required, other than trophic interactions. The host can tune the population of symbionts via the binding parameter ρ_{C_H} of carbohydrates to the assimilation SU of the symbiont.

The symbiosis can be simplified smoothly to a mixotroph with a single structure and reserve, by sacrificing the limited degree of freedom in composition. The explicit role of carbohydrates then disappears. A satisfactory description of the diurnal cycle requires separate carbohydrate and nitrogen reserves.

9.1.4 Biotrophy and parasitism

In a biotrophic relationship, the receiver lives off the host's body parts, without necessarily killing the host; it is a transition between a syntrophic and a predatory one. This definition includes most parasites, cows and excludes adult tapeworms (which are competitors). The pearlfish *Carapus* lives inside living sea cucumbers for shelter, where it feeds on the reproductive tissues. Many parasites, such as the avian schistosome *Trichobilharzia* which lives on the reproductive tissues of the pond snail *Lymnaea*, induce their host to increase its investment in growth, by increasing κ, cf. {87}; this, paradoxically, decreases short-term investment in reproduction, but increases the long-term investment via an increase in body size and so in feeding rate, cf. {295}. When the eggs are consumed a little further in their development, and are outside the body of the mother, as in the case of the snake *Dasypeltis* feeding on bird eggs, the relationship is usually called predatory, rather than parasitic. Parasites frequently have intimate metabolic and life history relationships with their host [163,781,994]. DNA sequencing reveals that the feared typhus bacterium *Rickettsia prowazekii* is the closest free-living relative of mitochondria [21], which are completely integrated into almost all eukaryotic cells [590].

9.1.5 Predation and saprotrophy

Although many heterotrophic species eat living prey individuals, most prey–predator models in ecology fail to recognize that the relationship is more complex than just the disappearance of prey individuals and the coupled production of predators. Predators usually have a strong preference for the less healthy prey individuals, and almost all predators are scavengers as well, i.e. they feed on dead biomass, which classifies them as saprotrophs. When a predator dies, a rich supply of substrates and nutrients becomes available in the form of its corpse, which directly or indirectly comes back to the prey. Accidental death or death from aging by the predator can be considered as maintenance-coupled substrate production processes at the population level. All organisms, therefore, have syntrophic

relationships with others at the population level. Predators also provide food for the prey via the release of nutrients (nitrogenous waste, faeces); if the prey happens to be algae or plants, the nutrients can be used directly, or these intermediate organisms will be directly or indirectly food for the prey. These indirect trophic relationships need to be included for a proper understanding of population dynamics.

Many carnivores have cannibalistic tendencies in periods of low prey abundance. This obviously reduces intra-species competition in the predator population, with more food available to the surviving individuals, while relieving the pressure on the prey. Cannibalism has a strong stabilizing effect on population dynamics. DEB models can be used to understand why dwarfs and giants can develop in cannibalistic populations [161].

Predation can also be beneficial to the prey, when ill individuals are preferred, and prey densities are kept low. This hampers the spreading of infectious diseases, which is frequently more devastating for the prey population than predation. Prey can develop intricate behavioural and physiological adaptations to avoid predation [839,964], and prey species that share a common predator can develop interrelationships [2].

9.2 Population dynamics

The significance of the population level for biological insight at all organization levels is manifold. It not only sets food availability and predation pressure for each individual, but it also defines the effect of all changes in life history, which is pertinent to evolutionary theory. All other individuals belong to the environment of the particular individual whose fitness is being judged. Fitness, whatever its detailed meaning, relates to the production of offspring, thus it changes the environment of the individual. This is one of the reasons why fitness arguments, which are central to evolutionary theories, should always involve the population level. Feeding on the same resource and being eaten are the major topics in population dynamics, but a real understanding requires analysis of all trophic interactions, as specified in the section on 'Canonical Communities', {352}.

Most models of population dynamics treat individuals as identical objects, so that a population is fully specified by its total number or total biomass. Such populations are called non-structured populations. This obviously leads to attractive simplicity; see e.g. Hastings [378] for an easy introduction. I discuss some doubts about their realism on {314}, doubts that can be removed by turning to structured populations. Structured populations are populations where the individuals differ from each other by one or more characteristics, such as age, which affect feeding, survival and/or reproduction. The DEB model provides an attractive, albeit somewhat complicated, structure. I will show the connection between non-structured and DEB-structured populations step by step.

V1-morphs have the unique property that they grow proportionally to their volume as individuals, which makes them an ideal paradigm for the connection between non-structured populations and structured ones. The definition of an individual is hard to make for V1-morphs and, in the DEB model, of no importance; it indeed makes no difference if the population consists of one single large V1-morph or many small ones. For isomorphs the situation is different, of course. The simplicity of non-structured population dynamics

comes with several unrealistic phenomena that have the potential to devalue any conclusion about real-world populations. I discuss some of them on {328}.

The introduction of a structure does not necessarily lead to realistic population models because of the effects of many environmental factors that typically operate at population level: spatial heterogeneity, seasonality, erratic weather, climatic changes, processes of adaptation and selection, subtle species interactions and so on. The occurrence of infectious diseases is perhaps one of the most common causes of decline and extinction of species, which typically operates in a density-dependent way. This means that population dynamics, as discussed in this chapter, still has to be embedded in a wider framework to arrive at realistic descriptions of population dynamics.

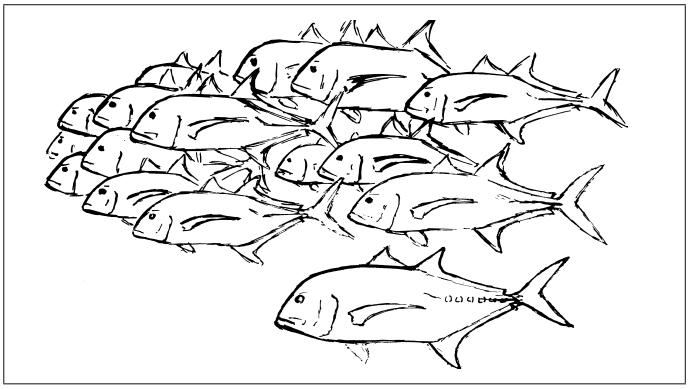

Spatial structure can profoundly modify population dynamics, as illustrated here for a compact school of fish, where only the individuals at the front actually feed, while the others starve and frequently interchange position with the individuals in the front. If the school increases its number of individuals, without changing shape, the feeding rate by the school is proportional to the number of individuals to the power 2/3 (based on the same argument as the DEB model uses for individuals), which implies that the feeding rate by the individual decreases for increasing numbers of individuals in the school. This is, however, not a proper population perspective, since this should include rules for the birth and death of schools; the school is here a 'super' individual.

The interaction between individuals of the same species is here restricted to feeding on the same resource. This point of view might seem a caricature in the eyes of a behavioural ecologist. The general idea, however, is not to produce population models that are as realistic as possible, but to study the consequences of feeding on the same resource. A comparison is then made with non-structured population dynamics and with real-world populations to determine the pay-off between realism and model complexity. If DEB-structured population dynamics predictions are not realistic, while the DEB model is at the individual level, this will give a key to factors that are important in this situation. The basic energetics and trophic interactions must be right before the significance of the more subtle factors can be understood. My fear is that most of the factors shown to be relevant will be specific for a particular species, a particular site and a particular period in time. This casts doubts on the extent to which general theory is applicable and on the feasibility of systems ecology. The main application of population dynamics theory here concerns a mental exercise pertaining to evolutionary theory, with less emphasis on direct testing in real-world populations. The theory should, however, be able to predict population behaviour in simplified environments, such as those found in laboratory setups, in bio-reactors and the like, so that it has potential practical applications.

9.2.1 Non-structured populations

The chemostat, a popular device in microbiological research, will be used to make the transition from the intensively studied non-structured populations to DEB-structured populations. In a chemostat, food (substrate) is supplied at a constant rate to a population, which is called a continuous culture. Food density in the inflowing medium is denoted by X_r and the medium is flowing through the chemostat at throughput rate $\dot{h}$ times the volume of the chemostat V_c. Together with the initial conditions (food and biomass density) these controls determine the behaviour of the system, in particular the food (substrate) density X_0 and the biomass density X_1 as functions of time. The index 0 in the notation for food density is added for reasons of symmetry with X_1: the biomass density of predators, i.e. the ratio of the sum of the individual masses and the volume of the chemostat, V_c. So $X_1 = \sum_{i=1}^{N} M_{Vi}/V_c$, if there are N individuals in the population. The reactor is assumed to be spatially homogenous, and is called a 'continuous flow stirred tank reactor' by engineers.

The chemostat as a model can also be realistic for particular situations outdoors [282, 301]. An important difference between chemostat models and many population dynamic models is that food (substrate) does not propagate in the formulation here, while exponential or logistic growth is the standard assumption in most literature [377,489,539,604]. I do not follow this standard, however, because I want to stick to mass and energy balance equations in a strict way. The growth rate of food should, therefore, depend on its resource levels, which should be modelled as well. In the section on food chains, {344}, higher trophic levels, X_2, $X_3 \cdots$ will be introduced, not lower ones.

Batch cultures, which do not have a supply of food other than that initially present, are a special case of chemostat cultures, where $\dot{h} = 0$. I start with the Lotka–Volterra model, which was and probably still is the standard prey–predator model in ecology. In a sequence of related models, the effect of the stepwise introduction of biological detail that leads to DEB-structured populations will be studied.

Lotka–Volterra

The Lotka–Volterra model assumes that the predation frequency is proportional to the encounter rate with prey (here substrate), on the basis of what is known as the law of mass action, i.e. the product of the densities of prey and predator. It can be thought of as a linear Taylor approximation of the hyperbolic functional response around food density 0: $f = (1+X_K/X_0)^{-1} \simeq X_0/X_K$ for $X_0 \ll X_K$. The ingestion rate is taken to be proportional to body volume, as is appropriate for V1-morphs, so that the sum of all ingestion rates by individuals in the population is found by adding the volumes of all individuals and applying the same proportionality constant.

The Lotka–Volterra model for chemostats with throughput rate $\dot{h}$ is

$$\frac{d}{dt}X_0 = \dot{h}X_r - j_{Xm}\frac{X_0}{X_K}X_1 - \dot{h}X_0 \tag{9.5}$$

$$\frac{d}{dt}X_1 = Yj_{Xm}\frac{X_0}{X_K}X_1 - \dot{h}X_1 \tag{9.6}$$

where Y stands for the yield factor, i.e. the conversion efficiency from prey to predator biomass; this is taken to be constant here. This model does not account for maintenance or energy reserves, so that in the context of the DEB model we have $Y = \kappa \frac{\mu_{AX}}{\mu_{GV}}$, with $[\dot{p}_M] = 0$ and $[E_m] = 0$. At the individual level, this model implicitly assumes that the feeding rate is proportional to the volume of the individual. This aspect corresponds with the V1-morph case of the DEB model. The analysis of the population dynamics can best be done with the dimensionless quantities $\tau \equiv t\dot{h}$, $\jmath_{Xm} \equiv j_{Xm}/\dot{h}$, $x_r \equiv X_r/X_K$, $x_0 \equiv X_0/X_K$, $x_1 \equiv X_1/X_K$. These substitutions turn (9.5) and (9.6) into

$$\frac{d}{d\tau}x_0 = x_r - \jmath_{Xm}x_0x_1 - x_0 \tag{9.7}$$

$$\frac{d}{d\tau}x_1 = Y\jmath_{Xm}x_0x_1 - x_1 \tag{9.8}$$

The equilibrium is found by solving x_0 and x_1 from $\frac{d}{d\tau}x_0 = \frac{d}{d\tau}x_1 = 0$. The positive solutions are $x_0^* = (Y\jmath_{Xm})^{-1}$ and $x_1^* = Yx_r - \jmath_{Xm}^{-1}$. The yield factor in this model has a double interpretation. It stands for the efficiency of converting food into biomass at both the individual and the population levels. To see this, one has to realize that food influx is at rate $\dot{h}X_Kx_r$ and food output is at rate $\dot{h}X_Kx_0^* = \frac{\dot{h}X_K}{Y\jmath_{Xm}}$ at equilibrium. So total food consumption is $\dot{h}X_K(x_r - \frac{1}{Y\jmath_{Xm}})$. Biomass output is $\dot{h}X_Kx_1^* = \dot{h}X_K(Yx_r - \jmath_{Xm}^{-1})$. The conversion efficiency at the population level thus amounts to $\frac{\dot{h}X_K(Yx_r - \jmath_{Xm}^{-1})}{\dot{h}X_K(x_r - (Y\jmath_{Xm})^{-1})} = Y$. This is so simple that it seems trivial. That this impression is false soon becomes obvious when we introduce more elements of the DEB machinery; the conversion efficiency at the population level then behaves differently from that at the individual level for non-V1-morphs.

The linear Taylor approximation around the equilibrium of the coupled system (9.7) and (9.8) equals for $\boldsymbol{x}^T \equiv (x_0, x_1)$ and $\boldsymbol{x}^{*T} \equiv (x_0^*, x_1^*)$

$$\frac{d}{d\tau}\boldsymbol{x} \simeq \begin{pmatrix} -\jmath_{Xm}x_1 - 1 & -\jmath_{Xm}x_0 \\ Y\jmath_{Xm}x_1 & Y\jmath_{Xm}x_0 - 1 \end{pmatrix}_{\boldsymbol{x}=\boldsymbol{x}^*} (\boldsymbol{x} - \boldsymbol{x}^*) \tag{9.9}$$

$$\simeq \begin{pmatrix} -Y\jmath_{Xm}x_r & -Y^{-1} \\ Y^2\jmath_{Xm}x_r - Y & 0 \end{pmatrix} \begin{pmatrix} x_0 - \frac{1}{Y\jmath_{Xm}} \\ x_1 - Y(x_r - \frac{1}{Y\jmath_{Xm}}) \end{pmatrix} \tag{9.10}$$

The eigenvalues of the matrix with coefficients, the Jacobian, are -1 and $-Y\jmath_{Xm}x_r + 1$, so that this system does not oscillate. See Edelstein-Keshet [248], and Yodzis [1025] for valuable introductions to this subject, and Hirsch and Smale [413], Ruelle [795], and Arrowsmith and Place [31,32] for more advanced texts. Mathematical texts on non-linear dynamics systems are now appearing at an overwhelming rate [65,232,352,445,917], especially with a focus on 'chaos'. Simple biological problems still seem too complex to analyse analytically, however, and one has to rely on numerical analyses. Figure 9.2 compares the dynamics of the Lotka–Volterra model with other simplifications of the DEB model.

Although this model cannot produce oscillations, with a minor change it can, by feeding the outflowing food (substrate) back into the bio-reactor. This is technically a simple operation. Most microbiologists even neglect the small outflow in open systems in their

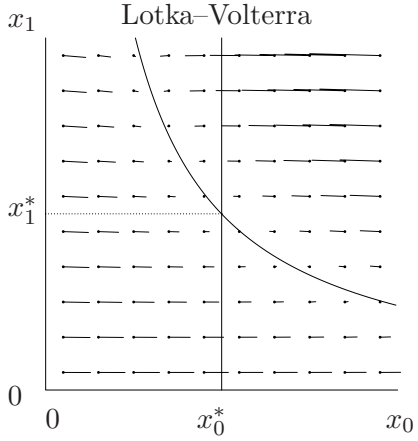

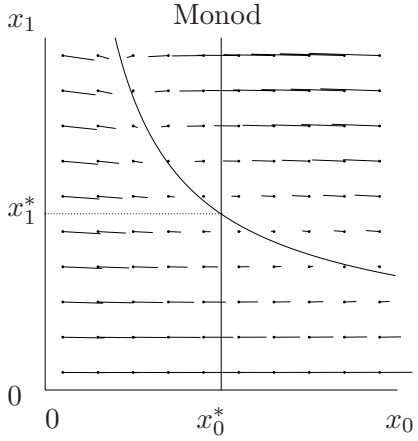

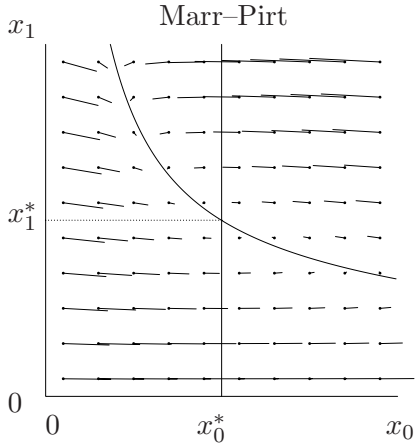

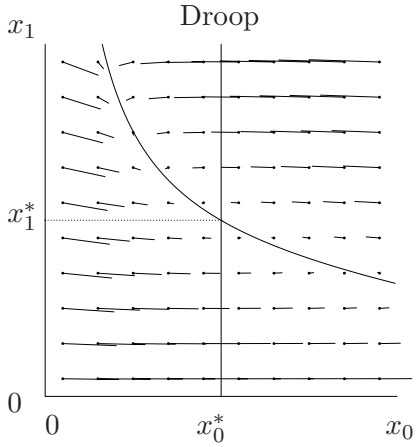

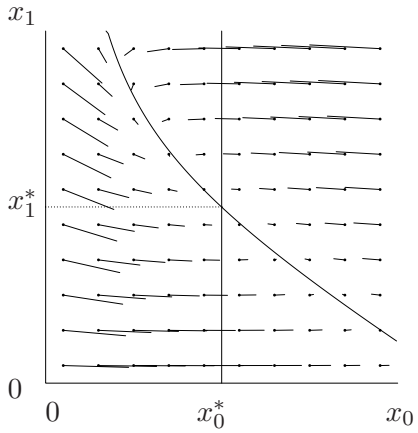

Equilibrium values for x_0 and x_1 and parameters

model	x_0^*	x_1^*	x_r	Y_g	$\jmath_{Xm}$	g	l_d
Lotka	0.39	8.17	10	0.85	3	-	-
Monod	0.65	7.95	10	0.85	3	-	-
Marr	0.97	6.12	10	0.85	3	-	0.1
Droop	1.82	4.23	10	0.85	3	1	-
DEB	4.25	2.37	10	0.85	3	1	0.1

Figure 9.2: The direction fields and isoclines for the DEB model for V1-morphs in a chemostat with reserves at equilibrium, and the various simplifications of this model. The lengths and directions of the line segments indicate the change in scaled food density x_0 and scaled biovolume x_1. The isoclines represent x_0, x_1-values where $\frac{d}{d\tau}x_0 = 0$ or $\frac{d}{d\tau}x_1 = 0$. All parameters and variables are made dimensionless, as indicated in the text. Figure 9.4 gives the direction field when the reserves are not in equilibrium.

mass balances. The situation is covered by deleting the third term in (9.7), i.e. $-x_0$. The eigenvalues of the Jacobian then become $-\frac{1}{2}Y_{\jmath Xm}x_r \pm \frac{1}{2}\sqrt{(Y_{\jmath Xm}x_r)^2 - 4Y_{\jmath Xm}x_r}$. For $Y_{\jmath Xm}x_r < 4$, the eigenvalues are complex, thus the system is oscillatory.

Monod, Marr–Pirt and Droop

If the hyperbolic functional response is used in the Lotka–Volterra model, rather than the linear Taylor approximation, we arrive with some reconstructions of the original formulations at the well-known model of Monod. Marr *et al.* [592] and Pirt [716] extended this model to account for maintenance, while Droop [234,236] extended it in another way to account for (nutrient) reserves. Maintenance or reserves have been introduced directly at the population level, however, which presents the problem of reconstructing the implicit assumptions at the individual level. This problem can most easily be solved with the DEB model for V1-morphs.

The energy reserve density follows the functional response according to a first-order process; see (3.14). So, if e_1 and e_2 denote the scaled energy density of two particular individuals, the difference decays exponentially with a relaxation time of $\dot{k}_E^{-1}$, because $\frac{d}{dt}(e_1 - e_2) = -\dot{k}_E(e_1 - e_2)$. Even if substrate density changes so rapidly that the energy reserve density is not at its equilibrium, and even if the initial energy densities of the individuals differ, the energy reserve densities of all individuals soon follow the same time-curve. It follows that $\frac{d}{dt}X_1 \propto \sum_i \frac{d}{dt}M_i \propto \frac{d}{dt}\sum_i M_i$. So the change of the sum of the masses equals the sum of the changes of each mass, which are simple functions of volumes in the DEB model for V1-morphs; see (3.38). The structured population of V1-morphs collapses to a non-structured one. In order to compare its dynamics with classic models, I now assume that the specific energy conductance is large enough with respect to changes of food density, $\frac{d}{dt}\ln X_0 \ll \dot{k}_E$, meaning that the energy reserves are close to their equilibrium value $e = f$. This condition will be removed in the subsection on DEB V1-morphs on {320}. The result is now that reconstructions of the models of Marr–Pirt, Droop and Monod are special cases of the DEB model for V1-morphs. It reads

$$\frac{d}{d\tau}x_0 = x_r - \jmath_{Xm} f x_1 - x_0 \tag{9.11}$$

$$\frac{d}{d\tau}x_1 = Y_{\jmath Xm} f x_1 - x_1 \tag{9.12}$$

with $f = (1+x_0^{-1})^{-1}$. The yield factor Y is only constant in the Monod model. The growth dynamics for V1-morphs, (3.38), can be used to show that the conversion efficiency equals

$[E_m]$ \ $[\dot{p}_M]$	0	$\neq 0$	0	$\neq 0$
0	Monod $\kappa\frac{\mu_{AX}}{\mu_{GV}}$	Marr–Pirt $\kappa\frac{\mu_{AX}}{\mu_{GV}}\frac{f-l_d}{f}$	Monod Y_g	Marr–Pirt $Y_g\frac{f-l_d}{f}$
$\neq 0$	Droop $\kappa\frac{\mu_{AX}}{\mu_{GV}}\frac{g}{f+g}$	DEB for V1s. $\kappa\frac{\mu_{AX}}{\mu_{GV}}\frac{g}{f}\frac{f-l_d}{f+g}$	Droop $Y_g\frac{g}{f+g}$	DEB for V1s. $Y_g\frac{g}{f}\frac{f-l_d}{f+g}$

In the microbiological literature, Y_g is known as the 'true' yield, i.e. the yield excluding maintenance losses. In the Lotka–Volterra and the Monod model, the (actual) yield equals the 'true' yield, $Y = Y_g$, but in the Marr–Pirt, Droop and DEB models we find that $Y < Y_g$ and that Y is a function of food density, while Y_g is a constant. The conversion from food into biomass cannot be constant for models allowing for maintenance; this is obvious if one realizes that maintenance has priority over growth. So if feeding conditions are poor, a larger fraction of the available energy is spent on maintenance, compared with good feeding conditions.

The biologically interesting equilibrium values x_0^* and x_1^* can easily be obtained from (9.11) and (9.12), but the result is line filling. The linear Taylor approximation in the equilibrium for the Monod case is:

$$\frac{d}{d\tau}\boldsymbol{x} \simeq \begin{pmatrix} -\frac{x_r+x_0^{*2}}{x_0^*+x_0^{*2}} & -\frac{1}{Y_g} \\ \frac{x_r-x_0^*}{\jmath_{Xm}x_0^{*2}} & 0 \end{pmatrix} (\boldsymbol{x}-\boldsymbol{x}^*) \tag{9.13}$$

The eigenvalues of the Jacobian are -1 and $-\frac{1}{Y_g\jmath_{Xm}}(x_r - \frac{1}{Y_g\jmath_{Xm}-1})(Y_g\jmath_{Xm}-1)^2$, so the system does not oscillate. The linear Taylor approximation of the functional response is accurate for small equilibrium values of food density, and thus a high value for $Y_g\jmath_{Xm}$, which means that the Monod and the Lotka–Volterra models for the chemostat are very similar. The Monod model has less tendency to oscillate than the Lotka–Volterra model. This becomes visible if the substrate is fed back to the bio-reactor. (Thus we omit the term $-x_0$ in (9.11).) Contrary to the Lotka–Volterra model, the eigenvalues of the Jacobian cannot become complex, so the system cannot oscillate.

Figure 9.2 gives the direction fields of the various simplifications of the DEB model and Figure 9.4 gives the direction field of the DEB model for V1-morphs in which energy reserves are allowed to deviate from their equilibrium values. The functional response in the equilibrium of the Monod model is only 0.4, for the chosen parameter values, which results in a close similarity with the Lotka–Volterra model. The direction fields of the Marr–Pirt and Droop models are rather similar, so the effects of introducting maintenance and reserves are more or less the same. When introduced simultaneously, as in the DEB model, the effect is enhanced. Note that the isocline $\frac{d}{d\tau}x_0 = 0$ hits the axis $x_1 = 0$ at $x_0 = x_r$, which is just outside the frame of the picture for the DEB model, but far outside for the Lotka–Volterra model. For very small initial values for x_0 and x_1, the direction fields show that x_0 will first increase very rapidly to x_r, without a significant increase of x_1, then the $\frac{d}{dt}x_0 = 0$-isocline is crossed and the equilibrium value x_0^*, x_1^* is approached with strongly decreasing speed. This means that x_0 falls back to a very small value for Lotka's model, but much less so for the DEB model. The most obvious difference between the models is in the equilibrium values, where $x_1^* \gg x_0^*$ in Lotka's model, but the reverse holds in the DEB model. The other models take an intermediate position. The approach of x_0, x_1 to the equilibrium value closely follows the $\frac{d}{dt}x_0 = 0$-isocline if $x_1 > x_1^*$ in all models. The speed in the neighbourhood of the isocline is much less than further away from the isocline, and the differences in speed are larger for Lotka's model than for the DEB model. These extreme differences in speed mean that the numerical integration of this type of differential equations needs special attention.

Death

The usefulness of the chemostat in microbiological research lies mainly in the continuous production of cells that are in a particular physiological state. This state depends on the dilution rate. In equilibrium situations, this rate is usually equated to the population growth rate. The implicit assumption being made is that cell death plays a minor role. As long as the dilution rate is high, this assumption is probably realistic, but if the dilution rate is low, its realism is doubtful. Low dilution rates go with low substrate densities and long inter-division intervals. In the section on aging {139}, the hazard rate for V1-morphs is tied to the respiration rate and so, indirectly, to substrate densities in (4.23). The law of large numbers states that the hazard rate can be interpreted as a mean (deterministic) death rate for large populations. The dynamics for the dead biovolume, $x_\dagger$ reads

$$\frac{d}{dt}x_\dagger = \dot{h}_a x_1 - \dot{h} x_\dagger \tag{9.14}$$

with $\dot{h}_a$ denoting the hazard rate. It can easily be seen that, in the equilibrium, we must have that $\dot{h} x_\dagger^* = \dot{h}_a x_1^*$, so the fraction of dead biovolume equals $\frac{x_\dagger^*}{x_1^*+x_\dagger^*} = \frac{\dot{h}_a}{\dot{h}+\dot{h}_a}$. The dynamics of the biomass should account for this loss, thus

$$\frac{d}{dt}x_1 = Y j_{Xm} f x_1 - (\dot{h} + \dot{h}_a) x_1 \tag{9.15}$$

Substitution of the expression for the hazard rate and the yield and the condition $\frac{d}{dt}x_1 = 0$ leads to the equilibrium value for f: $\frac{g(\dot{k}_M+\dot{h})}{\dot{k}_E-\dot{h}-\dot{h}_a(1+g)}$. Back-substitution into the hazard rate and the yield finally results in

$$\frac{x_\dagger^*}{x_1^*+x_\dagger^*} = \frac{\dot{k}_M + \dot{h}}{\dot{k}_M + (\dot{k}_M + \dot{r}_m^\circ)\dot{h}/\dot{h}_a} \tag{9.16}$$

where $\dot{r}_m^\circ = \frac{\dot{k}_E - \dot{k}_M g}{1+g}$ is the gross maximum population growth rate. (The net maximum population growth rate is $\dot{r}_m = \dot{r}_m^\circ - \dot{h}_a$ and $\dot{h} \leq \dot{h}_m \leq \dot{r}_m \leq \dot{r}_m^\circ$. The maximum throughput rate is $\dot{h}_m = \frac{\dot{k}_E - \dot{h}_a(1+g) - g\dot{k}_M(1+X_K/X_r)}{1+g(1+X_K/X_r)}$. Since most microbiological literature does not account for death, and saturation coefficients are usually small, these different maximum rates are usually not distinguished. The concept 'population growth rate' is introduced on {323}.) Figure 9.3 illustrates how the dead fraction depends on the population growth rate.

The significance of the fraction of dead cells is not only of academic interest. Since it is practically impossible to distinguish the living from the dead, it can be used to 'correct' the measured biomass for the dead fraction to obtain the living biomass.

In the section on aging, {139}, I speculate that prokaryotes might not die instantaneously, but first switch to a physiological state called 'stringent response'. The fraction (9.16) can then be interpreted as the fraction of individuals that is in the stringent response. A typical difference between both types of cells is the intracellular concentration of Guanosine 4-phosphate (ppGpp), which is usually expressed per gram of total biomass.

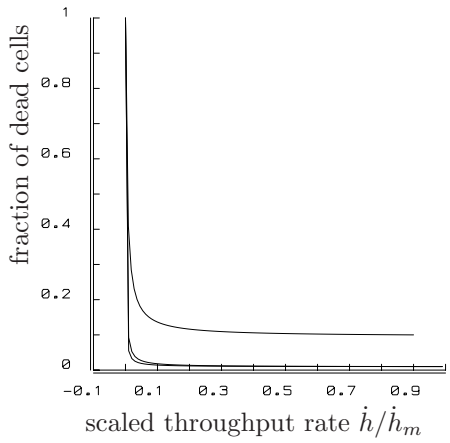

Figure 9.3: The fraction of dead cells depends hyperbolically on the population growth rate, and increases sharply for decreasing population growth rates. The three curves correspond with $\dot{k}_M/\dot{r}_m = 0.05$, $\dot{h}_a/\dot{r}_m = 0.01$ (lower), $\dot{k}_M/\dot{r}_m = 0.1$, $\dot{h}_a/\dot{r}_m = 0.01$ (middle) and $\dot{k}_M/\dot{r}_m = 0.05$, $\dot{h}_a/\dot{r}_m = 0.1$ (upper curve). For high growth rates, the dead fraction is close to $\dot{h}_a/\dot{r}_m$, which will be very small in practice. The curves make it clear that experimental conditions are extremely hard to standardize at low growth rates.

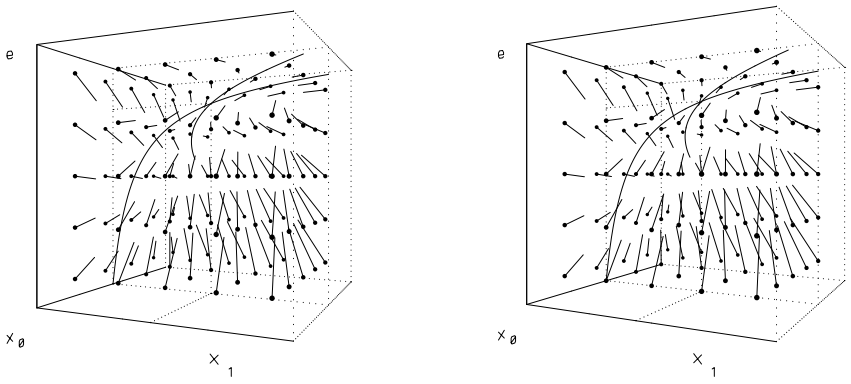

Figure 9.4: Stereo view of the direction field and isoclines for the DEB model for V1-morphs in a chemostat. The parameter values are the same as in Figure 9.2 and the projection of this direction field on the x, y-plane reduces to the direction field given in Figure 9.2, where the reserves are set at equilibrium.

This quantification implicitly assumes that all cells in the population behave in the same way physiologically, and not that the population can be partitioned into cells that are in the stringent response and those that are not. It remains to be determined which presentation is the more realistic.

Reserves and expo-logistic growth

The full DEB model for V1-morphs in chemostats is in need of an auxiliary equation for energy reserves, which amounts to the following three coupled equations

$$\frac{d}{d\tau}x_0 = x_r - \jmath_{Xm} f x_1 - x_0 \tag{9.17}$$

$$\frac{d}{d\tau}e = Y_g \jmath_{Xm} g(f - e) \tag{9.18}$$

$$\frac{d}{d\tau}x_1 = Y_g \jmath_{Xm} g \frac{e - l_d}{e + g} x_1 - x_1 - h_a \frac{1 + g}{e + g} e x_1 \tag{9.19}$$

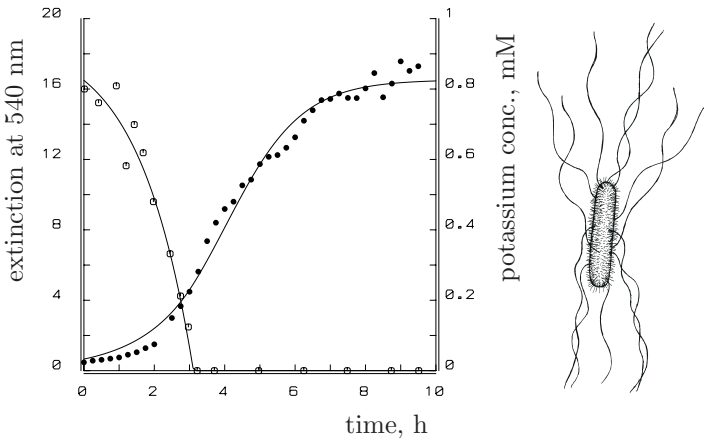

Figure 9.5: The potassium-limited growth of *E. coli* at 30 °C. Data from Mulder [646]. The expo-logistic growth is fully from reserves when potassium is depleted from the environment. Parameters for biomass in dimensionless extinction units: initial potassium concentration $X_0(0) = 0.825$ mM, initial biomass $x_1(0) = 0.657$, maximum specific uptake rate $j_{Xm} = 0.125$ mM h^{-1}, investment ratio $g = 0.426$, reserve turnover $\dot{k}_E = 0.925$ h^{-1}.

These coupled equations can be reduced to one integro-differential equation by integration of $\frac{d}{d\tau}e$ and $\frac{d}{d\tau}x_1$, and substitution of the results into the differential equation for x_0. This is of little help, however, because this equation also has to be solved numerically.

The direction field of this model is given in Figure 9.4. Mortality is excluded, $\dot{h}_a = 0$, to facilitate comparison with the situation where reserves are in equilibrium; see Figure 9.2.

A special case of conceptual interest can be solved analytically. This case relates to batch cultures, where no input or output (of substrate or biomass) exists, and the biomass just develops on the substrate that is present at the start of the experiment. If the saturation coefficient, the maintenance costs and aging rate are small, DEB V1-morphs will grow in a pattern that might be called expo-logistic. Initially they will grow exponentially and after a certain time (which corresponds to the depletion of the substrate) they switch to logistic growth, depleting their reserves. The biomass–time curve is smooth, even at the transition from one mode of growth to the other.

Worked out quantitatively, we get the following results. The functional response f is initially 1, since X_K is small with respect to X_0. If the inoculum is from a culture that has not suffered from substrate depletion, we have $e = 1$ and $X_1(t) = X_1(0)\exp\{\dot{r}_m t\}$, so the population growth rate is maximal, i.e. $\dot{r}_m = (\dot{k}_E - \dot{k}_M g)(1+g)^{-1}$. The substrate concentration develops as $X_0(t) = X_0(0) - \int_0^t j_{Xm} X_1(t_1)\,dt_1$. It becomes depleted at t_0, say, where $X_0(t_0) = 0$. Substitution gives

$$X_0(t) = X_0(0)(\exp\{\dot{r}_m t_0\} - \exp\{\dot{r}_m t\})(\exp\{\dot{r}_m t_0\} - 1)^{-1}$$

where depletion occurs at time $t_0 = \frac{1}{\dot{r}_m} \ln\left\{1 + \frac{X_0(0)}{X_1(0)} \frac{\dot{r}_m}{j_{Xm}}\right\}$. The reserves then decrease exponentially, i.e. $e(t_0 + t) = \exp\{-\dot{k}_E t\}$. The biovolume thus behaves as $X_1(t_0 + t) = X_1(t_0) \exp\left\{\int_0^t \frac{\dot{k}_E e(t_0+t_1) - \dot{k}_M g}{e(t_0+t_1)+g}\,dt_1\right\}$. For small maintenance costs, $\dot{k}_M \to 0$, this reduces to $X_1(t_0 + t) = X_1(t_0)\frac{1+g}{\exp\{-\dot{k}_E t\}+g}$. This is the solution of the well-known logistic growth equation $\frac{d}{dt}X_1 = \dot{k}_E\left(1 - \frac{X_1(t)}{X_1(0)}\frac{g}{1+g}\right)X_1$, see Figure 9.5. The equation originates from Pearl

[695] in 1927. If the maintenance costs are not negligibly small, the integral for $X_1(t)$ has to be evaluated numerically. Biomass will first rise to a maximum and then collapse at a rate that depends on the maintenance costs. This behaviour offers the possibility to determine these costs experimentally. The quantitative evaluation can easily be extended to include fed-batch cultures for instance, which have food (substrate) input and no output of food or biomass, but this does involve numerical work.

Similar biovolume–time curves can also arise if the reserve capacity rather than the saturation coefficient is small. If maintenance and aging are negligible as before, the batch culture can be described by $\frac{d}{dt}X_0 = -j_{Xm}fX_1$ and $\frac{d}{dt}X_1 = Y_g j_{Xm} f X_1$. We must also have $X_1(t) = X_1(0) + Y_g(X_0(0) - X_0(t))$. Substitution and separation of variables gives

$$j_{Xm}Y_g t = \frac{X_K Y_g}{X_1(\infty)} \ln \frac{X_1(t)(X_1(\infty) - X_1(0))}{X_1(0)(X_1(\infty) - X_1(t))} + \frac{1}{2} \ln \frac{X_1(t)}{X_1(0)}$$

Although this expression looks very different from the corresponding one for small saturation coefficients, the numerical values are practically indistinguishable, as shown in Figure 9.6, where both population growth curves have been fitted to data on *Salmonella*. The only way to distinguish a difference is in the simultaneous fit for both biomass and substrate. This illustrates the rather fundamental problem of model identification for populations, even in such a simple case as this with only four free parameters. (To reduce the number of free parameters, maintenance and aging were taken to be negligible for both special cases.) Although *Salmonella* is a rod-shaped bacterium, it is treated here as a V1-morph because of its small aspect ratio; full treatment of rods is much more complicated, as shown later in this chapter. The conclusion to be drawn is that these data are not very informative and models for individual dynamics are soon too complicated to be of much help with the interpretation.

If other information is available to allow a choice between various possibilities, such as in the case of very efficient histidine uptake by deficient *Salmonella* strains, cf. {214}, the growth of batch cultures can be used to estimate the reserve capacity. This has been done in Figure 9.7 to illustrate that under particular circumstances, the DEB model implies mass fluxes, as discussed in more detail on {125}.

9.2.2 Structured populations

It is not my intention to review the rapidly growing literature on structured population dynamics, but, for those who are unfamiliar with the topic, some basic notions are introduced below to help develop intuition. See Heijmans [388], Metz and Diekmann [622], Łomnicki [566], Ebenman and Persson [246], DeAngelis and Gross [202], Tuljapurkar and Caswell [934], Gurney and Nisbet [355], and Cushing [189] for reviews of recent developments.

In unstructured models, all individuals are treated as identical, so their state (the i-state) is degenerated, and the population state (the p-state) is simply the number of individuals. This is different in structured models, where a population exists of individuals that differ in their i-state, and the p-state is defined as the frequency distribution of the

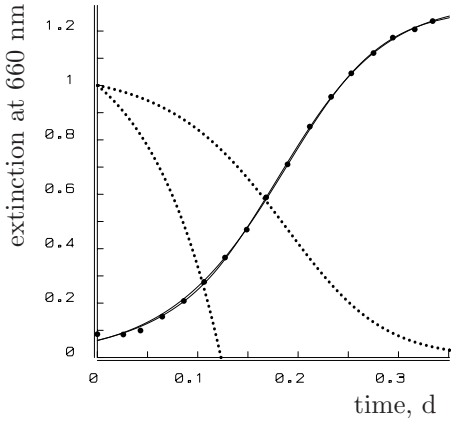

Figure 9.6: A batch culture of *Salmonella typhimurium* strain TA98 at 37 °C in Vogel and Bonner medium with glucose, (excess) histidine and biotin added. Two models have been fitted and plotted: one assumes that the saturation coefficient is negligibly small, but the reserves capacity is substantial, while the other does the opposite. Only the substrate density will tell the difference (stippled curves), but this is not measured. Parameters: $\dot{k}_E = 18.6$ (sd 0.37) d^{-1}, $g = 0.355$ (sd 0.063), $x_0(0)/j_{Xm} = 0.020$ (sd 0.0036) d or $x_1(\infty) = 1.28$ (sd 0.02), $Yx_K = 1.31$ (sd 0.86), $Yj_{Xm} = 23.6$ (sd 11.5).

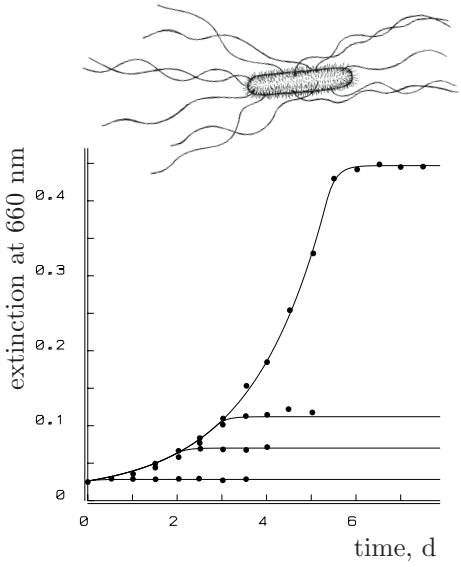

Figure 9.7: Batch cultures of a histidine-deficient strain of *S. typhimurium*, with initially only 0, 0.5, 1 or 5 μg histidine ml^{-1} in the medium, stop growing because of histidine depletion. The fit is based on the assumption of negligible maintenance requirements for histidine, which implies that the extinction plateau is a linear function of the added amount of histidine. The parameters are $j_{Xm} = 8$ (sd 0.44) $\mu\mathrm{g\,His\,ml^{-1}\,h^{-1}}$, $\dot{k}_E = 5.3$ (sd 1.2) h^{-1} and $g = 7.958$ (sd 0.00205). One extinction unit corresponds with 7.56×10^8 cells ml^{-1}, so that the yield is $Y_g = \frac{\dot{k}_E}{j_{Xm}g} = 0.0834$ ml μg His^{-1}. This corresponds with 1.1×10^{-10}g His cell^{-1} $= 3.15 \times 10^5$ molecules His cell^{-1} with a maximum of 4×10^4 molecules histidine in the reserve pool.

individuals over the i-state. Individuals with almost identical i-states are thus taken together in a cohort, and counted. I first consider a one-dimensional i-state (age), to illustrate the concept p-state. The significance of this particular i-state is that a multi-dimensional i-state can always be reduced to this one if the environment is constant (including food density).

Stable age distributions

If food density is constant or high (with respect to the saturation coefficient), the distribution of individual states in the population, such as age and volume, stabilizes, while the numbers grow exponentially. This distribution can be evaluated in a relatively simple way, which makes it possible to evaluate statistics such as the mean volume and its variance, mean life span, etc. Situations may occur where the individual states change cyclically, so that such a stable distribution does not exist. The distribution of individual states has a limited practical value, because it only holds at prolonged constant food densities. How

long food density must remain constant for state distributions to stabilize is hard to tell in specific cases and impossible in general. The main value of stable distributions lies in finding practical approximations for the behaviour of population models based on individuals. The derivation of stable state distributions is easiest when looking at the stable age distribution, which I will explain briefly. More extensive treatment is given by Frauenthal [295].

Let $\phi_N(a,t)\,da$ denote the number of females at time t aged somewhere in the interval $(a, a+da)$, where da is an infinitesimally small time increment. The total number of individuals is thus $N(t) = \int_0^\infty \phi_N(a,t)\,da$. Individuals that have age a at t must have been born at $t-a$ and must be still alive to be counted in N, so we have the recursive relationship $\phi_N(a,t) = \phi_N(0,t-a)\Pr\{\underline{a}_\dagger > a\}$, where $\phi_N(0,t)\,da$ denotes the number of births in $(t, t+da)$. The birth rate relates to the reproduction rate as $\phi_N(0,t) = \int_0^\infty \phi_N(a,t)\dot{R}(a)\,da$, where $\dot{R}(a)$ is the reproduction rate of an individual of age a. If we substitute the birth rate into the recursive relationship, we arrive at the integral equation

$$\phi_N(0,t) = \int_0^\infty \phi_N(0,t-a)\Pr\{\underline{a}_\dagger > a\}\dot{R}(a)\,da \tag{9.20}$$

Rather than specifying the number of births before the start of the observations at $t=0$, we specify the founder population $\phi_N(a,0) = \phi_0(a)$ and write

$$\phi_N(0,t-a) = \phi_0(a-t)/\Pr\{\underline{a}_\dagger > a-t\} \quad \text{for } a > t$$

The integral in (9.20) can now be partitioned and gives what is known as the renewal equation

$$\phi_N(0,t) = \int_0^t \phi_N(0,t-a)\Pr\{\underline{a}_\dagger > a\}\dot{R}(a)\,da + \int_t^\infty \frac{\Pr\{\underline{a}_\dagger > a\}}{\Pr\{\underline{a}_\dagger > a-t\}}\phi_0(a-t)\dot{R}(a)\,da \tag{9.21}$$

The second term thus relates to the contribution of the individuals that were present in the founder population. Depending on the survival probability and age-dependent reproduction rate, its importance decreases with time. Suppose that it is negligibly small at some time t_1 and that the solution of (9.21) is of the form $\phi_N(0,t) = \phi_N(0,0)\exp\{\dot{r}t\}$, for some value of $\dot{r}$ and $\phi_N(0,0)$. Substitution into (9.21) gives for $t > t_1$

$$\phi_N(0,0)\exp\{\dot{r}t\} = \int_0^{t_1} \phi_N(0,0)\exp\{\dot{r}(t-a)\}\Pr\{\underline{a}_\dagger > a\}\dot{R}(a)\,da \quad \text{or} \tag{9.22}$$

$$1 = \int_0^{t_1} \exp\{-\dot{r}a\}\Pr\{\underline{a}_\dagger > a\}\dot{R}(a)\,da \tag{9.23}$$

The latter equation is known as the characteristic equation. It is possible to show that, under some smoothness restrictions on reproduction as a function of age, this equation has exactly one real root for the population growth rate $\dot{r}_1$. The other roots are complex and have a real part smaller than $|\dot{r}_1|$. The general solution for $\phi_N(0,t)$ is a linear combination $\sum_i \phi_i(0,0)\exp\{\dot{r}_i t\}$. For large t, the exponential $\exp\{\dot{r}_1 t\}$ will be dominant, so the asymptotic solution will be $\phi_{N1}(0,0)\exp\{\dot{r}_1 t\}$; because the other roots are of little practical interest, the index will be dropped and $\dot{r}$ is thus taken to be the dominant root. The

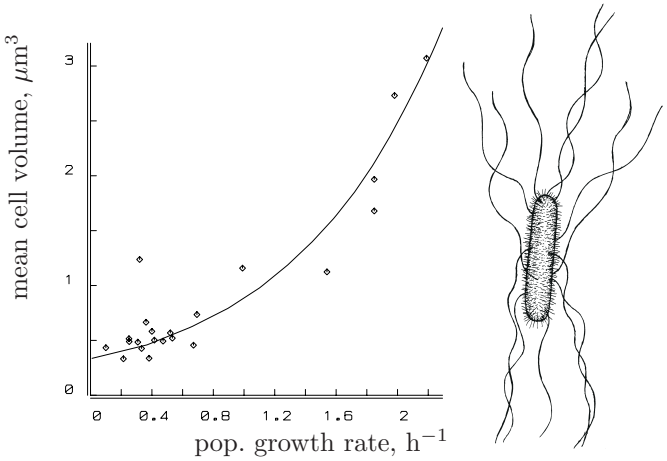

Figure 9.8: The mean volume of *E. coli* as a function of population growth rate at 37 °C. Data from Trueba [933]. For a chosen aspect ratio $\delta = 0.28$, a maintenance rate coefficient $\dot{k}_M = 0.05$ h^{-1} and an investment ratio $g = 1$, the least-squares estimates (with sd) of the volume at the start of DNA replication is $V_p = 0.454$ (sd 0.069) μm^3, the time required for division is $t_D = 1.03$ (sd 0.081) h and the energy conductance $\dot{v} = 31.3$ (sd 32) μm h^{-1}.

smoothness restrictions on $\dot{R}(a)$ are violated if, for instance, reproduction is only possible at certain ages. In this case, the information about the age distribution of the founder population is not lost.

The stable age distribution – i.e. the distribution of the ages of a randomly taken individual, $\underline{a}$ – is defined by $\phi_{\underline{a}}(a)\,da \equiv \phi_N(a,t)\,da/N(t)$ for $t \to \infty$. As before, we have for large t

$$\phi_N(a,t) = \phi_N(0,t-a)\Pr\{\underline{a}_\dagger > a\} = \phi_N(0,0)\exp\{\dot{r}(t-a)\}\Pr\{\underline{a}_\dagger > a\}$$

As $N(t) \equiv \int_0^\infty \phi_N(a,t)\,da$ serves only to normalize the distribution, we get the simple relationship between the age distribution and the survivor probability of the individuals

$$\phi_{\underline{a}}(a) = \frac{\exp\{-\dot{r}a\}\Pr\{\underline{a}_\dagger > a\}}{\int_0^\infty \exp\{-\dot{r}a_1\}\Pr\{\underline{a}_\dagger > a_1\}\,da_1} \tag{9.24}$$

Note that $\underline{a}$ is defined for the population level, while $\underline{a}_\dagger$ is the age at which a particular individual dies, so it is defined for the individual level. For a stable age distribution, the adage 'older and older, rarer and rarer' always holds. The mean age in the population is thus

$$\mathcal{E}\underline{a} = \int_0^\infty a\phi_{\underline{a}}(a)\,da = \frac{\int_0^\infty a\exp\{-\dot{r}a\}\Pr\{\underline{a}_\dagger > a\}\,da}{\int_0^\infty \exp\{-\dot{r}a\}\Pr\{\underline{a}_\dagger > a\}\,da} \tag{9.25}$$

Stable size distributions

Volume distribution is intimately related with the growth of dividing individuals, as has been widely recognized [167,216,375,593,956]. It can most easily be expressed in terms of its survivor function. If death plays a minor role, (9.24) gives the stable age distribution for $\Pr\{\underline{a}_\dagger > a\} = (a < a_d)$ with $a_d = \dot{r}^{-1}\ln 2$. For dividing individuals aged between 0 and a_d, the stable age distribution is given by $\phi_{\underline{a}}(a)\,da = 2\dot{r}\exp\{-\dot{r}a\}\,da = \frac{2\ln 2}{a_d}2^{-a/a_d}\,da$. For reproducing immortal individuals, the stable age distribution is $\phi_{\underline{a}}(a)\,da = \dot{r}\exp\{-\dot{r}a\}\,da$. The expected value of scaled length to the power i amounts to $\mathcal{E}\underline{l}^i = \int \phi_{\underline{a}}(a)l(a)^i\,da$.

The mean length increases less steeply with increasing substrate density or $\dot{r}$ than length at division, because the mean age reduces. Figure 9.8 shows that the mean volume of rods depends on population growth rate in the predicted way.

The survivor function of the stable age distribution is thus: $\Pr\{\underline{a} > a\} \equiv \int_a^{a_d} \phi_{\underline{a}}(a_1)\, da_1 = (a < \dot{r}^{-1} \ln 2)(2\exp\{-\dot{r}a\} - 1)$. The stable age distribution only exists at constant food densities, where volume increases if age increases. It was first derived by L. Euler in the eighteenth century [500]. The remarks on the need for scatter for stability of age distributions also apply to size distributions. See Diekmann *et al.* [214,215] for a more technical discussion.

If growth is deterministic and division occurs at a fixed size and the baby cells are of equal size, no stable age distribution exists. If there is some scatter in size at division, a stable age distribution exists, unless growth is exponential [66], because the information about the age distribution of the founder populations never gets lost. If sisters are not exactly the same size, a stable age distribution exists, even if growth is exponential. The age distribution has a weaker status, that of an eigenfunction: if the founder population has this particular age distribution, the age distribution will not change, while all other age distributions for the founder population will change cyclically with period a_d. In practice, however, scatter in growth rate and the size of baby cells will be more than sufficient for a rapid convergence to the stable age distribution.

The survivor function of the stable volume distribution is

$$\Pr\{\underline{V} > V\} = \Pr\{\underline{a} > t(V)\} = 2\exp\{-\dot{r}t(V)\} - 1 \quad \text{for } V \in (V_d/2, V_d]$$

where $t(V)$ is the age at which volume V is reached. The probability density is thus

$$\phi_{\underline{V}}(V)\, dV = (V \geq V_d/2)(V \leq V_d) 2\dot{r} \exp\{-\dot{r}t(V)\}\, dt \tag{9.26}$$

For isomorphs, $t(V)$ is given in (3.21). Since scaled length, l, has a monotonous relationship with volume; we have $\Pr\{\underline{l} > l\} = \Pr\{\underline{V} > V\}$. The survivor function of the stable length distribution for isomorphs that divide at scaled length l_d becomes

$$\Pr\{\underline{l} > l\} = 2^{1+\ln \frac{f-l}{f-l_b} / \ln \frac{f-l_b}{f-l_d}} - 1 \tag{9.27}$$

The same can be done for rods, which leads to

$$\Pr\{\underline{l} > l\} = 2^{\ln \frac{1-l_d/f}{(1-l_d/f-\delta/3)(l/l_d)^3+\delta/3} / \ln \frac{2(1-l_d/f)}{1-l_d/f+\delta/3}} - 1 \tag{9.28}$$

and for V1-morphs

$$\Pr\{\underline{l} > l\} = (l_1/l)^3 - 1 \tag{9.29}$$

These relationships can be important for testing assumptions about the growth process using the stable length distribution. Actual stable length distributions reveal that the scaled length at division, l_d, is not identical for all individuals, but has some scatter, which is close to a normal distribution [501]. It is assumed that the size-age curve does not depend on the size of the baby cell. As soon as a small baby cell has grown to the size of a larger baby cell, the rest of their growth curves are indistinguishable. Let $\phi_{\underline{V}_b}$ denote the probability density of the number of baby cells of volume V, i.e. cells of an age less than an arbitrarily small period Δt, and $\phi_{\underline{V}_d}$ the probability density of the number of mother cells of volume V, i.e. cells which will divide within the period Δt. A practical way to

determine $\phi_{\underline{V}_b}(V)\,dV$ and $\phi_{\underline{V}_d}(V)\,dV$ empirically is to make photographs at t and $t+\Delta t$ of the same group of cells and select cells that are divided at $t+\Delta t$, but not at t. The photograph at t can be used to obtain $\phi_{\underline{V}_d}(V)\,dV$ and that at $t+\Delta t$ to obtain $\phi_{\underline{V}_b}(V)\,dV$. When N denotes the total number of cells in the population, the number of cells with a volume in the interval $(V, V+dV)$ is $N\phi_{\underline{V}}(V)\,dV$. Painter and Marr [685] argued that the change in this number is given by

$$\frac{d}{dt}N\phi_{\underline{V}} = 2\frac{d}{dt}N\phi_{\underline{V}_b} - \frac{d}{dt}N\phi_{\underline{V}_d} - N\frac{\partial}{\partial V}\left(\phi_{\underline{V}}\frac{dV}{dt}\right) \tag{9.30}$$

The first term stands for the increase caused by birth, the second one for loss attributed to division and the third term for loss due to growth. Since the stable volume distributions do not depend on time and $\frac{d}{dt}N = \dot{r}N$, some rearrangement of terms gives

$$\frac{\partial}{\partial V}\left(\phi_{\underline{V}}\frac{dV}{dt}\right) = \dot{r}\left(2\phi_{\underline{V}_b} - \phi_{\underline{V}_d} - \phi_{\underline{V}}\right)$$

This is a linear inhomogeneous differential equation in $\phi_{\underline{V}}(V)$, with solution

$$\phi_{\underline{V}}(V) = \frac{dt}{dV}\dot{r}\exp\{-\dot{r}t(V)\}\int_{V_{\min}}^{V}\exp\{\dot{r}t(V_1)\}(2\phi_{\underline{V}_b}(V_1) - \phi_{\underline{V}_d}(V_1))\,dV_1 \tag{9.31}$$

where $V_{\min}$ is the smallest possible cell volume and, since $\phi_{\underline{V}}(V_{\max}) = 0$, $\dot{r}$ satisfies [956]

$$\int_{V_{\min}}^{V_{\max}}\exp\{\dot{r}t(V_1)\}(2\phi_{\underline{V}_b}(V_1) - \phi_{\underline{V}_d}(V_1))\,dV_1 = 0 \tag{9.32}$$

The connection with the previous deterministic rules for division can be made as follows. When mother cells divide into two equally sized baby cells, we have $\phi_{\underline{V}_b}(V) = 2\phi_{\underline{V}_d}(2V)$. So, $\phi_{\underline{V}_b}(V)\,dV = (V = V_d/2)$ and $\phi_{\underline{V}_d}(V)\,dV = (V = V_d)$ when division always occurs at V_d. Substitution into (9.31) gives (9.26) and into (9.32) gives $t_d^{-1}\ln 2$, as before. When division always occurs at V_d, so $\phi_{\underline{V}_d}(V)\,dV = (V = V_d)$, and the sizes of the baby cells are V_a and V_p, we have $\phi_{\underline{V}_b}(V)\,dV = (V = V_a)/2 + (V = V_p)/2$ with $V_a + V_p = V_d$ and $V_a < V_p$. Substitution into (9.31) gives

$$\phi_{\underline{V}}(V)\,dV = (V \geq V_a)(V \leq V_d)\dot{r}\exp\{\dot{r}(t(V_a) + t(V_p)(V \geq V_p) - t(V))\}\,dt$$

and substitution into (9.32) gives $1 = \exp\{-\dot{r}t_{da}\} + \exp\{-\dot{r}t_{dp}\}$.

Figure 9.9 gives the stable length distribution for *Escherichia coli*, together with the model fit with a log-normal distribution for the length at division. Since the curves approach the x-axis very closely for large cell lengths, the approximation $\dot{r} = t_d^{-1}\ln 2$ is appropriate. Although the goodness of fit is quite acceptable and only three parameters occur, the one relating to the growth process, V_∞, is not well fixed by the data. Again, the conclusion must be that this population response is consistent with what can be deduced from the individual level, but that the population behaviour gives poor access to that of individuals.

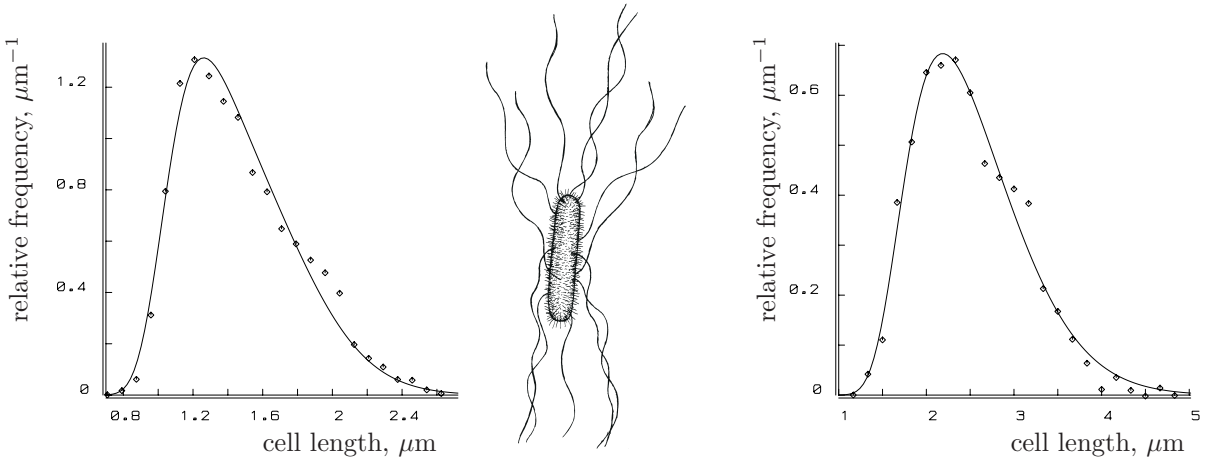

Figure 9.9: The probability density of the length of *E. coli* B/r A (left) and K (right) at a population growth rate of 0.38 and 0.42 h^{-1} respectively at 37 °C. Data from Koppes *et al.* [527]. For an aspect ratio of $\delta = 0.3$, the three parameters are $V_d = 0.506$ μm^3, $V_\infty = -0.001$ μm^3 and $\sigma^2 = 0.026$ and $V_d = 2.324$ μm^3, $V_\infty = -1$ μm^3 and $\sigma^2 = 0.044$. Because of the relatively large variance of the volume at division, these frequency distributions give poor access to the single parameter that relates to the growth process V_∞.

Reproducing neonates

There is no way to prevent neonates from giving rise to new neonates in unstructured populations. This artefact of the formulation can dominate population dynamics at lower growth rates. Comparison with a simple age-structured population, in which individuals reproduce at a constant rate after a certain age a_p, can illustrate this.

In a constant environment, any population grows exponentially given time, structured as well as non-structured. (Real populations will not do so because the environment will soon change because of food depletion.) Let $N(t)$ denote the number of individuals at time t. The numbers follow $N(t) = N(0)\exp\{\dot{r}t\}$, where the population growth rate $\dot{r}$ is found from the characteristic equation

$$1 = \int_0^\infty \Pr\{\underline{a}_\dagger > a\}\dot{R}(a)\exp\{-\dot{r}a\}\,da \tag{9.33}$$

Suppose that death plays a minor role, so $\Pr\{\underline{a}_\dagger > a\} \simeq 1$, and that reproduction is constant after age a_p, so $\dot{R}(a) = (a > a_p)\dot{R}$, where, with some abuse of notation, $\dot{R}$ in the right argument is taken to be a constant. Substitution into (9.33) gives

$$\exp\{-\dot{r}a_p\} = \dot{r}/\dot{R} \tag{9.34}$$

This equation ties the population growth rate $\dot{r}$ to the length of the juvenile period and the reproduction rate. It has to be evaluated numerically. For unstructured populations, where $a_p = 0$ must hold, the population growth rate equals the reproduction rate, $\dot{r} = \dot{R}$. For increasing a_p, $\dot{r}$ falls sharply; see Figure 9.10. This means that neonates giving birth to new neonates contribute significantly to unstructured populations.

Figure 9.10: For a constant reproduction rate $\dot{R}$ in the adult state, the population growth rate depends sensitively on the length of the juvenile period, as shown in the upper curve. The unit of time is $\dot{R}^{-1}$ and mortality is assumed to be negligible. The lower curve also accounts for the fact that individuals are discrete units of biomass. The required accumulation of reproductive effort to produce such discrete units reduces the population growth rate even further, especially for short juvenile periods. Note that the effect of food availability is not shown in this figure, because it only affects the chosen unit of time.

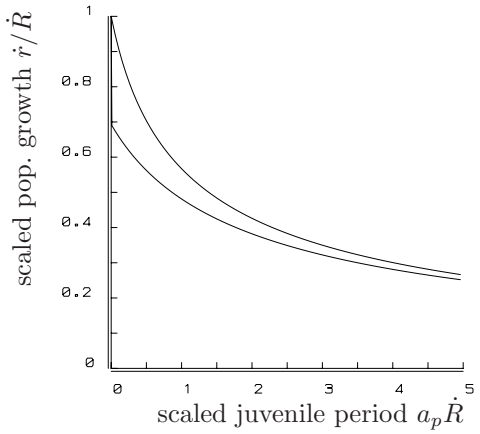

Discrete individuals

The formulation of the reproduction rate such as $\dot{R}(a) = (a > a_p)\dot{R}$ treats the number of individuals as a continuous variable. Obviously, this is unrealistic, because individuals are discrete units. It would be more appropriate to gradually fill a buffer with energy allocated to reproduction and convert it to a new individual as soon as enough energy has been accumulated. In that case, the reproduction rate becomes $\dot{R}(a) = (a = a_p + i/\dot{R})/da$, for $i = 1, 2, \cdots$. It is zero almost everywhere, but at regular time intervals it switches to ∞ over an infinitesimally small time interval da, such that the mean reproduction rate as an adult over a long period is $\dot{R}$ as before. Giving death a minor role, the characteristic equation becomes

$$1 = \sum_{i=1}^{\infty} \exp\{-\dot{r}(a_p + i/\dot{R})\} = \exp\{-\dot{r}/\dot{R} - \dot{r}a_p\} \left(1 - \exp\{-\dot{r}/\dot{R}\}\right)^{-1} \tag{9.35}$$

In analogy with (9.34) this can be re-written as

$$\exp\{-\dot{r}a_p\} = \exp\{\dot{r}/\dot{R}\} - 1 \tag{9.36}$$

to reveal the effect of individuals being discrete units rather than continuous flows of biomass; see Figure 9.10. The effect is most extreme for $a_p = 0$, where $\dot{r} = \dot{R}\ln 2$, which is a fraction of some 0.7 of the continuous biomass case. If young are not produced one by one, but in a litter, which requires longer accumulation times of energy, the discreteness effect is much larger. For a litter size n and a reproduction rate of $\dot{R}(a) = (a = a_p + in/\dot{R})n/da$, the population growth rate is $n^{-1}\ln\{1+n\}$ times the one for continuous biomass with the same mean reproduction rate and negligibly short juvenile period.

The effect of the discrete character of individuals is felt most strongly at low reproduction rates. Since populations tend to grow rapidly in situations where reproduction reduces sharply because of food limitation, this problem is rather fundamental. Reproduction, i.e. the conversion of the energy buffer into offspring, is usually triggered by independent factors (a two-day moulting cycle in daphnids, seasonal cycles in many other animals). If

reproduction is low, details of buffer handling become dominant for population dynamics. Energy that is not sufficient for conversion into the last young dominates population dynamics. Whether it gets lost or remains available for the next litter makes quite a difference and, unfortunately, we know little about what exactly does happen.

Population growth rates and division intervals

The relationship between the population growth rate and division interval can be obtained as follows. When the substrate density is constant for a sufficiently long period and death has little effect, the population of dividing individuals will grow exponentially at rate $\dot{r} = a_d^{-1} \ln 2$, where the division interval a_d tends to some fixed value at constant food densities. This relationship, which is well known in microbiology, is obvious if one realizes that, starting from a single, just divided, individual in an environment that has not changed over a long period, the development of the population in terms of cell numbers is given by $N(t) = 2^{t/a_d} = \exp\{\dot{r}t\}$ if the observations are done at $t = 0, a_d, 2a_d, \cdots$. Strictly, the development of cell numbers in continuous time is a step function. If we start from a large population rather than a single individual, the cell numbers will be close to $N(t) = N(0)2^{t/a_d} = N(0)\exp\{\dot{r}t\}$, but not exactly so, because of the deterministic nature of the growth and division process. This preserves information about the age distribution of the founder population, as explained on {325}. In practice more than enough scatter is found in almost all aspects of the growth and division process. We can, therefore, assume for practical purposes that information about the founder population rapidly fades, even without formulating these stochastic processes explicitly.

The relationship between population growth rate and the division interval can also be obtained from a formulation that allows for the production of neonates by letting the mother cell disappear at the moment of division, when two baby cells appear. Thus we write $\Pr\{\underline{a}_\dagger > a\} = (a \leq a_d)$ and $\dot{R}(a)\,da = 2(a = a_d)$. Substitution into the characteristic equation (9.33) gives $1 = 2\exp\{-\dot{r}a_d\}$.

The division interval a_d is given in (3.21), (3.40) or (3.43). Substitution gives the expressions for the population growth rates at constant substrate densities and for their relative values with respect to the maximum population growth rates, which are collected in Figure 9.11. The scaled length at division, l_d, is a function of f, because of the fixed period required to duplicate DNA. It has to be solved numerically from (3.54), but, for most practical purposes, it can probably be treated as a constant. For small aspect ratios, δ, the expressions for rods reduce to that for V1-morphs, while for an aspect ratio of $\delta = 0.6$ rods resemble isomorphs. The table in Figure 9.11 therefore illustrates how the population growth rate of dividing DEB isomorphs reduces stepwise to well known classic models. It also illustrates why many microbiologists do not like models that explicitly deal with substrate density; the saturation coefficient for uptake is usually very small for most combinations of micro-organisms and substrate types, and the saturation coefficient for population growth is even smaller, so that problems arise in measuring such low densities. Natural populations of micro-organisms tend either to grow at the maximum rate, or not to grow at all. This on/off behaviour is a major obstacle in the analysis of population dynamics.

Figure 9.11: The population growth rate $\dot{r}$ for dividing organisms as it simplifies when expressed as a fraction of its maximum $\dot{r}_m$ and small maintenance costs $[\dot{p}_M]$ and/or storage capacity $[E_m]$. The last three rows in the 'V1-morphs' column correspond to the models by Marr–Pirt, Droop and Monod. These models are graphically compared with the DEB model for V1-morphs in the figure below. The symbols l_1 and V_1 stand for l_d and V_d for $f = 1$.

	isomorphs	rods	V1-morphs
$\dot{r}$	$\frac{g\dot{k}_M}{f+g} \frac{\frac{1}{3}\ln 2}{\ln \frac{f-l_d 2^{-1/3}}{f-l_d}}$	$\frac{(1-\delta/3)f/l_d-1}{(f+g)/g\dot{k}_M} \frac{\ln 2}{\ln \frac{2(1-l_d/f)}{1-l_d/f+\delta/3}}$	$\frac{f/l_d-1}{(f+g)/g\dot{k}_M}$
$\frac{\dot{r}}{\dot{r}_m}$	$\frac{1+g}{f+g} \frac{\ln \frac{1-l_1 2^{-1/3}}{1-l_1}}{\ln \frac{f-l_d 2^{-1/3}}{f-l_d}}$	$\frac{1+g}{f+g} \frac{(1-\delta/3)f/l_d-1}{(1-\delta/3)/l_1-1} \frac{\ln \frac{2(1-l_1)}{1-l_1+\delta/3}}{\ln \frac{2(1-l_d/f)}{1-l_d/f+\delta/3}}$	$\frac{1+g}{f+g} \frac{f/l_d-1}{1/l_1-1}$
$\frac{\dot{r}}{\dot{r}_m}\Big\vert\, [E_m] \to 0$	$\frac{\ln \frac{1-l_1 2^{-1/3}}{1-l_1}}{\ln \frac{f-l_d 2^{-1/3}}{f-l_d}}$	$\frac{(1-\delta/3)f/l_d-1}{(1-\delta/3)/l_1-1} \frac{\ln \frac{2(1-l_1)}{1-l_1+\delta/3}}{\ln \frac{2(1-l_d/f)}{1-l_d/f+\delta/3}}$	$\frac{f/l_d-1}{1/l_1-1}$
$\frac{\dot{r}}{\dot{r}_m}\Big\vert\, [\dot{p}_M] \to 0$	$f\frac{1+g}{f+g}(\frac{V_1}{V_d})^{1/3}$	$f\frac{1+g}{f+g}(\frac{V_1}{V_d})^{1/3}$	$f\frac{1+g}{f+g}$
$\frac{\dot{r}}{\dot{r}_m}\Big\vert\, [E_m], [\dot{p}_M] \to 0$	$f(\frac{V_1}{V_d})^{1/3}$	$f(\frac{V_1}{V_d})^{1/3}$	f

In all models, Monod, Marr–Pirt, Droop and DEB, uptake as a fraction of its maximum depends hyperbolically on substrate density X as a fraction of the saturation coefficient X_K, as indicated by the thick curve. In the Monod model, $\dot{r} \propto \frac{x}{x+1}$, this curve coincides with the population growth rate $\dot{r}$ as a fraction of its maximum $\dot{r}_m$. The Marr–Pirt model, $\dot{r} \propto \frac{x-l_d/(1-l_d)}{x+1}$, which includes maintenance, has a translation to the right. The Droop model, $\dot{r} \propto \frac{x}{x+g/(1+g)}$, which includes storage, has a smaller saturation coefficient, whereas the DEB model for V1-morphs $\dot{r} \propto \frac{x-l_d/(1-l_d)}{x+g/(1+g)}$ has both. All four curves are hyperbolas with a horizontal asymptote of 1.

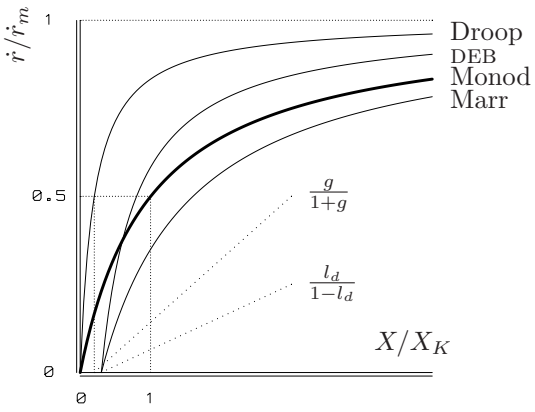

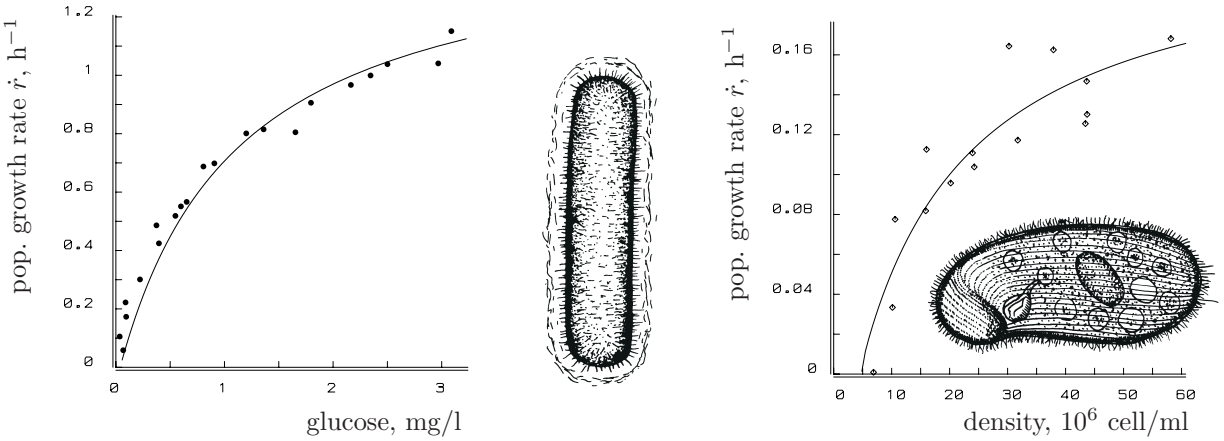

Figure 9.12: The population growth rate as a function of the concentration of substrate or food. The left figure concerns the rod *Klebsiella aerogenes* feeding on glucose at 35 °C. Data from Rutgers *et al.* [800]. The right figure concerns the isomorphic ciliate *Colpidium campylum* feeding on suspensions of *Enterobacter aerogenes* at 20 °C. Data from Taylor [910]. The functions are given in the table of Figure 9.11.

The population growth rate is plotted against the substrate concentration for the rods *Escherichia coli* and *Klebsiella aerogenes* in Figures 7.30 and 9.12, and for the isomorph *Colpidium* also in Figure 9.12. The curves closely resemble simple hyperbolic functions, which indicates that they contain little information about some of the parameter values of the individual-based DEB model, particularly the energy investment ratio g. Since the goodness of fit is quite acceptable, the modest conclusion can only be that these population responses give little reason to change assumptions about the energy behaviour of individuals. Figure 9.12 also illustrates that the scatter in population responses tends to increase dramatically with body size.

If propagation is via eggs, the population growth rate in constant environments has to be evaluated numerically from the characteristic equation (9.33).

Population structure

As long as food density remains constant and stable age distributions exist, it is possible to study most phenomena analytically, as illustrated in the preceding sections. For many purposes non-equilibrium situations should be considered, which requires computer simulation studies. Two strategies can be used to follow population dynamics: the family-tree method and the frequency method.

The family-tree method evaluates the changes of the state variables for each individual in the population at each time increment. For this purpose, the individuals are collected in a matrix, where each row represents an individual and each column the value of a state variable. At each time increment rows can be added and/or deleted and at regular time intervals population statistics, such as the total volume of individuals, are evaluated. The amount of required computer time is thus roughly proportional to the number of individuals in the population which must, therefore, be rather limited. This restricts the

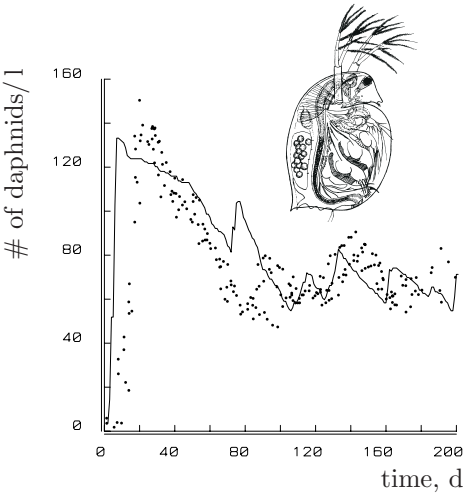

Figure 9.13: Computer simulation of a DEB-structured population of *Daphnia magna*, compared to a real laboratory population at 20 °C with a supply of 5×10^7 cells *Chlorella saccarophila* d^{-1}, starting from 5 individuals. Data from Fitsch [284]. The parameter values were obtained independently of the observations of individuals. Parameters:

$\{\dot{J}_{Xm}\}$	5×10^4 cells $\mathrm{mm}^{-2}\,\mathrm{h}^{-1}$	$g\dot{k}_M$	0.33 h^{-1}	g	0.033
X_K	3×10^5 cells ml^{-1}	l_b	0.133	l_p	0.417
$\ddot{h}_a$	1.1×10^{-6} h^{-2}	cv	0.5	κ_R	0.9

applicability of this method for analytical purposes, because at low numbers of individuals stochastic phenomena, such as those involved in survival, tend to dominate. The method is very flexible, however, which makes it easy to incorporate differences between individuals with respect to their parameter values. Such differences are realistic and appear to affect population dynamics substantially; see {335}. Kaiser [461,462] used the programming environment SIMULA successfully to study the population dynamics of individual dragon flies, mites and rotifers. Kreft *et al.* [531] simulated the spatial aspects of the individual-based population dynamics of bacteria.

The frequency method is based on bookkeeping in terms of (hyperbolic) partial differential equations. Several strategies exist to integrate these equations numerically. The method of the escalator boxcar train, perfected by de Roos [784,785], follows cohorts of individuals through the state space. The border of the state space where individuals appear at birth is partitioned into cells, which are allowed to collect a cohort of neonates for a specified time increment. The reduction of the number of individuals in the cohorts is followed for each time increment, as the cohort moves through the state space. The amount of computer time required is proportional to the number of cohorts, which relates to the volume of the state space as measured by the size of the cells. The number of cells must be chosen by trial and error. The escalator boxcar train is just one method of integrating the partial differential equation, but it appears to be an efficient one compared with methods that use a fixed partitioning of the state space into cells that transfer numbers of individuals among them.

A nasty problem of the (partial) differential equation approach to describe population dynamics is the continuity of the number of neonates if the reproduction rate is very small. This situation occurs in equilibrium situations, if the loss rate is small. The top predators especially are likely to experience very small loss rates. Details of the handling of energy reserves to produce or not produce a single young prove to have a substantial effect on population dynamics.

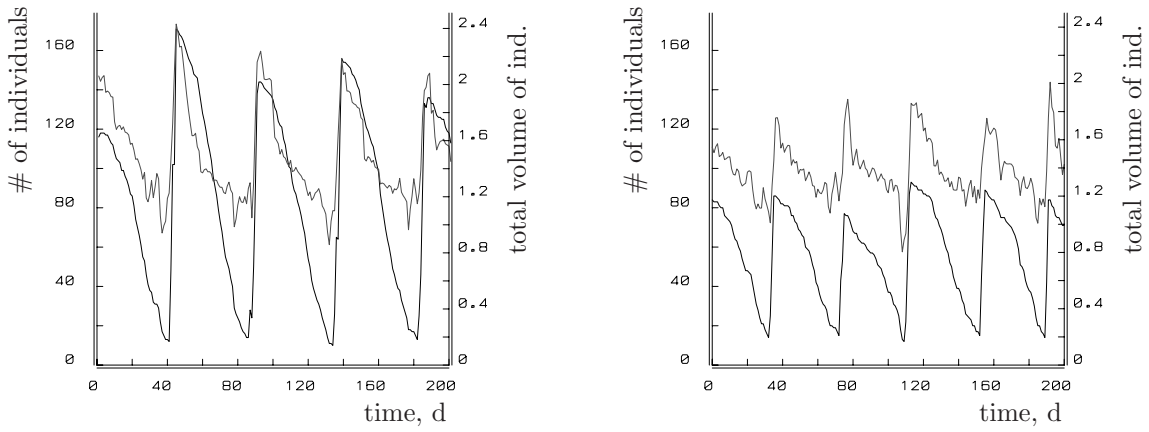

Figure 9.14: The number of individuals (black) and the total biovolume (grey) in a simulated batch culture of daphnids subjected to aging as the only method of harvesting. The individuals accumulate reproductive effort during the incubation time in the left figure, while they reproduce egg by egg in the right one. The parameters are $\dot{h}X_r = 7$ units d^{-1}, $l_b = 0.133$, $l_p = 0.417$, $\dot{J}_{Xm} = 4.99$ units d^{-1}, $\kappa = 0.3$, $\dot{k}_M = 10$ d^{-1}, $g = 0.033$, $\ddot{h}_a = 2.5 \times 10^{-5}$ d^{-2}.

Synchronization

Computer simulations of fed-batch cultures of reproducing isomorphs reveal a rather unexpected property of the DEB model. In these simulations the food supply to the population is taken to be constant and the population is harvested by the process of aging and in a random way. To reduce complicating factors as much as possible, only parthenogenetically reproducing females are considered, using realistic parameter values for *Daphnia magna* feeding on the green alga *Chlorella pyrenoidosa* at 20 °C. Reproduction in daphnids is coupled to moulting, which occurs every 2 to 3 days at 20 °C, irrespective of food availability. Just after moulting, the brood pouch is filled with eggs which hatch just before the next moult. So the intermoult period is beautifully adapted to the incubation time and the buffer for energy allocated to reproduction stays open during the intermoult period. These details are followed in the simulation study because many species produce clutches rather than single eggs.

Figure 9.14 shows a typical result of the population trajectory: the numbers oscillate substantially at low random harvesting rates. Closer inspection reveals that the shape of the number cycles closely follows the survival function of the aging process. The individuals appear to synchronize their life cycles, i.e. their ages, lengths and energy reserve densities, despite the fact that the founder population consists of widely different individuals. This synchronization is reinforced by the accumulation of reproductive effort in clutches, but it also occurs with single-egg reproduction. The path individuals take in their state space closely follows the no-growth condition. Growth in these populations can only occur via thinning by aging and the resultant amelioration of the food shortage. After reaching adult volumes, the individuals start to reproduce and mothers are soon outcompeted by their offspring, because they can survive at lower food densities. This has indeed been observed in experimental populations [339,913].

Table 9.3: Oscillations can affect crude population statistics. This table compares statistics for computer simulations, assuming that reproduction is by clutches, or by eggs laid one at a time, with statistics that assume the stable age distribution.

statistic	clutch	single-egg	stable age
mean scaled functional response, f	0.355	0.340	0.452
mean scaled biomass density, x	1.095	0.99	0.943
mean number of individuals, N	87.0	55.3	18.3
scaled yield coefficient, y	0.214	0.186	0.120

Having observed the synchronization of the individuals, it is not difficult to quantify population dynamics from an individual perspective when we now know that the scaled functional response cycles from $f = l_b$ to l_p. Starting from a maximum $N(0) = \frac{\dot{h}_p X_r g^2 \dot{k}_M^2}{\{\dot{J}_{Xm}\} l_b^3 \dot{v}^2}$ at time 0, the numbers drop according to $N(t) = N(0) \exp\{-\int_0^t \dot{h}(t_1)\, dt_1\}$, down to $N(t_n) = N(0)(l_b/l_p)^3$. The total biovolume is about constant at $X_1 = \frac{\dot{h}_p X_r V_m^{1/3}}{\kappa \{\dot{J}_{Xm}\}}$; see Table 9.3. At the brief period of take-over by the next generation, the population deviates a little from this regime. It is interesting to note that growth and reproduction are fully determined by the aging process in this situation. Length-at-age curves do not resemble the saturation curve that is characteristic of the von Bertalanffy growth curve; they are more or less exponential. Biovolume density and the yield are increased by the oscillatory dynamics, compared to expectation on the basis of the stable age distribution.

If the harvesting effort is increased, the population experiences higher food densities and the model details for growth and reproduction become important. The shape of the length-at-age curves switches from 'exponential' to von Bertalanffy, the cycle period shortens, the generations overlap for a longer period because competition between generations becomes less important, and the tendency to synchronize is reduced. All these changes result from the tendency of populations to grow and create situations of food shortage if the harvesting rates drop.

Similar synchronization phenomena are known for the bakers' yeast *Saccharomyces cerevisiae* [154,689]. It produces buds as soon the cell exceeds a certain size. This gives a synchronization mechanism that is closely related to that for *Daphnia*.

Variation between individuals

Although it is not unrealistic to have fluctuating populations at constant food input [855], the strong tendency of individuals to synchronize their life cycles seems to be unrealistic. Yet the model describes the input-output relationships of individuals rather accurately. A possible explanation is that at the population level some new phenomena play a role, such as slightly different parameter values for different individuals. This gives a stochasticity

of a different type than that of the aging process, which is effectively smoothed out by the law of large numbers. This way of introducing stochasticity seems attractive because the replicability of physiological measurements within one individual generally tends to be better than that between individuals. The exact source of variation in energy parameters, however, is far from obvious. This applies especially to parthenogenetically reproducing daphnids, where recombination is usually assumed not to occur. Hebert [384] however, has reported that (natural) populations of daphnids, which probably originate from a limited number of winter eggs, can have substantial genetic variation. Branta [110] was able to obtain a rapid response to selection in clones of daphnids, which could not be explained by the occurrence of spontaneous mutations. Cytoplasmic factors possibly play a much more important role in gene expression than is recognized at the moment. Koch [497] has discussed individual variability among bacteria.

In principle, it is possible to allow all parameters to scatter independently, but this seems neither feasible nor realistic. High ingestion rates, for instance, usually go with high assimilation rates and storage capacities. The parameter values of the DEB model for different species appear to be linked in a simple way, as discussed in the section on parameter variation {267}. We assume here that the parameters for the different individuals within a species are also linked in this way but vary within a narrow range. The parameters for a particular individual remain constant during its lifetime. In this way, we require only one simple individual-specific multiplier operating on (some of) the original parameters of the DEB model to produce the scatter. The way the scatter appears in the scaled parameters is even simpler [522].

Parameter variation between individuals has interesting effects on population dynamics: a log-normally distributed scatter with even a small coefficient of variation is enough to prevent death by starvation at the take-over of the new generation. Moreover, each generation becomes extinct only halfway through the period of the next generation and the amplitude of the population oscillations is significantly reduced; see Figure 9.14. This may be quantified by its effect on the coefficient of variation for population measures, defined as

$$c_j = \left(\frac{1}{t_n} \int_0^{t_n} \sum_i l_i^j(t)\, dt \right)^{-1} \sqrt{\frac{1}{t_n} \int_0^{t_n} \left(\sum_i l_i^j(t) - \frac{1}{t_n} \int_0^{t_n} \sum_i l_i^j(t_1)\, dt_1 \right)^2 dt} \qquad (9.37)$$

for $j = 0, 1, 2, 3$. Integration is taken over one typical cycle of length t_n and the summation over all individuals in the population. For values larger than 0.2, the coefficient of variation of the scatter parameter barely depresses the variation coefficient of the population measures further; see Figure 9.15.

Figure 9.13 demonstrates that computer simulations of DEB-structured daphnids closely match the dynamics of laboratory populations. The strength of the argument is in the fact that the parameter values for individual performance have been obtained independently.

The oscillations are also likely to be less if one accounts for spatial heterogeneities. This is realistic even for daphnids, because some of the algae adhere to the walls of the vessels and some (but not all) daphnids feed on them [304,429]. The general features of the dynamics of experimental populations are well captured by the DEB model. Emphasis is

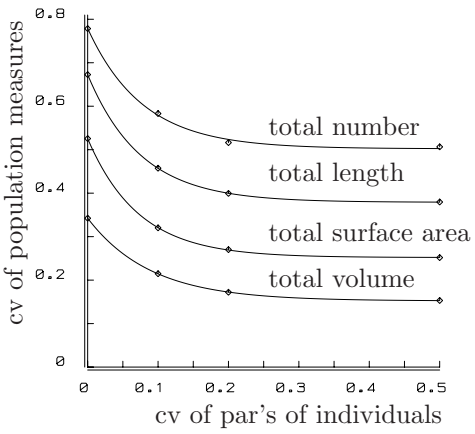

Figure 9.15: The coefficient of variation of the total number, length, surface area and volume of individuals in the population as functions of the coefficient of variation of the scatter parameter that operates on the parameters of individuals. The sharp initial reduction points to the limited realism of strictly deterministic models.

given to the competition for food, which Slobodkin [855] considered to be the only type of interaction operative in his experimental food-limited populations. He suggested that the competition between different age-size categories was responsible for the observed intrinsic oscillations, which is confirmed by this model analysis. Mrs N. van der Hoeven [419] has concluded, on the basis of a critical survey of the literature on experimental daphnid populations with constant food input, that some fluctuations are caused by external factors. Even populations that tend to stabilize do so, however, by way of a series of damped oscillations, while others seem to fluctuate permanently.

Adaptive dynamics

When parameter values for energy budgets vary among individuals, and rules about how the values carry over to new generations are formulated, selective forces are specified through competition for the same resources. Such selective forces need not be external, the DEB assumptions already imply these forces, namely how differences in feeding translate into differences in reproduction. These rules can obviously be modified as a result of interactions with other populations, such as predators, whose actions directly or indirectly relate to the parameter value of the individuals. Predators can select for particular body sizes, for instance, and body size is determined by DEB parameters. Given a specification of the environment in which the individuals live, the mean parameter values can evolve, and the (multivariate) frequency distribution can become multi-modal, reflecting the process of speciation. Many qualitative properties of this process can be evaluated, even without detailed specification of the models for individuals. This type of problem is called adaptive dynamics [213,318,624].

9.2.3 Mass transformation in populations

Mass fluxes in populations are the sum of the individual mass fluxes, but interactions between substrate and biomass densities through the processes of feeding and competition substantially complicate the conversion of substrate to biomass. The results for reproducers and dividers are discussed briefly in the following sections.

Propagation through reproduction

Let us consider a population of parthenogenetically reproducing individuals that develop through embryonic, juvenile and adult stages. Sexually reproducing animals can be included in a simple way, as long as the sex ratio is fixed. The population structure, derived from the collection of individuals that make up that population, is based on individual characteristics. Suppose that there is a maximum for the amount of structural body mass and reserves for individuals, and that we use the scaled length l, the scaled reserve density e and the age a to specify the state of the individual (the techniques to model the dynamics are readily available for an arbitrary number of state variables [360,361]).

Suppose that a population of individuals lives in a 'black box' and that the individuals only interact through competition for the same food resource. Food is supplied to the black box at a constant rate $\dot{h}_X M_X$, where $\dot{h}_X$ has dimension time^{-1} and M_X is the amount of food (in C-moles per black box volume). Eggs are removed from the black box at a rate $\dot{h}_e$; juveniles and adults are harvested at a rate $\dot{h}$ randomly, i.e. the harvesting process is independent of the state of the individuals (age a, reserves e, size l). Furthermore, the aging process harvests juveniles and adults at a state-dependent rate $\dot{h}_a$, which is beyond experimental control. Individuals harvested by the aging process leave the black box instantaneously.

The present purpose is to study how food supplied to the black box converts to body mass and reserves that leave the box in the form of harvested individuals, when the amounts of oxygen, carbon dioxide, nitrogenous waste and faeces in the black box are kept constant. This implies that these mass fluxes to and from the box equal the use or production by all individuals in the box. Food is not removed, which implies that the amount of food in the box depends on both the food supply and the harvesting rates of individuals.

Before analysing the conversion process in more detail, it is helpful to point out the fundamental difference between the population and the individual level. If no harvesting occurs at all, and food is supplied to the bio-reactor, the population will eventually grow to a size where food input just matches the maintenance needs of the individuals. In this situation no individual is able to grow or reproduce (otherwise we would not have a steady state). The conversion efficiency is then zero. Figure 9.16 illustrates this situation for experimental *Daphnia* populations. By increasing the harvesting rate, the conversion efficiency increases also, at least initially. This illustrates that the conversion process is controlled by the way the population is sandwiched between food input and harvesting. Individual energetics only set the constraints.

In many field situations, the harvesting rate will not be set intentionally. The process of aging can be considered, for instance, as one of the ways of harvesting through intrinsic causes, but this does not affect the principle. The present aim is to study the behaviour of the yield factor in steady-state situations, so $\dot{r} = 0$, and compare the different life styles: V1-morphs, rods and isomorphs, propagating via division and eggs. For this purpose, let us strip the population of as many details as possible and think of it in terms of the diagram given in Figure 9.17.

In summary, the conversion process has three control parameters, $\dot{h}_X$, $\dot{h}_e$ and $\dot{h}$, and the aim is now to evaluate all mass fluxes in terms of these three control parameters, given the

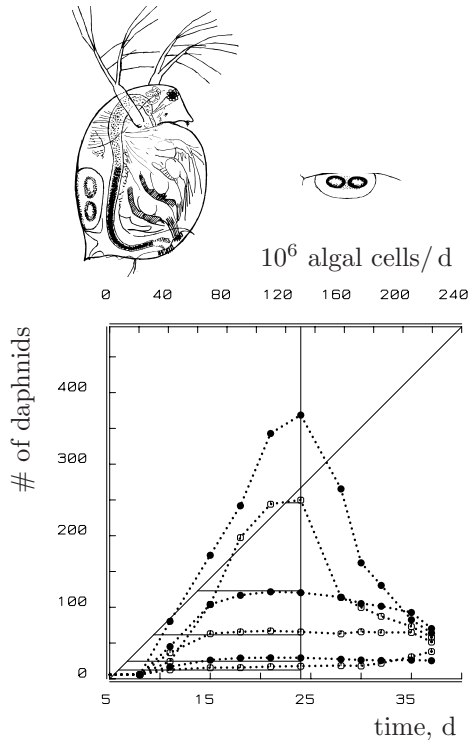

Figure 9.16: Populations of daphnids *Daphnia magna* fed a constant supply of food, the green alga *Chlorella pyrenoidosa* at 20 °C, grow to a maximum number of individuals that is directly proportional to food input [512]. From this experiment, it can be concluded that each individual requires six algal cells per second just for maintenance. No deaths occurred before day 24. A reduction of food input to 30×10^6 cells day^{-1} after day 24 resulted in almost instant death if the populations were at carrying capacity. The 240×10^6 cells day^{-1} population was still growing when the food supply was suddenly reduced, so the energy reserves were high, and it produced many winter eggs. The daily food supply related to the cumulated number of winter eggs as

240	120	60	30	12	6	10^6 cells d^{-1}
38	1	3	1	0	0	winter eggs

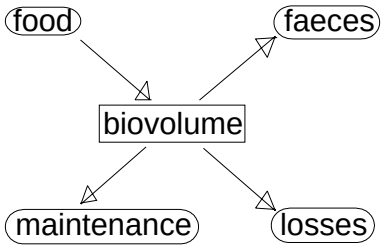

Figure 9.17: The population, quantified as the sum of the volumes of the individuals, converts food into faeces, while extracting energy. Part of this energy is lost in maintenance processes and part of it is deposited in losses, i.e. the cumulated harvest. The harvesting effort determines the allocation rules and sets the population size and so its impact on resources.

properties of the individuals. This result is of direct interest to particular biotechnological applications, and to the analysis of ecosystem behaviour, provided that the control parameters are appropriate functions of other populations and the degradation of faeces and dead individuals is specified to recycle the nutrients that are locked in these compounds.

The index + refers to the population, to distinguish fluxes at the population level from those at the individual level. Embryos are treated separately from juveniles and adults, not only because this allows different harvesting rates for both groups, but also because they do not eat, and therefore do not interact with the environment through food.

Given the initial conditions $\phi_e(0, a, e, l)$ and $\phi(0, a, e, l)$, the change in density of embryos and of juveniles plus adults over the state space is given by the McKendrick-von Foerster hyperbolic partial differential equation [289,849]

$$\begin{aligned} \frac{\partial}{\partial t}\phi_e(t,a,e,l) &= -\frac{\partial}{\partial l}\left(\phi_e(t,a,e,l)\frac{d}{dt}l\right) - \frac{\partial}{\partial e}\left(\phi_e(t,a,e,l)\frac{d}{dt}e\right) + \\ &\quad -\frac{\partial}{\partial a}\phi_e(t,a,e,l) - \dot{h}_e\phi_e(t,a,e,l) \end{aligned} \tag{9.38}$$

$$\frac{\partial}{\partial t}\phi(t,a,e,l) = -\frac{\partial}{\partial l}\left(\phi(t,a,e,l)\frac{d}{dt}l\right) - \frac{\partial}{\partial e}\left(\phi(t,a,e,l)\frac{d}{dt}e\right) + \\ -\frac{\partial}{\partial a}\phi(t,a,e,l) - (\dot{h}+\dot{h}_a(a,e,l))\phi(t,a,e,l) \tag{9.39}$$

where $\int_{a_1}^{a_2}\int_{l_1}^{l_2}\int_{e_1}^{e_2}\phi(t,a,e,l)\,de\,dl\,da$ is the number of individuals (juveniles plus adults) aged somewhere between a_1 and a_2, with a scaled energy density somewhere between e_1 and e_2 and a scaled length somewhere between l_1 and l_2. The total number of juveniles plus adults equals $N(t) = \int_0^\infty\int_{l_b}^1\int_0^1\phi(t,a,e,l)\,de\,dl\,da$. The total number of embryos likewise equals $N_e(t) = \int_0^\infty\int_0^{l_b}\int_0^\infty\phi_e(t,a,e,l)\,de\,dl\,da$. The boundary condition at $a=0$ reads

$$\phi_e(t,0,e_0,l)\frac{d}{dt}a = \delta(l=l_0)\int_0^\infty\int_{l_p}^1\dot{R}(e,l)\phi(t,a,e,l)\,dl\,da \quad \text{for all } e \tag{9.40}$$

where l_0 denotes the scaled length at $a=0$, which is taken to be infinitesimally small, l_b the scaled length at birth (i.e. the transition from embryo to juvenile), l_p the scaled length at puberty (i.e. the transition from juvenile to adult), and e_0 the scaled reserve at $a=0$, which can be a function of e of the mother. The function $\delta(l=l_0)$ is the Dirac delta function in l (dimension: l^{-1}). The boundary condition at $l=l_b$ reads

$$\phi(t,a,e,l_b)\frac{d}{dt}a = \phi_e(t,a,e,l_b)\frac{d}{dt}a \quad \text{for all } a,e \tag{9.41}$$

The individuals can differ at $a=0$, because e_0 can depend on e, and individuals can make state transitions at different ages and different scaled reserves. The dynamics for food amounts to

$$\frac{d}{dt}M_{X+} = \dot{h}_X M_X + \dot{J}_{X+} \tag{9.42}$$

$$\dot{J}_{X+} \equiv \int_0^\infty\int_{l_b}^1\int_0^1\phi(t,a,e,l)\dot{J}_X(e,l)\,de\,dl\,da \tag{9.43}$$

where M_{X+} denotes the food density in C-moles per black box volume, and $\dot{J}_X(e,l)$ the (negative) ingestion rate of an individual of scaled energy reserves e and scaled length l, as discussed in the previous section. The faecal flux $\dot{J}_{P+}$ is simply proportional to the ingestion flux, i.e. $\dot{J}_{P+}/\dot{J}_{X+} = \dot{J}_P/\dot{J}_X$.

The molar fluxes of body mass and reserves ($* = V, E$), are given by

$$\dot{J}_{*+} = \dot{h}_e\int_0^\infty\int_0^{l_b}\int_0^\infty\phi_e(t,a,e,l)M_*(e,l)\,de\,dl\,da + \tag{9.44}$$

$$+\int_0^\infty\int_{l_b}^1\int_0^1(\dot{h}+\dot{h}_a(a))\phi(t,a,e,l)M_*(e,l)\,de\,dl\,da \tag{9.45}$$

The mineral fluxes $\dot{\boldsymbol{J}}_{\mathcal{M}+}$ and the dissipating heat $\dot{p}_{T+}$ follow from (4.3) and (4.38)

$$\dot{\boldsymbol{J}}_{\mathcal{M}+} = -\boldsymbol{n}_{\mathcal{M}}^{-1}\boldsymbol{n}_{\mathcal{O}}\dot{\boldsymbol{J}}_{\mathcal{O}+} \tag{9.46}$$

$$0 = \dot{p}_{T+} + \boldsymbol{\mu}_{\mathcal{M}}^T\dot{\boldsymbol{J}}_{\mathcal{M}+} + \boldsymbol{\mu}_{\mathcal{O}}^T\dot{\boldsymbol{k}}_{\mathcal{O}+}. \tag{9.47}$$

Due to the linear relationships between mass and energy fluxes, the mass fluxes are simple metrics on the densities ϕ_e and ϕ, which are solutions of the partial differential equations (9.38) and (9.39); the determination of the solution generally requires numerical integration.

Steady-state situations

At steady state, the easiest approach is to relate the states of the individuals to age, and replace the density $\phi(t, a, e, l)$, by the relative density $\phi^\circ(t, a) = \phi(t, a)/N(t)$. This relative density no longer depends on time at steady state, so we omit the reference to time. $\dot{J}_*(a)$ denotes the flux of compound $*$ with respect to an individual of age a, where a_b is the age at birth and a_p the age at puberty. These ages might be parameters, but the DEB model obtains them from $M_V(a_b) = M_{Vb}$ and $M_V(a_p) = M_{Vp}$.

The characteristic equation applies at steady state

$$M_{E0} = \exp\{-\dot{h}_e a_b\} \int_{a_p}^{\infty} \exp\left\{-\dot{h}a - \int_0^a \dot{h}_a(a_1)\, da_1\right\} \dot{J}_{E_R}(a)\, da \tag{9.48}$$

The characteristic equation can be used to solve for the food density M_{X+}, and so the scaled functional response f. Given this food density, the trajectories of the state variables are fixed.

The age distributions of embryos and juveniles plus adults are given by

$$\phi_e^\circ(a) = \frac{\dot{h}_e \exp\{-\dot{h}_e a\}}{1 - \exp\{-\dot{h}_e a_b\}} \quad \text{for } a \in [0, a_b] \tag{9.49}$$

$$\phi^\circ(a) = \frac{(\dot{h} + \dot{h}_a(a)) \exp\{-\dot{h}a - \int_0^a \dot{h}_a(a_1)\, da_1\}}{\int_{a_b}^{\infty} \exp\{-\dot{h} - \int_0^a \dot{h}_a(a_1)\, da_1\}\, da} \quad \text{for } a \in [a_b, \infty) \tag{9.50}$$

We introduce the expectation operators $\mathcal{E}_e$ and $\mathcal{E}$, i.e. $\mathcal{E}_e Z \equiv \int_0^{a_b} Z(a)\phi_e^\circ(a)\, da$ and $\mathcal{E}Z \equiv \int_{a_b}^{\infty} Z(a)\phi^\circ(a)\, da$, for any function $Z(a)$ of age.

The harvesting rates of organic compounds equal their mass fluxes, i.e.

$$\dot{\boldsymbol{J}}_{\mathcal{O}+} \equiv \begin{pmatrix} \dot{J}_{X+} \\ \dot{J}_{V+} \\ \dot{J}_{E+} \\ \dot{J}_{P+} \end{pmatrix} = \boldsymbol{\eta} N \mathcal{E} \dot{\boldsymbol{p}} = \begin{pmatrix} -\dot{h}_X M_X \\ N_e \mathcal{E}_e \dot{h}_e M_V + N\mathcal{E}(\dot{h} + \dot{h}_a) M_V \\ N_e \mathcal{E}_e \dot{h}_e M_E + N\mathcal{E}(\dot{h} + \dot{h}_a) M_E \\ \dot{h}_X M_X \mu_{AX}/\mu_{AP} \end{pmatrix} \tag{9.51}$$

The numbers of juveniles plus adults in the population, N, and of embryos, N_e, are given by

$$N = \frac{\dot{J}_{X+}}{\mathcal{E}\dot{J}_X} \quad \text{and} \quad N_e = (1 - \exp\{-\dot{h}_e a_b\}) \frac{N\mathcal{E}\dot{J}_{E_R}}{\dot{h}_e M_{E0}}$$

Propagation through division

The aging rate of dividing organisms is taken to be independent of age and this hazard rate is included in the harvesting rate $\dot{h}$; the state variable age is not used, so the scaled

length l and the scaled reserve density e specify the state of the individual. The conversion process of substrate into biomass has two control parameters: $\dot{h}_X$ and $\dot{h}$.

Given the initial condition $\phi(0, e, l)$, the dynamics of density $\phi(t, e, l)$ is then given by

$$\frac{\partial}{\partial t}\phi(t,e,l) = -\frac{\partial}{\partial l}\left(\phi(t,e,l)\frac{d}{dt}l\right) - \frac{\partial}{\partial e}\left(\phi(t,e,l)\frac{d}{dt}e\right) - \dot{h}\phi(t,e,l) \tag{9.52}$$

with boundary condition

$$\phi(t,e,l_b)\left.\frac{d}{dt}l\right|_{l=l_b} = 2\phi(t,e,l_d)\left.\frac{d}{dt}l\right|_{l=l_d} \quad \text{for all } e \tag{9.53}$$

where the scaled length at 'birth' relates to the scaled length at division as $l_b = l_d 2^{-1/3}$. This dynamics implies that both daughters are identical.

Suppose now that the dynamics of the scaled reserves is independent of the scaled length, and that the dynamics of the scaled length is proportional to the scaled length. The scaled reserve density then has the property that all individuals will eventually have the same scaled reserve density, which may still vary with time. (The DEB model for V1-morphs is an example of such a model.) For simplicity's sake, we will assume that this also applies at $t = 0$, which removes the need for an individual structure. The consequence is that a population that consists of one giant individual behaves the same as a population of many small ones.

The partial differential equation (9.52) collapses to two ordinary differential equations, one of which is at the population level for the structural body mass

$$\frac{d}{dt}\ln M_{V+} = \frac{d}{dt}\ln l^3 - \dot{h} \tag{9.54}$$

where the scaled volume kinetics $\frac{d}{dt}l^3 = 3l^2\frac{d}{dt}l$ is given by the model for individuals. The other differential equation is at the individual level for the scaled reserve density kinetics $\frac{d}{dt}e$, which should also be specified by the model for individuals, see e.g. Table 3.6. The scaled reserve density kinetics specifies the (nutritional) state of a random individual.

The expressions for the dissipating heat (9.47), and mineral fluxes (9.46) still apply here, while $\dot{\boldsymbol{J}}_{\mathcal{O}+} = \boldsymbol{\eta}\dot{\boldsymbol{p}}_+$, with $\dot{\boldsymbol{p}}_+ = \int_{l_b}^{l_d}\int_0^1 \dot{\boldsymbol{p}}(e,l^3)\phi(t,e,l)\,de\,dl$, and $\dot{\boldsymbol{p}}(e,l^3)$ denotes $\dot{\boldsymbol{p}}$, evaluated at scaled energy reserve e and cubed scaled length l^3. (For V1-morphs it is more convenient to use l^3 as an argument, rather than l.) This result is direct because $\int_{l_b}^{l_d}\int_0^1 l^3\phi(t,e,l)\,de\,dl = M_{V+}/M_{Vm}$, so that

$$\dot{\boldsymbol{p}}_+ = \dot{\boldsymbol{p}}(e, \int_{l_b}^{l_d}\int_0^1 l^3\phi(t,e,l)\,de\,dl) = \dot{\boldsymbol{p}}(e, M_{V+}/M_{Vm}) = \dot{\boldsymbol{p}}(e,1)M_{V+}/M_{Vm}$$

The latter equality only holds for models such as the DEB model for 1S–V1-morphs, where all powers are proportional to structural body mass. The dynamics for food amounts to

$$\frac{d}{dt}M_{X+} = \dot{h}_X M_X + \dot{J}_{X+} = \dot{h}_X M_X - \frac{\dot{p}_A(e,1)}{\mu_{AX}}\frac{M_{V+}}{M_{Vm}} \tag{9.55}$$

where $\dot{p}_A(e,1)$ does not depend on the scaled reserves e, in the DEB model.

The environment for the population reduces to the chemostat conditions for the special choice of the harvesting rate $\dot{h}$ relative to the supply rate: $\dot{h}_X M_X = \dot{h}(M_X - M_{X+})$.

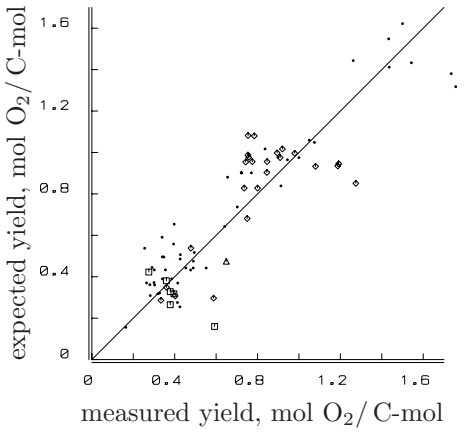

Figure 9.18: The expected molar yield of oxygen as a function of the measured value based on the assumption of a constant and common biomass composition of $n_{HW_1} = 1.8$, $n_{OW_1} = 0.5$ and $n_{NW_1} = 0.2$ for a wide variety of bacteria (•), yeasts (⋄), fungi (□) and the green alga *Chlorella* (△). The expectation is based on measured yields of biomass. Data gathered by Heijnen and Roels [391] from the literature on aerobic growth on a wide variety of substrates without product formation and NH_4^+ as nitrogen substrate.

Steady-state situations

The population growth rate must be zero at steady state. We use this to solve the value of the scaled functional response, i.e. $f = \frac{\dot{k}_M + \dot{h}}{\dot{k}_M/l_d - \dot{h}/g}$ in the case of the DEB model. This model has the nice property that $e = f$ at steady state; it then follows that $M_{X+} = M_K f/(1-f)$, where M_K is the saturation constant of the Holling type II functional response.

The stable age distribution amounts to

$$\phi^\circ(a) = 2\dot{h} \exp\{-\dot{h}a\} \quad \text{for } a \in [0, \dot{h}^{-1} \ln 2] \tag{9.56}$$

The number of individuals in the population, the total structural body mass and the organic fluxes are given by

$$N = \frac{\dot{J}_{X+}}{\mathcal{E}\dot{J}_X} = \frac{M_{V+}}{l_d^3 M_{Vm} \ln 2} \tag{9.57}$$

$$M_{V+} \equiv N\mathcal{E}M_V = \frac{\dot{h}_X M_X [M_V]}{f[M_X][\dot{J}_{Xm}]} \tag{9.58}$$

$$\dot{\boldsymbol{J}}_{\mathcal{O}+} = \boldsymbol{\eta}\dot{\boldsymbol{p}}_+ = \boldsymbol{\eta}\dot{\boldsymbol{p}}(f,1) M_{V+}/M_{Vm} \tag{9.59}$$

The mean mass per individual is thus $\mathcal{E}M_V = M_{V+}/N$.

The relationship (9.46) for the mineral fluxes still holds. Since the row of $\boldsymbol{n}_{\mathcal{M}}^{-1}$ that corresponds to oxygen, i.e. the third row, can be interpreted as the ratio of the reduction degrees of the elements to that of oxygen if the N substrate is ammonia (cf. {131}), the third row of $\boldsymbol{n}_{\mathcal{M}}^{-1}\boldsymbol{n}_{\mathcal{O}}$ can be interpreted as the ratio of the reduction degrees of the organic components to that of oxygen. It follows that $-\delta_O \dot{J}_{O+} = \boldsymbol{\delta}_{\mathcal{O}}^T \dot{\boldsymbol{J}}_{\mathcal{O}+}$, when $\boldsymbol{\delta}_{\mathcal{O}}$ denotes the reduction degrees of the organic compounds. If the structural biomass has the same composition as the reserves, and if no products are formed, this further reduces to $-\delta_O \dot{J}_{O+} = \delta_X \dot{J}_{X+} + \delta_W \dot{J}_{W+}$, or $-\delta_O Y_{OW} = \delta_X Y_{XW} + \delta_W$, where index W refers to the total biomass, i.e. the sum of the structural biomass and the reserves, and Y to yield coefficients. This result is well known from the microbiological literature [391,779] and follows directly from the general assumptions in Table 3.3.

Figure 9.18 compares the measured oxygen yield with the yield that has to be expected on the basis of this relationship and measured values of biomass yields for a wide variety of organisms and 15 substrates that differ in n_{HX} and n_{OX}, but all have $n_{NX} = 0$. The substantial scatter shows that the error of measurement is large and/or that the biomass composition is not equal for all organisms and is not independent of the growth rate. Generally $n_{*V} \neq n_{*E}$, and n_{*W} depends on the population growth rate $\dot{r}$.

9.3 Food chains and webs

Many ecosystems have consumers that are linked in a food web; the food chain being its simplest form. Bi- and tri-trophic chains are intensively studied [377,379,489,539,603, 604]. Most models, however, have growing zero-trophic levels, and are based on implicit assumptions about their food dynamics. This will be avoided here, to allow the application of mass and energy balances. Some popular models are even at odds with conservation principles [506,508].

A basic problem in the analysis of food web dynamics is the large number of parameters that show up, which reduces the value of the exhausting undertaking of a systematic approach to the analysis of the system's potential behaviour. Several strategies are required to minimise that problem. One of them is to use body size scaling relationships to tie parameter values across species. This reduces the problem of community dynamics in principle to that of particle size distributions in taxon-free communities, as reviewed by Damuth *et al.* [194].

The next sections explore transient and asymptotic behaviour of bi- and tri-trophic chains; the results are based on work by B. W. Kooi and M. P. Boer [94,95,96,366,507,510].

9.3.1 Transient behaviour of bi-trophic chains

The non-equilibrium dynamics of food chains can be rather complex and sensitively depends on the initial conditions. Figure 9.19 illustrates results for a substrate–bacteria–myxamoebae chain in a chemostat. B. W. Kooi has been able to fit the experimental data to the DEB model for V1-morphs with remarkable success. All parameters were estimated on the basis of a weighted least-squares criterion. The fitted system does not account for the digestion of reserves; its incorporation resulted in very similar fits, while the extra parameters were poorly fixed by the data. The main dynamic features are well described by the model. The myxamoebae decrease more rapidly in time than the throughput rate allows by shrinking during starvation. The type of equilibrium of this chain is known as a spiral sink, so that this chain ultimately stabilizes, and the period reduces with the amplitude. The numerical integration of the set of differential equations that describe the system was achieved using a fourth-order Runge–Kutta method.

This particular data set was used to illustrate the application of catastrophe theory by Saunders [808], who concluded that simple generalizations of the Lotka–Volterra model cannot fit this particular data set, because growth is fast when substrate is low. He suggested that the feeding rate for each individual myxamoeba is proportional to the

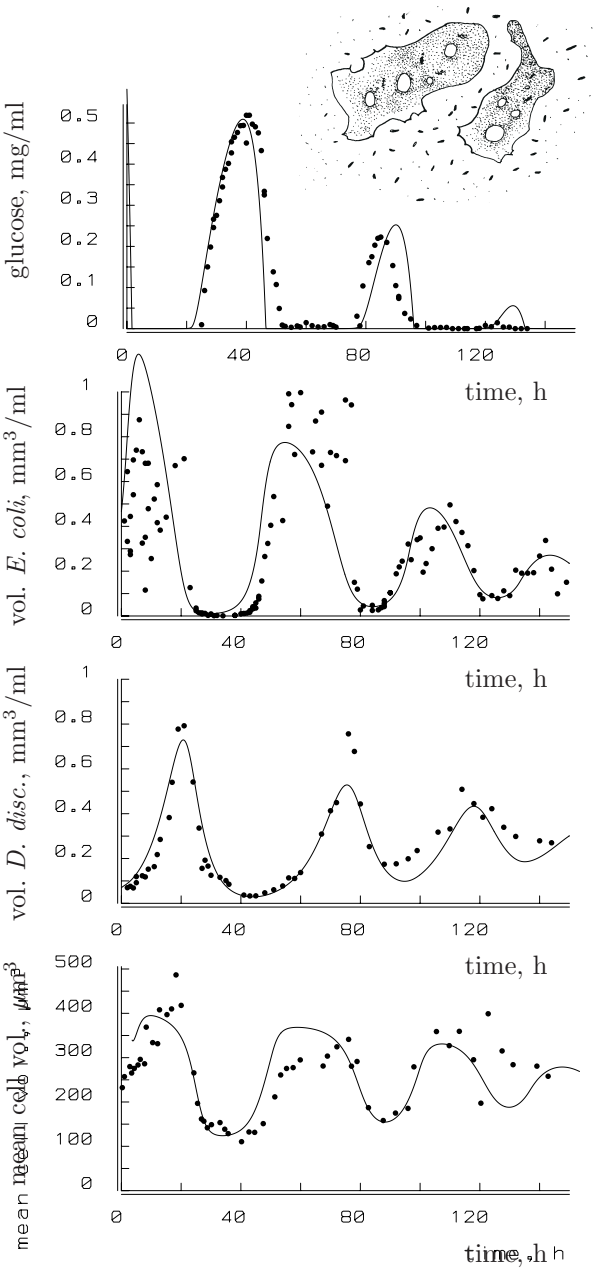

Figure 9.19: A chemostat with a bi-trophic chain of glucose X_0, the bacterium *Escherichia coli* X_1 and the cellular slime mould *Dictyostelium discoideum* X_2 at 25 °C, throughput rate $\dot{h} = 0.064\ \mathrm{h}^{-1}$ and a glucose concentration of $X_r = 1\ \mathrm{mg\,ml}^{-1}$ in the feed. The 4th graph gives the mean cell volumes of *Dictyostelium*. Data from Dent *et al.* [208].

The parameter values and equations are

$X_0(0)$	0.433			$\mathrm{mg\,ml}^{-1}$
$X_1(0)$	0.361	$X_2(0)$	0.084	$\mathrm{mm^3\,ml}^{-1}$
$e_1(0)$	1	$e_2(0)$	1	-
X_{K1}	0.40	X_{K2}	0.18	$\frac{\mu\mathrm{g}}{\mathrm{ml}}$, $\frac{\mathrm{mm^3}}{\mathrm{ml}}$
g_1	0.86	g_2	4.43	-
$\dot{k}_{M1}$	0.008	$\dot{k}_{M2}$	0.16	h^{-1}
$\dot{k}_{E1}$	0.67	$\dot{k}_{E2}$	2.05	h^{-1}
$j_{Xm,1}$	0.65	$j_{Xm,2}$	0.26	$\frac{\mathrm{mg}}{\mathrm{mm^3\,h}}$, h^{-1}

$$\begin{aligned}
\frac{d}{dt}X_0 &= \dot{h}(X_r - X_0) - \frac{X_0 X_1 j_{Xm,1}}{X_{K1} + X_0} \\
\frac{d}{dt}X_1 &= \left(\frac{\dot{k}_{E1}e_1 - \dot{k}_{M1}g_1}{e_1 + g_1} - \dot{h}\right) X_1 - \frac{X_1 X_2 j_{Xm,2}}{X_{K2} + X_1} \\
\frac{d}{dt}X_2 &= \left(\frac{\dot{k}_{E2}e_2 - \dot{k}_{M2}g_2}{e_2 + g_2} - \dot{h}\right) X_2 \\
\frac{d}{dt}e_1 &= \dot{k}_{E1}\left(\frac{X_0}{X_{K1} + X_0} - e_1\right) \\
\frac{d}{dt}e_2 &= \dot{k}_{E2}\left(\frac{X_1}{X_{K2} + X_1} - e_2\right)
\end{aligned}$$

Table 9.4: List of basic local bifurcations for ODEs: $dx/dt = f(x, \alpha)$, and maps: $y_{n+1} = f(y_n, \alpha)$ with normal forms. The bifurcation point is $\alpha = 0$. λ is the eigenvalue of the Jacobian matrix evaluated at the equilibrium ($\frac{d}{dt}x = 0$ and $y_{n+1} = y_n$) and μ is the Floquet multiplier evaluated at the limit cycle. The bifurcation type depends on the real (Re) parts of these characteristic exponents. With food web dynamics, a stable positive attractor originates at a supercritical transcritical bifurcation (superscript +) and an unstable positive equilibrium or limit cycle at a subcritical transcritical bifurcation (superscipt −). Superscript ± refers to supercritical and subtritical.

symbol	bifurcation	normal form	characteristic exponents
T_e	Tangent, of equilibrium	$\frac{d}{dt}x = \alpha - x^2$	Re $\lambda = 0$
T_c	Tangent, of limit cycle	$y_{n+1} = y_n + \alpha - y_n^2$	Re $\mu = 1$
$TC_e^{\pm}$	Transcritical, of equilibrium	$\frac{d}{dt}x = \alpha x \pm x^2$	Re $\lambda = 0$
$TC_c^{\pm}$	Transcritical, of limit cycle	$y_{n+1} = (1 + \alpha)y_n \pm y_n^2$	Re $\mu = 1$
$H^{\pm}$	Hopf	$\frac{d}{dt}x = -y + x(\alpha \pm (x^2 + y^2))$	
		$\frac{d}{dt}y = x + y(\alpha \pm (x^2 + y^2))$	Re $\lambda_{1,2} = 0$
$F^{\pm}$	Flip	$y_{n+1} = -(1 + \alpha)y_n \pm y_n^3$	Re $\mu = -1$

product of the bacteria and the myxamoebae densities. This implies an interaction between the myxamoebae; Bazin and Saunders [61] suggested that the myxamoebae measure their own density via folic acid. Although interactions cannot be excluded, the goodness of fit of the DEB model makes it clear that it is not necessary to include such interactions. The significance of realistic descriptions without interaction is in the extrapolation to other systems; if species-specific interactions do dominate systems behaviour, there can be hardly any hope for the feasibility of community ecology. Reserves cause a time delay in the reaction of the predator to fluctuations in prey and explain why a high growth rate can combine with low substrate densities in these oscillatory systems.

9.3.2 Asymptotic behaviour: bifurcation analysis

When the number of loosely coupled variables is sufficiently large in a system, the system is likely to have very complex asymptotic behaviour, including the occurrence of multiple attractors, possibly of the chaotic type. This is almost independent of the specific model; the behaviour has been observed in several models for tri-trophic food chains. Bifurcation analysis deals with qualitative changes in the asymptotic behaviour of the system, when a parameter is varied in value. Table 9.4 gives the possible bifurcation types, which all have been found in tri-trophic food chains. The bifurcation type depends on the value of the eigenvalue of the Jacobian matrix evaluated at the equilibrium and the Floquet multiplier, which is an eigenvalue of the Poincaré next-return map. If all complex values of the Floquet multipliers are within the unit circle, the dynamic system's orbit converges to a limit cycle.

Methods

The analysis of bifurcation behaviour must be done numerically, using specialized software: LOCBIF [480] and AUTO [221] can calculate bifurcation diagrams using continuation methods. The theory is documented in [538]. The analyses cannot be done on a routine basis, however, and the user must have a fairly good idea of what to expect and what to look for. Although the software is rapidly improving in quality, at present it is still deficient in computing certain types of global bifurcations, for instance, and one has to rely on 'in-house' software to fill in the gaps, see [94].

Results of bifurcation analyses are frequently reported in the form of bifurcation diagrams. These diagrams connect points where system's asymptotic behaviour changes in a similar way when the bifurcation parameters are varied. So, the system has similar asymptotic behaviour for values of bifurcation parameters within one region. The construction of such diagrams is only feasible if there are just one or two of such parameters. Many food chain studies take parameters that represent properties of species which cannot be changed experimentally. When the organisms live in a chemostat, two natural bifurcation parameters are the throughput rate and the concentration of substrate in the feed. Diagrams with these parameters are called operating diagrams.

Bifurcation diagrams for bi- and tri-trophic chains

Figure 9.20 shows the bifurcation diagram, as computed by B. W. Kooi and M. P. Boer for bi- and tri-trophic chains living in a chemostat. The reserve capacity is reduced to zero for all species, so they follow the Marr–Pirt model. The system amounts to

$$\begin{aligned}
\frac{d}{dt}X_0 &= (X_r - X_0)\dot{h} - j_{Xm,1}f_{0,1}X_1 \\
\frac{d}{dt}X_1 &= (j_{Xm,1}f_{0,1}Y_{g,1} - \dot{k}_{M,1} - \dot{h})X_1 - j_{Xm,2}f_{1,2}X_2 \\
\frac{d}{dt}X_2 &= (j_{Xm,2}f_{1,2}Y_{g,2} - \dot{k}_{M,2} - \dot{h})X_2 - j_{Xm,3}f_{2,3}X_3 \\
\frac{d}{dt}X_3 &= (j_{Xm,3}f_{2,3}Y_{g,3} - \dot{k}_{M,3} - \dot{h})X_3
\end{aligned}$$

where $j_{Xm,i}$ is the maximum specific feeding rate of species i; $f_{i,j} = (1 + X_{Kj}/X_i)^{-1}$ is the scaled function response; $Y_{g,i}$ is the 'true' yield coefficient, $\dot{k}_{M,i}$ the maintenance rate coefficient. The bifurcation parameters are X_r and $\dot{h}$.

The bi-trophic chain has simple asymptotic behaviour only. If the species are not washed out, they can either coexist in a single stable equilibrium, or in a single limit cycle. A supercritical Hopf bifurcation separates the corresponding parameter regions. The diagram beautifully illustrates the paradox of enrichment, which is the observed induction of oscillatory behaviour that follows an increase in resource levels [790].

Figure 9.20 illustrates that the bifurcation diagram of the tri-trophic chain is very complex in a small part of the parameter space. A detailed discussion is beyond the scope of this book, and is given in [509]. The diagram has an 'organizing centre' M_1, which is a codimension-two point; the transcritical curves $TC_{e,3}$ and $TC_{c,3}$ for equilibrium and

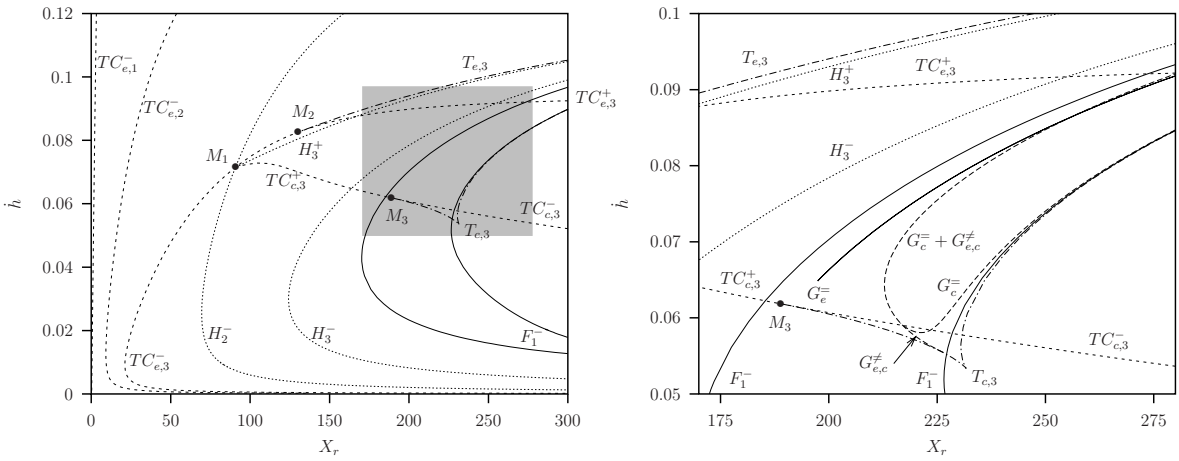

Figure 9.20: Bifurcation diagrams for Marr-Pirt model of bi- and tri-trophic chains. The right figure is a detail of the left one. The transcritical bifurcation curves $TC_{e,1}$, $TC_{e,2}$ and the supercritical Hopf bifurcation curve H_2^- relate to both bi- and tri-trophic chains, all others only to tri-trophic chains. The bifurcation parameters are the dilution rate $\dot{h}$ and the substrate concentration in the reservoir X_r. Left of the $TC^-_{e,2}$ curve, the predator is washed out; between this curve and the H_2^- curve, the bi-trophic chain has a stable equilibrium, and right of the curve H_2^- it has a stable limit cycle. The curves $TC^-_{e,3}$ and H_3^- mark similar regions for the tri-trophic chain. Within the folded (closed) flip-bifurcation curve F_1^- the limit cycle is unstable. Homoclinic $G^=_e$, $G^=_c$ and heteroclinic $G^{\neq}_{e,c}$ bifurcation curves denote global bifurcations to multiple attractors.

Parameters:

i	1	2	3	
X_K	8	9	10	$\mathrm{mg\,l^{-1}}$
j_{Xm}	1.25	0.33	0.25	$\mathrm{h^{-1}}$
Y_g	0.4	0.66	0.6	
$\dot{k}_M$	0.025	0.01	0.0027	$\mathrm{h^{-1}}$

limit cycles, where $X_3 = 0$, originate here. The points M_2 and M_3 on these curves are the origins of the tangent bifurcation curves $T_{e,3}$ and $T_{c,3}$ for equilibria and limit cycles. A pair of interior equilibria or limit cycles disappears simultaneously as the two bifurcation parameters passes a tangent bifurcation curve. The latter tangent bifurcation curve $T_{c,3}$ has a cusp bifurcation point N. This type of bifurcation is often associated with a so-called catastrophe.

Figure 9.21 presents part of the orbit of the three trophic levels in a chemostat, using the Monod model. The bifurcation parameters are in the chaotic region of the bifurcation diagram. The bifurcation diagram for the tri-trophic chain on the basis of the full DEB model for V1-morphs resembles that of the Marr–Pirt model [508].

Canonical map for tri-trophic chains

Many aspects of the bifurcation pattern of continuous-time systems can be understood from discrete-time systems, where the variables at time point $n + 1$ are taken to be functions of those at time point n. These systems are called maps. M. P. Boer [94] showed that the bifurcation behaviour of a tri-trophic chain of the Marr–Pirt and Monod type can be

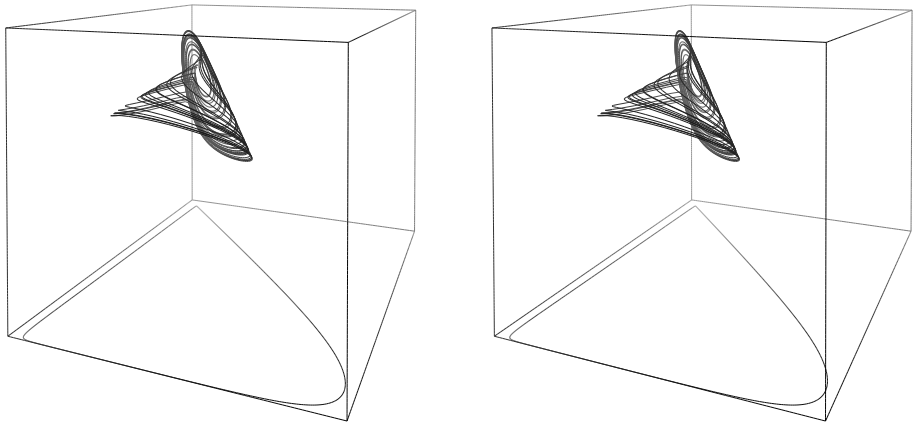

Figure 9.21: Stereo view of part of the orbit of the three trophic levels (x_1, x_2 and x_3 in the x-, y-, z-direction, respectively) of the Monod model for a food chain on a chaotic attractor (throughput rate $\dot{h} = 0.08732\,\mathrm{h}^{-1}$ and substrate level $X_r = 200\,\mathrm{mg\,l}^{-1}$).

understood from the one-dimensional map

$$x_{n+1} = f_{\alpha,\beta}(x_n) = 16\beta x_n^3 - 24\beta x_n^2 + 9\beta x_n - \beta + \alpha$$

where x is an abstract variable, and α and β bifurcation parameters; $f_{\alpha,\beta}$ is thus a cubic polynomial in x_n, which is not invertable. There are two critical points, $c_1 = \frac{1}{4}$ and $c_2 = \frac{3}{4}$; $f(c_1) = \alpha$ is a local maximum, and $f(c_2) = \alpha - \beta$ is a local minimum. The map does not have a corresponding one-dimensional continuous system, and the equivalence is abstract, involving a Poincaré next-return map, where subsequent intersections of the dynamic system's orbit are compared with a plane chosen at a suitable location in the state space. All the points of intersection appear to lie close to a single curve when plotted against the preceding points, as occurs in the Lorenz system [567]. The shape of this curve resembles a cubic polynomial. A useful way to construct such a map is to select the local minima of the highest trophic level and to plot subsequent values against each other. The significance of identifying this one-dimensional map as a canonical form of the multi-dimensional system is in the powerful mathematical theory that exists for one-dimensional maps [618,210,581,848,898].

Figure 9.22 gives the map $f_{\alpha,\beta}$ for $\alpha = \beta = 0.8$, for which the map has three fixed points, $p_1 < p_2 < p_3$, and is invariant on the interval $[p_1, p_3]$. The fixed points p_1 and p_3 are repellors, since $\frac{d}{dx} f(p_i) > 1$. Then with $q \in (p_1, c_1)$ we have $\lim_{n\to-\infty} f^n_{0.8,0.8}(q) \to p_1$ and with $r \in (c_2, p_3)$ we have $\lim_{n\to-\infty} f^n_{0.8,0.8}(r) \to p_3$, where superscript n denotes the number of times the map f is applied.

An orbit starting at a point $q \in (p_1, c_1)$ is called *homoclinic* if there exists an $n > 0$ such that $f^n(q) = p_1$. This homoclinic orbit is called degenerated if $\frac{d}{dx} f^n(q) = 0$, which is the case in Figure 9.22. An orbit starting at a point $r \in (c_2, p_3)$ is called *heteroclinic* if there exists an $n > 0$ such that $f^n(r) = p_1$. The heteroclinic orbit in Figure 9.22 is also degenerated, since $\frac{d}{dx} f^n(r) = 0$. For further background, see for instance [210].

Figure 9.23 shows a one-parameter bifurcation diagram with bifurcation parameter α, for $\beta = 0.8$. It is symmetrical with respect to the point $(\alpha, x) = ((1+\beta)/2, 1/2) = (0.9, 0.5)$. The unstable equilibrium values p_1 and p_3 are plotted.

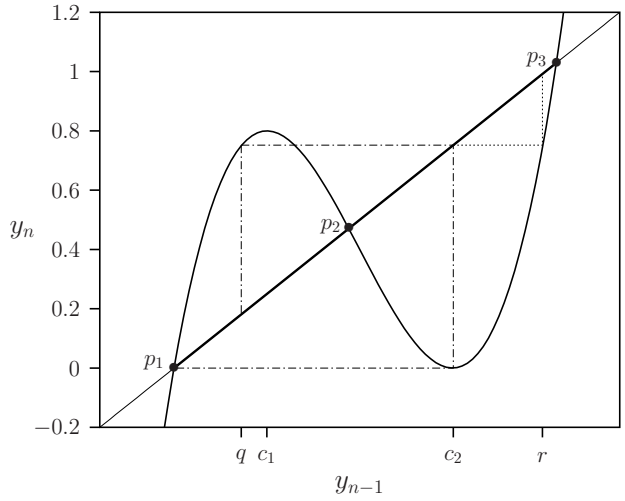

Figure 9.22: The function $f_{\alpha,\beta}$ for $\alpha = 0.8$ and $\beta = 0.8$. The points p_1, p_2 and p_3 are fixed points, and c_1 and c_2 are critical points. At point q a degenerate homoclinic orbit starts ($f^2_{0.8,0.8}(q) = p_1$ and $\lim_{n\to-\infty} f^n_{0.8,0.8}(q) \to p_1$ for $q \in (p_1, c_1)$). At point r a degenerate heteroclinic orbit starts ($f^2_{0.8,0.8}(r) = p_1$ and $\lim_{n\to-\infty} f^n_{0.8,0.8}(r) \to p_3$ for $r \in (c_2, p_3)$). The solid interval on the diagonal is the basin of attraction.

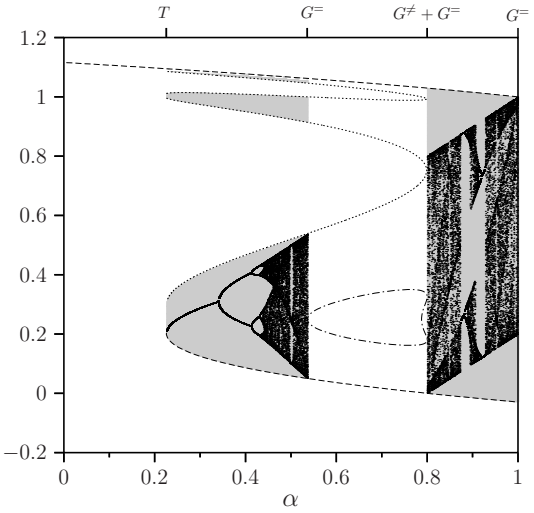

Figure 9.23: One-parameter bifurcation diagram of the canonical map for $\beta = 0.8$. The dashed curves indicate the repellors p_1 and p_3. The points on the dotted curves lie on a heteroclinic orbit. The points on the dashed-dotted curve lie on a homoclinic orbit. The attractors are plotted as points. The grey regions are the basin of attraction of these attractors. This diagram is point-symmetrical with respect to point $(0.9, 0.5)$.

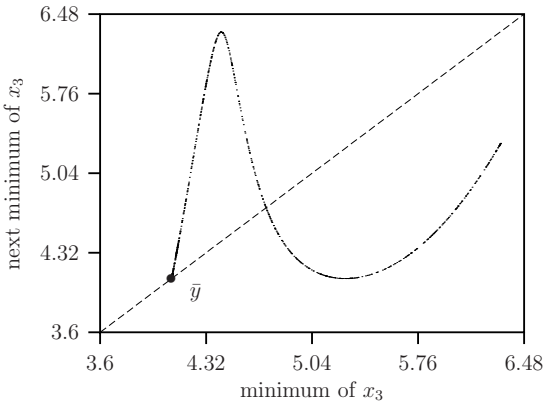

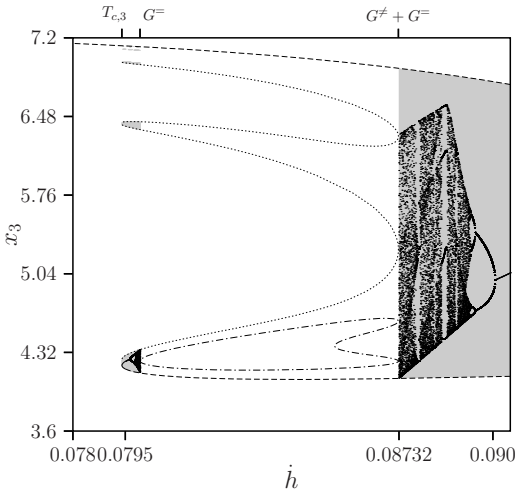

Figure 9.24: The left figure shows the next minimum of x_3 as a function of the current minimum for the Monod model, with dilution rate $\dot{h} = 0.08732\,\mathrm{h}^{-1}$ and concentration substrate in the feed $X_r = 200\ \mathrm{mg\,l}^{-1}$. The resulting map resembles the canonical cubic map with two critical points. The point $\overline{y}$ is the minimum of a limit cycle of the saddle type. The right figure shows the one-parameter bifurcation diagram of the Monod model, which again shows striking similarities with that of the canonical cubic map.

At the tangent bifurcation point T, at $\alpha \approx 0.2255$, the heteroclinic orbits disappear, together with the basin of attraction and the fixed points p_1 and p_2. In the region between this tangent bifurcation T and homoclinic bifurcation point $G^{=}$ ($\alpha \approx 0.5361$), the bifurcation diagram resembles the well-known bifurcation diagram of the (unimodal, with one critical point) logistic map $y_{n+1} = ry_n(1 - y_n)$ for $r \in [1, 4]$ discussed in [599].

For increasing α the fixed point becomes unstable and a cascade of period doubling leads to chaotic dynamics. As with the unimodal logistic map for $r = 4$, the strange attractor disappears suddenly at a homoclinic bifurcation point. In the interval $\alpha \in [0.8, 1.0]$ there is chaotic dynamics with abrupt destruction of the chaotic attractor and its basin of attraction at the end points of this interval in $\alpha = 0.8$ and $\alpha = 1.0$. Here homoclinic orbits to the equilibria p_1 and p_3, respectively, degenerate at the global bifurcation point (see Figure 9.22). With $\alpha = (1 + \beta)/2$ the equilibria p_3 and p_1 switch roles.

In the one-parameter bifurcation diagram of Figure 9.23 points on a heteroclinic orbit between p_3 and p_1 are plotted in the interval $\alpha \in [\approx 0.2255, 0.8]$. At the global bifurcation point $G^{\neq}$, the heteroclinic orbits between points p_3 and p_1 become degenerate. Figure 9.23 also gives the basin of attraction. In the absence of heteroclinic orbits, $\alpha \in [0.8, 1.0]$, the basin is connected. However, with heteroclinic orbits $\alpha \in [\approx 0.2255, 0.8]$ convergence to a positive attractor for $\alpha \in [\approx 0.2255, 0.5361]$ occurs in disconnected intervals with end points on heteroclinic orbits, and the basin boundary has a complex geometry close to the equilibrium p_3. In the 'hole' in the chaotic region there is convergence only for the countable points at the homoclinic and heteroclinic orbits and otherwise there is no convergence. At the tangent bifurcation point T the boundary basin is a vertical line where α is constant, that is the basin of attraction disappears abruptly at the tangent bifurcation together with the fixed points p_1 and p_2.

Figure 9.24 illustrates the next minimum map for the Monod model for a tri-trophic chain in the chemostat, and the one-parameter bifurcation diagram for the throughput rate. Both the map and the diagram have striking similarities with the canonical map given in Figures 9.22 and 9.23. A full analysis of the two-parameter bifurcation diagram can be found in [94].

Stability and invasion

Nisbet *et al.* [668] noted that the experimental system appears to be much more stable than is predicted by the bi-trophic Monod model. They concluded that the introduction of maintenance, as proposed by Marr–Pirt, increases the range of operation parameters that give stable chains; however, real-world chains still appear to be more stable. Consistent with the single trophic systems, compared in Figure 9.2, the DEB model for bi- and tri-trophic chains is much more stable than the Monod and the Marr–Pirt model. The experimental conditions which lead to the damped oscillation of Figure 9.19 are in the stable region of the bifurcation diagram, close to the supercritical Hopf bifurcation curve H_2^- in Figure 9.20. If the throughput rate were a little bit higher, the oscillations would not have been damped, but sustained.

A species can invade a trophic system in a chemostat if its per capita growth rate exceeds the throughput rate at an infinitesimally small population size. For most food web

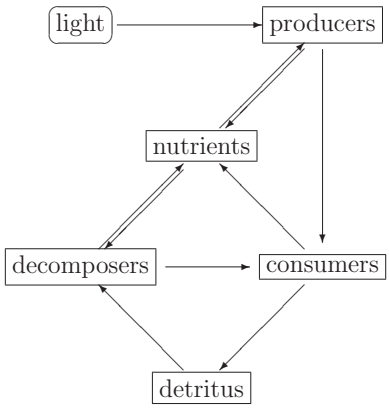

Figure 9.25: The Canonical Community consists of three 'species': producers that gain energy from light and take up nutrients to produce biomass, consumers that feed on producers and decomposers that recycle nutrients from producers and consumers. The community is rather closed for nutrients, but requires a constant supply of energy. Influx and efflux of nutrients largely determine the long-term behaviour of the community.

models, this occurs when the Lyapunov exponent, which is associated with the dynamics of the invader, is positive at the boundary of the attractor. The transcritical bifurcation point, when the Lyapunov exponent is zero, marks the region where invasion is possible. Using this criterion, numerical studies by B. W. Kooi showed that another level-two species can invade in a bi-trophic DEB chain. This means that the level-two species allows escape from the competitive exclusion principle, see [859], and the two competing species can coexist on a single substrate in the presence of a predator.

Before the 1970s the general insight was that an increase in diversity comes with an increase in stability. May [598] showed that the opposite holds for randomly connected Lotka–Volterra systems. Later, it became evident that the spatial scale is essential, and meta-population theory showed that instability at a small spatial scale can go with stability at a large spatial scale. We are now witnessing a new insight: diversity can go with stability in non-linear systems with more realistic dynamics, even in spatially homogeneous systems.

9.4 Canonical community

Figure 9.25 illustrates the structure of an idealized, simple, three-species ecosystem. Producers (algae) use light and nutrients to produce organic matter, which is transformed by consumers (grazers), while decomposers (bacteria) release nutrients from the organic matrix [880]. The system is 'open' to energy flow, but closed to inputs or removal of elemental matter. It might live in a closed bottle, for instance. Exchanges of mass with the rest of the world can be included at a later stage. It is found in many ecosystems, for example, and is very similar to the one used for material turnover in microbial flocs in sea-water plankton systems [332,586].

Microcosms are fairly realistic experimental models for ecosystems [83,337]. Kawabata and co-workers [307,469,654] studied a closed community consisting of the bacterium *Escherichia coli*, the ciliate *Tetrahymena thermophila* and the euglenoid *Euglena gracilis*, for direct and indirect effects of γ-rays. The ciliate grazes on the bacterium, and lives off organic products that are excreted by the euglenoid, which has mixotrophic capabilities. A stable coexistence developed for a period exceeding 130 days. The bacterium did not survive an irradiation of 500 Gy, but the two remaining species continued to exist at lower levels.

Table 9.5: The chemical compounds of the Canonical Community and their transformations and indices. The + signs mean appearance, the − signs disappearance. The signs of the mineral fluxes depend on the chemical indices and parameter values. The labels on rows and columns serve as indices to denote mass fluxes and powers. The table shows flux matrix $\dot{\boldsymbol{J}}^T$ rather than $\dot{\boldsymbol{J}}$ if the signs are replaced by quantitative expressions presented in Table 9.6.

compounds →			minerals					detritus				consumer		producer			decomp	
← transformations			L light	C carbon dioxide	H water	O oxygen	N ammonia	PP prod-faeces	PD decomp-faeces	PV dead cons-struc	PE dead cons-res	VC structure	EC reserves	VP structure	E_1P reserves 1	E_2P reserves 2	VD structure	ED reserves
consumer	assim 1	A_1C		+	+	−	+	+					+	−	−	−		
	assim 2	A_2C		+	+	−	+		+				+				−	−
	growth	GC		+	+	−	+					+	−					
	dissip	DC		+	+	−	+						−					
	death	HC								+	+	−	−					
prod	assim 1	A_1P	−	−	−	+									+			
	assim 2	A_2P	−	−	−	+	−									+		
	growth	GP		+	+	−	+							+	−	−		
	dissip 1	D_1P		+	+	−	+								−			
	dissip 2	D_2P		+	+	−	+									−		
decomposer	assim 1	A_1D		+	+	−	+	−										+
	assim 2	A_2D		+	+	−	+		−									+
	assim 3	A_3D		+	+	−	+			−								+
	assim 4	A_4D		+	+	−	+				−							+
	growth	GD		+	+	−	+										+	−
	dissip	DD		+	+	−	+											−
	carbon	C		1				1	1	1	1	1	1	1	1	1	1	1
	hydrogen	H			2		3	1.6	1.6	1.8	1.8	1.8	1.8	1.6	2	1.6	1.6	1.6
	oxygen	O		2	1	2		0.4	0.4	0.5	0.5	0.5	0.5	0.4	1	0.4	0.4	0.4
	nitrogen	N					1	0.1	0.1	0.2	0.2	0.2	0.2	0.2		0.4	0.2	0.4

The results presented here are from [526]. The Canonical Community differs from a prey–predator system by the inclusion of the zero-th trophic level in the dynamics of the system. Prey–predator systems that allow mass balances always require external supply of inert substrate. Many prey–predator systems in the literature, however, assume intrinsic growth of the prey, independent of its food, and, therefore, imply complex dynamics of variables that are excluded from the system. Another difference with a prey–predator system is that all components affect nutrients, which implies more complex trophic interactions between components, as discussed by e.g. Andersen [20].

9.4.1 Mass transformations in communities

The chemical compounds and their transformations in the Canonical Community are presented in Table 9.5. When we replace the signs by model-dependent quantitative expressions, such as in Table 9.6, this turns Table 9.5 into a matrix of fluxes that is known as a scheme matrix [754], which will be indicated by matrix $\boldsymbol{\dot{J}}$; element i, j of matrix $\boldsymbol{\dot{J}}$, called $\dot{J}_{i,j}$, gives the flux of compound i involved in transformation j. We quantify the compounds in terms of moles (for minerals) or C-moles (for organic compounds and biomass), and indicate the vector of moles of all compounds by $\boldsymbol{M}$.

The symbol $\boldsymbol{\dot{J}}_C$ denotes the vector of C-fluxes, while $\dot{J}_{C,GD}$ denotes the C-flux associated with the growth of decomposers. The flux $\dot{J}_C^+$ adds all positive contributions in $\boldsymbol{\dot{J}}_C$, and $\dot{J}_C^-$ all negative ones, so $\dot{J}_C^+ + \dot{J}_C^- = 0$; the quantity $\dot{J}_*^+/M_*$ quantifies the turnover rate of compound $*$ in the system. Index $\mathcal{M}$ collects the 4 minerals, $\mathcal{O}$ the 11 organic compounds; $\boldsymbol{\dot{J}}_{\mathcal{M},GD}$ denotes the 4 mineral fluxes that are associated with decomposer growth, $\boldsymbol{\dot{J}}_{\mathcal{O},GB}$ does the same for the 11 organic fluxes; $\boldsymbol{n}_{\mathcal{M}}$ collects the 4×4 chemical indices for minerals, $\boldsymbol{n}_{\mathcal{O}}$ is the 4×11 matrix of chemical indices for the organic compounds. Indices C, P and D refer to consumers, producers and decomposers.

When the transformations can be written as functions of the total amount of moles of the various compounds, $\boldsymbol{M}$, the dynamics of $\boldsymbol{M}$ can be written as $\frac{d}{dt}\boldsymbol{M} = \boldsymbol{\dot{J}}\mathbf{1}$, which just states that the change in masses equals the sum of the columns of the scheme matrix. The Jacobian $\frac{d}{d\boldsymbol{M}^T}\boldsymbol{\dot{J}}\mathbf{1}$ at steady state contains interesting information about the possible behaviour of the system close to the steady state.

Table 9.5 illustrates a case where decomposers and consumers have one type of reserve, and the producers have two, one with and one without nitrogen, to account for their larger metabolic flexibility. Consumers mainly feed on reserves, because they cannot digest cell wall material, which makes up a substantial part of structural mass, and faeces is only derived from structural mass (which implies that its composition does not depend on the nutritional status of the prey). Only ammonia is included, not because it is the most important nutrient, but because organisms excrete it. It makes little sense to include nitrate, for example, without including ammonia; the exclusion of nitrate is just for simplicity's sake.

The system is closed for mass, which means that $\boldsymbol{n}\boldsymbol{\dot{J}} = \mathbf{0}$. At steady state, we have

Table 9.6: (see next page) Fluxes in the Canonical Community of the consumers VC, producers VP, and decomposers VD that live in a confined environment, in which all are conceived as V1-morphs. The compounds and transformations are introduced in Table 9.5. Consumers and decomposers have one type of reserves (EC and ED, respectively), the producers have two types (E_1P and E_2P). Detritus includes producer-faeces PP, decomposer-faeces PD (both produced by consumers), and dead consumers (structural mass PV and reserves PE). Carbon dioxide (C) and ammonia (N) are obtained from the balance equation for carbon and nitrogen. The variables x refer to the scaled mass densities: $x_{PP} = M_{PP}/X_{K,PP}$, $x_{PD} = M_{PD}/X_{K,PD}$, $x_{PV} = M_{PV}/X_{K,PV}$, $x_{PE} = M_{PE}/X_{K,PE}$, $x_P = M_{VP}/X_{K,VP}$, $x_D = M_{VD}/X_{K,VD}$, $x_{Li} = \dot{J}_L/\dot{J}_{K,Li}$ $(i = 1, 2)$, $x_N = M_N/X_{K,N2}$, $x_{Ci} = M_C/X_{K,Ci}$ $(i = 1, 2)$, where $\dot{J}_L$ is the light flux that is supplied to the system to keep it going.

$$
\begin{aligned}
\dot{J}_{VP,\,A_1C} &= -M_{VC}\, j_{VP,\,AC,m}\frac{x_P}{1+x_P+x_D};\quad \dot{J}_{PP,\,A_1C} = -y_{PP,\,VP}\,\dot{J}_{VP,\,A_1C}\\
\dot{J}_{VD,\,A_2C} &= -M_{VC}\, j_{VD,\,AC,m}\frac{x_D}{1+x_P+x_C};\quad \dot{J}_{PD,\,A_2C} = -y_{PD,\,VD}\dot{J}_{VD,\,A_2C}\\
\dot{J}_{EC,\,A_iC} &= -\sum_{*} y_{EC,\,*}\dot{J}_{*,\,A_iC}\quad \text{for } (i,*)\in\{(1,VP),(1,E_1P),(1,E_2P),(2,VD),(2,ED)\}\\
\dot{J}_{E_iP,\,A_1C} &= m_{E_iP}\dot{J}_{VP,\,A_1C}\quad \text{for } i\in\{1,2\};\quad \dot{J}_{ED,\,A2C} = m_{ED}\dot{J}_{VD,\,A_2C}\\
\dot{J}_{VC,\,GC} &= M_{VC}\frac{m_{EC}\dot{k}_{EC}-j_{EC,\,MC}}{m_{EC}+y_{EC,\,VC}};\quad \dot{J}_{EC,\,DC} = -j_{EC,\,MC}M_{VC};\quad \dot{J}_{PE,\,HC} = m_{EC}\dot{J}_{PV,\,HC}\\
\dot{J}_{PV,\,HC} &= \dot{h}_a M_{VC}\frac{y_{VC,\,EC}\,m_{EC}}{1+y_{VC,\,EC}\,m_{EC}};\quad \dot{J}_{VC,\,HC} = -\dot{J}_{PV,\,HC};\quad \dot{J}_{EC,\,HC} = -\dot{J}_{PE,\,HC}\\
\dot{J}_{E_1P,\,A_1P} &= M_{VP}\, j_{E_1P,\,AP,m}\, f_{P_1}\quad \text{with}\quad f_{P_1} = \left(1+\sum_{*} x_*^{-1} - \left(\sum_{*} x_*\right)^{-1}\right)^{-1}\quad \text{for } *\in\{L,C\}\\
\dot{J}_{E_2P,\,A_2P} &= M_{VP}\, j_{E_2P,\,AP,m}\, f_{P_2}\quad \text{for } *\in\{L,N,C\}\\
f_{P_2} &= \left(1+\sum_{*} x_*^{-1} - \left(\sum_{*\notin L} x_*\right)^{-1} - \left(\sum_{*\notin N} x_*\right)^{-1} - \left(\sum_{*\notin C} x_*\right)^{-1} + \left(\sum_{*} x_*\right)^{-1}\right)^{-1}\\
\dot{J}_{VP,\,GP} &= \dot{r}_{VP,\,GP}M_{VP}\quad \text{with } \dot{r}_{VP,\,GP} = \left(\sum_i \dot{r}_{E_i}^{-1} - \left(\sum_i \dot{r}_{E_i}\right)^{-1}\right)^{-1}\quad \text{and}\\
\dot{r}_{E_i} &= \frac{m_{E_iP}(\dot{k}_{E_iP}-\dot{r}_{VP,\,GP}) - j_{E_iP,MP}}{y_{E_iP,\,VP}};\quad \dot{J}_{E_iP,\,GP} = -y_{E_iP,\,VP}\dot{J}_{VP,\,GP}\quad \text{for } i\in\{1,2\}\\
\dot{J}_{E_iP,\,D_iP} &= -j_{E_iP,\,MP}M_{VP} - (1-\kappa_{Ei})((\dot{k}_{E_iP}-j_{VP,\,GP})M_{E_iP} - (j_{E_iP,\,MP}+j_{VP,\,GP}\,y_{E_iP,\,VP})M_{VP})\\
\dot{J}_{*,\,A_iD} &= -M_{VD}\, j_{*,\,AD,m}\frac{x_*}{1+x_{PP}+x_{PD}+x_{PV}+x_{PE}}\\
\dot{J}_{ED,\,A_iD} &= -\dot{J}_{*,\,A_iD}y_{ED,\,*}\quad \text{for } (i,*)\in\{(1,PP),(2,PD),(3,PV),(4,PE)\}\\
\dot{J}_{VD,GD} &= M_{VD}\frac{m_{ED}\,\dot{k}_{ED}-j_{ED,\,MD}}{m_{ED}+y_{ED,\,VD}};\quad \dot{J}_{ED,\,DD} = -j_{ED,\,MD}M_{VD}
\end{aligned}
$$

$$
\begin{aligned}
\frac{d}{dt}M_{PP} &= \dot{J}_{PP} = \dot{J}_{PP,\,A_1C} + \dot{J}_{PP,\,A_1D};\quad \frac{d}{dt}M_{PD} = \dot{J}_{PD} = \dot{J}_{PD,\,A_2C} + \dot{J}_{PD,\,A_2D}\\
\frac{d}{dt}M_{PV} &= \dot{J}_{PV} = \dot{J}_{PV,\,HC} + \dot{J}_{PV,\,A_3D};\quad \frac{d}{dt}M_{PE} = \dot{J}_{PE} = \dot{J}_{PE,\,HC} + \dot{J}_{PE,\,A_4D}\\
\frac{d}{dt}M_{VC} &= \dot{J}_{VC} = \dot{J}_{VC,\,GC} + \dot{J}_{VC,\,HC};\quad \frac{d}{dt}M_{VP} = \dot{J}_{VP} = \dot{J}_{VP,\,GP} + \dot{J}_{VP,\,A_1C}\\
\frac{d}{dt}M_{EC} &= \dot{J}_{EC} = \dot{J}_{EC,\,GC} + \dot{J}_{EC,\,HC} + \dot{J}_{EC,\,DC} + \dot{J}_{EC,\,A_1C} + \dot{J}_{EC,\,A_2C}\\
\frac{d}{dt}M_{VP} &= \dot{J}_{VP} = \dot{J}_{VP,\,GP} + \dot{J}_{VP,\,A_1C};\quad \frac{d}{dt}M_{VD} = \dot{J}_{VD} = \dot{J}_{VD,\,A_2C} + \dot{J}_{VD,\,GD}\\
\frac{d}{dt}M_{E_iP} &= \dot{J}_{E_iP} = \dot{J}_{E_iP,\,A_1C} + \dot{J}_{E_iP,\,A_iP} + \dot{J}_{E_iP,\,GP} + \dot{J}_{E_iP,\,D_iP}\quad \text{for } i\in\{1,2\}\\
\frac{d}{dt}M_{ED} &= \dot{J}_{ED} = \dot{J}_{ED,\,A_2D} + \dot{J}_{ED,\,A_1D} + \dot{J}_{ED,\,A_2D} + \dot{J}_{ED,\,A_3D} + \dot{J}_{ED,\,A_4D} + \dot{J}_{ED,GD} + J_{ED,\,DD}\\
\frac{d}{dt}M_C &= \dot{J}_C = -\dot{J}_{PP} - \dot{J}_{PD} - \dot{J}_{PV} - \dot{J}_{PE} - \dot{J}_{VC} - \dot{J}_{EC} - \dot{J}_{VP} - \dot{J}_{E_1P} - \dot{J}_{E_2P} - \dot{J}_{VD} - \dot{J}_{ED}\\
\frac{d}{dt}M_N &= \dot{J}_N = -0.1\dot{J}_{PP} - 0.1\dot{J}_{PD} - 0.2\dot{J}_{PV} - 0.2\dot{J}_{PE} - 0.2\dot{J}_{VC} - 0.2\dot{J}_{EC} +\\
&\quad -0.2\dot{J}_{VP} - 0.4\dot{J}_{E_2P} - 0.2\dot{J}_{VP} - 0.4\dot{J}_{EP}
\end{aligned}
$$

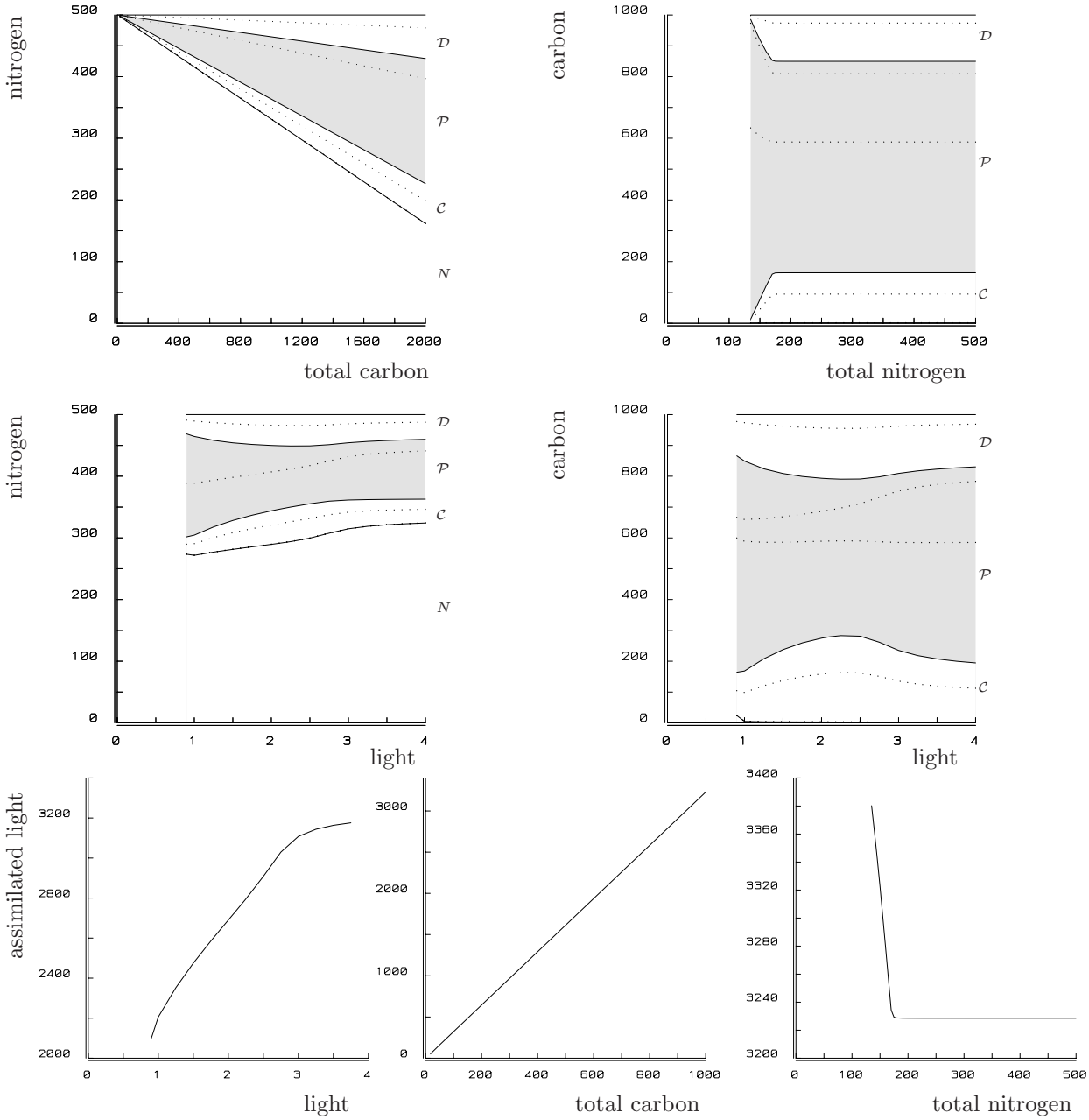

Figure 9.26: The steady-state distribution of carbon and nitrogen in the Canonical Community while increasing the total amount of carbon (upper left), nitrogen (upper right) or light (middle panels), using the DEB model for V1-morphs. The lower panels present the amounts of assimilated light (by the producers), which is proportional to the amount of dissipating heat. The non-changed amounts are 1000 units for carbon, 500 units for nitrogen, and 1000 for light. The amounts of carbon and nitrogen are plotted cumulatively, from bottom to top, for the minerals (carbon dioxide, C (very small, not labelled), or ammonia, N), detritus (very small, not labelled), consumers $\mathcal{C}$, (structure and reserve), producers $\mathcal{P}$ (structure, C- and N,C-reserves, grey shaded), decomposers $\mathcal{D}$ (structure and reserve). The producers have three carbon components, and two for nitrogen, because one reserve lacks nitrogen. An increase of light above 4 units has no effect (so all lines are horizontal).

$\frac{d}{dt}\boldsymbol{M} = \dot{\boldsymbol{J}}\mathbf{1} = \mathbf{0}$.

Figure 9.26 illustrates that an increase of total nitrogen, starting from a situation where nitrogen is limiting, shifts carbon proportionally from detritus and producers to carbon dioxide, consumers and decomposers, till it ceases to be limiting. A similar increase in carbon also results in a proportional increase in the biomass of all three living components, but ammonia decreases linearly, until it hits a threshold at which the community becomes extinct. An increase of the light level has a more complex effect on biomass. It results in a peak for the consumers and the decomposers, and a dip for the producers, while an increase beyond the level at which light ceases to be limiting has no effect at all. Assimilated light, in the lower panels of Figure 9.26, quantifies 'the rate of living'. It is curious to note that 'the rate of living' is *de*creasing for *in*creasing nitrogen, as long as nitrogen is limiting. Ammonia is practically absent if nitrogen is strongly limiting, all nitrogen is then fixed into the biota. This corresponds well with widely known qualitative observations: nitrogen minerals are extremely low in oligotrophic systems (lakes, oceans as well as rain forests).

The Canonical Community can be simplified to a two-species, or even a single-species, community of mixotrophs. Since grazing no longer limits life span, aging has to be taken into account for proper behaviour. The Canonical Community can also be extended in many ways: inclusion of exchange with the outside world and of spatial structure, and replacement of consumers by a food web of consumers, or of producers and decomposers by sets of competing producers and decomposers. Some of these extensions can be developed systematically.

9.5 Summary

This chapter deals with the metabolic interactions between individuals, and shows that individuals depend on each other in many ways; the boundaries between individuals can be somewhat vague, and the notion of ecosystem metabolism is developed.

Trophic interactions span a spectrum from competition, via syntrophy, symbiosis and biotrophy, to predation. The strength of the DEB theory is illustrated in the setup of a full quantitative specification of partners in a symbiontic relationship. The effects of calcification can be evaluated in corals, for instance, and environmental conditions specified where the host does not gain from the symbiont.

Populations can be considered as a set of individuals; their dynamics follows from the eco-physiological behaviour of individuals, when the environment in which they live is specified. Spatial structure is very important, but not considered in this text. The distinction between individuals and populations disappears for V1-morphs in the DEB theory. I show how popular models by Monod, Marr–Pirt, Droop, Lotka–Volterra and the logistic one can be considered as special cases of the DEB model, which also have intriguing implications for the internal dynamics of population structure. Synchronization of life cycles among individuals can occur spontaneously. Variations in parameter values, in combination with a set of rules that specify how the values carry over to new generations, imply selective forces that lead to speciation.

Food chains can show very complex dynamics if the chain length exceeds two. Multiple

attractors occur easily, sometimes of the chaotic type. Examples illustrate the application of bifurcation analysis, and a canonical one-dimensional map exists for tri-trophic chains. Contrary to general insight, an increase in diversity can go with an increase in stability in homogeneous environments for more realistic dynamics.

Canonical Communities serve to illustrate the metabolic interactions between producers, consumers and decomposers as quantified by the DEB theory. If fully closed for mass, the community seems to increase metabolic activity for decreasing nitrogen levels, up to a threshold value, while the activity is proportional to the carbon levels, and satiating in the light levels. The analysis of Canonical Communities unifies the traditionally separated characterizations of ecosystems in terms of structure and function; this separation makes no sense in the context of the DEB theory.

Chapter 10

Evaluation

The aim of this short chapter is to place the DEB model in the context of research in eco-energetics, and to evaluate some of its concepts. The chapter loops back to the general introduction in the first chapter, and especially to the section on modelling, cf. {7}. I first focus on the DEB theory, as presented in this book, then follows a comparison with some other approaches to the subject of energetics.

10.1 Energetics and metabolism

Metabolism can be defined as the chemical transformation of chemical compounds (in living systems), which has energetic aspects. These energetic aspects are sometimes particularly interesting themselves; for example, the thermal balance of endotherms, or the dissipation of heat in bioreactors, or particular stoichiometries in biochemical reactions. The main role of energy in the context of the DEB theory, however, is that of an abstract variable that has close links with transformations of chemical compounds. The fluxes of many compounds through organisms are frequently closely linked to each other, and rather than following one particular compound, energy is followed. This has several advantages in systems that can be understood with only one reserve component as state variable. If the fluxes of various compounds are not closely linked, such as in photoautotrophic systems, this simplification breaks down and we need to follow a set of compounds, as well as energy (in the form of light and dissipating heat). This extension can be considered as a multi-variate analogue of the mono-variate situation.

The significance of energy as the major player in the metabolic game, is that we can have little hope of understanding the multi-variate situation if we do not understand the mono-variate one. So energy itself is not considered to be much more important than any particular chemical compound, but the transformation of chemical compounds can be simplified in a particular way using energy as a descriptor. Although the thermodynamic basis of the detailed relationship between energy and compounds in living systems is incredibly complex, arguments are presented {35} that support a very simple approximate relationship that seems adequate for almost all practical purposes.

10.2 Principles of the DEB theory

Objective

The major objective of the DEB theory is to formulate a consistent framework for quantitative bioenergetics that helps us to connect the different levels of organization: from molecules to ecosystems. The core of the theory is a model for the energetics of an individual, as it changes during the life cycle. The objective implies that this model must not be species specific, and weighs the criterion 'generality' with respect to 'realism' and 'simplicity'. One might think that such a generic model must result in poor fits with experimental data, but this does not seem to be the case. The conclusion, therefore, must be that the DEB theory is very useful, for the time being. Much work remains to be done, however, both in terms of testing against experimental data and on further developing consistent theory for the molecular and the ecosystem levels.

Systems theory as the model language

All acceptable models about energetics should be formulated in terms of dynamic systems, or, at least, it must be possible to re-formulate them that way. The DEB model satisfies this requirement, as it has state variables, inputs and outputs, and explicit rules for changes of state. It is thus possible to represent the individual as a point in the state space, which is spanned by scaled length, scaled reserve density and accumulated damage. As time passes, the point moves through the state space. Individuals appear with zero scaled length, infinite scaled reserve density, and no damage, and disappear at death. In a population there are many individuals around, so many points are moving simultaneously through the state space for individuals. The population can be monitored as a changing frequency distribution of individuals in the state space for individuals.

Consistency

Consistency has priority over realism for judging mechanistic models. The first reason is that models are idealizations, so a certain lack of realism is to be expected. Second, the realism of an internally inconsistent model cannot be satisfactory, because of the absence of a link with explanatory mechanisms. Since an experienced modeller knows many ways to improve a fit for a particular data set, a good fit itself does not provide substantial support for the model. Although it is relatively easy to adapt a model, it is much more difficult to adapt the list of assumptions from which such a model should follow. Finally, a lack of realism does not necessarily imply a fault in the model; the data themselves may be suspect too. Lack of realism only says that model predictions and data are inconsistent, again underlining the importance of inconsistency. Nevertheless, lack of fit is certainly a good reason for reconsidering the model assumptions.

To illustrate the far-reaching implications of model assumptions, I want to point to a problem with the predecessor of the DEB model, which became known as the Kooijman–Metz model [524]. It is still applied because of its putative simplicity [56,786,787] and differs from the DEB model by disregarding reserves.

The problem concerns what happens if food is (during a very short period) insufficient for maintenance. The obvious route is to assume instantaneous death, but this is not realistic. One option is to decrease maintenance temporarily as far as necessary (although no biological arguments are known to me) and to assume that time until death follows an exponential distribution. Survival is then no longer coupled explicitly to the internal state of the organism. Although this problem can be solved by introducing an extra state variable, which could be called 'damage', the model then loses its simplicity. If maintenance is paid from food, if available, otherwise from biomass, problems become apparent as soon as one tries to set up mass balances using models that include maintenance but not reserves. We need at least one extra parameter, a switch, and a much more complex description of mass transformations. The price for refraining from modelling reserves is high; we have to give up modelling the embryonic stage, and new parameters appear that specify embryonic costs and incubation periods. Moreover, no useful body size scaling relationships can be based on a model without reserves. Furthermore, the modelling of product formation is problematic (because assimilation, maintenance and growth span up a vector space of two dimensions only), and modelling the kinetics of lipophilic compounds is hardly feasible. The conclusion is that, although the inclusion of reserves is not always essential for obtaining realism with all types of data (e.g. data on growth at one constant level of food availability), neglecting reserves greatly limits the scope of a model.

Consistency arguments easily lead to the conclusion that at least one reserve should consist of a generalized compound, rather than a set of pure compounds, to accommodate all essential nutrients that are not modelled explicitly. The same argument also implies that assimilation must be close to the minimum type, where a single nutrient limits growth, to avoid the unrealistic implication that non-modelled nutrients must be present at very high densities to guarantee that they do not affect assimilation. (The frequently applied multiplicative model for nutrient uptake fails this consistency test.) The requirement that reserves can be gradually coupled to reduce the number of freely varying reserves greatly restricts the class of possible dynamics for reserves. This consistency requirement is imposed by the process of evolution for reserves consisting of pure compounds, while the argument is basic for reserves consisting of generalized compounds. I have shown that the partionability requirement for reserves, in combination with the weak homeostasis assumption, not only fully determines reserve dynamics, but also imposes constraints on allocation rules.

Conservation laws

Cornerstones of the DEB theory are the mass and energy conservation laws. They constitute a special kind of consistency argument. This might seem trivial to non-biologists, but most existing theories and models in physiology and population dynamics do not observe these laws explicitly, and frequently violate them. The application of these conservation laws to very open systems, such as living organisms, is not always easy. It implies a strict homeostasis for each body component and a simple coupling between mass and energy fluxes.

The minimum number of body components for realistic models that cover all life stages

seems to be two. The description of nutrient limitations requires more than one type of reserve, plants require more than one type of structural body mass, because they use different organs for the uptake of the various nutrients and they are very flexible in the resource allocation to these organs. The assumption that mass fluxes are proportional to surface areas seems to be quite natural (i.e. it has an obvious physical interpretation), which makes the scaling between surface areas and body mass particularly important. This introduces a morphological element into the study of mass and energy fluxes. The representation of the complex chemical reaction that specifies the growth and reproduction process in terms of a vector of reaction rates, together with stoichiometric constraints, is a direct implication of the application of mass and energy conservation laws.

Apart from energy and mass, time is also a conserved quantity and time budgets play a central role in feeding behaviour. This conservation law is at the basis of the hyperbolic (Holling type II) functional response: the uptake system does not 'accept' arriving food particles when it is busy processing a food particle; one behavioural component excludes another at the same moment. In particular cases, it makes sense to elaborate on this and account for time lost for feeding because of social interactions, for instance. This approach is central to the optimal foraging theory [883], which deals with priorities that individuals have for activities that maximize some fitness measure. It is not difficult to see that behavioural components can in principle be optimized, because the individual has, to some extent, the freedom to choose. Even in this situation, however, there are doubts that this actually leads to profound insight [710]. Behavioural and physiological components are closely linked, and the individual has less freedom to choose from physiological options. A field that is known as life history theory [780,878] extends the argument to include physiological components in the evolutionary optimization of fitness. This is a grey area, where the success of such an approach depends sensitively on the constraints considered. The DEB theory provides such a set of constraints, which restricts optimization arguments to parameter values.

Generality

The DEB theory is extreme in the point of view that assumptions regarding the eco-physiological behaviour of organisms apply to all species in all life stages, unless it is obvious from the nature of the assumption that it applies only to a limited set of species and/or stages. Comparison of species helps to distinguish species-specific assumptions from the general ones. Models that restrict the maximum body size of female animals by allocating an increasing amount of resources to reproduction, for instance, are problematic because of the existence of males, which do have a restricted maximum body size but are not able to allocate this way; sex determination is frequently affected by environmental factors. Size control should be implemented in a way that applies to both females and males. Other examples: juveniles differ energetically from embryos only by feeding, heterotrophs only differ from autotrophs in the way they obtain the substrate for the formation of reserves. Observations of one species or stage are used to structure the modelling of the energetics of another. The approach has proven to be successful, in my judgement.

Mechanisms

The DEB theory is built on a relatively short list of assumptions that can be called 'mechanistic'. Although any statement has descriptive aspects, the easiest test for being mechanistic is in applications to other situations and in the possibility of formulating models at a lower level or organization that result in the model of interest, see {246}. Descriptive models only apply to the situation for which they are made; models based on mechanistic assumptions can be constructed for new situations, using supplementary situation-specific assumptions. The mathematical formulations differ from one situation to another, but the mechanistic assumptions remain the same. Many examples have been worked out in this book.

Hierarchy in metabolic organization

The types of assumptions used to specify the DEB model for the individual imply a supposed hierarchy in the organization of metabolism. The generation and use of ATP, for instance, is part of the machinery cells use to couple the degradation and formation of particular compounds, but ATP dynamics is not given an organizing role. ATP change is the focus of bioenergetics, mainly because it can be used to *measure* the difference in free energy between substrate and product. Hormones are considered to be compounds that organisms use to regulate and couple particular processes, by binding them to receptors to induce action. Hormones themselves do not organize metabolism; this is the task of model components higher up in the hierarchy, that controls the dynamics of the hormones. The hierarchy in metabolic control is a concept that is basic to understanding why the DEB model is appropriate for organisms that differ in the hormones they use. The concept is implied by the use of generalized compounds, such as structural body mass and reserves, rather then actual compounds, such as particular proteins. A full understanding of metabolism involves modules that show how actual compounds relate to generalized compounds in detail. Much work still has to be done to formulate such modules as part of the metabolic regulation system. It will be exciting to discover to what extent these regulation systems are not species specific.

Support and testability

A lot of effort went into empirical tests of evaluations on the basis of data collected from the literature. Adequate tests, however, require experimental programs specifically designed to test the theory.

Since models are simplifications and idealizations of the empirical world, it must always be possible to detect differences between model predictions and experimental data. This certainly applies to the DEB model, because it is really simple, while organisms are not.

When models have a large number of parameters, it usually implies that they are very flexible, and can always be fitted successfully to any experimental data set, even if the underlying assumptions lack any realism. This is why such effort has been invested to keep the DEB model as simple as possible. The possibility of testing the model for realism steeply increases if combinations of different types of data can be fitted *simultaneously*. If

the data only included weight as a function of age, for instance, a successful fit would give little support in the absence of knowledge about food availability, feeding rate, respiration, temperature, etc. If the data include information on all of these quantities, and the simultaneous fits are still satisfactory, the support increases substantially.

An important aspect of theoretical work is to classify the assumptions as general or specific. The general assumptions of the DEB model provide the theoretical basis for the mass–energy coupling, and for the empirical method of indirect calorimetry. The specific assumptions can be changed without affecting this theoretical basis. Any attempt to change the general assumptions, however, involves changes in the specific ones as well. Such changes should deal with the problem of understanding how the method of indirect calorimetry is so successful. Any attempt to change the strong homeostasis assumption, to allow for changes in the chemical composition of structural mass and/or reserves, should deal with the problem of how to quantify their amounts. Quantifications in terms of weights, volumes and carbon contents, for instance, are then no longer equivalent, and I can see no argument for a choice of one of these measures. (This is why more state variables should be introduced to increase the flexibility of chemical composition, rather than changing the strong homeostasis assumption.) These examples show the existence of a natural hierarchy in assumptions, which is most useful for developing a sound theoretical framework for metabolic organization. We can more easily change the specific assumptions and study the implications for the system's performance, while we need strong arguments to change the more general assumptions. Models that only differ in specific assumptions are more related to each other than models that differ in general assumptions. This can be a basis for the delineation of a family tree for models.

I consider the correct predictions for the body size scaling relationships as the strongest empirical support for the conclusion that the DEB model captures the main features in animal energetics quite realistically. The derivation of the body size scaling relationships applies to all models that allow a classification of the parameters as intensive and extensive, while the ultimate body size can be written as a function of parameters. The resulting relationships depend on the model, of course.

In each particular practical situation that requires interpretation of quantitative data, aspects and/or factors are involved that are specific for that particular situation, as are aspects that are more general and relate to general underlying principles. The significance of a mechanistic approach is to recognize these aspects, and decompose the signal into its various components. With the aid of a theory for the general aspects, the task of understanding the signal reduces to understanding the aspects that are specific for that situation. If the purpose is to test a theory for realism, it helps to select experimental conditions such that hardly any situation-specific aspects are involved. Testability is not a property of a theory only, but of the theory in combination with an experimental setup and the data collected from the experiments. Moreover, testability comes in gradations; it is simpler to study the various contributing processes one by one, rather than in combination. However, this is frequently not possible. The implication is that assumptions can usually only be tested for realism in bundles [487], which complicates the process of identifying the unrealistic assumption(s).

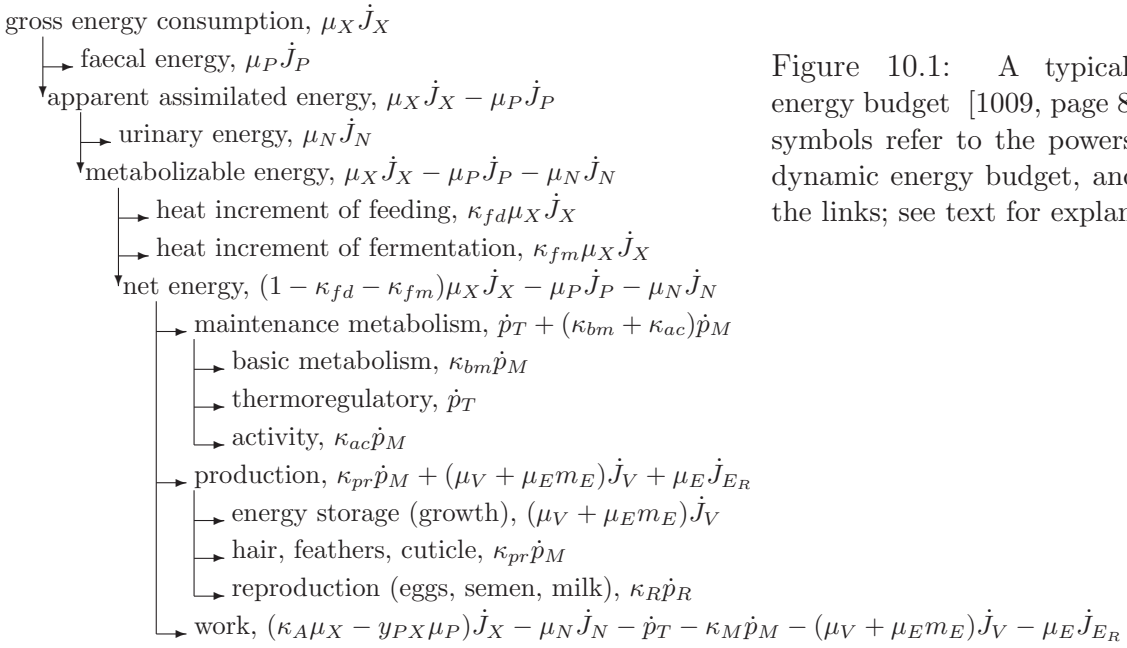

Figure 10.1: A typical static energy budget [1009, page 87]. The symbols refer to the powers in the dynamic energy budget, and reveal the links; see text for explanation.

10.3 Other approaches

10.3.1 Static Energy Budgets

Most of the literature on animal energetics concerns Static Energy Budgets (SEBs). The term budget refers to the conservation of energy, i.e. the various allocated powers add to the power input. SEBs can only be compared to DEBs at steady state, by averaging over a sufficient number of meals, but not so many that size changes. Figure 10.1 gives the relationship between both approaches. The following differences exist

- SEB deals with energies that are fixed in the different products, while DEB deals with energies allocated to assimilation, maintenance and growth; the difference is in the overhead costs. The reconstruction assumes that the SEB balance is complete, so no products are formed coupled to growth, and also that we are dealing with an adult, and are using a combustion frame of reference (the energy content of oxygen, carbon dioxide, water and ammonia is set to zero). Some of the mapping depends on details of how the quantities are actually measured. The total balance sheet amounts to $\mu_X \dot{J}_X = \mu_P \dot{J}_P + (\mu_V + \mu_E m_E) \dot{J}_V + \kappa_R \dot{p}_R + \mu_N \dot{J}_N + \dot{p}_{T+}$, or $\dot{p}_A = \dot{p}_M + \dot{p}_J + \dot{p}_T + (1 + m_E y_{VE}) \dot{p}_G + \dot{p}_R$.

- 'faecal energy' represents a fixed fraction of 'gross energy consumption' in DEB, so $\mu_P \dot{J}_P = \mu_P y_{PX} \dot{J}_X$.

- 'urinary energy' is decomposed in DEB into contributions from assimilation, maintenance and growth: $\dot{J}_N = \dot{J}_{N,A} + \dot{J}_{N,M} + \dot{J}_{N,G}$. Subtraction from the 'apparent assimilation energy' complicates the mapping of the remaining energy to maintenance and (re)production.

- 'heat increment of feeding' and of 'fermentation' are included in the overhead costs of assimilation and, therefore, fractions of the 'gross energy consumption'. The fractions κ_{fd} and κ_{fm} are constants.
- 'net energy' equals $\dot{p}_A - \mu_N(\dot{J}_{N,M} + \dot{J}_{N,G})$, assuming that both heat increments cover all assimilation overheads, except for the assimilation part of urinary energy. It follows that $\kappa_{fd} + \kappa_{fm} = \frac{1-y_{PX}\mu_P/\mu_X}{1+\mu_N\eta_{NA}}$.
- 'basic metabolism', 'activity', and 'hair, feather, cuticle' are all fractions of somatic maintenance costs in DEB, so $\kappa_{bm} + \kappa_{ac} + \mu_N \dot{J}_{NM}/\dot{p}_M = 1$. This mapping includes the overhead costs of maintenance in 'basic metabolism', the correctness depending on the way it is measured.
- 'energy storage' includes the energy fixed in new reserves and new structural mass. Notice that $\mu_V \dot{J}_V < \dot{p}_G$; the overhead costs of growth in DEB go into 'work' in SEB.
- 'milk production' (of female mammals) comes with a temporal change in the parameters $\{\dot{J}_{Xm}\}$ and $\{\dot{p}_{Am}\}$ in DEB.
- 'work' includes part of the overhead costs of growth and maintenance in SEBs' balance sheet. The abbreviations $\kappa_A = 1 - \kappa_{fd} - \kappa_{fm}$ and $\kappa_M = \kappa_{bm} + \kappa_{ac} + \kappa_{pr}$ have been made. Alternative expressions are: $\dot{p}_A - \dot{p}_M - \dot{p}_T - \kappa_R\dot{p}_R - \mu_N\dot{J}_{N,G} - (\mu_V + \mu_E m_E)\dot{J}_V = \dot{p}_G(1 + m_E y_{VE}) + \dot{p}_R(1 - \kappa_R) + \dot{p}_J - \mu_X\dot{J}_X + \mu_p\dot{J}_P + \kappa_R\dot{p}_R + \dot{p}_{T+} = \dot{p}_{T+} + \dot{p}_J + \dot{p}_R + \dot{p}_G(1 + y_{VE}m_E) + \mu_P\dot{J}_P - \mu_X\dot{J}_X$.

The significance of including certain energy allocations in the overhead of others is in the comparison of energy budgets, both between different organisms and with respect to changes in time. Such inclusions greatly simplify the structure of energy budgets, and reduce the flexibility, i.e. reveal patterns of covariation of allocations. It boils down to the sharp distinction that DEBs make between the power allocated to, for example, growth, and the power that is actually fixed in new biomass; SEBs can only handle the energy that is fixed in new biomass, because the energy allocated to growth can only be assessed indirectly via changes of the budget in time. The reconstruction beautifully shows that 'work' has many contributions in SEB, and cannot be interpreted easily. The term is misleading, by suggesting that the individual can spend it freely.

Von Bertalanffy [77] related the respiration rate to the rate of anabolism. I cannot follow this reasoning. At first sight, synthesis processes are reducing by nature, which makes catabolism a better candidate for seeking a relationship with respiration. In the standard static budget studies, respiration rates are usually identified with maintenance metabolism. These routine metabolic costs are a lump sum, including the maintenance of concentration gradients across membranes, protein turnover, regulation, transport (blood circulation, muscle tonus), and an average level of movement. The Scope For Growth (SFG) concept rests on this identification. The idea behind this concept is that energy contained in faeces and the energy equivalent of respiration are subtracted from energy derived from food, the remainder being available for growth [60]. The SFG concept is built on SEBs, {365}. In the DEB model, where energy derived from food is added to the reserves, the

most natural candidate for a relationship with respiration is the rate at which the reserves are used. This is underpinned on {135}.

Although respiration rates are measured over short periods (typically a couple of minutes) and the actual growth of the body is absolutely negligible, the energy investment in growth can still be substantial. Parry [688] estimates the cost of growth between 17 and 29% of the metabolism of an 'average' ectotherm population. The respiration rate includes routine metabolic costs as well as costs of growth [796]. This interpretation is, therefore, incompatible with the SFG concept. Since the DEB model does not use respiration rates as a primary variable, the interpretation problems concerning respiration rates only play a role in testing the model.

10.3.2 Net production models

The DEB model assumes that assimilates are added to reserves, and reserves are used to fuel other metabolic processes (maintenance, growth, development, reproduction). R. Nisbet proposed the term assimilation models for models based on this assumption, to distinguish them from net production models. The latter models first subtract maintenance costs from assimilates, before allocation to other metabolic processes occurs. Several net production models have been worked out [20,359,560,669,791]. Both types of models classify as DEB models, and it will not always be easy to use experimental data to choose between the two possibilities.

One problem is that only fully specified models can be tested with experimental data; one has to specify all allocation rules. The models then differ in more than one respect, because it is not possible to change the way of paying maintenance without changing the allocation to growth in the DEB model. This hampers firm conclusions with respect to the choice between assimilation and production models. Moreover, small differences in goodness of fit can hardly be used to make such a judgement. The cause of a lack of fit can be another assumption about allocation. Differences in goodness of fit are sometimes small [791].

The choice of an assimilation structure rather than a net production structure is primarily motivated by simplicity in several respects, including mechanistic arguments with respect to metabolic control. The first argument is that embryos do not feed, but nevertheless have to pay maintenance costs. Net production models then suffer from the choice of letting embryos differ from juveniles by allowing embryos to pay maintenance from reserves, or treating yolk as a new state variable that is typical for embryos [560]. The second argument is that if feeding is not sufficient to pay maintenance costs, they have to be paid from reserves; it does not seem realistic to assume that an animal dies from starvation while it has lots of reserves. Most animals feed on meals anyway, while the storage in the gut cannot explain the survival between the meals. Net production models must, therefore, contain elements of assimilation models, and switches have to be installed to pay maintenance from assimilates and/or from reserves. The analysis of the mathematical properties of models with switches rapidly becomes more problematic with the number of switches. The feeding and reproduction switch seems to be unavoidable for all energetic models. This set of arguments relates to the organization of metabolism, which is much

more independent of the environment in assimilation models than in net production models. This allows a simpler regulation system for metabolism, which is mainly driven by signals from the nutritional state of the organism itself, rather than from signals directly taken from the environment.

The net production models that are presently available have many more parameters than the assimilation model in this book; the simplest and best comparable production model is that formulated by Lika and Nisbet [560]. Besides structural mass, its state variables include yolk (in the embryonic stage), reserves and the maximum experienced reserve density in the juvenile and adult stages. Although it is possible to simplify net production models and reduce the number of parameters, I am convinced that they need more parameters and state variables than assimilation models with a comparable amount of detail. This is because they have to handle switches, and specify growth investment in a more complex way. The parameter κ of the assimilation model in this book specifies the investment in growth (plus somatic maintenance) versus reproduction (plus maturity maintenance); growth ceases automatically when the energy allocated to growth plus somatic maintenance is required for somatic maintenance. Reproduction can continue, while growth ceases. Net production models need at least one extra parameter to obtain this type of behaviour. Maintenance in net production models is paid for by food if possible, but from reserves if necessary, which requires an extra parameter for the maintenance costs. Maintenance is always paid from reserves in assimilation models (except in extreme starvation during shrinking). The number of parameters and state variables is a measure of the complexity of a model.

The mechanism for reserve dynamics and weak homeostasis that is proposed here, structural homeostasis {246}, does not apply to net production models. I expect that it is difficult to implement weak homeostasis mechanistically in net production models. If true, this means that biomass composition is changing, even at steady state, and structure always has to be disentangled from reserves in tests against experimental data. I also expect that it is difficult to derive realistic body size scaling relationships and to explain the method of indirect calorimetry on the basis of net production models.

Since reserves are wired prior to allocation to reproduction in production models, and not used for growth, they are hard to apply to dividing organisms, such as micro-organisms. The growth of plant biomass from tubers, and growth during starvation (cf. Figure 7.3), for instance, are also hard to implement; it needs an extra state variable similar to yolk in the embryo.

Toxic compounds, parasites or the light regime can change the value of κ, which has complex consequences (growth is reduced and development lasts for a shorter time and/or reproduction is greater because of the higher investment, which is partially cancelled by the reduction of assimilation due to reduced growth). These complex changes can be described realistically with effects on a single parameter in the present assimilation model, while net production models need a more complex description that involves effects on more parameters. This type of perturbation of metabolism is perhaps the strongest argument in favour of assimilation models.

Bibliography

[1] K. Aagaard. Profundal chironimid populations during a fertilization experiment in Langvatn, Norway. *Holarct. Ecol.*, **5**:325–331, 1982.

[2] P. Abrams. Indirect interactions between species that share a predator: varieties of indirect effects. In W. C. Kerfoot and A. Sih, editors, *Predation; direct and indirect impacts on aquatic communities*, pages 38–54. Univ. Press of New England, Hanover, 1987.

[3] R. A. Ackerman. Growth and gas exchange of embryonic sea turtles (*Chelonia*, *Caretta*). *Copeia*, **1981**:757–765, 1981.

[4] R. A. Ackerman. Oxygen consumption by sea turtle (*Chelonia*, *Caretta*) eggs during development. *Physiol. Zool.*, **54**:316–324, 1981.

[5] R. A. Ackerman, G. C. Whittow, C. V. Paganelli, and T. N. Pettit. Oxygen consumption, gas exchange, and growth of embryonic wedge-tailed shearwaters (*Puffinus pacificus chlororhynchus*). *Physiol. Zool.*, **53**:201–221, 1980.

[6] W. Agosta. *Bombardier beetles and fever trees.* Addison Wesley, 1995.

[7] D. L. Aksnes and J. K. Egge. A theoretical model for nutrient uptake in phytoplankton. *Mar. Ecol. Prog. Ser.*, **70**:65–72, 1991.

[8] A. H. Y. Al-Adhub and A. B. Bowers. Growth and breeding of *Dichelopandalus bonnieri* in Isle of Man Waters. *J. Mar. Biol. Assoc. U. K.*, **57**:229–238, 1977.

[9] A. W. H. Al-Hakim, M. I. A. Al-Mehdi, and A. H. J. Al-Salman. Determination of age, growth and sexual maturity of *Barbus grypus* in the Dukan reservoir of Iraq. *J. Fish Biol.*, **18**:299–308, 1981.

[10] M. Aleksiuk and I. M. Cowan. The winter metabolic depression in Arctic beavers (*Castor canadensis* Kuhl) with comparisons to California beavers. *Can. J. Zool.*, **47**:965–979, 1969.

[11] R. McN. Alex. *Energy for animal life.* Oxford University Press, 1999.

[12] R. McN. Alexander. *Dynamics of dinosaurs and other extinct giants.* Columbia Universty Press, New York, 1989.

[13] R. McN. Alexander. *Exploring biomechanics; animals in motion.* Scientific American Library, New York, 1992.

[14] V. Y. Alexandrov. *Cells, molecules and temperature.*, volume 21 of *Ecol. Stud.* Springer-Verlag, Berlin, 1977.

[15] A. L. Alldredge. Abandoned larvacean houses. A unique food source in the pelagic environment. *Science (New York)*, **177**:885–887, 1972.

[16] A. L. Alldredge. Discarded appendicularian houses as sources of food, surface habitats and particulate organic matter in planktonic environments. *Limnol. Oceanogr.*, **21**:14–23, 1976.

[17] A. L. Alldredge. House morphology and mechanisms of feeding in *Oikopleuridae* (*Tunicata*, *Appendicularia*). *J. Zool. Lond.*, **181**:175–188, 1977.

[18] T. F. H. Allen and T. B. Starr. *Hierarchy. Perspectives for ecological complexity.* University of Chicago Press, 1982.

[19] B. N. Ames, J. McCann, and E. Yamasaki. Methods for detecting carcinogens and mutagens with *Salmonella*/mammalian microsome mutagenicity test. *Mutat. Res.*, **31**:347–364, 1975.

[20] T. R. Andersen. *Pelagic nutrient nycles – Herbivores as sources and sinks.*, volume 129 of *Springer Ecological Studies.* Springer Verlag, Berlin, 1997.

[21] S. G. E. Anderson, A. Zomorodipour, J. O. Andersson, T. Sicheritz-Pontén, U. C. M. Alsmark, R. M. Podowski, A. K. Näslund, A.-S. Eriksson, H. H. Winkler, and C. G. Kurland. The genome sequence of *Rickettsia prowazekii* and the origin of mitochondria. *Nature*, **396**:133–140, 1998.

[22] A. W. Angulo y González. The prenatal growth of the albino rat. *Anat. Rec.*, **52**:117–138, 1932.

[23] A. D. Ansell. Reproduction, growth and mortality of *Venus striatula* (Da Costa) in Kames Bay, Millport. *J. Mar. Biol. Assoc. U. K.*, **41**:191–215, 1961.

[24] R. S. Appeldoorn. Variation in the growth rate of *Mya arenaria* and its relationship to the environment as analyzed through principal components analysis and the ω parameter of the von Bertalanffy equation. *J. Fish Biol.*, **81**:75–84, 1983.

[25] T. Appenzeller. Argentine dinos vie for heavyweight titles. *Science*, **266**:1085, 1994.

[26] A. Ar and H. Rahn. Interdependence of gas conductance, incubation length, and weight of the avian egg. In J. Piiper, editor, *Respiration function in birds*. Springer-Verlag, Berlin, 1978.

[27] K. Arbaĉiauskas and Z. Gasiūnaitė. Growth and fecundity of *Daphnia* after diapause and their impact on the development of a population. *Hydrobiologia*, **320**:209–222, 1996.

[28] R. Arking. *Biology of aging*. Sinauer Assoc. Inc., Sunderland, MA, 1998.

[29] E. A. Armstrong. *The wren*. The New Naturalist. Collins, London, 1955.

[30] N. Armstrong, R. E. Chaplin, D. I. Chapman, and B. Smith. Observations on the reproduction of female wild and park Fallow deer (*Dama dama*) in southern England. *J. Zool. Lond.*, **158**:27–37, 1969.

[31] D. K. Arrowsmith and C. M. Place. *An introduction to dynamical systems*. Cambridge University Press, 1990.

[32] D. K. Arrowsmith and C. M. Place. *Dynamical systems. Differential equations, maps and chaotic behaviour*. Chapman & Hall, London, 1992.

[33] P. W. Atkins. *Physical chemistry*. Oxford University Press, 1989.

[34] M. Atlas. The rate of oxygen consumption of frogs during embryonic development and growth. *Physiol. Zool.*, **11**:278–291, 1938.

[35] H. J. W. de Baar. von Liebig's law of the minimum and plankton ecology. *Prog. Oceanogr.*, **33**:347–386, 1994.

[36] F. G. Bader. Analysis of double-substrate limited growth. *Biotechnol. Bioeng.*, **20**:183–202, 1978.

[37] T. Baekken. Growth patterns and food habits of *Baetis rhodani*, *Capnia pygmaea* and *Diura nanseni* in a west Norwegian river. *Holarct. Ecol.*, **4**:139–144, 1981.

[38] T. B. Bagenal. The growth rate of the hake, *Merluccius merluccius* (L.), in the Clyde and other Scottish sea areas. *J. Mar. Biol. Assoc. U. K.*, **33**:69–95, 1954.

[39] T. B. Bagenal. Notes on the biology of the schelly *Coregonus lavaretus* (L.) in Haweswater and Ullswater. *J. Fish Biol.*, **2**:137–154, 1970.

[40] J. E. Bailey and D. F. Ollis. *Biochemical engineering fundamentals*. McGraw-Hill, London, 1986.

[41] R. Bakker. *The dinosaur heresies*. Longman, London, 1986.

[42] R. T. Bakker. Anatomical and ecological evidence of endothermy in dinosaurs. *Nature*, **238**:81–85, 1972.

[43] J. H. van Balen. A comparative study of the breeding ecology of the great tit *Parus major* in different habitats. *Ardea*, **61**:1–93, 1973.

[44] C. A. M. Baltus. De effekten van voedselregime en lood op de eerste reproduktie van *Daphnia magna*. Technical report, Dienst DBW/RIZA, 1990.

[45] M. C. Barber, L. A. Suárez, and R. R. Lassiter. Modeling bioconcentration of nonpolar organic pollutants by fish. *Environ. Toxicol. Chem.*, **7**:545–558, 1988.

[46] J. Barcroft. *Researches on pre-natal life.*, volume 1. Blackwell Sci. Publ., Oxford, 1946.

[47] J. Barcroft, R. H. E. Elliott, L. B. Flexner, F. G. Hall, W. Herkel, E. F. McCarthy, T. McClurkin, and M. Talaat. Conditions of foetal respiration in the goat. *J. Physiol. (Lond.)*, **83**:192–214, 1935.

[48] J. Barcroft, L. B. Flexner, W. Herkel, E. F. McCarthy, and T. McClurkin. The utilization of oxygen by the uterus in the rabbit. *J. Physiol. (Lond.)*, **83**:215–221, 1935.

[49] C. Barreto, R. M. Albrecht, D. E. Bjorling, J. R. Horner, and N. J. Wilsman. Evidence of the growth plate and the growth of long bones in juvenile dinosaurs. *Science*, **262**:2020–2023, 1993.

[50] G. A. Bartholomew and D. L. Goldstein. The energetics of development in a very large altricial bird, the brown pelican. In R. S. Seymour, editor, *Respiration and metabolism of embryonic vertebrates*, pages 347–357. Dr. W. Junk Publishers, Dordrecht, 1984.

[51] I. V. Basawa and B. L. S. P. Rao. *Statistical inference for stochastic processes*. Academic Press, London, 1980.

[52] G. C. Bateman and R. P. Balda. Growth, development, and food habits of young Pinon jays. *Auk*, **90**:39–61, 1973.

[53] J. F. Battey. Carbon metabolism in zooxanthellae-coelenterate symbioses. In W. Reisser, editor, *Algae and symbioses*, pages 153–187. Biopress Ltd, Bristol, 1992.

[54] E. H. Battley. Calculation of entropy change accompanying growth of *Escherichia coli* K-12 on succinic acid. *Biotechnol. Bioeng.*, **41**:422–428, 1993.

[55] B. Baule. Zu Mitscherlichs Gesetz der physiologischen Beziehungen. *Landw. Jahrb.*, **51**:363–385, 1917.

[56] H. Baveco. *Population dynamics in object-oriented and individual-based models*. PhD thesis, Amsterdam University, 1997.

[57] J. L. Baxter. A study of the yellowtail *Seriola dorsalis* (Gill). *Fish. Bull. (Dublin)*, **110**:1–96, 1960.

[58] B. L. Bayne, A. J. S. Hawkins, and E. Navarro. Feeding and digestion by the mussel *Mytilus edulis* L. (*Bivalvia*, *Mollusca*) in mixtures of silt and algal cells at low concentrations. *J. Exp. Mar. Biol. Ecol.*, **111**:1–22, 1987.

[59] B. L. Bayne, A. J. S. Hawkins, E. Navarro, and I. P. Iglesias. Effects of seston concentration on feeding, digestion and growth in the mussel *Mytilus edulis*. *Mar. Ecol. Prog. Ser.*, **55**:47–54, 1989.

[60] B. L. Bayne and R. C. Newell. Physiological energetics of marine molluscs. In A. S. M. Saleuddin and K. M. Wilbur, editors, *Physiology*, volume 4 of *The Mollusca*, chapter 1. Academic Press, London, 1983.

[61] M. J. Bazin and P. T. Saunders. Determination of critical variables in a microbial predator–prey system by catastrophe theory. *Nature (Lond.)*, **275**:52–54, 1978.

[62] R. C. Beason and E. C. Franks. Development of young horned larks. *Auk*, **90**:359–363, 1983.

[63] J. J. M. Bedaux and S. A. L. M. Kooijman. Stochasticity in deterministic models. In C. R. Rao, G. P. Patil, and N. P. Ross, editors, *Handbook of statistics 12: Environmental statistics.*, pages 561–581. Elsevier Science B. V., Amsterdam, 1994.

[64] W. N. Beer and J. J. Anderson. Modelling the growth of salmonid embryos. *J. theor. Biol.*, **189**:297–306, 1997.

[65] D. J. Bell. *Mathematics of linear and nonlinear systems.* Clarendon Press, Oxford, 1990.

[66] G. I. Bell and E. C. Anderson. Cell growth and division. *Biophys. J.*, **7**:329–351, 1967.

[67] D. B. Bennett. Growth of the edible crab (*Cancer pagurus* L.) off south-west England. *J. Mar. Biol. Assoc. U. K.*, **54**:803–823, 1974.

[68] A. A. Benson and R. F. Lee. The role of wax in oceanic food chains. *Sci. Am.*, **3**:77–86, 1975.

[69] T. G. O. Berg and B. Ljunggren. The rate of growth of a single yeast cell. *Biotechnol. Bioeng.*, **24**:2739–2741, 1982.

[70] C. Bergmann. Über die Verhältnisse der Wärmeökonomie der Tiere zu ihrer Grösse. *Goett. Stud.*, **1**:595–708, 1847.

[71] H. Bergmann and H. Helb. *Stimmen der Vögel Europas.* BLV Verlagsgesellschaft, München, 1982.

[72] H. H. Bergmann, S. Klaus, F. Muller, and J. Wiesner. *Das Haselhuhn.* Die Neue Brehm-Bücherei. A. Ziemsen-Verlag, Wittenberg Lutherstadt, 1978.

[73] J. Bernardo. Determinants of maturation in animals. *Trends Ecol. Evol.*, **8**:166–173, 1993.

[74] D. R. Berry, editor. *Physiology of industrial fungi.* Blackwell Sci. Publ., Oxford, 1988.

[75] H. H. Berry. Hand-rearing lesser flamingos. In J. Kear and N. Duplaix-Hall, editors, *Flamingos.* T. & A. D. Poyser, Berkhamsted, 1975.

[76] L. von Bertalanffy. A quantitative theory of organic growth. *Hum. Biol.*, **10**:181–213, 1938.

[77] L. von Bertalanffy. Quantitative laws in metabolism and growth. *Q. Rev. Biol.*, **32**:217–231, 1957.

[78] L. von Bertalanffy. *General systems theory.* George Braziller, New York, 1968.

[79] L. von Bertalanffy. Basic concepts in quantitative biology of metabolism. *Helgol. Wiss. Meeresunters.*, **9**:5–34, 1969.

[80] P. Berthold. Über den Einfluss der Nestlingsnahrung auf die Jugendentwickling, insbesondere auf das Flugelwachstum, bei der Mönchsgrasmücke (*Sylvia atricapilla*). *Vogelwarte*, **28**:257–263, 1976.

[81] J. Best. The influence on intracellular enzymatic properties for kinetics data obtained from living cells. *J. Cell. Comp. Physiol.*, **46**:1–27, 1955.

[82] R. J. H. Beverton and S. J. Holt. On the dynamics of exploited fish populations. *Fish. Invest. Ser. I*, **2**, 1957.

[83] R. J. Beyers. The metabolism of twelve aquatic laboratory microecosystems. *Ecol. Monogr.*, **33**:281–306, 1963.

[84] R. Bijlsma. *De boomvalk.* Kosmos vogelmonografieën. Kosmos, Amsterdam, 1980.

[85] R. J. Bijlsma. *Modelling whole-plant metabolism of carbon and nitrogen: a basis for comparative plant ecology and morphology.* PhD thesis, Vrije Universiteit, Amsterdam, 1999.

[86] T. Birkhead. *Great auk islands; a field biologist in the Arctic.* T. & A. D. Poyser, London, 1993.

[87] E. C. Birney and D. D. Baird. Why do some mammals polyovulate to produce a litter of two? *Am. Nat.*, **126**:136–140, 1985.

[88] D. G. Blackburn. Convergent evolution of viviparity, matrotrophy and specializations for fetal nutrition in reptiles and other vertebrates. *Am. Zool.*, **32**:313–321, 1992.

[89] F. F. Blackman. Optima and limiting factors. *Ann. Bot.*, **19**:281–295, 1905.

[90] W. Bland and D. Rolls. *Weathering; an introduction to the scientific principles.* Arnold, London, 1998.

[91] J. H. S. Blaxter and J. R. Hunter. The biology of the clupoid fishes. In J. H. S. Balxter, F. S. Russell, and M. Yonge, editors, *Advances in marine biology*, volume 20, pages 1–223. Academic Press, London, 1982.

[92] K. Blaxter. *Energy metabolism in animals and man.* Cambridge University Press, 1989.

[93] H. Blumel. *Die Rohrammer.* Die Neue Brehm-Bücherei. A. Ziemsen-Verlag, Wittenberg Lutherstadt, 1982.

[94] M. P. Boer. *The dynamics of tri-trophic food chains.* PhD thesis, Vrije Universiteit, Amsterdam, 2000.

[95] M. P. Boer, B. W. Kooi, and S. A. L. M. Kooijman. Food chain dynamics in the chemostat. *Math. Biosci.*, **150**:43–62, 1998.

[96] M. P. Boer, B. W. Kooi, and S. A. L. M. Kooijman. Homoclinic and heteroclinic orbits in a tri-trophic food chain. *J. Math. Biol.*, **39**:19–38, 1999.

[97] P. D. Boersma, N. T. Wheelwright, M. K. Nerini, and E.S. Wheelwright. The breeding biology of the fork-tailed storm-petrel (*Oceanodroma furcata*). *Auk*, **97**:268–282, 1980.

[98] S. Bohlken and J. Joosse. The effect of photoperiod on female reproductive activity and growth of the fresh water pulmonate snail *Lymnaea stagnalis* kept under laboratory conditions. *Int. J. Invertebr. Reprod.*, **4**:213–222, 1982.

[99] C. Bohr and K. A. Hasselbalch. Über die Kohlensäureproduction des Hühnerembryos. *Skand. Arch. Physiol.*, **10**:149–173, 1900.

[100] J. T. Bonner. *Size and cycle: an essay on the structure of biology.* Princeton University Press, 1965.

[101] T. A. Bookhout. Prenatal development of snowshoe hares. *J. Wildl. Manage.*, **28**:338–345, 1964.

[102] T. Borchardt. Influence of food quantity on the kinetics of cadmium uptake and loss via food and seawater in *Mytilus edulis*. *Mar. Biol.*, **76**:67–76, 1983.

[103] T. Borchardt. Relationships between carbon and cadmium uptake in *Mytilus edulis*. *Mar. Biol.*, **85**:233–244, 1985.

[104] F. van den Bosch. *The velocity of spatial population expansion.* PhD thesis, Rijksuniversiteit Leiden, 1990.

[105] F. van den Bosch, J. A. J. Metz, and O. Diekmann. The velocity of spatial population expansion. *J. Math. Biol.*, **28**:529–565, 1990.

[106] A. B. Bowers. Breeding and growth of whiting (*Gadus merlangus* L.) in Isle of Man waters. *J. Mar. Biol. Assoc. U. K.*, **33**:97–122, 1954.

[107] C. R. Boyden. Trace element content and body size in molluscs. *Nature (Lond.)*, **251**:311–314, 1974.

[108] A. E. Brafield and M. J. Llewellyn. *Animal energetics.* Blackie, Glasgow, 1982.

[109] B. W. Brandt and S. A. L. M. Kooijman. Two parameters account for the flocculated growth of microbes in biodegradation assays. *Biotech. & Bioeng.*, **70**:677–684, 2000.

[110] A. M. Branta. Studies on the physiology, genetics and evolution of some *Cladocera*. Technical report, Carnegie Institute, Washington, 1939.

[111] P. R. Bregazzi and C. R. Kennedy. The biology of pike, *Esox lucius* L., in southern eutrophic lake. *J. Fish Biol.*, **17**:91–112, 1980.

[112] W. W. Brehm. Breeding the green-billed toucan at the Walsrode Bird park. *Int. Zoo Yearb.*, **9**:134–135, 1969.

[113] H. Bremer and P. P. Dennis. Modulation of chemical composition and other parameters of the cell by growth rate. In F. C. Neidhardt, editor, Escherichia coli *and* Salmonella typhimurium, pages 1527–1542. Am. Soc. Microbiol., Washington, 1987.

[114] H. Brendelberger and W. Geller. Variability of filter structures in eight *Daphnia* species: mesh sizes and filtering areas. *J. Plankton Res.*, **7**:473–486, 1985.

[115] J. R. Brett. The relation of size to rate of oxygen consumption and sustained swimming speed of sockeye salmon (*Oncorhynchus nerka*). *J. Fish. Res. Board Can.*, **22**:1491–1497, 1965.

[116] F. H. van den Brink. *Zoogdierengids.* Petersons veldgidsenserie. Elsevier, Amsterdam, 1955.

[117] I. L. Brisbin Jr and L. J. Tally. Age-specific changes in the major body components and caloric value of growing Japanese quail. *Auk*, **90**:624–635, 1973.

[118] M. S. Brody and L. R. Lawlor. Adaptive variation in offspring size in the terrestrial isopod *Armadillium vulgare*. *Oecologia (Berlin)*, **61**:55–59, 1984.

[119] S. Brody. *Bioenergetics and growth.* Rheinhold, New York, 1945.

[120] S. Broekhuizen. *Hazen in Nederland.* PhD thesis, Landbouw Hogeschool, Wageningen, 1982.

[121] M. Brooke. *The manx shearwater.* T. & A. D. Poyser, London, 1990.

[122] J. L. Brooks and S. I. Dodson. Predation, body size, and composition of plankton. *Science (New York)*, **150**:28–35, 1965.

[123] S. P. J. Brooks, A. de Zwaan, G. van den Thillart, O. Cattani, and Corti. Differential survival of *Venus gallina* and *Scapharca inaequivalvis* during anoxic stress: Covalent modification of phosphofructokinase and glycogen phosphorylase during anoxia. *J. Comp. Physiol.*, **161**:207–212, 1991.

[124] D. J. Brousseau. Analysis of growth rate in *Mya arenaria* using the von Bertalanffy equation. *Mar. Biol.*, **51**:221–227, 1979.

[125] E. Brouwer. On simple formulae for calculating the heat expenditure and the quantities of carbohydrate and fat metabolized in ruminants from data on gaseous exchange and urine N. In *1st Symposium on energy metabolism*, pages 182–194. European association for animal production, Rome, 1958.

[126] R. Brouwer and C. T. de Wit. A simulation model of plant grwoth with special attention to root growth and its consequences. In W. J. Whittington, editor, *Root growth*, pages 224–279. Butterworth, London, 1969.

[127] G. H. Brown and J. J. Wolken. *Liquid crystals and biological structures.* Academic Press, London, 1979.

[128] W. Y. Brown. Growth and fledging age of sooty tern chicks. *Auk*, **93**:179–183, 1976.

[129] W. A. Bruggeman, L. B. J. M. Martron, D. Kooiman, and O. Hutzinger. Accumulation and elimination kinetics of di-, tri-and tetra chlorobiphenyls by goldfish after dietary and aqueous exposure. *Chemosphere*, **10**:811–832, 1981.

[130] L. W. Bruinzeel and T. Piersma. Cost reduction in the cold: heat generated by terrestrial locomotion partly substitutes for thermoregulation costs in knot *Calidris canutus*. *Ibis*, **140**:323–328, 1998.

[131] B. Bruun. *Gids voor de vogels van Europa.* Elsevier, Amsterdam, 1970.

[132] C. Bryant. *Metazoan life without oxygen.* Chapman & Hall, London, 1991.

[133] M. M. Bryden. Growth of the south elephant seal *Mirounga leonina* (Linn.). *Growth*, **33**:69–82, 1969.

[134] T. L. Bucher. Parrot eggs, embryos, and nestlings: patterns and energetics of growth and development. *Physiol. Zool.*, **56**:465–483, 1983.

[135] L. J. Buckley. RNA–DNA ratio: an index of larval fish growth in the sea. *Mar. Biol.*, **80**:291–298, 1984.

[136] J. J. Bull. Sex determination mechanisms: an evolutionary perspective. In S. C. Stearns, editor, *The evolution of sex and its consequences*, pages 93–114. Birkhäuser, Basel, 1987.

[137] P. C. Bull and A. H. Whitaker. The amphibians, reptiles, birds and mammals. In G. Kuschel, editor, *Biogeography and ecology in New Zealand*, pages 231–276. W. Junk b.v., Den Haag, 1975.

[138] B. A. Bulthuis. *Stoichiometry of growth and product-formation by* Bacillus licheniformis. PhD thesis, Vrije Universiteit, Amsterdam, 1990.

[139] S. Bunney. Some dinosaurs liked it cold. *New Sci.*, (8 April):27, 1989.

[140] C. W. Burns. The relationship between body size of filterfeeding cladocera and the maximum size of particles ingested. *Limnol. Oceanogr.*, **13**:675–678, 1968.

[141] R. Burton. *Egg: nature's miracle of packaging.* W. Collins, London, 1987.

[142] D. K. Button. Biochemical basis for whole-cell uptake kinetics: specific affinity, oligotrophic capacity, and the meaning of Michaelis constant. *Appl. Environ. Microbiol.*, **57**:2033–2038, 1991.

[143] M. Byrne. Viviparity and intragonadal cannibalism in the diminutive asterinid sea stars *Patiriella vivipara* and *P. parvivipara*. *Mar. Biol.*, **125**:551–567, 1996.

[144] P. L. Cadwallader and A. K. Eden. Food and growth of hatchery-produced chinook-salmon, *Oncorhynchus tschawytscha* (Walbaum), in landlocked lake Purrumbete, Victoria, Australia. *J. Fish Biol.*, **18**:321–330, 1981.

[145] W. A. Calder III. The kiwi and egg design: evolution as a package deal. *Bioscience*, **29**:461–467, 1979.

[146] W. A. Calder III. *Size, function and life history.* Harvard University Press, 1984.

[147] H. B. Callen. *Thermodynamics.* J. Wiley & Sons, Inc., Chichester, 1960.

[148] P. Calow and C. R. Townsend. Resource utilization in growth. In C. R. Townsend and P. Calow, editors, *Physiological ecology*, pages 220–244. Blackwell Sci. Publ., 1981.

[149] N. Cameron. *The measurement of human growth.* Croom Helm, London, 1984.

[150] R. N. Campbell. The growth of brown trout, *Salmo trutta* L. in northern Scottish lochs with special reference to the improvement of fisheries. *J. Fish Biol.*, **3**:1–28, 1971.

[151] H. Canter-Lund and J. W. G. Lund. *Freshwater algae; Their microscopic world explored.* Biopress Ltd, Bristol, 1995.

[152] T. J. Case. Speculations on the growth rate and reproduction of some dinosaurs. *Paleobiology*, **4**:320–328, 1978.

[153] M. Cashel and K. E. Rudd. The stringent response. In F. C. Neidhardt, editor, Escherichia coli *and* Salmonella typhimurium, volume 2, pages 1410–1438. American Society for Microbiology, 1987.

[154] L. Cazzador. Analysis of oscillations in yeast continuous cultures by a new simplified model. *Bull. Math. Biol.*, **53**:685–700, 1991.

[155] T. R. Cech, A. J. Zaug, and P. J. Grabowski. In vitro splicing of the ribosomal RNA precursor of *Tetrahymena*: involvement of a guanosine nucleotide in the excision of the intervening sequence. *Cell*, **27**:487–496, 1981.

[156] D. J. Chapman and J. W. Schopf. Biological and chemical effects of the development of an aerobic environment. In J. W. Schopf, editor, *Earth's earliest biosphere: its origin and evolution*, pages 302–320. Princeton, New York, 1983.

[157] B. Charlesworth. *Evolution in age-structured populations.* Cambridge University Press, 1980.

[158] E. L. Charnov and D. Berrigan. Dimensionless numbers and the assembly rules for life histories. *Philos. Trans. R. Soc. Lond. B Biol. Sci.*, **332**:41–48, 1991.

[159] F. F. Chehab, K. Mounzih, R. Lu, and M. E. Lim. Early onset of reproductive function in normal female mice treated with leptin. *Science (New York)*, **275**:88–90, 1997.

[160] K. Christoffersen and A. Jespersen. Gut evacuation rates and ingestion rates of *Eudiaptomus graciloides* measured by means of gut fluorescence method. *J. Plankton Res.*, **8**:973–983, 1986.

[161] D. Claessen, A. M. de Roos, and L. Persson. Dwarfs and giants: cannibalism and competition in size-structured populations. *Am. Nat.*, 1999. in press.

[162] A. Clarke. Temperature and embryonic development in polar marine invertebrates. *Int. J. Invertebr. Reprod.*, **5**:71–82, 1982.

[163] D. H. Clayton and J. Moore. *Host-parasite evolution; general principles & avian models.* Oxford University Press, 1997.

[164] G. A. Clayton, C. Nixey, and G. Monaghan. Meat yield in turkeys. *Br. Poult. Sci.*, **19**:755–763, 1978.

[165] J. S. Clegg. Cellular infrastructure and metabolic organization. *Curr. Top. Cell. Regul.*, **33**:3–14, 1992.

[166] J. H. L. Cloethe. Prenatal growth in the merino sheep. *Onderstepoort J. Vet. Sci. Anim. Ind.*, **13**:417–558, 1939.

[167] J. F. Collins and M. H. Richmond. Rate of growth of *Bacillus cereus* between divisions. *J. Gen. Microbiol.*, **28**:15–33, 1962.

[168] A. Comfort. *The biology of senescence.* Churchill Livingstone, Edinburgh, 1979.

[169] J. D. Congdon, D. W. Tinkle, and P. C. Rosen. Egg components and utilization during development in aquatic turtles. *Copeia*, **1983**:264–268, 1983.

[170] D. W. Connell and D. W. Hawker. Use of polynomial expressions to describe the bioconcentration of hydrophobic chemicals by fish. *Ecotoxicol. Environ. Saf.*, **16**:242–257, 1988.

[171] R. J. Conover. Transformation of organic matter. In O. Kinne, editor, *Marine Ecology.* J. Wiley & Sons, Inc., Chichester, 1978.

[172] G. D. Constanz. Growth of nestling rufous hummingbirds. *Auk*, **97**:622–624, 1980.

[173] C. L. Cooney, D. I. C. Wang, and R. I. Mateles. Measurement of heat evolution and correlation with oxygen consumption during microbial growth. *Biotechnol. Bioeng.*, **11**:269–281, 1968.

[174] S. Cooper. The constrained hoop: an explanation of the overschoot in cell length during a shift-up of *Escherichia coli*. *J. Bacteriol.*, **171**:5239–5243, 1989.

[175] S. Cooper. *Bacterial growth and division.* Academic Press, London, 1991.

[176] J. D. Coronios. Development of behaviour in fetal cat. *Genet. Psychol. Monogr.*, **14**:283–330, 1933.

[177] R. R. Coutts and I. W. Rowlands. The reproductive cycle of the skomer vole (*Clethrionomys glareolus skomerensis*). *J. Zool. Lond.*, **158**:1–25, 1969.

[178] D. R. Cox. *Renewal theory.* Methuen & co Ltd, London, 1962.

[179] D. R. Cox and D. Oakes. *Analysis of survival data.* Monographs on statistics and applied probability. Chapman & Hall, London, 1984.

[180] R. C. Crabtree and F. A. Bazzaz. Seedling response of four birch species to simulated nitrogen deposition – ammonium versus nitrate. *Ecol. Appl.*, **3**:315–321, 1993.

[181] D. Cragg-Hine and J. W. Jones. The growth of dace *Leuciscus leuciscus* (L.), roach *Rutilus rutilus* (L.) and chub *Sqalius cephalus* (L.) in Willow Brook, Northhamptonshire. *J. Fish Biol.*, **1**:59–82, 1969.

[182] J. F. Craig. A note on growth and mortality of trout, *Salmo trutta* L., in afferent streams of Windermere. *J. Fish Biol.*, **20**:423–429, 1982.

[183] G. Creutz. *Der Weiss-storch.* Die Neue Brehm-Bücherei. A. Ziemsen-Verlag, Wittenberg Lutherstadt, 1985.

[184] E. G. Crichton. Aspects of reproduction in the genus *Notomys* (*Muridae*). *Aust. J. Zool.*, **22**:439–447, 1974.

[185] J. R. Cronmiller and C. F. Thompson. Experimental manipulation of brood size in red- winged blackbirds. *Auk*, **97**:559–565, 1980.

[186] C. J. Crossland and D. J. Barnes. The role of metabolic nitrogen in coral calcification. *Mar. Biol.*, pages 325–332, 1974.

[187] H. Crum. *A focus on peatlands and peat mosses.* The University of Michican Press, Ann Abor, 1992.

[188] E. H. Curtis, J. J. Beauchamp, and B. G. Blaylock. Application of various mathematical models to data from the uptake of methyl mercury in bluegill sunfish (*Lepomis macrochirus*). *Ecol. Modell.*, **3**:273–284, 1977.

[189] J. M. Cushing. *An introduction to structured population dynamics.*, volume 71 of *CBMS-NSF regional conference series in applied mathematics*. SIAM, Philadelphia, 1998.

[190] H. Cyr and M. L. Pace. Allometric theory: extrapolations from individuals to communities. *Ecology*, **74**:1234–1245, 1993.

[191] W. B. Dade, P. A. Jumars, and D. L. Penry. Supply-side optimization: maximizing absorptive rates. In R. N. Hughes, editor, *Behavioural mechanisms of food selection*, volume 20 of *NATO ASI*, pages 531–555. Springer-Verlag, Berlin, 1990.

[192] M. J. Dagg. Complete carbon and nitrogen budgets for the carnivorous amphipod, *Calliopius laeviusculus* (Kroyer). *Int. Rev. Gesamten Hydrobiol.*, **61**:297–357, 1976.

[193] J. D. Damuth. Of size and abundance. *Nature (Lond.)*, **351**:268–269, 1991.

[194] J. D. Damuth. Taxon-free characterization of animal comminuties. In A. K. Behrensmeyer, J. D. Damuth, W. A. DiMichele, R. Potts, H.-D. Sues, and S. L. Wing, editors, *Terrestrial ecosystems through time; evolutionary paleoecology of terrestrial plants and animals*, pages 183–203. University of Chicago Press, 1992.

[195] N. Dan and S. E. R. Bailey. Growth, mortality, and feeding rates of the snail *Helix aspersa* at different population densities in the laboratory, and the depression of activity of helicid snails by other individuals, or their mucus. *J. Molluscan Stud.*, **48**:257–265, 1982.

[196] M. C. Dash and A. K. Hota. Density effects on the survival, growth rate, and metamorphosis of *Rana tigrina* tadpoles. *Ecology*, **61**:1025–1028, 1980.

[197] H. A. David and M. L. Moeschberger. *The theory of competing risks.*, volume 39 of *Griffin's Statistical Monographs & Courses*. C. Griffin & Co Ltd, 1978.

[198] P. J. Davoll and M. W. Silver. Marine snow aggregates: life history sequence and microbial community of abandoned larvacean houses from Monterey Bay, California. *Mar. Ecol. Prog. Ser.*, **33**:111–120, 1986.

[199] E. A. Dawes. The constrained hoop: an explanation of the overschoot in cell length during a shift-up of *Escherichia coli*. In T. R. Gray and J. R. Postgate, editors, *The survival of vegetative microbes*, pages 19–53. Cambridge University Press, 1976.

[200] W. R. Dawson. Evaporative losses of water by birds. *Biochem. Physiol.*, **71**:495–509, 1982.

[201] T. Day and P. D. Taylor. Von Bertalanff's growth equation should not be used to model age and size at maturity. *Am. Nat.*, **149**:381–393, 1997.

[202] D. L. DeAngelis and L. J. Gross, editors. *Individual-based models and approaches in ecology*. Chapman & Hall, London, 1992.

[203] D. C. Deeming and M. W. J. Ferguson. Environmental regulation of sex determination in reptiles. *Phil. Rans. R. Soc. Lond. Biol.*, **322**:19–39, 1988.

[204] D. C. Deeming and M. W. J. Ferguson. Effects of incubation temperature on growth and development of embryos of *Alligator mississippiensis*. *J. Comp. Physiol.*, **B159**:183–193, 1989.

[205] T. E. DeLaca, D. M. Karl, and J. H. Lipps. Direct use of dissolved organic carbon by agglutinated benthic foraminifera. *Nature (Lond.)*, **289**:287–289, 1981.

[206] M. W. Demment and P. J. van Soest. A nutritional explanation for body size patterns of ruminant and non-ruminant herbivores. *Am. Nat.*, **125**:641–672, 1985.

[207] W. R. Demott. Feeding selectivities and relative ingestion rates of *Daphnia* and *Bosmina*. *Limnol. Oceanogr.*, **27**:518–527, 1982.

[208] V. E. Dent, M. J. Bazin, and P. T. Saunders. Behaviour of *Dictyostelium discoideum* amoebae and *Escherichia coli* grown together in chemostat culture. *Arch. Microbiol.*, **109**:187–194, 1976.

[209] A. J. Desmond. *The hot-blooded dinosaurs*. Futura Publications Ltd., London, 1975.

[210] R. L. Devaney. *An introduction to chaotic dynamical systems*. Addison-Wesley, Redwood City, CA, 1989.

[211] A. W. Diamond. The red-footed booby on Aldabra atoll, Indian Ocean. *Ardea*, **62**:196–218, 1974.

[212] J. M. Diamond and R. K. Buddington. Intestinal nutrient absorption in herbivores and carnivores. In P. Dejours, L. Bolis, C. R. Taylor, and E. R. Weibel, editors, *Comparative physiology: life in water and on land*. IX-Liviana Press, 1987.

[213] U. Dieckmann and R. Law. The mathematical theory of coevolution: a derivation from stochastic processes. *J. Math. Biol.*, **34**:579–612, 1996.

[214] O. Diekmann, H. J. A. M. Heijmans, and H. R. Thieme. On the stability of the cell size distribution. *J. Math. Biol.*, **19**:227–248, 1984.

[215] O. Diekmann, H. J. A. M. Heijmans, and H. R. Thieme. On the stability of the cell size distribution II: time periodic developmental rates. *Comp. & Math. with Appls.*, **12A**:491–512, 1985.

[216] O. Diekmann, H. A. Lauwerier, T. Aldenberg, and J. A. J. Metz. Growth, fission and the stable size distribution. *J. Math. Biol.*, **18**:135–148, 1983.

[217] I. Dietzel, V. Kolb, and W. Boos. Pole cap formation in *Escherichia coli* following induction of the maltose-binding protein. *Arch. Microbiol.*, **118**:207–218, 1978.

[218] C. Dijkstra. *Reproductive tactics in the kestrel* Falco tinnunculus*; a study in evolutionary biology*. PhD thesis, University of Groningen, The Netherlands, 1988.

[219] F. A. Dipper, C. R. Bridges, and A. Menz. Age, growth and feeding in the ballan wrasse *Labrus bergylta* Ascanius 1767. *J. Fish Biol.*, **11**:105–120, 1977.

[220] H. Dittberner and W. Dittberner. *Die Schafstelze.* Die Neue Brehm-Bücherei. A. Ziemsen-Verlag, Wittenberg Lutherstadt, 1984.

[221] E. J. Doedel, A. R. Champneys, T. F. Fairgrieve, Y. A. Kuznetsov, B. Sandstede, and X. Wang. Auto 97: Continuation and bifurcation software for ordinary differential equations. Technical report, Concordia University, Montreal, Canada, 1997.

[222] D. Dolmen. Growth and size of *Triturus vulgaris* and *T. cristatus* (*Amphibia*) in different parts of Norway. *Holarct. Ecol.*, **6**:356–371, 1983.

[223] S. L. Domotor and C. F. D'Elia. Nutrient uptake kinetics and growth of zooxanthellae. *Marine Biology*, **80**:93–101, 1984.

[224] W. D. Donachie. Relationship between cell size and time of initiation of DNA replication. *Nature (Lond.)*, **219**:1077–1079, 1968.

[225] W. D. Donachie, K. G. Begg, and M. Vicente. Cell length, cell growth and cell division. *Nature (Lond.)*, **264**:328–333, 1976.

[226] F. Dörr. Energetic and statistical relations. In W. Hoppe, W. Lohmann, H. Markl, and H. Ziegler, editors, *Biophysics*, chapter 8, pages 316–371. Spinger-Verlag, Berlin, 1983.

[227] Q. Dortch. The interaction between ammonium and nitrate uptake in phytoplankton. *Mar. Ecol. Prog. Ser.*, **61**:183–201, 1990.

[228] P. G. Doucet and N. M. van Straalen. Analysis of hunger from feeding rate observations. *Anim. Behav.*, **28**:913–921, 1980.

[229] A. Douglas, P. J. McAuley, and P. S. Davies. Algal symbiosis in cnidaria. *J. Zool., Lond.*, **231**:175–178, 1993.

[230] W. L. Downing and J. A. Downing. Molluscan shell growth and loss. *Nature (Lond.)*, **362**:506, 1993.

[231] R. L. Draper. The prenatal growth of the guinea-pig. *Anat. Rec.*, **18**:369–392, 1920.

[232] P. G. Drazin. *Nonlinear systems.* Cambridge University Press, 1992.

[233] R. H. Drent. Functional aspects of incubation in the herring gull. *Behaviour, Suppl.*, **17**:1–132, 1970.

[234] M. R. Droop. Some thoughts on nutrient limitation in algae. *J. Phycol.*, **9**:264–272, 1973.

[235] M. R. Droop. The nutrient status of algal cells in continuous culture. *J. Mar. Biol. Assoc. U. K.*, **54**:825–855, 1974.

[236] M. R. Droop. 25 years of algal growth kinetics. *Bot. Mar.*, **26**:99–112, 1983.

[237] G. L. Dryden. Growth and development of *Suncus murinus* in captivity on Guam. *J. Mammal.*, **49**:51–62, 1968.

[238] E. Duclaux. Vie aérobie et anaérobie. In *Traité de microbiologie*, volume 1, pages 208–212. Masson et cie., Paris, 1898.

[239] W. E. Duellman. Reproductive strategies of frogs. *Sci. Am.*, **7**:58–65, 1992.

[240] W. E. Duellman and L. Trueb. *Biology of amphibians.* McGraw-Hill, 1986.

[241] G. C. A. Duineveld and M. I. Jenness. Difference in growth rates of the sea urchin *Echiocardium cordatum* as estimated by the parameter ω of the von Bertalanffy equation to skeletal rings. *Mar. Ecol.*, **19**:65–72, 1984.

[242] E. H. Dunn. Growth, body components and energy content of nestling double-crested cormorants. *Condor*, **77**:431–438, 1975.

[243] C. de Duve. *Blueprint for a cell: the nature and origin of life.* Neil Patterson Publishers, Burlington, NC, 1991.

[244] M. Dworkin. *Developmental biology of the bacteria.* Benjamin-Cummings Publ. Co., California, 1985.

[245] O. N. Eaton. Weight and length measurements of fetuses of karakul sheep and of goats. *Growth*, **16**:175–187, 1952.

[246] B. Ebenman and L. Persson. *Size-structured populations. Ecology and evolution.* Springer-Verlag, Berlin, 1988.

[247] R. Eckert, D. Randall, and G. Augustine. *Animal physiology.* W. H. Freeman and Company, New York, 1988.

[248] L. Edelstein-Keshet. *Mathematical models in biology.* Random House, New York, 1988.

[249] D. A. Egloff and D. S. Palmer. Size relations of the filtering area of two *Daphnia* species. *Limnol. Oceanogr.*, **16**:900–905, 1971.

[250] J. F. Eisenberg. *The mammalian radiations. An analysis of trends in evolutions, adaptation, and behaviour.* University of Chicago Press, 1981.

[251] R. C. Elandt-Johnson and N. L. Johnson. *Survival models and data analysis.* J. Wiley & Sons, Inc., Chichester, 1980.

[252] R. H. E. Elliott, F. G. Hall, and A. St. G. Huggett. The blood volume and oxygen capacity of the foetal blood in the goat. *J. Physiol. (Lond.)*, **82**:160–171, 1934.

[253] G. W. Elmes, J. A. Thomas, and J. C. Wardlaw. Larvae of *Maculinea rebeli*, a large-blue butterfly, and their *Myrmica* host ants: wild adoption and hehaviour in ant-nests. *J. Zool. Lond.*, **223**:447–460, 1991.

[254] S. Emerson. The growth phase in *Neurospora* corresponding to the logarithmic phase in unicellular organisms. *J. Bacteriol.*, **60**:221–223, 1950.

[255] L. H. Emmons and F. Feer. *Neotropical rainforest mammals.* The University of Chicago Press, 1990.

[256] J. Emsley. Potent painkiller from poisonous frog. *New Sci.*, **30**(May):14, 1992.

[257] R. H. Emson and P. V. Mladenov. Studies of the fissiparous holothurian *Holothuria parvula* (Selenka) (Echinodermata: Holothuroidea). *J. Exp. Mar. Biol. Ecol.*, **111**:195–211, 1987.

[258] H. Engler. *Die Teichralle.* Die Neue Brehm-Bücherei. A. Ziemsen-Verlag, Wittenberg Lutherstadt, 1983.

[259] L. Enserink. *Food mediated life history strategies in* Daphnia magna*: their relevance to ecotoxicological evaluations.* PhD thesis, Agricultural University Wageningen, 1995.

[260] G. Ernsting and J. A. Isaaks. Accelerated ageing: a cost of reproduction in the carabid beetle *Notiophilus biguttatus* F. *Funct. Ecol.*, **5**:229–303, 1991.

[261] G. Ernsting and J. A. Isaaks. Effects of temperature and season on egg size, hatchling size and adult size in *Notiophilus biguttatus*. *Ecol. Entomol.*, **22**:32–40, 1997.

[262] A. A. Esener, J. A. Roels, and N. W. F. Kossen. Dependence of the elemental composition of *K. pneumoniae* on the steady-state specific growth rate. *Biotechnol. Bioeng.*, **24**:1445–1449, 1982.

[263] A. A. Esener, J. A. Roels, and N. W. F. Kossen. Theory and applications of unstructured growth models: kinetic and energetic aspects. *Biotechnol. Bioeng.*, **25**:2803–2841, 1983.

[264] E. Evers and S. A. L. M. Kooijman. Feeding and oxygen consumption in *Daphnia magna*; a study in energy budgets. *Neth. J. Zool.*, **39**:56–78, 1989.

[265] N. Fairall. Prenatal development of the impala *Aepyceros melampus*. *Koedoe*, **12**:97–103, 1969.

[266] U. Falkengren-Grerup and H. Lakkenborg-Kristensen. Importance of ammonium an nitrate to the performance of herb-layer species from deciduous forests in southern Sweden. *Environ. Exp. Bot.*, **34**:31–38, 1994.

[267] P. G. Falkowski and J. A. Raven. *Aquatic photosynthesis.* Blackwell Science, Oxford, 1997.

[268] J. O. Farlow. A consideration of the trophic dynamics of a late Cretaceous large-dinosaur community (Oldman Formation). *Ecology*, **57**:841–857, 1976.

[269] J. O. Farlow and M. K. Brett-Surman. *The complete dinosaur.* Indiana University Press, 1997.

[270] G. D. Farquhar. Models describing the kinetics of ribulose riphosphate carboxylase-oxygenase. *Arch. Biochem. Biophys.*, **193**:456–468, 1979.

[271] G. D. Farquhar, S. von Caemmerer, and J. A. Berry. A biochemical model of photosynthetic CO_2 assimilation in leaves of C_3 species. *Planta*, **149**:78–90, 1980.

[272] H. S. Fawcett. The temperature relations of growth in certain parasitic fungi. *Univ. Calif. Berkeley Publ. Agr. Sci.*, **4**:183–232, 1921.

[273] M. A. Fedak and H. J. Seeherman. Reappraisal of energetics of locomotion shows identical cost in bipeds and quadrupeds including ostrich and horse. *Nature (Lond.)*, **282**:713–716, 1979.

[274] R. Fenaux. Rhythm of secretion of oikopleurid's houses. *Bull. Mar. Sci.*, **37**:498–503, 1985.

[275] R. Fenaux and G. Gorsky. Cycle vital et croissance de l'appendiculaire *Oikopleura longicauda*. *Ann. Inst. Oceanogr.*, **59**:107–116, 1983.

[276] T. Fenchel. Intrinsic rate of natural increase: the relationship with body size. *Oecologia (Berlin)*, **14**:317–326, 1974.

[277] T. Fenchel. Eukaryotic life: Anaerobic physiology. In D. McL. Roberts, P. Sharp, G. Alderson, and M Collins, editors, *Evolution of microbial life*, pages 185–203. Cambridge University Press, 1996.

[278] T. Fenchel and B. J. Finlay. *Ecology and evolution in anoxic worlds.* Oxford University Press, 1995.

[279] M. W. J. Ferguson. Palatal shelf elevation in the Wistar rat fetus. *J. Anat.*, **125**:555–577, 1978.

[280] S. Fernandez-Baca, W. Hansel, and C. Novoa. Embryonic mortality in the alpaca. *Biol. Reprod.*, **3**:243–251, 1970.

[281] C. E. Finch. *Longevity, senescence, and the genome.* University of Chicago Press, 1990.

[282] B. J. Finlay and T. Fenchel. An anaerobic ciliate as a natural chemostat for the growth of endosymbiotic methanogens. *Eur. J. Protistol.*, **28**:127–137, 1992.

[283] R. A. Fisher and L. H. C. Tippitt. Limiting forms of the frequency distribution of the largest or the smallest memeber of a sample. *Proc. Cambridge Phil. Soc.*, **24**:180–190, 1928.

[284] V. Fitsch. *Laborversuche und Simulationen zur kausalen Analyse der Populationsdynamik von* Daphnia magna. PhD thesis, Rheinisch-Westfälischen Technischen Hochschule Aachen, 1990.

[285] L. B. Flexner and H. A. Pohl. The transfer of radioactive sodium across the placenta of the white rat. *J. Cell. Comp. Physiol.*, **18**:49–59, 1941.

[286] P. R. Flood. Architecture of, and water circulation and flow rate in, the house of the planktonic tunicate *Oikopleura labradoriensis*. *Mar. Biol.*, **111**:95–111, 1991.

[287] G. L. Flynn and S. H. Yalkowsky. Correlation and prediction of mass transport across membranes I: Influence of alkyl chain length on flux-determining properties of barrier and diffusant. *J. Pharmacol. Sci.*, **61**:838–852, 1972.

[288] K. J. Flynn, M. J. R. Fasham, and C. R. Hipkin. Modelling the interactions between ammonium and nitrate in marine phytoplankton. *Phil. Trans. R. Soc. Lond. B*, **352**:1625–1645, 1997.

[289] H. von Foerster. Some remarks on changing populations. In F. Stohlman, editor, *The kinetics of cellular proliferation*. Grune and Stratton, 1959.

[290] J. Forsberg and C. Wiklund. Protandry in the green-veined white butterfly, *Pieris napi* L. (*Lepidoptera*; *Pieridae*). *Funct. Ecol.*, **2**:81–88, 1988.

[291] B. L. Foster Smith. The effect of concentration of suspension and inert material on the assimilation of algae by three bivalves. *J. Mar. Biol. Assoc. U. K.*, **55**:411–418, 1975.

[292] B. L. Foster Smith. The effect of concentration of suspension on the filtration rates and pseudofaecal production for *Mytilus edulis* L., *Cerastoderma edule* L. and *Venerupsis pullastra* (Montagu). *J. Exp. Mar. Biol. Ecol.*, **17**:1–22, 1975.

[293] P. da Franca. Determinacao da idade em *Gambusia holbrookii* (Girard). *Arq. Mus. Bocage*, **24**:87–93, 1953.

[294] D. R. Franz. Population age structure, growth and longevity of the marine gastropod *Uropalpinx cinerea* Say. *Biol. Bull. (Woods Hole)*, **140**:63–72, 1971.

[295] J. C. Frauenthal. Analysis of age-structured models. In T. G. Hallam and S. A. Levin, editors, *Mathematical ecology*, pages 117–147. Springer-Verlag, Berlin, 1986.

[296] J. J. R. Fraústo da Silva and R. J. P. Williams. *The biological chemistry of the elements. The inorganic chemistry of life.* Clarendon Press, Oxford, 1993.

[297] A. G. Fredrickson, R. D. Megee III, and H. M. Tsuchiy. Mathematical models for fermentation processes. *Adv. Appl. Microbiol.*, **13**:419–465, 1970.

[298] B. Friedich. Genetics of energy converting systems in aerobic chemolithotrophs. In H. G. Schlegel and E. Bowien, editors, *Autotrophic bacteria*, pages 415–436. Springer-Verlag, 1989.

[299] E. Frommhold. *Die Kreuzotter.* Die Neue Brehm-Bücherei. A. Ziemsen-Verlag, Wittenberg Lutherstadt, 1969.

[300] B. W. Frost. Effects of size and concentration of food particles on the feeding behaviour of the marine copepod *Calanus pacificus*. *Limnol. Oceanogr.*, **17**:805–815, 1972.

[301] B. W. Frost and N. C. Franzen. Grazing and iron limitation in the control of phytoplankton stock and nutrient concentration: a chemostat analogue of the pacific equatorial upwelling zone. *Mar. Ecol. Prog. Ser.*, **83**:291–303, 1992.

[302] W. E. Frost and C. Kipling. The growth of charr, *Salvinus willughbii* Gunther, in Windermere. *J. Fish Biol.*, **16**:279–289, 1980.

[303] F. E. J. Fry. The effect of environmental factors on the physiology of fish. In W. S. Hoar and D. J. Randall, editors, *Fish physiology*, volume 6, pages 1–87. Academic Press, London, 1971.

[304] G. Fryer. Evolution and adaptive radiation in *Macrothricidae* (*Crustacea*: *Cladocera*): a study in comparative functional morphology and ecology. *Proc. R. Soc. Lond. B Biol. Sci.*, **269**:142–385, 1974.

[305] E. Fuller, editor. *Kiwis*. Swan-Hill Press, Shrewsbury, 1991.

[306] T. W. Fulton. *The Sovereignty of the seas*. Edinburgh, 1911.

[307] S. Fuma, H. Takeda, K. Miyamoto, K. Yanagisawa, Y. Inoue, N. Sato, M. Hirano, and Z. Kawabata. Effects of γ-rays on the populations of the steady state ecological microcosm. *Int. J. Radiat. Biol.*, **74**:145–150, 1998.

[308] R. W. Furness. *The skuas*. T. & A. D. Poyser, Calton, 1987.

[309] V. F. Gallucci and T. J. Quinn. Reparameterizing, fitting, and testing a simple growth model. *Trans. Am. Fish. Soc.*, **108**:14–25, 1979.

[310] A. J. Gaston. *The ancient murrelet.* T. & A. D. Poyser, London, 1992.

[311] R. E. Gatten, K. Miller, and R. J. Full. Energetics at rest and during locomotion. In M. E. Feder and W. W. Burggren, editors, *Environmental physiology of the amphibians*, chapter 12, pages 314–377. The University of Chicago Press, 1992.

[312] M. Gatto, C. Ricci, and M. Loga. Assessing the response of demographic parameters to density in a rotifer population. *Ecol. Modell.*, **62**:209–232, 1992.

[313] V. Geist. Bergmann's rule is invalid. *Can. J. Zool.*, **65**:1035–1038, 1987.

[314] W. Geller. Die Nahrungsaufname von *Daphnia pulex* in Aghängigkeit von der Futterkonzentration, der Temperatur, der Köpergrösse und dem Hungerzustand der Tiere. *Arch. Hydrobiol./ Suppl.*, **48**:47–107, 1975.

[315] W. Geller and H. Müller. Seasonal variability in the relationship between body length and individual dry weight as related to food abundance and clutch size in two coexisting *Daphnia*. *J. Plankton Res.*, **7**:1–18, 1985.

[316] R. B. Gennis. *Biomembranes. Molecular structure and function.* Springer-Verlag, Berlin, 1989.

[317] M. Genoud. Energetic strategies of shrews: ecological constraints and evolutionary implications. *Mammal Rev.*, **4**:173–193, 1988.

[318] S. A. H. Geritz, É. Kisdi, G. Meszna, and J. A. J. Metz. Evolutionarily singular strategies and the adaptive growth and branching of the evolutionary tree. *Evol. Ecol.*, **12**:35–57, 1998.

[319] R. D. Gettinger, G. L. Paukstis, and W. H. N. Gutzke. Influence of hydric environment on oxygen consumption by embryonic turtles *Chelydra serpentina* and *Trionyx spiniferus*. *Physiol. Zool.*, **57**:468–473, 1984.

[320] W. Gewalt. *Der Weisswal (*Delphinapterus leucas*)*. Die Neue Brehm-Bücherei. A. Ziemsen-Verlag, Wittenberg Lutherstadt, 1976.

[321] R. N. Gibson. Observations on the biology of the giant goby *Gobius cobitis* Pallas. *J. Fish Biol.*, **2**:281–288, 1970.

[322] R. N. Gibson and I. A. Ezzi. The biology of a Scottish population of Fries' goby, *Lesueurigobius friesii*. *J. Fish Biol.*, **12**:371–389, 1978.

[323] R. N. Gibson and I. A. Ezzi. The biology of the scaldfish, *Arnoglossus laterna* (Walbaum) on the west coast of Scotland. *J. Fish Biol.*, **17**:565–575, 1980.

[324] R. N. Gibson and I. A. Ezzi. The biology of the Norway goby, *Pomatoschistus norvegicus* (Collett), on the west coast of Scotland. *J. Fish Biol.*, **19**:697–714, 1981.

[325] A. Gierer. *Hydra* as a model for the development of biological form. *Sci. Am.*, **12**:44–54, 1974.

[326] M. A. Gilbert. Growth rate, longevity and maximum size of *Macoma baltica* (L.). *Biol. Bull. (Woods Hole)*, **145**:119–126, 1973.

[327] S. Glasstone, K. J. Laidler, and H. Eyring. *The theory of rate processes.* McGraw-Hill, London, 1941.

[328] Z. M. Gliwicz. Food thresholds and body size in cladocerans. *Nature (Lond.)*, **343**:638–640, 1990.

[329] F. A. P. C. Gobas, A. Opperhuizen, and O. Hutzinger. Bioconcentration of hydrophobic chemicals in fish: relationship with membrane permeation. *Environ. Toxicol. Chem.*, **5**:637–646, 1986.

[330] K. Godfrey. *Compartment models and their application.* Academic Press, New York, 1983.

[331] L. Godfrey, M. Sutherland, D. Boy, and N. Gomberg. Scaling of limb joint surface areas in anthropoid primates and other mammals. *J. Zool. Lond.*, **223**:603–625, 1991.

[332] J. C. Goldman. Conceptual role for microaggregates in pelagic waters. *Bull. Mar. Sci.*, **35**:462–476, 1984.

[333] J. C. Goldman and E. J. Cerpenter. A kinetic approach of temperature on algal growth. *Limnol. Oceanogr.*, **19**:756–766, 1974.

[334] C. R. Goldspink. A note on the growth-rate and year-class strength of bream, *Abramis brama* (L.), in three eutrophic lakes, England. *J. Fish Biol.*, **19**:665–673, 1981.

[335] B. Gompertz. On the nature of the function expressive of the law of mortality, and on a new method of determining the value of life contingencies. *Philos. Trans. R. Soc.*, **27**:513–585, 1825.

[336] M. Gophen and W. Geller. Filter mesh size and food particle uptake by *Daphnia*. *Oecologia (Berlin)*, **64**:408–412, 1984.

[337] R. W. Gordon, R. J. Beyers, E. P. Odum, and R. G. Eagon. Studies of a simple laboratory microecosystem: bacterial activities in a heterotrophic succession. *Ecology*, **50**:86–100, 1969.

[338] S. J. Gould. *Ontogeny and phylogeny.* Belknap Press, Cambridge, 1977.

[339] C. E. Goulden, L. L. Henry, and A. J. Tessier. Body size, energy reserves, and competitive ability in three species of cladocera. *Ecology*, **63**:1780–1789, 1982.

[340] C. E. Goulden and L. L. Hornig. Population oscillations and energy reserves in planktonic cladocera and their consequences to competition. *Proc. Natl. Acad. Sci. U. S. A.*, **77**:1716–1720, 1980.

[341] B. W. Grant and W. P. Porter. Modelling global macroclimatic constraints on ectotherm energy budgets. *Am. Zool.*, **32**:154–178, 1992.

[342] C. J. Grant and A. V. Spain. Reproduction, growth and size allometry of *Liza vaigiensis* (Quoy & Gaimard) (*Pisces*: *Mugilidae*) from North Queensland inshore waters. *Aust. J. Zool.*, **23**:475–485, 1975.

[343] C. J. Grant and A. V. Spain. Reproduction, growth and size allometry of *Valamugil seheli* (Forskal) (*Pisces*: *Mugilidae*) from North Queensland inshore waters. *Aust. J. Zool.*, **23**:463–474, 1975.

[344] J. Gray. The growth of fish I. The relationship between embryo and yolk in *Salmo fario*. *J. Exp. Biol.*, **4**:215–225, 1926.

[345] R. H. Green. *Birds.* The fauna of Tasmania. Potoroo Publishing, Launceton, 1995.

[346] W. Greve. Ökologische Untersuchungen an *Pleurobrachia pileus* 1. Freilanduntersuchungen. *Helgol. Wiss. Meeresunters.*, **22**:303–325, 1971.

[347] W. Greve. Ökologische Untersuchungen an *Pleurobrachia pileus* 2. Laboratoriumuntersuchungen. *Helgol. Wiss. Meeresunters.*, **23**:141–164, 1972.

[348] P. Groeneveld. *Control of specific growth rate and physiology of the yeast* Kluyveromyces marxianus*; a biothermokinetic approach.* PhD thesis, Vrije Universiteit, Amsterdam, 1999.

[349] W. T. de Groot. Modelling the multiple nutrient limitation of algal growth. *Ecol. Modell.*, **18**:99–119, 1983.

[350] R. K. Grosberg. Life-history variation within a population of the colonial ascidian *Botryllus schlosseri.* I. The genetic and environmental control of seasonal variation. *Evolution*, **42**:900–920, 1988.

[351] R. Grundel. Determinants of nestling feeding rates and parental investment in the mountain chickadee. *Condor*, **89**:319–328, 1987.

[352] J. Guckenheimer and P. Holmes. *Nonlinear oscillations, dynamical systems, and bifurcations of vector fields.*, volume 42 of *Applied Mathematical Sciences.* Springer-Verlag, 1983.

[353] C. A. W. Guggisberg. *The crocodiles.* David and Charles, Newton Abbot, 1980.

[354] R. Günther. *Die Wasserfrösche Europas.* Die Neue Brehm-Bücherei. A. Ziemsen-Verlag, Wittenberg Lutherstadt, 1990.

[355] W. S. C Gurney and R. M. Nisbet. *Ecological dynamics.* Oxford University Press, 1998.

[356] R. Haase. *Thermodynamics of irreversible processes.* Dover Publications, New York, 1990.

[357] U. Halbach. Einfluss der Temperatur auf die Populationsdynamik der planktischer Radertieres *Brachionus calyciflorus* Pallas. *Oecologia (Berlin)*, **4**:176–207, 1970.

[358] D. O. Hall and K. K. Rao. *Photosynthesis.* Cambridge University Press, 1999.

[359] T. G. Hallam, R. R. Lassiter, and S. A. L. M. Kooijman. Effects of toxicants on aquatic populations. In S. A. Levin, T. G. Hallam, and L. F. Gross, editors, *Mathematical ecology.*, pages 352–382. Springer, London, 1989.

[360] T. G. Hallam, R. R. Lassiter, J. Li, and W. McKinney. An approach for modelling populations with continuous structured models. In D. L. DeAngelis and L. J. Gross, editors, *Individual based approaches and models in ecology*, pages 312–337. Springer-Verlag, 1992.

[361] T. G. Hallam, R. R. Lassiter, J. Li, and L. A. Suarez. Modelling individuals employing an integrated energy response: application to *Daphnia.* *Ecology*, **71**:938–954, 1990.

[362] T. G. Hallam and J. L. de Luna. Effects of toxicants on population: a qualitative approach. III. Environmental and food chain pathways. *J. Theor. Biol.*, **109**:411–429, 1984.

[363] B. Halliwell and J. M. C. Gutteridge. *Free radicals in biology and medicine.* Oxford University Press, 1999.

[364] P. Hallock. Algal symbiosis: a mathematical analysis. *Mar. Biol.*, **62**:249–255, 1981.

[365] P. P. F. Hanegraaf. *Mass and energy fluxes in microorganisms according to the Dynamic Energy Budget theory for filaments.* PhD thesis, Vrije Universiteit, Amsterdam, 1997.

[366] P. P. F. Hanegraaf, B. W. Kooi, and S. A. L. M. Kooijman. The role of intracellular components in food chain dynamics. *C. R. Acad. Sci. Ser. III*, **323**:99–111, 2000.

[367] R. J. F. van Haren and S. A. L. M. Kooijman. Application of the dynamic energy budget model to *Mytilus edulis* (L). *Neth. J. Sea Res.*, **31**:119–133, 1993.

[368] D. Harman. Role of free radicals in mutation, cancer, aging and maintenance of life. *Radiat. Res.*, **16**:752–763, 1962.

[369] D. Harman. The aging process. *Proc. Natl. Acad. Sci. U. S. A.*, **78**:7124–7128, 1981.

[370] F. M. Harold. *The vital force. A study of bioenergetics.* Freeman, New York, 1986.

[371] J. L. Harper. *Population biology of plants.* Academic Press, London, 1977.

[372] M. P. Harris. The biology of an endangered species, the dark-rumped petrel (*Pterodroma phaeopygia*), in the Galapagos Islands. *Condor*, **72**:76–84, 1970.

[373] C. Harrison. *A field guide to the nests, eggs and nestlings of European birds.* Collins, London, 1975.

[374] R. Harrison and G. G. Lunt. *Biological membranes. Their structure and function.* Blackie, Glasgow, 1980.

[375] R. J. Harvey, A. G. Marr, and P. R. Painter. Kinetics of growth of individual cells of *Escherichia coli* and *Azotobacter agilis. J. Bacteriol.*, **93**:605–617, 1967.

[376] K. A. Hasselbalch. Über den respiratorischen Stoffechsel des Hühnerembryos. *Skand. Arch. Physiol.*, **10**:353–402, 1900.

[377] A. Hastings. What equilibrium behaviour of Lotka–Volterra models does not tell us about food webs. In G. A. Polis and K. O. Winemiller, editors, *Food webs*, pages 211–217. Chapman & Hall, London, 1996.

[378] A. Hastings. *Population biology; concepts and models.* Springer, New York, 1997.

[379] A. Hastings and T. Powell. Chaos in a three-species food chain. *Ecology*, **72**:896–903, 1991.

[380] F. Haverschmidt. Notes on the life history of *Amazilia fimbriata* in Surinam. *Wilson Bull.*, **61**:69–79, 1952.

[381] D. W. Hawker and D. W. Connell. Relationships between partition coefficient, uptake rate constant, clearance rate constant, and time to equilibrium for bioaccumulation. *Chemosphere*, **14**:1205–1219, 1985.

[382] D. W. Hawker and D. W. Connell. Bioconcentration of lipophilic compounds by some aquatic organisms. *Ecotoxicol. Environ. Saf.*, **11**:184–197, 1986.

[383] A. J. S. Hawkins and B. L. Bayne. Seasonal variations in the balance between physiological mechanisms of feeding and digestion in *Mytilus edulis* (*Bivalvia*, *Mollusca*). *Mar. Biol.*, **82**:233–240, 1984.

[384] P. D. N. Hebert. The genetics of *Cladocera*. In W. C. Kerfoot, editor, *Evolution and ecology of zooplankton communities*, pages 329–336. University of New England Press, 1980.

[385] P. D. N. Hebert. Genotypic characteristic of cyclic parthenogens and their obligately asexual derivates. In S. C. Stearns, editor, *The evolution of sex and its consequences*, pages 175–195. Birkhäuser, Basel, 1987.

[386] H. Heesterbeek. R_0. PhD thesis, Rijksuniversiteit Leiden, 1992.

[387] H. J. A. M. Heijmans. Holling's 'hungry mantid' model for the invertebrate functional response considered as a Markov process. Part III: Stable satiation distribution. *J. Math. Biol.*, **21**:115–1431, 1984.

[388] H. J. A. M. Heijmans. *Dynamics of structured populations.* PhD thesis, University of Amsterdam, 1985.

[389] J. J. Heijnen. A new thermodynamically based correlation of chemotrophic biomass yields. *Antonie van Leeuwenhoek*, **60**:235–256, 1991.

[390] J. J. Heijnen and J. P. van Dijken. In search of a thermodynamic description of biomass yields for the chemotrophic growth of micro organisms. *Biotechnol. Bioeng.*, **39**:833–858, 1992.

[391] J. J. Heijnen and J. A. Roels. A macroscopic model describing yield and maintenance relationships in aerobic fermentation. *Biotechnol. Bioeng.*, **23**:739–761, 1981.

[392] B. Heinrich. *The hot-blooded insects; strategies and mechanisms of thermoregulation.* Harvard Universitiy Press, Cambridge, MA, 1993.

[393] R. Heinrich and S. Schuster. *The regulation of cellular systems.* Chapman & Hall, New York, 1996.

[394] J. M. Hellawell. Age determination and growth of the grayling *Thymallus thymallus* (L.) of the River Lugg, Herefordshire. *J. Fish Biol.*, **1**:373–382, 1969.

[395] M. A. Hemminga. *Regulation of glycogen metabolism in the freshwater snail* Lymnaea stagnalis. PhD thesis, Vrije Universiteit, Amsterdam, 1984.

[396] A. M. Hemmingsen. Energy metabolism as related to body size and respiratory surfaces, and its evolution. *Rep. Steno. Mem. Hosp. Nordisk Insulinlaboratorium*, **9**:1–110, 1969.

[397] A. J. Hendriks. Modelling non-equilibrium concentrations of microcontaminants in organisms: comparative kinetics as a function of species size and octanol-water partitioning. *Chemosphere*, **30**:265–292, 1995.

[398] V. Henri. Théorie générale de l'action de quelques diastases. *CR Hebd. Séances Acad. Sci. (Paris)*, **135**:916–919, 1902.

[399] W. G. Heptner and A. A. Nasimowitsch. *Der Elch (*Alces alces*).* Die Neue Brehm-Bücherei. A. Ziemsen-Verlag, Wittenberg Lutherstadt, 1974.

[400] D. Herbert. Some principles of continuous culture. In G. Tunevall, editor, *Recent progress in microbiology, Symposium of the 7th International Congress for Microbiology*, volume 7, pages 381–396, Stockholm, 1958. Almqvist and Wiksell.

[401] S. L. Herendeen, R. A. VanBogelen, and F. C. Neidhardt. Levels of major proteins of *Escherichia coli* during growth at different temperatures. *J. Bacteriol.*, **138**:185, 1979.

[402] C. F. Herreid II and B. Kessel. Thermal conductance in birds and mammals. *Comp. Biochem. Physiol.*, **21**:405–414, 1967.

[403] H. C. Hess. The evolution of parental care in brooding spirorbid polychaetes: the effect of scaling constraints. *Am. Nat.*, **141**:577–596, 1993.

[404] D. J. S. Hetzel. The growth and carcass characteristics of crosses between alabio and tegal ducks and moscovy and pekin drakes. *Br. Poult. Sci.*, **24**:555–563, 1983.

[405] H. R. Hewer and K. M. Backhouse. Embryology and foetal growth of the grey seal, *Halichoerus grypus*. *J. Zool. Lond.*, **155**:507–533, 1968.

[406] C. J. Hewett. Growth and moulting in the common lobster (*Homarus vulgaris* Milne-Edwards). *J. Mar. Biol. Assoc. U. K.*, **54**:379–391, 1974.

[407] P. S. Hewlett and R. L. Plackett. *The interpretation of quantal responses in biology.* Edward Arnold, London, 1979.

[408] L. C. Hewson. Age, maturity, spawning and food of burbot, *Lota lota*, in Lake Winnipeg. *J. Fish. Res. Board Can.*, **12**:930–940, 1955.

[409] R. W. Hickman. Allometry and growth of the green-lipped mussel *Perna canaliculus* in New Zealand. *Mar. Biol.*, **51**:311–327, 1979.

[410] R. Hile. Age and growth of the cisco *Leuchichthys artedi* (Le Sueur) in lake of the north-eastern High Land Eisconsian. *Bull. Bur. Fish., Wash.*, **48**:211–317, 1936.

[411] R. Hill and C. P. Whittingham. *Photosynthesis.* Methuen & Co., London, 1955.

[412] T. L. Hill. *An introduction to statistical thermodynamics.* Dover Publications, New York, 1986.

[413] M. W. Hirsch and S. Smale. *Differential equations, dynamical systems, and linear algebra.* Academic Press, London, 1974.

[414] P. W. Hochachka. *Living without oxygen.* Harvard University Press, 1980.

[415] P. W. Hochachka and M. Guppy. *Metabolic arrest and the control of biological time.* Harvard University Press, 1987.

[416] P. W. Hochachka and G. N. Somero. *Biochemical adaptation.* Princeton University Press, 1984.

[417] P. A. R. Hockey. Growth and energetics of the African black oystercatcher *Haematopus moquini*. *Ardea*, **72**:111–117, 1984.

[418] J. K. M. Hodasi. The effects of different light regimes on the behaviour biology of *Achatina (Achatina) achatina* (Linne). *J. Molluscan Stud.*, **48**:283–293, 1982.

[419] N. van der Hoeven. The population dynamics of daphnia at constant food supply: a review, re-evaluation and analysis of experimental series from the literature. *Neth. J. Zool.*, **39**:126–155, 1989.

[420] N. van der Hoeven, S. A. L. M. Kooijman, and W. K. de Raat. Salmonella test: relation between mutagenicity and number of revertant colonies. *Mutat. Res.*, **234**:289–302, 1990.

[421] M. Hoffman. Yeast biology enters a surprising new phase. *Science (New York)*, **255**:1510–1511, 1992.

[422] M. A. Hofman. Energy metabolism, brain size and longevity in mammals. *Q. Rev. Biol.*, **58**:495–512, 1983.

[423] M. J. Holden. The growth rates of *Raja brachyura*, *R. clavata* and *R. montaqui* as determined from tagging data. *J. Physiol. (Lond.)*, **34**:161–168, 1972.

[424] C. S. Holling. Some characteristics of simple types of predation and parasitism. *Can. Entomol.*, **91**:385–398, 1959.

[425] B. Holmes. The perils of planting pesticides. *New Sci.*, **28**:34–37, 1993.

[426] N. J. Horan. *Biological wastewater treatment systems.* J. Wiley & Sons Inc., Chichester, 1990.

[427] J. R. Horner. The nesting behaviour of dinosaurs. *Sci. Am.*, **4**:92–99, 1984.

[428] H. J. Horstmann. Sauerstoffverbrauch und Trockengewicht der Embryonen von *Lymnaea stagnalis* L. *Z. Vgl. Physiol.*, **41**:390–404, 1958.

[429] R. A. Horton, M. Rowan, K. E. Webster, and R. H. Peters. Browsing and grazing by cladoceran filter feeders. *Can. J. Zool.*, **57**:206–212, 1979.

[430] M. A. Houck, J. A. Gauthier, and R. E. Strauss. Allometric scaling in the earliest fossil bird, *Archaeopteryx lithographica*. *Science (New York)*, **247**:195–198, 1990.

[431] S. E. L. Houde and M. R. Roman. Effects of food quality on the functional ingestion response of the copepod *Acartia tonsa*. *Mar. Ecol. Prog. Ser.*, **48**:69–77, 1987.

[432] J. Hovekamp. *On the growth of larval plaice in the North Sea.* PhD thesis, University of Groningen, 1991.

[433] R. A. How. Reproduction, growth and survival of young in the mountain possum, *Trichosurus caninus* (*Marsupialia*). *Aust. J. Zool.*, **24**:189–199, 1976.

[434] A. St. G. Huggett and W. F. Widdas. The relationship between mammalian foetal weight and conception age. *J. Physiol. (Lond.)*, **114**:306–317, 1951.

[435] R. E. Hungate. The rumen microbial ecosystem. *Ann. Rev. Ecol. Syst.*, **6**:39–66, 1975.

[436] P. C. Hunt and J. W. Jones. Trout in Llyn Alaw, Anglesey, North Wales II. Growth. *J. Fish Biol.*, **4**:409–424, 1972.

[437] R. von Hutterer. Beobachtungen zur Geburt und Jugendentwicklung der Zwergspitzmaus, *Sorex minutus* L. (*Soricidae- Insectivora*). *Z. Saeugetierkd.*, **41**:1–22, 1976.

[438] J. S. Huxley. *Problems of relative growth.* Methuen & Co., London, 1932.

[439] H. L. Ibsen. Prenatal growth in guinea-pigs with special reference to environmental factors affecting weight at birth. *J. Exp. Zool.*, **51**:51–91, 1928.

[440] T. D. Iles and P. O. Johnson. The correlation table analysis of a sprat (*Clupea sprattus* L.) year-class to separate two groups differing in growth characteristics. *J. Cons. Int. Explor. Mer.*, **27**:287–303, 1962.

[441] H. Ineichen, U. Riesen-Willi, and J. Fisher. Experimental contributions to the ecology of *Chironomus* (*Diptera*) II. Influence of the photoperiod on the development of *Chironomus plumosus* in the 4th larval instar. *Oecologia (Berlin)*, **39**:161–183, 1979.

[442] L. Ingle, T. R. Wood, and A. M. Banta. A study of longevity, growth, reproduction and heart rate in *Daphnia longispina* as influenced by limitations in quantity of food. *J. Exp. Zool.*, **76**:325–352, 1937.

[443] J. L. Ingraham. Growth of psychrophillic bacteria. *J. Bacteriol.*, **76**:75–80, 1958.

[444] R. Ivell. The biology and ecology of a brackish lagoon bivalve, *Cerastoderma glaucum* Bruguiere, in Lago Lungo, Italy. *J. Molluscan Stud.*, **45**:364–382, 1979.

[445] E. A. Jackson. *Perspectives of nonlinear dynamics.*, volume I, II. Cambridge University Press, 1991.

[446] J. A. Jacquez. *Compartment analysis in biology and medicine.* Elsevier Publ. Co., Amsterdam, 1972.

[447] M. R. James. Distribution, biomass and production of the freshwater mussel, *Hyridella menziesi* (Gray), in Lake Taupo, New Zealand. *Freshwater Biol.*, **15**:307–314, 1985.

[448] M. J. W. Jansen and J. A. J. Metz. How many victims will a pitfall make? *Acta Biotheor.*, **28**:98–122, 1979.

[449] G. Janssen. *On the genetical ecology of springtails.* PhD thesis, Vrije Universiteit, Amsterdam, 1985.

[450] J. W. Jeong, J. Snay, and M. M. Ataai. A mathematical model for examining growth and sporulation processes of *Bacillus subtilus*. *Biotechnol. Bioeng.*, **35**:160–184, 1990.

[451] M. Jobling. Mathematical models of gastric emptying and the estimation of daily rates of food consumption for fish. *J. Fish Biol.*, **19**:245–257, 1981.

[452] A. W. B. Johnston, J. L. Firmin, and L. Rosen. On the analysis of symbiotic genes in *Rhizobium*. *Symp. Soc. Gen. Microbiol.*, **42**:439–455, 1988.

[453] A. Jones. Studies on egg development and larval rearing of turbot, *Scophthalmus maximus* L. and brill, *Scophthalmus rhombus* L., in the laboratory. *J. Mar. Biol. Assoc. U. K.*, **52**:965–986, 1972.

[454] G. P. Jones. Contribution to the biology of the red-banded perch, *Ellerkeldia huntii* (Hector), with a discussion on hermaphroditism. *J. Fish Biol.*, **17**:197–207, 1980.

[455] H. G. Jones. *Plant and microclimate. A quantitative approach to environmental plant physiology.* Cambridge University Press, 1992.

[456] J. W. Jones and H. B. N. Hynes. The age and growth of *Gasterosteus aculeatus*, *Pygosteus pungitius* and *Spinachia vulgaris*, as shown by their otoliths. *J. Anim. Ecol.*, **19**:59–73, 1950.

[457] E. N. G. Joosse and J. B. Buker. Uptake and excretion of lead by litter-dwelling Collembola. *Environ. Pollut.*, **18**:235–240, 1979.

[458] E. N. G. Joosse and E. Veltkamp. Some aspects of growth, moulting and reproduction in five species of surface dwelling *Collembola*. *Neth. J. Zool.*, **20**:315–328, 1970.

[459] D. M. Joubert. A study of pre-natal growth and development in the sheep. *J. Agric. Sci.*, **47**:382–428, 1956.

[460] J. Juget, V. Goubier, and D. Barthélémy. Intrisic and extrinsic variables controlling the productivity of asexual populations of *Nais spp*, (*Naididae*, *Oligochaeta*). *Hydrobiologia*, **180**:177–184, 1989.

[461] H. Kaiser. Populationsdynamik und Eigenschaften einzelner Individuen. *Verh. Ges. Ökol. Erlangen*, pages 25–38, 1974.

[462] H. Kaiser. The dynamics of populations as result of the properties of individual animals. *Fortschr. Zool.*, **25**:109–136, 1979.

[463] J. D. Kalbfleisch and R. L. Prentice. *The statistical analysis of failure time data.* J. Wiley & Sons, Inc., Chichester, 1980.

[464] G. Kapocsy. *Weissbart- und Weissflugelseeschwalbe.* Die Neue Brehm-Bücherei. A. Ziemsen-Verlag, Wittenberg Lutherstadt, 1979.

[465] W. H. Karasov. Dailey energy expenditure and the cost of activity in mammals. *Am. Zool.*, **32**:238–248, 1992.

[466] V. V. Kashkin. Heat exchange of bird eggs during incubation. *Biophysics*, **6**:57–63, 1961.

[467] L. Kaufman. Innere und Äussere Wachstumsfactoren. Untersuchungen an Hühnern und Tauben. *Wilhelm Roux' Arch. Entwicklungsmech. Org.*, **6**:395–431, 1930.

[468] N. Kautsky. Quantitative studies on gonad cycle, fecundity, reproductive output and recruitment in a baltic *Mytilus edulis* population. *Mar. Biol.*, **67**:143–160, 1982.

[469] Z. Kawabata, K. Matsui, K. Okazaki, M. Nasu, N. Nakano, and T. Sugai. Synthesis of a species-defined microcosm with protozoa. *J. Protozool. Res.*, **5**:23–26, 1995.

[470] C. Kayser and A. Heusner. Étude comparative du métabolisme énergétiques dans la série animale. *J. Physiol. (Paris)*, **56**:489–524, 1964.

[471] B. D. Keller. Coexistence of sea urchins in seagrass meadows: an experimental analysis of competition and predation. *Ecology*, **64**:1581–1598, 1983.

[472] C. M. Kemper. Growth and development of the Australian musid *Pseudomys novaehollandiae*. *Aust. J. Zool.*, **24**:27–37, 1976.

[473] S. C. Kendeigh. Factors affecting the length of incubation. *Auk*, **57**:499–513, 1940.

[474] M. Kennedy and P. Fitzmaurice. Some aspects of the biology of gudgeon *Gobio gobio* (L.) in Irish waters. *J. Fish Biol.*, **4**:425–440, 1972.

[475] R. A. Kent and D. Currie. Predicting algal sensitivity to a pesticide stress. *Environ. Toxicol. Chem.*, **14**:983–991, 1995.

[476] A. Kepes. Etudes cinetiques sur la galactoside-permease d'*Escherichia coli*. *Biochim. Biophys. Acta*, **40**:70–84, 1960.

[477] K. Kersting and W. Holterman. The feeding behaviour of *Daphnia magna*, studied with the coulter counter. *Mitt. Int. Ver. Theor. Angew. Limnol.*, **18**:1434–1440, 1973.

[478] M. Kessel and Y. Cohen. Ultrastructure of square bateria from a brine pool in southern Sinai. *J. Bacteriol.*, **150**:851–860, 1982.

[479] A. Keve. *Der Eichelhaher.* Die Neue Brehm-Bücherei. A. Ziemsen-Verlag, Wittenberg Lutherstadt, 1985.

[480] A. I. Khibnik, Yu. A. Kuznetsov, V. V. Levitin, and E. V. Nikolaev. Continuation techniques and interactive software for bifurcation analysis of ODEs and iterated maps. *Physica D*, **62**:360–371, 1993.

[481] P. Kindlmann and A. F. G. Dixon. Developmental constraints in the evolution of reproductive strategies: telescoping of generations in parthenogenetic aphids. *Funct. Ecol.*, **3**:531–537, 1989.

[482] C. M. King. *The natural history of weasels & stoats.* C. Helm, London, 1989.

[483] P. Kingston. Some observations on the effects of temperature and salinity upon the growth of *Cardium edule* and *Cardium glaucum* larvae in the laboratory. *J. Mar. Biol. Assoc. U. K.*, **54**:309–317, 1974.

[484] F. C. Kinsky. The yearly cycle of the northern blue penguin (*Eudyptula minor novaehollandiae*) in the Wellington Harbour area. *Rec. Dom. Mus. (Wellington)*, **3**:145–215, 1960.

[485] T. Kiørboe, F. Møhlenberg, and O. Nøhr. Effect of suspended bottom material on growth and energetics in *Mytilus edulis*. *Mar. Biol.*, **61**:283–288, 1981.

[486] T. B. L. Kirkwood, R. Holliday, and R. F. Rosenberger. Stability of the cellular translation process. *Int. Rev. Cytol.*, **92**:93–132, 1984.

[487] P. Kitcher. *Abusing science; the case against creationism.* MIT Press, Cambridge, MA, 1982.

[488] M. Klaassen, G. Slagsvold, and C. Beek. Metabolic rate and thermostability in relation to availability of yolk in hatchlings of black-legged kittiwake and domestic chicken. *Auk*, **104**:787–789, 1987.

[489] A. Klebanoff and A. Hastings. Chaos in a three-species food chain. *J. Math. Biol.*, **32**:427–451, 1994.

[490] M. Kleiber. Body size and metabolism. *Hilgardia*, **6**:315–353, 1932.

[491] O. T. Kleiven, P. Larsson, and A. Hobæk. Sexual reproduction in *Daphnia magna* requires three stimuli. *Oikos*, **64**:197–206, 1992.

[492] C. Klok and A. M. de Roos. Population level consequences of toxicological influences on individual growth and reproduction in *Lumbricus rubellus* (Lumbricidae, Oligochaeta). *Ecotoxicol. Environ. Saf.*, **33**:118–127, 1996.

[493] A. J. Kluyver and H. J. L. Donker. Die einheit in der biochemie. *Chem. Zelle Gewebe*, **13**:134–191, 1926.

[494] H. N. Kluyver. Food consumption in relation to habitat in breeding chickadees. *Auk*, **78**:532–550, 1961.

[495] A. L. Koch. Overall controls on the biosynthesis of ribosomes in growing bacteria. *J. Theor. Biol.*, **28**:203–231, 1970.

[496] A. L. Koch. The macroeconomics of bacterial growth. In M. Fletcher and G. D. Floodgate, editors, *Bacteria in their natural environment*, volume 16 of *Special publication of the Society for General Microbiology*, pages 1–42. Academic press, 1985.

[497] A. L. Koch. The variability and individuality of the bacterium. In F. C. Neidhardt, editor, Escherichia coli *and* Salmonella typhimurium*. Cellular and molecular biology*, pages 1606–1614. American Society for Microbiology, Washington, 1987.

[498] A. L. Koch. Diffusion. the crucial process in many aspects of the biology of bacteria. *Adv. Microb. Ecol.*, **11**:37–70, 1990.

[499] A. L. Koch. Quantitative aspects of cellular turnover. *Antonie van Leeuwenhoek*, **60**:175–191, 1991.

[500] A. L. Koch. Biomass growth rate during the prokaryote cell cycle. *Crit. Rev. Microbiol.*, **19**:17–42, 1993.

[501] A. L. Koch and M. Schaechter. A model for the statistics of the division process. *J. Gen. Microbiol.*, **29**:435–454, 1962.

[502] A. C. Kohler. Variations in the growth of Atlantic cod (*Gadus morhua* L.). *J. Fish. Res. Board Can.*, **21**:57–100, 1964.

[503] M. Konarzewski. A model of growth in altricial birds based on changes in water content of the tissues. *Ornis Scand.*, **19**:290–296, 1988.

[504] W. H. Könemann. *Quantitative structure–activity relationships for kinetics and toxicity of aquatic pollutants and their mixtures in fish.* PhD thesis, Utrecht University, the Netherlands, 1980.

[505] W. H. Könemann. Quantitative structure–activity relationships in fish toxicity studies. 1. Relationship for 50 industrial pollutants. *Toxicology*, **19**:209–221, 1981.

[506] B. W. Kooi, M. P. Boer, and S. A. L. M. Kooijman. Mass balance equation versus logistic equation in food chains. *J. Biol. Syst.*, **5**(1):77–85, 1997.

[507] B. W. Kooi, M. P. Boer, and S. A. L. M. Kooijman. Consequences of population models on the dynamics of food chains. *Math. Biosci.*, **153**:99–124, 1998.

[508] B. W. Kooi, M. P. Boer, and S. A. L. M. Kooijman. On the use of the logistic equation in food chains. *Bull. Math. Biol.*, **60**:231–246, 1998.

[509] B. W. Kooi, M. P. Boer, and S. A. L. M. Kooijman. Resistance of a food chain to invasion by a top predator. *Math. Biosci.*, **157**:217–236, 1999.

[510] B. W. Kooi and S. A. L. M. Kooijman. Invading species can stabilize simple trophic systems. *Ecological Modelling*, **133**:57–72, 2000.

[511] S. A. L. M. Kooijman. Statistical aspects of the determination of mortality rates in bioassays. *Water Res.*, **17**:749–759, 1983.

[512] S. A. L. M. Kooijman. Toxicity at population level. In J. Cairns, editor, *Multispecies toxicity testing.*, pages 143–164. Pergamon Press, New York, 1985.

[513] S. A. L. M. Kooijman. Population dynamics on the basis of budgets. In J. A. J. Metz and O. Diekmann, editors, *The dynamics of physiologically structured populations.*, Springer Lecture Infos in Biomathematics., pages 266–297. Springer-Verlag, Berlin, 1986.

[514] S. A. L. M. Kooijman. What the hen can tell about her egg; egg development on the basis of budgets. *J. Math. Biol.*, **23**:163–185, 1986.

[515] S. A. L. M. Kooijman. The von Bertalanffy growth rate as a function of physiological parameters; a comparative analysis. In T. G. Hallam, L. J. Gross, and S. A. Levin, editors, *Mathematical ecology.*, pages 3–45. World Scientific, Singapore, 1988.

[516] S. A. L. M. Kooijman. *Dynamic energy budgets in biological systems. Theory and applications in ecotoxicology.* Cambridge University Press, 1993.

[517] S. A. L. M. Kooijman. The stoichiometry of animal energetics. *J. Theor. Biol.*, **177**:139–149, 1995.

[518] S. A. L. M. Kooijman. The synthesizing unit as model for the stoichiometric fusion and branching of metabolic fluxes. *Biophys. Chem.*, **73**:179–188, 1998.

[519] S. A. L. M. Kooijman and J. J. M. Bedaux. *The analysis of aquatic toxicity data.* VU University Press, Amsterdam, 1996.

[520] S. A. L. M. Kooijman and J. J. M. Bedaux. Analysis of toxicity tests on *Daphnia* survival and reproduction. *Water Res.*, **30**:1711–1723, 1996.

[521] S. A. L. M. Kooijman and R. J. F. van Haren. Animal energy budgets affect the kinetics of xenobiotics. *Chemosphere*, **21**:681–693, 1990.

[522] S. A. L. M. Kooijman, N. van der Hoeven, and D. C. van der Werf. Population consequences of a physiological model for individuals. *Funct. Ecol.*, **3**:325–336, 1989.

[523] S. A. L. M. Kooijman, B. W. Kooi, and T. G. Hallam. The application of mass and energy conservation laws in physiologically structured population models of heterotrophic organisms. *J. Theor. Biol.*, **197**:371–392, 1999.

[524] S. A. L. M. Kooijman and J. A. J. Metz. On the dynamics of chemically stressed populations; the deduction of population consequences from effects on individuals. *Ecotox. Environ. Saf.*, **8**:254–274, 1983.

[525] S. A. L. M. Kooijman, E. B. Muller, and A. H. Stouthamer. Microbial dynamics on the basis of individual budgets. *Antonie van Leeuwenhoek*, **60**:159–174, 1991.

[526] S. A. L. M. Kooijman and R. M. Nisbet. How light and nutrients affect life in a closed bottle. In S. E. Jørgensen, editor, *Thermodynamics and ecological modelling.*, pages 19–60. CRC Publ., Boca Raton, FL, USA, 2000.

[527] L. J. H. Koppes, C. L. Woldringh, and N. Nanninga. Size variations and correlation of different cell cycle events in slow-growing *Escherichia coli. J. Bacteriol.*, **134**:423–433, 1978.

[528] A. Kowald and T. B. L. Kirkwood. Towards a network theory of ageing: a model combining the free radical theory and the protein error theory. *J. Theor. Biol.*, **168**:75–94, 1994.

[529] A. Kowald and T. B. L. Kirkwood. A network theory of ageing: the interactions of defective mitochondria, aberrant proteins, free radicals and scavengers in the ageing process. *Mutat. Res.*, **316**:209–235, 1996.

[530] K. B. Krauskopf and D. K. Bird. *Introduction to geochemistry.* McGraw-Hill Internat. Editions, New York, 1995.

[531] J.-U. Kreft, G. Booth, and W. T. Wimpenny. BacSim, a simulator for individual-based modelling of bacterial colony growth. *Microbiology*, **144**:3275–3287, 1998.

[532] F. Kreit and W. Z. Black. *Basic Heat Transfer.* Harper and Row, 1980.

[533] H. J. Kreuzer. *Nonequilibrium thermodynamics and its statistical foundations.* Clarendon Press, Oxford, 1981.

[534] H. J. Kronzucker, M. Y. Siddiqi, and A. D. M. Glass. Conifer root discrimination against soil nitrate and the ecology of forest succession. *Nature*, **385**:59–61, 1997.

[535] M. Kshatriya and R. W. Blake. Theoretical model of migration energetics in the blue whale, *Balaenoptera musculus. J. Theor. Biol.*, **133**:479–498, 1988.

[536] H. E. Kubitschek. Cell growth and abrupt doubling of membrane proteins in *Escherichia coli* during the division cycle. *J. Gen. Microbiol.*, **136**:599–606, 1990.

[537] S. W. Kuffler, J. G. Nicholls, and A. R. Martin. *From neuron to brain.* Sinauer, Sunderland, MA, 1984.

[538] Yu. A. Kuznetsov. *Elements of applied bifurcation theory.*, volume 112 of *Applied Mathematical Sciences.* Springer-Verlag, Berlin, 1995.

[539] Yu. A. Kuznetsov and S. Rinaldi. Remarks on food chain dynamics. *Math. Biosci.*, **134**:1–33, 1996.

[540] D. Lack. *Ecological adaptations for breeding in birds.* Methuen & Co., London, 1968.

[541] A. K. Laird. Dynamics of tumor growth. *Br. J. Cancer*, **18**:490–502, 1964.

[542] H. Lambers, F. S. Chapin III, and T. L. Pons. *Plant physiological ecology.* Springer-Verlag, New York, 1998.

[543] A. R. G. Lang and J. E. Begg. Movements of *Helianthus annuus* leaves and heads. *J. Appl. Ecol.*, **16**:299–306, 1979.

[544] E. Lanting. *Een wereld verdwaald in de tijd. Madagascar.* Fragment Uitgeverij, 1990.

[545] R. R. Lassiter and T. G. Hallam. Survival of the fattest: a theory for assessing acute effects of hydrophobic, reversibly acting chemicals on populations. *Ecology*, **109**:411–429, 1988.

[546] D. M. Lavigne, W. Barchard, S. Innes, and N. A. Oritsland. *Pinniped bioenergetics.*, volume IV of *FAO Fisheries Series No 5.* FAO, Rome, 1981.

[547] R. M. Laws. The elephant seal (*Mirounga leonina* Linn) I. Growth and age. *RIDS Sci. Rep.*, **8**:1–37, 1953.

[548] R. M. Laws. Age criteria for the African elephant, *Loxodonta a. africana* E. *Afr. Wildl.*, **4**:1–37, 1966.

[549] M. LeCroy and C. T. Collins. Growth and survival of roseate and common tern chicks. *Auk*, **89**:595–611, 1972.

[550] A. L. Lehninger. *Bioenergetics.* Benjamin/Cummings Publ. Co., Mnlo Park, Calif., 1973.

[551] R. A. Leigh and D. Sanders. *The plant vacuole.*, volume 25 of *Advances in botanical research.* Academic Press, San Diego, 1997.

[552] W. A. Lell. The relation of the volume of the amniotic fluid to the weight of the fetus at different stages of pregnancy in the rabbit. *Anat. Rec.*, **51**:119–123, 1931.

[553] J. W. Lengeler, G. Drews, and H. G. Schlegel. *Biology of the prokaryotes.* Thieme, Stuttgart, 1999.

[554] R. Leudeking and E. L. Piret. A kinetic study of the lactic acid fermentation. *J. Biochem. Microbiol. Technol. Eng.*, **1**:393, 1959.

[555] G. Levy. Demonstration of michaelis-menten kinetics in man. *J. Pharm. Sci.*, **54**:496, 1965.

[556] G. Levy, A.W. Vogel, and L.P. Amsel. Capacity-limited salicylurate formation during prolonged administration of aspirin to healthy human subjects. *J. Pharm. Sci.*, **58**:503–504, 1969.

[557] J. von Liebig. *Chemistry in its application to agriculture and physiology.* Taylor and Walton, London, 1840.

[558] N. Lifson and R. McClintock. Theory of use of the turnover rates of body water for measuring energy and material balance. *J. Theor. Biol.*, **12**:46–74, 1966.

[559] J. D. Ligon. Still more responses of the poor-will to low temperatures. *Condor*, **72**:496–498, 1970.

[560] K. Lika and R. M. Nisbet. A dynamic energy budget model based on partitioning of net production. *J. Math. Biol.*, 1999. in press.

[561] G. N. Ling. *In search of the physical basis of life.* Plenum Press, New York, 1984.

[562] C. Lockyer. Growth and energy budgets of large baleen whales from the southern hemisphere. In *Mammals in the seas*, volume III of *FAO Fisheries series No 5.* FAO, Rome, 1981.

[563] B. E. Logan and J. R. Hunt. Bioflocculation as a microbial response to substrate limitations. *Biotechnol. Bioeng.*, **31**:91–101, 1988.

[564] B. E. Logan and D. L. Kirchman. Uptake of dissolved organics by marine bacteria as a function of fluid motion. *Mar. Biol.*, **111**:175–181, 1991.

[565] H. Lohrl. *Die Tannemeise.* Die Neue Brehm-Bücherei. A. Ziemsen-Verlag, Wittenberg Lutherstadt, 1977.

[566] A. Łomnicki. *Population ecology of individuals.* Princeton University Press, 1988.

[567] E. N. Lorenz. Deterministic non-periodic flow. *J. Atmospher. Sci.*, **20**:130–141, 1963.

[568] B. G. Loughton and S. S. Tobe. Blood volume in the African migratory locust. *Can. J. Zool.*, **47**:1333–1336, 1969.

[569] G. Louw. *Physiological animal ecology.* Longman, London, 1993.

[570] B. Lovegrove. *The living deserts of Southern Africa.* Fernwood Press, Vlaeberg, 1993.

[571] B. G. Lovegrove and C. Wissel. Sociality in molerats: Metabolic scaling and the role of risk sensitivity. *Oecologia (Berlin)*, **74**:600–606, 1988.

[572] Y. Loya and L. Fishelson. Ecology of fish breeding in brackish water ponds near the Dead Sea (Israel). *J. Fish Biol.*, **1**:261–278, 1969.

[573] A. G. Lyne. Observations on the breeding and growth of the marsupial *Pelametes nasuta* geoffroy, with notes on other bandicoots. *Aust. J. Zool.*, **12**:322–339, 1964.

[574] J. W. MacArthur and W. H. T. Baillie. Metabolic activity and duration of life. I. Influence of temperature on longevity in *Daphnia magna*. *J. Exp. Zool.*, **53**:221–242, 1929.

[575] R. H. MacArthur and E. O. Wilson. *The theory of island biogeography.* Princeton University Press, 1967.

[576] D. MacDold. *European mammals; evolution and behaviour.* HarperCollins Publishers, London, 1995.

[577] B. A. MacDonald and R. J. Thompson. Influence of temperature and food availability on ecological energetics of the giant scallop *Placopecten magellanicus* I. Growth rates of shell and somatic tissue. *Mar. Ecol. Prog. Ser.*, **25**:279–294, 1985.

[578] E. C. MacDowell, E. Allen, and C. G. Macdowell. The prenatal growth of the mouse. *J. Gen. Physiol.*, **11**:57–70, 1927.

[579] D. MacKay. Correlation of bioconcentration factors. *Environ. Sci. Technol.*, **16**:274–278, 1982.

[580] D. MacKay and S. Paterson. Calculating fugacity. *Environ. Sci. Technol.*, **15**:1006–1014, 1981.

[581] R. S. MacKay and C. Tresser. Some flesh on the skeleton: the bifurcations of bimodal maps. *Physica D*, **27**:412–422, 1987.

[582] T. H. Mague, E. Friberg, D. J. Hughes, and I. Morris. Extracellular release of carbon by marine phytoplankton; a physiological approach. *Limnol. Oceanogr.*, **25**:262–279, 1980.

[583] S. P. Mahoney and W. Threlfall. Notes on the eggs, embryos and chick growth of the common guillemots *Uria aalge* in Newfoundland. *Ibis*, **123**:211–218, 1981.

[584] A. P. Malan and H. H. Curson. Studies in sex physiology, no. 15. Further observations on the body weight and crown-rump length of merino foetuses. *Onderstepoort J. Vet. Sci. Anim. Ind.*, **7**:239–249, 1936.

[585] S. E. Manahan. *Environmental chemistry.* Lewis Publishers, 1994.

[586] K. H. Mann and J. R. N. Lazier. *Dynamics of marine ecosystems.* Blackwell Science, Oxford, 1996.

[587] R. H. K. Mann. The growth and reproductive stategy of the gudgeon, *Gobio gobio* (L.), in two hard-water rivers in southern England. *J. Fish Biol.*, **17**:163–176, 1980.

[588] S. C. Manolis, G. J. W. Webb, and K. E. Dempsey. Crocodile egg chemistry. In G. J. W. Webb, S. C. Manolis, and P. J. Whitehead, editors, *Wildlife management: crocodiles and alligators*, pages 445–472. Beatty, Sydney, 1987.

[589] D. A. Manuwal. The natural history of Cassin's auklet (*Ptychoramphus aleuticus*). *Condor*, **76**:421–431, 1974.

[590] L. Margulis. *Symbiosis in cell evolution.* W. H. Freeman & Co., New York, 1993.

[591] D. M. Maron and B. N. Ames. Revised methods for the *Salmonella* mutagenicity test. *Mutat. Res.*, **113**:173–215, 1983.

[592] A. G. Marr, E. H. Nilson, and D. J. Clark. The maintenance requirement of *Escherichia coli*. *Ann. N. Y. Acad. Sci.*, **102**:536–548, 1962.

[593] A. G. Marr, P. R. Painter, and E. H. Nilson. Growth and division of individual bacteria. *Symp. Soc. Gen. Microbiol.*, **19**:237–261, 1969.

[594] M. M. Martin. *Invertebrate–microbial interactions: ingested fungal enzymes in arthropod biology.* Explorations in chemical ecology. Comstock Publ. Associates, Ithaca, 1987.

[595] D. Masman. *The annual cycle of the kestrel* Falco tinnunculus*; a study in behavioural energetics.* PhD thesis, University of Groningen, The Netherlands, 1986.

[596] J. Mauchline and L. R. Fisher. *The biology of euphausids.*, volume 7 of *Advances in Marine Biology.* Academic Press, 1969.

[597] J. E. Maunder and W. Threlfall. The breeding biology of the black-legged kittiwake in Newfoundland. *Auk*, **89**:789–816, 1972.

[598] R. M. May. *Stability and complexity in model ecosystems.* Princeton University Press, 1973.

[599] R. M. May. Simple mathematical models with very complicated dynamics. *Nature*, **261**:459, 1976.

[600] J. R. von Mayer. Über die Kräfte der unbelebten Natur. *Ann. Chem. Pharm.*, **42**:233, 1842.

[601] W. V. Mayneord. On a law of growth of Jensen's rat sarcoma. *Am. J. Cancer*, **16**:841–846, 1932.

[602] G. M. Maynes. Growth of the Parma wallaby, *Macropus parma* Waterhouse. *Aust. J. Zool.*, **24**:217–236, 1976.

[603] K. McCann and P. Yodzis. Nonlinear dynamics and population disappearances. *Am. Nat.*, **144**:873–879, 1994.

[604] K. McCann and P. Yodzis. Bifurcation structure of a tree-species food chain model. *Theor. Pop. Biol.*, **48**:93–125, 1995.

[605] E. McCauley, W. W. Murdoch, and R. M. Nisbet. Growth, reproduction, and mortality of *Daphnia pulex* leydig: Life at low food. *Funct. Ecol.*, **4**:505–514, 1990.

[606] P. McCullagh and J. A. Nelder. *Generalized linear models.* Monographs on statistics and applied probability. Chapman & Hall, London, 1983.

[607] E. H. McEwan. Growth and development of the barren-ground caribou II. Postnatal growth rates. *Can. J. Zool.*, **46**:1023–1029, 1968.

[608] S. B. McGrew and M. F. Mallette. Energy of maintenance in *Escherichia coli*. *J. Bacteriol.*, **83**:844–850, 1962.

[609] M. D. McGurk. Effects of delayed feeding and temperature on the age of irreversible starvation and on the rates of growth and mortality of pacific herring larvae. *Mar. Biol.*, **84**:13–26, 1984.

[610] J. W. McMahon. Some physical factors influencing the feeding behavior of *Daphnia magna* Straus. *Can. J. Zool.*, **43**:603–611, 1965.

[611] T. A. McMahon. Size and shape in biology. *Science (New York)*, **179**:1201–1204, 1973.

[612] T. A. McMahon and J. T. Bonner. *On size and life.* Scientific American Library. Freeman, 1983.

[613] B. K. McNab. On the ecological significance of Bergmann's rule. *Ecology*, **52**:845–854, 1971.

[614] B. K. McNab. Energy expenditure: a short history. In T. E. Tomasi and T. H. Horton, editors, *Mammalian energetics*, pages 1–15. Comstock Publ. Assoc., Ithaca, 1992.

[615] E. M. Meijer, H. W. van Verseveld, E. G. van der Beek, and A. H. Stouthamer. Energy conservation during aerobic growth in *Paracoccus denitrificans*. *Arch. Microbiol.*, **112**:25–34, 1977.

[616] T. H. M. Meijer. *Reproductive decisions in the kestrel* Falco tinnunculus*; a study in physiological ecology.* PhD thesis, University of Groningen, The Netherlands, 1988.

[617] T. H. M. Meijer, S. Daan, and M. Hall. Family planning in the kestrel (*Falco tinnuculus*): the proximate control of covariation of laying data and clutch size. *Behaviour*, **114**:117–136, 1990.

[618] W. de Melo and S. J. van Strien. *One-dimensional dynamics.* Springer-Verlag, Berlin, 1993.

[619] M. L. Mendelsohn. Cell proliferation and tumor growth. In L. F. Lamerton and R. J. M. Fry, editors, *Cell proliferation.* Blackwell, Oxford, 1963.

[620] J. A. J. Metz and F. H. D. van Batenburg. Holling's 'hungry mantid' model for the invertebrate functional response considered as a Markov process. Part I: The full model and some of its limits. *J. Math. Biol.*, **22**:209–238, 1985.

[621] J. A. J. Metz and F.H. D. van Batenburg. Holling's 'hungry mantid' model for the invertebrate functional response considered as a Markov process. Part II: Negligible handling time. *J. Math. Biol.*, **22**:239–257, 1985.

[622] J. A. J. Metz and O. Diekmann. *The dynamics of physiologically structured populations.*, volume 68 of *Lecture Notes in Biomathematics.* Springer-Verlag, Berlin, 1986.

[623] J. A. J. Metz and O. Diekmann. Exact finite dimensional representations of models for physiologically structured populations. I: The abstract foundations of linear chain trickery. In J. A. Goldstein, F. Kappel, and W. Schappacher, editors, *Differential equations with applications in biology, physics, and engineering*, pages 269–289. Marcel Dekker, New York, 1991.

[624] J. A. J. Metz, S. A. H. Geritz, G. Meszna, F. J. A. Jacobs, and J. S. van Heerwaarden. Adaptive dynamics, a geometrical study of the consequences of nearly faithful reproduction. In S. J. van Strien and S. M. Verduyn Lunel, editors, *Stochastic and spatial structures of dynamical systems*, pages 183–231. North-Holland, Amsterdam, 1996.

[625] D. E. Metzler. *Biochemistry; the chemical reactions of living cells.* Academic Press, New York, 1977.

[626] E. A. Meuleman. Host-parasite interrelations between the freshwater pulmonate *Biomphalaria pfeifferi* and the trematode *Schistosoma mansoni*. *Neth. J. Zool.*, **22**:355–427, 1972.

[627] H. Meyer and L. Ahlswede. Über das intrauterine Wachstum und die Körperzusammensetzung von Fohlen sowie den Nährstoffbedarf tragender Stuten. *Übersicht. Tierernähr.*, **4**:263–292, 1976.

[628] D. G. Meyers. Egg development of a chydorid cladoceran, *Chydorus sphaericus*, exposed to constant and alternating temperatures: significance to secondary productivity in fresh water. *Ecology*, **61**:309–320, 1984.

[629] L. Michaelis and M. L. Menten. Die Kinetik der Invertwirkung. *Biochem. Z.*, **49**:333–369, 1913.

[630] H. Mikkola. *Der Bartkauz.* Die Neue Brehm-Bücherei. A. Ziemsen-Verlag, Wittenberg Lutherstadt, 1981.

[631] T. T. Milby and E. W. Henderson. The comparative growth rates of turkeys, ducks, geese and pheasants. *Poult. Sci.*, **16**:155–165, 1937.

[632] J. S. Millar. Post partum reproductive characteristics of eutherian mammals. *Evolution*, **35**:1149–1163, 1981.

[633] A. R. Millard. The body temperature of *Tyrannosaurus rex*. *Science*, **267**:1666–1667, 1995.

[634] P. J. Miller. Age, growth, and reproduction of the rock goby, *Gobius paganellus* L., in the Isle of Man. *J. Mar. Biol. Assoc. U. K.*, **41**:737–769, 1961.

[635] P. Milton. Biology of littoral blenniid fishes on the coast of south-west England. *J. Mar. Biol. Assoc. U. K.*, **63**:223–237, 1983.

[636] A. Mira. Why is meiosis arrested? *J. Theor. Biol.*, **194**:275–287, 1998.

[637] J. M. Mitchison. The growth of single cells III *Streptococcus faecalis*. *Exp. Cell Res.*, **22**:208–225, 1961.

[638] G. G. Mittelbach. Predation and resource patitioning in two sunfishes (*Centrarchidae*). *Ecology*, **65**:499–513, 1984.

[639] J. Monod. *Recherches sur la croissance des cultures bacteriennes.* Hermann, Paris, 2nd edition, 1942.

[640] J. L. Monteith and M. H. Unsworth. *Principles of environmental physics.* E. Arnold, London, 1990.

[641] N. Moran and P. Baumann. Phylogenetics of cytoplasmically inherited microorganisms of arthropods. *Trends Ecol. Evol.*, **9**:15–20, 1994.

[642] S. Moreno, P. Nurse, and P. Russell. Regulation of mitosis by cyclic accumulation of $p80^{cdc25}$ mitotic inducer in fission yeast. *Nature (Lond.)*, **344**:549–552, 1990.

[643] J. A. Morrison, C. E. Trainer, and P. L. Wright. Breeding season in elk as determined from known-age embryos. *J. Wildl. Manage.*, **23**:27–34, 1959.

[644] B. S. Muir. Comparison of growth rates for native and hatchery-stocked populations of *Esox masquinongy* in Nogies Creek, Ontario. *J. Fish. Res. Board Can.*, **17**:919–927, 1960.

[645] Y. Mukohata, editor. *New era of bioenergetics.* Academic Press, London, 1991.

[646] M. M. Mulder. *Energetic aspects of bacterial growth: a mosaic non-equilibrium thermodynamic approach.* PhD thesis, Amsterdam Universiteit, 1988.

[647] E. B. Muller. *Bacterial energetics in aerobic wastewater treatment.* PhD thesis, Vrije Universiteit, 1994.

[648] M. T. Murphy. Ecological aspects of the reproductive biology of eastern kingbirds: geographic comparisons. *Ecology*, **64**:914–928, 1983.

[649] A. W. Murray and M. W. Kirschner. What controls the cell cycle? *Sci. Am.*, **3**:34–41, 1991.

[650] L. Muscatine, L. R. McCloskey, and R. E. Marian. Estimating the daily contribution of carbon from zooxanthellae to coral animal respiration. *Limnol. Oceanogr.*, **26**:601–611, 1981.

[651] L. Muscatine and V. Weis. Productivity of zooxanthellae and biogeochemical cycles. In P. G. Falkowski and A. D. Woodhed, editors, *Primary productivity and biochemical cycles in the sea*, pages 257–271. Plenum Press, New York, 1992.

[652] S. Nagasawa. Parasitism and diseases in chaetognats. In Q. Bone, H. Kapp, and A. C. Pierrot-Bults, editors, *The biology of chaetognats.* Oxford University Press, 1991.

[653] S. Nagasawa and T. Nemoto. Presence of bacteria in guts of marine crustaceans on their fecal pellets. *J. Plankton Res.*, **8**:505–517, 1988.

[654] H. Nakajima and Z. Kawabata. Sensitivity analysis in microbial cummunities. In Colwell *et al.* editor, *Microbial diversity in time and space*, pages 85–91. Plenum Press, New York, 1996.

[655] R. D. M. Nash. The biology of Fries' goby, *Lesueurigobius friesii* (Malm) in the Firth of Clyde, Scotland, and a comparison with other stocks. *J. Fish Biol.*, **21**:69–85, 1982.

[656] S. Nee, A. F. Read, J. D. Greenwood, and P. H. Harvey. The relationship between abundance and body size in British birds. *Nature (Lond.)*, **351**:312–313, 1991.

[657] F. C. Neidhardt, J. L. Ingraham, and M. Schaechter. *Physiology of the bacterial cell: a molecular approach.* Sinauer Assoc. Inc., Sunderland, MA, 1990.

[658] J. A. Nelder. The fitting of a generalization of the logistic curve. *Biometrics*, **17**:89–110, 1961.

[659] B. Nelson. *The gannet.* T. & A. D. Poyser, Berkhamsted, 1978.

[660] E. Nestaas and D. I. C. Wang. Computer control of the penicillum fermentation using the filtration probe in conjunction with a structured model. *Biotechnol. Bioeng.*, **25**:781–796, 1983.

[661] M. C. Newman and D. K. Doubet. Size dependence of mercury (II) accumulation in the mosquitofish *Gambusia affinis* (baird and girard). *Arch. Environ. Contam. Toxicol.*, **18**:819–825, 1989.

[662] M. C. Newman and S. V. Mitz. Size dependence of zinc elimination and uptake from water by mosquitofish *Gambusia affinis* (baird and girard). *Aquatic Toxicol.*, **12**:17–32, 1988.

[663] D. G. Nicholls. *Bioenergetics. An introduction to the chemiosmotic theory.* Academic Press, New York, 1982.

[664] A. J. Niimi and B. G. Oliver. Distribution of polychlorinated biphenyl congeners and other hydrocarbons in whole fish and muscle among Ontario salmonids. *Environ. Sci. Technol.*, **23**:83–88, 1989.

[665] K. J. Niklas. *Plant allometry; the sacling of form and process.* Chicago University Press, Chicago, 1994.

[666] B. Nisbet. *Nutrition and feeding strategies in protozoa.* Croom Helm, London, 1984.

[667] E. G. Nisbet, J. R. Cann, and C. L. van Dover. Origins of photosynthesis. *Nature*, **373**:479–480, 1995.

[668] R. M. Nisbet, A. Cunningham, and W. S. C. Gurney. Endogenous metabolism and the stability of microbial prey-predator systems. *Biotechnol. Bioeng.*, **25**:301–306, 1983.

[669] R. M. Nisbet, A. H. Ross, and A. J. Brooks. Empirically-based dynamic energy budget models: theory and application to ecotoxicology. *Nonlinear World*, **3**:85–106, 1996.

[670] P. S. Nobel. *Physicochemical and environmental plant physiology*. Academic Press, San Diego, 1999.

[671] G. North. Back to the RNA world and beyond. *Nature (Lond.)*, **328**:18–19, 1987.

[672] T. H. Y. Nose and Y. Hiyama. Age determination and growth of yellowfin tuna, *Thunnus albacares* Bonnaterre by vertebrae. *Bull. Jpn. Soc. Sci. Fish.*, **31**:414–422, 1965.

[673] W. J. O'Brian. The dynamics of nutrient limitation of phytoplankron algae: a model reconsidered. *Ecology*, **55**:135–141, 1974.

[674] A. Okubo. *Diffusion and ecological problems: Mathematical models.*, volume 10 of *Biomathematics*. Springer-Verlag, Berlin, 1980.

[675] K. Okunuki. Denaturation and inactivation of enzyme proteins. *Adv. Enzymol. Relat. Areas Mol. Biol.*, **23**:29–82, 1961.

[676] B. G. Oliver and A. J. Niimi. Trophodynamic analysis of polychlorinated biphenyl congeners and other chlorinated hydrocarbons in Lake Ontario ecosystem. *Environ. Sci. Technol.*, **22**:388–397, 1988.

[677] R. V. O'Neill, D. L. DeAngelis, J. B. Waide, and T. F. H. Allen. *A hierarchical concept of ecosystems.*, volume 23 of *Monographs in population biology*. Princeton University Press, 1986.

[678] A. Opperhuizen. *Bioconcentration in fish and other distribution processes of hydrophobic chemicals in aquatic environments*. PhD thesis, University of Amsterdam, 1986.

[679] C. B. Osmond and W. S. Chow. Ecology of photosynthesis in sun and shade: summary and prognosticications. *Aust. J. Plant Physiol.*, **15**:1–9, 1988.

[680] A. Y. Ota and M. R. Landry. Nucleic acids as growth rate indicators for early developmental stages of *Calanus pacificus* Brodsky. *J. Exp. Mar. Biol. Ecol.*, **80**:147–160, 1984.

[681] M. J. Packard, G. C. Packard, and W. H. N. Gutzke. Calcium metabolism in embryos of the oviparous snake *Coluber constrictor*. *J. Exp. Biol.*, **110**:99–112, 1984.

[682] M. J. Packard, G. C. Packard, J. D. Miller, M. E. Jones, and W. H. N. Gutzke. Calcium mobilization, water balance, and growth in embryos of the agamid lizard *Amphibolurus barbatus*. *J. Exp. Zool.*, **235**:349–357, 1985.

[683] M. J. Packard, T. M. Short, G. C. Packard, and T. A. Gorell. Sources of calcium for embryonic development in eggs of the snapping turtle *Chelydra serpentina*. *J. Exp. Zool.*, **230**:81–87, 1984.

[684] R. T. Paine. Growth and size distribution of the brachiopod *Terebratalia transversa* Sowerby. *Pac. Sci.*, **23**:337–343, 1969.

[685] P. R. Painter and A. G. Marr. Mathematics of microbial populations. *Annu. Rev. Microbiol.*, **22**:519–548, 1968.

[686] J. E. Paloheimo, S. J. Crabtree, and W. D. Taylor. Growth model for *Daphnia*. *Can. J. Fish. Aquat. Sci.*, **39**:598–606, 1982.

[687] J. R. Parks. *A theory of feeding and growth of animals*. Springer-Verlag, Berlin, 1982.

[688] G. D. Parry. The influence of the cost of growth on ectotherm metabolism. *J. Theor. Biol.*, **101**:453–477, 1983.

[689] S. J. Parulekar, G. B. Semones, M. J. Rolf, J. C. Lievense, and H. C. Lim. Induction and elimination of oscillations in continuous cultures of *Saccharomyces cerevisiae*. *Biotechnol. Bioeng.*, **28**:700–710, 1986.

[690] C. S. Patlak. Energy expenditure by active transport mechanisms. *Biophys. J.*, **1**:419–427, 1961.

[691] M. R. Patterson. A chemical engineering view of cnidarian symbioses. *Amer. Zool.*, **32**:566–582, 1992.

[692] M. R. Patterson. A chemical engineering view of cnidarian symbioses. *Am. Zool.*, **32**:566–582, 1993.

[693] D. Pauly and P. Martosubroto. The population dynamics of *Nemipterus marginatus* (Cuvier & Val.) off Western Kalimantan, South China Sea. *J. Fish Biol.*, **17**:263–273, 1980.

[694] P. R. Payne and E. F. Wheeler. Growth of the foetus. *Nature (Lond.)*, **215**:849–850, 1967.

[695] R. Pearl. The growth of populations. *Q. Rev. Biol.*, **2**:532–548, 1927.

[696] T. J. Pedley. *Scale effects in animal locomotion*. Academic Press, London, 1977.

[697] D. L. Penry and P. A. Jumars. Chemical reactor analysis and optimal digestion. *Bioscience*, **36**:310–315, 1986.

[698] D. L. Penry and P. A. Jumars. Modeling animal guts as chemical reactors. *Am. Nat.*, **129**:69–96, 1987.

[699] B. Peretz and L. Adkins. An index of age when birthdate is unknown in *Aplysia californica*: shell size and growth in long-term maricultured animals. *Biol. Bull. (Woods Hole)*, **162**:333–344, 1982.

[700] R. H. Peters. *The ecological implications of body size*. Cambridge University Press, 1983.

[701] T. N. Pettit, G. S. Grant, G. C. Whittow, H. Rahn, and C. V. Paganelli. Respiratory gas exchange and growth of white tern embryos. *Condor*, **83**:355–361, 1981.

[702] T. N. Pettit, G. S. Grant, G. C. Whittow, H. Rahn, and C. V. Paganelli. Embryonic oxygen consumption and growth of laysan and black-footed albatross. *Am. J. Physiol.*, **242**:121–128, 1982.

[703] T. N. Pettit and G. C. Whittow. Embryonic respiration and growth in two species of noddy terns. *Physiol. Zool.*, **56**:455–464, 1983.

[704] T. N. Pettit, G. C. Whittow, and G. S. Grant. Caloric content and energetic budget of tropical seabird eggs. In G. C. Whittow and H. Rahn, editors, *Seabird energetics*, pages 113–138. Plenum Press, New York, 1984.

[705] H. G. Petzold. *Die Anakondas.* Die Neue Brehm-Bücherei. A. Ziemsen-Verlag, Wittenberg Lutherstadt, 1984.

[706] J. Phillipson. Bioenergetic options and phylogeny. In C. R. Townsend and P. Calow, editors, *Physiological ecology.* Blackwell Sci. Publ., Oxford, 1981.

[707] E. R. Pianka. On r and K selection. *Am. Nat.*, **104**:592–597, 1970.

[708] E. R. Pianka. *Evolutionary ecology.* Harper & Row Publ. Inc., London, 1978.

[709] E. R. Pianka. *Ecology and natural history of desert lizards; analyses of the ecological niche of community structure.* Princeton University Press, 1986.

[710] G. J. Pierce and J. G. Ollason. Eight reasons why optimal foraging theory is a complete waste of time. *Oikos*, **49**:111–118, 1987.

[711] T. Piersma. Estimating energy reserves of great crested grebes *Podiceps cristatus* on the basis of body dimensions. *Ardea*, **72**:119–126, 1984.

[712] T. Piersma, N. Cadée, and S. Daan. Seasonality in basal metabolic rate and thermal conductance in a long-distance migrant shorebird, the knot (*Calidris canutus*). *J. Comp. Physiol. B*, **165**:37–45, 1995.

[713] T. Piersma and R. I. G. Morrison. Energy expenditure and water turnover of incubating ruddy turnstones: high costs under high arctic climatic conditions. *Auk*, **111**:366–376, 1994.

[714] J. Pilarska. Eco-physiological studies on *Brachionus rubens* ehrbg (*Rotatoria*) I. Food selectivity and feeding rate. *Pol. Arch. Hydrobiol.*, **24**:319–328, 1977.

[715] E. M. del Pino. Marsupial frogs. *Sci. Am.*, **5**:76–84, 1989.

[716] S. J. Pirt. The maintenance energy of bacteria in growing cultures. *Proc. R. Soc. Lond. B Biol. Sci.*, **163**:224–231, 1965.

[717] S. J. Pirt. *Principles of microbe and cell cultivation.* Blackwell Sci. Publ., Oxford, 1975.

[718] S. J. Pirt and D. S. Callow. Studies of the growth of *Penicillium chrysogenum* in continuous flow culture with reference to penicillin production. *J. Appl. Bacteriol.*, **23**:87–98, 1960.

[719] G. Pohle and M. Telford. Post-larval growth of *Dissodactylus primitivus* Bouvier, 1917 (*Brachyura*: *Pinnotheridae*) under laboratory conditions. *Biol. Bull. (Woods Hole)*, **163**:211–224, 1982.

[720] J. S. Poindexter. Oligotrophy: fast and famine existence. *Adv. Microb. Ecol.*, **5**:63–89, 1981.

[721] A. Polle. Mehler reaction: friend or foe in photosynthesis? *Bot. Acta*, **109**:84–89, 1996.

[722] D. E. Pomeroy. Some aspects of the ecology of the land snail, *Helicella virgata*, in South Australia. *Aust. J. Zool.*, **17**:495–514, 1969.

[723] R. W. Pomeroy. Infertility and neonatal mortality in the sow. III: Neonatal mortality and foetal development. *J. Agric. Sci.*, **54**:31–56, 1960.

[724] W. E. Poole. Breeding biology and current status of the grey kangaroo, *Macropus fuliginosus fuliginosus*, of Kangaroo Island, South Australia. *Aust. J. Zool.*, **24**:169–187, 1976.

[725] D. Poppe and B. Vos. *De buizerd.* Kosmos Vogelmonografieën. Kosmos, Amsterdam, 1982.

[726] K. G. Porter, J. Gerritsen, and J. D. Orcutt. The effect of food concentration on swimming patterns, feeding behavior, ingestion, assimilation and respiration by *Daphnia*. *Limnol. Oceanogr.*, **27**:935–949, 1982.

[727] K. G. Porter, M. L. Pace, and J. F. Battey. Ciliate protozoans as links in freshwater planktonic food chains. *Nature (Lond.)*, **277**:563–564, 1979.

[728] R. K. Porter and M. D. Brand. Body mass dependence of H^+ leak in mitochondria and its relevance to metabolic rate. *Nature (Lond.)*, **362**:628–630, 1993.

[729] L. Posthuma, R. F. Hogervorst, E. N. G. Joosse, and N. M. van Straalen. Genetic variation and covariation for characteristics associated with cadmium tolerance in natural populations of the springtail *Orchesella cincta* (l.). *Evolution*, **47**:619–631, 1993.

[730] L. Posthuma, R. F. Hogervorst, and N. M. van Straalen. Adaptation to soil pollution by cadmium excretion in natural populations of *Orchesella cincta*(l.) (*Collembola*). *Arch. Environ. Contam. Toxicol.*, **22**:146–156, 1992.

[731] E. Postma, W. A. Scheffers, and J. P. van Dijken. Kinetics of growth and glucose transport in glucose-limited chemostat cultures of *Saccharomyces cerevisiea* cbs 8086. *Yeast*, **5**:159–165, 1989.

[732] E. Postma, C. Verduyn, W. A. Scheffers, and J. P. van Dijken. Enzyme analysis of the crabtree effect in glucose-limited chemostat cultures of *Saccharomyces cerevisiea*. *Appl. Environ. Microbiol.*, **55**:468–477, 1989.

[733] D. M. Prescott. Relations between cell growth and cell division. In D. Rudnick, editor, *Rythmic and synthetic processes in growth*, pages 59–74. Princeton University Press, 1957.

[734] G. D. Prestwich. The chemical defences of termites. *Sci. Am.*, **249**:68–75, 1983.

[735] H. H. Prince, P. B. Siegel, and G. W. Cornwell. Embryonic growth of mallard and pekin ducks. *Growth*, **32**:225–233, 1968.

[736] W. G. Pritchard. Scaling in the animal kingdom. *Bull. Math. Biol.*, **55**:111–129, 1993.

[737] D. R. Prothero and W. A. Berggren, editors. *Eocene-Oligocene climatic and biotic evolution.* Princeton University Press, 1992.

[738] L. Psihoyos. *Hunting dinosaurs.* Random House, New York, 1994.

[739] D. M. Purdy and H. H. Hillemann. Prenatal growth in the golden hamster (*Cricetus auratus*). *Anat. Rec.*, **106**:591–597, 1950.

[740] A. Pütter. Studien über physiologische Ähnlichkeit. VI Wachstumsähnlichkeiten. *Arch. Gesamte Physiol. Mench. Tiere*, **180**:298–340, 1920.

[741] P. A. Racey and S. M. Swift. Variations in gestation length in a colony of pipistrelle bats (*Pipistrellus pipistrellus*) from year to year. *J. Reprod. Fertil.*, **61**:123–129, 1981.

[742] E. C. Raff, E. M. Popodi, B. J. Sly, F. R. Turner, J. T. Villinski, and R. A. Raff. A novel ontogenetic pathway in hybrid embryos between species with different modes of development. *Development*, **126**:1937–1945, 1999.

[743] U. Rahm. *Die Afrikanische Wurzelratte.* Die Neue Brehm-Bücherei. A. Ziemsen-Verlag, Wittenberg Lutherstadt, 1980.

[744] H. Rahn and A. Ar. The avian egg: incubation time and water loss. *Condor*, **76**:147–152, 1974.

[745] H. Rahn, A. Ar, and C. V. Paganelli. How bird eggs breathe. *Sci. Am.*, **2**:38–47, 1979.

[746] H. Rahn and C. V. Paganelli. Gas fluxes in avian eggs: Driving forces and the pathway for exchange. *Comp. Biochem. Physiol.*, **95A**:1–15, 1990.

[747] H. Rahn, C. V. Paganelli, and A. Ar. Relation of avian egg weight to body weight. *Auk*, **92**:750–765, 1975.

[748] K. Raman. *Transport phenomena in plants.* Narosa Publ. House, London, 1997.

[749] J. E. Randall, G. R. Allen, and R. C. Steen. *Fishes of the great barrier reef and coral sea.* University of Hawai Press, Honolulu, 1990.

[750] C. Ratledge. Biotechnology as applied to the oils and fats industry. *Fette Seifen Anstrichm.*, **86**:379–389, 1984.

[751] J. A. Raven. *Energetics and transport in aquatic plants.*, volume 4 of *MBL lectures in biology.* Alan R. Liss, Inc., New York, 1984.

[752] J. A. Raven. The vacuole: a cost-benefit analysis. In R. A. Leigh and D. Sanders, editors, *The plant vacuole.*, pages 59–86. Academic Press, San Diego, 1997.

[753] P. J. Reay. Some aspects of the biology of the sandeel, *Ammodytes tobianus* L., in Langstone Harbour, Hampshire. *J. Mar. Biol. Assoc. U. K.*, **53**:325–346, 1973.

[754] C. Reder. Metabolic control theory: a structural approach. *J. Theor. Biol.*, **135**:175–201, 1988.

[755] A. C. Redfield. The biological control of chemical factors in the environment. *Am. Sci.*, **46**:205–221, 1958.

[756] M. R. Reeve. The biology of *Chaetognatha* I. Quantitative aspects of growth and egg production in *Sagitta hispida*. In J. H. Steele, editor, *Marine food chains.* University of California Press, Berkeley, 1970.

[757] M. R. Reeve and L. D. Baker. Production of two planktonic carnivores (Chaetognath and Ctenophore) in south Florida inshore waters. *Fish. Bull. (Dublin)*, **73**:238–248, 1975.

[758] M. J. Reiss. *The allometry of growth and reproduction.* Cambridge University Press, 1989.

[759] W. Reisser. *Algae and symbioses.* Biopress Ltd, Bristol, 1992.

[760] H. Remmert. *Artic animal ecology.* Springer-Verlag, Berlin, 1980.

[761] F. J. Richards. A flexible growth function for empirical use. *J. Exp. Bot.*, **10**:290–300, 1959.

[762] S. W. Richards, D. Merriman, and L. H. Calhoun. Studies on the marine resources of southern New England. IX. The biology of the little skate, *Raja erinacea* Mitchill. *Bull. Bingham Oceanogr. Collect. Yale Univ.*, **18**:5–67, 1963.

[763] D. Richardson. *The vanishing lichens: their history, biology and importance.* David and Charles, Newton Abbot, 1975.

[764] S. Richman. The transformation of energy by *Daphnia pulex*. *Ecol. Monogr.*, **28**:273–291, 1958.

[765] R. E. Ricklefs. Patterns of growth in birds. *Ibis*, **110**:419–451, 1968.

[766] R. E. Ricklefs. Patterns of growth in birds III. Growth and development of the cactus wren. *Condor*, **77**:34–45, 1975.

[767] R. E. Ricklefs. Adaptation, constraint, and compromise in avian postnatal development. *Biol. Rev. Camb. Philos. Soc.*, **54**:269–290, 1979.

[768] R. E. Ricklefs and T. Webb. Water content, thermoregulation, and the growth rate of skeletal muscles in the European starling. *Auk*, **102**:369–377, 1985.

[769] R. E. Ricklefs, S. White, and J. Cullen. Postnatal development of Leach's storm-petrel. *Auk*, **97**:768–781, 1980.

[770] U. Riebesell, D. A. Wolf-Gladrow, and V. Smetacek. Carbon dioxide limitation of marine phytoplankton growth rates. *Nature (Lond.)*, **361**:249–251, 1993.

[771] F. H. Rigler. Zooplankton. In W. T. Edmondson, editor, *A manual on methods for the assessment of secondary productivity in fresh waters*, number 17 in IBP handbook, pages 228–255. Bartholomew Press, Dorking, 1971.

[772] H. U. Riisgård, E. Bjornestad, and F. Møhlenberg. Accumulation of cadmium in the mussel *Mytilus edulis*: kinetics and importance of uptake via food and sea water. *Mar. Biol.*, **96**:349–353, 1987.

[773] H. U. Riisgård and F. Møhlenberg. An improved automatic recording apparatus for determining the filtration rate of *Mytilus edulis* as a function of size and algal concentration. *Mar. Biol.*, **66**:259–265, 1979.

[774] H. U. Riisgård and A. Randløv. Energy budgets, growth and filtration rates in *Mytilus edulis* at different algal concentrations. *Mar. Biol.*, **61**:227–234, 1981.

[775] C. T. Robbins and A. N. Moen. Uterine composition and growth in pregnant white-tailed deer. *J. Wildl. Manage.*, **39**:684–691, 1975.

[776] D. V. Roberts. *Enzyme kinetics.* Cambridge University Press, 1977.

[777] J. R. Robertson and G. W. Salt. Responses in growth, mortality, and reproduction to variable food levels by the rotifer *Asplanchna girodi*. *Ecology*, **62**:1585–1596, 1981.

[778] P. G. Rodhouse, C. M. Roden, G. M. Burnell, M. P. Hensey, T. McMahon, B. Ottway, and T. H. Ryan. Food resource, gametogenesis and growth of *Mytilus edulis* on the shore and in suspended culture: Killary Harbour, Ireland. *Mar. Biol.*, **64**:513–529, 1984.

[779] J. A. Roels. *Energetics and kinetics in biotechnology.* Elsevier Biomedical Press, Amsterdam, 1983.

[780] D. A. Roff. *The evolution of life histories.* Chapman & Hall, New York, 1992.

[781] K. Rohde. *Ecology of marine parasites.* CAB International, Wallingford, 1993.

[782] A. L. Romanov. *The avian embryo.* MacMillan Publ. Co., New York, 1960.

[783] C. Romijn and W. Lokhorst. Foetal respiration in the hen. *Physiol. Zool.*, **2**:187–197, 1951.

[784] A. de Roos. Numerical methods for structured population models: the escalator boxcar train. *Num. Meth. Part. Diff. Eq.*, **4**:173–195, 1988.

[785] A. M. de Roos. Escalator boxcar train package (version 2.0). `ftp://toranaga.bio.uva.nl/pub/andre/programs/old/escbox-2.0/escbox2.tar%.Z`, 1996.

[786] A. M. de Roos. A gentle introduction to physiologically structured population models. In S. Tuljapurkar and H. Caswell, editors, *Structured-population models in marine, terrestrial, and freshwater systems*, pages 119–204. Chapman & Hall, New York, 1996.

[787] A. M. de Roos, O. Diekmann, and J. A. J. Metz. Studying the dynamics of structured population models: a versatile technique and its application to *Daphnia*. *Am. Nat.*, **139**:123–147, 1992.

[788] M. R. Rose. Laboratory evolution of postponed senescence in *Drosophila melanogaster*. *Evolution*, **38**:1004–1010, 1984.

[789] J. L. Roseberry and W. D. Klimstra. Annual weight cycles in male and female bobwhite quail. *Auk*, **88**:116–123, 1971.

[790] M. L. Rosenzweig. Paradox of enrichment: destabilization of exploitation ecosystems in ecological time. *Science*, **171**:385–387, 1971.

[791] A. H. Ross and R. M. Nisbet. Dynamic models of growth and reproduction of the mussel *Mytilus edulis* L. *Funct. Ecol.*, **4**:777–787, 1990.

[792] J. A. Ruben, W. J. Hillenius, N. R. Geist, A. Leitch, T. D. Jones, P. J. Currie, J. R. Horner, and G. Espe III. The metabolic status of some late cretaceous dinosaurs. *Science*, **273**:1204–2023, 1996.

[793] M. Rubner. Über den Einfluss der Körpergrösse auf Stoff- und Kraftwechsel. *Z. Biol.*, **19**:535–562, 1883.

[794] W. Rudolph. *Die Hausenten.* Die Neue Brehm-Bücherei. A. Ziemsen-Verlag, Wittenberg Lutherstadt, 1978.

[795] D. Ruelle. *Elements of differentiable dynamics and bifurcation theory.* Academic Press, San Diego, 1989.

[796] P. C. de Ruiter and G. Ernsting. Effects of ration on energy allocation in a carabid beetle. *Funct. Ecol.*, **1**:109–116, 1987.

[797] R. W. Russel and F. A. P. C. Gobas. Calibration of the freshwater mussel *Elliptio complanata*, for quantitative monitoring of hexachlorobenzene and octachlorostyrene in aquatic systems. *Bull. Environ. Contam. Toxicol.*, **43**:576–582, 1989.

[798] R. L. Rusting. Why do we age? *Sci. Am.*, **12**:86–95, 1992.

[799] M. Rutgers. *Control and thermodynamics of microbial growth.* PhD thesis, University of Amsterdam, 1990.

[800] M. Rutgers, M. J. Teixeira de Mattos, P. W. Postma, and K. van Dam. Establishment of the steady state in glucose-limited chemostat cultures of *Kleibsiella pneumoniae*. *J. Gen. Microbiol.*, **133**:445–453, 1987.

[801] A. J. Rutter and F. H. Whitehead. *The water relations of plants.* Blackwell, London, 1963.

[802] I. Ružić. Two-compartment model of radionuclide accumulation into marine organisms. I. Accumulation from a medium of constant activity. *Mar. Biol.*, **15**:105–112, 1972.

[803] T. L. Saaty. *Elements of queueing theory with applications.* Dover Publications, New York, 1961.

[804] S. I. Sandler and H. Orbey. On the thermodynamics of microbial growth processes. *Biotechnol. Bioeng.*, **38**:697–718, 1991.

[805] J. R. Sargent. Marine wax esters. *Sci. Prog.*, **65**:437–458, 1978.

[806] Sarrus and Rameaux. Mémoire adressé à l'Académie Royale. *Bull. Acad. R. Med.*, **3**:1094–1100, 1839.

[807] J. Sarvala. Effect of temperature on the duration of egg, nauplius and copepodite development of some freshwater benthic copepoda. *Freshwater Biol.*, **9**:515–534, 1979.

[808] P. T. Saunders. *An introduction to catastrophe theory.* Cambridge University Press, 1980.

[809] H. Schatzmann. *Anaerobes Wachstum von* Saccharomyces cervisiae*: Regulatorische Aspekte des glycolytischen und respirativen Stoffwechsels.* Diss. eth 5504, ETH, Zürich, 1975.

[810] H. G. Schegel. *Algemeine Mikrobiologie.* Thieme, 1981.

[811] H. Scheufler and A. Stiefel. *Der Kampflaufer.* Die Neue Brehm-Bücherei. A. Ziemsen-Verlag, Wittenberg Lutherstadt, 1985.

[812] D. W. Schindler. Feeding, assimilation and respiration rates of *Daphnia magna* under various environmental conditions and their relation to production estimates. *J. Anim. Ecol.*, **37**:369–385, 1968.

[813] I. I. Schmalhausen and E. Syngajewskaja. Studien über Wachstum und Differenzierung. I. Die individuelle Wachtumskurve von *Paramaecium caudatum. Roux's Arch. Dev. Biol.*, **105**:711–717, 1925.

[814] U. Schmidt. *Vampirfledermäuse.* Die Neue Brehm-Bücherei. A. Ziemsen-Verlag, Wittenberg, 1978.

[815] K. Schmidt-Nielsen. *Scaling: why is animal size so important?* Cambridge University Press, 1984.

[816] R. Schneider. Polychlorinated biphenyls (PCBs) in cod tissues from the Western Baltic: significance of equilibrium partitioning and lipid composition in the bioaccumulation of lipophilic pollutants in gill-breathing animals. *Meeresforschung*, **29**:69–79, 1982.

[817] S. A. Schoenberg, A. E. Maccubbin, and R. E. Hodson. Cellulose digestion by freshwater microcrustacea. *Limnol. Oceanogr.*, **29**:1132–1136, 1984.

[818] P. F. Scholander. Evolution of climatic adaptation in homeotherms. *Evolution*, **9**:15–26, 1955.

[819] M. Schonfeld. *Der Fitislaubsanger.* Die Neue Brehm-Bücherei. A. Ziemsen-Verlag, Wittenberg Lutherstadt, 1982.

[820] S. Schonn. *Der Sperlingskauz.* Die Neue Brehm-Bücherei. A. Ziemsen-Verlag, Wittenberg Lutherstadt, 1980.

[821] R. M. Schoolfield, P. J. H. Sharpe, and C. E. Magnuson. Non-linear regression of biological temperature-dependent rate models based on absolute reaction-rate theory. *J. Theor. Biol.*, **88**:719–731, 1981.

[822] H. N. Schulz, T. Brinkhoff, T. G. Ferdelman, M. Hernández Marineé, A. Teske, and B. B. Jørgensen. Dense populations of a giant sulfur bacterium in Namibian shelf sediments. *Science*, **284**:493–495, 1999.

[823] K. L. Schulze and R. S. Lipe. Relationship between substrate concentration, growth rate, and respiration rate of *Escherichia coli* in continuous culture. *Arch. Mikrobiol.*, **48**:1–20, 1964.

[824] W. A. Searcy. Optimum body sizes at different ambient temperatures: an energetics explanation of Bergmann's rule. *J. Theor. Biol.*, **83**:579–593, 1980.

[825] L. A. Segel. *Modeling dynamic phenomena in molecular and cellular biology.* Cambridge University Press, 1984.

[826] L. A. Segel. *Biological kinetics.*, volume 12 of *Cambridge studies in mathematical biology.* Cambridge University Press, 1991.

[827] H. P. Senn. *Kinetik und Regulation des Zuckerabbaus von* Escherichia coli *ML 30 bei tiefen Zucker Konzentrationen.* PhD thesis, Techn. Hochschule Zurich, 1989.

[828] M. Shafi and P. S. Maitland. The age and growth of perch (*Perca fluviatilis* L.) in two Scottish lochs. *J. Fish Biol.*, **3**:39–57, 1971.

[829] J. A. Shapiro. Bacteria as multicellular organisms. *Sci. Am.*, **6**:62–69, 1988.

[830] P. J. H. Sharpe and D. W. DeMichele. Reaction kinetics of poikilotherm development. *J. Theor. Biol.*, **64**:649–670, 1977.

[831] J. E. Shelbourne. A predator–prey relationship for plaice larvae feeding on *Oikopleura*. *J. Mar. Biol. Assoc. U. K.*, **42**:243–252, 1962.

[832] J. C. Sherris, N. W. Preston, and J. G. Shoesmith. The influence of oxygen and arginine on the motility of a strain of *Pseudomonas sp. J. Gen. Microbiol.*, **16**:86–96, 1957.

[833] J. M. Shick. *A functional biology of sea anemones.* Chapman & Hall, London, 1991.

[834] R. Shine. Why is sex determined by nest temperature in many reptiles? *TREE*, **14**:186–189, 1999.

[835] R. Shine and E. L. Charnov. Patterns of survival, growth, and maturation in snakes and lizards. *Am. Nat.*, **139**:1257–1269, 1992.

[836] Y. Shlesinger and Y. Loya. Coral community reproductive pattern: Red Sea versus the Great Barrier Reef. *Science*, **228**:1333–1335, 1985.

[837] R. V. Short. Species differences in reproductive mechanisms. In C. R. Austin and R. V. Short, editors, *Reproductive fitness*, volume 4 of *Reproduction in mammals.*, pages 24–61. Cambridge University Press, 1984.

[838] L. Sigmund. Die Postembryonale Entwicklung der Wasserralle. *Sylvia*, **15**:85–118, 1958.

[839] A. Sih. Predators and prey lifestyles: an evolutionary and ecological overview. In W. C. Kerfoot and A. Sih, editors, *Predation; direct and indirect impacts on aquatic communities*, pages 203–224. University of New England Press, Hanover, 1987.

[840] D. T. H. M. Sijm, K. W. Broersen, D. F. de Roode, and P. Mayer. Bioconcentration kinetics of hydrophobic chemicals in different densities of *Chlorella pyrenoidosa*. *Environ. Toxicol. Chem.*, **17**:1695–1704, 1998.

[841] D. T. H. M. Sijm and A. van der Linde. Size-dependent bioconcentration kinetics of hydrophobic organic chemicals in fish based on diffusive mass transfer and allometric relationships. *Environ. Sci. Technol.*, **29**:2769–2777, 1995.

[842] D. T. H. M. Sijm, G. Schüürmann, P. J. Vries, and A. Opperhuizen. Aqueous solubility, octanol solubility, and octanol/water partition coefficient of nine hydrophobic dyes. *Environ. Toxicol. Chem.*, **18**:1109–1117, 1999.

[843] D. T. H. M. Sijm, W. Seinen, and A. Opperhuizen. Life-cycle biomagnification study in fish. *Environ. Sci. Technol.*, **26**:2162–2174, 1992.

[844] D. T. H. M. Sijm, M. E. Verberne, W. J. de Jonge, P. Pärt, and A. Opperhuizen. Allometry in the uptake of hydrophobic chemicals determined *in vivo* and in isolated perfused gills. *Toxicol. Appl. Pharmacol.*, **131**:130–135, 1995.

[845] G. G. Simpson. *Penguins. Past and present, here and there.* Yale University Press, 1976.

[846] M. R. Simpson and S. Boutin. Muskrat life history: a comparison of a northern and southern population. *Ecography*, **16**:5–10, 1993.

[847] B. Sinervo. The evolution of maternal investment in lizard. An experimental and comparative analysis of egg size and its effect on offspring performance. *Evolution*, **44**:279–294, 1990.

[848] D. Singer. Stable orbits and bifurcation of maps of the interval. *SIAM J. Appl. Math.*, **35**:260–267, 1978.

[849] J. W. Sinko and W. Streifer. A model for populations reproducing by fission. *Ecology*, **52**:330–335, 1967.

[850] P. Sitte, S. Eschbach, and M. Maerz. The role of symbiosis in algal evolution. In W. Reisser, editor, *Algae and symbioses*, pages 711–733. Biopress Ltd, Bristol, 1992.

[851] S. Sjöberg. Zooplankton feeding and queueing theory. *Ecol. Modell.*, **10**:215–225, 1980.

[852] J. G. Skellam. The formulation and interpretation of mathematical models of diffusionary processes in population biology. In M. S. Bartlett and R. W. Hiorns, editors, *The mathematical theory of the dynamics of biological populations*, pages 63–85. Academic Press, San Diego, 1973.

[853] R. O. Slatyer. *Plant-water relationships.* Academic Press, London, 1967.

[854] W. Slob and C. Janse. A quantitative method to evaluate the quality of interrupted animal cultures in aging studies. *Mech. Ageing Dev.*, **42**:275–290, 1988.

[855] L. B. Slobodkin. Population dynamics in *Daphnia obtusa* Kurz. *Ecol. Monogr.*, **24**:69–88, 1954.

[856] J. F. Sluiters. *Parasite–host relationship of the avian schistosome* Trichobilharzia ocellata *and the hermaphrodite gastropod* Lymnea stagnalis. PhD thesis, Vrije Universiteit, Amsterdam, 1983.

[857] G. L. Small. *The blue whale.* Columbia Univesity Press, 1971.

[858] F. A. Smith and N. A. Walker. Photosynthesis by aquatic plants: effects of unstirred layers in relation to assimilation of CO_2 and HCO_3^- and to carbon isotopic discrimination. *New Phytol.*, **86**:245–259, 1980.

[859] H. L. Smith and P. Waltman. *The theory of the chemostat.* Cambridge University Press, 1994.

[860] M. L. Smith, J. N. Bruhn, and J. B. Anderson. The fungus *Armillaria bulbosa* is among the largest and oldest living organsism. *Nature (Lond.)*, **356**:428–431, 1992.

[861] S. Smith. Early development and hatching. In M. E. Brown, editor, *The physiology of fishes*, volume 1, pages 323–359. Academic Press, San Diego, 1957.

[862] S. M. Smith. *The black-capped chickadee. Behavioral ecology and natural history.* Comstock Publishing Associates, Ithaca, 1991.

[863] S. V. Smith. The Houtman Abrolhos Islands: Carbon metabolism of coral reefs at high latitude. *Limnol. Oceanogr.*, **26**:612–621, 1981.

[864] S. V. Smith and D. W. Kinsey. Calcium carbonate production, coral reef growth, and sea level change. *Science*, **194**:937–939, 1976.

[865] O. Snell. Die Abhängigkeit des Hirngewichtes von dem Körpergewicht und den geistigen Fähigkeiten. *Arch. Psychiatr. Nervenkr.*, **23**:436–446, 1891.

[866] D. W. Snow. The natural history of the oilbird, *Steatornis caripensis* in Trinidad, W.I. part 1. General behaviour and breeding habits. *Zoologica (N. Y.)*, **46**:27–48, 1961.

[867] G. M. Southward. A method of calculating body lengths from otolith measurements for pacific halibut and its application to Portlock-Albatross Grounds data between 1935 and 1957. *J. Fish. Res. Board Can.*, **19**:339–362, 1962.

[868] G. R. Southworth, J. J. Beauchamp, and P. K. Schmieder. Bioaccumulation potential and acute toxicity of synthetic fuel effluents in freshwater biota: Azaarenes. *Environ. Sci. Technol.*, **12**:1062–1066, 1978.

[869] A. L. Spaans. On the feeding ecology of the herring gull *Larus argentatus* Pont. in the northern part of the Netherlands. *Ardea*, **59**:75–188, 1971.

[870] G. Spitzer. Jahreszeitliche Aspekte der Biologie der Bartmeise (*Panurus biarmicus*). *J. Ornithol.*, **11**:241–275, 1972.

[871] J. R. Spotila and E. A. Standora. Energy budgets of ectothermic vertebrates. *Am. Zool.*, **25**:973–986, 1985.

[872] J. B. Sprague. Measurement of pollutant toxicity to fish i. bioassay methods for acute toxicity. *Water Res.*, **3**:793–821, 1969.

[873] M. Sprung. Physiological energetics of mussel larvae (*Mytilus edulis*) I. Shell growth and biomass. *Mar. Ecol. Prog. Ser.*, **17**:283–293, 1984.

[874] M. W. Stanier, L. E. Mount, and J. Bligh. *Energy balance and temperature regulation.* Cambridge University Press, 1984.

[875] R. Y. Stanier, E. A. Adelberg, and J. L. Ingraham. *General microbiology.* MacMillan Press, London, 1976.

[876] R. Y. Stanier, J. L. Ingraham, M. L. Wheelis, and P. R. Painter. *The microbial world.* Prentice Hall, Englewood Cliffs, 1986.

[877] P. Starke-Reed. Oxygen radicals and aging. In C. E. Thomas and B. Kalyanaman, editors, *Oxygen radicals and the disease process.* Hardwood, Australia, 1997.

[878] S. C. Stearns. *The evolution of life histories.* Oxford University Press, 1992.

[879] G. G. Steel. *Growth kinetics of tumors.* Clarendon Press, Oxford, 1977.

[880] J. H. Steele. *The structure of marine ecosystems.* Oxford University Press, 1993.

[881] R. G. Steen. The bioenergetics of symbiotic sea anemones (*Anthozoa: Actinaria*). *Symbiosis*, **5**:103–142, 1988.

[882] R. S. Stemberger and J. J. Gilbert. Body size, food concentration, and population growth in planktonic rotifers. *Ecology*, **66**:1151–1159, 1985.

[883] D. W. Stephens and J. R. Krebs. *Foraging theory.* Monographs in behavior and ecology. Princeton University Press, 1986.

[884] M. N. Stephens. The otter report. Universal Federation of Animal Welfare, Hertfordshire, 1957.

[885] J. D. Stevens. Vertebral rings as a means of age determination in the blue shark (*Prionace glauca* L.). *J. Mar. Biol. Assoc. U. K.*, **55**:657–665, 1975.

[886] J. R. Stewart. Placental structure and nutritional provision to embryos in predominantly lecithotrophic viviparous reptiles. *Am. Zool.*, **32**:303–312, 1992.

[887] B. Stonehouse. The emperor penguin. I: Breeding behaviour and development. F.I.D.S. Scientific Reports 6, 1953.

[888] B. Stonehouse. The brown skua of South Georgia. F.I.D.S. Scientific Reports 14, 1956.

[889] B. Stonehouse. The king penguin of South Georgia I. Breeding behaviour and development. F.I.D.S. Scientific Reports 23, 1960.

[890] J. M. Stotsenburg. The growth of the fetus of the albino rat from the thirteenth to the twenty-second day of gestation. *Anat. Rec.*, **9**:667–682, 1915.

[891] A. H. Stouthamer. Metabolic pathways in *Paracoccus denitrificans* and closely related bacteria in relation to the phylogeny of prokaryotes. *Antonie van Leeuwenhoek*, **61**:1–33, 1992.

[892] A. H. Stouthamer, B. A. Bulthuis, and H. W. van Verseveld. Energetics of growth at low growth rates and its relevance for the maintenance concept. In R. K. Poole, M. J. Bazin, and C. W. Keevil, editors, *Microbial growth dynamics*, pages 85–102. IRL Press, Oxford, 1990.

[893] A. H. Stouthamer and S. A. L. M. Kooijman. Why it pays for bacteria to delete disused DNA and to maintain megaplasmids. *Antonie van Leeuwenhoek*, **63**:39–43, 1993.

[894] N. M. van Straalen, T. B. A. Burghouts, M. J. Doornhof, G. M. Groot, M. P. M. Janssen, E. N. G. Joosse, J. H. van Meerendonk, J. P. J. J. Theeuwen, H. A. Verhoef, and H. R. Zoomer. Efficiency of lead and cadmium excretion in populations of *Orchesalla cincta* (*Collembola*) from various contaminated forest soils. *J. Appl. Ecol.*, **24**:953–968, 1987.

[895] R. Strahan, editor. *The complete book of Australian mammals.* Angus and Robertson Publ., London, 1983.

[896] R. R. Strathmann and M. F. Strathmann. The relationship between adult size and brooding in marine invertebrates. *Am. Nat.*, **119**:91–1011, 1982.

[897] J. R. Strickler. Calanoid copepods, feeding currents and the role of gravity. *Science (New York)*, **218**:158–160, 1982.

[898] S. J. van Strien. *Structures in dynamics*, chapter Interval Dynamics, pages 111–160. Elsevier, Amstrdam, 1991.

[899] T. Strömgren and C. Cary. Growth in length of *Mytilus edulis* L. fed on different algal diets. *J. Mar. Biol. Assoc. U. K.*, **76**:23–34, 1984.

[900] W. C. Summers. Age and growth of *Loligo pealei*, a population study of the common Atlantic coast squid. *Biol. Bull. (Woods Hole)*, pages 189–201, 1971.

[901] D. W. Sutcliffe, T. R. Carrick, and L.G. Willoughby. Effects of diet, body size, age and temperature on growth rates in the amphipod *Gammarus pulex*. *Freshwater Biol.*, **11**:183–214, 1981.

[902] A. Suwanto and S. Kaplan. Physical and genetic mapping of the *Rhodobacter sphaeroides* 2.4.1. genome: presence of two unique circular chromosomes. *J. Bacteriol.*, **171**:5850–5859, 1989.

[903] C. Swennen, M. F. Leopold, and M. Stock. Notes on growth and behaviour of the Americam razor clam *Ensis directus* in the Wadden Sea and the predation on it by birds. *Helgol. Wiss. Meeresunters.*, **39**:255–261, 1985.

[904] E. Syngajewskaja. The individual growth of protozoa: *Blepharisma lateritia* and *Actinophrys sp. Trav. Inst. Zool. Biol. Acad. Sci. Ukr.*, **8**:151–157, 1935.

[905] W. M. Tattersall and E. M. Sheppard. Observations on the asteriod genus *Luidia*. In *James Johnstone memorial volume*. Liverpool University Press, 1934.

[906] C. R. Taylor, K. Schmidt-Nielsen, and J. L. Raab. Scaling of energetic costs of running to body size in mammals. *Am. J. Physiol.*, **219**:1104–1107, 1970.

[907] D. L. Taylor. Symbiotic marine algae: taxonomy and biological fitness. In W. B. Vernberg, editor, *Symbiosis in the sea*, pages 245–262. University of South Carolina Press, 1974.

[908] J. M. Taylor and B. E. Horner. Sexual maturation in the Australian rodent *Rattus fuscipes assimilis*. *Aust. J. Zool.*, **19**:1–17, 1971.

[909] R. H. Taylor. Growth of adelie penguin (*Pygoscelis adeliae* Hombron and Jacquinot) chicks. *N. Z. J. Sci.*, **5**:191–197, 1962.

[910] W. D. Taylor. Growth responses of ciliate protozoa to the abundance of their bacterial prey. *Microb. Ecol.*, **4**:207–214, 1978.

[911] D. W. Tempest and O. M. Neijssel. The states of Y_{atp} and maintenance energy as biologically interpretable phenomena. *Annu. Rev. Microbiol.*, **38**:459–486, 1984.

[912] H. Tennekes. *De wetten van de vliegkunst; over stijgen, dalen, vliegen en zweven.* Aramith Uitgevers, Bloemendaal, 1992.

[913] A. J. Tessier and C. E. Goulden. Cladoceran juvenile growth. *Limnol. Oceanogr.*, **32**:680–685, 1987.

[914] A. J. Tessier, L. L. Henry, C. E. Goulden, and W. W. Durand. Starvation in *Daphnia*: energy reserves and reproductive allocation. *Limnol. Oceanogr.*, **28**:489–496, 1983.

[915] H. R. Thieme. Well-posedness of physiologically structured population models for *Daphnia magna*. *J. Math. Biol.*, **26**:299–317, 1988.

[916] T. W. Thomann and J. A. Mueller. *Principles of surface water quality modeling and control.* Harper & Row Publ. Inc., London, 1987.

[917] J. M. T. Thompson and H. B. Stewart. *Nonlinear dynamics and chaos.* J. Wiley & Sons, Inc., Chichester, 1986.

[918] K. S. Thompson. *Living fossil: the story of the coelacanth.* Hutchinson Radius, London, 1991.

[919] M. B. Thompson. Patterns of metabolism in embryonic reptiles. *Respir. Physiol.*, **76**:243–256, 1989.

[920] J. H. M. Thornley. *Mathematical models in plant physiology.* Academic Press, London, 1976.

[921] S. T. Threlkeld. Starvation and the size structure of zooplankton communities. *Freshwater Biol.*, **6**:489–496, 1976.

[922] E. V. Thuesen. The tetrodotoxin venom of chaetognaths. In Q. Bone, H. Kapp, and A. C. Pierrot-Bults, editors, *The biology of chaetognaths*. Oxford University Press, 1991.

[923] R. R. Tice and R. B. Setlow. DNA repair and replication in aging organisms and cells. In C. E. Finch and E. L. Schneider, editors, *Handbook of the biology of aging*, pages 173–224. Van Nostrand, New York, 1985.

[924] W. L. N. Tickell. *The biology of the great albatrosses,* Diomedea exulans *and* Diomedea epomophora, pages 1–55. Antarctic Research series No 12. American Geophysical Union, Washington, DC, 1968.

[925] A. G. M. Tielens. Energy generation in parasitic helminths. *Parasitol. Today*, **10**:346–352, 1994.

[926] A. G. M. Tielens and J. J. van Hellemond. Differences in energy metabolism between *Trypanosomatidae*. *Parasitol. Today*, **14**:265–271, 1998.

[927] A. G. M. Tielens and J. J. van Hellemond. The electron transport chain in anaerobically functioning eukaryotes. *Biochim. Biophys. Acta*, **1365**:71–78, 1998.

[928] K. Tiews. Biologische Untersuchungen am Roten Thun (*Thunnus thynnus* [Linnaeus]) in der Nordsee. *Ber. Dtsch. Wiss. Komm. Meeresforsch.*, **14**:192–220, 1957.

[929] H. Topiwala and C. G. Sinclair. Temperature relationship in continuous culture. *Biotechnol. Bioeng.*, **13**:795–813, 1971.

[930] N. R. Towers, J. K. Raison, G. M. Kellerman, and A. W. Linnane. Effects of temperature-induced phase changes in membranes on protein synthesis by bound ribosomes. *Biochim. Biophys. Acta*, **287**:301–311, 1972.

[931] A. P. J. Trinci. A kinetic study of the growth of *Aspergillus nidulans* and other fungi. *J. Gen. Microbiol.*, **57**:11–24, 1969.

[932] A. P. J. Trinci, G. D. Robson, M. G. Wiebe, B. Cunliffe, and T. W. Naylor. Growth and morphology of *Fusarium graminearum* and other fungi in batch and continuous culture. In R. K. Poole, M. J. Bazin, and C. W. Keevil, editors, *Microbial growth dynamics*, pages 17–38. IRL Press, Oxford, 1990.

[933] F. J. Trueba. *A morphometric analysis of* Escherichia coli *and other rod-shaped bacteria.* PhD thesis, University of Amsterdam, 1981.

[934] S. Tuljapurkar and H. Caswell. *Structured-population models in marine, terrestrial, and freshwater systems.* Chapman & Hall, New York, 1996.

[935] A. W. H. Turnpenny, R. N. Bamber, and P.A. Henderson. Biology of the sand-smelt (*Atherina presbyter* Valenciennes) around Fawlay power station. *J. Fish Biol.*, **18**:417–427, 1981.

[936] H. Tyndale-Biscoe. *Life of marsupials.* E. Arnold, London, 1973.

[937] D. E. Ullrey, J. I. Sprague, D. E. Becker, and E. R. Miller. Growth of the swine fetus. *J. Anim. Sci.*, **24**:711–717, 1965.

[938] F. A. Urquhart. *The monarch butterfly: international traveler.* Nelson Hall, Chicago, 1987.

[939] E. Ursin. A mathematical model of some aspects of fish growth, respiration, and mortality. *J. Fish. Res. Board Can.*, **24**:2355–2453, 1967.

[940] K. Uvnäs-Moberg. The gastrointestinal tract in growth and reproduction. *Sci. Am.*, **7**:60–65, 1989.

[941] H. A. Vanderploeg, G.-A. Paffenhöfer, and J. R. Liebig. Concentration-variable interactions between calanoid copepods and particles of different food quality: Observations and hypothesis. In R. N. Hughes, editor, *Behavioural mechanisms of food selection*, volume G 20 of *NATO ASI*, pages 595–613. Springer-Verlag, Berlin, 1990.

[942] N. Verboven and T. Piersma. Is the evaporative water loss of knot *Calidris canutus* higher in tropical than in temperate climates? *Ibis*, **137**:308–316, 1995.

[943] C Verduyn. *Energetic aspects of metabolic fluxes in yeasts.* PhD thesis, Technical Univertsity, Delft, 1992.

[944] L. J. Verme. Effects of nutrition on growth of white-tailed deer fawns. *Trans. N. Am. Widl. Nat. Resour. Conf.*, **28**:431–443, 1963.

[945] K. Vermeer. The importance of plankton to Cassin's auklets during breeding. *J. Plankton Res.*, **3**:315–329, 1981.

[946] H. W. van Verseveld, M. Braster, F. C. Boogerd, B. Chance, and A. H. Stouthamer. Energetic aspects of growth of *Paracoccus denitrificans*: oxygen-limitation and shift from anaerobic nitrate-limitation to aerobic succinate-limitation. *Arch. Microbiol.*, **135**:229–236, 1983.

[947] H. W. van Verseveld and A. H. Stouthamer. Oxidative phosphorylation in *Micrococcus denitrificans*; calculation of the P/O ration in growing cells. *Arch. Microbiol.*, **107**:241–247, 1976.

[948] H. W. van Verseveld and A. H. Stouthamer. Growth yields and the efficiency of oxydative phosphorylation during autotrophic growth of *Paracoccus denitrificans* on methanol and formate. *Arch. Microbiol.*, **118**:21–26, 1978.

[949] H. W. van Verseveld and A. H. Stouthamer. Two-(carbon) substrate-limited growth of *Paracoccus denitrificans* on mannitol and formate. *FEMS Microbiol. Lett.*, **7**:207–211, 1980.

[950] J. Vidal and T. E. Whitledge. Rates of metabolism of planktonic crustaceans as related to body weight and temperature of habitat. *J. Plankton Res.*, **4**:77–84, 1982.

[951] J. Vijverberg. Effect of temperature in laboratory studies on development and growth of *Cladocera* and *Copepoda* from Tjeukemeer, The Netherlands. *Freshwater Biol.*, **10**:317–340, 1980.

[952] C. M. Vleck, D. F. Hoyt, and D. Vleck. Metabolism of embryonic embryos: patterns in altricial and precocial birds. *Physiol. Zool.*, **52**:363–377, 1979.

[953] C. M. Vleck, D. Vleck, and D. F. Hoyt. Patterns of metabolism and growth in avian embryos. *Am. Zool.*, **20**:405–416, 1980.

[954] D. Vleck, C. M. Vleck, and R. S. Seymour. Energetics of embryonic development in the megapode birds, mallee fowl *Leipoa ocellata* and brush turkey *Alectura lathami*. *Physiol. Zool.*, **57**:444–456, 1984.

[955] N. J. Volkman and W. Trivelpiece. Growth in pygoscelid penguin chicks. *J. Zool. Lond.*, **191**:521–530, 1980.

[956] W. J. Voorn and A. L. Koch. Characterization of the stable size distribution of cultured cells by moments. In J. A. J. Metz and O. Diekmann, editors, *The dynamics of physiologically structured populations*, volume 68 of *Springer Lecture Notes in Biomathematics.*, pages 430–440. Springer-Verlag, Berlin, 1986.

[957] J. G. Wagner. The kinetics of alcohol elimination in man. *Acta Pharmacol. Toxicol.*, **14**:265–289, 1958.

[958] J. G. Wagner. A modern view in pharmacokinetics. *J. Pharmacokinet. Biopharm.*, **1**:363–401, 1973.

[959] J. G. Wagner. Do you need a pharmacokinetic model, and, if so, which one? *J. Pharmacokinet. Biopharm.*, **3**:457–478, 1975.

[960] J. G. Wagner. Time to reach steady state and prediction of steady-state concentrations for drugs obeying Michaelis-Menten elimination kinetics. *J. Pharmacokinet. Biopharm.*, **6**:209–225, 1978.

[961] C. H. Walker. Kinetic model to predict bioaccumulation of pollutant. *Funct. Ecol.*, **4**:295–301, 1990.

[962] E. P. Walker. *Mammals of the world.* Johns Hopkins University Press, Baltimore, 1975.

[963] G. M. Walker. *Yeast; physiology and biotechnology.* J. Wiley & Sons Inc., Chichester, 1998.

[964] M. Walls, H. Caswell, and M. Ketola. Demographic costs of Chaoborus-induced defences in *Daphnia pulex*. *Oecologia*, **87**:43–50, 1991.

[965] A. E. Walsby. A square bacterium. *Nature (Lond.)*, **283**:69–73, 1980.

[966] N. Walworth, S. Davey, and D. Beach. Fission yeast chk1 protein kinase links the rad checkpoint pathway to cdc2. *Nature (Lond.)*, **363**:368–371, 1993.

[967] J. Warham. The crested penguins. In B. Stonehouse, editor, *The biology of penguins*, pages 189–269. MacMillan Publishing Co., London, 1975.

[968] B. L. Warwick. Prenatal growth of swine. *J. Morphol.*, **46**:59–84, 1928.

[969] I. Watanabe and S. Okada. Effects of temperature on growth rate of cultured mammalian cells (l5178y). *J. Cell Biol.*, **32**:309–323, 1967.

[970] L. Watson. *Whales of the world.* Hutchinson & Co. Ltd., London, 1981.

[971] E. Watts and S. Young. Components of *Daphnia* feeding behaviour. *J. Plankton Res.*, **2**:203–212, 1980.

[972] J. van Waversveld, A. D. F. Addink, and G. van den Thillart. The anaerobic energy metabolism of goldfish determined by simultaneous direct and indirect calorimetry during anoxia and hypoxia. *J. Comp. Physiol.*, **159**:263–268, 1989.

[973] J. van Waversveld, A. D. F. Addink, G. van den Thillart, and H. Smit. Heat production of fish: a literature review. *Comp. Biochem. Physiol.*, **92A**:159–162, 1989.

[974] H. Wawrzyniak and G. Sohns. *Die Bartmeise.*, volume 553 of *Die Neue Brehm-Bücherei*. A. Ziemsen-Verlag, Wittenberg Lutherstadt, 1986.

[975] G. J. W. Webb, D. Choqeunot, and P. J. Whitehead. Nests, eggs, and embryonic development of *Carettochelys insculpta* (*Chelonia*: *Carettochelidae*) from Northern Australia. *J. Zool. Lond.*, **B1**:521–550, 1986.

[976] G. J. W. Webb, S. C. Manolis, K. E. Dempsey, and P. J. Whitehead. Crocodilian eggs: a functional overview. In G. J. W. Webb, S. C. Manolis, and P. J. Whitehead, editors, *Wildlife management: crocodiles and alligators*, pages 417–422. Beatty, Sydney, 1987.

[977] T. P. Weber and T. Piersma. Basal metabolic rate and the mass of tissues differing in metabolic scope: migration-related covariation between individual knots *Calidris canutus*. *J. Avian Biol.*, **27**:215–224, 1996.

[978] W. Weibull. A statistical distribution of wide applicability. *J. Appl. Mech.*, **18**:293–297, 1951.

[979] A. P. Weinbach. The human growth curve. I: Prenatal. *Growth*, **5**:217–233, 1941.

[980] J. Weiner. Physiological limits to sustainable energy budgets in birds and mammals: ecological implications. *Trends Ecol. Evol.*, **7**:384–388, 1992.

[981] E. Weitnauer-Rudin. Mein Vogel. aus dem Leben der Mauerseglers *Apus apus*. Basellandschaftlicher Natur- und Vogelschutzverband, Liestal., 1983.

[982] M. J. Wells. Cephalopods do it differently. *New Sci.*, **3**:333–337, 1983.

[983] D. F. Werschkul. Nestling mortality and the adaptive significance of early locomotion in the little blue heron. *Auk*, **96**:116–130, 1979.

[984] G. B. West, J. H. Brown, and B. J. Enquist. A general model for the origin of allometric scaling laws in biology. *Science*, **276**:122–126, 1997.

[985] I. C. West. *The biochemistry of membrane transport.* Chapman & Hall, London, 1983.

[986] P. Westbroek. *Life as a geological force; dynamics of the Earth.* W. W. Norton & Co, New York, 1991.

[987] H. V. Westerhoff and K. van Dam. *Thermodynamics and control of biological free energy transduction.* Elsevier, Amsterdam, 1987.

[988] K. Westerterp. The energy budget of the nestling starling *Sturnus vulgaris*, a field study. *Ardea*, **61**:137–158, 1973.

[989] D. F. Westlake. Some effects of low-velocity currents on the metabolism of aquatic macrophytes. *J. Exp. Bot.*, **18**:187–205, 1967.

[990] R. Wette, I. N. Katz, and E. Y. Rodin. Stochastic processes for solid tumor kinetics: surface-regulated growth. *Math. Biosci.*, **19**:231–225, 1974.

[991] T. C. R. White. *The inadequate environment; nitrogen and the abundance of animals.* Springer-Verlag, Berlin, 1993.

[992] P. J. Whitehead. Respiration of *Crocodylus johnstoni* embryos. In G. J. W. Webb, S. C. Manolis, and P. J. Whitehead, editors, *Wildlife management: crocodiles and alligators*, pages 473–497. Beatty, Sydney, 1987.

[993] P. J. Whitehead, G. J. W. Webb, and R. S. Seymour. Effect of incubation temperature on development of *Crocodylus johnstoni* embryos. *Physiol. Zool.*, **63**:949–964, 1990.

[994] P. J. Whitfield. *The biology of parasitism: an introduction to the study of associating organisms.* E. Arnold, London, 1979.

[995] A. P. Wickens. *The causes of aging.* Harwood Academic Publishers, Australia, 1998.

[996] J. Widdows, P. Fieth, and C. M. Worral. Relationship between seston, available food and feeding activity in the common mussel *Mytilus edulis*. *Mar. Biol.*, **50**:195–207, 1979.

[997] E. Widmark and J. Tandberg. Über die bedingungen für die akkumulation indifferenter narkoliken theoretische bereckerunger. *Biochem. Z.*, **147**:358–369, 1924.

[998] P. Wiersma and T. Piersma. Effects of microhabitat, flocking, climate and migratory goal on energy expenditure in the annual cycle of red knots. *Condor*, **96**:257–279, 1994.

[999] H. Wijnandts. Ecological energetics of the long-eared owl (*Asio otus*). *Ardea*, **72**:1–92, 1984.

[1000] M. Wilbrink, M. Treskes, T. A. de Vlieger, and N.P.E. Vermeulen. Comparative toxicokinetics of 2,2'- and 4,4'-dichlorobiphenyls in the pond snail *Lymnaea stagnalis* (L.). *Arch. Environ. Contam. Toxicol.*, **19**:69–79, 1989.

[1001] H. M. Wilbur. Interactions of food level and population density in *Rana sylvatica*. *Ecology*, **58**:206–209, 1977.

[1002] L. W. Wilcox and G. J. Wedemayer. Dinoflagellate with blue-green chloroplasts derived from an ensosymbiotic eukaryote. *Science*, **227**:192–194, 1985.

[1003] D. I. Williamson. *Larvae and evolution.* Chapman & Hall, London, 1992.

[1004] P. Williamson and M. A. Kendall. Population age structure and growth of the trochid *Monodonta lineata* determined from shell rings. *J. Mar. Biol. Assoc. U. K.*, **61**:1011–1026, 1981.

[1005] D. B. Wingate. First successful hand-rearing of an abondoned Bermuda petrel chick. *Ibis*, **114**:97–101, 1972.

[1006] J. E. Winter. The filtration rate of *Mytilus edulis* and its dependence on algal concentrations, measured by a continuous automatic recording apparatus. *Mar. Biol.*, **22**:317–328, 1973.

[1007] L. M. Winters and G. Feuffel. Studies on the physiology of reproduction in the sheep. IV. Fetal development. *Techn. Bull. Minn. Agric. Exp. Station*, **118**:1–20, 1936.

[1008] L. M. Winters, W. W. Green, and R. E. Comstock. Prenatal development of the bovine. *Techn. Bull. Minn. Agric. Exp. Station*, **151**:1–50, 1942.

[1009] P. C. Withers. *Comparative animal physiology.* Saunders College Publishing, Fort Worth, 1992.

[1010] P. C. Withers and J. U. M. Jarvis. The effect of huddling on thermoregulation and oxygen consumption for the naked mole-rat. *Comp. Biochem. Physiol.*, **66**:215–219, 1980.

[1011] M. Witten. A return to time, cells, systems, and aging III: Gompertzian models of biological aging and some possible roles for critical elements. *Mech. Ageing Dev.*, **32**:141–177, 1985.

[1012] W. de Wolf, J. H. Canton, J. W. Deneer, R. C. C. Wegman, and J. L. M. Hermens. Quantitative structure-activity relationships and mixture–toxicity studies of alcohols and chlorohydrocarbons: reproducibility of effects on growth and reproduction of *Daphnia magna*. *Aquatic Toxicol.*, **12**:39–49, 1988.

[1013] D. Wolf-Gladrow and U. Riebesell. Diffusion and reactions in the vicinity of plankton: a refined model for inorganic carbon transport. *Mar. Chem.*, **59**:17–34, 1997.

[1014] D. A. Wolf-Gladrow, J. Bijma, and R. E. Zeebe. Model simulation of the carbonate chemistry in the micro-environment of symbiont bearing foraminifera. *Marine Chemistry*, 1999. to appear.

[1015] F. I. Woodward. *Climate and plant distribution.* Cambridge studies in ecology. Cambridge University Press, 1987.

[1016] R. J. Wootton. *Ecology of teleost fishes.* Chapman & Hall, London, 1990.

[1017] J. P. Wourms. Viviparity: the maternal–fetal relationship in fishes. *Am. Zool.*, **21**:473–515, 1981.

[1018] J. P. Wourms and J. Lombardi. Reflections on the evolution of piscine viviparity. *Am. Zool.*, **32**:276–293, 1992.

[1019] G. A. Wray. Punctuated evolution of embryos. *Science (New York)*, **267**:1115–1116, 1995.

[1020] G. A. Wray and A. E. Bely. The evolution of echinoderm development is driven by several distinct factors. *Development*, **suppl.**:97–106, 1994.

[1021] G. A. Wray and R. A. Raff. The evolution of developmental strategy in marine invertebrates. *Trends Ecol. Evol.*, **6**:45–50, 1991.

[1022] J. R. Wright and R. G. Hartnoll. An energy budget for a population of the limpet *Patella vulgata*. *J. Mar. Biol. Assoc. U. K.*, **61**:627–646, 1981.

[1023] I. Wyllie. *The cuckoo*. B.T. Batsford Ltd., London, 1981.

[1024] A. Ykema. *Lipid production in the oleaginous yeast* Apiotrichum curvantum. PhD thesis, Vrije Universiteit, Amsterdam, 1989.

[1025] P. Yodzis. *Introduction to theoretical ecology*. Harper & Row Publ. Inc., London, 1989.

[1026] E. Zeuthen. *Body size and metabolic rate in the animal kingdom.* H. Hagerup, Copenhagen, 1947.

[1027] S. H. Zinder. Physiological ecology of methanogens. In J.G. Ferry, editor, *Methanogenesis; ecology, physiology, biochemistry and genetics*, pages 128–206. Chapman & Hall, London, 1993.

[1028] C. Zonneveld and S. A. L. M. Kooijman. Application of a general energy budget model to *Lymnaea stagnalis*. *Funct. Ecol.*, **3**:269–278, 1989.

[1029] C. Zonneveld and S. A. L. M. Kooijman. Body temperature affects the shape of avian growth curves. *J. Biol. Syst.*, **1**:363–374, 1993.

[1030] C. Zonneveld and S. A. L. M. Kooijman. Comparative kinetics of embryo development. *Bull. Math. Biol.*, **3**:609–635, 1993.

Glossary

acidity The negative logarithm, with base 10, of the proton concentration expressed in mole dm^{-3}. It is known as the pH

alga An autotrophic (or mixotrophic) protoctist

allometry The group of analyses based on a linear relationship between the logarithm of some physiological or ecological variable and the logarithm of the body weight of individuals

altricial A mode of development where the neonate is still in an early stage of development and requires attention from the parents. Typical altricial birds and mammals are naked and blind at birth. The opposite of altricial is precocial

anabolism The collection of biochemical processes involved in the synthesis of structural body mass

animal Metazoan, ranging from sponges to chordates

Arrhenius temperature The value of the slope of the linear graph one gets if the logarithm of a physiological rate is plotted against the inverse absolute temperature. It has dimension temperature, but it does not relate to a temperature that exists at a site

aspect ratio The dimensionless ratio between the length and the diameter of an object with the shape of a cylinder (filaments, rods). The length of rods includes both hemispheres

assimilation Generation of reserves from substrates (food)

ATP Adenosine triphosphate is a chemical compound that is used by all cells to store or retrieve energy via hydrolysis of one or two phosphate bonds

Avogadro constant The number of C-atoms in 12 g of $^{12}\mathrm{C}$, which is $6.02205\,10^{23}$ mol^{-1}

Bernoulli equation A differential equation of the type $\frac{d}{dx}y + f(x)y = g(x)y^a$, where a is any real number and f and g are arbitrary functions of x. Bernoulli found a solution technique for this type of equation

C-mole Ratio of the number of carbon atoms of a compound to the Avogadro's constant, where the frequencies of non-carbon elements are expressed relative to carbon

canonical Relating to the simplest form to which various equations and schemata can be reduced without loss of generality

catabolism The collection of biochemical processes involved in the decomposition of compounds for the generation of energy and/or source material for anabolic processes; here used for the use of reserves for metabolism (maintenance and growth)

chemical potential The change in the total free energy of a mixture of compounds per mole of substance when an infinitesimal amount of a substance is added, while temperature, pressure and all other compounds are constant

coefficient of variation The dimensionless ratio of the (sample) standard deviation and the mean. It is a useful measure for the scatter of realizations of a random variable that has a natural origin. The measure is useless for temperatures measured in degrees Celsius, for example

combustion reference In this frame of reference, the chemical potentials of H_2O, HCO_3^-, NH_4^+, H^+ and O_2 are taken to be 0. The chemical potentials of organic compounds in the standard thermodynamic frame of reference (pH=7, 298 K, unit molarity) are corrected for this setting by equating the dissipation free energy in both frames of reference, when the compound is fully oxidized. The chemical potential of compound $CH_xO_yN_z$ in the combustion frame of reference is expressed in the standard frame of reference as $\mu_{CH_xO_yN_z} = \mu^\circ_{CH_xO_yN_z} + \frac{1}{2}(2 - x + 3z)\mu^\circ_{H_2O} - \mu^\circ_{HCO_3^-} - (1 - z)\mu^\circ_{H^+} - z\mu^\circ_{NH_4^+} + \frac{1}{4}(4 + x - 2y - 3z)\mu^\circ_{O_2}$

compound parameter A function of original parameters. It is usually a simple product and/or ratio

cubic spline function A function consisting of a number of third-degree polynomials glued together in a smooth way for adjacent intervals of the argument. This is done by requiring that polynomials which meet at a particular argument value x_i have the same value y_i, and the same first two derivatives at that point. The points x_i, y_i, for $i = 1, 2, \cdots, n$ with $n \geq 4$ are considered as the parameters of the cubic spline. For descriptive purposes, splines have the advantage over higher order polynomials because their global behaviour is much less influenced by local behaviour

DEB Initials of the Dynamic Energy Budget model or theory, which is discussed in this book. The term 'dynamic' refers to the contrast with the frequently used Static Energy Budget models, where the specifications of the individual do not change explicitly in time

density The ratio of two masses; but these masses are not necessarily homogeneously mixed, contrary to the concept 'concentration'

dissociation constant The negative logarithm, with base 10, of the ratio of the product of the proton and the ion concentration, to the molecule concentration. It is known as the pK

DNA Deoxyribonucleic acid, the carrier of genetic information in all living cells

eclosion Hatching of imago from pupa (of a holo-metabolic insect)

ectotherm An organism that is not an endotherm

eigenvalue If a special vector, an eigenvector, is multiplied by a square matrix, the result is the same as multiplying that vector by a scalar value, known as the eigenvalue. Each square matrix has a number of different independent eigenvectors. This number is less than or equal to the number of rows (or columns). Each eigenvector has its own eigenvalue, but some of the eigenvalues may be equal

endotherm An animal that usually keeps its body temperature within a narrow range by producing heat. Birds and mammals do this for most of time that they are active. Some other species (insects, tuna fish) have endothermic tendencies

enthalpy Heat content with dimension energy mole^{-1}. The enthalpy of a system increases by an amount equal to the energy supplied as heat if the temperature and pressure do not change

entropy The cumulative ratio of heat capacity to temperature of a body when its temperature is gradually increased from zero (absolute) temperature to the temperature of observation. Its dimension is energy$\times$(temperature mole)$^{-1}$. The equivalent definition of the ratio of enthalpy minus free energy to temperature is more useful in biological applications

estimation The use of measurements to assign values to one or more parameters of a model. This is usually done in some formalized manner that allows evaluation of the uncertainty of the result

eukaryote An organism that has a nucleus; it contrasts with prokaryote, and includes protoctists, plants and animals

expectation The theoretical mean of a function of a random variable. For a function g of a random variable $\underline{x}$ with probability density $\phi_{\underline{x}}$, its formal definition is $\mathcal{E}g(\underline{x}) \equiv \int_x^g (x)\phi_{\underline{x}}(x)\,dx$. For $g(\underline{x}) = \underline{x}$, the expectation of $\underline{x}$ is the theoretical mean

exponential distribution The random variable $\underline{t}$ is exponentially distributed with parameter $\dot{r}$ if the probability density is $\phi_{\underline{t}}(t) = \dot{r}\exp\{-\dot{r}t\}$. The mean of $\underline{t}$ equals $\dot{r}^{-1}$

filament An organism with the shape of a cylinder that grows in length only. The aspect ratio is so small that the caps can be neglected in its energetics

first-order process A process that can be described by a differential equation where the change of a quantity is linear in the quantity itself

flux An amount of mass or energy per unit of time. An energy flux is physically known as a power

free energy The maximum amount of energy of a system that is potentially available for 'work'. In biological systems, this 'work' usually consists of driving chemical reactions against the direction of their thermodynamic decay

functional response The ingestion rate of an organism as a function of food density

generalized compound Mixture of chemical compounds that does not change in composition: fixed stoichiometries for synthesis (organic substrate, reserves and structural mass are generalized compounds)

growth Increase in structural body mass, measured as an increase in volume in most organisms. I do not include anabolic processes that are part of maintenance

hazard rate The probability per time increment that death strikes at a certain age, given survival up to that age

heat capacity The mole-specific amount of heat absorbed by a substance to increase one Kelvin in temperature. Heat capacity typically depends on temperature and has dimension energy mole^{-1}

heterotroph An organism that uses organic compounds as a source of energy

homeostasis The ability of most organisms to keep the chemical composition of their body constant, despite changes in the chemical composition of the environment

iteroparous Able to reproduce several times, rather than just once

isomorph An organism that does not change its shape during growth

large number law The strong law of large numbers states that the difference between the mean of a set of random variables and its theoretical mean is small, with an overwhelming probability, given that the set is large enough

maintenance A rather vague term denoting the collection of energy-demanding processes that life seems to require to keep going, excluding all production processes. I also exclude heat production in endotherms

mass action law The law that states that the meeting frequency of two types of particles is proportional to the product of their densities, i.e. number of particles per unit of volume

morph Organism in which surface area that is involved in uptake grows proportional to volume^0 (V0-morph) or to volume^1 (V1-morph)

NADPH Nicotinamide adenine dinucleotide phosphate is a chemical compound that is used by all cells to accept pairs of electrons

nutrients Inorganic substrates used for the synthesis of reserves; carbon dioxide and ammonia are examples, and light is also included for convenience

ODE Ordinary differential equation, which is an equation of the type $\frac{d}{dt}y = f(t, y)$, for some function f of t and y

ovoviviparous Having embryos that develop energetically independent from, but inside the mother

parameter A quantity in a model that describes the behaviour of state variables. It is usually assumed to be a constant

parthenogenesis The mode of reproduction where females produce eggs that hatch into new females without the interference of males

partition coefficient The ratio of the equilibrium concentrations of a compound dissolved in two immiscible solvents, which is taken to be independent of the actual concentrations. The concentrations are here expressed per unit of weight of solvent (not per unit of volume or per mole of solvent)

phylum A taxon that collects organisms with the same body plan

plant Embryophyte, which includes mosses, ferns and relatives, gymnosperms and flowering plants

Poisson distribution A random integer-valued variable $\underline{X}$ is Poisson distributed with parameter (mean) λ if $\Pr\{\underline{X} = x\} = \frac{\lambda^x}{x!}\exp\{-\lambda\}$. If intervals between independent events are exponentially distributed, the number of events in a fixed time period will be Poisson distributed

polynomial A polynomial of degree n of argument x is a function of the type $\sum_{i=0}^{n} c_i x^i$, where $c_0, c_0, \cdots, c_n$ with $c_n \neq 0$ are fixed coefficients

precocial A mode of development where the neonate is in an advanced state of development and usually does not require attention from the parents. Typical precocial birds and mammals have feathers or hair and gather food by themselves. The opposite of precocial is altricial

probability density function A non-negative function, here called ϕ, belonging to a continuous random variable, $\underline{x}$ for instance, with the property that $\int_{x_1}^{x_2} \phi_{\underline{x}}(x)\,dx = \Pr\{x_1 < \underline{x} < x_2\}$

prokaryote An organism that does not have a nucleus, i.e. a eubacterium or archaebacterium; it contrasts with an eukaryote

protoctist An eukaryote that is not a plant or animal

reduction degree A property of a molecule. Its value equals the sum of the valences of the atoms minus the electrical charge

relaxation time A characteristic time that indicates how long a dynamic system requires to return to its equilibrium after perturbation. It is a compound parameter with the dimension time, standing for the first term of the Taylor expansion of the differential equation that describes the dynamics of the system, evaluated in its equilibrium

respiration quotient The ratio between carbon dioxide production and oxygen consumption, expressed on a molar basis

rod A bacterium with the shape of a croquette or sausage, that grows in length only, at a certain substrate density. It is here idealized by a cylinder with hemispheres at both ends

sd Standard deviation, estimated by the square root of the variance

state variable A variable which determines, together with other state variables, the behaviour of a system. The crux of the concept is that the collection of state variables, together with the input, determines the behaviour of the system completely

survivor function A rather misleading term standing for the probability that a given random variable exceeds a specified value. All random variables have a survivor function, even those without any connection to life span. It equals one minus the distribution function. The term is sometimes synonymous with upper tail probability

taxon A systematic unit, which is used in the classification of organisms. It can be species, genus, family, order, class, phylum, kingdom

Taylor expansion The approximation of a function by a polynomial of a certain degree that is thought to be accurate for argument values around a specified value. The coefficients of the polynomial are obtained by equating the function value and its first n derivatives at the specified value to that of the n degree polynomial

volumetric length The cubic root of the volume of an object. It has dimension length

weighted sum The sum of terms that are multiplied with weight coefficients before addition. If the terms do not have the same dimension, the dimensions of the different weight coefficients convert the dimensions of weighted terms to the same dimension

zero-th order process A process that can be described by a differential equation where the change of a quantity is constant

zooplankter An individual belonging to the zooplankton, i.e. a group of usually small aquatic animals that live in free suspension and do not actively move far in the horizontal direction

Notation and symbols

Some readers will be annoyed by the notation, which sometimes differs from that typically used in a particular specialization. One problem is that conventions in microbiology, for example, differ from those in ecology, so not all conventions can be observed at the same time. The symbol D, for example, is used by microbiologists for the dilution rate in chemostats, but by chemists for diffusivity. A voluminous literature on population dynamics exists, where it is standard to use the symbol l for survival probability. This works well as long as one does not want to use lengths in the same text! Another problem is that most literature does not distinguish structural biomass from energy reserves, which both contribute to dry weight, for example. So the conventional symbols actually differ in meaning from those used here. Few texts deal with such a broad spectrum of phenomena as this book. A consequence is that any symbol table is soon exhausted if one carelessly assigns new symbols to all kinds of variables that show up.

The following conventions are used to reduce this problem and to aid memory.

Symbols

- Variables denoted by symbols that differ only in indices have the same dimensions. For example M_E and M_V are both moles.

- The interpretation of the leading character does not relate to that of the index character. For example, the M in M_E stands for mass in moles, but in $\dot{k}_M$ it stands for maintenance.

- Lowercase symbols frequently relate to uppercase ones via scaling; e is a scaled E. Likewise, this applies to J, L, M, W and X. Exceptions are F, P, R and T.

- Analogous to the tradition in chemistry, quantities which are expressed per unit of biovolume have square brackets, $[\,]$. Quantities per unit of biosurface area have braces, $\{\,\}$. Quantities per unit of weight have angles, $\langle\,\rangle$, (with indices w and d for wet and dry weight). This notation is chosen to stress that these symbols refer to relative quantities, rather than absolute ones. They do not indicate concentrations in the chemical sense, because most of the compounds concerned are not soluble.
  Parentheses, square brackets and braces around numbers refer to equations, references and pages respectively.

- Rates have dots, which merely indicate the dimension 'per time'. Dots (and primes) do *not* stand for the derivative as in some mathematical and physical texts (see the subsection 'Expressions'). Dots, brackets and braces allow an easy test for some dimensions, and reduce the number of different symbols for related variables. If time has been scaled, i.e. the time unit is some particular value making scaled time dimensionless, the dot has been removed from the rate that is expressed in scaled time.

- Random variables are underscored. The notation $\underline{x}|\underline{x} > x$ means the random variable $\underline{x}$ given that it is larger than the value x. It can occur in expressions for the probability, $\Pr\{\}$, or for the probability density function, $\phi()$, or the distribution function, $\Phi()$.

- Vectors and matrices are printed in bold face. A bold number represents a vector or matrix of elements with that value; so $\dot{\boldsymbol{J}}\mathbf{1}$ is the summation of matrix $\dot{\boldsymbol{J}}$ across columns and $\mathbf{1}^T\dot{\boldsymbol{J}}$ across rows; $\boldsymbol{x} = \mathbf{0}$ means that all elements of $\boldsymbol{x}$ are 0.

Indices

Indices are catenated, the first subscript frequently specifying the variable to which the symbol relates. For example M_V stands for a mole of structural biomass, where V is structural biovolume. Some indices have a specific meaning

$*$	indicates that several other symbols can be substituted. It is known as a 'wildcard' in computer science. As superscript it denotes the equilibrium value of the variable.
$'$	indicates a scaling as superscript.
i, j	are counters that refer to types or species; they can take the values $1, 2, \cdots$.
m	stands for 'maximum'. For example $\dot{J}_{Am}$ is the maximum value that $\dot{J}_A$ can attain.
$+$	can refer to the sum of elements, such as $V_+ = \sum_i V_i$, or to addition, such as X_{i+1}, *ortoaspecialr*

Indices for compounds refer to

C	carbon dioxide	$C-$	bicarbonate	E	reserves	E_R	reprod. reserves
H	water	$\mathcal{M}$	minerals	N_H	ammonia	N_O	nitrate
O	dioxygen	$\mathcal{O}$	org. compounds	P	product (faeces)	Q	toxic compound
V	structural mass	X	food				

Indices for processes refer to

a	aging	A	assimilation	C	catabolism	D	dissipation
F	feeding	G	growth	J	matur. maintenance	M	som. maintenance
R	reproduction	$T+$	dissipating heat	T	heating (endotherms)		

Expressions

- An expression between parentheses with an index '+' means: take the maximum of 0 and that expression, so $(x - y)_+ \equiv \max\{0, x - y\}$. The symbol '$\equiv$' means 'is per definition'. It is just another way of writing, you are not supposed to understand that the equality is true.

- Although the mathematical standard for notation should generally be preferred over that of any computer language, I make one exception: the logic boolean, e.g. $(x < x_s)$. It always comes with parentheses and has value 1 if true or value 0 if false. It appears as part of an expression. Simple rules apply, such as

  $(x \leq x_s)(x \geq x_s) = (x = x_s)$

  $(x \leq x_s) = (x = x_s) + (x < x_s) = 1 - (x > x_s)$

  $\int_{x_1=-\infty}^{x} (x_1 = x_s)\, dx_1/dx = (x \geq x_s)$

  $\int_{x_1=-\infty}^{x} (x_1 \geq x_s)\, dx_1 = (x - x_s)_+$

- The following operators occur

$\frac{d}{dt}X\|_{t_1}$	derivative of X with respect to t evaluated at $t = t_1$
$\frac{\partial}{\partial t}X\|_{t_1}$	partial derivative of X with respect to t evaluated at $t = t_1$
$\mathcal{E}g(\underline{x})$	expectation of a function g of the random variable $\underline{x}$
var $\underline{x}$	variance of the random variable $\underline{x}$: $\mathcal{E}(\underline{x} - \mathcal{E}\underline{x})^2$
cv $\underline{x}$	coefficient of variation of the random variable $\underline{x}$: $\sqrt{\text{var } \underline{x}}/\mathcal{E}\underline{x}$
cov $(\underline{x}, \underline{y})$	covariance between the random variables $\underline{x}$ and $\underline{y}$: $\mathcal{E}(\underline{x} - \mathcal{E}\underline{x})(\underline{y} - \mathcal{E}\underline{y})$
cor $(\underline{x}, \underline{y})$	correlation between $\underline{x}$ and $\underline{y}$: cov $(\underline{x}, \underline{y})/\sqrt{\text{var } \underline{x} \text{ var } \underline{y}}$
$\boldsymbol{x}^T$	transpose of vector or matrix $\boldsymbol{x}$ (interchange rows and colums)
$\vdots$	catenation across columns: $\boldsymbol{n} = (\boldsymbol{n}_{\mathcal{M}} \vdots \boldsymbol{n}_{\mathcal{O}})$

Units, dimensions and types

The SI system is used to present units of measurements. My experience is that some readers are unfamiliar with the symbol 'a' for year.

In the description of the dimensions in the list of symbols, the following symbols are used

–	no dimension	L	length (of individual)	e	energy ($\equiv ml^2t^{-2}$)
t	time	l	length (of environment)	T	temperature
#	number (mole)	m	mass (weight)		

These dimension symbols just stand for an abbreviation of the dimension, and differ in meaning from symbols in the symbol column. A difference between the dimensions l and L is that the latter involves an arbitrary choice of the length to be measured (e.g. including or excluding a tail). The morph interferes with the choice. The dimensions differ because the sum of lengths of objects for which l and L apply does not have any useful meaning. The list below does not include symbols that are used in a brief description only. The page number refers to the page where the symbol is introduced.

The choice of symbols relates to dimensions, and not to types. Three types are specified in the description in the list: constant, c, variable, v, and function, f. This classification cannot be rigorous, however. The temperature T, for example, is indicated to be a constant, but it can also be considered as a function of time, in which case all rate constants are functions of time as well. On the other hand, variables such as food density, X, can be held

constant in particular situations. Variables such as structural biovolume V are constant for a short period, such as is relevant to the study of the process of digestion, but not for a longer period, such as is relevant for the study of life cycles. The choice of type can be considered as a default, deviations being mentioned in the text.

Table 3.4 gives useful relationships between energies, volumes and masses.

List of frequently used symbols

symbol	dim	type	page	interpretation
a	t	v	{324}	age, i.e. time since gametogenesis of fertilization
a_b	t	v	{97}	age at birth (hatching), i.e. end of embryonic stage
a_p	t	v	{255}	age at puberty, i.e. end of juvenile stage
$a_\dagger$	t	v	{139}	age at death (life span)
$\dot{b}_\dagger$	$l^3 \# ^{-1} t^{-1}$	c	{205}	killing rate by xenobiotic compound
$B_x(a,b)$	-	f	{107}	incomplete beta function
c_0	$\# l^{-3}$	c	{206}	no-effect concentration of xenobiotic compound in the environment
c_d	$\# l^{-3}$	v	{189}	concentration of xenobiotic compound in the water (dissolved)
c_X	$\# l^{-3}$	v	{197}	concentration of xenobiotic compound in food
c_V	$\# l^{-3}$	v	{190}	scaled concentration of xenobiotic compound in tissue: $[M_Q]P_{dV}$
d_*	$m\,L^{-3}$	c	{23}	density of compound $*$
$\dot{D}$	$l^2 t^{-1}$	c	{235}	diffusivity
e	-	v	{105}	scaled energy density: $[E]/[E_m] = m_E/m_{Em}$
e_0	-	v	{107}	scaled energy costs of one egg/foetus: E_0/E_m
e_b	-	v	{107}	scaled energy density at birth
e_R	-	v	{117}	scaled energy allocated to reproduction: $E_R E_m^{-1}$
E	e	v	{82}	non-allocated energy in reserve
E_0	e	v	{97}	energy costs of one egg/foetus
E_m	e	c	{107}	maximum non-allocated energy in reserve: $[E_m]V_m$
E_R	e	v	{31}	energy in reserve with allocation reproduction
$[E]$	$e\,L^{-3}$	v	{83}	energy density: E/V
$[E_b]$	$e\,L^{-3}$	v	{97}	energy density at birth
$[E_G]$	$e\,L^{-3}$	c	{94}	volume-specific costs of structure
$[E_m]$	$e\,L^{-3}$	c	{85}	maximum energy density
f	-	v	{73}	scaled functional response: $f = \frac{X}{X_K+X} = \frac{x}{1+x}$
$\dot{F}$	$l^3 t^{-1}$	v	{74}	filtering rate
$\dot{F}_m$	$l^3 t^{-1}$	c	{75}	maximum filtering rate
g	-	c	{94}	energy investment ratio: $\frac{[E_G]}{\kappa[E_m]}$
$\dot{h}$	t^{-1}	v	{141}	number-specific predation probability rate (hazard rate)
$\dot{h}_a$	t^{-1}	c	{144}	aging rate for unicellulars: $\frac{[E_G]}{\kappa\mu_{QC}} \frac{\dot{k}_E+\dot{k}_M}{g+1}$
$\ddot{h}_a$	t^{-2}	c	{141}	aging acceleration: $\propto \frac{[E_G]}{\kappa\mu_{QC}}$
$\dot{h}_m$	t^{-1}	c	{319}	max. throughput rate in a chemostat without complete washout
j_*	$\# \#^{-1} t^{-1}$	v	{120}	structure-specific flux of compound $*$: $\dot{J}_*/M_V$
$\dot{J}_*$	$\# t^{-1}$	v	{130}	flux of compound $*$

$\dot{J}_{*_1,*_2}$	$\#\,t^{-1}$	v	{169}	flux of compound $*_1$ associated with process $*_2$
$\dot{\boldsymbol{J}}$	$\#\,t^{-1}$	v	{130}	matrix of fluxes of compounds $\dot{J}_{*_1,*_2}$
$\{\dot{J}_{Xm}\}$	$\#L^{-2}t^{-1}$	c	{75}	surface-area-specific max ingestion rate
$[\dot{J}_{Xm}]$	$\#L^{-3}t^{-1}$	c	{76}	volume-specific maximum ingestion rate: $\{\dot{J}_{Xm}\}V_d^{-1/3}$
$\dot{k}_e$	t^{-1}	c	{190}	elimination rate of xenobiotic compound
$\dot{k}_E$	t^{-1}	c	{86}	specific-energy conductance: $\{\dot{p}_{Am}\}V_d^{-1/3}[E_m]^{-1} = [\dot{p}_{Am}]/[E_m]$
$\dot{k}_M$	t^{-1}	c	{94}	maintenance rate coefficient: $[\dot{p}_M]/[E_G]$
l	-	v	{105}	scaled body length: $(V/V_m)^{1/3}$
l_b	-	c	{107}	scaled body length at birth: $(V_b/V_m)^{1/3}$
l_d	-	c	{119}	scaled cell length at division: $(V_d/V_m)^{1/3} = \dot{k}_M g/\dot{k}_E$
l_h	-	c	{95}	scaled heating length: $(V_h/V_m)^{1/3}$
l_p	-	c	{112}	scaled body length at puberty: $(V_p/V_m)^{1/3}$
L	L	v	{23}	length: $V^{1/3}/\delta_{\mathcal{M}}$
L_b	L	c	{117}	length at birth: $V_b^{1/3}/\delta_{\mathcal{M}}$
L_d	L	c	{29}	length at cell division
L_m	L	c	{117}	maximum length: $V_m^{1/3}/\delta_{\mathcal{M}}$
L_p	L	c	{117}	length at puberty: $V_p^{1/3}/\delta_{\mathcal{M}}$
m_*	$\#\#^{-1}$	v	{34}	mass of compound $*$ in moles relative to M_V: M_*/M_V
m_{Em}	$\#\#^{-1}$	v	{120}	max molar reserve density: $M_{Em}/M_V = [M_{Em}]/[M_V]$
M_*	$\#$	v	{33}	mass of compound $*$ in moles
$\mathcal{M}(V)$	-	f	{27}	shape (morph) correction function: $\frac{\text{real surface area}}{\text{isomorphic surface area}}$
$[M_{Em}]$	$\#\,L^{-3}$	c	{35}	maximum reserve density in non-embryos in C-moles $[E_m]/\mu_E$
$[M_{sm}]$	$\#\,L^{-3}$	c	{80}	maximum volume-specific capacity of the stomach for food
$[M_V]$	$\#\,L^{-3}$	c	{34}	number of C-atoms per unit of structural body volume V
$n_{*_1*_2}$	$\#\#^{-1}$	c	{126}	number of atoms of element $*_1$ present in compound $*_2$
$\boldsymbol{n}$	$\#\#^{-1}$	c	{126}	matrix of chemical indices $n_{*_1*_2}$
N	$\#$	v	{324}	(total) number of individuals: $\int_a \phi_N(a)\,da$
$\dot{p}_*$	$e\,t^{-1}$	v	{82}	energy flux (power) of process $*$
$\dot{p}_{T+}$	$e\,t^{-1}$	v	{153}	total dissipating heat
$\dot{\boldsymbol{p}}$	$e\,t^{-1}$	v	{129}	vector of basic powers: $(\dot{p}_A\,\dot{p}_D\,\dot{p}_G)$
$\{\dot{p}_{Am}\}$	$e\,L^{-2}t^{-1}$	c	{81}	surface-area-specific maximum assimilation rate
$[\dot{p}_{Am}]$	$e\,L^{-3}t^{-1}$	c	{86}	volume-specific maximum assimilation rate: $\{\dot{p}_{Am}\}V_d^{-1/3}$
$[\dot{p}_M]$	$e\,L^{-3}t^{-1}$	c	{91}	volume-specific maintenance rate: $\dot{p}_M/V$
$\{\dot{p}_T\}$	$e\,L^{-2}t^{-1}$	c	{93}	surface-area-specific heating rate: $\dot{p}_T\,V^{-2/3}$
$P_{*_1*_2}$	-	c	{197}	partition coeff. of a compound in matrix $*_1$ and $*_2$ (moles per volume)
P_{ow}	-	c	{191}	octanol/water partition coefficient of a compound
P_{PX}	-	c	{197}	faeces/food partition coefficient of a compound
P_{Vd}	l^3L^{-3}	c	{190}	biomass/water (dissolved fraction) partition coefficient of a compound
P_{VW}	-	c	{197}	structural/total body mass partition coefficient of a compound
$q(c,t)$	-	v	{206}	survival probability to a toxic compound
$\dot{r}$	t^{-1}	c	{324}	number-specific population growth rate
$\dot{r}_B$	t^{-1}	c	{95}	von Bertalanffy growth rate: $(3/\dot{k}_M + 3fV_m^{1/3}/\dot{v})^{-1} = \dot{k}_M g/3(f+g)$
$\dot{r}_m$	t^{-1}	c	{319}	(net) maximum number-specific population growth rate
$\dot{r}_m^\circ$	t^{-1}	c	{319}	gross maximum number-specific population growth rate

$\dot{R}$	$\# t^{-1}$	v	{114}	reproduction rate, i.e. number of eggs or young per time
$\dot{R}_m$	$\# t^{-1}$	c	{115}	max reproduction rate
s	-	v	{213}	stress value
s_0	-	c	{217}	stress value without effect
t	t	v	{20}	time
t_d	t	v	{243}	inter division period
t_D	t	c	{118}	DNA duplication time
t_g	t	v	{80}	gut residence time
t_R	t	v	{198}	time at spawning
t_s	t	v	{80}	mean stomach residence time
T	T	c	{53}	temperature
T_A	T	c	{53}	Arrhenius temperature
T_b	T	c	{92}	body temperature
T_e	T	c	{92}	environmental temperature
$\dot{v}$	$L\, t^{-1}$	c	{85}	energy conductance (velocity): $\{\dot{p}_{Am}\}/[E_m]$
V	L^3	v	{31}	structural body volume
V_b	L^3	c	{111}	structural body volume at birth (transition embryo/juvenile)
V_d	L^3	c	{29}	structural cell volume at division
V_h	L^3	c	{94}	structural volume reduction due to heating: $\{\dot{p}_T\}^3[\dot{p}_M]^{-3}$
V_m	L^3	c	{94}	maximum structural body volume: $(\kappa\{\dot{p}_{Am}\})^3[\dot{p}_M]^{-3} = (\dot{v}/\dot{k}_M g)^3$
V_p	L^3	c	{111}	structural body volume at puberty (transition juvenile/adult)
V_w	L^3	c	{23}	physical volume
V_∞	L^3	c	{110}	ultimate structural body volume
$\mathcal{V}$	L^3	v	{272}	maximum structural body volume compared to reference: $z^3 V_{m1}$
w_*	$m\,\#^{-1}$	c	{34}	molar weight of compound $*$
W_d	m	v	{31}	dry weight of (total) biomass
W_w	m	v	{23}	wet weight of (total) biomass
x	-	v	{315}	scaled biomass density in environment: X/X_K
X_*	$\# l^{-3 \text{ or } -2}$	v	{73}	biomass density of compound $*$ in environment; default: food
X_{K*}	$\# l^{-3 \text{ or } -2}$	c	{73}	saturation coefficient of compound $*$; default: food
X_r	$\# l^{-3}$	c	{314}	substrate density in feed of chemostat
$y_{*_1*_2}$	$\#\#^{-1}$	c	{147}	coefficient that couples mass flux $*_1$ to mass flux $*_2$
Y	$\#\#^{-1}$	c	{315}	yield factor
z	-	v	{270}	zoom factor to compare body sizes
$\Gamma(x)$	-	f	{255}	gamma function
δ	-	c	{29}	aspect ratio
δ_l	-	c	{260}	shape parameter of generalized logistic growth
$\delta_{\mathcal{M}}$	-	c	{23}	shape (morph) coefficient: $V^{1/3}/L$
$\eta_{*_1*_2}$	$\# e^{-1}$	c	{130}	coefficient that couples mass flux $*_1$ to energy flux $*_2$: $\mu^{-1}_{*_2*_1}$
$\boldsymbol{\eta}$	$\# e^{-1}$	c	{130}	matrix of coefficients that couple mass to energy fluxes
θ	-	v	{42}	fraction of a number of items: $0 \leq \theta \leq 1$
κ	-	c	{65}	fraction of catabolic power energy spent on maintenance plus growth
κ_A	-	c	{162}	fraction of assimilation that originates from well-fed-prey reserves
κ_E	-	c	{170}	fraction of rejected flux of reserves that returns to reserves
κ_R	-	c	{114}	fraction of reproduction energy fixed in eggs
μ_*	$e\,\#^{-1}$	c	{151}	chemical potential of compound $*$

$\mu_{*_1*_2}$	$e\,\#^{-1}$	c	{130}	coefficient that couples energy flux $*_1$ to mass flux $*_2$: $\eta^{-1}_{*_2*_1}$
$\boldsymbol{\mu}_{\mathcal{M}}$	$e\,\#^{-1}$	c	{153}	vector of chemical potentials of 'minerals'
$\boldsymbol{\mu}_{\mathcal{O}}$	$e\,\#^{-1}$	c	{153}	vector of chemical potentials of organic compounds
ρ	-	c	{43}	binding probability of substrate
τ	-	v	{222}	scaled time
$\phi_N(a)$	$\#\,t^{-1}$	v	{324}	number of individuals of age in interval $(a, a+da)$
$\phi_{\underline{x}}(x)dx$	-	f	{44}	probability density of $\underline{x}$ evaluated in x
$\Phi_{\underline{x}}(x)$	-	f	{46}	distribution function of $\underline{x}$ evaluated in x: $\int_0^x \phi_{\underline{x}}(x_1)\,dx_1$
$\zeta_{*_1*_2}$	$\#\,\#^{-1}$	c	{148}	coefficient that couples mass flux $*_1$ to energy flux $*_2$: $\mu_E m_{Em} \mu^{-1}_{*_2*_1}$

Taxonomic index

Index